Application of sequence stratigraphic concepts to the cretaceous Urgonian carbonate platform, southeast France

Hunt, David William

Application Of Sequence Stratigraphic Concepts To The Cretaceous Urgonian Carbonate Platform, Southeast France.

David William Hunt.

A thesis submitted to the University of Durham for the degree of Doctor of Philosophy.

Department of Geological Sciences February, 1992.

Declaration.

The content of this thesis is the original work of the author and has not previously been submitted for a degree at this or any other university. Other people's work is acknowledged by reference.

David Hunt

Department of Geological Sciences,

University of Durham.

Copyright.

My parents, to whom this thesis is dedicated, enjoying the views and early morning sunshine Charmont Sommet, Chartreuse, July, 1990.

Application Of Sequence Stratigraphic Concepts To The Cretaceous Urgonian Carbonate Platform, Southeast France.

Carbonate platforms are increasingly being studied using sequence stratigraphic concepts and models borrowed from the study of siliciclastic shelves in passive margin settings. The direct transposition of the stratigraphic model for a siliciclastic shelf to its carbonate counterpart, the carbonate shelf, assumes that the two systems respond in a very similar way to changes of relative sea-level, the interpreted major control upon depositional stacking patterns. Current models depicting the sequence stratigraphic evolution of carbonate shelves are and have been frequently applied without regard for the differences between the siliciclastic and carbonate shelf depositional systems. It is the purpose of this study to test the current sequence stratigraphic model and its assumptions for a carbonate shelf.

Carbonate shelves do differ quite fundamentally from their siliciclastic equivalents. The carbonate shelf has the capacity to respond in quite different ways to changes in relative sea-level, compared to siliciclastic systems, as a result of the strong physio-chemical control upon carbonate sedimentation and the potential high rates of carbonate production at the shelf margin in comparison to rates of relative sea-level rise. Carbonate sedimentation rates are also differential across a shelf and highly sensitive to slight 'environmental' changes such as nutrient upwelling and temperature increases or decreases. This can lead to abrupt changes of sedimentation rate not necessarily related to changes of relative sea-level. Because of these differences carbonate shelves can develop stratal patterns similar to siliciclastic settings, but in the majority of cases they are very different.

In direct contrast to siliciclastic systems the lowstand systems tract is normally impoverished on the flanks of carbonate shelves. Two different end-members of lowstand sedimentation are distinguished for carbonate shelves and these reflect the inherited morphology of the slope: low angle, mud-dominated slopes are characterized by basin-floor slides and debrites during times of falling relative sea-level and by a relatively large volume autochthonous slope wedge. In direct contrast, high angle slopes are characterized by basin-floor megabreccias and volumetrically very small or even absent autochthonous slope wedges. The carbonate transgressive systems tract can also develop a wide variety of stratal patterns, a reflection of the often complex interplay of variable sedimentation rates and rates of relative sea-level rise. Two different types of geometric stacking pattern are distinguished: *type 1 geometries*, developed when sedimentation rates are less than rates of relative sea-level rise, and *type 2 geometries* formed when sedimentation rates are equal to or greater than rates of relative sea-level rise. The highstand systems tract is the time of maximum carbonate production potential and is normally associated with rapid basinwards progradation. For the highstand systems tract two different types of foreslope progradation are distinguished, *slope aprons* and *toe-of-slope aprons*. These differences between carbonate and siliciclastic depositional models suggest that simple application of the previously published models can lead to incorrect interpretation of systems tracts, sequences and therefore relative sea-level curves.

Sequence stratigraphic models and concepts are tested by application to the spectacular seismic scale exposures of the mid-Cretaceous Urgonian platform, SE France. The platform is divided into a lower 'regressive' part, the Glandasse Formation and an upper 'transgressive' part the Urgonian Limestone Formation. These are dominated by progradational outer-shelf grainstone facies and aggradational shelf-lagoonal facies respectively. Criteria are developed to identify key surfaces and stratal packages upon the Urgonian platform. On the shelf sequence boundaries are readily defined and are marked by sub-aerial exposure surfaces associated with meteoric diagenesis. Lowstand sedimentation is generally absent, but can be represented by lacustrine facies. Strong erosional truncation is only developed on the shelf if siliciclastics are introduced during lowstand of sea-level. Thus, the transgressive and highstand systems tracts dominate shelf sedimentation but can only be distinguished if a clear flooding surface is developed, and this is not always the case. On the slope large-scale erosional surfaces developed by sedimentary bypass and/or slope collapse can develop at any stage of a sequence and make identification of the sequence boundary more difficult. Similarly, on the basin-floor allochthonous debris derived from slope collapse and/or bypassing is not restricted to times of falling relative sea-level. From the criteria developed for identification of key stral surfaces and packages a sequence stratigraphy for the Urgonian platform is built. This is placed within the time scale of Haq *et al.* (1987), and relative sea-level curves for the platform are constructed. These are compared to the eustatic sea-level charts from which they differ significantly. Minimum aggradation rates are also compared to other well known ancient carbonate platforms, from which the Urgonian is shown to have very high sedimentation rates.

'So Dave are you still here? Just how many PhD's are you doing?'

-Lee Margetts

Acknowledgements.

-First and foremost I have to thank my parents for their great support during this PhD without which much, if not all of it would not have been possible. I'm sure you're pretty glad this most prolonged education has at last ended.

-Maurice Tucker (sorry you only made it to second place) is thanked for his constant help and input to this thesis, without which it would be particularly lacking in the appropriate background reading, spelling, punctuation etc. and laying a sound foundation for a geological career in carbonate sedimentology.

-Jenny Robb is acknowledged for her company in Durham and assistance in the field.

-Annie Arnaud-Vanneau and Hubert Arnaud contributed greatly to the field study upon the Urgonian platform. The unselfish use of their time, resources in the field and numerous discussions in the bars and restaurants of Dauphinois are very much appreciated.

-John Hirst and Rod Graham at BP are thanked for a crash-course introduction to sequence stratigraphy in the field and six course slap up meals accompanied by ample vin de table.

-I am most grateful to all the technicians in geology at Durham for their help. Special thanks must go to Alan Carr for removing the numerous obstacles to successful photography, Karen who drafted many figures for publication (some of which are included here), Dave Asberry for his 'Jim'll fix it' like powers and his occasional blind eye and Ron Lambert for his numerous encounters with the dark force.

-Carole Blair and Lynne Gilchrist are thanked for numerous favours and occasional abuse of their typing skills.

-George Randall and Ron Lambert supplied endless patience and thin sections from the dungeon. These greatly aided this project.

-Gerald Roberts, Jon Henton, Steve Moss, Dougy Forbes and Jon Booler are thanked for their gracious submission of room 216 to me. S. Moss is thanked for his removal

services and particular not having used them on me. G. Roberts deserves special thanks for opening the 'escape tunnel'.

-Rob and Cath Gawthorpe helped enormously in preparation of the passport from Durham in December 1990 for which I am most grateful. Rob was also pretty enthusiastic whilst at Durham and this certainly helped.

-I must also thank Hugh Sinclair for numerous stimulating conversations concerning enigmatic parts of sequence stratigraphy, and Dick Swarbrick for reviewing early drafts of manuscripts and introducing me to the Geology of Cyprus.

-Ian Parkinson, Mike 'bruised knuckles' Curtis, Mark Wharton and Tim Allsop are also thanked, for reasons only they surely know.

-Finally I must mention Cherry Walker for special rent concessions, numerous lifts and for putting up with me during the most tormented last stages of writing up and my sisters.

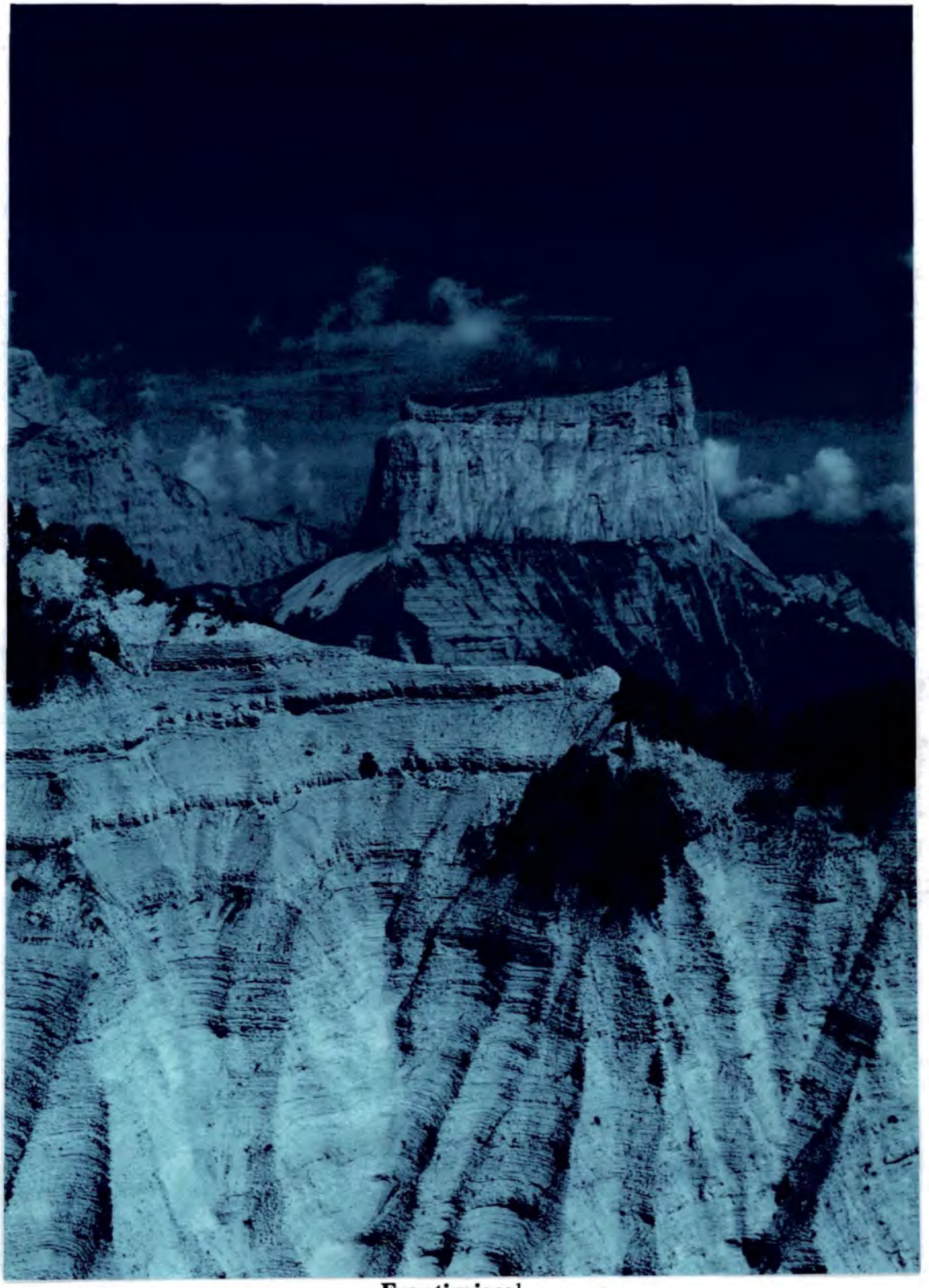

Frontispiece[1] **.**

The spectacular south face of Mont Aiguille to the east of the southern Vercors, southeast France. This mountain first ascended in 1492 at the order of the King of Savoie marks the birth of Alpinism. Note the downlap of clinoforms at the base of the cliff, further discussed in Chapter 5.

[1] Photograph from print courtesy of Gerald Roberts.

Contents.

2.3. A Critique Of Sequence Stratigraphic Models And Alternatives.

Chapter 3.

Sequence Stratigraphic Models For Carbonate Shelves.

6.2. Sequence Stratigraphic Evolution Of The Urgonian Platform.

pgs. 282-369

Chapter 1.
Thesis Objectives And Outline.

In recent years sequence stratigraphic models have become an increasingly widespread tool in basin analysis, particularly within the hydrocarbon industry (eg. Vail *et al.*, 1977; Haq *et al.*, 1987; 1988; Van Wagoner *et al.*, 1990 etc.). These models were developed from the study of stratigraphic packages in seismic sections and attempt to predict facies associations in the sub-surface from stratal termination patterns and the geometric relationships of stratal packages. Sequence stratigraphic models depict the conceptual stratigraphic development of a siliciclastic shelf through a cycle of relative sea-level change (eg. Vail *et al.*, 1977; Posamentier & Vail, 1988; Van Wagoner *et al.*, 1990). Characteristically, sedimentation through a cycle of relative sea-level change develops three distinct stratal packages termed systems tracts from lowstand of relative sea-level through times of rapidly rising sea-level (transgressive phase) to highstand of relative sea-level. These are named the lowstand, transgressive and highstand systems tracts respectively and each is a stratal package with unique position and stratal termination patterns upon the basin-floor, slope or shelf. The geometric relationships of these systems tracts are used to predict facies associations in the sub-surface and have also been used to build sea-level charts (eg. Vail *et al.*, 1977; Haq *et al.*, 1987; 1988)

Increasingly, these and similar sequence stratigraphic models are being used to predict facies associations and interpret relative sea-level changes upon carbonate shelves, and they are commonly applied with little or no modification both in the subsurface and at outcrop (eg. Vail, 1987; Sarg, 1988; Eberli & Ginsburg, 1989; Rudolph & Lehmann, 1989; Jacquin *et al.*, 1991). However, it is well known that carbonate and siliciclastic sediments originate, are deposited and are lithified in very different ways so that the siliciclastic and carbonate depositional systems may differ fundamentally in their response to relative sea-level changes and so develop different and unique geometries from each other.

It is the first objective of this thesis to explore the differences and similarities of these two depositional systems and, where necessary, to develop new models which account for the differences between carbonate and siliciclastic shelves in open ocean settings. The second objective of this thesis is to apply the new, revised sequence stratigraphic models developed in this thesis to the outcrop where they can be tested, compared and evaluated next to other sequence stratigraphic models and other workers sequence stratigraphic schemes. For this second part of the study the well known and spectacularly exposed Urgonian platform of the French Sub-Alpine Chains was chosen. This platform was selected for study as it offers a combination of seismic scale exposures and a relatively well known, recently studied stratigraphy (eg. Arnaud-Vanneau, 1980; Arnaud, 1981).

An understanding of the various controls upon the geometric stacking patterns and facies associations developed by carbonate shelves in open ocean settings is particularly important to the hydrocarbon industry, for carbonate platforms contain approximately 42% of the worlds known hydrocarbon reserves. The development of sequence stratigraphic models specific to carbonate shelves in open ocean settings, and a better understanding of the various factors which control stacking patterns upon carbonate shelves should help to predict more accurately and precisely facies associations from geometric relationships developed on these platforms.

Thesis Outline.

- Chapter 2.

This chapter introduces the assumptions, concepts and sequence stratigraphic models of Vail (1987), Haq *et al.* (1987, 1988) Posamentier & Vail (1988), Posamentier *et al.* (1988) and Van Wagoner *et al.* (1990), and discusses the relationship of stratal packages to changes of relative sea-level. The latter part of the chapter discusses the alternative sequence stratigraphic scheme of Galloway (1989), introduces new systematics for times of falling and lowstand of relative sea-level and

illustrates alternative stratal geometries and relationships which can be developed by the lowstand wedge.

- Chapter 3.

This chapter examines the application of sequence stratigraphic models conceptually developed for siliciclastic shelves to carbonate shelves. The carbonate sequence stratigraphic controversy is introduced, followed by a comparison of siliciclastic and carbonate depositional systems where the differences between the two are highlighted. The role of environmental changes in the development of distinctive stratal packages is also discussed and it is argued that these can have a role as great or even greater than relative sea-level changes on the development of stratal packages upon a carbonate shelf. From this introduction new models are developed for carbonate shelves in open ocean settings. These models account for the greater variability of geometries that can be developed on a carbonate shelf. Different geometries developed by carbonate shelves reflect the high, variable and differential sediment production potential unique to the carbonate shelf. These new, alternative models are discussed and illustrated using well known examples, primarily from the sub-surface. Finally, the development of a conceptual carbonate shelf is discussed and illustrated. This conceptual development of a carbonate shelf highlights the differences that can be developed between a carbonate and a siliciclastic shelf.

- Chapter 4.

The geological background to the Urgonian platform is introduced. Firstly the general tectonostratigraphic evolution of the passive margin is discussed from the onset of extension through to its subsequent inversion during Alpine orogenesis. In particular the tectonic evolution of the External Zone and its component palaeogeographic domains, the Jura Platform, Dauphinois Basin and Vocontian Basin are discussed, highlighting their development during the late Jurassic and early Cretaceous. The history of Urgonian research is briefly reviewed and the Urgonian

palaeontological controversy discussed before the general stratigraphy of the platform is introduced. This is accompanied by the original conceptual development of the platform as devised by Arnaud-Vanneau (1980) and Arnaud (1981) prior to the application of sequence stratigraphic concepts. The main microfacies in the framework of the facies model of Arnaud-Vanneau (1980) and Arnaud (1981) are also briefly introduced and discussed.

- Chapter 5.

The criteria used to identify the sequence boundary and other major stratal surfaces upon the Urgonian platform are detailed in this Chapter. Contrasts are drawn between geometric and sedimentological criteria for the identification of sequence boundaries, in particular using a seismic scale example from the southern Vercors. The characteristic stratal patterns and development of systems tracts and parasequences are discussed for the shelf, slope and basin-floor in-turn.

- Chapter 6.

The sequence stratigraphic evolution of the Urgonian carbonate platform is discussed in this Chapter using the models and concepts introduced in the preceding Chapters of this thesis. The sequences of the platform are each discussed in the stratigraphic order of their development and contrasts are drawn to alternative schemes and the sequence stratigraphic model for a siliciclastic shelf. A relative sea-level curve is constructed from the Urgonian platform, compared to other charts for the platform and the 'eustatic' chart of Haq *et al.* (1987).

- Chapter 7.

This chapter lists the principal conclusions of the thesis.

Chapter 2.
Sequence Stratigraphy.

2.1. Introduction.

The recognition of seismic-scale repetitive sedimentary units with characteristic internal geometries has led to the development of sequence stratigraphy. A *sequence* is bounded above and below by regionally extensive unconformities and their correlative basinal conformities, termed *sequence boundaries* (Mitchum *et al.*, 1977) (Fig. 2.1). Each sequence is interpreted to form as a result of sedimentation during a cycle of relative sea-level change, from a lowstand, through times of rising sea-level (transgressive), to a relative sea-level highstand (eg. Vail *et al.*, 1977; Vail *et al.*, 1984; Haq *et al.*, 1987; Posamentier *et al.*, 1988). As relative sea-level changes, sediment bodies (*systems tracts*) with characteristic position (eg. shelf, slope, basin-floor) and distinctive internal stacking patterns (eg. progradational, aggradational, retrogradational) develop. These are named according to the sea-level stand during which they are interpreted to have developed, ie. *lowstand/shelf margin wedge*, *transgressive* and *highstand systems tracts* (Fig. 2.1).

Recognition of the characteristic geometries of sequences and systems tracts and their initial interpretation to represent globally synchronous eustatic sea-level changes led to the erection of global sea-level curves (eg. Vail *et al.*, 1977; Haq *et al.*, 1987, 1988), a powerful tool for the prediction of stratal geometry and facies associations in the sub-surface. The eustatic or 'Vail / Haq' curves were originally proposed as a seismic correlation tool in 'frontier' basins where seismic data were available, but the geological control was poor. Proponents of the eustatic curves argued that the global synchroneity of eustatic cycles and their role as the fundamental control upon basin stratigraphy enabled stratigraphic correlation purely upon the basis of sub-surface geometric stacking patterns (eg. Vail *et al.*, 1977; Haq *et al.*, 1987, 1988 etc).

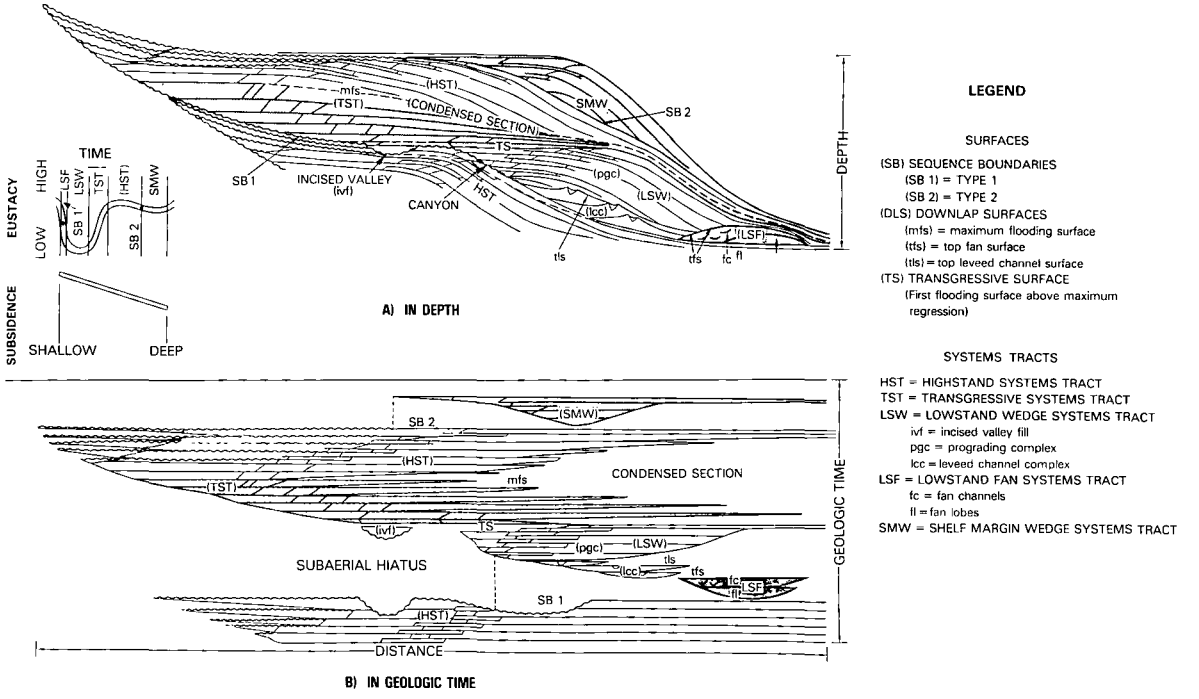

Figure 2.1. Summary stratigraphic sequence model illustrating the component systems tracts (here five) for a siliciclastic shelf. The lower sequence has a type 1 sequence boundary and the upper a type 2 boundary. The lower figure (B) illustrates the chronostratigraphic relationships of the stratal units depicted in A. From Haq *et al.* (1988).

This approach appears to be particularly successful for the late Tertiary which, for the most part is characterized by high amplitude, high frequency eustatic sea-level variations related to fluctuations in ice-sheet volumes (eg. Williams, 1988). Comparison of the Tertiary eustatic curves of Haq *et al.* (1987, 1988) to independent data such as ^{18}O stratigraphies shows favourable correlation (eg. Fig. 2.2). This compatibility suggests that for similar times (eg. icehouse times) the approach of Vail *et al.* (1977) and Haq *et al.* (1987, 1988) can be useful as assumptions concerning global synchroneity of sea-level cycles appear to be applicable in all but the most tectonically active basins.

The extrapolation of high-amplitude 'eustatic' sea-level changes interpreted from seismic sections (eg. Haq *et al.*, 1987, 1988) into the supposedly ice-free Early Tertiary and Mesozoic (eg. see Barron *et al.*, 1981; Sloan & Barron, 1990) is,

however, a matter of some contention. The inference of 'icehouse' type eustasy into the early Cenozoic and Mesozoic where evidence for glaciation is absent suggested to many workers (eg. Pitman, 1978; Parkinson & Summerhayes, 1985; Miall, 1986; Carter, 1988; Hubbard, 1988) that the 'eustatic' stratal patterns of Vail *et al.* (1977) and Haq *et al.* (1987, 1988) could be developed by other mechanisms such as changes in the rate and spatial distribution of tectonic subsidence. Evidence is now overwhelming that sequences develop during changes of *relative sea-level*; the combination of tectonic subsidence and eustasy, and at different times and/or places the relative importance of either eustatic or tectonic components differs.

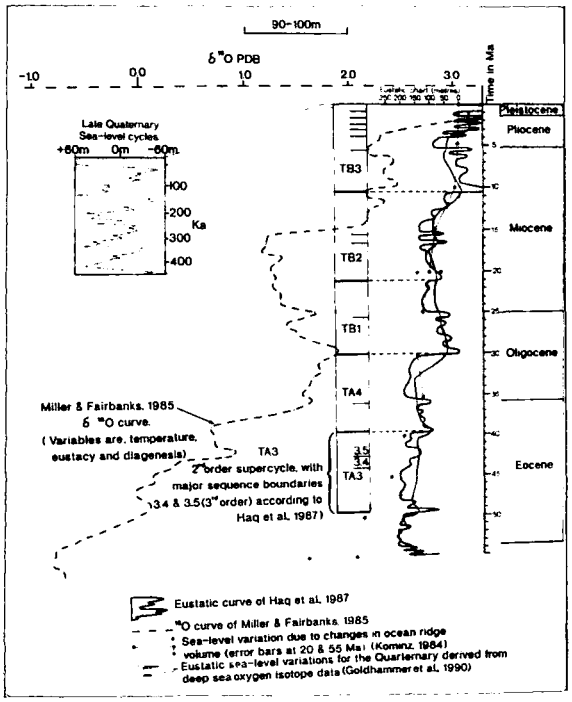

Figure 2.2. Comparison of the Tertiary 'eustatic' sea-level chart as developed from seismic stratigraphic methodology (Haq, 1987) with the ^{18}O stratigraphy of Miller & Fairbanks (1985).

The 'relaxation' of the 'eustatic' interpretations of sequence stratigraphy led to a general acceptance of sequence stratigraphic models and a rapid expansion of their usage in both the hydrocarbon industry and academia. Application of sequence stratigraphy (eg. Bally *et al.*, 1987) forced a re-evaluation of strata in the context of a dynamically linked shelf-slope-basin system with respect to changes of relative sea-level. Initial outcrop studies, predominantly upon siliciclastic exposures of the western USA, illustrated how the seismic scale geometries could be recognized and interpreted in the context of the 'Exxon' model (eg. see Wilgus *et al.*, 1988).

More recently, the application of sequence stratigraphic models and concepts to Quaternary and Holocene deposits where the rates, amplitude and frequency of sea-level changes are well constrained has allowed a rigorous testing of the models (eg. Thorne & Swift in press). Initial attempts to apply the sequence stratigraphic model to carbonate depositional systems have been extremely controversial (eg. Shanmugam & Moiola, 1982: Mullins, 1983; Sarg, 1988; Schlager, 1991; Jacquin *et al.*, 1991; Hunt & Tucker, 1992) and is the subject of Chapter 3.

New concepts and models are introduced later in this chapter but firstly the 'Exxon' model is introduced. The following Section (2.2) describes the theoretical development of a siliciclastic shelf: the 'Exxon' sequence stratigraphic template.

2.2. Sequence Stratigraphic Terminology, Definitions, Models and Concepts of the Exxon Model.

2.2.1. Introduction.

Sequence stratigraphic models and concepts have evolved considerably since their initial publication (Vail *et al.*, 1977) although the controversial interpretation of a eustatic control upon sequences and their global correlation has been a linking theme between many of their revisions and refinements (eg. Vail & Todd, 1981; Vail

et al., 1984; Haq *et al.*, 1987; Posamentier *et al.*, 1988; Posamentier & Vail, 1988). The ongoing working hypothesis of the Exxon group that sea-level changes exert the fundamental control upon stratal patterns and has led to a partly interpretative terminology of geometric stratal stacking patterns. Discrete stratal packages bound by stratal discontinuities (systems tracts) are named according to the sea-level stance for which they are interpreted to have developed (eg. *lowstand*, *transgressive* and *highstand systems tracts*).

2.2.2. Interpretations and assumptions.

A sequence is interpreted to develop during a cycle of relative sea-level change from an initial fall of sea-level (lowstand), through times of rapid sea-level rise (transgression) followed by a period of time when the rate of rise is reduced, the highstand. The 'Exxon' models and concepts of sequence stratigraphy have several important assumptions, and these are summarised below:

1) The depositional setting is a passive margin setting, where the physiography is characterized by a shelf, slope and basin. The shelf has basinward dips at less than $0{\cdot}5^{\circ}$, the slope 3° to 6° with dips of 10° locally developed along canyon walls. The transition from shallow to deep water is abrupt (Van Wagoner *et al.*, 1990).

2) The trend of the eustatic curve is approximately sinusoidal (Posamentier *et al.*, 1988; Posamentier & Vail, 1988).

3) Relative sea-level change contains a strong eustatic component as this is the only variable thought to fluctuate at a sufficient rate to produce the frequency (1-10Ma) of sequences (Vail *et al.*, 1977; Posamentier *et al.*, 1988; Posamentier & Vail, 1988).

4) Sequence stratigraphic patterns result from the interaction of eustasy and tectonic subsidence which reduces or increases the space available for the *accommodation* of

sediments (Posamentier *et al.*, 1988; Posamentier & Vail, 1988). Other factors such as sedimentation rates and major oceanographic changes, are secondary variables and as such do not significantly modify the signature resulting from changes in accommodation. Thus, each systems tract may be correlated with a segment of the 'eustatic curve', although locally the timing of its development will be modified by local rates of subsidence and/or sedimentation (Vail *et al.*, 1984; Parkinson & Summerhayes, 1985; Posamentier *et al.*, 1988; Posamentier & Vail, 1988).

5) Rates of tectonic subsidence are assumed constant as a function of time throughout the deposition of a sequence, and increase in a basinwards direction.

6) Sedimentation rates remain relatively constant with time, but are enhanced during times of falling sea-level.

7) The differences of depositional pattern between different depositional systems are secondary factors and do not modify stacking patterns which contain the essentially eustatic signature (This theme is explored further specifically for carbonate shelves in chapter 3).

Posamentier & Vail (1988) acknowledged that these assumptions are simplistic, but allowed the construction of a general model which would need modification to be successfully applied to specific basins.

2.2.3. Terminology, definition and conceptual development of stratal packages.

[1]A *sequence* is the fundamental unit of sequence stratigraphy and was originally defined as 'a relatively conformable succession of genetically related strata bounded by unconformities or their correlative conformities' (Mitchum, 1977), the sequence bounding unconformities and their correlative conformities are termed

[1] The text of Sections 2.2.3-2.2.6 is accompanied by Figures 2.1 & 2.5.

sequence boundaries. This definition has subsequently been modified (eg. Van Wagoner *et al.*, 1988) and restricted, re-defining an unconformity as 'a surface separating younger from older strata, along which there is evidence of subaerial erosional truncation (and in some areas, correlative submarine erosion) or subaerial exposure, with a significant hiatus indicated. This definition restricts the usage of the term unconformity to significant subaerial surfaces'. As Schlager (1991) points out this usage is too restrictive as it is not sufficiently broad to include sequence boundaries which develop due to major environmental changes.

Each sequence is divisible into three of four possible (or 4 of 5; see Sections 2.2.4. & 2.3.2) *depositional systems tracts* of which all but one (shelf-margin wedge) are named according to the stance of sea-level during which they are interpreted to have developed: the *lowstand / shelf margin wedge*, the *transgressive* and the *highstand* systems tracts. Each systems tract can be recognized from its position along the depositional surface (shelf, slope, or basin-floor), internal stratal termination patterns and the stacking patterns of its component members, termed *parasequences.*

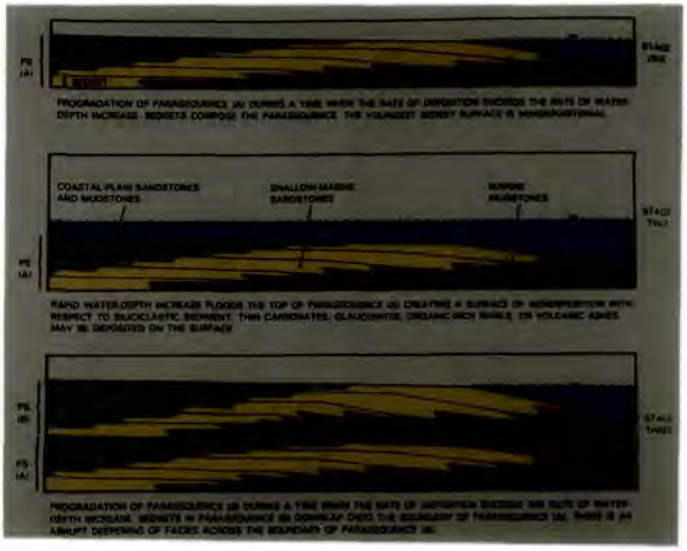

Figure 2.3. Progressive conceptual development of a siliciclastic parasequence in relation to relative sea-level rise(s). Sedimentation rates are assumed constant. From Van Wagoner *et al.* (1990).

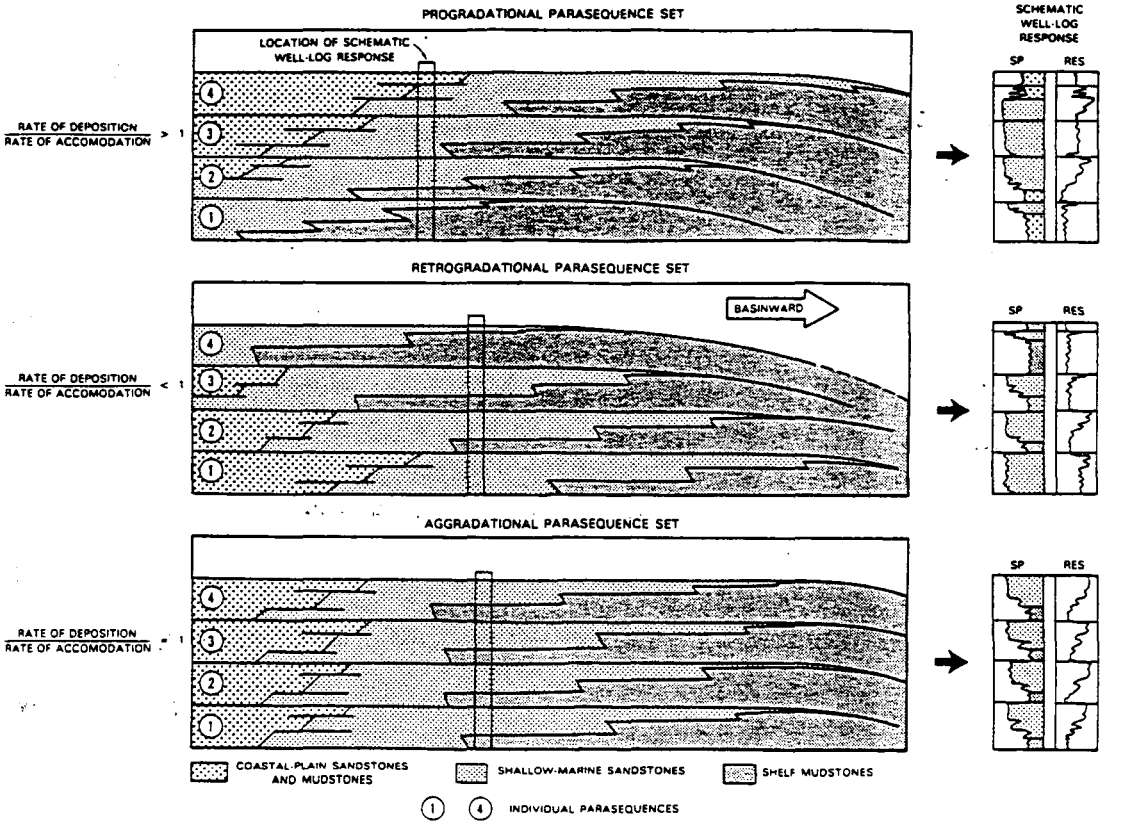

Figure 2.4. Parasequence stacking patterns in parasequence sets and the relation of sedimentation rates to rates of relative sea-level rise in each case. From Mitchum & Van Wagoner (1991), after Van Wagoner *et al.* (1990).

A parasequence is composed of 'a genetically related succession of beds or bedsets bounded by marine-flooding surfaces or their correlative surfaces' (Van Wagoner, 1985; Van Wagoner *et al.*, 1988). The progressive conceptual development of a parasequence is illustrated in Figure 2.3. Parasequences 'build-up' or 'stack' to form *parasequence sets* which have progradational, aggradational or retrogradational stacking patterns. The different patterns reflect the ammount of accommodation or space generated by each transgressive event (Fig. 2.4). A depositional systems tract consists of either 1 or 2 parasequence sets (eg. aggradational and progradational parasequence sets are depicted for the highstand systems tract of Figure 2.1).

2.2.4. Dynamics of sequence development.

The following description of a type 1 and type 2 sequence is based upon the stacking patterns and systems tract nomenclature of Haq *et al.* (1987, 1988) and the concepts and sediment dynamics of Posamentier *et al.* (1988) and Posamentier & Vail (1988). A sequence develops during a cycle of eustatic sea-level change which is sinusoidal in form and has a third order periodicity (1-10Ma) such that tectonic subsidence can be considered constant. The combination of eustasy and tectonic subsidence is relative sea-level although the eustatic signature is considered the most important component controlling stratal stacking patterns (Posamentier *et al.*, 1988; Posamentier & Vail, 1988; Haq *et al.*, 1987, 1988 etc.). Different stratal patterns develop in response to changes in the rate and amplitude of relative sea-level change and distinctive stratal boundaries (of the systems tracts) tend to develop at the steepest parts of the curve when the rates of change are highest (Posamentier *et al.*, 1988; Posamentier & Vail, 1988).

Sequence boundaries are interpreted to develop in response to a lowering of relative sea-level either to the vicinity of, or below the shelf-slope break. A range of sequence boundaries are theoretically possible although practically two end-members are generally recognized, *type 1* and *type 2* boundaries. A sequence boundary passes from a subaerial unconformity on the shelf basinwards to a correlative conformity. In the case of a type 1 sequence boundary the unconformity is developed in both subaerial and marine environments (eg. Fig. 2.1). Contrastingly, in the case of type 2 sequence boundaries unconformities are only developed subaerially (on the shelf) and do not extend into the marine environment (the slope).

The type of sequence boundary developed is believed to reflect both the rate and amplitude of relative sea-level fall. High amplitude and/or high rates of relative sea-level fall drop sea-level below the shelf-slope break to develop a type 1 sequence boundary (Vail, 1987; Van Wagoner *et al.*, 1990 etc). Type 2 sequence boundaries are developed when sea-level falls at a slower rate and/or has a lower amplitude so that the shelf is exposed to the vicinity of, but not below the shelf-slope break (Figs

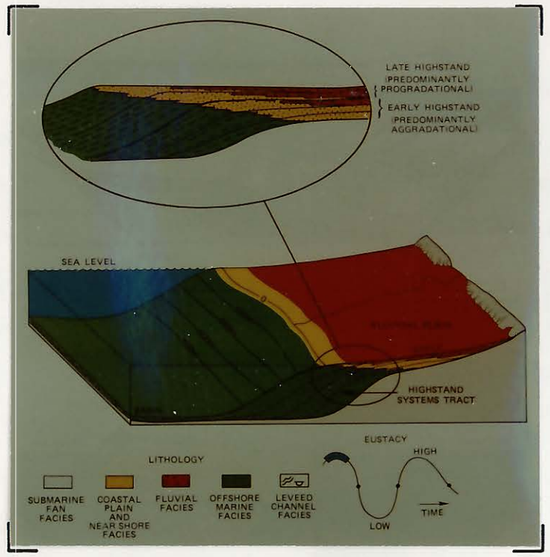

a. Highstand systems tract I.

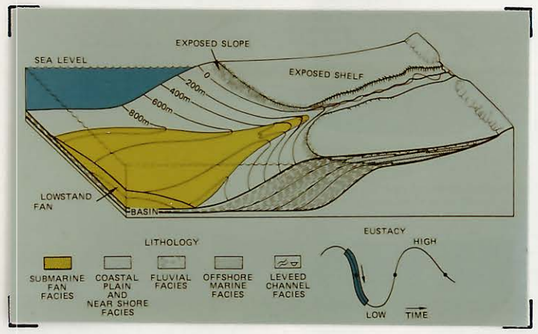

b. Lowstand fan systems tract.

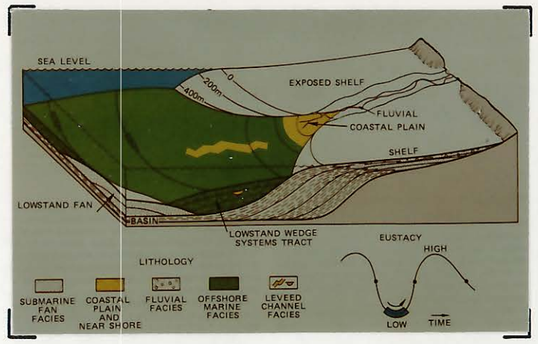

c. Lowstand wedge systems tract.

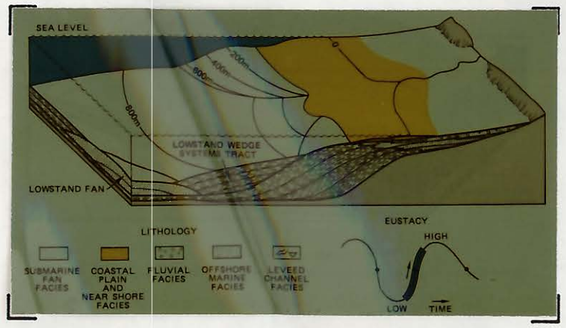

d. Transgressive systems tract.

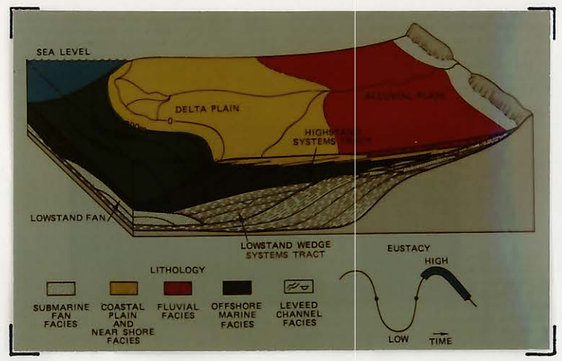

e. Highstand systems tract II.

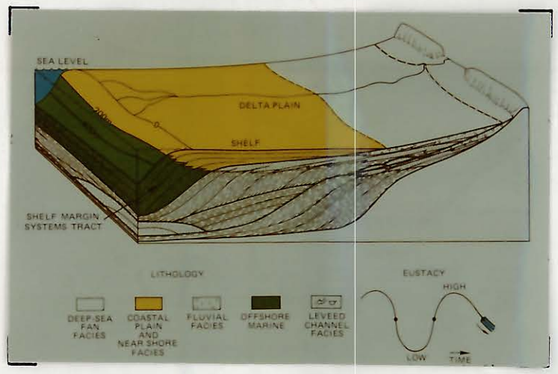

f. Shelf margin wedge systems tract.

Figure 2.5. Conceptual three dimensional diagrams depicting the development of lowstand, transgressive, highstand and shelf margin systems tracts in relation to eustatic sea-level change. From Posamentier & Vail (1988). Nomenclature after Haq *et al.* (1987;1988), see Fig 2.1.

2.1 & 2.5). Common to both type 1 and 2 sequence boundaries is a basinward and downward shift of both the facies and the locus of deposition.

Before discussing the development of a type 1 sequence it is useful to point out that there is some confusion in the literature concerning the stratal units associated with times of falling and lowstand of relative sea-level. Three distinct stratal packages are differentiated in the stratigraphic model illustrated in Figure 2.1: the basin-floor fan, slope fan and slope wedge. The lowermost stratal unit, the fan, is downlapped by the stratigraphically younger slope fan and wedge (Figs 2.1 & 2.5). This stratal discontinuity is termed the top fan surface (tfs).

Vail (1987), and most proponents of the 'Exxon' model (eg. Posamentier & Vail, 1988; Van Wagoner *et al.*, 1990 etc.) include all three stratal packages within the general umbrella of the *lowstand systems tract.* Haq *et al.* (1987; 1988) mark a departure from this approach separating the basin-floor fan into its own systems tract (*lowstand fan systems tract*) distinct from both the slope fan and wedge which are placed into their own systems tract; the *lowstand wedge systems tract.* The boundary between the two is the tfs, a stratal discontinuity separating times of falling from times of rising sea-level. This scheme, although far less cited is followed here.

2.2.5. Dynamics of sedimentation during development of a type 1 sequence.

2.2.5. A. *Lowstand fan systems tract.*

As sea-level falls at the beginning of a type 1 sequence the shelf moves above depositional base-level and becomes increasingly exposed. As the shelf is exposed fluvial systems extend basinwards across the shelf and sit abruptly upon marine sediments. The drop of base-level rejuvenates the fluvial systems which incise and cannibalise the preceding highstand (eg. Fig. 2.5a). The fluvial systems which, in the preceding sequence had deposited their load in coastal plains and deltas upon the shelf are forced to carry their load (itself enhanced from cannibalisation of the highstand) through and across the shelf via incised valleys (eg. Fig. 2.5a). The sediment budget

upon the shelf is reversed from positive to negative as the fluvial systems both incise and bypass sediment through it.

In seismic sequence stratigraphy the fall of relative sea-level *appears* to be almost instantaneous (eg. see Vail *et al.*, 1977); no stratigraphic units are normally resolved between the highstand and the lowstand. This accounted for the initial publication of saw-toothed sea-level curves interpreted from seismic sections (eg. Vail *et al.*, 1977). With the application of sequence stratigraphic concepts and models to outcrop, units developed during 'forced regression' (falling sea-level) situated between the highstand and lowstand systems tract have become increasingly recognized and are termed *stranded parasequences* (eg. Van Wagoner *et al.*, 1990).

Stranded parasequences develop as sea-level does not fall to its lowest point instantaneously. As, for example, sea-level falls on the third order time scale, shorter periodicity cycles (4th-5th order) are superimposed upon it, alternately accelerating and decelerating the lower order fall. During times when the fall is decelerated (eg. stillstand or relative sea-level rise) 'stranded deltas' or 'stranded parasequences' are deposited (Van Wagoner *et al.*, 1990). Depending upon the position of relative sea-level, stranded parasequences can be developed either on the shelf or slope. The term 'stranded parasequences' refers to the fact that these are not genetically linked to the highstand; however they are included with this systems tract since they are currently placed below the sequence boundary (Van Wagoner *et al.*, 1990, pg. 36) (see 2.3.2. for discussion of this point). As sea-level then resumes its general fall these parasequences are soon abandoned and incised. Stranded parasequences form only a minor part of a sequence, and particularly in siliciclastic systems they have a poor preservation potential.

During times of falling sea-level the vast *majority* of sediment is forced to bypass both the shelf and slope to the basin-floor. The slope is bypassed by a submarine canyon which passes upslope through the incised shelf-slope break to the major fluvial axis, itself confined to an incised valley. Incision of the bypass system into the shelf and slope is interpreted to be approximately synchronous and developed

as sea-level falls. Sediments are funnelled through the slope as high density turbidity currents confined to the slope canyon and deposited upon the basin-floor as a submarine (lowstand) fan (eg. Mitchum, 1985). The lowstand fan has a high sand/mud ratio as coarse sands which would have been deposited in alluvial and coastal environments are forced to bypass these areas which are either significantly reduced or even eliminated (eg. Fig. 2.5b).

The amount of erosional truncation developed on both the shelf and slope during times of falling sea-level (forced regression) is thought to reflect the sediment load of the fluvial systems; major fluvial axes are characterized by strong erosional truncation which weakens or is even absent away from these areas (eg. Brown & Fischer, 1980, their fig. 37) (Fig. 2.5b). Thus, although the model for a type 1 sequence boundary depicts strong erosion of the shelf and slope, and bypassing of sediments to the basin-floor, this is likely to be localised to the vicinity of major fluvial axes. Correspondingly, basin-floor fans are localised to areas of high sedimentation rate and will correlate laterally to slope fans where erosional truncation is much reduced.

The stratal relationships that characterise the lowstand fan systems tract are shown in Figures 2.1 and 2.5b. Upon the shelf the most diagnostic feature is erosional truncation which, on the scale of the sequence is very localised to fluvial axes. The vast majority of the shelf will be characterized by parallel stratal relationships with the overlying systems tracts. Small stranded parasequences may be developed upon either shelf or slope and will be characterized by local onlap/downlap relationships. The slope, like the shelf, is locally characterized by strong erosional truncation, weaker or absent away from the main fluvial axes. The basin-floor is the main site of deposition and is characterized in both dip and strike sections by mounded stratal patterns developed by lobes of the distributary fan system (Mitchum, 1985). Erosional truncation is thus the diagnostic feature of this systems tract on both shelf and slope and mounded stratal patterns on the basin-floor. As a whole the

systems tract represents the basinward and downward shift of the depocenter from the shelf to the basin-floor.

2.2.5. *B. Lowstand wedge sytems tract.*

As the rate of eustatic sea-level fall decreases towards the lowest point of the curve a 'eustatic stillstand' is reached but *relative* sea-level begins to rise as tectonic subsidence temporarily becomes the dominant control upon relative sea-level. The systems tract is characterized by the change of both shelf and slope sediment budgets from negative to positive. As relative sea-level slowly rises during the development of the *lowstand wedge*, fluvial systems begin to aggrade to maintain their equilibrium profile and begin to fill the valleys incised during the *lowstand fan systems tract.* A similar development takes place on the slope (slope fans) (Fig. 2.5c).

Although there is some aggradation within incised valleys the shelf remains essentially a region of sediment bypass to the slope. A direct result of aggradation within river valleys is that the amount of coarse sediment supplied to the slope decreases as this preferentially is sedimented in the aggrading river valleys on the shelf. Early in the development of the prograding wedge turbidities are channelised by the relict canyon inherited from the preceding systems tract. As the wedge develops the canyon fills by aggradation of slope fans and eventually becomes abandoned (Fig. 2.5c). Sediments of the lowstand wedge become increasingly muddy as, increasingly, coarse sediment becomes sedimented in river valleys.

Upon the upper slope deltas begin to build-out. Sediments continue to be redeposited downslope to the basin-floor, but they become increasingly mud-rich as coarse sediment is preferentially deposited as the aggradational fill of river valleys and in coastal delta complexes (eg. Fig. 2.4c-d). This means that submarine fan sedimentation is mud dominated and characterized by the development of aggrading slope fans which downlap the basin-floor fan(s) and progressively shift up the slope (eg. Figs 2.1 & 2.5c). Because the deltas pass abruptly into deep waters there is no dampening of waves and currents so that the sediment tends to be dispersed along the

shoreline and a wedge rather than a fan is developed (Posamentier *et al.*, 1988; Posamentier & Vail, 1988). The wedge has a sediment budget greater than the rates of relative sea-level rise and is thus characterized by basinward progradation (Figs 2.1 & 2.5c).

As the lowstand wedge is developed the rate of relative sea-level rise increases so that each parasequence is characterized by the thicker development of toplapping strata than its precursor. As the rate of aggradation progressively increases so, correspondingly, the rate of facies progradation falls. The very last package(s) of the lowstand prograding wedge is characterized by the halt of facies progradation and development of an aggradational parasequence or parasequence set.

Upon the shelf the characteristic stratal pattern of the systems tract is the partial onlap of incised valleys, but this is a very minor component. The most readily recognizable stratal pattern of the systems tract is slope onlap and basinward downlap onto the *lowstand fan systems tract* by the slope fan and wedge (eg. Figs 2.1 & 2.5c). Onlap of the slope is both coastal and submarine and associated with well developed clinoforms of the prograding slope delta complex. Internally, the wedge is characterized by a strongly progradational lower part with well developed oblique-sigmoid clinoforms and an upper progradational-aggradational parasequence set with sigmoid clinoforms and well developed toplapping strata. As a whole the lowstand wedge is characterized by a gradual landward shift of slope onlap accompanied by facies regression which reflects the creation of space during the lowstand but at a lesser rate than sediment is supplied.

2.2.5. *C. The transgressive systems tract.*

The transgressive systems tract is developed during times of rapidly rising relative sea-level and is characterized by a series of punctuated flooding events and the transgression of the shelf. Rapid rates of relative sea-level rise result from the combination of both tectonic subsidence and most importantly rapidly rising eustatic

sea-level (Posamentier *et al.*, 1988; Posamentier & Vail, 1988) (Fig. 2.1 & 2.5d). The base of the systems tract is the point/time at which the rate of relative sea-level rise exceeds the rate of sediment supply and is marked by the *transgressive surface*, a downlap surface across the top of the lowstand wedge systems tract (Fig. 2.1). This surface separates the aggradational/progradational parasequence of the lowstand wedge systems tract from the retrogradational (backstepping) parasequence set diagnostic of the transgressive systems tract.

On the shelf the initial stages of the systems tract are localised to the fill of incised valleys and the later stages by widespread marine transgression. The backstepping (retrogradational) parasequence set develops as landwards space available for the accumulation of sediments is created at a greater rate than it can be filled. This results in a progressive landwards stepping of facies, shoreline and the depocenter onto and across the shelf (eg. Figs 2.1 & 2.5). Parasequences represent minor regressive events during a general facies transgression developed during 4th-5th order stillstands.

As the shelf is transgressed the fluvial systems aggrade at an increasing rate as the fluvial system attempts to maintain its equilibrium profile, filling the incised valleys created during the lowstand fan systems tract. Thus, increasingly, coarse sediment is deposited in the non-marine environment and the marine sediments become finer. The gradual landward stepping of the depositional locus is associated with the development of a *condensed section* upon the outer shelf and slope above the lowstand wedge (depocenter of the preceding systems tract). The condensed section developed in these regions is starved of terrigenous input and characterized by periplatform/pelagic sedimentation and deposits indicative of reduced sedimentation rates (eg. glauconite and phosphate). The upper bounding surface to the transgressive systems tract is the *maximum flooding surface* which marks the most landward encroachment of marine facies onto the shelf and correlates basinward with the condensed section (eg. Fig. 2.1).

The transgressive systems tract laps out basinwards by downlap onto the lowstand wedge systems tract and older parasequences of the transgressive systems tract itself. Landwards the systems tract laps out by onlap against the erosional topography of the preceding sequence (Fig. 2.1). Any topography upon the shelf inherited from the lowstand systems tract is interpreted to be filled during the transgressive systems tract (eg. the filling of incised valleys developed during the lowstand). The overall geometry of the systems tract is a basinwards tapering wedge, with landward thinning fingers representing the fill of incised valleys. Internally the systems tract is typified by a single stacking pattern: the retrogradational parasequence set (eg. Figs 2.1 & 2.5d).

2.2.5. *D. The highstand systems tract.*

The highstand is developed as the rate of relative sea-level decreases firstly to match then fall behind the rate of sediment supply. Eustatic sea-level is interpreted to reach a relative stillstand and for a second time tectonic subsidence becomes the main component of the *relative* sea-level rise. The base of the systems tract is the *maximum flooding surface* (mfs) which represents the maximum encroachment of marine facies on to the shelf (Figs 2.1 & 2.5d). Subsequent to the development of the mfs rate of relative sea-level rise reduces to match that of sedimentation to develop an aggradational parasequence set which is characteristic of the early stages of the systems tract (Fig. 2.5a). With time the rate of relative sea-level rise reduces further and a progradational parasequence set is developed as sedimentation rates exceed those of sea-level rise (Fig. 2.5a). The relative timing of stratal package development above the maximum flooding surface, i.e. the aggradational and progradational parasequence sets, is a function of both sedimentation rate and that of relative sea-level rise (eg. the highstand will begin earlier and in a more basinwards position in an area characterized by higher than average sedimentation rates). The highstand systems tract is interpreted to be the time at which the alluvial and coastal plain systems are best developed and are most widespread (eg. compare a-f, Fig. 2.5).

2.2.6. Development of a type 2 sequence.

A type two sequence differs by virtue of the extent of the unconformity at the base of the sequence. This type of sequence has no 'lowstand' deposits (Posamentier & Vail, 1988). The *shelf-margin wedge* is the lowest systems tract of the sequence and may be deposited anywhere on the shelf and consists of one or more weakly progradational to aggradational parasequences. Type 2 unconformities are soley subaerial but are characterized by widespread denudation, and not with bypass to the basin-floor or shelf incision (eg. Fig. 2.5f). Type 2 sequence boundaries are associated with a basinward shift of fluvial facies. This type of sequence boundary passes from a non-incisive unconformity upon the shelf to a conformity landwards of the shelf-slope break; the only downward shift of onlap occurs within the fluvial successions. The change of stratal pattern associated with this type of sequence boundary is from strongly progradational to aggradational parasequence sets. The transgressive and highstand systems tracts are similar to those of a type 1 sequence. Type 2 sequences have an overall aggradational stratal pattern when compared to type 1 sequences which are associated with significant basinward progradation.

2.2.7. General discussion.

The above description of type 1 and 2 sequences and their component members is based largely upon the concepts and model of Posamentier *et al.* (1988), Posamentier & Vail (1988) and Haq *et al.* (1987; 1988). Many geologists, whilst applying the model do not accept the strong 'eustatic' component of relative sea-level change interpreted by Vail *et al.* (1977), Haq *et al.* (1987; 1988), Posamentier *et al.* (1988) etc. For this thesis and for many geologists the term 'relative sea-level' is simply the sum of tectonic subsidence and eustatic sea-level changes. The dominance of neither component is inferred unless specified. Thus, *the application of sequence stratigraphic concepts and models does not infer a eustatic interpretation of stratal patterns.* Consequences of the assumptions of the model are explored in the following Section (2.3).

2.3. A Critique Of Sequence Stratigraphic Models And Alternatives.

2.3.1. Introduction.

The detailed geometric models for the development of sequences introduced in Section 2.2 have a through-going logic which is conceptually appealing, relating the falls of base-level to the timing of shelf-slope incision, development of basin-floor fans and basinwards facies shifts. It should, however, be noted that these models are theoretical, developed to explain the stacking patterns observed from seismic sections. Thus, there are no 'type' examples where the model has been critically applied to real geological situations. Sequence stratigraphic models can only be appraised by application to real, well exposed and understood examples. From applying the model(s) to outcrop examples weaknesses of the model can be highlighted, evaluated and used to develop new models suitable for specific geological settings.

The sequence stratigraphic models themselves have only relatively recently come under close scrutiny from independent siliciclastic workers, who have suggested revisions, refinements and alternatives to the 'Exxon' siliciclastic model (Galloway 1989a, b; Thorne & Swift in press). The acceptance of new and/or alternative models for sequence stacking patterns have often suffered from a lack of detail and/or the introduction of new cumbersome terminology. The latter problem is becoming particularly acute from the abuse of Exxon terminology and the development of numerous different terminologies produced from different workers (eg. Thorne & Swift in press). The following section critically examines the systematics, stacking patterns and major surfaces in the context of the development of an 'Exxon' sequence. This is followed by a resume of the systematics of Galloway (1989a, b).

2.3.2. An exploration of the 'Exxon' model.

2.3.2. *A. The lowstand and shelf margin wedge systems tract.*

The lowstand deposits are divided into two end member geometries of a whole spectrum of possible stratal patterns. Type 1 and 2 sequence boundaries are distinguished on the basis of position upon the depositional surface (shelf, slope, or basin-floor), and internal termination and stacking patterns.

2.3.2. *A1.* Dynamics of sedimentation during forced regression and lowstand of relative sea-level.

One of the major problems with the present Exxon model is the timing of surfaces and dynamics of sedimentation during 'forced regression'. Using the current model and systematics chronostratigraphically-equivalent stratal packages deposited upon the shelf/slope or basin-floor are placed either below or above the sequence boundary respectively (eg. Fig. 2.6A). This problem is particularly acute for high-resolution outcrop studies and has been highlighted from application of the 'Exxon' model to the Urgonian platform (eg. Hunt & Tucker, 1992) and the subject of the later part of this thesis. The situation where sediments deposited under identical conditions of sea-level change upon the slope/shelf but are placed within different systems tract suggests that a revision of the present model is timely and this is presented below.

2.3.2. *A2.* Current systematics

During third-order relative sea-level falls higher order cycles (4th-5th order) are superimposed upon the general fall resulting in acceleration and deceleration of the third order signature. During times of decelerated fall (or even rise), parasequence-scale bodies are deposited and then subsequently abandoned, exposed and incised as the third order fall continues. Such deposits are termed 'stranded'

parasequences (eg. see Fig. 2.6A[2]), and since they are deposited during the sea-level fall, but prior to the lowest point of sea-level they are therefore placed below the sequence boundary in the highstand systems tract (Van Wagoner *et al.*, 1990. pg. 36).

The stratal patterns and chronostratigraphy of both 'stranded' parasequences, and the lowstand systems tract (sensu Vail, 1987; Haq *et al.*, 1987, 1988; Posamentier *et al.*, 1988; Posamentier & Vail, 1988) in relation to the 'Exxon' sequence boundary are summarised in Figure 2.6A. On the slope, 'stranded' parasequences are placed below the sequence boundary as they are developed prior to the lowest point of sea-level at which time the sequence boundary is formed (Van Wagoner *et al.*, 1990, pg. 36). Basin-floor, time-equivalent deposits (the basin-floor fan/allochthonous debris Fig. 2.6A) to the 'stranded' slope parasequences are placed above the sequence boundary so that, by way of contrast, the formation of the sequence boundary on the basin-floor occurs prior to the lowest point of relative sea-level (sl_2 Fig 2.6A). Thus, in this model, the position of the sequence boundary is chronostratigraphically ambiguous (Fig. 2.6A).

2.3.2. *A3.* Revised systematics.

This scheme is based on the models of a type 1 sequence of Van Wagoner *et al.* (1990) and earlier authors. The most significant revisions are the subdivision of the current lowstand systems tract into two newly named systems tracts and the alteration of the sequence boundary position on the basin-floor to above sediments deposited during forced regression so it is now everywhere coincident with the lowest point of relative sea-level and most extensive subaerial unconformity. New systems tract boundaries are chosen to coincide with changes of both the rate and the direction of relative sea-level change (eg. compare Figs 2.6A & B).

---

[2] This diagram and 2.6B are based upon a carbonate rimmed shelf where the shelf-slope break has aggraded to within a few meters of relative sea-level. Thus, stranded parasequences are developed only upon the slope as the shelf moves above depositional base-level with the first increment of sea-level fall. In other cases stranded parasequences can be developed both on the shelf and slope.

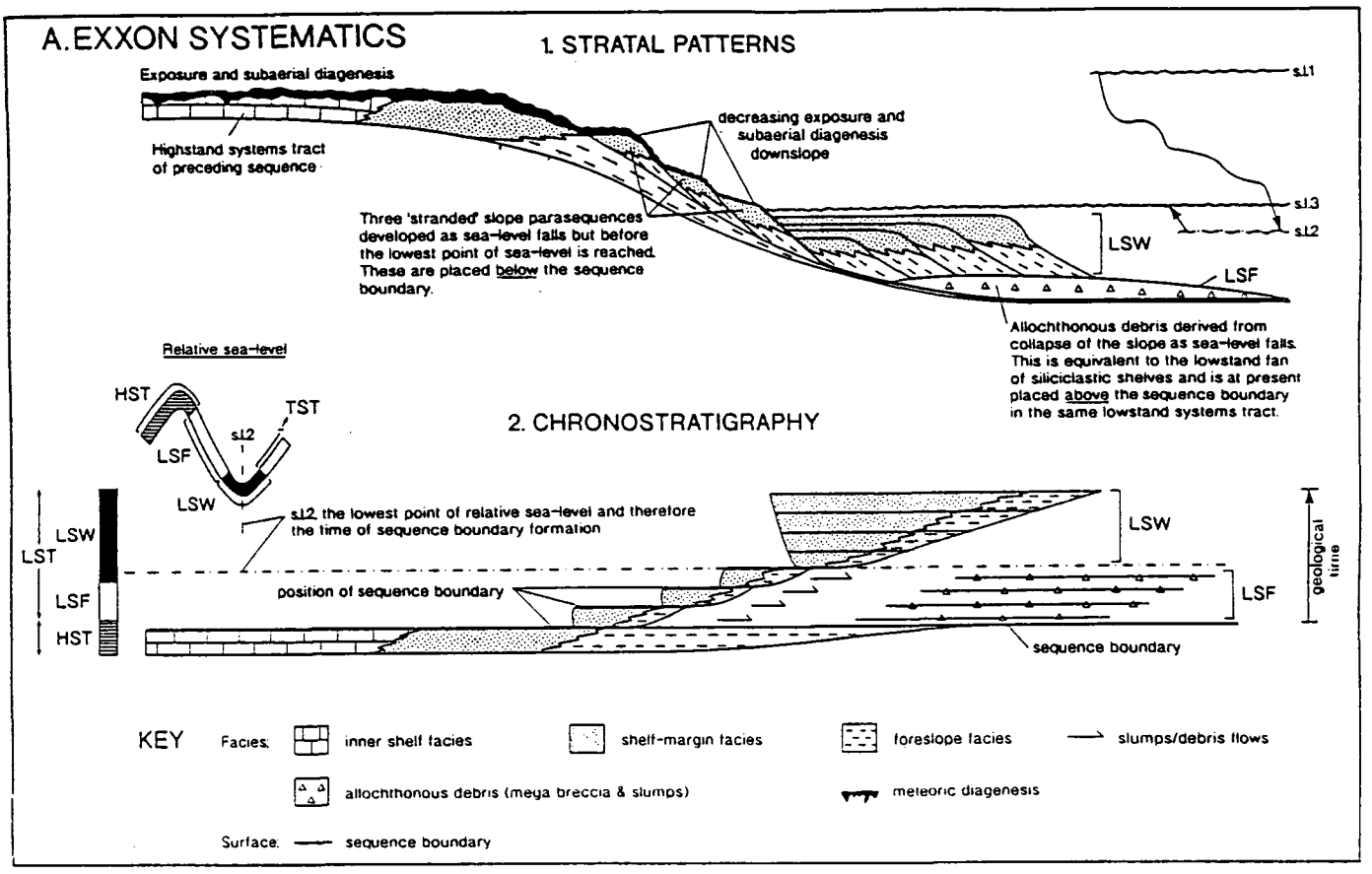
A. EXXON SYSTEMATICS
1. STRATAL PATTERNS
Exposure and subaerial diagenesis
Highstand systems tract of preceding sequence
decreasing exposure and subaerial diagenesis downslope
s.l.1
s.l.3
s.l.2
Three 'stranded' slope parasequences developed as sea-level falls but before the lowest point of sea-level is reached. These are placed below the sequence boundary.
LSW
LSF
Allochthonous debris derived from collapse of the slope as sea-level falls. This is equivalent to the lowstand fan of siliciclastic shelves and is at present placed above the sequence boundary in the same lowstand systems tract.
Relative sea-level
HST
TST
LSF
s.l.2
LSW
2. CHRONOSTRATIGRAPHY
LSW
LST
LSF
HST
s.l.2 the lowest point of relative sea-level and therefore the time of sequence boundary formation
position of sequence boundary
LSW
LSF
sequence boundary
geological time
KEY
Facies:
inner shelf facies
shelf-margin facies
foreslope facies
slumps/debris flows
allochthonous debris (mega breccia & slumps)
meteoric diagenesis
Surface:
sequence boundary

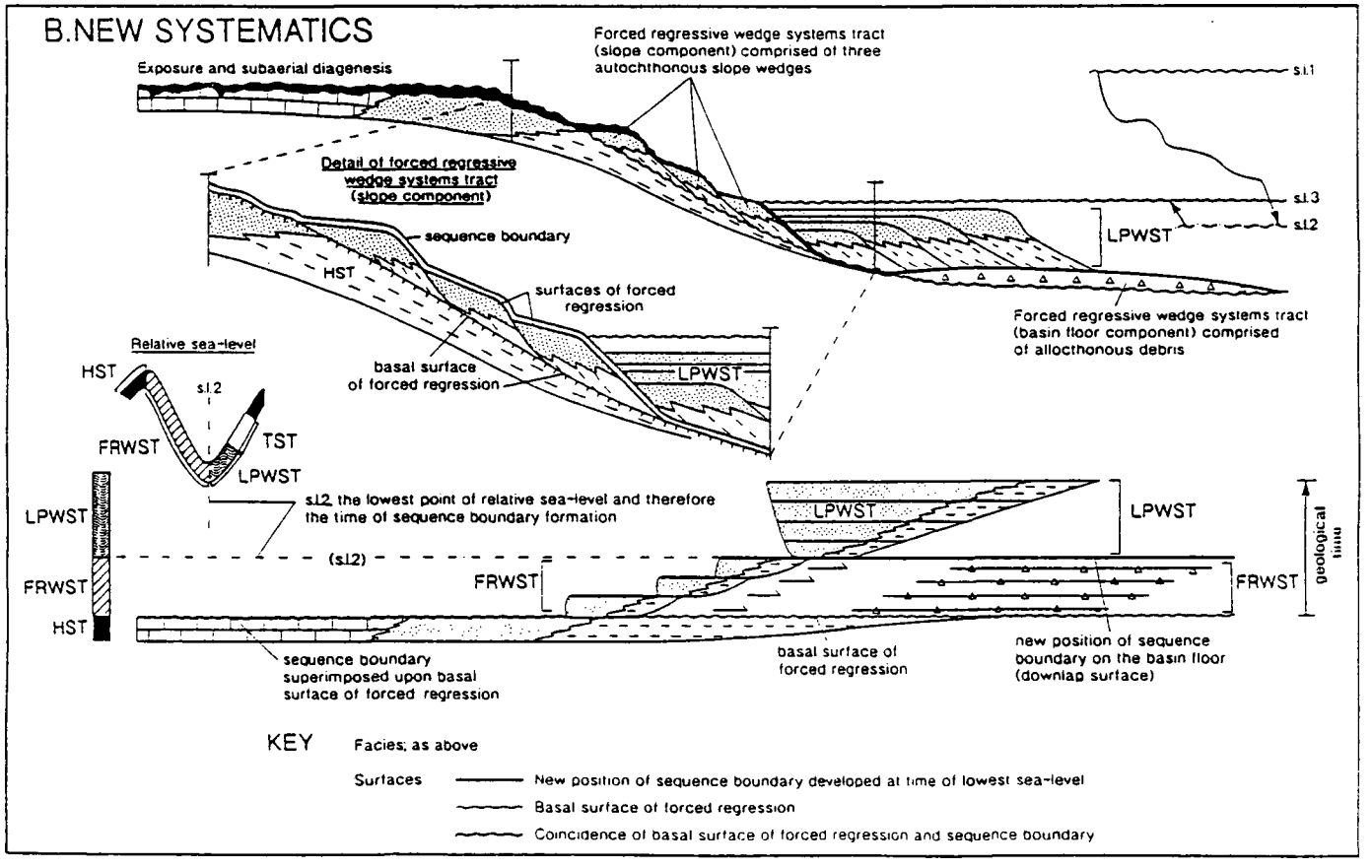
B. NEW SYSTEMATICS
Exposure and subaerial diagenesis
Forced regressive wedge systems tract (slope component) comprised of three autochthonous slope wedges
s.l.1
Detail of forced regressive wedge systems tract (slope component)
s.l.3
s.l.2
sequence boundary
LPWST
HST
surfaces of forced regression
Forced regressive wedge systems tract (basin floor component) comprised of allochthonous debris
Relative sea-level
HST
s.l.2
basal surface of forced regression
LPWST
FRWST
TST
LPWST
s.l.2 the lowest point of relative sea-level and therefore the time of sequence boundary formation
LPWST
LPWST
(s.l.2)
FRWST
FRWST
FRWST
HST
geological time
sequence boundary superimposed upon basal surface of forced regression
basal surface of forced regression
new position of sequence boundary on the basin floor (downlap surface)
KEY
Facies: as above
Surfaces
New position of sequence boundary developed at time of lowest sea-level
Basal surface of forced regression
Coincidence of basal surface of forced regression and sequence boundary

Systematics developed below originate from high resolution outcrop studies on the Urgonian platform presented later and are envisaged to be of use at a similar scale to other successions. In application this scheme is no easier to use than its predecessors and is of little or no use to seismic stratigraphers where recognition of the systems tracts is often difficult and distinction of stranded parasequences is impracticable, if not impossible. The new systems tract and sequence boundaries introduced appear to eliminate many of the contradictions and ambiguities associated with falling and lowstand of relative sea-level in the previous models (eg. see above). Where possible current terminology is retained, but new terms are introduced where it is felt that recycling of the previous term(s) would only precipitate (further) confusion.

Sediments deposited during forced regression (i.e. falling relative sea-level), but prior to the lowest point of relative sea-level are placed within the *forced regressive wedge systems tract* (FRWST) (Fig. 2.6B). The base of this systems tract is the *basal surface of forced regression* (BSRF) (Fig. 2.6B), a chronostratigraphic surface which separates older sediments of the preceding highstand systems tract from younger sediments deposited during falling relative sea-level (Fig. 2.6B). The systems tract has a slope component termed the *forced regressive slope wedge* (after which the systems tract is named), and a basin-floor component, the *forced regressive basin-floor fan/apron.* Both components are schematically illustrated in Figure 2.6B. These terms are developed specifically for a carbonate shelf and are approximately equivalent to the lowstand fan systems tract and lowstand wedge systems tract

Figure 2.6. (preceding page) Comparison of stratigraphic sequence depositional models for times of falling relative sea-level upon a carbonate shelf using Exxon systematics and new systematics proposed in this Chapter. In each figure stratal patterns are illustrated in the upper diagram (1) and their chronostratigraphic relationships below (2). Note the new position of the systems tract boundaries in relation to the relative sea-level curve, revised position of the sequence boundary, now placed above sediments deposited during times of falling sea-level and the distinction of two systems tracts separated by the sequence boundary. See text for further discussion.

discussed in Section 2.2.

The slope wedge component of the FRW systems tract consists of one or more 'stranded' parasequences all bound below by the basal surface of forced regression, and above by the sequence boundary (Fig. 2.6B). These surfaces are also common to the base and top of the basin-floor component of the systems tract where the *sequence boundary* is moved from the base to top of these deposits and is replaced by the basal surface of forced regression (eg. compare Figs 2.6A & B). Slope and basin-floor elements of the forced regressive wedge systems tract are not necessarily developed together during an individual forced regression so that the systems tract may be represented by just the slope or basin-floor components. Alternatively, the systems tract may be totally absent due to no sedimentation during forced regression (eg. sea-level fall too rapid) or post-depositional erosion (eg. upon the slope).

The upper surface of the forced regressive wedge systems tract is the *sequence boundary* which represents the lowest point of relative sea-level, thus, the most extensive unconformity (Van Wagoner *et al.*, 1990) (Fig. 2.6A & B). The position of the sequence boundary on the shelf-top is unchanged from previous models, but, on the basin-floor it is now placed above sediments (if any) deposited during the sea-level fall so that it is now truly a chronostratigraphic surface in that all sediments below it are older and those above younger (eg. compare positions of the sequence boundary in Fig. 2.6A & B). Any sediments deposited at, or after sea-level has reached its lowest position are placed above the sequence boundary and are thus part of the *lowstand prograding wedge* (LPW) *systems tract*, developed from the time relative sea-level is at its lowest point and is beginning to rise (Fig. 2.6B), but prior to the transgressive systems tract. The LPW systems tract downlaps the sequence boundary in a basinwards direction and onlaps it landwards (Fig. 2.6B).

Conceptually, since the FRW systems tract lies below the sequence boundary it becomes the fourth and final systems tract of a sequence, bounded by the sequence boundary. Thus, the first three systems tracts (LPW, TST and HST) of a sequence are now all formed during times of rising relative sea-level (Fig. 2.6B) after the

lowest point of relative sea-level (eg. Figure 2.6B). The new, final, fourth systems tract of a sequence (FRW) forms during times of falling relative sea-level (Fig. 2.6B). Therefore, the upper and lower bounding surfaces of a sequence remain the sequence boundary, but it is now more precisely defined *everywhere* to form at the lowest point of relative sea-level.

2.3.2. *A4.* Types of 'lowstand' prograding wedge.

Currently, the lowstand wedge is normally depicted to 'fill' to the shelf-slope break of the preceding sequence (eg. Fig. 2.1) prior to the development of the transgressive systems tract in a type 1 sequence. This would appear to be a consequence of the sinusoidal form of the sea-level curve and the point at which sea-level is taken to accelerate.

The size of the LPW systems tract will reflect the ratio of the rate of relative sea-level rise to the sedimentation rate. If the sedimentation rate is high and/or rates of relative sea-level rise low then the LPW will be volumetrically significant and can fill up to the shelf-slope break (eg. Figs 2.1 & 2.7) or even 'overfill' this interface (Fig. 2.7). In the case of an 'overfilled' 'lowstand' prograding wedge, then marine transgression of the shelf occurs prior to the commencement of the TST (eg. Fig. 2.7). By way of contrast, if the sedimentation rate is low and/or relative sea-level rises rapidly from the time of sequence boundary formation then the LPW will be volumetrically small and 'underfill' the slope (Fig. 2.7).

2.3.2. *A5.* An alternative sequence boundary.

Galloway (1989a) suggested that the sequence boundary chosen by the Exxon group is misplaced. Working predominantly upon the Gulf Coast, USA, Galloway (1989a, b) also identified repetitive progradational, aggradational, retrogradational sedimentary cycles, but, contrastingly, divided up the stratigraphic succession into 'genetic' stratigraphic sequences using flooding surfaces. These, he argued are

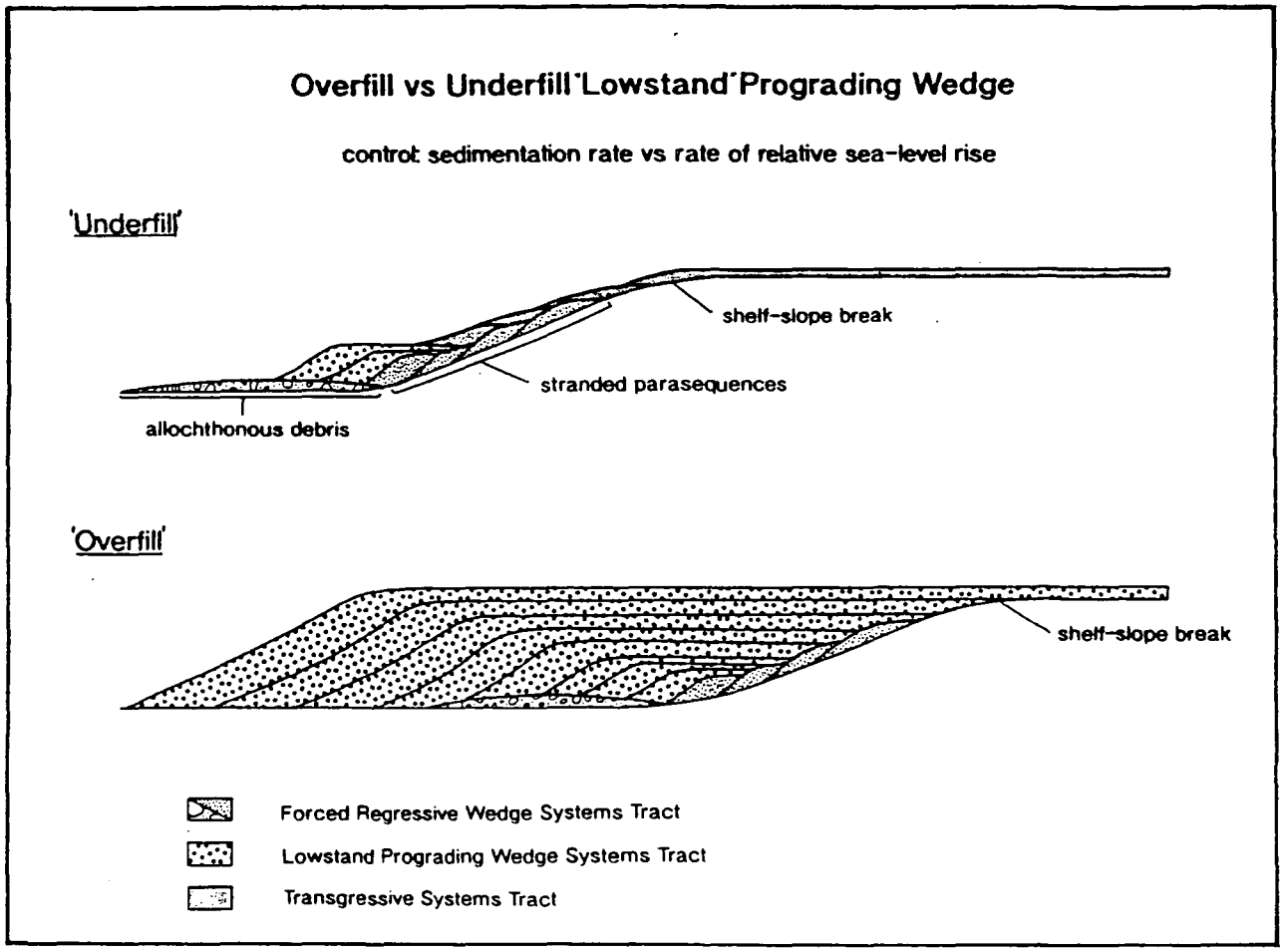

Figure 2.7. The two types of 'lowstand' prograding wedge (LPW), 'underfill' and 'overfill' wedges. An 'underfill' wedge is developed when the rate of relative sea-level rise exceeds sedimentation rates prior to onlap of the LPW having reached the shelf-slope break of the preceding sequence. In the case of an 'overfilled' LPW the wedge fills past the preceding shelf-slope break before the TST is developed. Thus, marine transgression of the shelf occurs during the LPW systems tract, not the TST. Note that these geometries are depicted for a carbonate shelf system so that the LPW is associated with gradually increasing sedimentation rates as the area available for sedimentation is enlarged.

developed independently of subsidence rates and are the most readily identified and is widely developed stratal surface which are easily datable. He also suggested that the time of maximum flooding is a time of frequent extensive mass wasting of the slope with resedimentation to the toe of clinoforms (eg. Fig 2.8). This is also coincident with major palaeogeographic adjustments such as the relocation of major fluvial axes on the shelf (Galloway, 1989a, b).

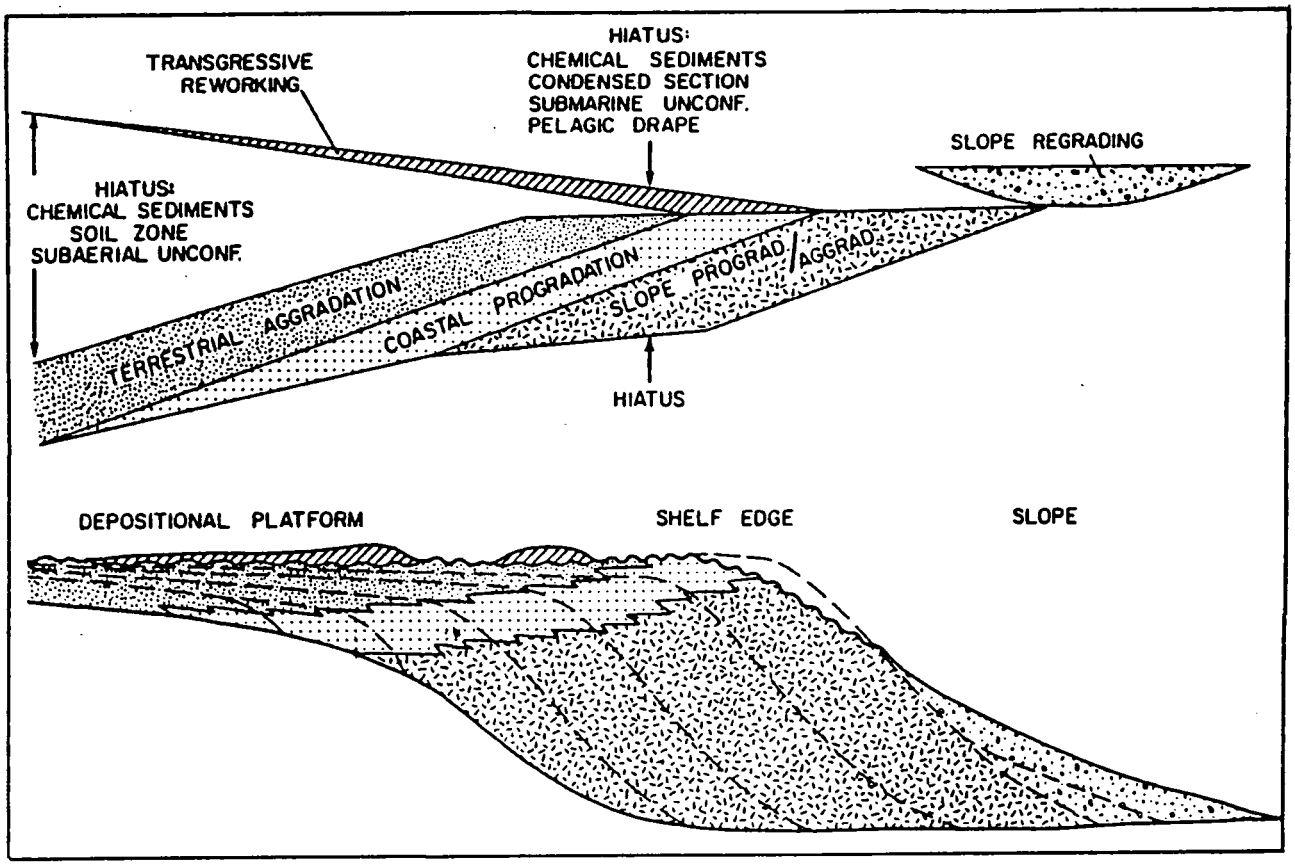

Figure 2.8. Idealised stratigraphic architecture of the genetic stratigraphic sequence of Galloway (1989a). Upper diagram illustrates chronostratigraphy of the strata and the lower their stratal patterns. See text for further discussion.

2.3.2. *B.* The transgressive systems tract.

The transgressive systems tract is characterized by a retrogradational parasequence set (eg. Fig 2.1). Galloway (1989a) described a similar geometry upon the shelf to the Exxon model, namely a backstepping wedge, but as discussed in the preceding Section (2.3.2. *A5*) he suggested that the slope retrogrades by mass-wasting and a toe of slope wedge is developed during the transgressive systems tract (Fig. 2.8).

Using Holocene examples from the western USA Thorne & Swift (in press) demonstrated that during rapid rates of relative sea-level rise valleys cut during lowstand of relative sea-level are only partially filled by fluvial aggradation during

the transgressive systems tract. Mostly they are filled by marine muds and sands. These authors also highlighted a secondary major erosive surface that is frequently developed during transgression (ie. the shoreface ravinement surface) and this can commonly rival erosional truncation developed during lowstands. This surface is equivalent to the transgressive surface upon siliciclastic shelves (Thorne & Swift, in press)

2.3.2. *C. The highstand systems tract.*

The highstand systems tract is typified by an aggradational to progradational wedge (eg. Fig. 2.1). Galloway (1989a) described a similar geometry but it differs in detail in that as soon as the deltas prograde to the shelf-slope break then resedimentation of the delta front to the basin-floor resumes to deposit base-of-slope lobes.

2.3.3. Discussion.

The strength of the Exxon approach is that it has forced a major re-evaluation of strata as part of a linked and interdependent shelf-slope-basin system. The Exxon model describes the architectural development of a sequence formed from sedimentation during a cycle of relative sea-level change. This model has several important assumptions (Section 2.2) which should be considered when applying the model: eustatic sea-level control and constancy of sedimentation rates. These assumptions of the model are to many workers the archilles heel of the model as when applied to real geological situations stacking patterns reflect the complex interplay of sediment supply (sediment production in the case of carbonate platforms, see Chapter 3), sediment transport rate, tectonic subsidence and eustasy. Each of these can vary in both time and space so that their relative importance can change both along a depositional surface and through a vertical succession of strata. In applying the model to analyse sediment stacking patterns many (and probably the majority)

workers do not accept the model's assumptions, particularly concerning the role of eustasy and constancy of sediment supply/production.

The strength of alternative sequence stratigraphic schemes (eg. Galloway, 1989) is their recognition of the important role played by variables assumed constant in the Exxon model and how these rather than relative sea-level changes can control architecture of a depositional sequence. The problems of these schemes is, however, a general lack of detail. Integration of the more realistic assumptions such as those discussed above into the Exxon model can only strengthen its role as a template for stratigraphic analysis. Its general world-wide acceptance ahead of rival or successor schemes has put it in an unrivalled position in basin analysis.

Acceptance of stratigraphic schemes which account for differences observed in different basins and/or depositional systems must therefore, be put in the context of the Exxon model if they are to be successfully communicated. The application of the Exxon model to carbonate shelves in open ocean settings is the subject of the following Chapter.

Chapter 3.
Sequence Stratigraphic Models For Carbonate Shelves

3.1. Introduction.

The direct application of sequence stratigraphic models developed conceptually for siliciclastic depositional systems to carbonate platforms is a subject of some controversy. Development of sequence stratigraphic models for carbonate platforms has focused upon carbonate shelves, physiographically the most similar type of platform to a siliciclastic shelf for which the models were originally developed. Proponents of the Exxon model (eg. Sarg, 1988; Jacquin *et al.*, 1991) argue that models developed for siliciclastic shelves can be successfully applied to carbonate shelves without need for modification. Other workers (eg. Mullins, 1983; Schlager, 1991; Hunt & Tucker, 1991, 1992) suggest that current models need modification to account for the differences between the two depositional systems.

In this chapter the various diagnostic features of the different types of carbonate platform are introduced and followed by a discussion of the general differences between siliciclastic and carbonate depositional systems. In Section 3.7 these differences are used to construct new sequence stratigraphic models for carbonate shelves in open ocean settings. New models are illustrated by applying them to well known geological examples. These account for the differences between carbonate and siliciclastic shelves and explain the different stratal patterns (eg. buildups) commonly associated with carbonate platforms. Models developed in this Chapter are later used in discussion of the Urgonian carbonate platform.

3.2. Physiographic Types Of Carbonate Platform.

3.2.1. Introduction.

Different 'types' of carbonate platform can be recognized on the basis of their cross-sectional profile and basinal setting, as summarised in Figure 3.1. All but epeiric platforms are identified in the modern oceans.

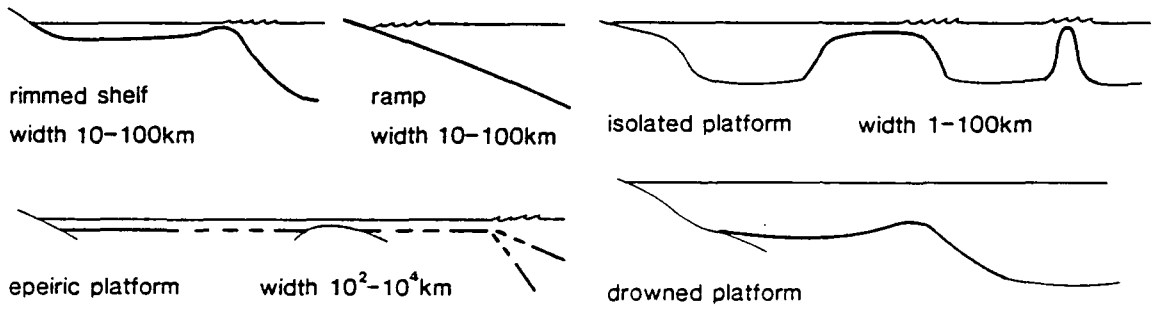

Figure 3.1. Different physiographic types of carbonate platform and approximate basinal settings. From Tucker & Wright (1990).

3.2.2. Epeiric platforms.

Epeiric platforms cover very wide areas, aggrade very near to sea-level and are only recognized in the rock record during times of globally high sea-level (eg. Late Cretaceous, Hancock & Kaufmann, 1979; Haq *et al.*, 1987, 1988) when large stable cratonic areas of the continents were flooded by shallow seas. During such times the budget of siliciclastic sediments was probably reduced. Conversely, the carbonate budget would have been increased due to interpreted globally higher temperatures promoting carbonate precipitation (eg. 6-12°C warmer for the Cretaceous, Barron *et al.*, 1981).

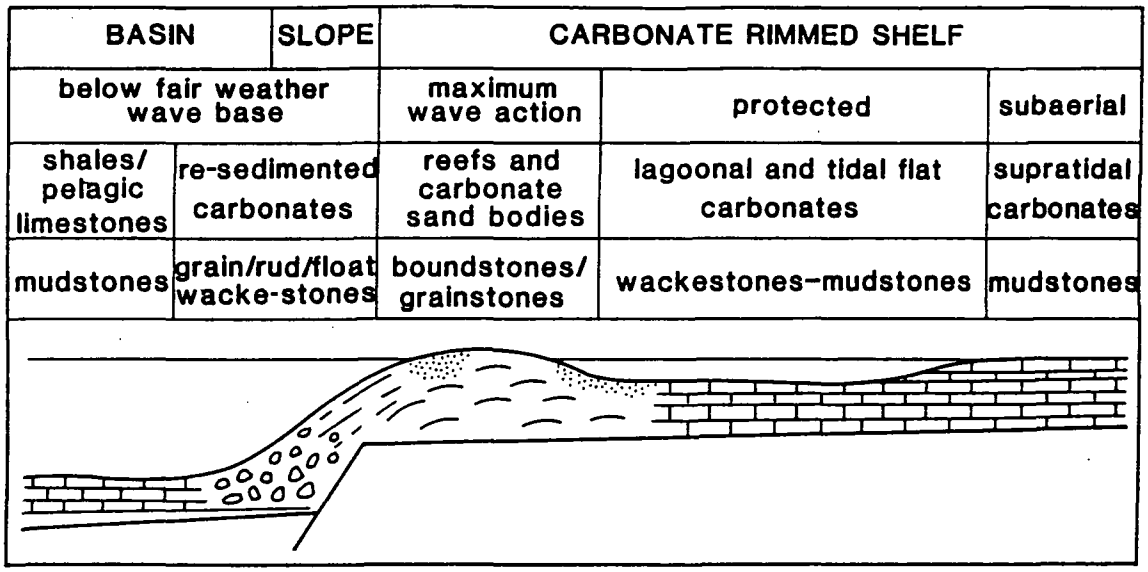

Figure 3.2. Idealised cross section across a rimmed shelf. Note that the shelf rim is shallower than the protected shelf-lagoon/inner shelf. From Hunt & Tucker (1992).

3.2.3. Shelves.

Carbonate shelves are shallow platforms with an abrupt change in gradient that marks their outer edge (Figs 3.1 & 3.2). The shelf margin is subject to high wave energy and current activity and is typically rimmed by a continuous-semicontinuous barrier of reefs and/or carbonate sands. Landwards of the margin is the inner shelf/shelf-lagoon; protected from vigorous current activity it may be 1-100's of km in width. Faunal and textural changes shorewards reflect the increasingly restricted circulation of the shelf (Jordan, 1978; Tucker, 1985). Modern examples of shelves include the Great Barrier Reef and shelf-lagoon (eg. Davies *et al.*, 1989) and the East Florida shelf (eg. Enos, 1977).

Three categories of shelf can be distinguished: *rimmed shelves*, where the shelf is delineated by high energy facies and a protected lagoon (Fig. 3.2); *aggraded shelves*, where the whole expanse of the inner shelf behind the margin has little topography and is at or within a few metres of sea-level (eg. Fig. 3.3) and '*drowned shelves*' an intermittent stage in platform evolution where the shelf has passed below the euphotic zone after a particularly rapid relative sea-level rise and/or major

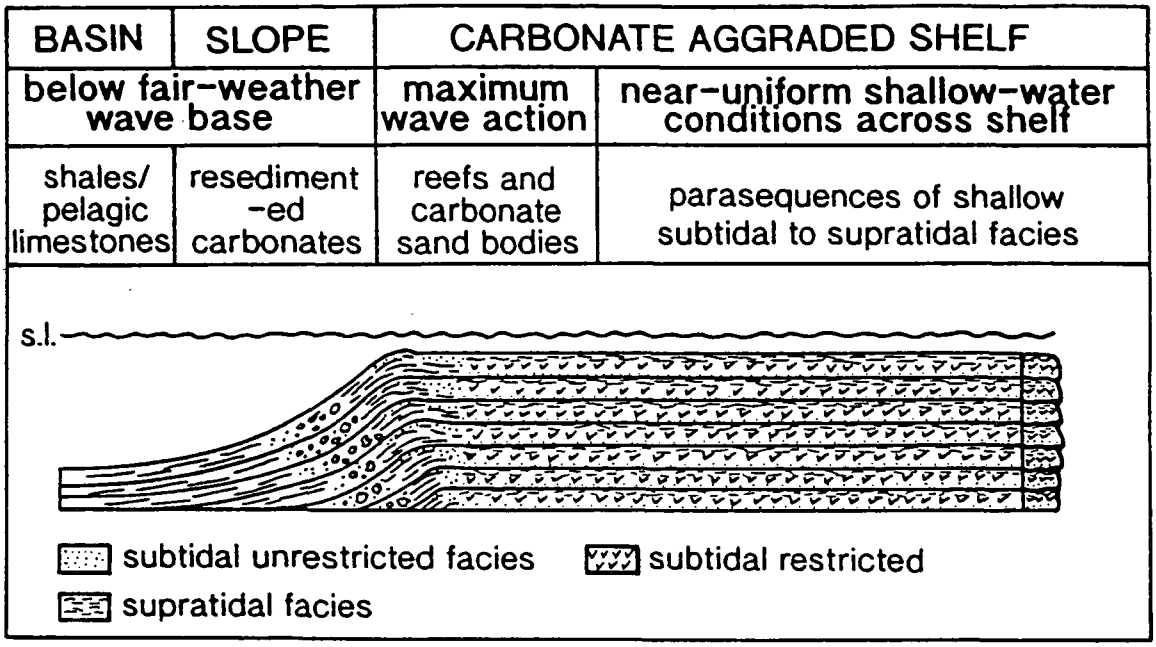

Figure 3.3. Idealised cross section across an aggraded shelf where there is little topography behind the platform margin and facies tend to be time specific. From Hunt & Tucker (1992).

environmental change. Rimmed shelves are characterized by a greater facies differentiation than aggraded shelves; upon aggraded shelves facies tend to accrete vertically and so are generally time specific (eg. Fig. 3.3) whereas upon rimmed shelves facies belts tend to migrate, albeit with an element of aggradation.

3.2.4. Ramps.

Carbonate ramps are a type of carbonate platform where there is no major break of slope in shallow water and water depth increases gradually with distance from the shoreline (Fig. 3·4). Two categories of ramp can be identified: *homoclinal ramps*, where there is a gentle gradient into the basin, and *distally steepened ramps*, where there is an increase in gradient in the outer, deep ramp region (Read, 1982, 1985). High energy sedimentation is characteristic of the inner ramp where patch reefs and/or carbonate sand bodies are normally developed, behind which there may be more restricted facies. Outer ramp sediments are more muddy and often dominated by storm deposits. Modern examples of ramps include the Trucial coast

of the Arabian Gulf (papers in Purser, 1973), the eastern Yucatan coast of Mexico (Ward *et al.*, 1985), and the West Florida ramp (Mullins *et al.*, 1988: Gardaluski *et al.*, 1990).

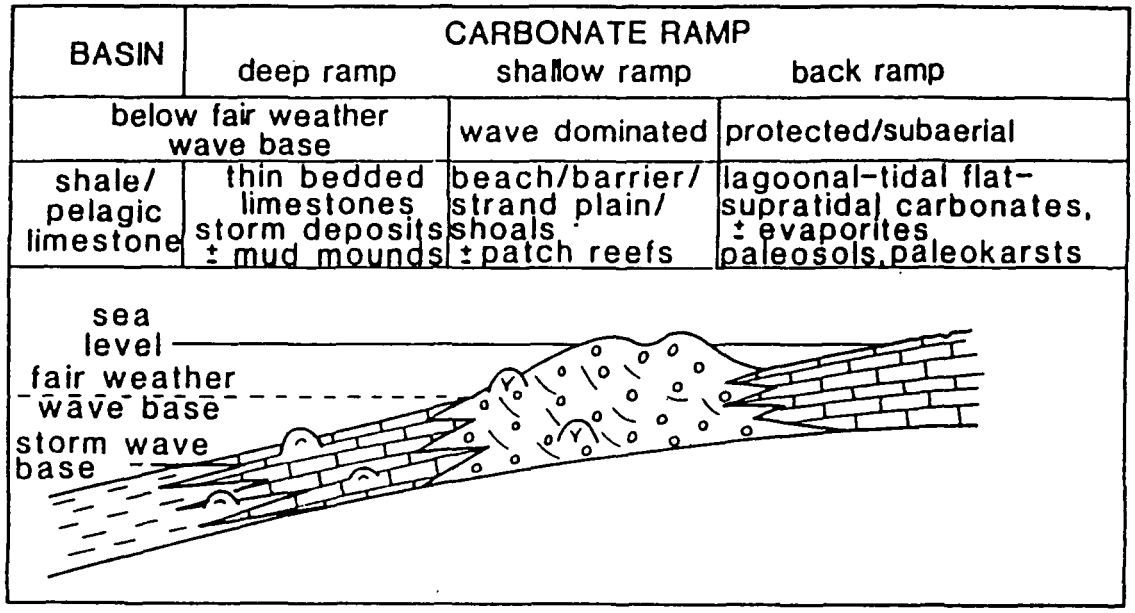

Figure 3.4. Idealised cross section across a ramp type platform (from Tucker & Wright, 1990).

3.2.5. Isolated platforms.

Isolated platforms are not attached to a landmass and are thus surrounded on all sides by the sea (Fig. 3.1). They can vary in size from 1-100's of km across (eg. The Bahama banks). Their outer margin is often rimmed by continuous to semicontinuous reefs and/or carbonate sands and marked by an abrupt change in gradient to the basin-floor. The size of isolated platforms is important in terms of facies and sedimentary budget. The slopes to these platforms tend to be extremely steep which reflects their building of topography compared to surrounding areas (Fig. 3.1). The protected inner parts of large isolated platforms tend to be dominated by muddy facies (eg. Weins, 1962). Modern examples of isolated platforms include the Bahama banks (eg. Gebelin, 1974), Coral Sea Plateau (Read, 1985), Glovers Reef off the Belize shelf (James & Ginsburg, 1979) and the numerous Pacific atolls (eg. Weins, 1962).

3.3. Current Sequence Stratigraphic Models For Carbonate Platforms.

3.3.1. Introduction.

At present, the most widely used models for sequence stratigraphic analysis of carbonate platforms are those produced by Exxon Production Research (eg. Vail, 1987; Sarg, 1988, Fig. 3.5) which focus upon the dynamics of carbonate shelf sedimentation. A comparison between the sequence stratigraphic models produced by this group for carbonate and siliciclastic shelves (eg. Fig. 3.5 A & B) illustrates how the precursor siliciclastic models were used as a template from which their carbonate equivalents have been derived (eg. Vail, 1987; Sarg, 1988).

The identical position and stratal packaging of systems tracts for carbonate and siliciclastic shelf sequences (eg. Fig. 3·5 A & B) demonstrates the belief of the models proponents that both systems respond in much the same way to relative sea-level changes. This suggests that the differences between depositional systems are 'secondary factors' and do not modify the response of depositional systems to *relative sea-level changes*, the interpreted primary control upon stratal packaging (eg. Sarg, 1988; Jacquin *et al.*, 1991; Vail *et al.*, in press).

Sarg (1988) demonstrated several important ways in which carbonate systems, and shelves in particular, respond differently from their siliciclastic equivalents but interpreted these differences to have a secondary importance compared to the role of relative sea-level change(s) in developing stratal patterns (eg. Fig 3.5 A & B). When sea-level falls below the shelf-slope break (a type 1 sequence) Sarg (1988) recognized two genetically distinct types of deposit: *allochthonous debris*, calciclastic sediments derived mechanically from gravitational collapse of the preceding highstand, and *autochthonous wedges*, formed *in situ* on the modified/unmodified slope of the preceding highstand (Fig. 3.5 B).

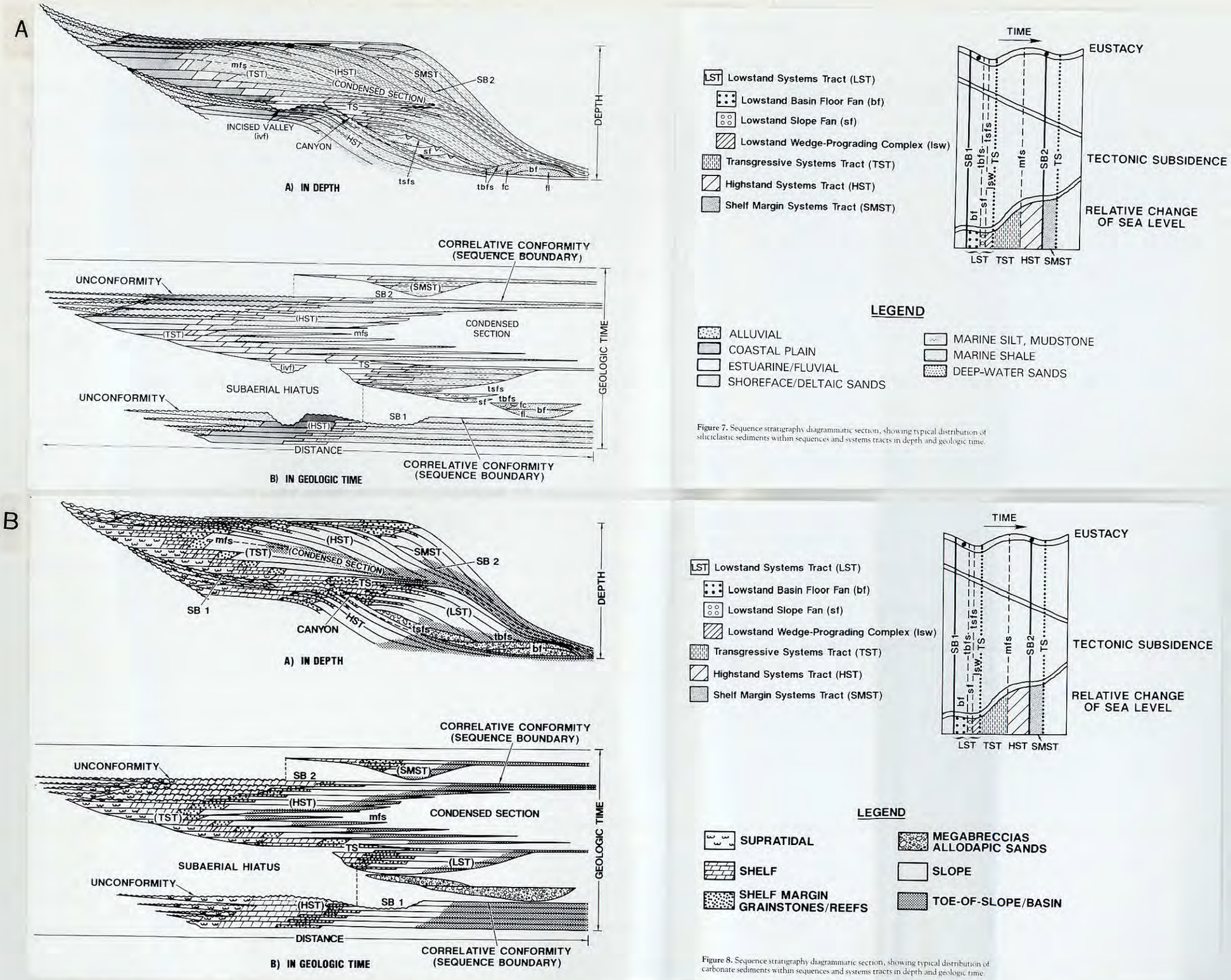

Figure 7. Sequence stratigraphy diagrammatic section, showing typical distribution of siliciclastic sediments within sequences and systems tracts in depth and geologic time.

Figure 8. Sequence stratigraphy diagrammatic section, showing typical distribution of carbonate sediments within sequences and systems tracts in depth and geologic time.

Figure 3.5. Sequence stratigraphic models for siliciclastic (A) and carbonate (B) shelves from Vail (1987). Note that the position of stratal packages and the stratal termination patterns of these two models is identical.

Building upon the concepts of Kendall & Schlager (1981) Sarg (1988) also identified two different 'modes' of sedimentation for the transgressive and highstand systems tracts. These reflect the ratio of the sedimentation rate to the rate of relative sea-level rise, and are: *keep-up*, when sedimentation rates are equal to or greater than periodic rises of relative sea-level and, *catch-up*, when sedimentation rates are lower than periodic rises of relative sea-level. The different modes of the highstand and transgressive systems tracts are characterized by different patterns of progradation at the shelf-margin. Sigmoidal and oblique clinoform geometries are interpreted to represent times of catch-up and keep-up respectively (Sarg, 1988). Sarg (1988) did not consider the role of environmental changes upon sedimentation rates.

3.3.2. The controversy.

Carbonate depositional systems do differ from siliciclastic systems and these differences can be recognized in both modern and ancient patterns of sedimentation. The current debate centers upon the relative importance of these differences in the development of stratal patterns (eg. Vail *et al.*, in press; Schlager, 1991; Hunt & Tucker, 1992): namely, whether the disparities or 'depositional bias' of different depositional systems can exert a control upon the development of stratal packaging of lesser, equal, or greater importance than relative sea-level changes.

Currently, opinion is strongly divided into the 'sequence stratigraphers', proponents of the Exxon model and 'carbonate sedimentologists'. The 'sequence stratigraphers' believe that the differences between the carbonate and siliciclastic systems are 'secondary factors' which do not alter the form of stacking patterns in response to relative sea-level changes (eg. see Vail *et al.*, in press). Thus, the primary control upon stratal geometry is interpreted to be relative sea-level change (eg. Vail *et al.*, 1977; VanWagoner *et al.*, 1990 etc.).

The 'carbonate sedimentologists' (eg. Schlager, 1991; Hunt & Tucker, 1992) have mostly approached sequence stratigraphy from a sedimentological background. These workers argue that the direct superimposition of geometries developed for one

depositional system to another (eg. Fig. 3.5) is overly simplistic and does not account for the differences between depositional systems. Such differences are, at certain times, considered to have a role of equal or greater importance than relative sea-level changes in the development of stratal patterns/packages. Therefore, the response of a depositional system to relative sea-level is altered and different sequence architectures can be developed (eg. carbonate buildups). These workers also suggest that environmental changes can at times drastically alter sedimentation rates and can rival relative sea-level changes in the development of stratal patterns (eg. Schlager, 1991; Hunt & Tucker, 1992).

If the differences between depositional systems (eg. carbonate and siliciclastic) and/or environmental changes can be of equal or greater importance than relative sea-level changes in the development of stratal patterns then geometry alone cannot be reliably used to determine relative sea-level curves/changes from the subsurface and/or at outcrop (Hunt & Tucker, 1992).

3.4. Patterns And Processes Of Carbonate Sedimentation.

In this Section the major controls which determine the distribution of carbonate platforms are introduced.

3.4.1. Major controls of carbonate sedimentation.

Unlike the occurrence and deposition of siliciclastic sediments modern shallow-water carbonate platform sedimentation shows a marked environmental sensitivity. The situation and facies patterns of modern carbonate platforms reflect the complex interplay of a number of variables such as *climate* (temperature, seasonality, ratio of precipitation to evaporation), *oceanographic setting* (wind and tidal energy/polarity, nutrient supply) and *basinal setting* (tectonics and siliciclastic

input). Such variables interact to determine the situation, physiography, budget and facies patterns of a carbonate platform.

3.4.2. Geographic distribution of carbonate platform sedimentation.

Modern carbonate platforms are relatively young, immature systems having become established only within the last few thousand years (3000 to 6000 yrs^{-1}). Modern platforms are mostly developed upon the karstified relicts of Pleistocene platforms whose antecedent topography exerts a strong control upon patterns and facies of platform sedimentation observed today (Purdy, 1974; Longman, 1981). Thus, direct analogies with the rock record should be used with an appreciation for the relative immaturity and architectural inheritance of modern platforms.

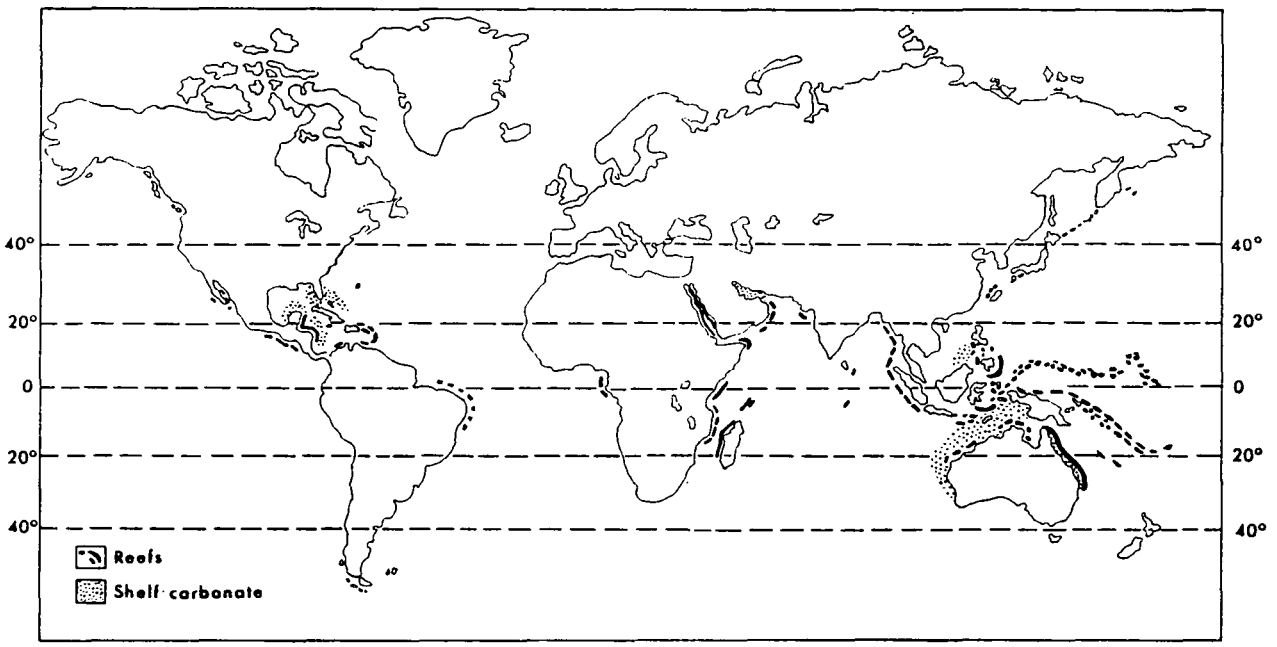

Figure 3.6. The present day distribution of reefs and carbonate platforms. Note that almost all carbonate platforms are restricted to 30° north and south of the equator. From Wilson (1975).

Contemporary carbonate platform sedimentation is concentrated between 30° north and south of the equator (eg. Fig. 3.6). This reflects both the greater supersaturation of $CaCO_3$ in seawater with increasing temperature and the equatorial habitat of the major modern carbonate secreting organisms. Within the equatorial

Sequence Stratigraphic Models For Carbonate Shelves.

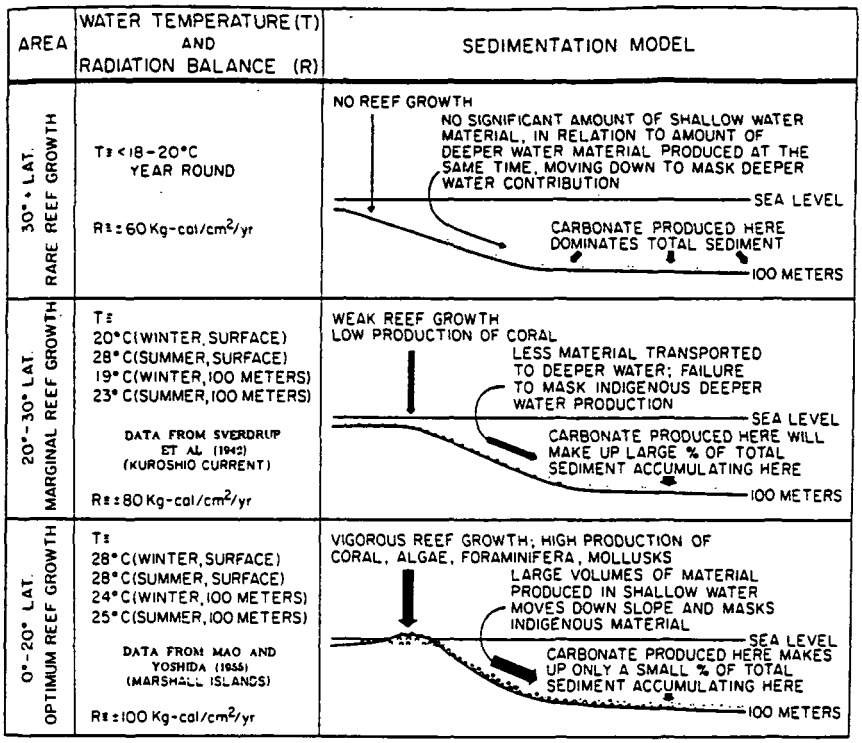

Figure 3.7. Ecology and profile of reefs from the Pacific Ocean. With increasing latitude the profile of platforms changes, most notably at the shelf margin. This illustrates the decreasing production potential of carbonates with increasing latitude, where platform margins have been unable to aggrade and keep pace with the Holocene sea-level rise. These profiles also demonstrate the effects that major environmental change(s) can have on a shelf/isolated platform. For example, upwelling of cold waters at low latitude would result in a loss of production potential and the protective barrier reef complex, opening the shelf-lagoon to the effects of storms. From Schlanger & Konishini (1975).

zone of carbonate platforms (in the absence of other factors) differences of water temperature and seasonality control the ecology of carbonate secreting organisms, production potential and in-turn the platform profile (eg. Fig. 3.7) (Schlanger & Konishi, 1975).

The modern range of carbonate platform sedimentation does appear to provide a fair guide to the rock record. For example, during the Mesozoic the northwards continental drift of N. America is marked by the drowning of carbonate platforms on the eastern continental margin at the approximate time a particular area passed through 30° north (eg. Schlager, 1981, his fig. 14). During times of globally higher temperature, such as during the late Cretaceous (interpreted to be 6-12°C warmer, Barron *et al.*, 1981) the range of carbonate secreting organisms and the

supersaturation of $CaCO_3$ in seawater was probably significantly expanded and so, correspondingly, was the development of carbonate platforms.

3.4.3. Siliciclastic contamination.

Siliciclastic sediments tend to have a detrimental effect upon carbonate sedimentation and particularly organically-produced carbonate. Thus, siliciclastics are often said to 'contaminate' carbonate platforms. The present day distribution of carbonate platforms in the equatorial zone reflects this sensitivity: regions of high terrigenous input are generally unfavourable sites for carbonate sedimentation, and conversely regions of low input with otherwise favourable conditions are often sites of carbonate platforms (eg. see Acker & Stearn, 1990). With the exception of the Bahamas and most Pacific atolls all modern carbonate platforms are associated with varying degrees of siliciclastic contamination.

In the northern Gulf of Mexico carbonate sedimentation upon the West Florida platform is inhibited by the relatively constant input of siliciclastic muds from the Mississippi (eg. Ginsburg & James, 1974). Upon platforms developed in more arid climates input of siliciclastic sediments is normally sporadic. Siliciclastic input tends to be either very coarse grained and so quickly sedimented and localised and/or so infrequent it is only a hindrance to carbonate production for a few days a year or less (eg. Roberts & Murray, 1988; Friedman, 1988). The development of depressions on carbonate platforms can also act to localise carbonate sedimentation by trapping siliciclastic input(s) into discrete areas (eg. northeastern Australia, Davies *et al.*, 1989). Alternatively, shallow-water carbonate sedimentation may be isolated upon tectonic highs between which siliciclastics are deposited, confined to the troughs (eg. western Red Sea, Purser *et al.* 1987).

3.4.4. Climate.

Within the equatorial zone (Fig. 3.6) two distinctive climates in which carbonate platforms are developed can be recognized from characteristic facies

associations. Sub-humid climates are typified by a high precipitation to evaporation ratio for most of the year promoting hyposalinty where circulation is restricted (eg. the Bahamas, Gelebein, 1974, east Florida shelf, Jordan, 1978). In sub-arid to arid climates the evaporation to precipitation ratio is high for most of the year and hypersalinities are promoted where circulation is poor (eg. Trucial coast, Purser, 1973).

The modifying effect of climate upon carbonate sedimentation is particularly notable in intertidal to supratidal areas of a platform. Here circulation is generally restricted and in humid environments reduction of salinity (hyposalinity) is promoted by freshwater run-off during the wet season (eg. Florida Bay seasonal run-off from the Everglades) and/or by high rates of precipitation (eg. Gebelein, 1974). Hyposaline conditions favour the development of algal marsh, mangrove swamp and subsurface karstification (Jordan, 1978; Enos, 1983). Hypersaline conditions developed in sub-arid and arid climates are distinguished by microbial mats in peritidal environments and formation of displacive evaporites (halite and gypsum) in supratidal regions of a platform (eg. Kinsman & Park, 1976) (see Section 3.4.7).

3.4.5. Carbonate productivity.

The production of calcium carbonate in seawater is, for a given latitude (eg. Fig. 3.7), a function of water depth. Maximum productivity is limited to within 10m of sea-level decreasing by approximately half between 10 and 20m (Schlager, 1981) (Fig. 3.8). Thus, the production potential for a given platform can be related to the area of a platform with water depths of less than 10m (for a given latitude). Regions of a shelf or isolated platform which pass below depths of 10m are considered 'drowned' as these areas are thought to be unable to aggrade sufficiently fast to keep pace with further relative sea-level rise(s) (Schlager, 1981) (Fig. 3.9).

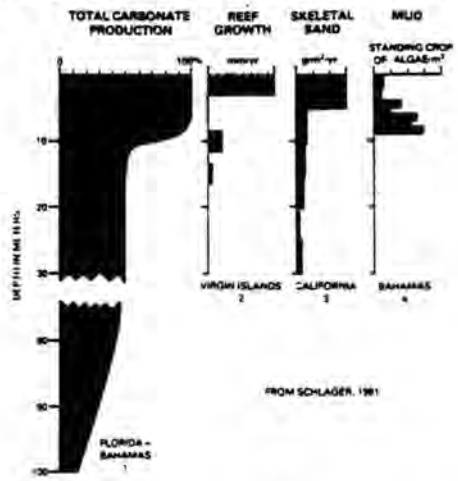

Figure 3.8. Carbonate production in relation to depth below sea-level. Note that the production potential is reduced by approximately half in water depths greater than 10m. The margins of shelves or isolated platforms submerged below 10-20m are often termed 'drowned' or 'incipiently' drowned (eg. Fig. 3.9). From Schlager (1981).

Areas of modern platforms below depths of 10m (euphotic zone) are considered either 'drowned' or 'incipiently drowned' (eg. Fig. 3.9) (eg. Dominguez *et al.*, 1988). The drowning of Bahamian banks during the Holocene sea-level rise is a reflection of both the situation (eg. windward v leeward orientation) and size of a bank (Dominguez *et al.*, 1988). Smaller banks such as Cay Sal Bank (Hine & Steinmetz, 1984) and Cat Island (leeward side) were selectively drowned during the Holocene (Dominguez *et al.*, 1988). This directly reflects both the production potential and windward-leeward orientation of these banks. More recent studies do, however, show that areas of modern platforms submerged below 10-20m and classically considered 'drowned' can still be 'healthy'. For example, carbonate banks upon the Nicaragua Rise are submerged to depths of 20-30m but are still producing excess sediment which is exported to the surrounding slopes and basin-floor (Glaser & Droxler, 1991).

Within the upper 10m of the water column potential for carbonate production is also a function of water energy; high energy areas of platforms, eg. inner ramps and shelf margins have the greatest current activity which promotes biogenic and abiogenic grain/cement production/formation. Away from high energy regions sediment production rates tend to decrease, both basinwards and landwards (Fig.3.13)

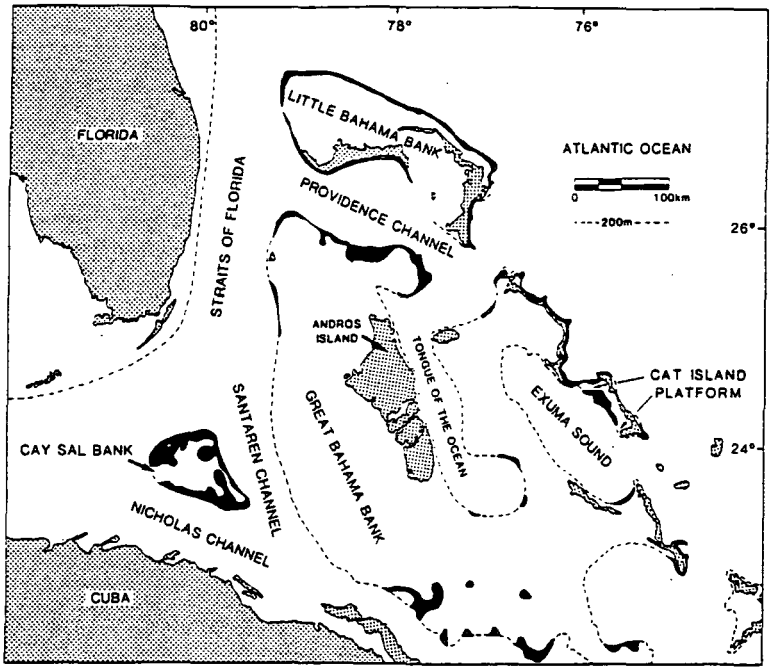

Figure 3.9. General map of the northwestern Bahama region. Areas shaded in black are banktops submerged below 10m, suggesting these areas are drowned. Note the location of Cay Sal Bank and Cat Island, mentioned in text (Section 3.4.5). From Dominguez *et al.* (1988).

Differentiation of platform production potential can be clearly illustrated by the profiles of modern shelves and isolated platforms where the high energy rims are often elevated to within a few metres of sea-level but are backed by deeper water lagoons (eg. Fig. 3.10) (Hunt & Tucker, 1992). More quantitatively, Holocene vertical accretion rates of reefs average about 1m 1000 yr^{-1}, but can reach 6m 1000yr^{-1} (Enos, 1977; Longman, 1981). This compares with average rates of between 0.2-0.5m 1000 yr^{-1} for the inner shelf although locally mudbank buildups can match rates reported from reefs (1m 1000yr^{-1} upon the Florida shelf, Bosence *et al.*, 1985; Mullins *et al.*, 1981).

3.4.6. Reef productivity and environmental sensitivity of carbonate secreting organisms.

Much carbonate sediment is produced by reefs and exported to lower energy surrounding areas (eg. slope and inner shelf). Reefs are normally situated in the high-energy regions of platforms where circulation is unrestricted and these are most

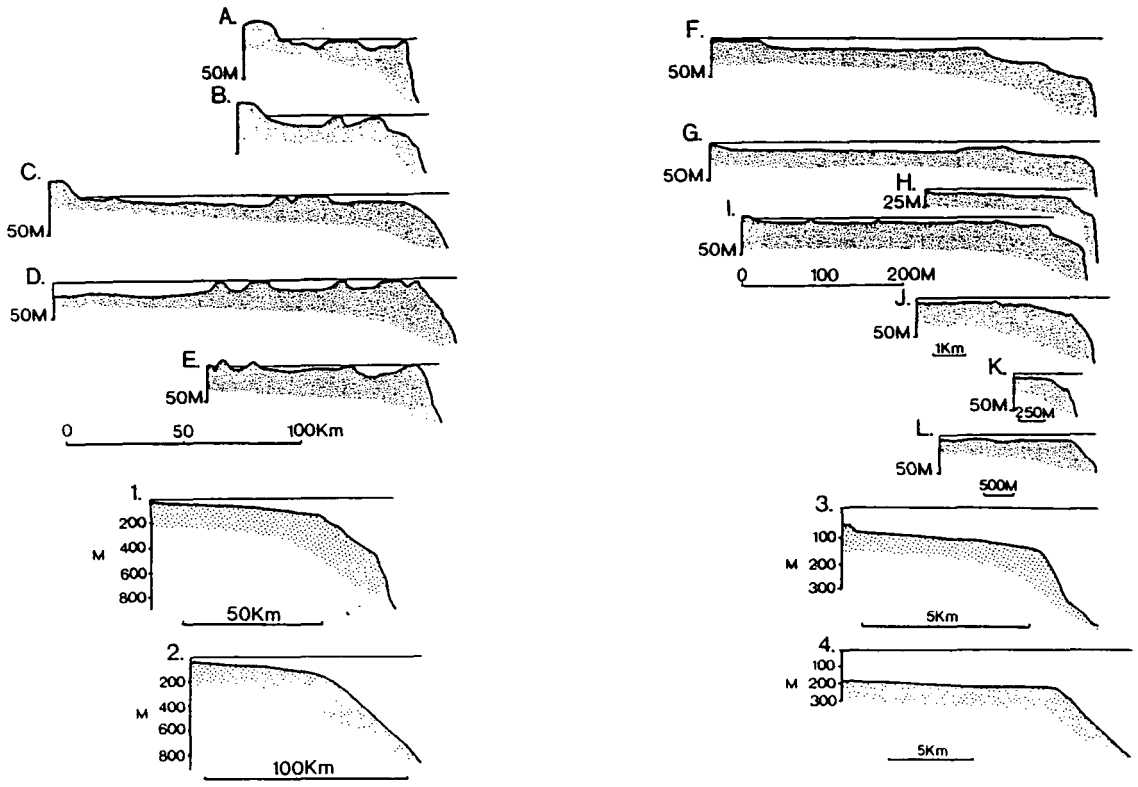

Figure 3.10. Comparison of depth below sea-level of the shelf-slope break between siliciclastic and carbonate Holocene shelves (1-4 and A-L respectively). Carbonate shelf-slope breaks are all at less than 50m and typically less than 10m. This compares with depths of between 100 and 400m on siliciclastic shelves, which average 130m (Curray, 1965). Thus, a fall of typically 10-20m is needed to develop a type 1 sequence boundary on a carbonate shelf and 100-400m on a siliciclastic shelf. (From Hunt & Tucker, 1992).

typically windward margins (eg. Bahamas, Gebelein, 1974; Great Barrier Reef, Davies *et al.*, 1989). Because of the hydrodynamic protection afforded to the platform (particularly isolated platforms and shelves) by reefs and their overproduction of sediment the health of the reef ecosystem is particularly crucial to that of the whole platform.

Because of their prolific productivity it is intuitive to think of reefs as prospering in waters anomalously rich in nutrients. In fact the opposite is more typically the case. Excess of nutrients (eg. phosphates and nitrates) from any source

(eg. freshwater river input, oceanic upwelling or even sewage outflow) is normally detrimental to a reef, reducing or even terminating its growth (Hallock & Schlager, 1986). This 'inverse' relationship reflects the more rapid growth of non-reefal organisms such as plankton which reduce water transparency, fleshy non-calcareous algae which attach themselves to reefs and smother them, and 'blooms' of reef grazers/bioeroders such as starfish which attack living corals and bioerode the reef (Hallock & Schlager, 1986).

Other changes in environment have also been attributed to the termination or reduction of Holocene reef growth and accompanying reef and/or platform drowning. Neumann & Macintyre (1985) suggested that reef growth can be suppressed by the passage of inmicable lagoon waters over reefs reducing both their efficiency and ability to aggrade (as happens/happened when Florida Bay was flooded and the channels through the Florida Keys brought hypo/hypersaline waters onto the Florida Shelf killing reefs). Glynn (1977) related the drowning of Holocence reef complexes to the upwelling of cool waters which should be marked by a change in reef community (eg. Fig. 3.7). Very recently, occurrences of reef whitings and species extinctions have been reported from the Panamic Pacific Province (Glynn & De Weerdt, 1991). These extinctions have been related to the 1982-83 El Niño warming event during which water temperatures were elevated by 2-3° for a six month period. This illustrates the very low tolerance of tropical carbonate secreting organisms to environmental changes, a reflection of the very stable climatic conditions to which these organisms have become adapted. Thus, relatively little variation of temperature for example (up or down) as an environmental variable can result in widespread extinctions. In the geological record it is almost impossible to pinpoint such events to their cause.

An important consequence of the termination of reefs is that relatively quickly (on a geological time scale) the platform (eg. inner-shelf, inner-ramp or isolated platform) loses its protective rim which had acted as a hydrodynamic buffer zone protecting the backreef environment from the full intensity and force of wind and/or

tidal energy. This can have particularly important consequences for shelves or isolated platforms where the demise of reefs would be associated with an opening up of conditions, increase of energy and a major hydrodynamic reorganisation of the shelf-lagoon. The lack of an effective rimming complex is well illustrated by the most southerly region of the West Florida platform (Brooks & Holmes, 1989). Here the absence of a shelf-rimming complex allows incursion of the Florida Loop current onto the platform and the uninterrupted off-shelf passage of storm currents which move significant amounts of shallow-water sediments to the slope.

3.4.7. Cementation.

Rather differently from siliciclastic depositional systems, carbonate platform sediments are often subject to early cementation and lithification. The occurrence and intensity of cementation on a platform generally corresponds closely to regions of maximum water energy, namely the shelf-margin. The degree of early marine cementation is also a reflection of sediment permeability and/or stability, so, for example, stable permeable sediments such as reefs are cemented more readily than permeable but mobile carbonate sand shoals. The development of both early marine cements and meteoric diagenesis is also highly sensitive to climate.

The precipitation of cements is promoted by CO_2 degassing which is normally associated with turbulence. Organic activity also promotes changes of pH and CO_2 degassing and thus precipitation. Primary regions of a platform subject to the most intense early cementation are high energy areas such as reefs and/or carbonate sand shoals and peritidal regions. Secondary regions often associated with early cementation are the flanks of the platform which can interact with oceanic currents. These are frequently associated with cementation, slope stabilisation and where currents are strongest, ferruginised hardgrounds are commonly developed (eg. Mullins *et al.*, 1984; Gardaluski *et al.*, 1990). Early diagenesis can have a direct and important effect upon the flanks of carbonate platforms as it increases shear strength

and thus promotes slope stability, increasing slope angles (Kenter, 1990) (see Sections 3.5.2 & 3.6.4).

Arid platforms appear to be prone to more intense and a different style of early submarine diagenesis than humid platforms (Hird & Tucker, 1988). This probably reflects the hypersalinities of sea-water in regions of restricted circulation on arid platforms. Meteoric diagenesis in particular tends to be very sensitive to climate (eg. Hird & Tucker, 1988; Wright, 1988; Tucker, 1992). Humid climates tend to favour rapid dissolution, particularly of aragonite by hyposaline porewaters, and karst may be developed. The rate of dissolution appears to be a direct reflection of precipitation (rainfall) rate (James & Choquette, 1984). Hypersaline porewaters in arid climates tend to favour reflux dolomitization and evaporite cementation (see Tucker, 1992 for a review of diagenesis in a sequence stratigraphic framework).

3.5. External Controls Upon the Position, Size and Geometry of Stratal Units.

3.5.1. Introduction.

To a sequence stratigrapher 'external controls' are those changes other than relative sea-level which can cause changes in stratal packaging. These are normally considered to assume a secondary role to relative sea-level changes (eg. Vail *et al.*, in press). It is the aim of this section to illustrate briefly how in some situations these changes can play an important, if not the dominant role in the development of stratal patterns.

Under the umbrella of 'external controls' are environmental changes such as upwelling and the influence of currents (oceanic, storm, tidal) on sedimentation patterns. Factors which also could be considered here are long term changes of sea-water chemistry and organism evolution but since these are rather specific to

carbonate platforms they are discussed in Section 3.6. Examples in this section are chosen solely from carbonate depositional settings.

3.5.2. Oceanic currents.

Common to both the Florida and Bahamas platform is the Loop current, renamed the Florida current as it passes between Florida and the Bahamas. This current developed during the mid Miocene due to a major reorganisation of oceanic currents related to tectonic closure farther south (Mullins *et al.*, 1988). Inception of the current is associated with truncation of clinoforms, blocking of basinwards progradation, upwelling of cool waters along the slope and (probable) increased slope cementation and therefore higher slope stability along the western slope of the Florida platform (Mullins *et al.*, 1988; Gardaluski *et al.*, 1990; Brooks & Holmes, 1989).

Along the Straits of Florida between the Bahamas and Florida the same current is associated with development of basin-floor hardgrounds, lithoherms and the along slope movement of sediment which is deposited at the northwestern tip of Great Bahama and Little Bahama banks as toe-of-slope wedges ('sediment drifts', Mullins & Neumann, 1979). These toe-of-slope wedges onlap the slope and downlap on to the basin-floor: the geometry of a lowstand wedge in seismic stratigraphy, but developed primarily in response to a change in oceanographic circulation, not relative sea-level changes.

The northeast slope of Little Bahama Bank is also affected by the Antilles current (Mullins *et al.*, 1984). This current is responsible for the degree of early cementation along the slope which in turn controls the facies and position of submarine canyons, gullies and depositional processes acting on the various parts of the upper slope (Mullins *et al.*, 1984). Early cementation associated with this current also indirectly controls the mechanism(s) and type of sediment reworked from the upper slope to the basin-floor (eg. see Mullins *et al.*, 1984)

3.5.3. Windward v leeward platform orientation and the influence of tidal currents.

One of the most obvious features of the modern Bahamas is the marked asymmetry of reefs which are preferentially developed on the windward side of banks. Carbonate sand shoals are also developed in windward locations, but in addition they occur on both leeward sides of banks and in areas which experience strong reversing tidal currents (eg. Gebelein, 1974). This asymmetry is also reflected upon the flanks of the Bahamian banks. Leeward facing slopes tend to be accretionary and characterized by high sedimentation rates and coarse sands swept leewards and off-bank by storms. Rather differently, windward margins tend to have low sedimentation rates with shelf-margin sediment carried back on to the platform and, thus, slopes which are dominated by the deposition of calcitic pelagic oozes (Mullins *et al.*, 1984). Such asymmetry is also evident in the rock record of the Bahamas (Fig. 3.11). Since the mid-Cretaceous sediment has been preferentially exported to leeward (westerly) slopes (eg. Fig. 3.11) (Eberli & Ginsburg, 1989). Today the leeward flanks of the Bahamas are characterized by accretionary low relief progradational slopes whereas windward sides are typically high-relief erosional slopes (Fig. 3.12, Ginsburg & Schlager, 1981). This reflects the long-term aggradation of the platform coupled with the preferential leeward export of sediment.

The effects of tide and wind domination along a shelf-margin are well illustrated by the Florida Keys (eg. Tucker & Wright, 1990, their figs 3.26 & 3.27). The Keys are formed of exposed Pleistocene limestone and the form of these islands demonstrates the southward change from a wind-dominated to a tidally-dominated shelf-margin complex. Southwards, along strike, the Pleistocene shelf-margin changes from a narrow wind-dominated reef complex (Key Largo Limestone) to a considerably broader tide-dominated oolite shoal complex (the Miami Oolite) of Sugarloaf Key, Big Pine Key, and Key West.

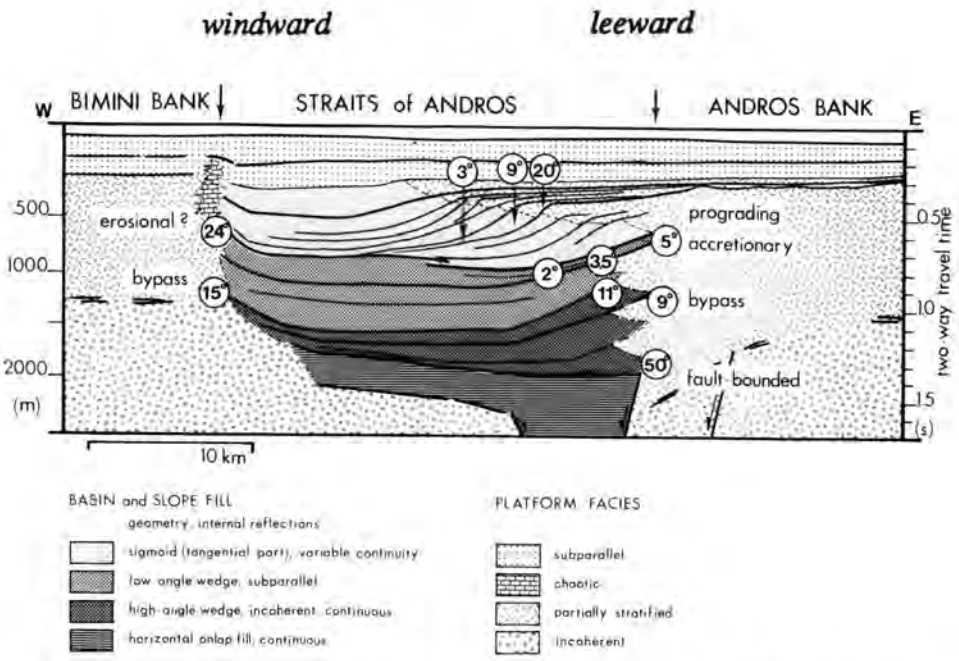

Figure 3.11. Interpreted section across the Straits of Andros from Eberli & Ginsburg (1989). The windward margin is reef dominated and characterized by bypass and erosional slopes. This contrasts markedly with the leeward slope which evolves from a stationary bypass to a prograding accretionary slope as the platform to basin-floor relief reduced. The base of the coherent reflectors is interpreted to be mid-Cretaceous and the change form leeward aggradation to progradation mid-Miocene.

3.5.4. Discussion.

The preceding two sections clearly demonstrate the important roles, both direct (eg. Florida Loop current blocking progradation of the Florida ramp) and indirect (eg. Antilles current controlling cementation and in turn slope processes on northeast Little Bahama Bank) which the so called 'external controls' can have in the development of stratal patterns of carbonate platforms. These processes, with the exception of the differences between wind and tidally dominated margins are not, however, considered in the development of new sequence stratigraphic models for carbonate shelves which only consider the movement of sediment parallel to dip sections.

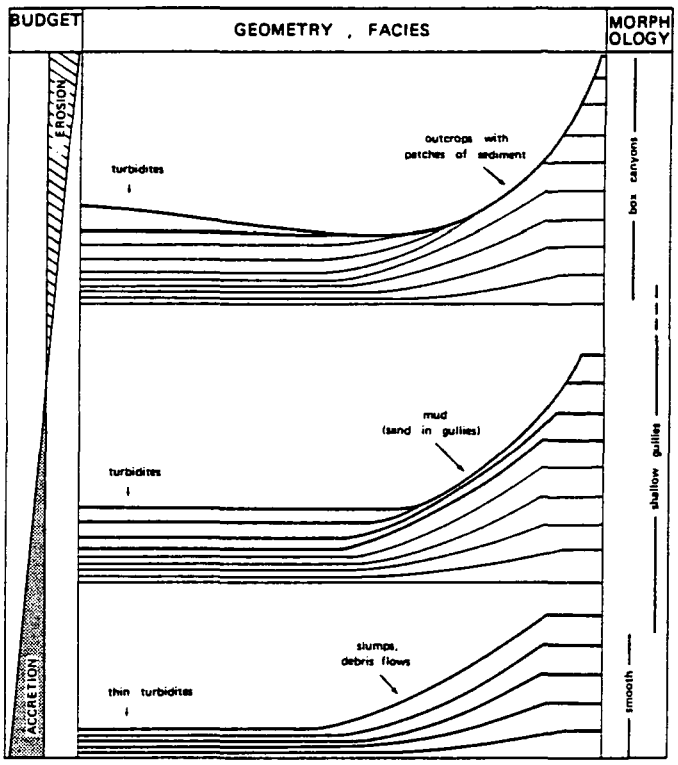

Figure 3.12. Accretionary, bypass and erosional slope profiles as found upon the flanks of the modern Bahamas. Note the increasing platform to basin-floor relief and change of slope profile from accretionary to erosional slopes. This is associated with a change of the slope budget from positive (accretionary) through neutral (bypassing) to negative (erosional). From Schlager (1989), after Schlager & Ginsburg (1981).

3.6. Contrasts Between Carbonate And Siliciclastic Depositional Systems Of Particular Importance To Sequence Stratigraphy.

3.6.1. Introduction.

In the 'Exxon' carbonate sequence stratigraphic models published to date (eg. Fig. 3.5B) differences between siliciclastic and carbonate depositional systems are considered to be of secondary importance. In this section differences between the two systems of particular relevance to the development of sequence stratigraphic models for carbonate shelves in open ocean settings are explored. These differences are used as a basis for the revised carbonate sequence stratigraphic models developed in Section 3.7.

The contrasts between carbonate and siliciclastic depositional systems may be differentiated into those which can alter stacking patterns on a sequence (i.e. 3rd

order) or smaller scale (eg. slope morphology, sediment source) and, secondly, those changes which can be considered evolutionary (2^{nd}-1^{st} order) such as organism evolution/demise and/or changes of sea-water chemistry.

3.6.2. Present bathymetry of the shelf-slope break.

Present day morphology of the shelf-slope break may be significantly different from the geological record because of the high amplitude sea-level variations during the Quaternary and the relative immaturity of most shelves having been transgressed during the Holocene (eg. Thorne & Swift, in press). However, as both carbonate and siliciclastic depositional systems have experienced the same changes of sea-level a comparison of the present day morphology can elucidate the different responses of the two systems to changes of relative sea-level.

Figure 3.10 (p. 50), is a comparative diagram illustrating both modern siliciclastic and carbonate shelf profiles. As an initial contrast, it is interesting to note that across the width of carbonate shelves the shelf as a whole is much shallower than siliciclastic counterparts. Secondly, the bathymetry of the shelf-slope break occurs at depths of less than 50m (normally <20m) upon carbonate shelves whereas this interface *normally* occurs at depths of between 87 and 183m (averaging 130m, Curray, 1965) upon siliciclastic shelves (Van Wagoner *et al.*, 1990). The different profiles for siliciclastic and carbonate shelves may be explained by a combination of differential erosion between siliciclastic and carbonate shelves upon exposure and differential sedimentation rates during Holocene transgression allowing carbonate platforms to build close to sea-level.

Purdy (1974) demonstrated that modern carbonate platforms, particularly those in humid climates have inherited much of their present day architecture from the karstified relicts of Pleistocene platforms. High resolution seismic profiles of the Bahamas (eg. see Mullins & Neumann, 1979) illustrate how rimming reef complexes have aggraded and for the most part, kept pace with rates of sea-level rise during Holocene transgression. This contrasts with inner parts of the platform where

Holocene sediments are a thinner veneer resting upon the previously exposed Pleistocene limestones. This relationship suggests that outer platform areas were able to keep pace with the rates of relative sea-level rise during transgression but, more importantly, carbonate shelves underwent comparatively little denudation during the preceding lowstand of sea-level.

In terms of comparative sequence stratigraphic models between carbonate and siliciclastic shelves perhaps the most important conclusion from this comparison of shelf profiles is that a lesser magnitude of sea-level fall is needed to develop a type 1 sequence boundary (eg. fall of sea-level below the shelf-slope break) upon a carbonate shelf. Upon a siliciclastic shelf the average would be 130m, compared to a fall of typically less than 10m upon a carbonate shelf. The elevated rim of carbonate shelves implies that this region will become exposed with only small amplitude sea-level falls (<10m). However, such falls do not necessarily expose the inner-shelf/shelf-lagoon which is often deeper (eg. Fig. 3.10). Thus, defining a sequence boundary (type 1) on the basis of dropping sea-level below the shelf-slope break upon a carbonate shelf is not always adequate and should include documentation of the unconformity within the shelf-lagoon succession.

3.6.3. The origin and budget of siliciclastic and carbonate sediments.

3.6.3. A. Source of sediments and relationship of sediment budget to sea-level.

Upon carbonate platforms most sediment is produced in shallow waters (<10m Fig. 3.8, see Section 3.4.5) and normally relatively close or actually in its depositional environment. As previously discussed (Section 3.4.5 & 3.4.6) production is differential across a carbonate platform (excepting epeiric platforms/aggraded shelves) and is mostly produced in shallow water high energy regions (eg. inner ramps, outer shelf margins) and exported to other, lower energy regions of the platform (Fig. 3.13).

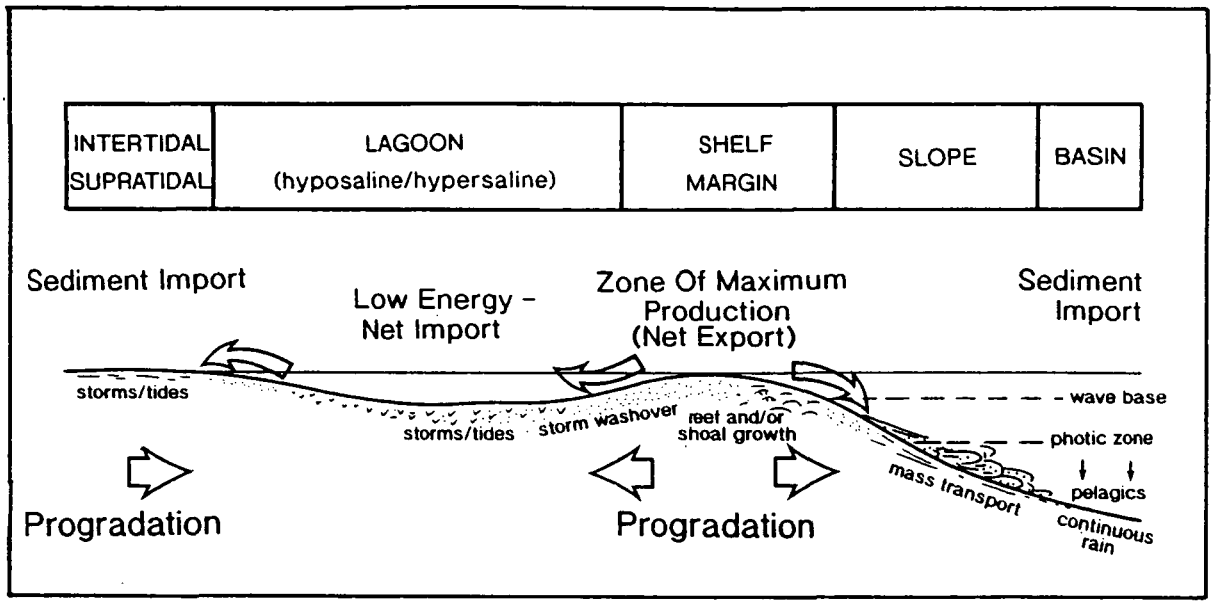

Figure 3.13. Idealised cross section of a carbonate shelf showing areas of net sediment export.

By way of contrast, in siliciclastic depositional systems sediments are generally introduced into their depositional environment by a point source and are normally transported great distances from their provenance. The sediment budget of a siliciclastic shelf tends to reflect the size of its hinterland so that an enlargement (as occurs when sea-level falls) increases the sediment flux. Contrastingly, carbonate platforms have a largely submarine sediment source; the production potential of a carbonate platform tends to reflect the area of the platform with water depths of less than 10m (see Section 3.4.5.). Exposed areas of a platform are 'shutdown' and rapidly cemented so that no (or volumetrically insignificant) sediment is created and/or exported from such areas. A fall of sea-level upon a carbonate shelf or isolated platform thus reduces the area suitable for sedimentation to a narrow ramp-like strip upon the slope (eg. Bahamas, Boardman *et al.*, 1986; Droxler & Schlager, 1985 and the south Florida platform, Brooks & Holmes, 1989). Thus, since carbonate production is related to the area of shallow water sedimentation (Section 3.4.5) and this is vastly reduced during the lowstand of sea-level sedimentation rates will be at their lowest at these times. [3]

[3] Variation of the production potential of a carbonate platform need not be related to relative sea-level changes. Carbonate sedimentation rates are sensitive to environmental changes which can vary independently of sea-level (eg. see Section 3.4.6)

3.6.3. B. Aggradational vs progradational origin of carbonate parasequences.

Both siliciclastic and carbonate marine and marginal marine deposits commonly develop shallowing-up cycles or parasequences. In siliciclastic systems these are formed by the migration of facies belts as sedimentation rates exceed the rate of relative sea-level rise and/or during relative sea-level stillstands (Fig. 2.3, p. 11). The development of shallowing-up cycles upon some carbonate platforms (eg. epeiric platforms or aggraded shelves) cannot always be explained by the same progradational mechanism since such cycles can develop simply from *in situ*, upward growth (aggradation) rather than from lateral progradation of sediment.

Carbonate platforms often have the capacity to produce carbonate sediments at rates greater than common rates of relative sea-level rise (eg. Schlager, 1981, his fig. 5), although this production potential is highly differentiated across an individual platform. The ability to produce large volumes of sediment is related to water depths, water energy and nutrient supply (see Sections 3.4.5 & 3.4.6). Two strongly progradational areas are generally recognized upon carbonate shelves; the shelf-margin and tidal flats (eg. Fig. 3.13). Progradation of the shelf-margin is related to the overproduction and export of sediment into surrounding slopes and basinal areas by a variety of mechanisms (eg. clinoform progradation of high-energy shelf-margin facies into deeper water by gravity driven processes). This contrasts with the progradation of most tidal flats which accrete laterally as mud is thrown on to them from the adjacent lagoon during storms. Progradation of these areas (shelf margin and tidal flats) during relative stillstands of relative sea-level develops parasequences.

3.6.4. Carbonate v siliciclastic slopes.

Siliciclastic slopes are usually characterized by a submarine canyon-fan system (eg. see review, Shanmugam & Moiola, 1991); sediments supplied to the slope are typically funnelled via a major canyon eroded into the slope to a basin-floor. Here sediments are distributed upon lobes of a discrete fan. In carbonate depositional systems direct analogues are relatively rare (Mullins & Cook, 1986). More typically,

carbonate slopes are characterized by a series of relatively small canyons and gullies which act as a line source so that an apron of small interfingered lobes is developed around the platform on the slope or basin-floor as opposed to a discrete point-sourced fan (eg. Mullins & Cook, 1986).

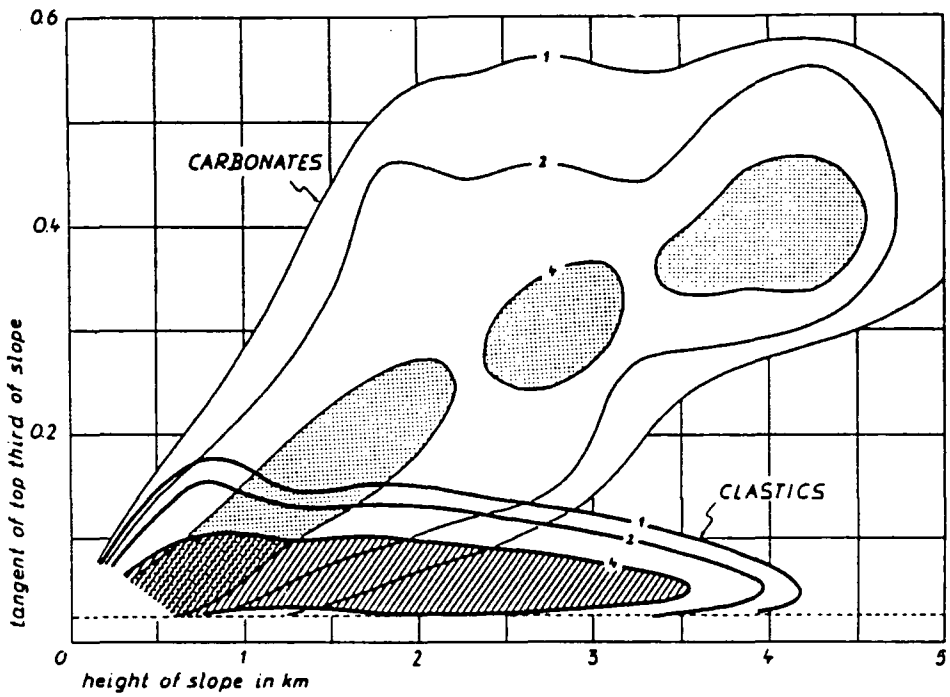

Figure 3.14. Angle of upper one-third of slope versus slope height. Contours indicate concentrations of 0.5, 1 and 2 % of total sample in unit area of 0.25 x 0.005 tan S, measured as a moving average of 9 unit cells. Carbonate samples includes Bahamas and central Pacific atolls (n=413); siliciclastic sample is based on Atlantic continental slopes (n=72). Carbonate slopes steepen with heights of 5 000m or more; siliciclastics follow this trend only to 500m; over 500m slope height has no influence on declivity of siliciclastic slopes. From Schlager & Camber (1986).

Modern carbonate slopes are generally characterized by higher angles than those of siliciclastics (Fig. 3.14). The angles attained upon modern carbonate slopes in the Pacific and Atlantic have a direct relationship to the slope height. Upon siliciclastic slopes this relationship breaks down upon slopes greater than 500-800m (Fig. 3.14) (Schlager & Camber, 1986). The close relationship between slope height and morphology was first illustrated from the Bahamas by Schlager & Ginsburg (1981) as illustrated in Figure 3.12. With increasing height between the platform and

basin-floor the slope changes profile becoming increasingly concave-up (eg. Fig 3.12). Correspondingly, the slope profile, processes and dynamics of sedimentation evolve. With increasing height the slope sediment budget changes from positive (accretionary) to neutral (bypass) to negative (erosional) (Schlager & Ginsburg, 1981; Camber & Schlager, 1986; Schlager, 1989, Fig. 3.12). Bypass and erosional slopes are characterized by the development of a toe-of-slope apron composed of sediments bypassed through and eroded from the slope and platform. The toe-of-slope apron has a positive budget and is aggradational, onlapping the slope (eg. Fig. 3.12). Upon bypass slopes most sediment is shed to the toe-of-slope apron during highstands (the highstand shedding of Droxler and Schlager, 1985). Thus, in such situations slope onlap is developed during highstands of sea-level on bypass slopes (Fig 3.12, p. 57).

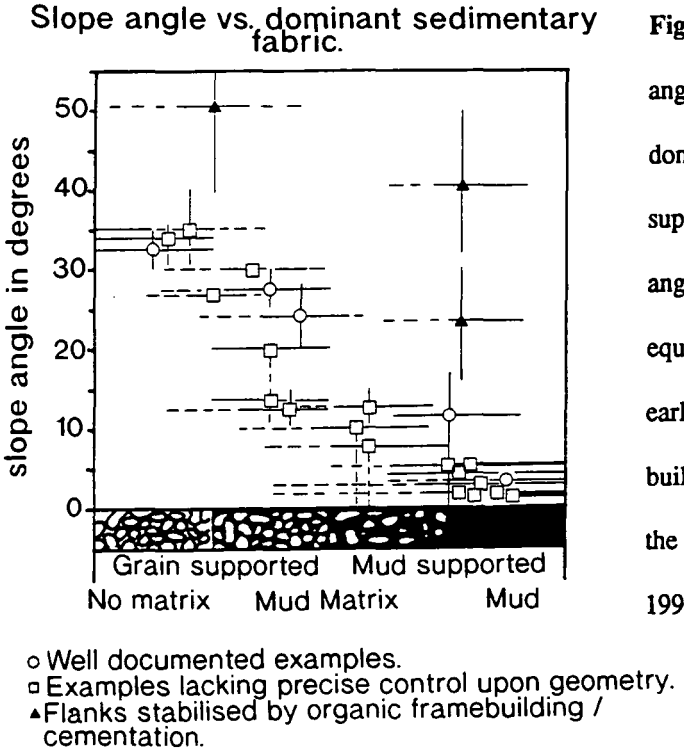

Figure 3.15. Relationship of foreslope angle of carbonate platforms to the dominant sedimentary fabric. Grain supported slopes tend to have higher angle slopes than mud supported equivalents in the absence of early cementation and/or frame building organisms which plot above the general trend (adapted from Kenter, 1991).

Although there is a well documented relationship between the height of a carbonate slope and its morphology (eg. Schlager & Ginsburg, 1981, Fig. 3.12) other factors can modify this general trend, and these include sea-level changes, subsidence, climate, windward/leeward orientation, currents and oceanographic setting (eg. open ocean, a seaway, or an embayment etc) (eg. Schlager & Chermak, 1979; Schlager & Ginsburg, 1981; Mullins *et al.*, 1984; Schlager & Camber, 1986). Kenter (1990) (Fig. 3.15, preceding page) has shown that the dips of carbonate slopes are directly related to sediment fabric in the absence of organic framebuilding and/or early cementation. The sediment fabric itself reflects the type of sediment supplied to the slope (eg. sands on leeward flanks and muds on windward flanks, Mullins *et al.*, 1984), the depositional mechanism by which the sediment is deposited and the role of oceanic currents (if any) which can promote deep water cementation and/or framebuilding (eg. Mullins & Neumann, 1979, Section 3.5.2).

3.6.5. Carbonates through geologic time: organic and geochemical changes.

Carbonate depositional systems have evolved considerably through geological time in response to changes in the chemistry of sea-water, and to changes of the major carbonate secreting organisms (eg. Tucker, 1992; James, 1983). Evolutionary patterns are particularly important at platform margins where the type and relative abundance of reef-forming organisms have varied considerably.

The study of inorganic carbonate deposits through the geological record has revealed cyclic changes in the dominant mineralogy of calcium carbonate precipitated from sea-water (Sandberg, 1983; Tucker, 1985; Tucker, 1992) (Fig 3.16). Sandberg (1983) showed that at different times in the geological record precipitation of either aragonite, or calcite is preferred (eg. Fig. 3.16). These changes are thought to reflect the first order tectono-eustatic sea-level curve and the change from icehouse (times of glaciation) to greenhouse conditions (ice-free times characterized by high sea-level / CO_2). Similar trends have also been noted in skeletal carbonates (Wilkinson, 1979).

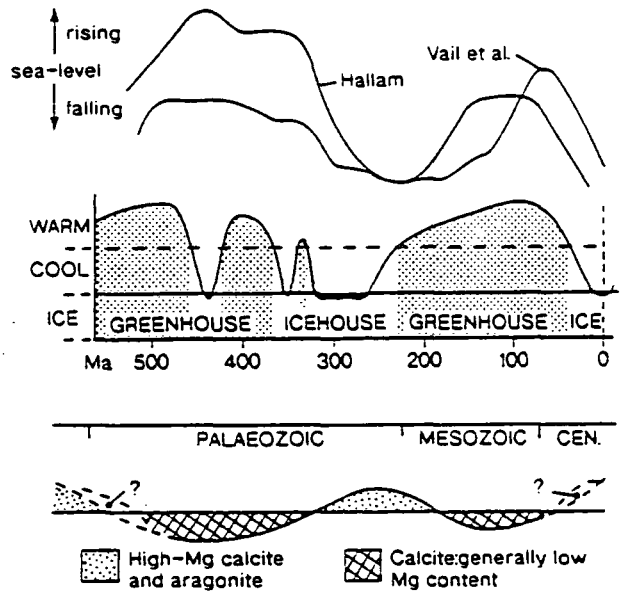

Figure 3.16. Change of predominant carbonate mineralogy with time from the Late Precambrian to present day compared to the sea-level curves of Hallam (1977) and Vail *et al.* (1977). Adapted from Tucker (1992).

These changes in carbonate mineralogy appear to relate to the first order sea-level curve of Vail *et al.* (1977). Variations of mineralogy are important as they alter the 'diagenetic potential' of a carbonate sediments. During times when aragonite is preferentially precipitated (icehouse times) the potential for the diagenetic alteration of carbonates is high in both the vadose and burial environments (Tucker, 1992).

Carbonate secreting organisms have evolved with geological time so that different organisms predominate as the major carbonate secreting organisms at different times (Fig. 3.17). The rise and demise of different reef-forming organisms can have a dramatic effect upon the type and distribution of high energy facies. In-turn, this can affect the geometries developed both at a shelf-margin and upon its adjacent foreslope(s). At certain times in the geological record (eg. Fig. 3.17) reef forming organisms were relatively rare so that shelf margins for instance tended to be dominated by sand-shoal complexes. Such changes can have a profound effect upon the geometry of platforms world-wide that will not be related to changes of sea-level.

A possible example of such a change is from the mid-Devonian to Lower Carboniferous when there was a major extinction of reef-forming organisms (eg.

James, 1983) (Fig. 3.17). The dearth of reef forming organisms contributed to the abundance of bioclastic/oolite dominated ramps and generally reduced slope angles at shelf margins in the early Carboniferous. Ahr, (1989) observed that the change from sand-dominated ramps to reef-rimmed shelves during the Carboniferous was accompanied by a change in the geometry of the Mississippian platform of New Mexico. Ahr (1989) noted that similar changes take place world-wide at the same time. Such changes in geometry appear to relate to organism evolution rather than global sea-level change and may well have produced different sequence stratigraphic geometries in the lower and upper Carboniferous upon carbonate platforms.

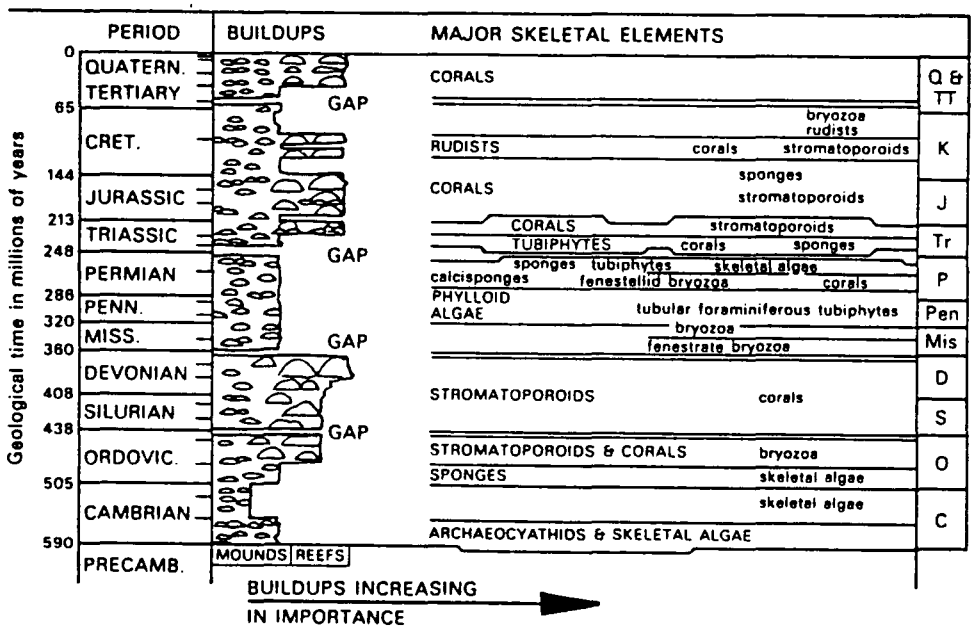

Figure 3.17. Idealised stratigraphic column for the Phanerozoic illustrating the relative importance of reef forming organisms and relative abundance of reefs and bioherms. Note four major gaps, between the Ordovician and Silurian, the Devonian and Carboniferous, the Permian and Triassic and in the lower Tertiary. The second gap, between the Devonian and Carboniferous is discussed in the text. From Reading (1986) after James (1983).

3.7. Revised Models For The Sequence Stratigraphic Evolution Of Carbonate Shelves.

3.7.1. Introduction.

The models presented here for carbonate shelves in open ocean settings build upon and from the sequence stratigraphic concepts introduced in Chapter 2. The basic background for these has been introduced in the earlier sections of this chapter where the differences between siliciclastic and carbonate depositional systems have been highlighted. These differences are incorporated to build new or revised sequence stratigraphic models for carbonate shelves in open ocean settings that account for the variation found in the carbonate depositional system.

It is the thesis of this section that these differences can, and normally do significantly modify stratal patterns developed by carbonate shelves in response to changes of relative sea-level and/or sedimentation rate. It is shown that stratal variation is not solely related to changes of relative sea-level. Environmental changes can produce profound variations in sedimentation rates and these can be as important as relative sea-level changes in the development of stratal patterns. Models developed for carbonate shelves can be equally applied to isolated, aggraded and epeiric platforms. Models for carbonate shelves in intracratonic settings are discussed by Tucker (1991) and models for carbonate ramps are developed in Tucker *et al.* (1992, see inclusions).

Models developed here are two dimensional and do not consider movement of sediment in or out of dip section(s).

3.7.2. Carbonate shelves.

The different types of carbonate shelf and their diagnostic physiographies are summarised in Section 3.2 and Figures 3.1, 3.2 and 3.3.

3.7.2. A. Processes and depositional dynamics upon carbonate shelves associated with falling and lowstand of relative sea-level: *the lowstand fan and lowstand wedge systems tracts*.

Exposure of carbonate shelf tops rarely results in mechanical reworking of the shelf but, more typically a chemical reworking (cementation/dissolution) in the form of early meteoric diagenesis that will tend to be climatically controlled (eg. humid-karstification, arid-dolomitisation). The extent of early diagenesis will reflect the amplitude of sea-level fall and the diagenetic potential (see Tucker, 1992 for review). Exposure of the shelf thus does not typically result in an increased sediment supply to the adjacent slope/basin, but the reverse, as negligible sediment is supplied off the shelf top (eg. Crevello & Schlager, 1980) (see also 3.6.3. A). During the lowstand, rates of periplatform mud sedimentation are therefore likely to decrease as the shelf top's capacity to overproduce carbonate mud is terminated or drastically reduced (Mullins, 1983; Crevello & Schlager, 1980; Droxler & Schlager, 1985; Boardman *et al.*, 1986; Wilber *et al.*, 1990). Because sedimentation becomes areally restricted to a narrow margin of the slope during lowstand these times are normally associated with the lowest overall sedimentation rates. In most cases lowstand will be impoverished or event absent on many carbonate platforms due to the restricted area of potential carbonate production (Fig. 3.18). In the basin proximal to the platform lowstand of relative sea-level is likely to be associated with development of a condensed section and a shift from periplatform muds to pelagic sedimentation.

Lowstand sedimentation on carbonate platforms is characterized by two genetically distinct types of deposit: *allochthonous debris*, calciclastic sediments derived mechanically from the preceding highstand, and *autochthonous wedges*, formed *in situ* on the modified/unmodified slope to the preceding highstand (Sarg,

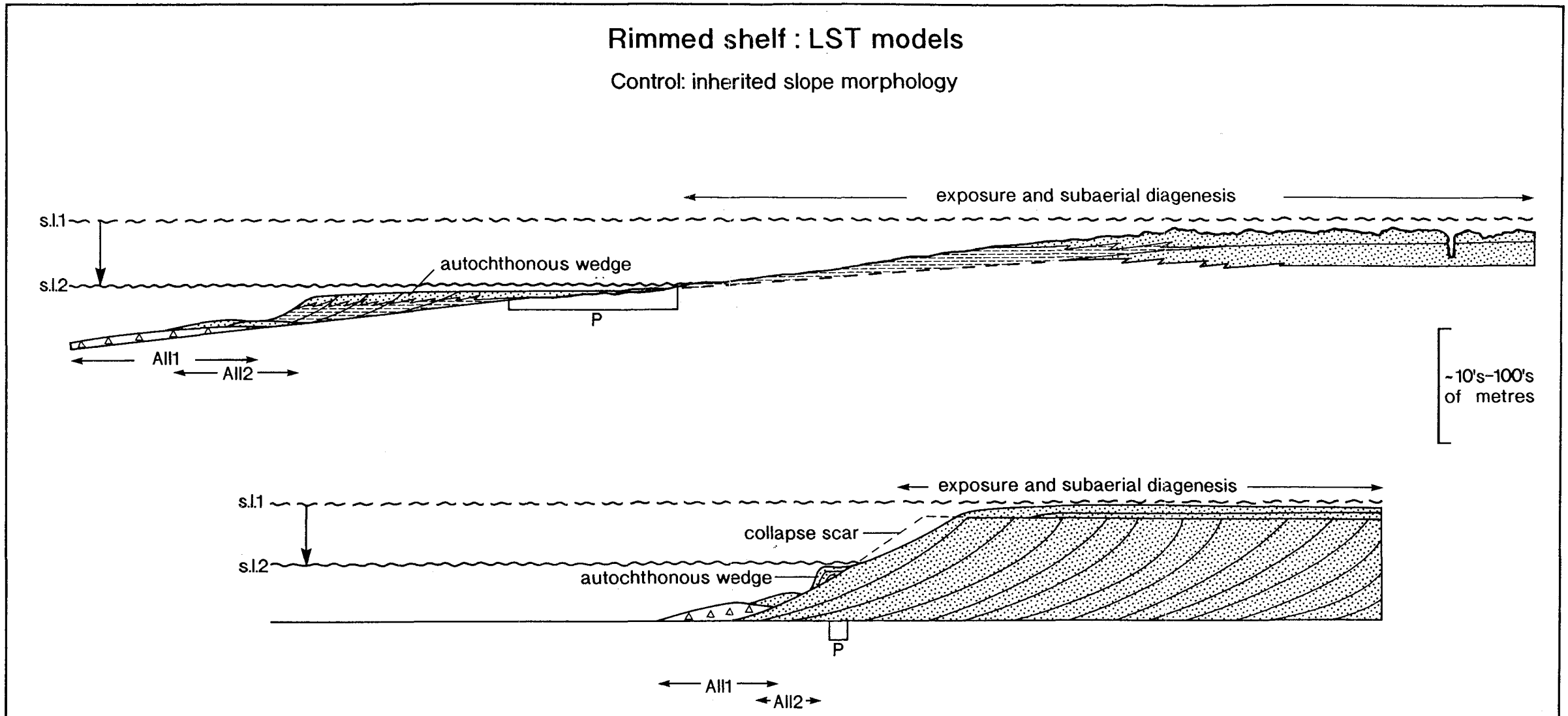

Figure 3.18. The two end-member models for lowstand of relative sea-level upon carbonate shelves. As relative sea-level falls the foreslope collapsed as storm wave base lowered and loaded the slope. Collapsed slope sediments are reworked to the basin floor as slumps/debris flows (AII1, allochthonous debris). Upon exposure the shelf undergoes chemical reworking that is climatically controlled. When sea-level reaches its lowest point the sequence boundary is formed and relative sea-level begins to rise slowly. It is at this time that the prograding autochthonous wedge is developed. The size of the autochthonous wedge reflects the area available for sediment production (P), and increases as slope angle decreases. Thus, the high angle slope is associated with a smaller autochthonous wedge than the low angle slope. Secondary basin-floor allochthonous debris is developed if the slope to the autochthonous wedge is itself bypassed. The two slope end-members, high and low angle foreslopes, develop contrasting styles of allochthonous debris and lowstand wedge. Low angle slopes are associated with mud dominated slumps, debrites and turbidites from slope collapse, whereas high angle slopes will tend to develop megabreccias formed of coherent blocks of foreslope limestones. High angle slopes also tend to develop narrow autochthonous wedges whereas low angle slopes tend to form wider, more volumetrically significant autochthonous wedges.

1988). Two types of allochthonous debris can be differentiated; the turbidite fans and/or aprons, which are analogous to the lowstand systems tract of siliciclastic systems, and, megabreccia or slump sheets, formed by catastrophic collapse of the preceding highstand. Either and/or both can form during times of falling or the lowstand of relative sea-level. In the rest of this thesis the term allochthonous debris is broadened to include sediments reworked from the preceding highstand and the autochthonous wedge(s) to the basin-floor.

Turbidite fan depositional systems are relatively rare in carbonate settings although they have been documented (eg. Wright & Wilson, 1984). Examples of incision and development of basin-floor fans interpreted to have formed during lowstands of sea-level are the Lower Barremian of the French Sub-Alpine Chains (Jacquin *et al.*, 1991), and the Triassic of Arabia (Watts, 1988). Both formed as sea-level fell below the slope-break upon distally-steepened ramps where canyons incised into the break of slope to supply the lowstand fans (type 1 sequence boundary). Similar development may be applicable to drowned carbonate shelves when the fall of relative sea-level is particularly large exposing the shelf-slope break.

More commonly, mechanical reworking of the preceding highstand on carbonate shelves takes the form of megabreccia sheets as the shelf margin undergoes catastrophic failure to form allochthonous debris. Megabreccias tend to be formed upon relatively steep slopes (>25°), and as such are more likely to have formed upon mud-free, grain supported slopes, or those subject to early cementation/framebuilding (Kenter, 1990). Collapse of the slope is probably triggered by increased storm wave pounding and/or pore pressure disequilibrium as sea-level falls (Hilbrecht, 1990) Examples of such lowstand deposits include the Permian megabreccia at Trow Point of sequence ZS2, NE England (Tucker, 1991), the Marmolada Breccia in the Triassic of N. Italy (Bosellini, 1984; Doglioni *et al.*, 1990), debrites in the late Cretaceous-Eocene platforms of southern Italy (Bosellini, 1989), and the late Sangamon age debrite (80-120 000 yr^{-1}) in Exuma sound described by Crevello & Schlager (1980). A possible example of a scar left at the shelf margin is seen in the classic face of

Windjana gorge, Australia where a paleokarstic surface developed on subhorizontal limestones passes basinwards into a subvertical erosion surface (Playford, 1980, his fig. 8).

Caution should, however, be used if attempting to use megabreccias as lowstand 'predictors' as they are not lowstand specific. Aggradation during the transgressive systems tract (eg. see Section 3.7.2. B) can lead to oversteepening and collapse of the shelf margin (eg. Mclreath, 1977; Saller *et al.*, 1989); faulting can also generate megabreccias to, especially in active rift basins (Colacicchi *et al.*, 1975; Eberli, 1987). On lower angle mud dominated slopes, allochthonous wedges will tend to take the form of large slump sheets and disorganised debrites (eg. Hilbrecht, 1990), but such redeposited units upon low angle slopes are likely to be less volumetrically important than the autochthonous lowstand wedge (eg. see Fig 3.18). On steep slopes the reverse situation is likely to be developed (Fig. 3.18).

The occurrence and volume of sediment deposited during a lowstand as an autochthonous wedge owes much to the morphology of the preceding highstand and to any subsequent modification of the slope during sea-level fall (eg. collapse, as discussed above). Lowering of sea-level below the shelf top drastically reduces the area available for the production of shallow water carbonates (eg. Mullins, 1983; Droxler & Schlager, 1985; Goldhammer & Harris, 1989) and is schematically illustrated in Figure 3.18. Depending upon the situation of the platform small or even large volumes of siliciclastic sediments may bypass the shelf at this time (eg. Saller *et al.*, 1989; Arnaud-Vanneau & Arnaud, 1990) (eg. Fig. 3.19).

A critical factor in determining the volume of the lowstand wedge is the angle and profile of the slope (Fig. 3.18). Two end-member situations can be envisaged for carbonate platform flanks: mud-dominated slopes which have low basinward dips and grain/clast supported slopes with high angle dips (Fig. 3.15 & 3.18). Steep grain-supported accretionary, or bypass/erosional slopes are more likely to produce allochthonous debris, with volumetrically small (eg. Doglioni *et al.*, 1990, Bosellini 1989) or even no autochthonous lowstand wedges. Contrastingly, mud-dominated

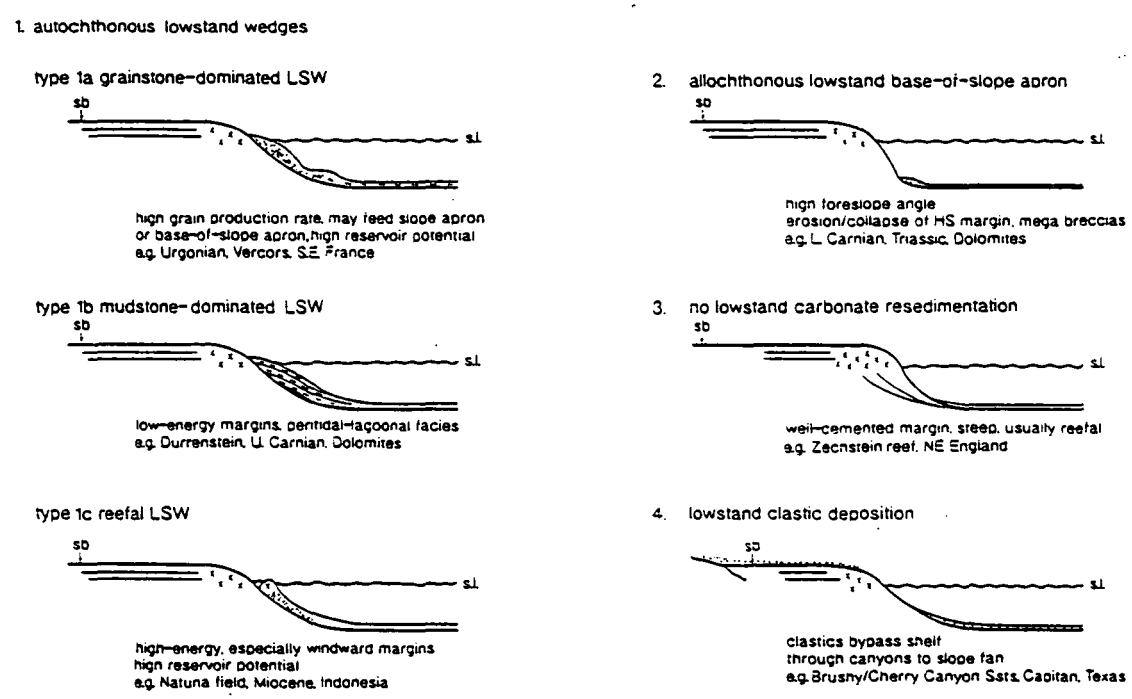

Figure 3.19. Examples of the different types of deposit associated with times of falling and lowstand of relative sea-level on carbonate shelves. From Tucker & Hunt (in prep).

accretionary/low angle bypass slopes will tend to be the sites of extensive autochthonous carbonate production leading to significant lowstand wedges without megabreccias (eg. Arnaud-Vanneau & Arnaud, 1990) (eg. Fig. 3.18 & 3.19). Secondary basin-floor sediments may be deposited in association with an autochthonous wedge if the wedge itself builds up steep angles so that it becomes a bypass system depositing a second basin-floor allochthonous fan/apron/sheet (All2-Fig. 3.18).

3.7.2. B. *The transgressive systems tract.*

The transgressive systems tract (*sensu* Vail, 1987 etc.) is defined at its base by the first backstepping parasequence (eg. Fig. 2.1), two or more of which form a retrogradational parasequence set as the rate of relative sea-level rise is greater than that of deposition/sediment supply (see Section 2.2.5. C). The current definition of the transgressive systems tract is thus based upon a single geometric stacking pattern (eg. Vail, 1987; Sarg, 1988). Such a narrow definition needs to be broadened for carbonate systems, as during the 'transgressive' phase of sequence development

several different stacking patterns can be developed (Fig. 3.20). Different geometries are developed because of the high and differential production potential across a carbonate shelf (eg. see Section 3.4.5). Hunt (1991) and Hunt & Tucker (1991, 1992) propose a new scheme relating changes in stratal geometry developed during relative sea-level rises to the ratio of the sedimentation rate : the rate of relative sea-level rise.

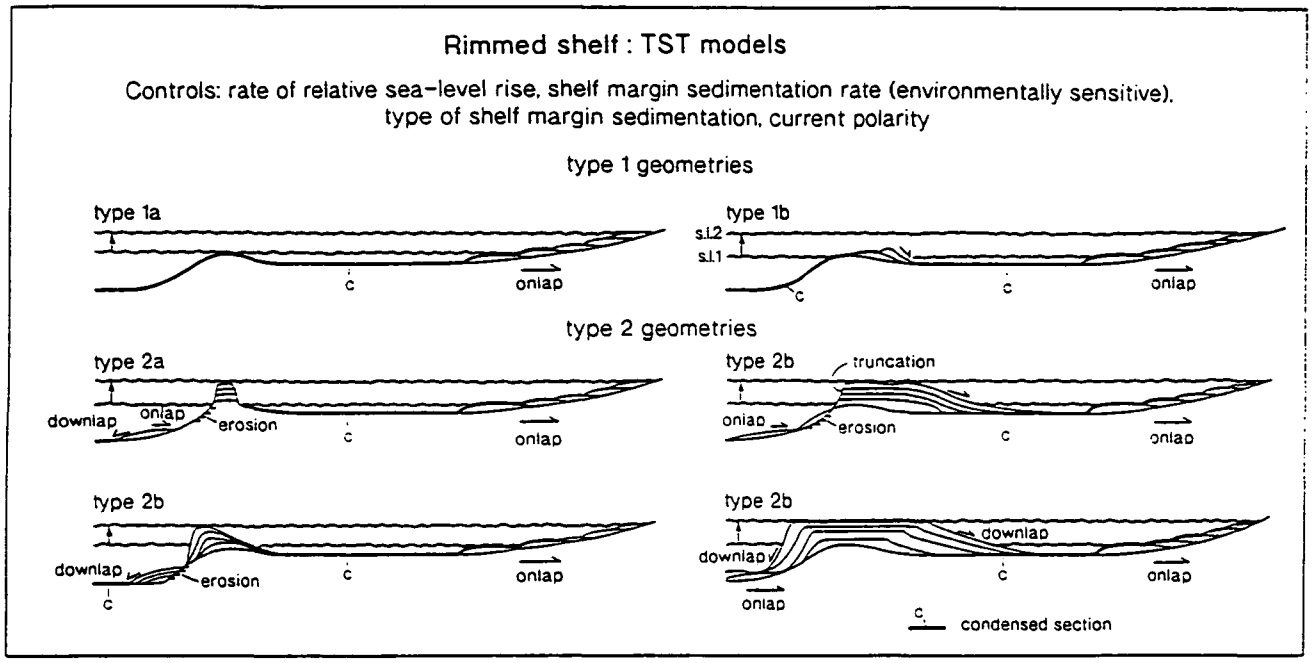

Figure 3.20. Theoretical geometries that can be developed upon carbonate shelves during the TST. The different geometries reflect the ratio of the sedimentation rate to that of relative sea-level rise. Individual geometries are depicted to have developed throughout the whole TST. Different geometries can become superimposed upon each other during an individual TST as the rate of sedimentation and/or the rate of relative sea-level varies. It should be noted that these models are depicted for when lowstand sedimentation has 'filled' to the preceding shelf-slope break or alternatively if there actually was no lowstand. Different geometries can be developed if this is not the case.

The most significant difference between carbonate and siliciclastic depositional systems highlighted during the transgressive systems tract is the high growth potential of shelf-rimming complexes (sand shoal and/or reef) and the often highly differential production potential across a shelf as discussed in Section 3.4.5.

During the TST different geometries develop as a response to relative sea level rises and/or variation of the sedimentation rate. Changes of the sedimentation rate are particularly sensitive to environmental changes as discussed in Section 3.4.6. These can cause changes of both facies and stacking patterns without need for relative sea-level rises *sensu* Vail (1987) or Sarg (1988).

The sensitivity of carbonate sedimentation to environmental changes demands caution if attempting to relate differences of the geometric stacking pattern to acceleration(s)/deceleration(s) of the rate of relative sea-level rise as identical patterns can develop from environmental degradation and/or improvement. Thus, changes of stacking pattern need not necessarily be related to changes of relative sea-level rise (Hunt, 1991; Hunt & Tucker, 1992; Hallock & Schlager, 1986; Schlager, 1981; Schlager, 1991). This applies equally at any point during development of a sequence.

As with the terminology for relative sea-level falls (type 1/type 2) an attempt has been made to relate the changes in the geometric stacking patterns to the rate of relative sea-level rise, although, as mentioned above both rates of sedimentation and relative sea-level rise can vary independently, both in time and space. As discussed in Section 2.2, different rates and/or magnitudes of relative sea-level fall are distinguished by the Exxon approach. Fast rates and/or high magnitude falls of sea-level develop type 1 sequence boundaries and slower and/or lower magnitude decreases type 2 boundaries (eg. Van Wagoner *et al.*, 1990). Such an approach and simple terminology has been transposed for the different geometries developed during the transgressive systems tract (Hunt, 1991; Hunt & Tucker, 1991, 1992).

When the rate of relative sea-level rise is greater than the sedimentation rate geometries developed are similar to those depicted for siliciclastic depositional systems (eg. Van Wagoner *et al.*, 1990) (eg. type 1 TST geometries; compare Figs 2.1 & 3.20), whereas when the sedimentation rate at the shelf-margin is either equal to or greater than that of relative sea-level rise geometries formed are very different (type 2 geometries Fig. 3.20) (Hunt, 1991; Hunt & Tucker, 1991, 1992). The different geometries can be developed at a variety of scales representing the whole

transgressive systems tract, a single parasequence or on regional seismic sections at the sequence set scale (see later examples).

3.7.2. B1. Type 1 geometries.

As discussed above type 1 geometries are developed when the rate of sedimentation at the shelf-margin and across the platform is less than that of relative sea-level rise. Two different stratal patterns are differentiated within this category, types 1a and 1b. A type 1a geometry is developed when the shelf-margin 'drowns' with little or no evidence of aggradation as relative sea-level began to rise. The lack of an aggradational element before drowning suggests that sedimentation was inhibited by rapid environmental deteoriation, and as such is most likely to be developed by reef-rimmed platforms (eg. see Section 3.4.6). Sand rimmed shelves, where sediment is relatively mobile, are more prone to backstep and aggrade before drowning, and this type of geometry is termed 1b (Fig. 3.20).

Both type 1 geometries can be associated with a landwards 'jump' of high-energy facies to the shoreline so that two zones of high-energy facies may be present at the same time, separated by a drowned shelf-lagoon. Depending upon the inherited topography and whether the sequence is 3^{rd} or 4^{th} order, the transgressive unit may form a single transgressive sheet sand complex above the underlying sequence boundary, or a series of retrogradational parasequences. The differences between type 1a and 1b geometries appear to reflect the mobility of the shelf rimming complex (eg. sand vs reef), the sensitivity of carbonate systems to environmental stresses and antecedent topography. The condensed section is best developed on the outer shelf and slope in a similar position to that depicted for siliciclastic shelves (eg. Compare Figs 2.1 & 3.20).

3.7.2. B2. Type 2 geometries.

Type 2 geometries develop when the rates of relative sea-level rise are either equal to, or less than those of sedimentation at the high energy shelf-rim but greater

than those of the shelf-lagoon. Type 2 geometries, where growth of the shelf-margin complex is maintained, suggest that environmental stresses are a secondary factor and the shelf-margin is essentially 'healthy' and responding to changes of relative sea-level. The termination of type 2 geometries is, however, often associated with a marked environmental deterioration (see later examples of 3.6.3. B3 & B4). It is during the development of type 2 geometries that the differential production potential across a carbonate shelf becomes most evident as the shelf-lagoon drowns and sedimentation is areally restricted to the highest energy areas (eg. shelf-margin and shoreline).

Due to the ability of the shelf-rim to keep-up with rising sea-level considerable shelf-margin topography can be built with respect to both the basin-floor and the drowned shelf, the latter forming an intra-platform basin (eg. Figs 3.20 & 3.21). Such buildups are economically extremely significant since they contain approximately 70% of the worlds known carbonate hydrocarbon reserves (Greenlee & Lehmann, 1990). Examples of productive fields in this type of buildup include the Devonian reef complexes of Alberta, Canada (eg. Stoakes, 1980) (Figs 3.20, 3.21 & 3.22), the Cretaceous Stuart City build-up of the Gulf of Mexico U.S.A. (Bay, 1977) (Fig. 3.22) and the Miocene of the South China Sea (eg. May & Eyles, 1985; Rudolph & Lehmann, 1989; Erilch *et al.*, 1990) (Fig. 3.22).

3.7.2. B3. Type 2a geometries.

A type 2a geometry is developed when the rate of aggradation at the shelf-

---

Figure 3.21. (next page) Reinterpreted cross-section of the Upper Devonian of Alberta, Canada. Adapted from Stoakes (1980). This platform developed a type 2a geometry during the TST, associated with development of a secondary zone of high energy facies. See text for further discussion (Sections 3.7.2.B & 3.7.3D).

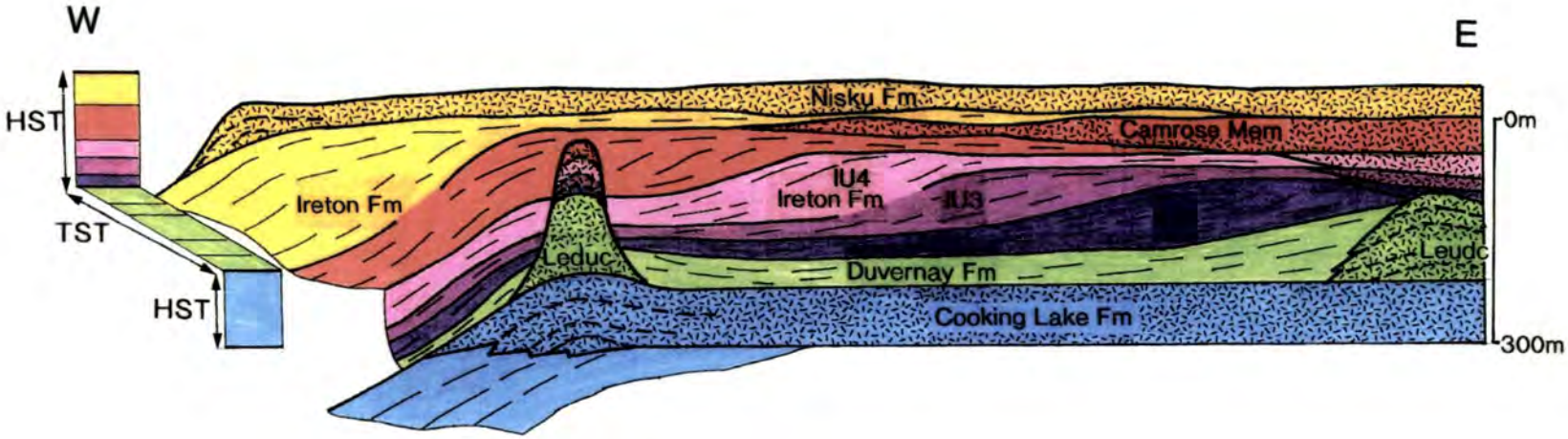

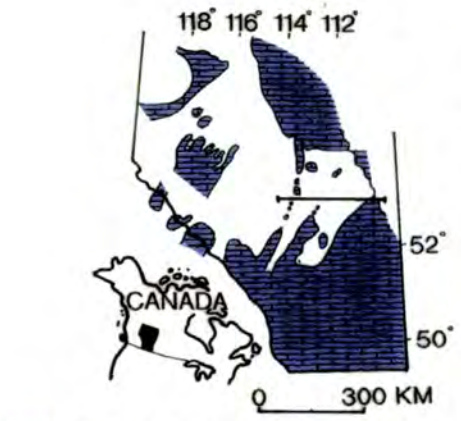

1. Cooking Lake Fm = HST aggrading.
2. Leduc & Duvernay Fm's = TST retrogradational parasequence set.
3. Ireton Fm Camrose Mem & Nisku Fm = HST progradational parasequence set.

* Note that geometries of basinal shales to Camrose Mem and Nisku Fm are identical to sequence boundaries (slope onlap), but are not associated with basinwards facies shifts. These are analogous to drowning unconformities.

margin is approximately equal to the rate of relative sea-level rise. This type of geometry appears to be most commonly developed by reef-rimmed shelves which have the ability to build steep slopes (eg. see Fig. 3.15). Significant build-up of the shelf-rim can lead to oversteepening, collapse and formation of debrite and/or turbidite complexes. These can be deposited both basinward and landward of the buildup and complex onlap/downlap patterns can be developed (eg. Fig. 3.20). The condensed section is not developed at the shelf-margin which is characterized by high sedimentation rates (eg. Fig. 3.20). On the slope development of the condensed section will reflect the complex patterns of sedimentation and erosion. Where slope erosion is frequent and/or where sediments are regularly bypassed (gullies and channels) the condensed section is likely to be poorly developed. Thus, the condensed section is likely to be best developed on the shelf top in the intra-platform basin which is sediment starved (eg. Fig. 3.20). This is the opposite relationship to type 1 geometries where development of the condensed section is similar in position to models proposed for siliciclastics (eg. compare Figs 2.1 & 3.20).

A classic example of this type of geometry is developed in the subsurface Devonian of Alberta, Canada (Stoakes, 1980) and illustrated in Figure 3.21. In this example, the onset of the transgressive systems tract is recorded by some buildup of the rimmed shelf of the Cooking Lake Formation. This Formation otherwise is considered to represent the highstand systems tract as sedimentation rates for the inner-shelf are not exceeded (see Fig. 3.21). The highstand is developed during a relative stillstand during a second order relative sea-level rise. No lowstand systems tract is developed. The development of the Leduc Formation marks an acceleration in the rate of relative sea-level rise as the shelf drowns. Contemporaneously, the shelf-margin (Leduc Formation) aggrades, keeping pace with relative sea-level and a secondary zone of shelf-margin type facies are established, having 'jumped' back on to the shelf. This reflects the substantial fetch of approximately 300Km across the intra-shelf basin (Fig. 3.21).

The westerly Leduc Formation at the 'shelf-margin' appears simply to aggrade during the relative sea-level rise and does not overproduce much sediment or any known collapse breccias. The basal part of the reef is onlapped by contemporaneous periplatform lime muds of the Duvernay Formation. The fact that these only very locally thicken around the westerly Leduc reefs (Fig. 3.21) suggests that the majority of lime muds deposited at this time were derived from the easterly, backstepped Leduc reef. Foreslope muds to the easterly Leduc complex downlap on to the drowned shelf-lagoon of the Cooking Lake Formation (Fig. 3.21).

Highstand sedimentation following the type 2 TST is represented by the Ireton Formation (IU2-4), Camrose Member and Nisku Formation (Fig. 3.21). Foreslope mudstones of the Ireton Formation onlap the isolated Leduc buildup forming a type of 'drowning unconformity'. Upward growth of the westerly Leduc reef continued through the early part of the highstand until 'contaminated' and terminated by foreslope mudstones of the Camrose Member and Nisku Formation (Fig. 3.21).

3.7.2. B4. Type 2b geometries.

These are developed when the sedimentation rates at the shelf-margin are greater than the rates of relative sea-level rise so that excess sediment is produced in this region and is either redistributed basinwards allowing progradation and/or is 'backshed' onto the shelf. The shelf-lagoon is drowned and a condensed section is developed in this area. As with type 2a geometries a consequence of continued aggradation of isolated high-energy facies at the shelf-margin is an increasing topography of the complex with respect to both the basin-floor and/or the shelf (eg. by 50m during the TST to sequence ZS2 of the English Zechstein, Tucker, 1991).

Stratal patterns developed when this type of geometry dominates the TST will reflect both the type of shelf-margin complex (eg. sand vs reef) and the hydrodynamics of this region. Three possible 'end member' geometries can be envisaged: aggradation with basinwards progradation, aggradation and shelfwards 'progradation' and, thirdly, aggradation with both basinwards and shelfwards

'progradation' of the shelf-margin facies (Fig. 3.20). Examples of these include the Devonian (Frasnian) Ramparts and Kee Scarp buildup, Alberta Canada (eg. Muir *et al.*, 1985, KIA-K3B, their fig 17), the Devonian Swan Hills buildup, Alberta, Canada (Viau, 1983) both of which are examples of aggradation associated with basinwards progradation; the Lower Miocene Liuhua platform, offshore China (Erlich *et al.*, 1991, see Fig. 3.22) and the TST to sequence ZS2 of the English Zechstein (Tucker, 1991, his fig. 6) both examples of shelf-margin aggradation associated with leeward 'backshedding' of sediment; and the Las Pilas Member, Devils River Formation, Lower Cretaceous Mexico (Bay, 1977), an example of shelf margin aggradation associated with both backshedding and basinwards progradation (Fig. 3.22).

Reef and sand dominated shelf-margin complexes will tend to develop different stacking patterns that both reflect the mobility of sands compared to reefs and the preferred windward orientation of reefs. Reef dominated margins can be crudely divided into those which produce large excesses of sands such as the Lower Miocene of China (eg. Erlich *et al.*, 1990) and TST to sequence ZS2 of the English Zechstein (Tucker, 1991) and those which only produces small amounts of sand. The Kee Scarps and Ramparts reefs (Muir *et al.*, 1985) is a good example of a reef which

Figure 3.22. (facing page) Examples of Type 2 TST geometries from the subsurface. (A) The Devonian Swan Hills buildup of Alberta Canada from Wright & Tucker (1990), after Viau (1983). This reef developed a type 2b geometry during a relative sea-level rise (the TST). The preferential basinward progradation of the reef reflects environmental differences across the shelf-margin. (B) The Lower Cretaceous Devils River and Las Pilas Members of Texas and New Mexico from Tucker & Wright (1990), after Bay, (1977). A type 2b geometry is developed by the Las Pilas member. This developed as the rate of relative sea rise increased and shelf-lagoon facies (Salmon Peak) drowned. Contrastingly, the shelf-margin rudist facies were able to keep pace with and exceeded rates of relative sea-level rise. Thus the platform margin shed excess sediments both basinwards and back onto the drowned shelf. As the fetch of the platform was sufficient a secondary zone of outer shelf type facies developed within/on the flanks of the intra-platform basin. (C) The Lower Miocene from offshore China. On this isolated platform relative sea-level rise led to vertical aggradation of the windward reef dominated margin. This windward margin shed large amounts of sand in a leeward direction and these downlap onto on-shelf type facies (Adapted from Erlich *et al.* (1990).

A

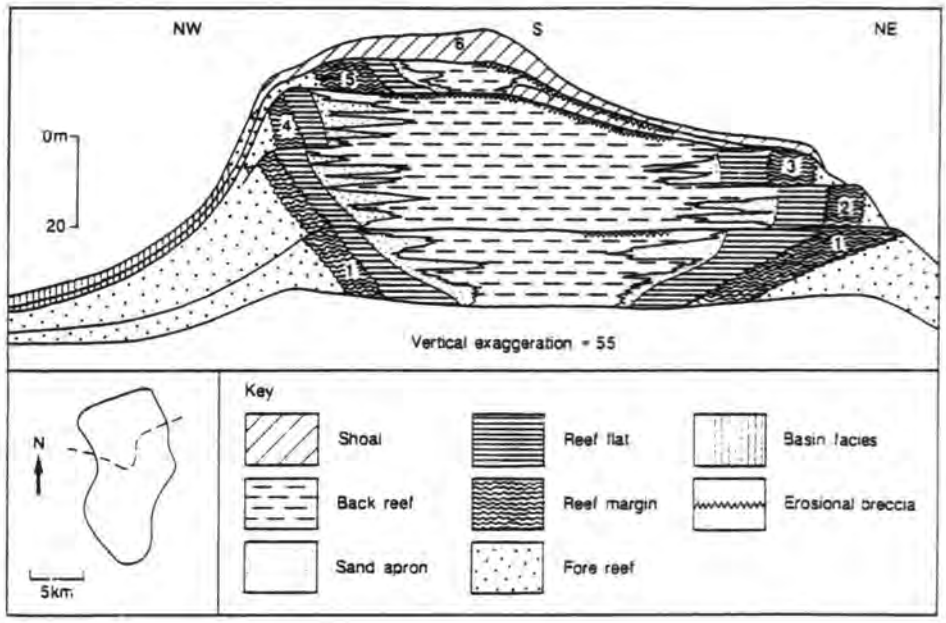
NW
S
NE
0m
20
6
5
4
3
2
1
Vertical exaggeration = 55
N
5km
Key
Shoal
Reef flat
Basin facies
Back reef
Reef margin
Erosional breccia
Sand apron
Fore reef

B

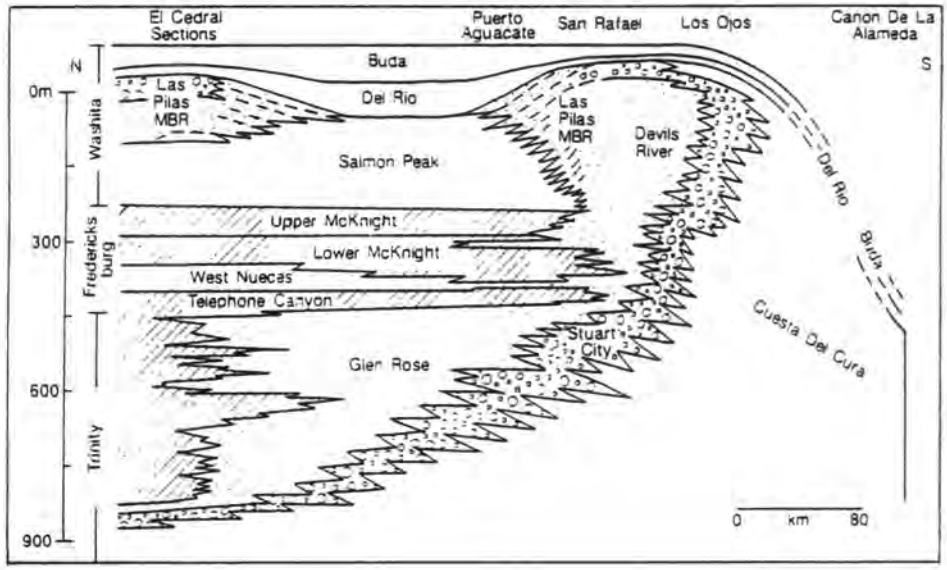
El Cedral Sections
Puerto Aguacate
San Rafael
Los Ojos
Canon De La Alameda
N
S
0m
300
600
900
Washita
Fredericksburg
Trinity
Buda
Del Rio
Las Pilas MBR
Salmon Peak
Upper McKnight
Lower McKnight
West Nueces
Telephone Canyon
Glen Rose
Devils River
Stuart City
Cuesta Del Cura
0 km 80

C

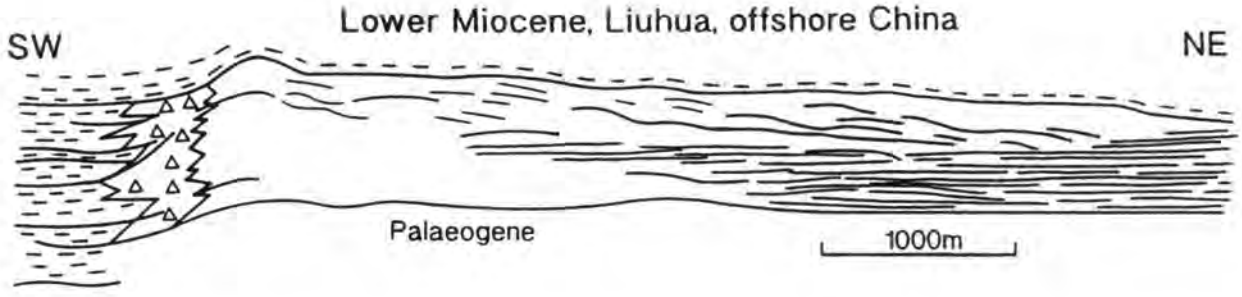
Lower Miocene, Liuhua, offshore China
SW
NE
Palaeogene
1000m

produced only a small excess of sands. Stratal patterns are dominated by the preferential outward growth of the reef complex (Muir *et al.*, 1985, their fig. 17). The Swan Hills reef of Alberta provides a second excellent example of this geometry (Viau, 1983, Fig. 3.22). This type of geometry reflects the environmental differences developed across the shelf margin, with faster rates of accretion in a basinwards direction (Fig. 3.22). Where the redistribution of overproduced sediments (particularly sands) is bi-polar and of approximately equal magnitude both on-shelf and off-shelf offlap and downlap are equally developed (eg. Lower Cretaceous Las Pilas Member, northern Cohuila, Mexico Bay, 1977, Fig. 3.22).

3.7.2. B5. Other common stratal patterns.

When either type 1 or 2 geometries typify the TST a 'jump' of high energy facies to the shoreline or an intermediate position can take place at any time as relative sea-level rises. The occurrence (timing and position) of such a jump will reflect both the inherited topography and hydrodynamics of the shelf. Establishment at an intermediate point on the shelf will generally be topographically controlled as is the case for many Holocene reefs (Purdy, 1974). Such a 'jump' of facies to an intermediate position on the platform is developed during the Frasnian (Upper Devonian) in the Canning Basin, western Australia (Playford, 1980, his fig 14).

The condensed section is typically a key surface upon carbonate platforms. Frequently, it is represented by a strong reflection in seismic sections (eg. Erlich *et al.*, 1990), and is also readily identified in wireline logs (Van Wagoner *et al.*, 1990). Where type 1 geometries characterize the whole of TST development the condensed section closely resembles patterns proposed for siliciclastic systems (eg. compare Fig. 2.1 & 3.20). The development of condensed sections where type 2 geometries dominate the whole transgressive systems tract are more complex and, conversely, the condensed section will tend to be best developed within the intra-platform basin on the drowned shelf (eg. Figs 3.20, 3.21 & 3.22).

The 'drowning unconformity' is a feature common to many carbonate platforms and, as its name suggests is normally developed during and/or after relative sea-level rises. It can also be developed when platforms are covered by siliciclastics (Schlager & Camber, 1986; Schlager 1989, 1991). In purely carbonate depositional systems these unconformities generally develop when sediments with mud supported fabrics overlie sediments with grain supported fabrics which have a higher internal shear strength and correspondingly greater dips (eg. Kenter, 1990, Fig. 3.15). Such unconformities are common to both type 1 and type 2 geometries.

3.7.2. B6. Superimposition of different geometries.

During the formation of an individual transgressive systems tract both the rates of sedimentation and relative sea-level rise can change with time. Thus, a single geometry as described in the preceding section need not represent the whole systems tract. The Upper Devonian reefs from Alberta and Northwest Territories, Canada (Muir *et al.*, 1985, their fig. 17; Viau, 1983, Fig. 3.22) demonstrate variability of geometry on the parasequence scale. The reef develops different geometries as the ratio of the rates of sedimentation : relative sea-level rise varied. In addition, for an individual platform the response of a platform margin can vary along strike due to different sedimentation rates, oceanographic setting, environmental factors etc.

3.7.2. B7. Discussion of the transgressive systems tract.

The two most significant questions which this approach raises concern the nature and role of the different controlling variables upon the geometries and stratal patterns developed during the transgressive systems tract:

1) Is it possible to distinguish what are the major factors 'forcing' different geometries to develop ? and,

2) How can geometries developed in response to environmental change be separated from those resulting from a rapid relative sea-level rise?

Clearly, there is at present no unequivocal answer but it would appear that for type 2 geometries when the shelf-margin complex can keep pace or even outstrip the rates of relative sea-level rise, 'environmental changes' are secondary factors in the shelf margin response to relative sea-level changes. Secondly, following this line of argument the development of type 1 geometries suggests that environmental stresses played an important role contributing to shelf drowning as often argued by Schlager (1981, 1991) and/or glacio-eustatic rates of sea-level rise outstripped sedimentation rates. Where environmental changes have played an important role in the development of stratal patterns during the TST faunal changes and deposition of phosphates may occur.

3.7.2. C. *The Highstand systems tract.*

The Highstand systems tract is, classically, developed above the maximum flooding surface. It is the last systems tract formed as relative sea-level rises (see Section 2.3). Highstand sedimentation 'begins' when sedimentation rates exceed those of relative sea-level rise for both shelf-margin and shelf-lagoon facies. The topography inherited by this systems tract can reflect both that developed during the lowstand (eg. Purdy, 1974), and/or any developed during the TST (eg. where type 2 geometries dominate the TST). The systems tract marks the return to the normal 'bankfull' stage of the platform, although after particularly large rises of relative sea-level it may take some time for normal shelf-lagoon sedimentation to resume across the shelf top (eg. Camrose member to Nisku Formations, Fig. 3.21)

The highstand tends to be the time in a sequence of maximum sediment production as the area of shallow water suitable for carbonate sediment production tends to be the greatest. Correspondingly, platforms tend to expand most rapidly during the highstand by clinoform progradation at the shelf-margin which can be spectacular (eg. see Bosellini, 1984; Doglioni *et al.*, 1990). Two different styles of progradation can be distinguished as portrayed in Figure 3.23, and these are: *slope aprons* and *toe-of-slope aprons*. The latter type is particularly well developed in the

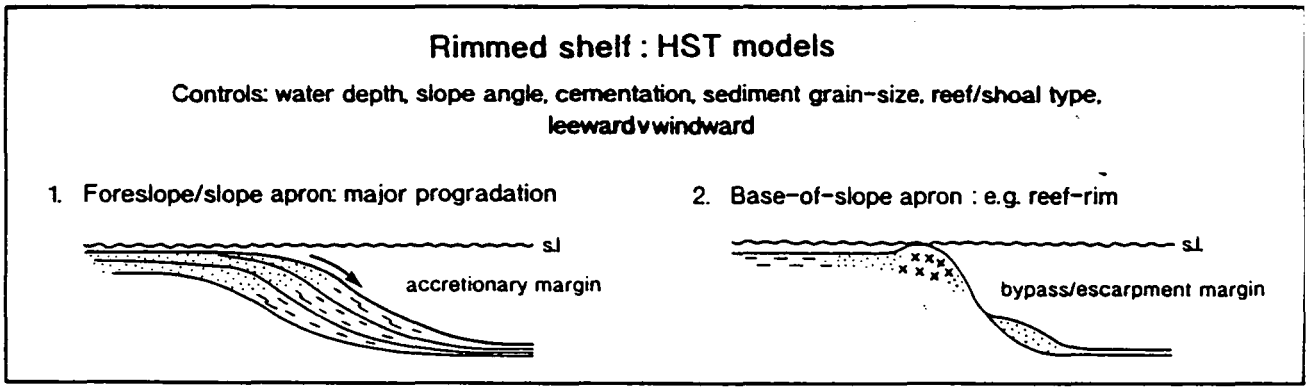

Figure 3.23. The two different patterns of highstand slope progradation. The slope apron is characterized by the trapping of shallow-water grains on the upper and mid-slope (1). Sedimentation rates decrease progressively down the slope with periplatform muds deposited at the toe-of-slope. (2) Toe-of-slope patterns are characterized by the deposition of shallow bank-derived sediments at the toe of slope, having bypassed the upper and mid slope. The basin-floor is the depositional locus and aggrades to onlap the toe of clinoforms. These two patterns are characterized by horizontal/descending and ascending clinoform packages respectively (from Hunt & Tucker, 1992).

modern Bahamas where in many areas (eg. The Tongue of the Ocean) banktop derived sediments bypass the slope to form the major component of basin-floor sedimentation (eg. Schlager & Chermak, 1979; Droxler & Schlager, 1985). Observations on the basin-floors of the Bahamas lead to the concepts of 'highstand shedding' (eg. Mullins, 1983; Droxler & Schlager, 1985, Boardman *et al.,* 1986; Wilber *et al.,* 1990) where basin-floor redeposition is 180° out of phase to that predicted for siliciclastic depositional systems. This pattern of 'highstand shedding' appears to be a function of both the foreslope morphology and high rates of banktop production and has become the subject of intense controversy (eg. Mullins, 1983; Schlager, 1991; Jacquin *et al.*, 1991). The toe-of-slope apron progradational pattern characteristic of highstand shedding in the Bahamas (eg. Droxler & Schlager, 1985) (eg. Fig 3.12 & 3.23) results in an ascending geometry developed by clinoform packages (eg. similar to Fig. 3.24B). Geometrically, this pattern of clinoform progradation is similar to that described from the Carnian Sella platform, Italy where basinal sedimentation rates are high (Bosellini, 1984, Fig. 3.24B).

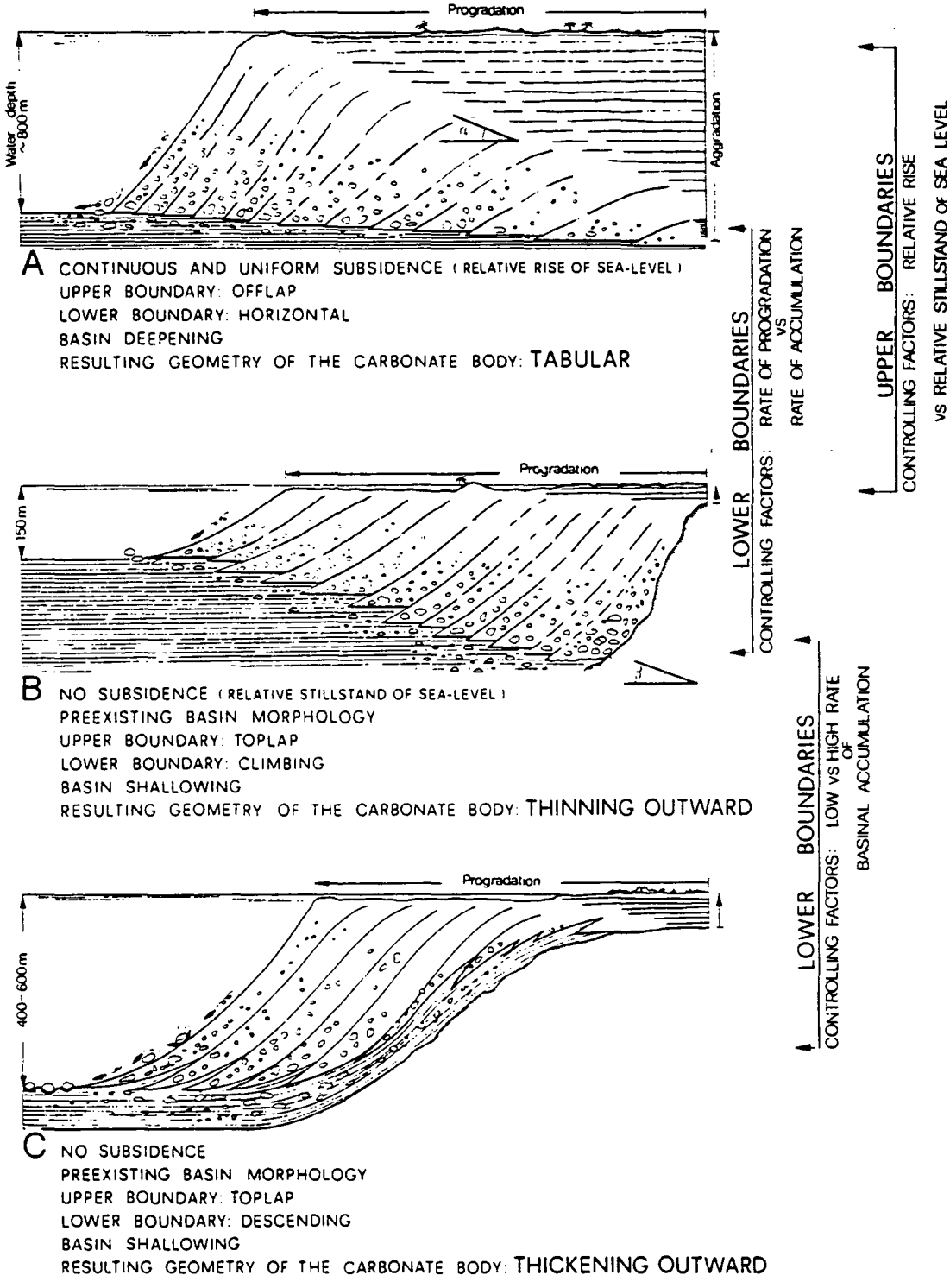

Figure 3.24. The different basal relationships developed at the toe-of-slope of prograding clinoform packages (from Bosellini, 1984). The different relationships reflect the budget of basin-floor sedimentation and the inherited basin-floor morphology.

The second distinctive pattern of highstand progradation is the slope apron, where shallow bank-top derived sediment is mainly deposited on the upper-mid foreslope. Toe-of-slope sedimentation is dominated by periplatform muds (Fig. 3.23), and the overall pattern is to develop subhorizontal to descending lower boundaries to clinoform packages (Fig. 3.24). The upper surface of the highstand systems tract is the basal surface of forced regression that represents the turn-around point of relative sea-level from times of rising sea-level to times of falling relative sea-level.

3.8. Conceptual Development Of A Type 1 Sequence Upon A Carbonate Sand-Shoal Rimmed Shelf.

3.8.1. Introduction.

In this Section the conceptual development of a carbonate sequence is presented. It is the aim here to illustrate how the models developed in Section 3.7 can fit together in the development of a type one sequence. The conceptual model uses the systematics for times of falling and lowstand of relative sea-level introduced in Section 2.3.2.A and illustrated in Figure 2.6B (p. 26).

3.8.2. Assumptions.

1. The 'starting point' or 'template' for the sequence is an accretionary carbonate rimmed shelf in an open ocean setting. The climate is humid.

2. The sequence is developed during a 3^{rd} order cycle of relative sea-level change. The varying roles of eustasy and subsidence are not differentiated. The relative sea-level curve is sinusoidal in form (see accompanying figures). The general sinusoidal third order sea-level curve has higher order cycles (4^{th}-5^{th} order) superimposed upon

it. These alternately accelerate and decelerate the 3rd order signature to develop parasequences.

3. There is no differential subsidence across the platform during development of the sequence.

4. Relative sea-level changes are the fundamental control upon changes of both the rate and position of space made available for the accommodation of sediments. Environmental changes can cause dramatic changes in sedimentation rates as discussed in Section 3.4.6, but are here assumed 'constant' for the development of this conceptual sequence.

3.8.3. Summary.

Upon an accretionary rimmed shelf third order relative sea-level falls. This fall has higher order cycles (4^{th} order) superimposed upon it. These decelerate the fall allowing the development of autochthonous slope wedges during the *Forced regressive wedge systems tract.* These slope wedges are chronostratigraphically equivalent to basin-floor allochthonous debris derived from collapse of the slope (eg. see Fig. 2.7B). The sequence boundary is developed at the lowest point of relative sea-level and is the most widespread unconformity associated with the deepest and most basinwards shift of meteoric diagenesis.

From the lowest point of relative sea-level (the time of sequence boundary formation) relative sea-level begins to rise. As relative sea-level begins to rise at a rate initially less than the sedimentation rate, the lowstand prograding wedge (LPW) is developed as an autochthonous slope wedge. This systems tract 'underfills' the slope as the rate of relative sea-level rise increases so that all but the highest energy area of the autochthonous wedge drowns. The selective drowning of the autochthonous wedge discriminates between the LPW and transgressive systems tracts (TST).

The TST is characterized by a balance between sedimentation rates of high-energy facies and rates of relative sea-level rise. Thus, a type 2 geometry is developed at the slope break of the lowstand prograding wedge (see Section 3.7.2.B). As relief grows between the buildup of high-energy facies and the basin-floor sediments are increasingly bypassed through and eroded from the foreslope and deposited as a toe-slope-apron upon the basin-floor. Also during the TST the shelf is transgressed and sedimentation starts-up across the shelf. As sea-level continues to rise only higher-energy facies situated upon karstic topographic highs on the shelf are able to keep pace with the relative sea-level rise. Elsewhere, the shelf is drowned and outer slope type facies are deposited and/or a hardground is developed on the shelf and a condensed section on the basin-floor and slope.

The highstand systems tract is developed when the rate of relative sea-level rise slows to allow the aggradation and progradation of the shelf-lagoon. This slowing rate of sea-level rise means that the high-energy facies produce much excess sediment which bypasses the slope to the basin-floor. Eventually, aggradation of the basin-floor reduces the shelf to basin-floor topography so that foreslope declivity is reduced and the platform once more progrades.

3.8.4. Sequential development.

The following discussion is accompanied by nine conceptual diagrams of Figure 3.25.

3.8.4. *A. Highstand systems tract.*

The highstand systems tract is bound below by the maximum flooding surface (mfs) and above by the basal surface of forced regression (BSFR) (Section 2.3.2). The highstand shelf template is illustrated in Figure 3.25.1 and is characterized by an accretionary foreslope (as discussed in Section 3.7.2.C, Fig. 3.23) which passes upwards to a sand shoal rimmed margin. This has an elevated topography which affords protection to the deeper water shelf-lagoon (>10m water depths), itself bound

1. Highstand systems tract.

Rimmed shelf with accretionary slope apron pattern of progradation.

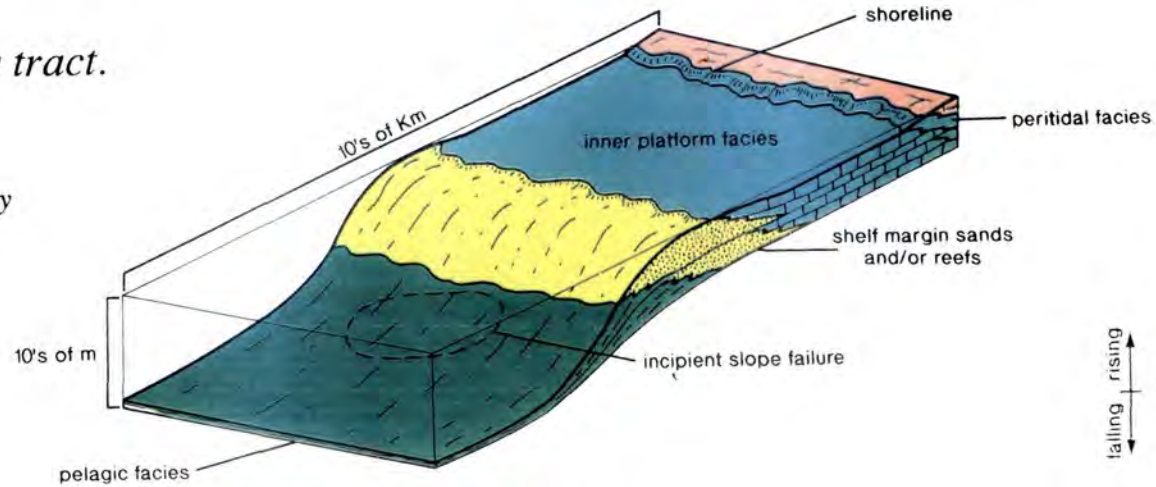

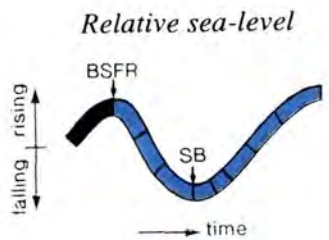

2a. Forced regressive wedge systems tract.

Shelf is exposed and shutdown and the area available for shallow water sedimentation is greatly reduced. Failure as sea-level falls transports slope sediments onto the basin-floor. Locally, the slope is bypassed where it steepens into slump scar(s).

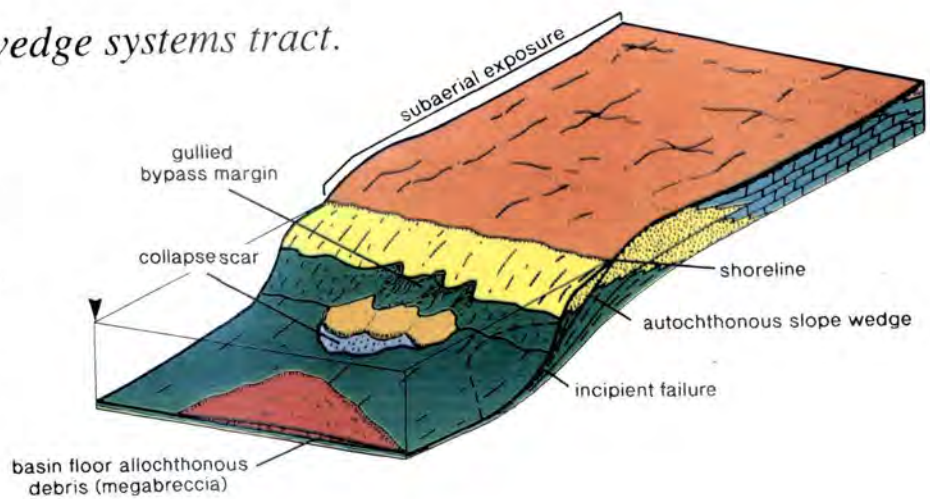

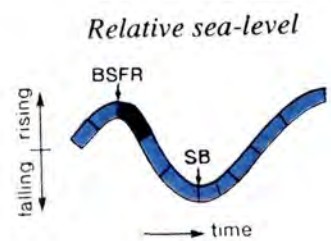

landwards by the supratidal environment. The highstand systems tract is developed when the rate of relative sea-level rise is less than sedimentation rates across the shelf.

3.8.4. *B1. Forced regressive wedge systems tract.*

The forced regressive wedge systems tract (FRWST) is developed during times of falling relative sea-level and is bounded below by the BSFR and above by the sequence boundary as discussed in Section 2.3, Fig. 2.6 (p. 26). During the third order relative sea-level fall three higher order (4^{th} order) cycles (parasequences) are superimposed on the fall. These alternately accelerate and decelerate the fall. During times of relative stillstand (or even rise) during the overall third order fall autochthonous slope wedges are developed (eg. Fig. 2.6B). These are chronostratigraphically equivalent to basin-floor allochthonous debris.

3.8.4. *B2. Dynamics of the shelf during forced regression.*

During the preceding highstand the shelf was aggraded close (<10m) to relative sea-level, so that the initial sea-level fall of the FRW systems tract exposes both the shelf-margin and inner-shelf (Fig. 3.25.2a). Thus, this is a type 1 sequence as sea-level has fallen below the shelf-slope break. Two distinct types of deposit can be distinguished during the forced regression and these are: *autochthonous wedges* or *stranded parasequences*, shallow water high-energy sediments developed on the narrow strip of the slope and *allochthonous debris*, calciclastic sediments derived from collapse of the slope to the preceding highstand and/or from sands which bypassed the foreslope of the autochthonous slope wedges to the basin-floor (eg. Fig. 3.25.2a-c).

Figure 3.25. (preceding page) Diagrams 1, 2a, of this Figure illustrating the highstand prograding accretionary shelf template and the first unit of the forced regressive wedge systems tract. See text for further discussion.

2b. Forced regressive wedge systems tract.

As relative sea-level continues to fall the preceding slope wedge is exposed. Antecedant topography exerts a strong control upon patterns of sedimentation.

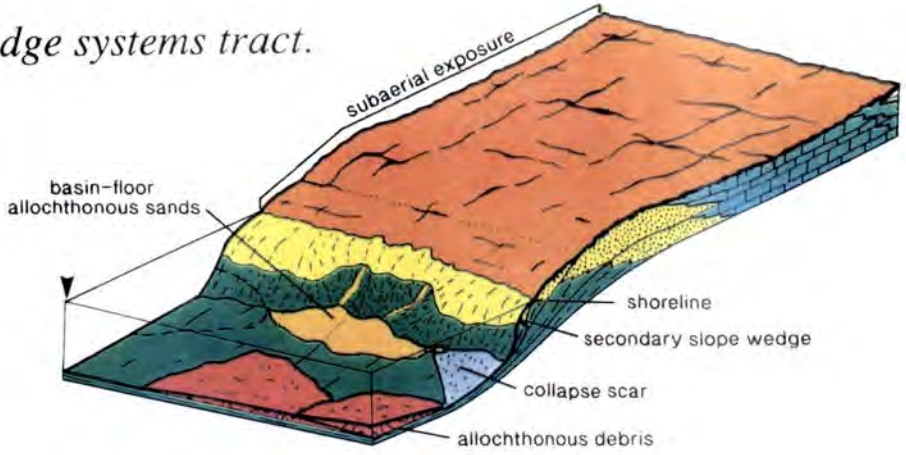

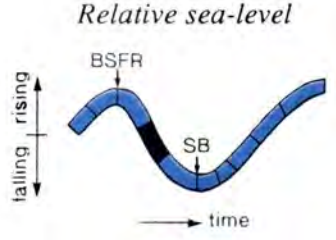

2c. Forced regressive wedge systems tract and sequence boundary formation.

At the end of the third slope wedge sea-level is at its lowest point and the greatest area of the platform is exposed. The sequence boundary thus passes above slope and basin-floor sediments formed during forced regression. Sedimentation patterns reflect inherited topography.

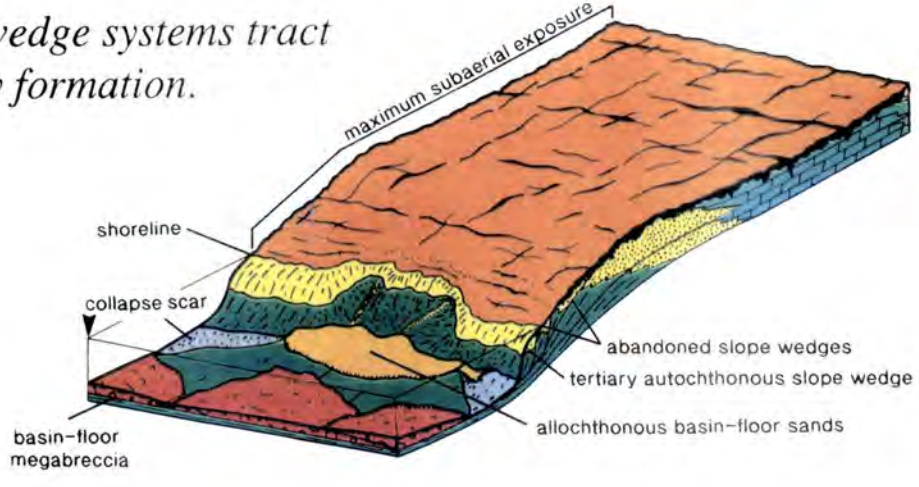

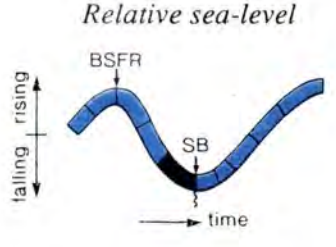

Upon exposure, the shelf undergoes rapid cementation and lithification stabilising the shelf so little (if any) sediment is moved off-shelf to the slope whilst it is exposed. For the rest of the systems tract (and the LPW and early part of the TST) the shelf is subaerially exposed and subject to meteoric diagenesis. Penetration of karstification is greatest when the hydraulic potential is highest. This is the time at which relative sea-level is at its lowest i.e. at the sequence boundary. As sea-level rises the hydraulic head is reduced, lower levels of the karst are abandoned and upper levels reworked (LPW-TST) (Esteban, 1991).

As sea-level falls, storm wave base is lowered down the foreslope and this is interpreted to trigger its collapse (Section 3.7.2.A). Slope sediments are reworked as debris flows and turbidity currents and redeposited on the basin-floor as discrete lobes of allochthonous debris (3.25.2a-c). Chronostratigraphically, slope collapse is essentially instantaneous (eg. Fig. 2.6). This pattern is repeated for each of the three falls of relative sea-level depicted for the forced regressive wedge systems tract so that three discrete slump/debrite units are deposited on the basin-floor at the time of sequence boundary formation (Fig. 3.25.2c). Generally, basin-floor sedimentation rates are drastically reduced and condensed sections are developed across much of the basin-floor as the periplatform ooze is terminated and pelagic oozes deposited.

Shallow-water carbonate sedimentation is areally restricted to a narrow strip on the foreslope (i.e. in autochthonous slope wedge or stranded parasequences). Three autochthonous slope wedges are developed during the 4^{th} order stillstands within the general 3^{rd} order sea-level fall (Fig. 3.25.2a-c). Each slope wedge onlaps the slope of either the preceding highstand or an earlier autochthonous slope wedge (coastal onlap) and downlaps on to the slope and/or basin-floor (Figs 2.6B & 3.25.2a-c).

Figure 3.25. (preceding page) Diagrams 2b and 2c of this Figure illustrating the forced regressive wedge through to the lowest point of relative sea-level fall, the time of sequence boundary formation See text for further discussion.

During forced regression, locally small quantities of sand derived from the autochthonous slope wedges are bypassed to the basin-floor (Fig. 3.25.2a-c). Bypass is restricted to areas where the slope is steepened, such as in the vicinity of collapse scars formed as storm wavebase was lowered (Section 3.7.2.A). Steepened areas of the foreslope are inherited by each succeeding autochthonous wedge and, progressively, shallow water sedimentation is restricted to a narrower area (coloured yellow on Figure. 3.25.2a-c). This results in a progressively decreasing sediment budget for each slope wedge.

The sequence boundary is developed at the lowest point of relative sea-level and is associated with the most basinward shift of subaerial exposure and coastal onlap (Fig. 3.25.2c). The sequence boundary passes above the autochthonous slope wedges (the first two of which are now exposed and subject to meteoric diagenesis, Fig. 3.25.2c) and above allochthonous basin-floor debris developed during the forced regression. On the basin-floor the sequence boundary is a downlap surface to the succeeding lowstand prograding wedge systems tract (LPWST). On the slope it is onlapped (coastally) by the LPW systems tract. On the shelf subaerial exposure continues throughout the LPW and into the early part of the TST so that here the sequence boundary is diagenetically modified from the time of its formation (eg. Fig. 3.25.3-4).

In summary, the forced regressive wedge systems tract is associated with a drastic reduction of overall sedimentation rates and with the development of slope wedges that locally onlap and downlap on the slope. Collapse of the slope redeposits slope facies as disorganised slumps and debrites on the basin-floor ('lowstand' megabreccis). Collapse scars locally steepen the foreslope allowing the bypass of sands to the basin-floor.

Figure 3.25. (next page) Diagrams 3a and 3b/4 of this Figure illustrating the onset of the LPW systems tract characterized by slowly rising relative sea-level passing into the TST when rates of relative sea-level rise were higher.

3a. Lowstand prograding wedge systems tract.

As relative sea-level begins to rise the area available for sedimentation increases.

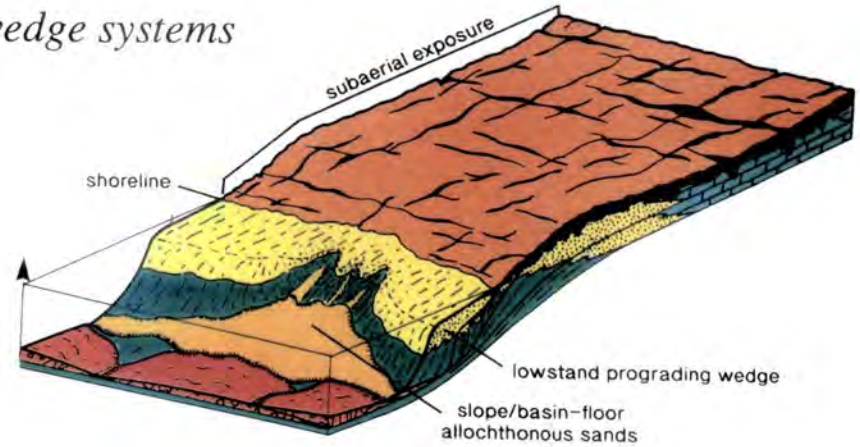

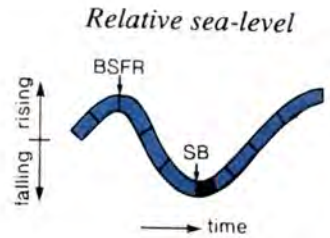

3b/4. Lowstand prograding wedge systems tract and beginning of transgressive systems tract.

As the rate of relative sea-level rise accelerates only the region with the highest sedimentation rates keeps pace. By-pass becomes common along the slope due to increased topography, and clinoform packages have an ascending geometry on the basin-floor from this point on.

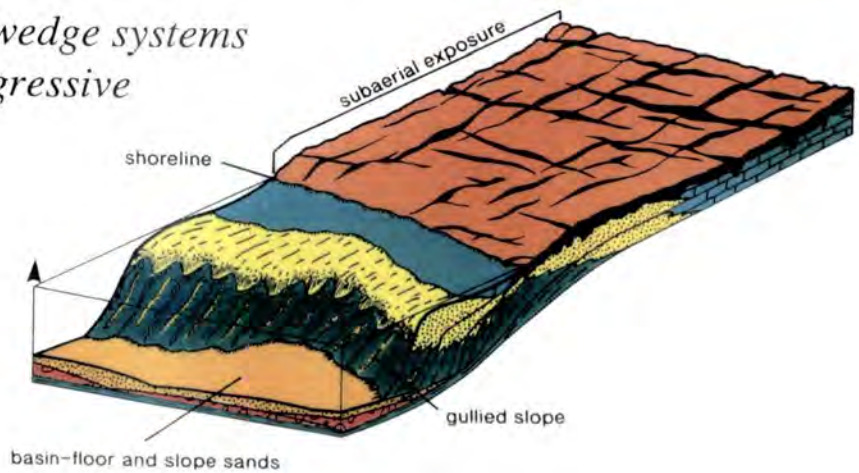

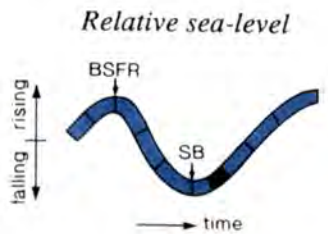

3.8.3. *C. The lowstand prograding wedge systems tract.*

The lowstand prograding wedge (LPW) systems tract is developed after sequence boundary formation, as relative sea-level slowly begins to rise (Figs 2.6B & 3.25.3a). The area available for shallow water sedimentation increases as coastal onlap shifts landwards and up the slope (Fig. 3.25.3a), so that the overall sedimentation rate of the autochthonous wedge increases. Thus, rates of sedimentation are initially able to outpace rates of relative sea-level rises and facies prograde basinwards (3.25.3a).

The morphology of the LPW systems tract is largely inherited from the preceding systems tract. The foreslope continues to locally bypass sands formed on the autochthonous wedge to the basin-floor. Larger amounts of sand are deposited on the basin-floor and at the toe-of-slope as the shallow-water area of the LPW increases and, correspondingly, so does the sediment budget (Fig. 3.25.3a). It should be stated here that the lowstand prograding wedge systems tract is not present in all carbonate systems, it is in fact rare as sedimentation rates are generally low during these times due to the decreased potential area for carbonate production (see Section 3.7.2A).

3.8.3. *D. The transgressive systems tract.*

The transgressive systems tract (TST) is depicted in Figure 3.25.4, 4a & 4b. The TST is developed as the rate of relative sea-level rise accelerates and only the highest energy facies are able to keep pace. In the case illustrated the TST commences prior to the 'filling' of the LPW systems tract to the shelf-slope break of

---

Figure. 3.25. (next page) Diagrams 4a and 4b illustrate the latter stages of the TST characterized by the transgression and subsequent drowning of much of the shelf. See text for further discussion.

4a. Transgressive systems tract.

The shelf is transgressed and locally sedimentation resumes. Oversteepening of the slope causes collapse that can extend upto the shelf margin.

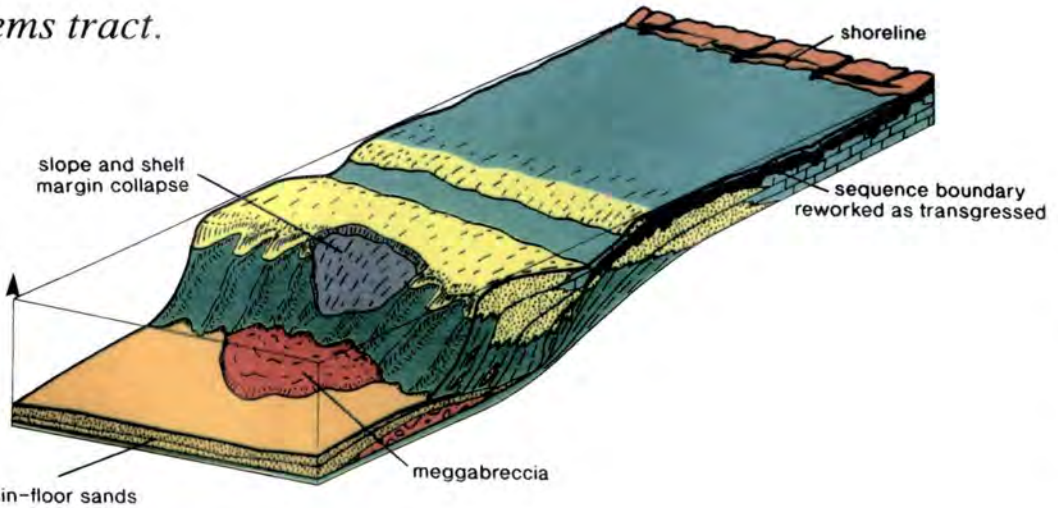

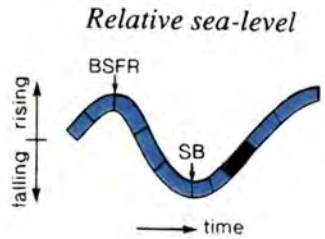

4b. Transgressive systems tract.

Most of the shelf drowns as sedimentation is outpaced by relative sea-level rise, and a condensed section develops across the shelf. Shelf margin is scalloped due to frequent collapse.

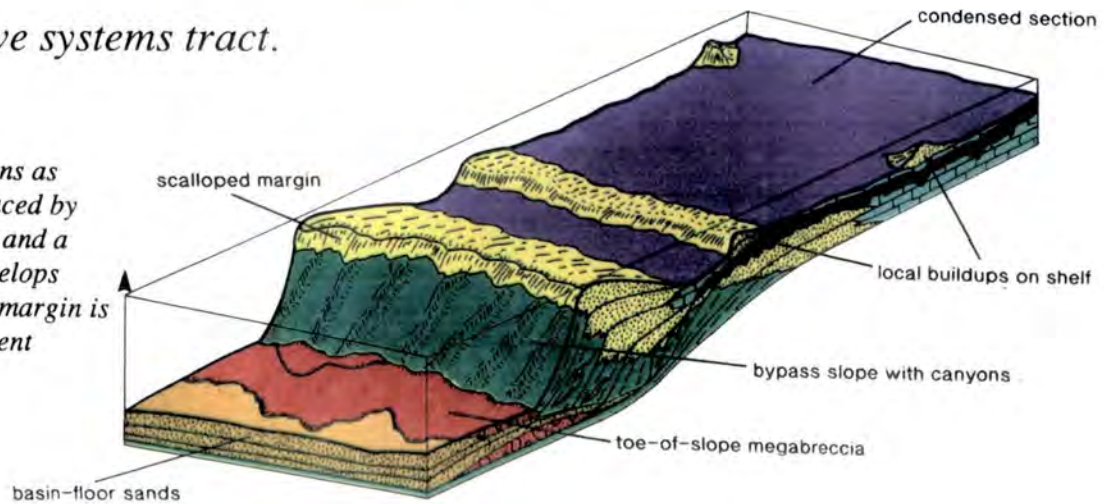

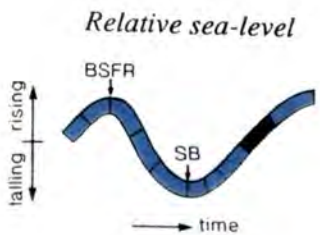

the preceding sequence, developing an 'underfilled' geometry (eg. Fig. 2.7, p. 30 & 3.25.3a-b), and a type 2a geometry develops throughout the systems tract. As relative sea-level continues to rise the shelf becomes transgressed and eventually drowned, developing a condensed section.

The transgressive systems tract is differentiated from the LPW systems tract by the change from offlap to localised aggradation at the basinwards margin of the preceding LPW. Thus, during the systems tract sedimentation is mostly areally restricted to the margin of the preceding LPW (eg. Figs 3.25.3a-4b), although as the shelf is transgressed sedimentation 'starts-up' in other areas but is subsequently drowned (Fig. 3.25.4, 4a, 4b). The region behind the aggrading marginal edge of the antecedent LPW has sedimentation rates lower than the rate of relative sea-level rise and is eventually drowned. Initially, however, marginal aggradation affords protection to this area and shelf-lagoon type facies are temporarily developed (Fig. 3.25.4, 4a).

At the margin of the proceeding LPW, aggradation during the TST is associated with the building of topography and a gradual steepening of the foreslope. The latter correspondingly evolves from a locally bypassed margin, funnelling shallow water sands to a basin-floor fan (Fig. 3.25.3a) to an extensively gullied bypass margin, which feeds a basin-floor apron (Fig. 3.25.4a) and, finally, to an erosional, scalloped foreslope associated with toe-of-slope megabreccias comprised of cemented shelf-margin and foreslope facies (Fig. 3.25.4b). This evolution of the basin-floor and foreslope is contemporaneous with the transgression of the shelf (Fig. 3.25.4, 4a, 4b).

On the shelf transgression is associated with the 'start-up' of carbonate sedimentation (eg. Fig. 3.25.4a). Initially, inner shelf facies are widely developed,

---

Figure 3.25. (next page) Diagram 5 of this figure illustrating the highstand systems tract (see text for further discussion).

5. *Highstand systems tract.*

Normal shelf sedimentation resumes as the rate of relative sea-level rise decreases. Facies on the shelf reflect inherited topography from the lowstand (eg. karst) and transgression (eg. build-ups). Shallow shelf-sediments bypass the slope to the basin-floor which aggrades, decreasing relief and correspondingly slope angles (highstand shedding).

protected by a second 'buffer' of high-energy facies developed upon an inherited topographic high (eg. see Section 3.7.2.B5, Fig. 3.25.4a-b). As relative sea-level continues to rise sedimentation is restricted to high-energy areas across the shelf as shelf-lagoon type facies are drowned. Isolated buildups are at this time developed across the shelf (Fig. 3.25.4b) and surrounded by a condensed section of slope type facies and/or a hardground.

The stratal patterns and relative timing of sedimentation developed across the platform during the TST is complex. Perhaps the most characteristic stratal pattern associated with this type 2a geometry TST is the development of buildups, both at the margin of the platform and to a lesser degree upon the shelf (Fig. 3.25.4, 4a, 4b). Volumetrically, most sediment is deposited at the margin of the platform and upon the basin-floor. This is associated with the development of gullies and erosional truncation upon the slope which extends up into the high-energy facies. The basin-floor is characterized by an increase of sedimentation rates and widespread toe-of-slope onlap as the sediment source evolves from a point to a line source (eg. Fig. 3.25.4b).

3.8.3. *E. The Highstand systems tract.*

This systems tract is illustrated in Figure 3.25.5 and is developed when the rate of relative sea-level rise has slowed, allowing the aggradation and progradation of shelf-lagoon facies and the shelf-margin. Upon both the shelf and slope the highstand systems tract on this scenario (HST) inherits the physiography developed mainly by the TST (eg. compare Fig. 3.25.4b &5).

The slowing of the rate of relative sea-level rise is associated at the platform margin with a change from sedimentation rates being in balance with the rate of relative sea-level rise to a large excess of sediment being formed. This excess is redeposited via the gullied bypass slope to the basin-floor which aggrades and onlaps the slope (toe-of-slope pattern, see Section 3.7.2. D & Fig. 3.24). This is termed highstand shedding (eg. Droxler & Schlager, 1985, see Section 3.7.3.C). As the

basin-floor aggrades the declivity of the foreslope decreases and the platform gradually progrades basinwards with an ascending basal relationship at the toe of clinoforms (eg. Figs. 3.24 & 3.25.5).

3.9. Conclusions.

A. General.

1. Sequence stratigraphic models developed for siliciclastic shelves need modification if they are to be successfully applied to carbonate platforms and in particular carbonate shelves.

2. On carbonate shelves the development of distinctive stratal packages and patterns reflects both the inherited platform architecture and interplay of rates of relative sea-level change and sedimentation.

3. The environmental sensitivity of carbonate sedimentation, and in particular that of carbonate secreting organisms means that sedimentation rates cannot be assumed constant upon carbonate platforms; environmental changes alone can cause development of different stratal packages/patterns.

4. Upon Holocene siliciclastic shelves the shelf-slope break is developed at an average depth of 130m. Contrastingly, on carbonate shelves and isolated platforms the shelf-slope break normally occurs within 10-20m of sea-level. Thus, a lesser magnitude of relative sea-level fall is needed to develop a type 1 sequence boundary upon a carbonate shelf than upon most siliciclastic shelves.

B. Lowstand systems tract.

1. Currently, a type 1 sequence boundary is developed when sea-level falls below the shelf-slope break. Such a definition is not sufficiently broad upon many carbonate shelves as the shelf margin has an elevated topography compared to its shelf-lagoon. Thus, a fall of sea-level below the shelf-slope break does not necessarily expose the shelf-lagoon. Definition of a sequence boundary needs to be broadened to include the subaerial exposure of the shelf-lagoon on a carbonate rimmed shelf.

2. The production potential of a carbonate platform reflects the area with water depths of less than 10m. A reduction of this area results in a fall of sedimentation rates. Upon a carbonate shelf a reduction of the production potential is associated with times of falling and lowstand of sea-level, the opposite relationship to that suggested for siliciclastic shelves. Unlike a siliciclastic shelf which when exposed augments sediment supply exposure of a carbonate shelf results in its 'shutting down'.

3. Following on from the previous point 'lowstands' are commonly impoverished or even absent on carbonate shelves and will be associated with the development of condensed pelagic sections on the basin-floor.

4. Exposure of a carbonate platform generally results in chemical rather than mechanical reworking in the form of subaerial diagenesis that will be climatically controlled.

5. Times of falling relative sea-level promote slope collapse through increased storm wave base loading on the slope. Reworked slope sediments are deposited by turbidity currents and debris flows on the basin-floor and at the toe-of-slope (allochthonous debris). Mud dominated, uncemented slopes will tend to be low angle and associated with mud dominated turbidites and plastically deformed debrites whereas high angle cemented or grain dominated slopes will tend to develop megabreccias.

6. The development of lowstand autochthonous wedges reflects the inherited slope morphology. Two end-members of autochthonous wedge are differentiated, those deposited on low angle slopes and those developed on high angle slopes. Low angle slopes are associated with wide volumetrically significant autochthonous wedges and high angle slopes with narrow volumetrically insignificant autochthonous wedges.

C. The transgressive systems tract.

1. The transgressive systems tract is currently defined on the basis of a single geometric stacking pattern, the retrogradational parasequence set. Upon carbonate platforms and shelves in particular this definition needs to be broadened as several different stacking patterns can be developed during the systems tract. The different geometries reflect the ratio of the rate of relative sea-level rise to the rate of sedimentation. Two different geometries are distinguished for the systems tract, type 1 and type 2 geometries. Type 1 geometries are developed when the rate of relative

rise exceeds sedimentation rates. Type 2 geometries are developed when the rate of relative sea-level rise is either equal to or less than the sedimentation rates of high energy facies, but greater than for shelf-lagoon type facies. Different geometries develop in response to relative sea-level rise(s) and/or environmental changes. Environmental changes appear to be the most important factor in the development of type 1 geometries.

2. When type 1 geometries typify the TST the stratal patterns developed are similar to those proposed for siliciclastic shelves (eg. retrogradational parasequence set). Type 2 geometries develop very different stratal patterns, characterized by the buildup of topography at the shelf margin, and possibly across the platform. The development of buildups at the shelf margin can lead to oversteepening and the deposition of basin-floor megabreccias. Type 2 geometries are characterized by the development of carbonate buildups both at the shelf margin and possibly across the shelf.

3. Toe-of-slope mega-breccias are not specific to times of falling relative sea-level; they can also be formed when type 2 geometries dominate the TST or in association with active faulting.

4. During the TST both the rates of sedimentation and relative sea-level rise can vary. This can lead to the superimposition of two or more of the different geometries (types 1-2) during the transgressive systems tract.

5. During the systems tract the shelf becomes transgressed and sedimentation can start up, but normally falls behind the rates of rising sea-level and is drowned.

D. The highstand systems tract.

1. The highstand systems tract inherits topography from both times of lowstand and possibly from the TST. Antecedent topography often plays an important role in the architecture of the HST.

2. This systems tract is normally the time at which there is the greatest area suitable for the production of carbonate sediment. Thus, it is normally the time at which the platform expands most rapidly.

3. Two different patterns of highstand slope sedimentation are recognised and these are slope aprons and toe-of-slope aprons. These are associated with descending/horizontal and ascending basal clinoform package relationships respectively.

Chapter 4.
The Geological Background Of The Urgonian Platform.

4.1. Introduction.

The Urgonian carbonate platform developed on the European passive margin to Ligurian Tethys and today crops out in the South-East Basin of France. The passive margin underwent rifting during the lower-mid Jurassic. From the late Jurassic the onset of oceanic spreading is associated with a change to thermal subsidence upon the passive margin. Late Cretaceous closure of Ligurian Tethys is marked by the development of compressional structures on the European passive margin and culminated in the Tertiary with continent-continent collision. This resulted in the telescoping and stacking of the two passive margins which loaded and downwarped the crust developing a foreland basin. Convergence ended in the late Miocene-Pliocene since when thermal re-equilibration of the depressed lithosphere has resulted in the isostatic uplift of the two collided margins.

The Urgonian platform formed during the early Cretaceous as the passive margin underwent thermal subsidence. The Urgonian limestones form the most extensive platform developed on this margin. Prior to the Urgonian platform shallow water carbonate sedimentation was restricted to the Jura Platform. In this chapter the general evolution of the passive margin is introduced and particular emphasis is placed upon the Cretaceous dynamics of the 'external zone' where the Urgonian platform developed.

4.2. Dynamics Of Passive Margin Formation And Inversion.

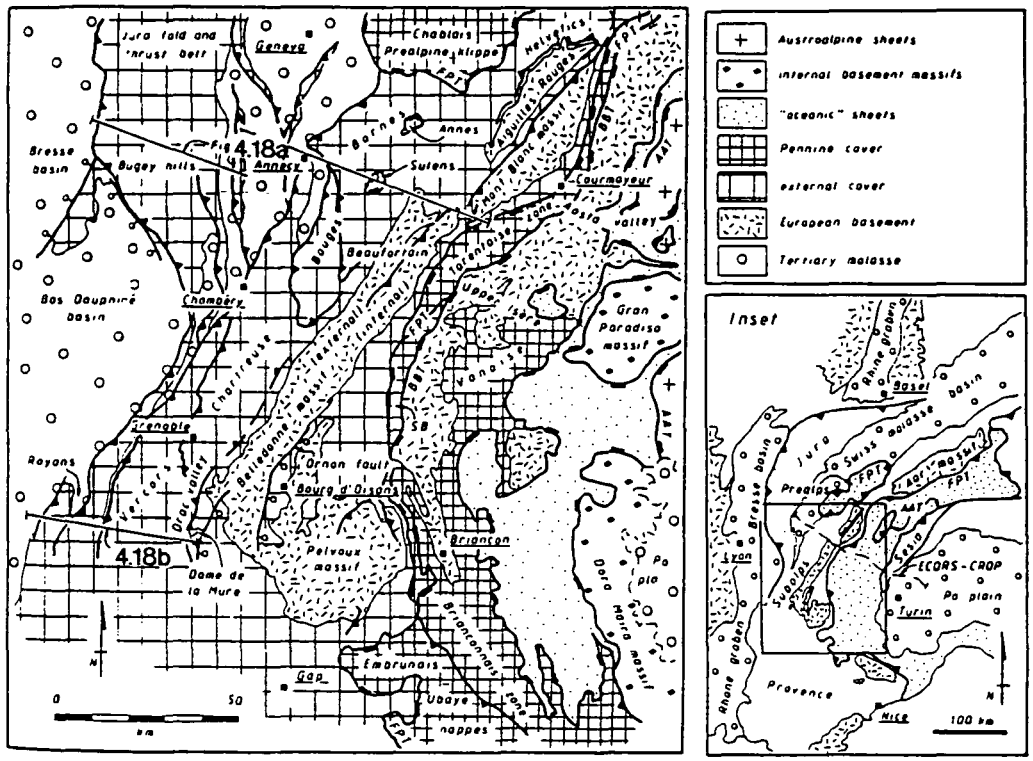

Figure 4.1. Simplified map of the northwestern Alps illustrating the main tectonostratigraphic units. The boundary between the Jura-Bas Dauphiné platform and the Dauphinois Basin of the external zone approximately follows the trend of the mountain belt from Royans NNE through Chambery to Annecy. This is also coincident with the geographic western margin of the Sub-Alpine Chains. The eastern margin to these mountains is approximately coincident at this scale with the western edge the Belledonne basement Massif. FPT, Frontal Pennine Thrust; BBT, Basal Briançonnais Thrust; AAT Austro-alpine Thrust. The position of Figures 4.18a and b are also shown (From Butler, 1989).

4.2.1. Introduction.

The External zone of the alpine province is the most proximal and least deformed part of the European Mesozoic passive margin to Ligurian Tethys. It is bounded today by the basement of the Massif Central to the west and the internal or Penninic zones to the east (Fig. 4.1). The Frontal Pennine Thrust is the western, basal surface delimiting the Internal alpine zones which represent the distal, sediment starved, underfilled part of the passive margin (eg. Fig. 4.2). The Penninic zones are themselves structurally overlain by ophiolitic thrust sheets which represent the ocean-

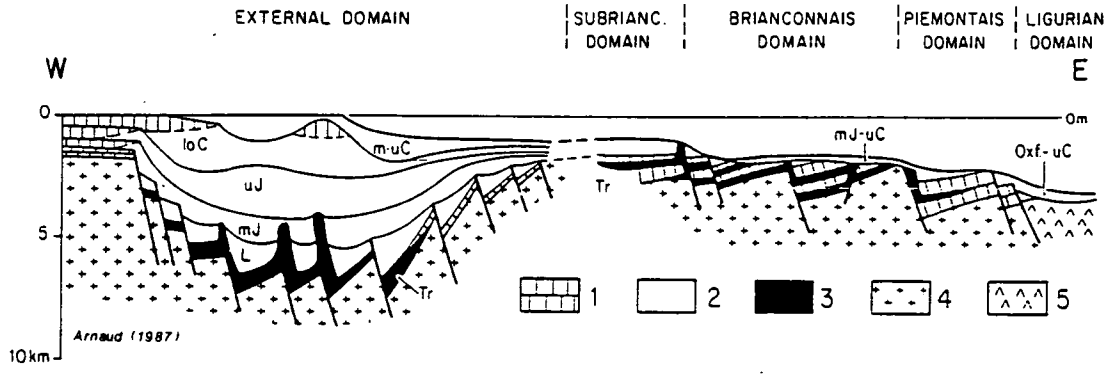

Figure 4.2. Schematic restored cross-section through the European passive margin. The Urgonian platform is represented by the upper most carbonate platform which extends farthest into the basin. 1: platform carbonates; 2: basin formations (clays, marls, marly limestones, limestones, detrital formations); 3: evaporites; 4: continental crust; 5: oceanic crust; L: Lias; mJ: middle Jurassic; uJ: upper Jurassic; Oxf: Oxfordian; loC: lower Cretaceous; m-uC: middle-upper Cretaceous. From Mascle *et al.* (1988).

floor that separated the two passive margin successions: the European passive margin to the north and the Apulian-Adriatic continental block to the south or southeast. The Austroalpine sheets which crop out tectonically above and to the west of the oceanic sheets represent the southern, Apulian passive margin (Lemoine *et al.*, 1986; Butler, 1989) (Fig. 4.1).

The External zone is itself divisible into three discrete palaeogeographic domains, the Jura-Bas Dauphiné platform, the Provençal platform and the Dauphinois Basin (Fig. 4.3). These domains are separated by major NNW-SSE trending lineaments such as the Isère-Cevennes and Durance faults (Fig 4.3) The Dauphinois Basin is itself cut by the more highly subsident east-west trending Vocontian Basin (Fig. 4.4).

4.2.2. Development and inversion of the European continental margin to Ligurian Tethys.

The sedimentary succession of the continental margin series is generally starved of terrigenous input (particularly the External zone) and as such is characterized by the development of carbonate platforms and their lateral basinal

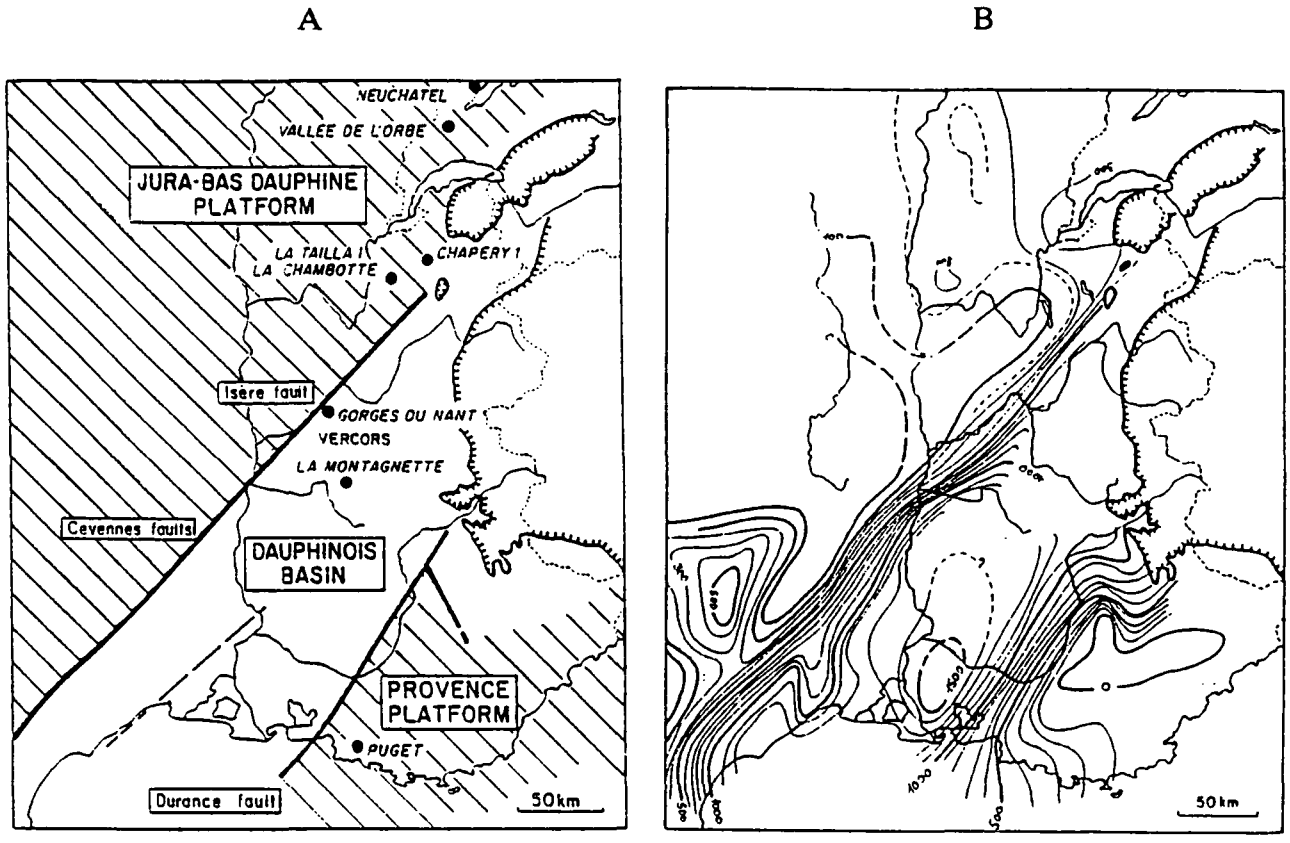

Figure 4.3. Paired maps showing the major palaeogeographic domains (a) and Liassic isopachs (b) for the South-East Basin or External zone. (a) The hatched areas, the Jura-Bas Dauphiné and the Provençe platforms represent the so-called 'stable' areas and the unhatched area between is the Dauphinois Basin, the 'unstable' areas (Arnaud, 1988). (b) The isopach map shows a NNW-SSE trend with maximum thicknesses corresponding to the Dauphinois Basin. Note that at this time (Liassic) the Vocontian Basin had not become palaeogeographically distinct (eg. Fig. 4.4) (From Arnaud-Vanneau *et al.*, 1987).

equivalents. The passive margin succession is deposited onto a pre-Triassic 'basement' which includes Variscan (and older) high grade gneisses, granitoids and Permo-Carboniferous continental deposits. Carboniferous coal deposits are of both economic and geological importance. Stephanian coals were deposited in en-echelon, NNW-SSE to NW-SE trending pull-apart basins formed during the very late stages of Variscan orogenesis (eg. Blès *et al.*, 1989). The trends of these major Variscan strike slip faults exerted a strong control upon the later dip-slip extensional structure(s) developed during Mesozoic stretching (Blès *et al.*, 1989). By the onset of extension,

in the Triassic and lower Jurassic much of the topography associated with the Variscan orogeny was subdued (eg. Fig. 4.5). Across the European passive margin (from internal to external zones) sedimentation ubiquitously begins with Triassic siliciclastics which pass upwards into shallow water Triassic carbonates and associated evaporites.

The development and subsequent demise of the European passive margin and in particular the External zone can be divided into a six fold tectono-stratigraphic evolution recognised across the passive margin; (1) onset of subsidence in the Triassic and Hettangian, associated with a shut off of siliciclastic input and development of carbonate platform sedimentation (2) lower to mid-Jurassic initiation of highly differential subsidence as major tilt blocks developed, associated with a general deepening (3) mid-late Jurassic onset of oceanic spreading coupled with an acceleration of subsidence on the passive margin (4) late Jurassic-mid Cretaceous thermal subsidence phase of the passive margin (5) Late Cretaceous onset of compression and inversion (6) continent-continent collision during the Tertiary, crustal thickening with large horizontal displacements and development of foreland basins.

The above evolution of the European passive margin to Ligurian Tethys can be related approximately to the opening history of the Atlantic (Fig. 4.6). In the early Triassic displacement associated with opening of the mid-north Atlantic was transferred by a major transform structure to the area which contemporaneously underwent extension to become Ligurian Tethys. Rifting associated with stretching of both the mid-Atlantic and Ligurian areas continued to the late Jurassic-early Cretaceous when the first oceanic sea-floor was formed (Fig. 4.6). Subsequent to the onset of sea-floor spreading both the mid-Atlantic and the western, European Ligurian passive margin entered the 'thermal subsidence' phase of passive margin development. In the late Cretaceous evolution of the mid-Atlantic and European passive margins diverged. Whilst the mid-Atlantic continued to subside the northward propagation of rifting in the southern Atlantic caused a major

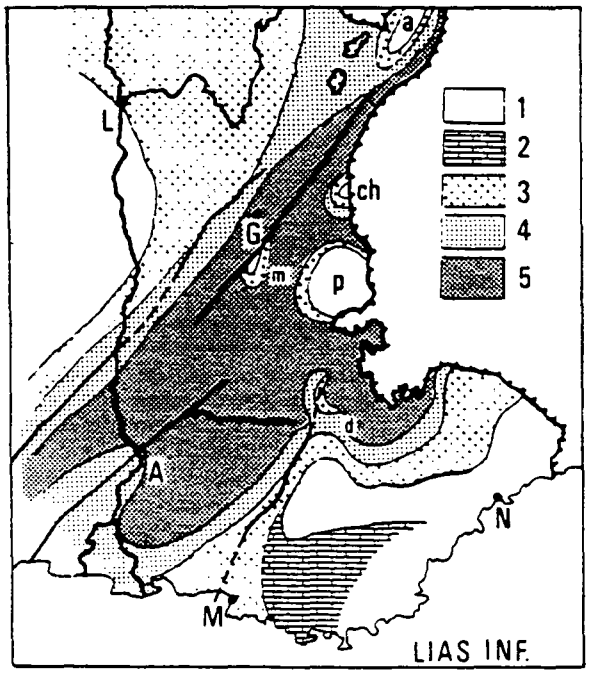
a
L
ch
G
m
p
d
A
N
M
1
2
3
4
5
LIAS INF.

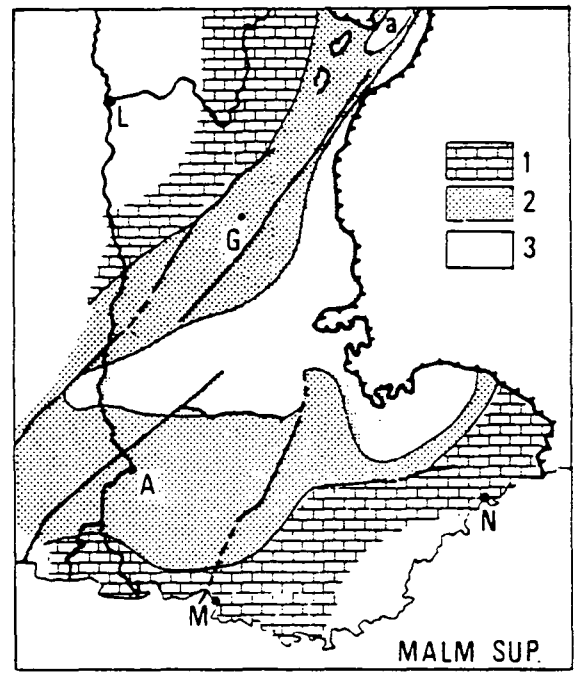
a
L
G
A
N
M
1
2
3
MALM SUP.

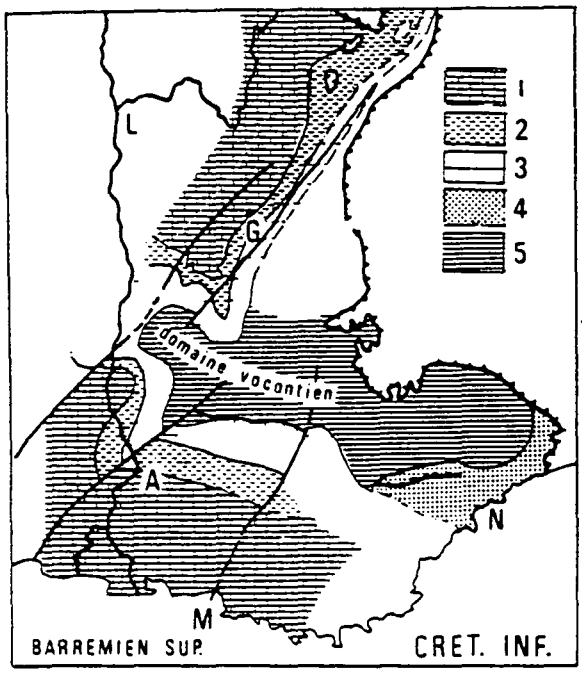
L
G
domaine vocontien
A
N
M
1
2
3
4
5
BARREMIEN SUP.
CRET. INF.

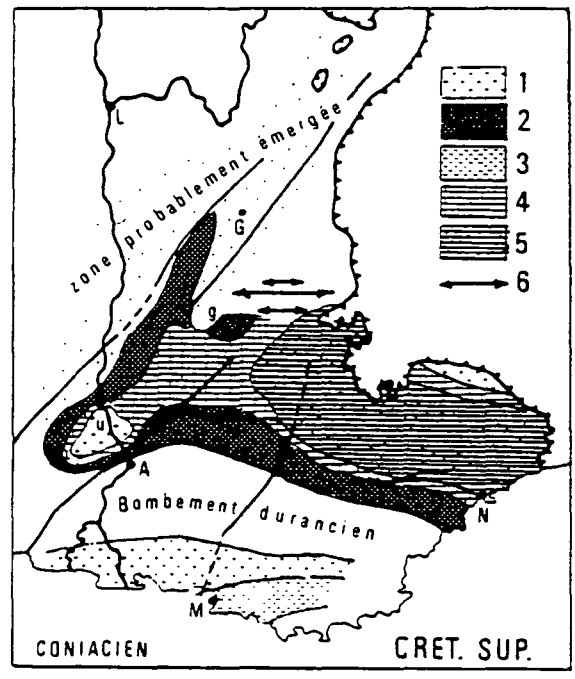
L
zone probablement émergée
G
g
u
A
Bombement durancien
N
M
1
2
3
4
5
6
CONIACIEN
CRET. SUP.

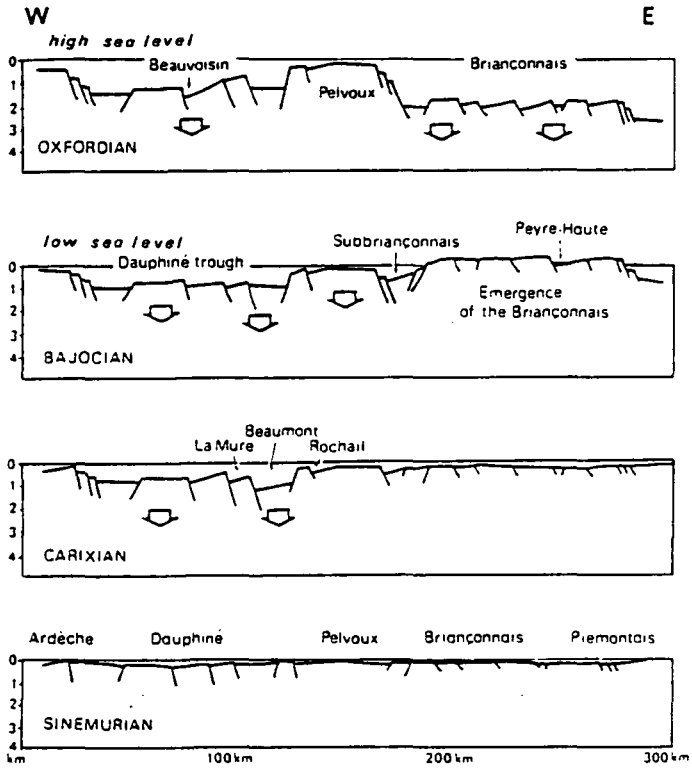

Figure 4.5. Reconstruction of the Bathymetric evolution of the European passive margin to Ligurian Tethys for the Lower Jurassic. Note that from Sinemurian-Bajocian times subsidence was concentrated in the External zone, the proximal part of the passive margin. The western elevated margin to the Dauphiné trough in these figures corresponds approximately to the Isère fault. From Roux *et al.* (1988).

Figure 4.4. (preceeding page) Four simplified palaeogeographic maps of southeast France. In each map the major normal faults which controlled the palaeogeography in the Mesozoic are marked. These are from NW to SE; the Cevennes-Isère fault, the Cléry fault, the Nîmes fault and the Durance fault.

A: Avignon; G: Grenoble; L: Lyon; M: Marseille; N: Nice.

Lias Inf: Lower Lias; 1: above sea-level; 2: intertidal-supratidal dolomites; 3: shallow-water fossiliferous facies; 4: limestones and shales with ammonites and *Gryphaea* (Digne), of average thickness; 5: limestones and shales with ammonites (very thick).

Malm Sup: upper Malm; 1: often dolomitized reefal facies; 2: pelagic facies; 3: very deep water pelagic facies.

Cret. Inf: upper Barremian: Urgonian facies (1. rudist limestones; 2. shelf margin facies); 3: limestones and shales with sponge spicules; 4: micritic limestones with glauconite and phosphate; 5: limestones and shales with ammonites (Vocontian facies *sensu stricto*).

Cret. Sup: upper Cretaceous: 1: rudist limestones; 2: glauconitic sands and conglomerates (g: conglomerates des Gâs, near Châtillion-en-Dios); 3: sandy limestones; 4: calcareous sands; 5: limestones and shales with ammonites; 6: folds (Diois, Dévoluy).

From Debelmas, (1983).

---

reorganisation of plate motion vectors (Fig. 4.6). A consequence of the northward propagation of south Atlantic opening was the anti-clockwise rotation of the African plate leading to the contraction of the Ligurian Tethys.

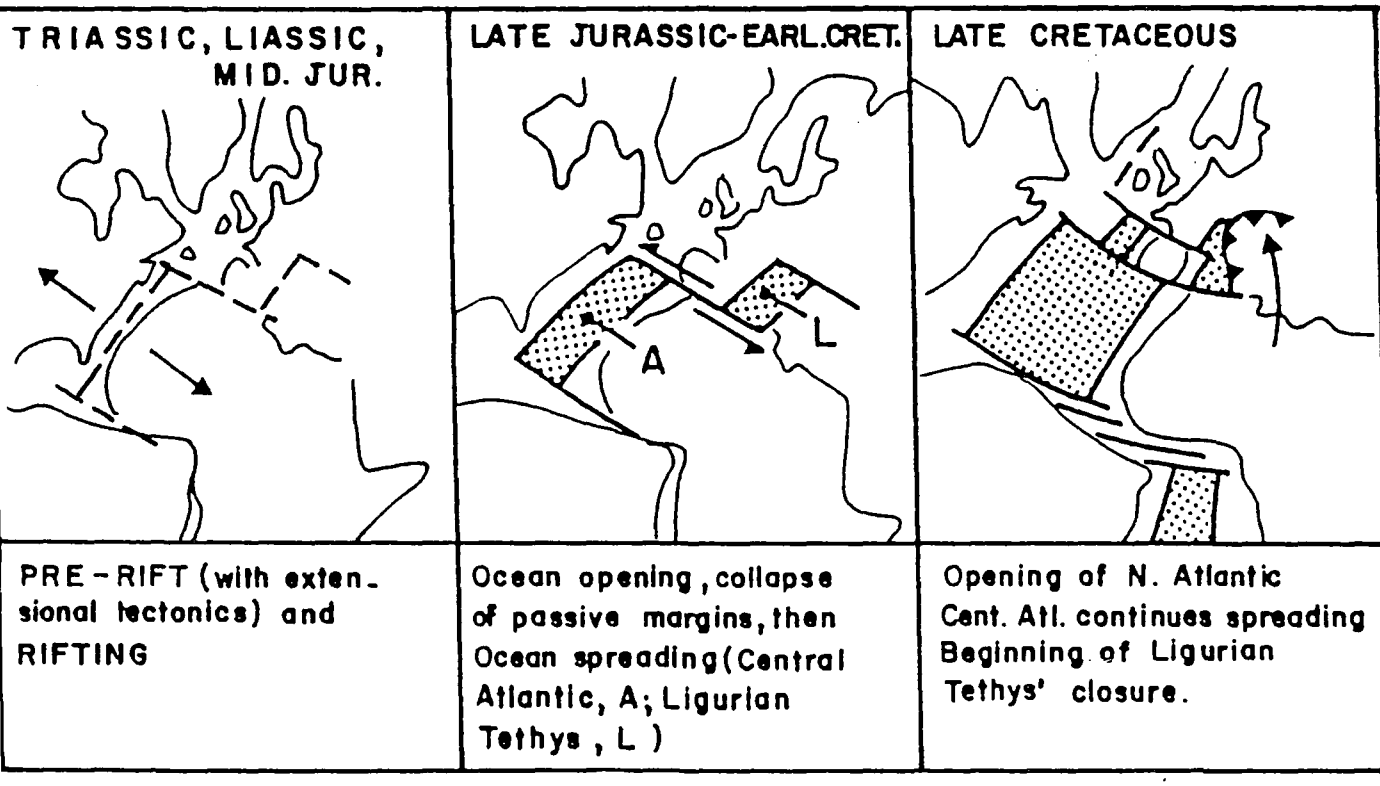

Figure 4.6. The three main stages of development of the Ligurian Tethys and their close relationship to the progressive opening of the Atlantic. The initial stages were characterized by the transference of extension via a transform from the mid-Atlantic to the northern Tethyan realm. Continued stretching throughout the lower and mid-Jurassic led to the onset of sea-floor spreading in both the mid-Atlantic and Ligurian Tethys in the upper Jurassic. In the late Cretaceous the northward propagation of south Atlantic opening caused the anti-clockwise rotation of Africa with respect to Europe, beginning the contraction of Ligurian Tethys. (From Lemoine *et al.*, 1986).

4.2.2. A. Triassic-early Jurassic.

The initial stages of passive margin subsidence occurred during the Triassic and early Hettangian. Subsidence was generally widespread, gentle and

undifferentiated across the area to become the two passive margins (Rudkiewicz, 1988) (Fig. 4.5). The intercalation of alkaline volcanics within the sedimentary succession at this time is suggestive of the early stages of continental extension, thought to be coupled to the initial stages of Atlantic rifting (eg. Lemoine *et al.*, 1986, Fig. 4.6).

During the Triassic sedimentation generally passes up from siliciclastic fluvial and shallow marine deposits to a shallow-water, arid carbonate platform and associated evaporite basin(s) over almost the entire area undergoing stretching (eg. Curnelle & Dubois, 1986, their fig. 1). The Triassic-lower Hettangian carbonate-evaporite basins indicate an arid climate and suggest that connection to the open ocean was poor. By way of contrast, the mid-upper Hettangian is characterized by a halt of terrigenous input to the proximal parts (External zone) of the passive margin and a change from arid to humid climatic conditions as subsidence began to accelerate and general transgression and/or deepening occurred (Elmi, 1990) (eg. Fig. 4.5).

4.2.2. B. Early to late middle-Jurassic.

During this second stage of passive margin development, beginning in the mid-late Hettangian continued stretching and extension was accommodated by the formation of tilted fault blocks which fragmented the Triassic and early Jurassic platform(s) (Fig. 4.5) (eg. Elmi, 1990). Subsidence became highly differentiated across the European passive margin; concentrated to within the External zone of the passive margin subsidence was localised further to several major lineaments, notably the Isère and Durance faults (eg. Figs 4.3, 4.4 & 4.5). These structures delineate the margins of the stable platform areas (Jura-Bas Dauphiné & Provençal, Figs 4.3, 4.4 & 4.5) between which the more highly subsident basinal area, the Dauphinois Basin developed (Figs 4.2, 4.3, 4.4 & 4.5). Within the Dauphinois Basin extension was accommodated by the formation of tilted fault blocks several km to 10's of km wide and generally downthrowing to the east (eg. Figs 4.3, 4.5 & 4.7)

(Barfety & Gidon, 1983; Lemoine & Trümpy, 1987; Lemoine *et al.*, 1986; Elmi, 1990).

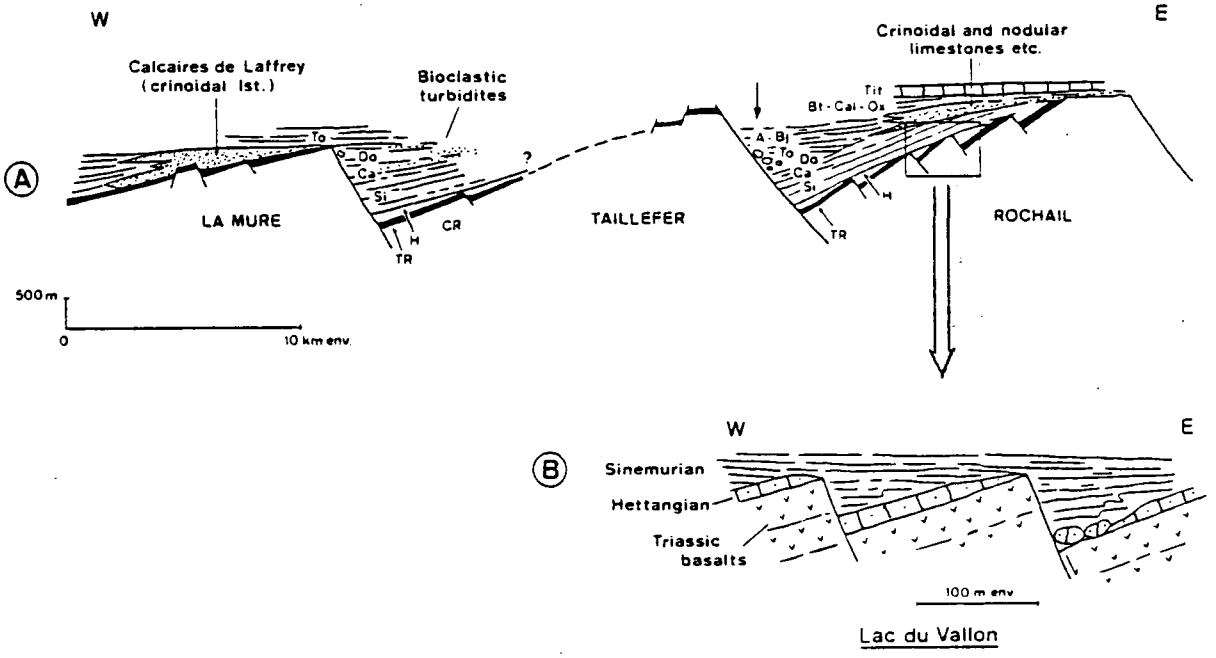

Figure 4.7. Schematic reconstruction of the fault bounded extensional tilted blocks of the southern Belledonne Massif of the external Alps. Note the development of crinoidal sand shoals on the shoulders of the blocks. The grabens were classically underfilled during active extension. Note that the Tithonian is approximately horizontal and blankets the half-grabens. This is interpreted to represent the break-up unconformity. See text for further discussion (From Lemoine & Trümpy, 1987).

Within the Dauphinois Basin extensional fault bound tilted blocks are exceptionally well preserved within the Belledonne Massif (eg. Barfety & Gidon, 1983; Lemoine *et al.*, 1986, their fig 6). The hanging walls of fault blocks are filled predominantly by pelagic and hemipelagic sediments, interbedded with gravity deposits derived from the uplifted footwall block (eg. the Ornon fault, Lemoine *et al.*, 1986, Fig. 4.7, arrowed). Contrastingly, the uplifted footwalls were the sites of deposition of shallow-water crinoidal sand bodies which often rest with marked angular unconformity upon the rotated earlier syn-rift deposits (eg. Barfety & Gidon, 1983, their figs 14-17). In areas more proximal to the main bounding faults (eg. Isère-Cevennes lineament) of the Dauphinois Basin such as the Ardèche the uplifted

footwalls of fault blocks commonly became elevated above sea-level and subaerially exposed (eg. Elmi, 1990).

Across the External zone, both the 'unstable' basinal areas and the 'stable' platform were 'drowned', and deep water (eg. 500m in Dauphinois Basin, Rudkiewicz *et al.*, 1988, their fig. 6) and often organic rich shales were deposited (Arnaud, 1988) (Figs 4.5 & 4.8). This resulted from the marked Toarcian and Aalenian acceleration of tectonic subsidence which was clearly concentrated in the external zone (eg. Arnaud, 1988; Roux, 1988; Rudkiewicz, 1988, Fig 4.5). Contrastingly, contemporaneously, the Briançonnais zone was either very shallow water or subaerially exposed (Fig. 4.5).

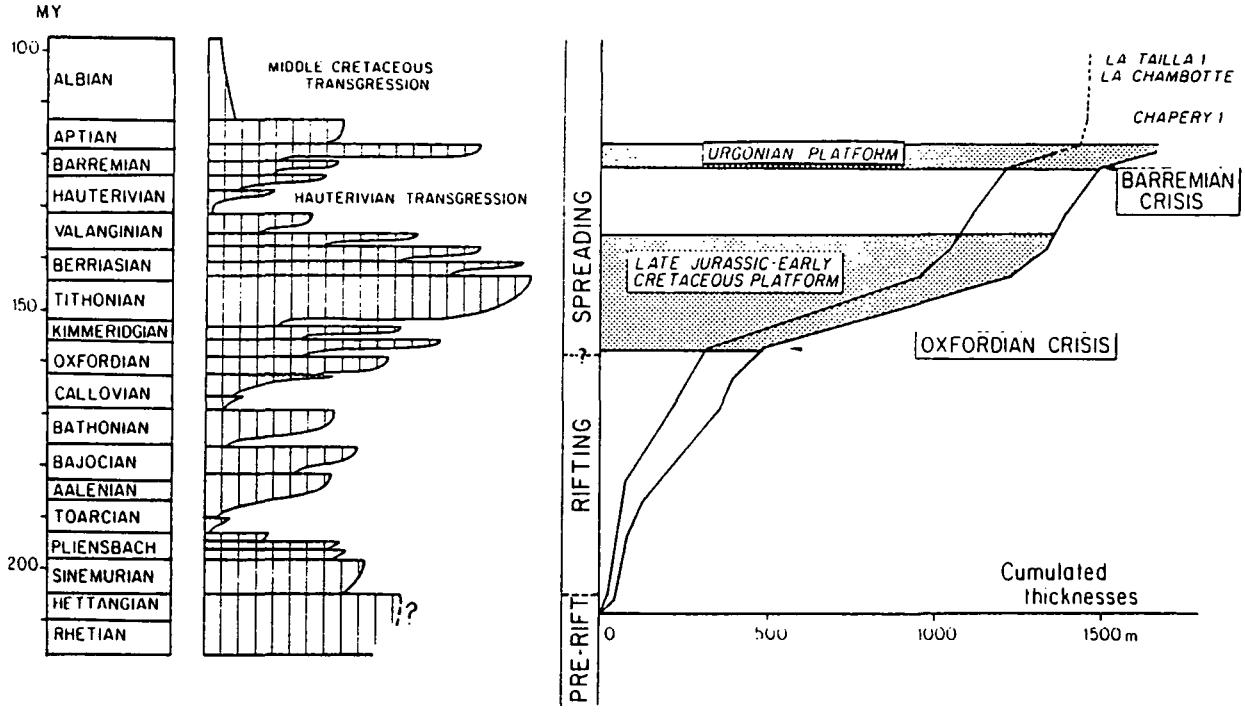

Figure 4.8. Schematic facies evolution curve (deepest to left) and accumulated sediment thickness for the Jura Platform during the rifting (Lias-Dogger), and spreading (lower Cretaceous-upper Cretaceous) of the Ligurian ocean. (From Arnaud, 1988).

4.2.2. C. Late mid-late Jurassic.

The late middle Jurassic to early late Jurassic times are characterized by a major palaeogeographic change, with the formation of true oceanic sea-floor upon which radiolarian cherts were deposited in the Ligurian zone (eg. Fig. 4.2). The formation of ocean crust is associated with a second major acceleration of subsidence upon the European passive margin between the Callovian and Oxfordian (Rudkiewicz, 1988; Arnaud, 1988, Figs 4.5 & 4.8). This third phase of subsidence is again strongly differentiated across the passive margin, concentrated to the distal, eastern part of the passive margin (internal zones, Roux *et al.*, 1988, Fig. 4.5).

Within the external zones this acceleration of subsidence corresponds to the 'Oxfordian crisis' of Arnaud (1988) which in the Jura is marked by an increase of sedimentation rates (Fig. 4.8). In the Dauphinois Basin the Callovian-Oxfordian subsidence event is also characterized by the first palaeogeographic distinction of the east-west trending Vocontian Basin (eg. Curnelle & Dubois, 1986, Fig. 4.4), here interpreted as a failed rift arm off Ligurian Tethys.

Shallow-water carbonate sedimentation by this time was limited to a few tectonic highs, the stable platforms of the passive margin (the Jura and Provençal platforms, Arnaud-Vanneau *et al.*, 1987, Figs 4.3 & 4.4). Mostly, carbonate sedimentation was drowned and such areas are characterized by hemipelagic and pelagic sediments. This illustrates the high subsidence rates across the margin and the attenuation of the basin-and-shoal topography across the whole passive margin during the lower and mid Jurassic (eg. Figs 4.2, 4.4 & 4.5).

4.2.2. D. Late Jurassic-early Cretaceous.

Following on from the onset of oceanic spreading, thermal subsidence dominated the next phase of passive margin formation, characterized by the gentle subsidence of the passive margin, interpreted to be a time of tectonic quiescence. Certainly, the supply of detrital sediment to the passive margin was most reduced at this time (Arnaud-Vanneau *et al.*, 1987). The break-up unconformity is classically

interpreted to be represented by the widespread Tithonian carbonate platform as this 'blankets' or 'seals' the tilted blocks in the Belledonne Massif (eg. Lemoine *et al.*, 1986; Lemoine & Trümpy, 1987, Fig. 4.7). However, active extension of the half-grabens could certainly have halted earlier as for most of their evolution the grabens appear to have been underfilled.

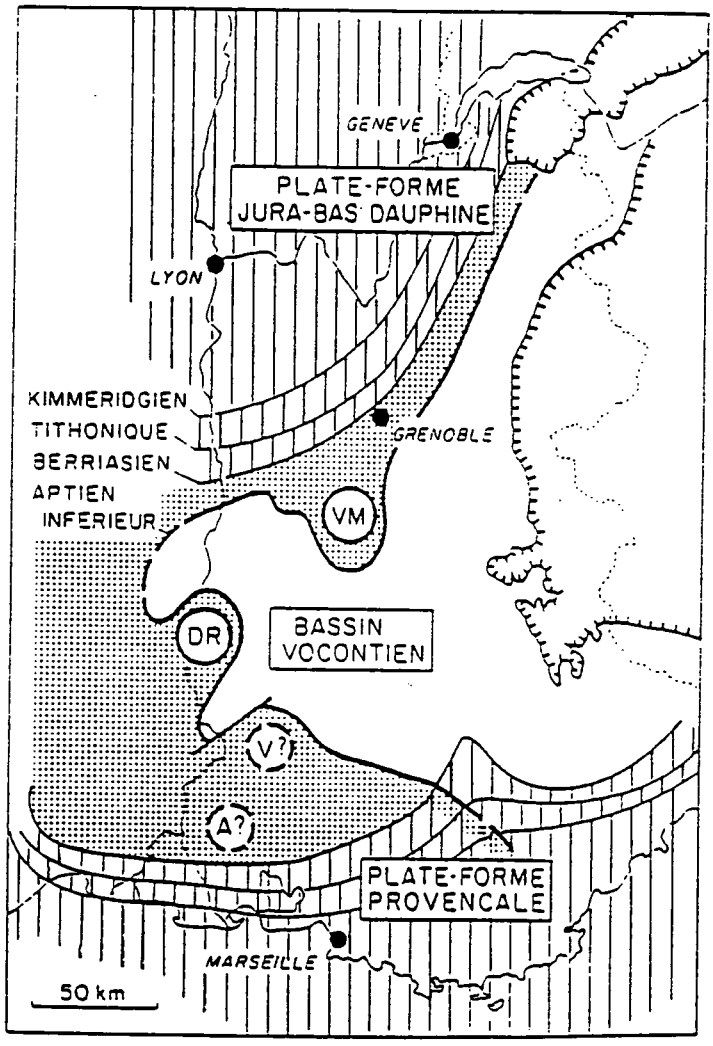

Figure 4.9. The progressive progradation of shallow water platform sedimentation during the late Jurassic and Cretaceous. The two progradational events (Tithonian-Berriasian and Barremian-Aptian) are separated by a flooding event (see Figure 4.8). From Arnaud-Vanneau *et al.* (1987).

In the External zone this time is characterized by the aggradation and progradation of carbonate platforms. The first progradational event is marked by progradation of shallow-water platform sedimentation in the Tithonian-Berriasian

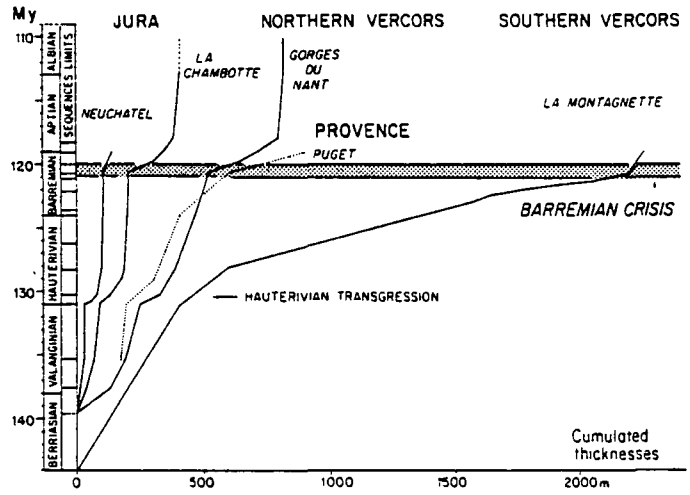

Figure 4.10. Curves of minimal sedimentation rates during the Lower Cretaceous on the Jura Platform, the Vercors, to the NW of the Vocontian Basin and the Provence platform. Note the acceleration of sedimentation at the La Montagnette section at the beginning of the Hauterivian, continuing into the Lower Barremian, then slowing in the upper Barremian. Conversely, the sections for the northern Vercors and Jura show the opposite trend in the upper Barremian and for most of the Hauterivian. Sections are located on Fig. 4.3A, p. 108 (From Arnaud, 1988).

southeast across the Jura Platform to the borders of the Dauphinois Basin (eg. Figs 4.2, 4.4 & 4.9, eg. Arnaud-Vanneau *et al.*, 1987). Restriction of shallow-water carbonate platform sedimentation to the north of the Isère lineament suggests that either the antecedent topography inherited from Jurassic rifting across this structure was still significant and/or that subsidence continued to be localised along this structure in the upper Jurassic and/or lower Cretaceous. The second major progradation of carbonate platform sedimentation is, however, characterized by development of shallow-water platform facies across the Isère lineament and a considerable distance into the Dauphinois Basin and onto the flanks of the Vocontian Basin (Fig. 4.9). This is the Barremian-Aptian Urgonian carbonate platform (Figs 4.2, 4.4 & 4.9). This second phase of platform development is characterized by the Barremian subsidence crisis of Arnaud (1988), an abrupt increase of sediment thickness which occurs at this time from the Jura Platform to the northern margin of the Vocontian Basin (eg. Figs 4.8 & 4.10). The demise of the Urgonian platform sedimentation is characterized by a general decrease of sedimentation rates (with the

exception of the Vocontian Basin, Section 4.3) and return to deeper water sedimentation across much of the external zone.

4.2.2. E. Late Cretaceous-late Miocene.

In the mid-late Cretaceous a major reorganisation of plate motion vectors between the European and African plate resulted from the northward propagation of rifting in the south Atlantic (Fig. 4.6). The anti-clockwise rotation of Africa led to the closure of Ligurian Tethys (Lemoine *et al.*, 1986; Lemoine & Trümpy, 1987).

The first indications of this plate reorganisation were a renewal of detrital sedimentation over much of the external domain and the formation of folds and thrusts in some areas (eg. Dèvoluy, Arnaud, 1981; Debelmas, 1983; Arnaud-Vanneau *et al.*, 1987). Deposition during this phase is characterized by a gradual, diachronous return to siliciclastic sedimentation and the development of flysch in the Internal zones from the late Cretaceous and, subsequently molasse basins (Tertiary) as the mountain belt progressively migrated westwards (eg. Mugnier *et al.*, 1990, their fig. 1), stacking and telescoping the passive margins (eg. Butler, 1989).

4.2.2. F. Post-Miocene.

Collision and hence folding/thrusting halted in the late Miocene in the Sub-Alpine Chains (Roberts, 1990) and Pliocene in the Jura (Mugnier *et al.*, 1990). Since this time the crust, which was depressed during the stacking of the two passive margin successions became thermally re-equilibrated and isostatically rebounded. This resulted in the isostatic rebound of the Sub-Alpine Chains by about 700m (eastern Vercors, Chartreuse) and approximately 300m in the Jura-Bas Dauphiné (Roberts, 1990). In more internal areas of the Alps this figure is likely to be greater. Isostatic uplift since the Miocene aided by Pleistocene glaciation has eroded a series of steep sided valleys which afford spectacular exposures of the Mesozoic passive margin successions.

4.3. The External Zone Structure And Mesozoic Tectono-Stratigraphic Evolution.

4.3.1. Introduction.

The general dynamics of passive margin evolution have been discussed in the preceding section. In this section the evolution of the external zone in particular is discussed, establishing the template and stratigraphic framework upon and within which the Urgonian platform developed. The external zone is divided into three discrete palaeogeographic regions, the Jura/Provençal platforms, the Dauphinois and the Vocontian Basins (Figs 4.3 & 4.4). The structure and stratigraphy of each are introduced, beginning with the Vocontian Basin as this contains the least deformed and stratigraphically most complete Mesozoic succession.

4.3.2. The Vocontian Basin.

4.3.2. A. Introduction.

The Vocontian Basin became palaeogeographically distinct during the Callovian-Oxfordian (see Section 4.2, Fig. 4.4). From this time to the late Cretaceous the basin is characterized by a predominantly pelagic fill of limestone-shale couplets which is unusually thick (3.5km, Fig. 4.11), attesting to the considerable input of fine terrigenous sediment (Ferry & Rubino, 1989). During the Cretaceous periplatform sediments of the surrounding carbonate platforms prograded into the basin, progressively contracting it (Figs 4.4, 4.9 & 4.12). Within the pelagic succession of the basin there is a marked correspondence between the progradation of carbonate platforms in the Jura and a shift to limestone dominated pelagic sedimentation (Tithonian-Berriasian and Barremian-Aptian, eg. compare Figs 4.8 & 4.11) (Arnaud, 1981; Arnaud-Vanneau *et al.*, 1987; Ferry & Rubino, 1989). During the Barremian-

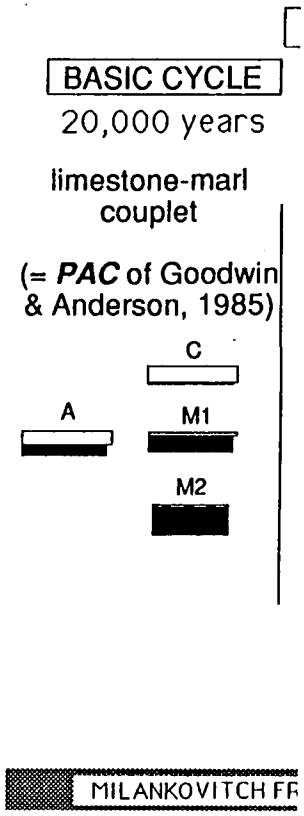

Figure 4.11. The lower Jurassic to upper Cretaceous stratigraphy of the Vocontian Basin showing the superimposed cyclicities which can be recognized building from the basic limestone shale couplet (left). Three types of basic limestone-shale couplet are recognised A: limestone and shale in approximately equal proportion; C: carbonate dominated; M: shale dominated. These basic couplets have been built into units thought to represent the parasequences, parasequence sets, sequences and sequence sets of the Exxon paradigm (From Ferry & Rubino, 1989).

Aptian, the Urgonian platform developed upon the flanks of the Vocontian Basin and radically altered the palaeogeography and the type, patterns and rates of sedimentation on the slopes and floor of the basin (eg. Figs 4.4, 4.9 & 4.12) (eg.

Ferry & Rubino 1989; Arnaud, 1981; Arnaud-Vanneau & Arnaud, 1990; Jacquin *et al.*, 1991; Hunt & Tucker, 1992).

4.3.2. B. Structure.

The Mesozoic structural framework of the Vocontian Basin is complex. During the late Jurassic (Oxfordian-Callovian) extension associated with the onset of sea-floor spreading developed east-west trending Vocontian or Provençal extensional faults which overprinted onto the NNE-SSW 'Cevenol' or 'Dauphiné' structure characteristic of the external zone (Figs 4.3 & 4.13). Thus, within the basin three main families of Mesozoic fault can be recognized (Fig. 4.13) (1) the NNE-SSW to NE-SW trending Cevenol or Dauphiné faults such as the Nimes, Menée, Durance, Clery and Gigors faults, (2) the E-W to NW-SE trending Provençal or Vocontian faults such as the Clavelière, Tourettes faults and the Ventoux-Lure fault which bounds the Vocontian Basin to the south, and (3) the N-S faults (Saillans, Die and Bonneval faults) which are associated with diapirism since the Oxfordian of Triassic evaporites (Joseph *et al.*, 1989).

In the southern part of the basin the E-W Provençal faults predominate, whereas in the northern part of the basin (north of the Tourettes fault) N-S and NE-SW Dauphiné faults are more important (Fig. 4.13). This emphasises the gradual northwards transition from the Vocontian Basin to the Dauphinois Basin. Contrastingly, the southern basin-margin, the Ventoux-Lure fault is rather abrupt (eg. Figs 4.12 & 4.13). During late Cretaceous-Tertiary Alpine orogenesis E-W trending

Figure 4.12. (next page) Late Jurassic to mid-Cretaceous palaeogeographic evolution of the Vocontian Basin. Note the gradual swinging of major channels from a N-S orientation towards an E-W orientation towards the centre of the basin and major changes of patterns of basin-floor sedimentation during the development of the Urgonian platform. (From Joseph *et al.*, 1989).

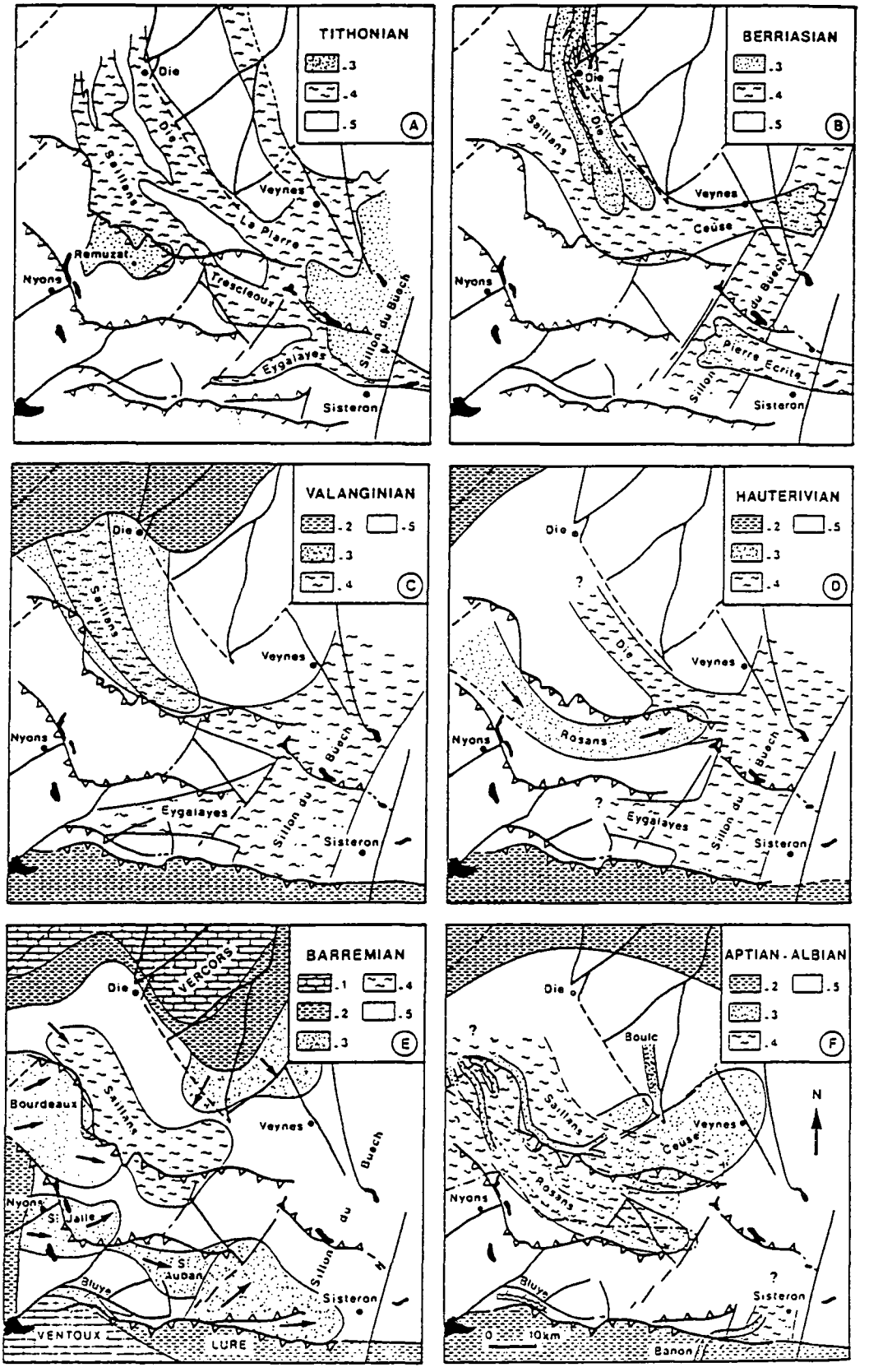
TITHONIAN
.3
.4
.5
A
Die
Saillans
Veynes
Le Pierre
Remuzat
Nyons
Trescleoux
Eygalayes
Sillon du Buech
Sisteron
BERRIASIAN
.3
.4
.5
B
Die
Saillans
Veynes
Ceüse
Nyons
Sillon du Buech
Pierre Ecrite
Sisteron
VALANGINIAN
.2
.3
.4
.5
C
Die
Saillans
Veynes
Nyons
Eygalayes
Sillon du Buech
Sisteron
HAUTERIVIAN
.2
.3
.4
.5
D
Die
?
Veynes
Rosans
Nyons
Eygalayes
Sillon du Buech
Sisteron
BARREMIAN
.1
.2
.3
.4
.5
E
VERCORS
Die
Bourdeaux
Saillans
Veynes
Buech
Nyons
St Jalle
St Auban
Sillon du
Bluyes
Sisteron
VENTOUX
LURE
APTIAN - ALBIAN
.2
.3
.4
.5
F
Die
?
Boulc
Saillans
Veynes
Ceüse
Rosans
Nyons
Bluyes
?
Sisteron
0
10km
Banon
N

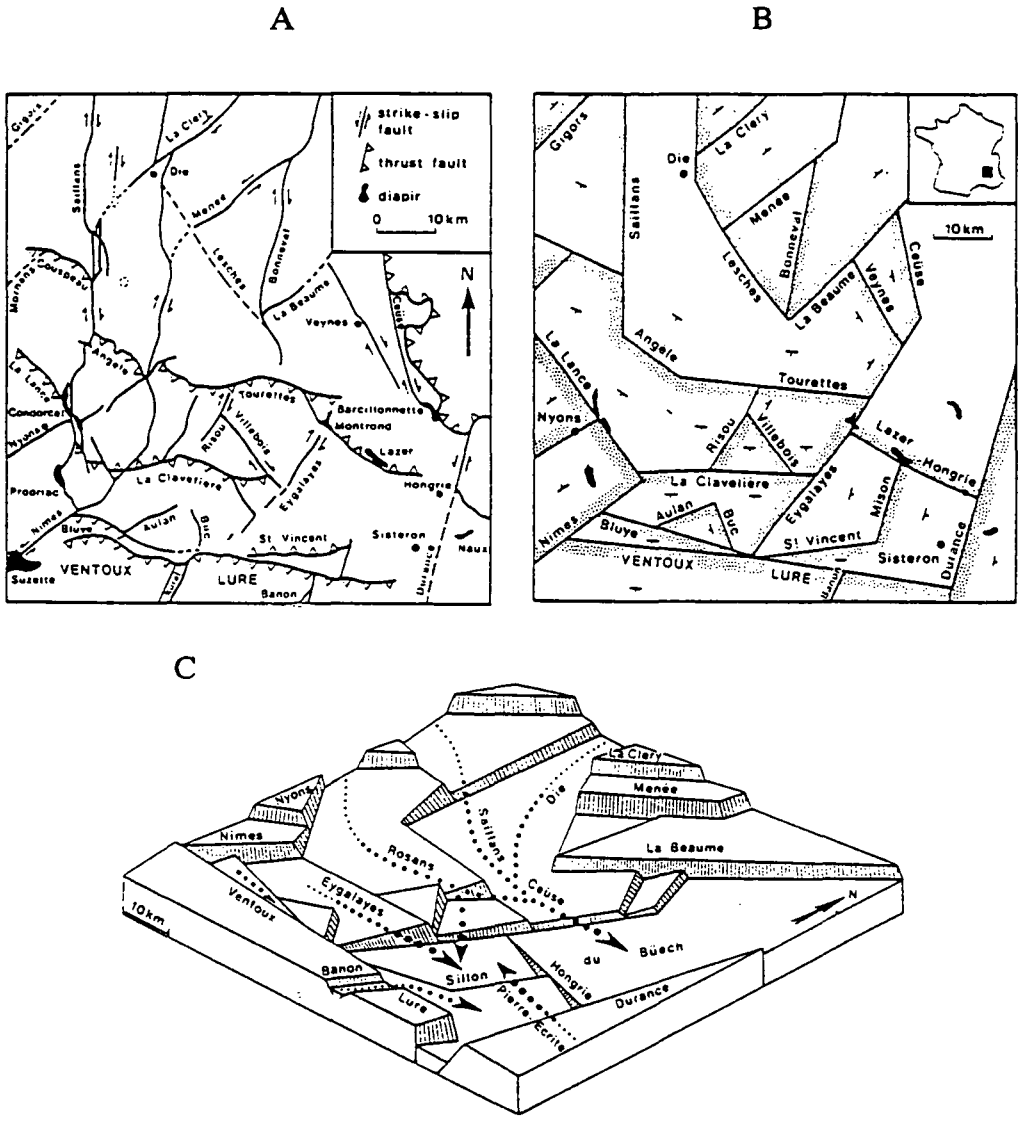

Figure 4.13. Structural summary maps of the Vocontian Basin. (A) The present day structural framework. Note that E-W Provençal structures are thrust faults and N-S to NW-SE structures strike-slip faults. (B) The interpreted pattern of lower Cretaceous extensional fault blocks. Shading on the uplifted footwall of fault blocks. (C) Reconstructed block diagram of the basin-floor palaeotopography and position of the major submarine canyons. Note the dominance of E-W Provençal structures in the southern part of the basin and N-S to NE-SW trending Dauphiné structures in the north of the basin (From Joseph *et al.*, 1989).

structures acted to localise thrust faults whereas the N-S to NNE-SSW faults were reactivated with a strike-slip motion. (Fig. 4.13, Joseph *et al.*, 1989). Into the Vercors Massif the N-S and NNW-SSE Dauphiné structures have acted to localise thrust faults (Butler, 1989; Roberts, 1990) (eg. Fig. 4.18b).

4.3.2. C. Stratigraphy.

The basin stratigraphy contains a near continuous record of sedimentation through passive margin development. Basinal facies are characterized by 0.3-1m thick limestone-shale couplets, the basic stratigraphic unit of the basin (Ferry & Rubino, 1989). These couplets are interpreted to represent 20 000 year climatic cycles (Cotillion *et al.*, 1980; Cotillion, 1987) (Section for 4.3.2. D for further discussion of cyclicities). The limestone-shale couplets have a distinctive mineralogical evolution from $CaCO_3$ poor, kaolinite rich shale interbeds to smectite rich limestone beds typically composed of 60-70% nannonfossils. These carbonate-shale cycles are almost identical to upper Pleistocene/Holocene high frequency ocean basin pelagic cycles where smectite rich limestones alternate with kaolinite rich interbeds (Ferry & Rubino, 1989, their figs 88 & 89); the limestones developed during warm and interbeds during cool climatic conditions. Such an interpretation is extended to the Vocontian limestone shale couplets (eg. Cotillion *et al.*, 1980; Cotillion, 1987; Ferry & Rubino, 1989).

On the basis of the relative proportion of limestone to shale and clay mineralogy three major asymmetric cycles can be recognized from the late Jurassic to late Cretaceous (Figs. 4.11 & 4.14): Oxfordian-Tithonian/Berriasian (Megasequence I), Valanginian-lower Aptian (Megasequence II) and lower Aptian-Turonian (Megasequence III) (Deconinck, 1984; Jospeh *et al.*, 1985; Ferry & Rubino, 1989). The cycles pass from shale dominated smectite-poor couplets to limestone dominated smectite-rich couplets. The shift to limestone dominated sedimentation is associated with a decrease of the overall sedimentation rates in the Vocontian Basin (Fig. 4.15). This suggests that a decrease of the input to the basin of clays rather than an increase of pelagic carbonate productivity is responsible for the shift to limestone dominated sedimentation in the Vocontian Basin. It is interesting to note here that the tops of the megasequences I and II correspond to the progradation of shallow-water carbonate platform facies in the Tithonian-Berriasian and Urgonian (Barremian-Aptian)

respectively in the Jura (eg. compare Figs 4.8 & 4.14, Arnaud, 1981; Arnaud-Vanneau *et al.*, 1987; Ferry & Rubino, 1989).

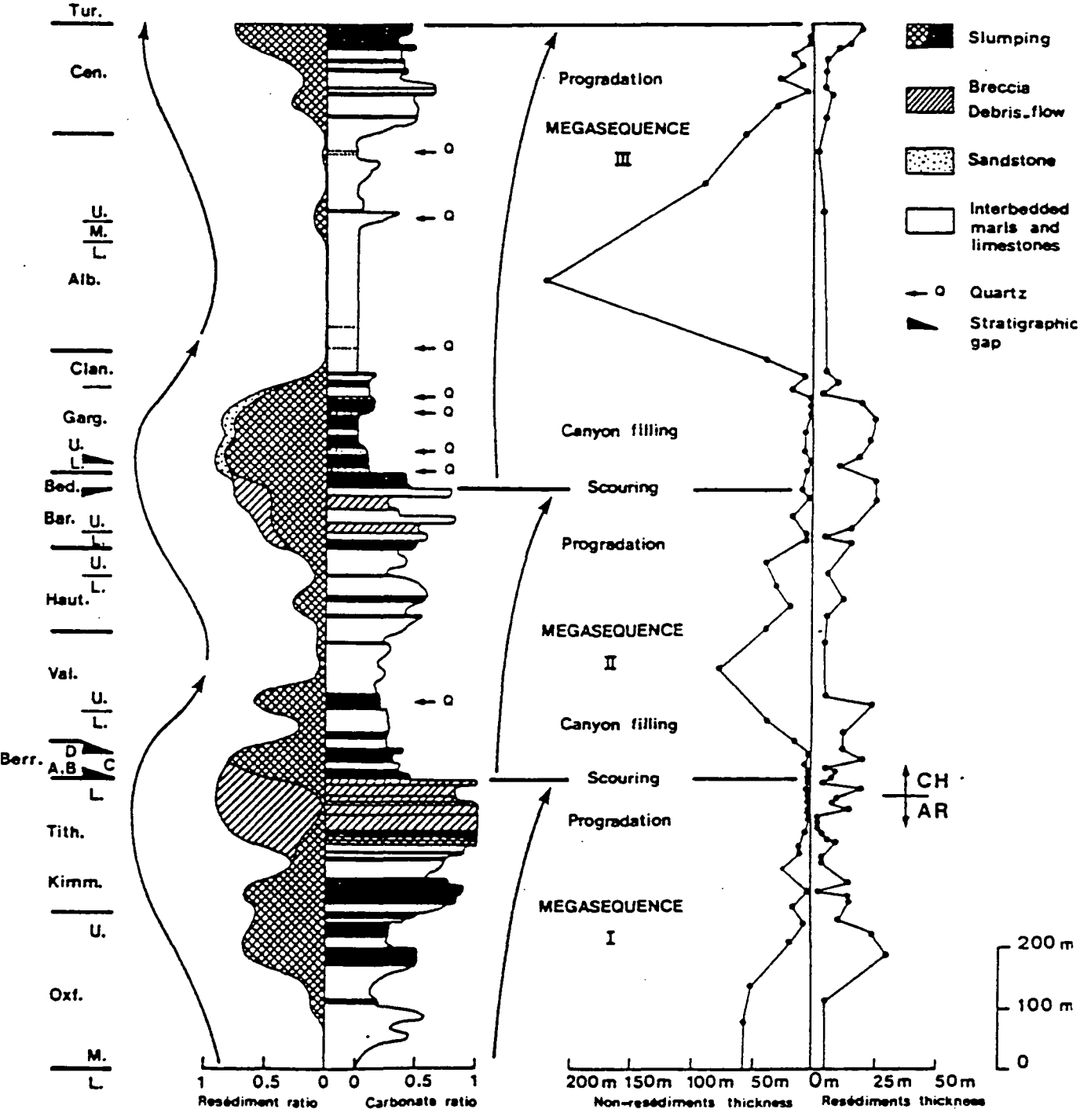

Figure 4.14. Relationship of the asymmetric limestone-shale and clay mineral megasequences to the rates and types of resedimentation (From Joseph *et al.* 1985).

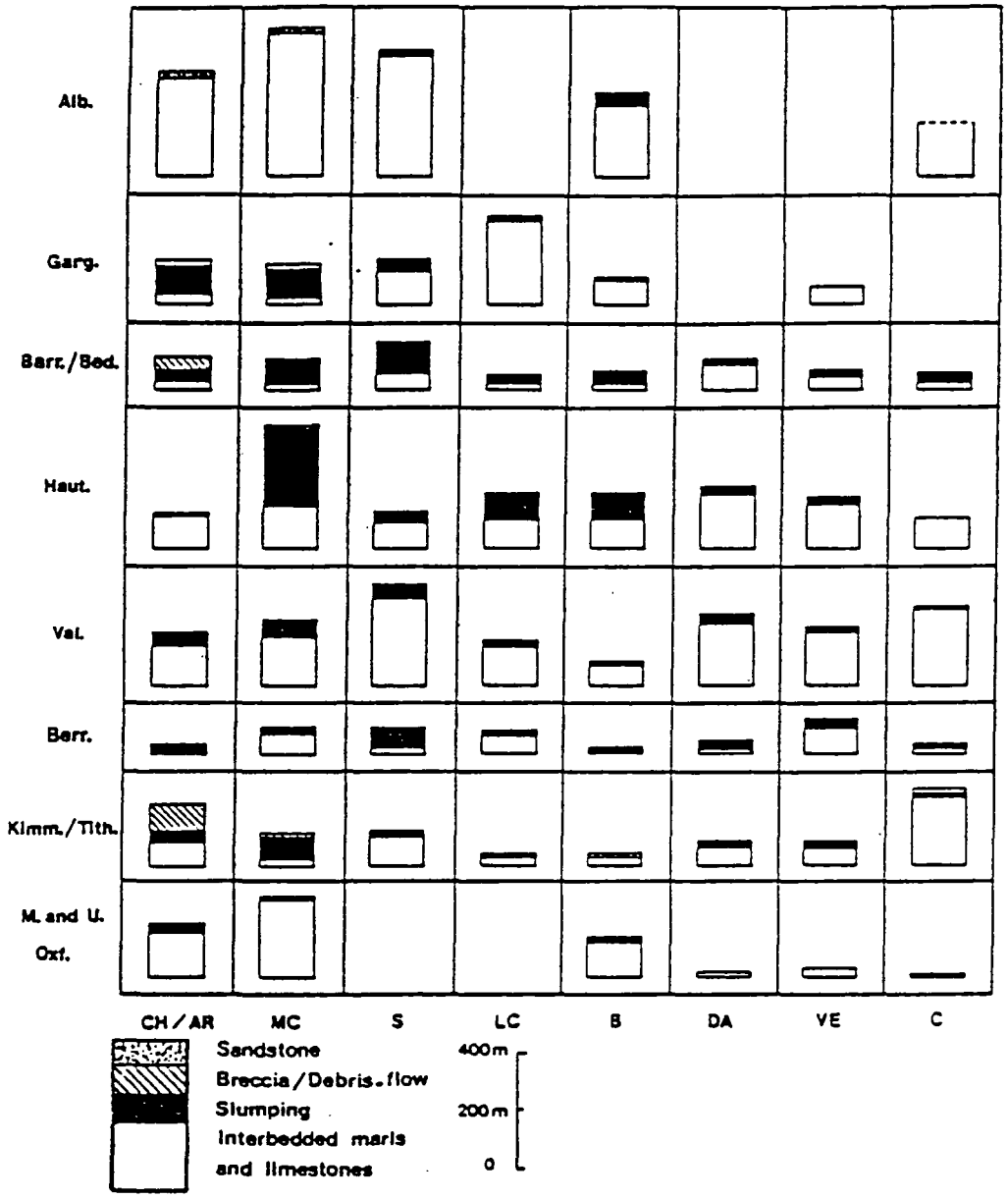

Figure 4.15. Ratio of resedimentation to pelagic sedimentation during the lower Cretaceous and thicknesses of sedimentation during each stage. Note that during times of carbonate platform progradation the thickness of pelagic sedimentation was much reduced (From Joseph *et al.*, 1985).

Pelagic sediments of the basin are cut by submarine channels and canyons which tend to be localised along the hanging walls of extensional fault-blocks (Fig. 4.12, Jospeh *et al.*, 1989). Thus, the channels mainly trend E-W in the southern part of the basin and have a N-S or NW-SE orientation in the northern part of the basin (Fig. 4.12). The main canyons which enter the basin from the north (eg. Die and Saillnas canyons, Fig. 4.12) tend to swing to an E-W orientation as they reach towards the centre of the basin (Joseph *et al.*, 1988; Joseph *et al.*, 1989; Graciansky & Lemoine, 1988).

The progressive development of the flanks and basin-floor of the Vocontian Basin during the late Jurassic and Cretaceous is summarised in Figure 4.12. From the Tithonian to the Valanginian most redeposition was derived from the north via N-S or NNW-SSE canyons and channels (Joseph *et al.*, 1988,; Joseph *et al.*, 1989). In the Hauterivian this pattern continued, although of lesser importance and was augmented by the easterly Rosans canyon (Fig. 4.12, Joseph *et al.*, 1989). By way of contrast during the Barremian and the Aptian patterns of basin-floor resedimentation were radically altered: bioclastic sands were deposited as discrete fans such as the St. Jalle, St. Auban, Bordeaux and Borne fans at the basin margins rather than being transported significant distances within elongate channels or canyons (Fig. 4.12 E). In the Aptian-Albian with the demise of the Urgonian platform basin-floor reworked sedimentation once more became concentrated to the centre of the basin (eg. Fig. 4.12 F).

In contrast to the asymmetric cycles defined by pelagic limestone-shale ratios and clay mineralogy, three distinct symmetrical cycles of resedimentation can be distinguished from the late Jurassic to late Cretaceous as shown in Figure 4.14. The proportion of resedimentation increases gradually to coincide with the maximum progradation of carbonate platforms but symmetrically decreases above the megasequence boundaries defined on the basis of the limestone shale ratio and clay mineralogy (eg. Fig. 4.14). The greatest proportion of resedimentation coincides with the highest proportion of limestone, and approximately with the most basinward progradation of platform facies on the Jura Platform (eg. compare Figs 4.8, 4.11 & 4.14). The gradual decline of the resedimentation ratio above the megasequence boundary contrasts markedly with the pronounced asymmetric cycles, coincident with the abrupt top of the megasequences.

4.3.2. D. Discussion.

As discussed in the preceding section the basic limestone-shale couplets which characterise the Vocontian Basin are interpreted by Cotillion *et al.* (1980) and

Cotillion (1987) to represent 20 000yr climatic cycles. Ferry & Rubino (1989) note that these basic couplets in the field are commonly grouped into bundles of 3 or 5 which could represent the 100 000yr Milankovitch climatic signal. However, the Fourier transform analysis of Rio *et al.* (1989) upon the lower Cretaceous (Fig. 4.16) failed to resolve the Milankovitch 100 000yr eccentricity or the 400 000yr eccentricity supercycle although distinct clusters do occur. Such a poor muting of the astronomical signals may reflect the diminished role of glacio-eustasy during the Cretaceous.

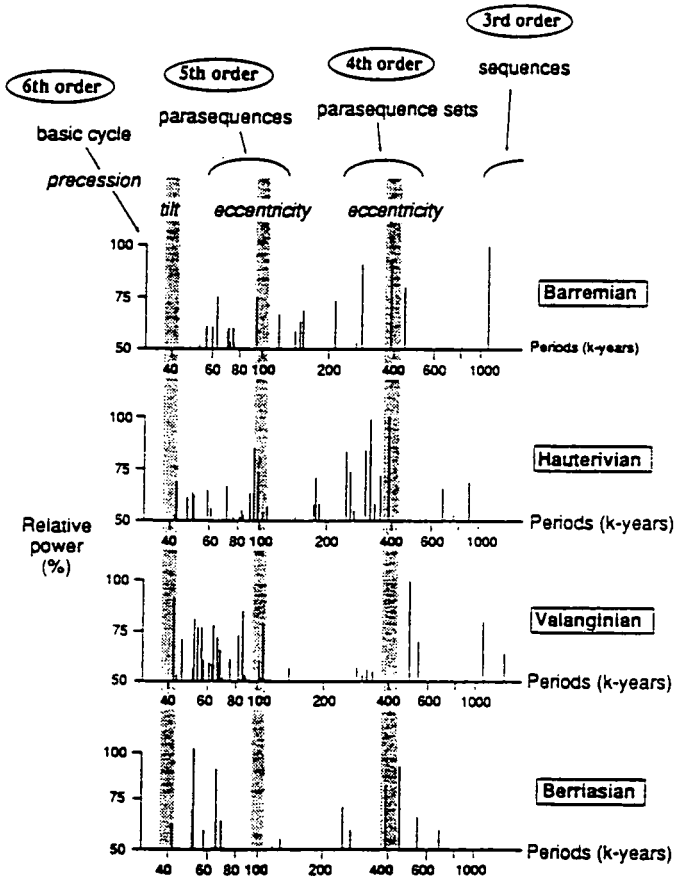

Figure. 4.16. Fourier transform analysis of the lower Cretaceous limestone-shale alternations of the Vocontian Trough and possible correspondance with cycle orders of sequence stratigraphy. Note that there is no strong 100 or 400 000 yr eccentricity astronomical signature (From Ferry & Rubino, 1989, after Rio *et al.*, 1989).

In the Vocontian Basin the pelagic carbonate-shale ratio defines three distinct asymmetric cycles or megasequences from shale to limestone dominated times during the late Jurassic and Cretaceous (Ferry & Rubino, 1989, Figs 4.11 & 4.14) and these are closely matched to clay mineral cycles (Deconinck, 1984). Analogy of the basic

limestone-shale couplets to well known Pleistocene counterparts strongly suggests that limestones correspond to warmer climatic conditions and vice versa. Arnaud (1981) and Ferry & Rubino (1989) demonstrated that times of carbonate dominated sedimentation in the Vocontian Basin correspond to times of carbonate platform progradation on the Jura Platform.

Comparison of the stacking patterns and facies to clay mineral trends from the Vocontian Basin to northern Europe for the Tithonian suggests that carbonate platform progradation occurred under more arid climate across much of northern Europe (Ruffel & Batten, 1990). A similar stratigraphic pattern and clay mineral shift is developed in the Vocontian Basin during the Barremian when the Urgonian platform developed (Fig. 4.14, Deconinck, 1984; Ferry & Rubino, 1989; Ruffel & Batten, 1990). This association suggests that the progradation of carbonate platforms (Tithonian-Berriasian, Urgonian) is a response to climatic variation and platforms are best developed when a warmer, arid climate prevailed and precipitation rates and hence the supply of fine siliciclastics were reduced. This relationship is also suggested by sedimentation rates in the basin which are reduced during times of platform progradation (eg. Fig. 4.15). Such a relationship suggests that a reduction of the rate of input to the basin of fine siliciclastic clays rather than an increase of pelagic carbonate production is responsible for the shift to limestone dominated sedimentation during times of carbonate platform progradation.

Resedimentation of slope and shallow-water bioclastics onto the basin-floor during the three asymmetric megasequence shows a more symmetrical variation (Fig. 4.14). Resedimentation generally increases progressively towards the top of a megasequence and similarly decreases above the boundary. This suggests that as carbonate platform sedimentation prograded, slopes became increasingly unstable and, following the maximum progradation of a platform, slopes gradually re-equilibrated by collapse. Development of the Urgonian platform on the flanks of the basin is associated with major palaeogeographic reorganisations in the basin. The

Urgonian platform is associated with the change from elongate channels and fans to discrete lobes of sediment at the toe-of-slope (eg. Joseph *et al.*, 1989, Fig. 4.12).

4.3.3. The Dauphinois Basin and the Jura Platform. Geographic and geological setting.

The Dauphinois Basin is today bound to the northwest by the Cevennes-Isère lineament and to the east by the Internal Alpine zones (Fig. 4.3) and is represented by the Belledonne Massif and the Sub-Alpine Chains (Vercors and Chartreuse) to the north of the Vocontian Basin (Fig. 4.1). The Jura Platform lies to the northwest of the Cevennes-Isère lineament, approximately coincident with the western geographical boundary of the Sub-Alpine Chains. The Massif de Vercors is bound on its eastern side by the Drac valley as is Massif de Chartreuse bound on its eastern side by the sill on subalpin (Fig. 4.17). The northern boundary of the Massif de Vercors is the Cluse d'Iseran, the NW-SE trending U-shaped valley in which the city of Grenoble is situated. The Massif de Chartreuse extends northeast from the northern side of this valley and is bounded to the north by the NW-SE trending U-shaped valley in which the city of Chambery is located (Fig. 4.17).

Both Vercors and Chartreuse Massifs represent the western part of the Dauphinois Basin, dominated by lower Cretaceous stratigraphy deposited during the thermal subsidence phase of passive margin formation. The eastern part, to the east of the Drac valley and sillon subalpin, the Belledonne Massif, is characterized by well preserved extensional tilt blocks of the rifting stage of the passive margin development (eg. Fig. 4.7) (Lemoine *et al.*, 1986, See section 4.2).

4.3.3. A. Structure.

During the Miocene and Pliocene the Sub-Alpine Chains and Jura accommodated the last few kilometres of Alpine shortening (Butler, 1989; Mugnier *et al.*, 1990), mostly contained to the east of the Isère lineament. The Isère fault limited the western propagation of Alpine thrusting and folding in the southern

A = Cirque d' Archiane
BE = Balcon des Ecouges
BG = Borne Gorge
BM = Montagne de Belle Motte
BOR = Borne
CED = Chatillion-en-Diois
CL = Combe Laval
CP = Col du Pionnier
CR = Col de Rousset
FR = Font Renard
FU = Font d'Urle
G = Gigors
GF = Gorge du Frou
GG = Grands Goulets
GN = Gorge du Nant
LC = La Chambotte
LCH = La Chaudiere
LCL = Les Clappiers
LM = La Montagnette
LN = Le Neron
LR = Les Rimets
MA = Mont Aiguille
MG = Mont Granier
MN = Mont Noir
PE = Pas de l'Echelle
PES = Pas de Essaure
RC = Rocher du Combau
SA = Saillans
TC = Tete Chevaliere
TM = Tunnel du Mortier
TO = Le Toussiere
TP = Tete Praorzel

Lines of section.

1 = 5.3 & 6.37
2 = 6.23
3 = 6.32
4 = 6.30
5 = 6.29
6 = 6.28
7 = 5.20, 5.39 & 5.40
8 = 5.52
9 = 5.49 & 6.45
10 = 6.13
11 = 5.7 & 6.15
12 = 5.23 & 6.10
13 = 5.21, 5.23, 6.16, 6.17 & 6.18
14 = 5.22, 5.30, 5.33, 5.35 & 5.37
15 = 6.31
16 = 6.43
17 = 5.43
18 = 6.4 & 6.9

Location

France

JURA
BAS DAUPHINE
JURA
LC
Aix-les-Bains
Chambery
0 10 20km
MG
GF
PE
PO
CHARTREUSE
Cluse d'Iseran
Sillon subalpin
TM
LN
FR
LCL
BE
Autrans
Grenoble
GN
MN
LR
VERCORS
BG
Villard-de-Lans
Vif
BELLEDONNE
Romans-sur-Isere
GG
Isere fault
CL
CP
18
Drac valley
3
4
FU
5
Clery Fault
Jasneuf Fault
CR
6
MA
7
TC
PE
10
Menee Fault
Mens
G
9
8
LM
RC
TP
12
11
14
15
DEVOLUY
Die
Crest
A
13
BM
BOR
SA
DIOIS
CED
Jocou Fault
BORNE
TO
16
18
17
LCH

Chartreuse and Vercors (Butler, 1989; Roberts, 1990) (Fig. 4.18b). In both the Sub-Alpine Chains and Jura Platform there is little evidence of the E-W trending upper Cretaceous folding and thrusting characteristic of the southerly Vocontian Basin and Provence, although the Isère lineament was reactivated as a strike-slips fault with local inversion along its length at this time (Arnaud, 1981). More importantly, within the Dauphinois Basin and Jura Platform prior to Alpine orogenesis is Oligocene E-W extension associated with development of the Rhône-Bresse graben. This extension was associated in both the Jura and much of the Dauphinois Basin with reactivation of the major NNE-SSW and N-S trending Mesozoic lineaments such as the Isère-Cevennes lineament (Blès *et al.*, 1989).

Along the strike of the Massifs de Vercors and Chartreuse the trend of Alpine fold and thrust structures changes (Fig. 4.19). The Vercors to the south of Villard-de-Lans and west of Autrans (Fig. 4.19) is characterized by N-S trending folds and thrusts whose Alpine are displacements are normally small (1-2km) and generally decrease southwards. These N-S trending structures intersect with and are bound to the west by the NNE-SSW trending mountain front. Contrastingly, the northern Vercors and the Chartreuse Massifs are characterized by NNE-SSW trending Alpine fold-thrust structures which parallel the Dauphiné trend of the mountain front (Figs 4.1 & 4.19).

In much of the Vercors the location and orientation of the main Alpine fold-thrust structures owes much to the pre-existing Mesozoic and Cenozoic (Oligocene) basin structure (Butler, 1989; Roberts, 1990). An example of this control upon the location of Alpine structures is the N-S trending Rencurel thrust of the central and northern Vercors (Fig. 4.19). The thrust displacement of this fault tips out

Figure 4.17. (preceding page) Location map showing the Massifs de Vercors and Chartreuse, separated from the eastern Dauphinois Basin by the Drac valley and sillon subalpin respectively. Note that the front of the Sub-Alpine Chains (Vercors and Chartreuse Massifs) is approximately coincident with the Isère fault.

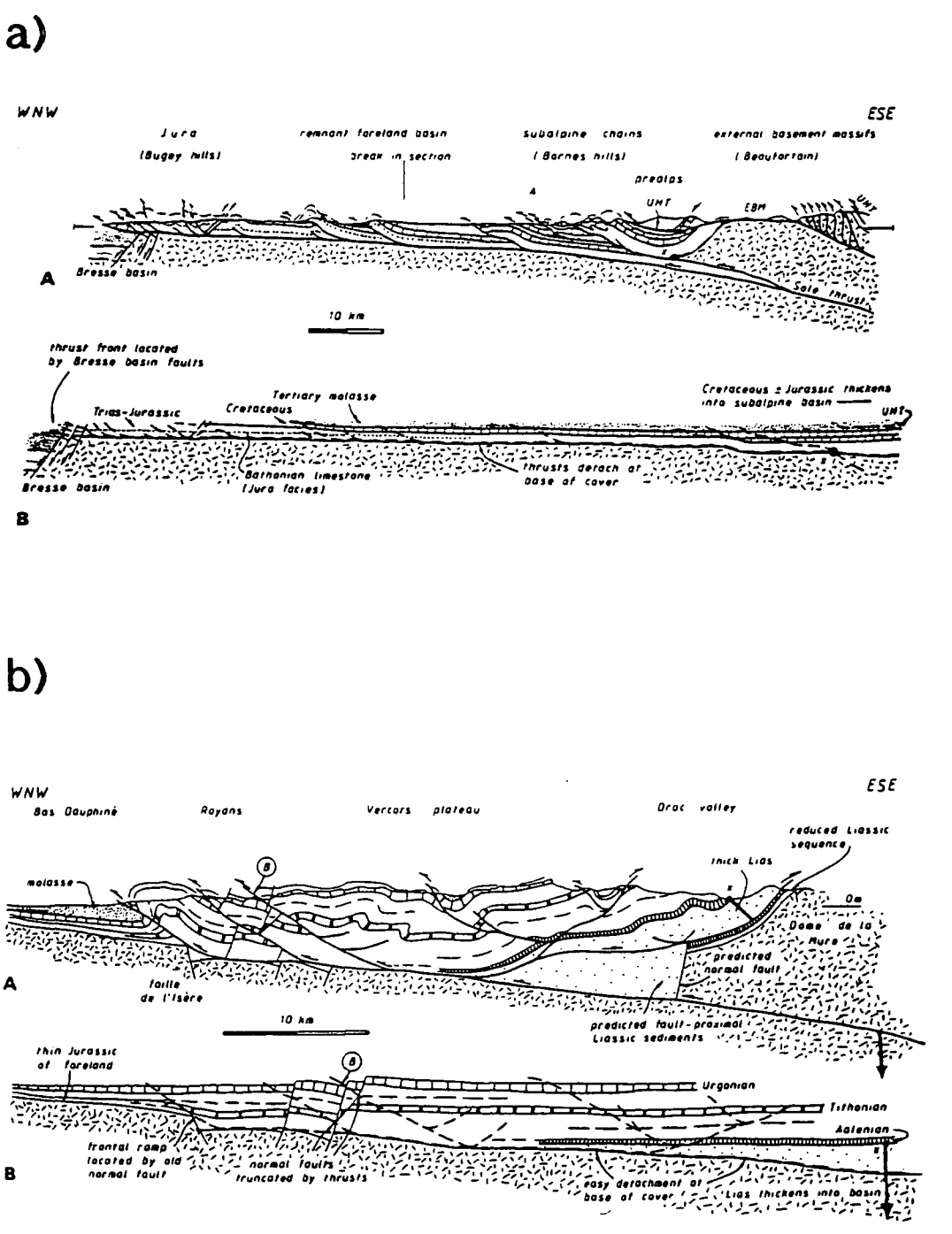

Figure 4.18. Cross-sections across the Sub-Alpine Chains as located on Figure 4.1. These two sections illustrate the constant 30km of shortening ahead of the Belledonne massif. Note the difference in structural style from the Borne-Aravis to the Vercors Massifs. In the northern section (a) almost all shortening is taken up by foreland directed thrusting whereas in the Vercors most displacement is taken up by backthrusting (b). Pre-existing basin structure exerts a strong control upon the location of subsequent inversion structures in the Vercors as can be seen on the restored template of this section. (From Butler, 1989)

southwards as it passes into the Faille de Rochers de Chironne which acted to locate the Rencurel thrust fault further north. Joseph *et al.* (1989) interpreted this fault to have controlled the position of the Die canyon during the lower Cretaceous (eg. Figs 4.12 & 4.13). Perhaps the best example of the influence of pre-existing basin structure upon the location of Alpine fold-thrust structures is the Isère lineament which acted to localise the mountain front of the Sub-Alpine Chains from the southern Vercors to northern Chartreuse (Butler, 1989; Roberts, 1990) (eg. Figs. 4.1, 4.18 & 4.19).

In the northern Vercors (north of Villard-de-Lans and east of Autrans, Fig. 4.19) and Chartreuse where foreland directed thrust displacements are more substantial the role of pre-existing basin structure upon the location of Alpine structures is ambiguous. It is worthy of note, however, that the NNE-SSW orientation of Alpine folds and thrusts in this area closely match the Dauphiné trend of the Isère lineament. By way of contrast, the southern Jura is characterized by N-S to NW-SE trending Alpine fold-thrust structures (Fig. 4.1). The orientation of these structures reflects the increasing northward displacements within the Jura mountains which rotated the southern Jura structures anti-clockwise to their present orientation as the northerly thrusts propagated farther into the foreland (eg. See Mugnier *et al.*, 1990).

Arguments developed from crustal scale section balancing of the Alpine Sole Thrust upon which the Belledonne Massif is interpreted to have been carried (eg. Fig. 4.18), suggest a constant 30km of displacement along the length of the Massif (Butler, 1989). This shortening was accommodated within the Sub-Alpine Chains but differentially along their strike (Butler, 1989). In the northern Chartreuse, where the Jura mountains swing into the front of the Sub-Alpine Chains (Fig. 4.1) displacement was almost entirely taken up by foreland directed thrusting, contained to the east of the Isère lineament, which approximately marks the mountain front of the Sub-Alpine Chains (Butler, 1989) (Figs 4.1 & 4.18). Only 1-2km of shortening was accommodated by folding and thrusting in the Jura in this area (eg. Butler, 1989).

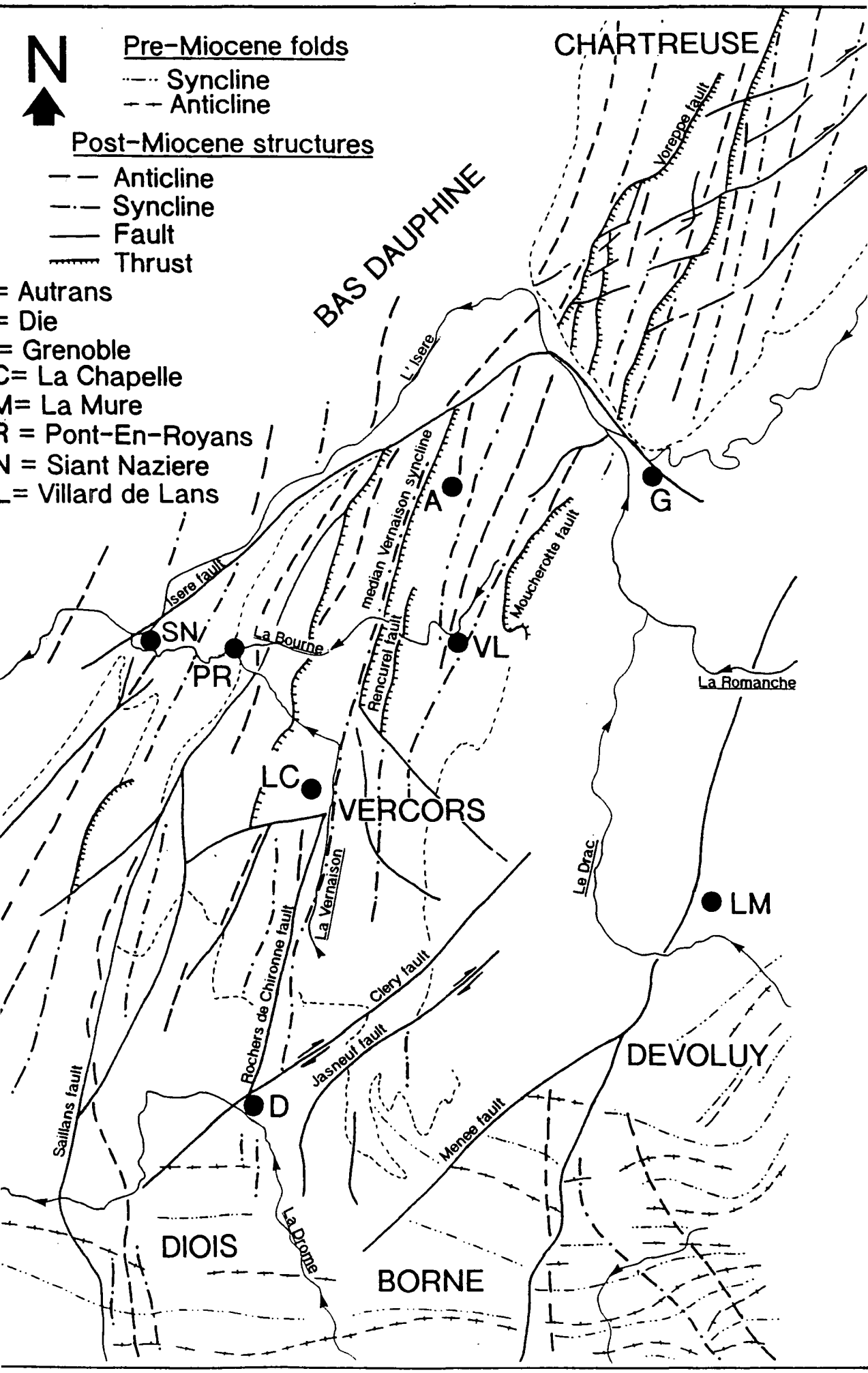
N
Pre-Miocene folds
Syncline
Anticline
Post-Miocene structures
Anticline
Syncline
Fault
Thrust
= Autrans
= Die
= Grenoble
C= La Chapelle
M= La Mure
R = Pont-En-Royans
N = Siant Naziere
L= Villard de Lans
CHARTREUSE
Voreppe fault
BAS DAUPHINE
L' Isere
median Vernaison syncline
A
G
Isere fault
SN
PR
La Bourne
Rencurel fault
VL
Moucherolle fault
La Romanche
LC
VERCORS
La Vernaison
Le Drac
LM
Rochers de Chironne fault
Clery fault
Jasneuf fault
DEVOLUY
Saillans fault
D
Menee fault
DIOIS
La Drome
BORNE

Southwards, in the southern Chartreuse and Vercors the Isère lineament acted as a very efficient buttressing structure as very little shortening was accommodated to the west of this fault (Butler, 1989; Roberts, 1990).

Southwards, along the strike of the Sub-Alpine Chains from the southern Chartreuse to the south of the Vercors the amount of displacement from the Alpine Sole Thrust was increasingly accommodated by backthrusting as the amount of foreland directed thrusting decreased (Butler, 1989; Roberts, 1990) (eg. Fig. 4.18). In the southern Vercors almost all shortening is interpreted to have been taken up by backthrusting which moved the cover stratigraphy eastwards over the top of the advancing thrust wedge (Butler, 1989, Fig. 4.18).

4.3.3. B. Comparative late Jurassic-Cretaceous stratigraphy and dynamics of the Jura Platform and Dauphinois Basin.

As discussed in Section 4.2 the Jura Platform is characterized by slower subsidence rates and separated from the Dauphinois Basin by the Isère lineament which localised subsidence during Mesozoic extension (eg. Figs 4.3, 4.4 & 4.5) (Arnaud, 1988). Shallow-water carbonate sedimentation dominates the Jura Platform for much of the Cretaceous whilst the more highly subsident Dauphinois Basin mostly received the periplatform carbonate muds off the Jura Platform (eg. Fig. 4.20). The progradation of shallow-water carbonate sedimentation across the Jura Platform and eventually into the Dauphinois Basin is coincident with the shift to limestone

Figure 4.19. (preceding page) Structural summary map of the Vercors and southern Chartreuse Massifs. Note the difference in the trend of Alpine fold and thrust structures between the southern Vercors and northern Vercors/Chartreuse massifs. The mountain front of the Sub-Alpine Chains (Vercors and Chartreuse Massifs) trends approximately NNE-SSW and is interpreted to be localised along the Isère lineament. This trend is oblique to most Alpine structures of the southern Vercors but parallels those of the northern Vercors and Chartreuse. Adapted from Arnaud (1981).

dominated sedimentation in the Vocontian Basin (eg. Tithonian-Berriasian, and Barremian-Aptian, compare Figs. 4.8, 4.9 and 4.11, see Section 4.3.2). However, whereas the shifts to limestone dominated sedimentation in the Vocontian Basin are

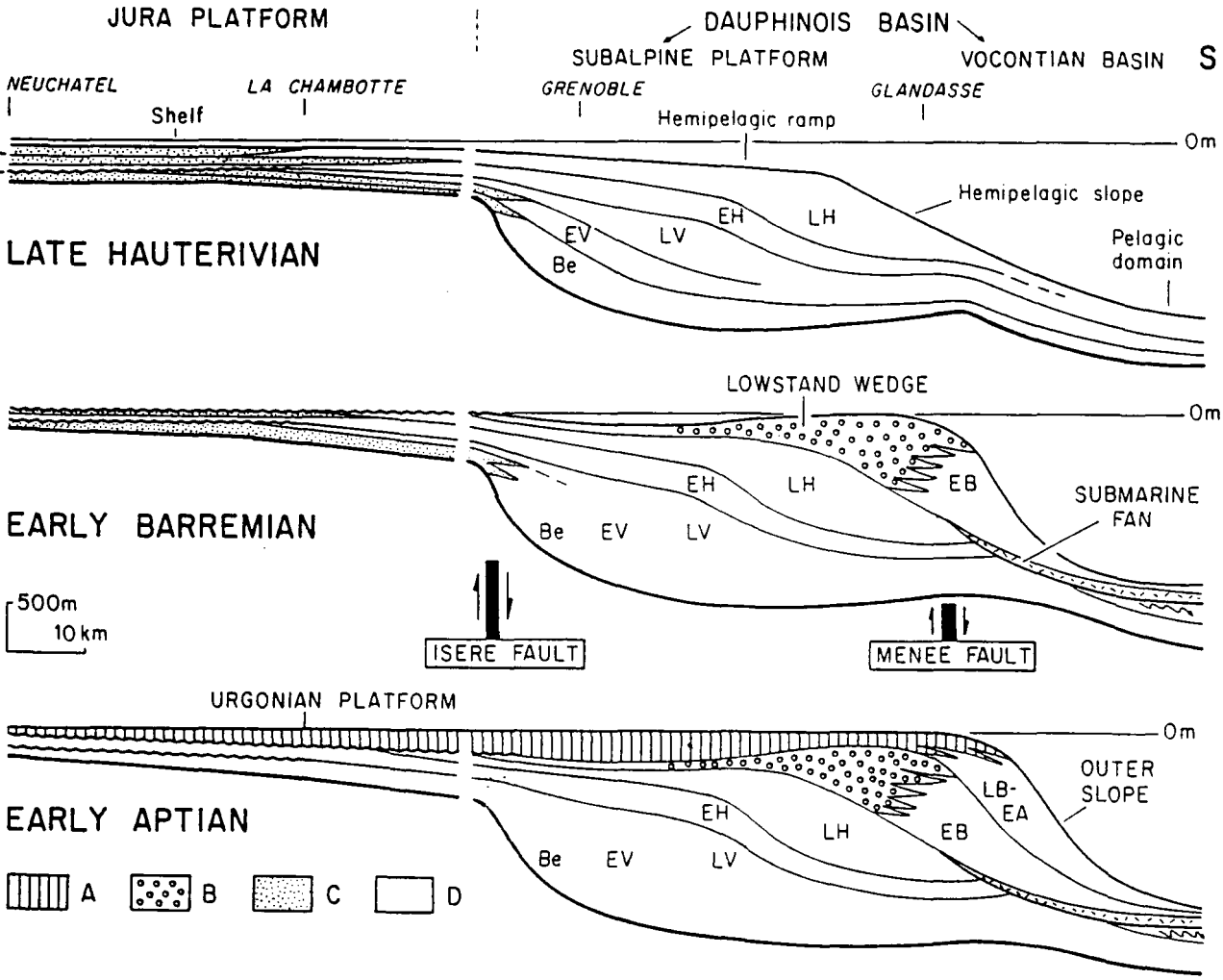

Figure 4.20. Schematic cross-sections showing the progressive development of the Jura Platform and Dauphinois Basin (Neuchâtel-southeastern Vercors). (A) Urgonian Limestone Formation; (B) Glandasse Bioclastic Limestone Formation; (C) Berriasian-Hauterivian platform facies; (D) basinal periplatform to pelagic facies. (1) Erosion surface above the Valanginian platform in the Neuchâtel area (Swiss Jura); (2) Pierre Jaune de Neuchâtel Formation (bioclastic limestone). Be = Berriasian; EV = early Valanginian; LV = late Valanginian; EH = early Hauterivian; LH = late Hauterivian; EB = early Barremian; LB-EA = late Barremian - early Aptian. From Arnaud-Vanneau & Arnaud (1990).

marked by a decrease of sedimentation rates (Fig. 4.15) in the Jura and proximal parts of the Dauphinois Basin the converse is true (eg. Figs 4.8 & 4.10).

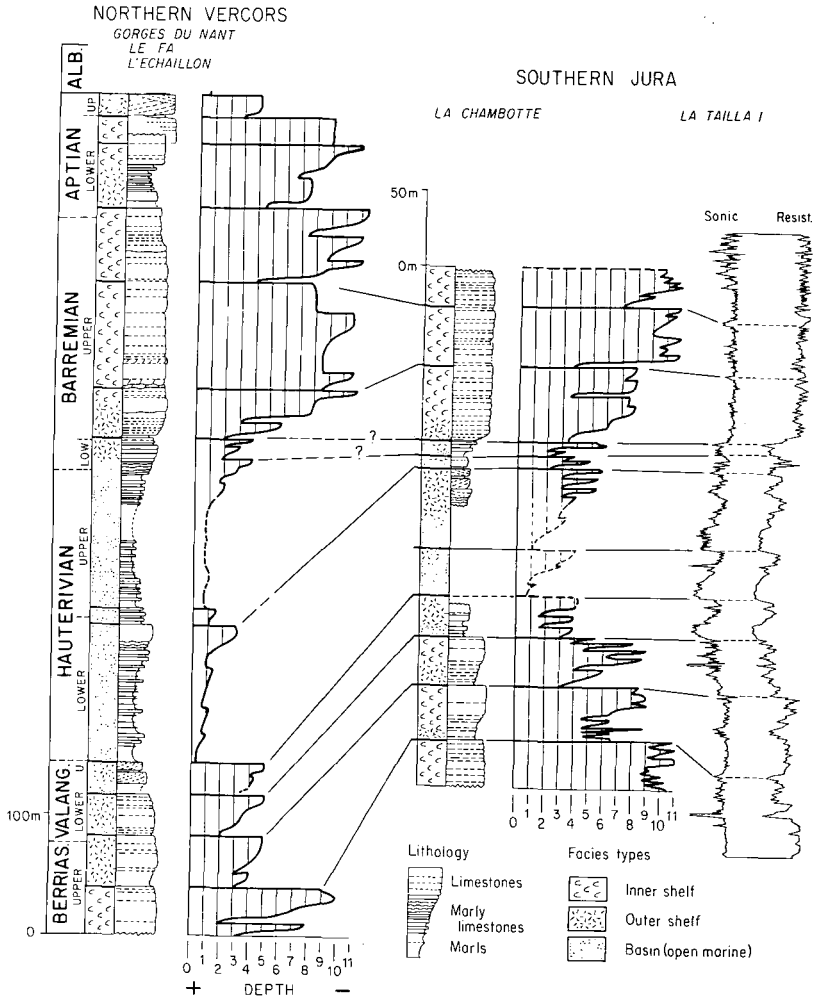

Figure 4.21. Facies evolution curves and stratigraphic correlations of Arnaud (1988) between the northern Vercors and southern Jura. Facies 0: biomicrite with radiolaria and ammonites; 1: biomicrite with sponge spicules; 2: biopelmicrite with echinoids; 3: biomicrite-biosparite with echinoderm debris and small foraminifera; 4: biomicrites-sparites with bryozoans and crinoids; 5: biosparites with large rounded grains; 6: oosparites and bio-oosparites; 7: biosparites with corals or boundstones; 8: biosparites-micrites with large foraminifera and occasional large rudists; 9: biosparites-micrites with miliolids and rudists; 10: biosparites-biomicrites with oncolites; 11; biomicrites-sparites with birdseye fenestrae and/or keystone vugs.

The upper Jurassic and lower Cretaceous stratigraphy of the Dauphinois Basin and southern Jura Platform is summarised in Figures 4.20 & 4.21. As an immediate contrast it is evident that the stratigraphy of the Dauphinois Basin is considerably thicker than that of the southern Jura Platform. This contrast is reflected by the minimum sedimentation rates for these areas as illustrated in Figure 4.10 (Arnaud, 1988). For the lower Cretaceous (Berriasian-Barremian) in the Jura minimum sedimentation rates vary between 13 and 31m per million years whereas in the Dauphinois Basin this figure is approximately double, between 31 and 80m per million years (Fig. 4.10) (Arnaud, 1988). Arnaud (1988) suggested that as the minimum sedimentation rates were differential across the Isère fault this lineament and similarly the more southerly Menée fault (close to the location of the Montagnette Section, Fig. 4.10) (Fig. 4.19, 4.20) were reactivated and localised subsidence during the lower Cretaceous.

The lower Cretaceous minimum sedimentation rates for both the Jura Platform and Dauphinois Basin form three distinct asymmetric cycles of sedimentation rate which can be correlated from the Jura to the northern margin of the Vocontian Basin (eg. Fig. 4.10, sections located on Fig 4.3A) (Arnaud, 1988). Each cycle (eg. upper Berriasian-Hauterivian, lower Hauterivian-upper Barremian and upper Barremian-Albian, Fig. 4.10) is characterized by an initial, rapid acceleration of the sedimentation rate followed by a gradual decrease and a long period of time when sedimentation rates were approximately constant. These asymmetric, cyclic accelerations and decelerations of sedimentation rate are coincident with abrupt facies changes upon the Jura Platform and in the Dauphinois Basin, but are not obviously related to megasequences of the Vocontian basin (eg. compare Figs. 4.10 & 4.14).

The minimum sedimentation rates of the southern Vercors (marginal to the Vocontian Basin) varied independently during the Hauterivian and Lower Barremian compared to those of the Jura Platform and northwestern Dauphinois Basin (eg. Fig. 4.10). The acceleration of sedimentation rates at the base of the Hauterivian in the southern Vercors is similar to that of the northwestern Dauphinois Basin and Jura

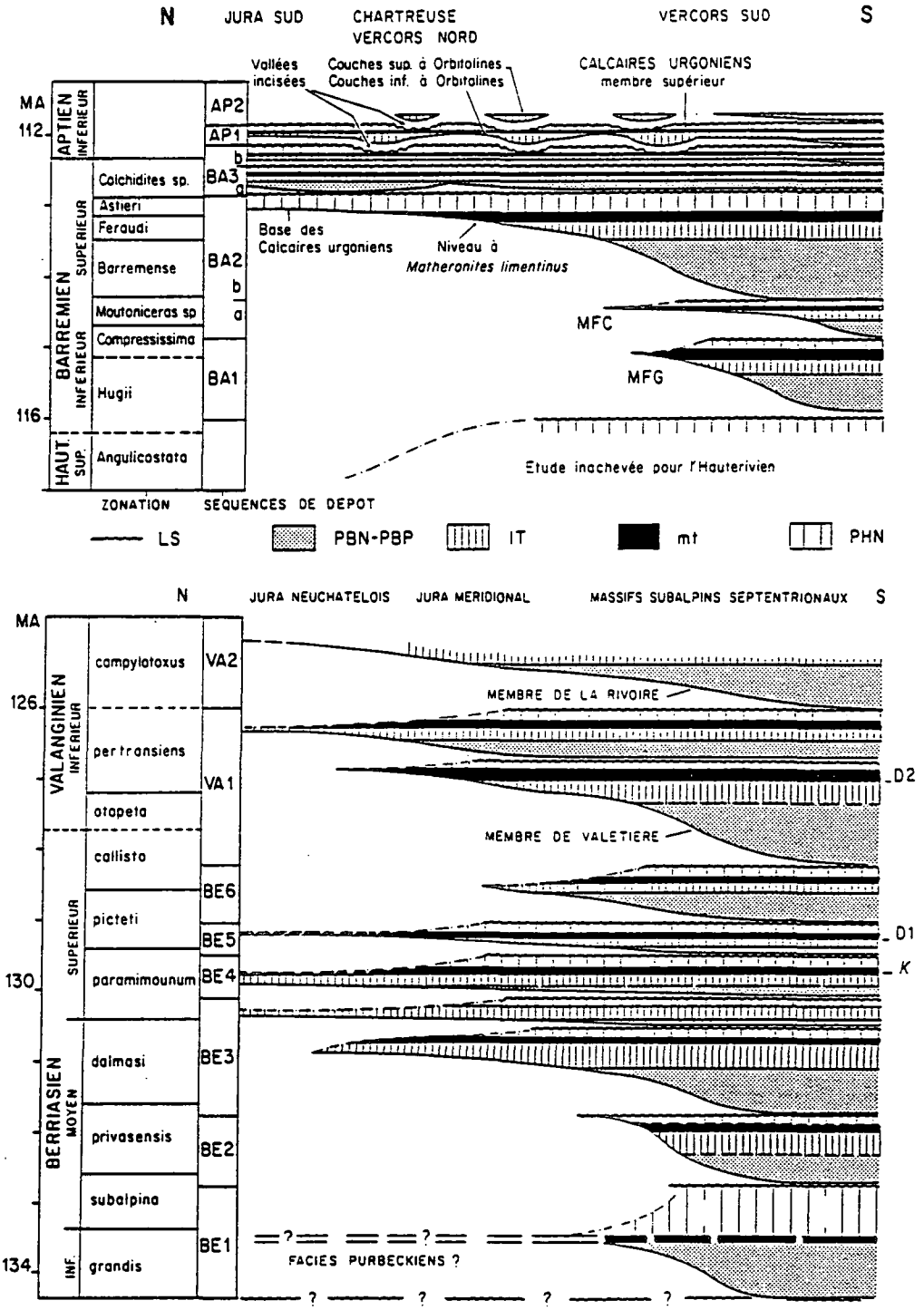

Figure. 4.22. Sequence stratigraphy of the Berriasian-early Valanginian and Barremian-early Aptian in geologic time (time scale according to Haq *et al.*, 1987, slightly modified). LS: Sequence boundary; PBN-PBP: lowstand wedge-shelf margin wedge systems tract; IT: transgressive systems tract; mt: maximum flooding surface; PHN: highstand systems tract. CIO: Lower *Orbitolina* beds; CSO: upper *Orbitolina* beds; MFG: Fontaine Graillère marls; MFC Fontaine Colombette marls; D1, D2: discontinuities according to Darsac (1983); K: *Keramosphera allobrogensis* level (From Arnaud-Vanneau & Arnaud, 1991). The sequence boundary BE5 between level K and D1 is illustrated in Figure 4.23.

Platform (Fig. 4.10). However, during the Hauterivian and lower Barremian by way of contrast to the northern Dauphinois Basin and Jura Platform sedimentation continued to be high and even accelerated in the southern Vercors. At the beginning of the upper Barremian rather differently from the northern Dauphinois Basin and Jura Platform sedimentation rates in the southern Vercors decreased (Arnaud, 1988) (Fig. 4.10). Arnaud (1988) suggested that the differences of sedimentation rate between the northern and southern Vercors (Dauphinois Basin) show that these two regions had become tectonically independent and argued for the reactivation of the Isère and Menée faults (Fig. 4.19) during the Hauterivian and Barremian.

Upon the Jura Platform upper Jurassic and lower Cretaceous sedimentation is characterized by the progradation, aggradation, retrogradation and subaerial exposure of carbonate platforms. Three major stratigraphic gaps exist on the Jura Platform in the lower Cretaceous as illustrated in Figure 4.22 and these are: the lower Berriasian, *grandis* zone to mid *dalmasi* zone, upper Berriasian *callisto* zone to lower Valanginian *otopeta* zone and the upper Hauterivian *angulicostata* zone to upper Barremian *feraudi* zone (Arnaud-Vanneau & Arnaud, 1991). By way of contrast the stratigraphy of the Dauphinois Basin is relatively complete (eg. Fig. 4.22) and few stratigraphic gaps exist with the notable exception of the uppermost Hauterivian-lower Barremian (*angulicostata* to *feraudi* zones) (Arnaud & Arnaud-Vanneau, 1989; Arnaud-Vanneau & Arnaud, 1990; Arnaud-Vanneau & Arnaud, 1991) (Fig. 4.22) (see Section 4.4 for further discussion of Barremian stratigraphy).

On the Jura Platform these stratigraphic omissions correspond to subaerial hiatuses (eg. sequence boundaries, Figs 4.22 & 4.23). During the Berriasian and the Valanginian relative sea-level lowstands much, if not all of the Jura Platform is interpreted to have become exposed (Arnaud-Vanneau & Arnaud, 1991) and shallow water carbonate sedimentation was localised upon the northeastern slopes of the Dauphinois Basin (eg. Gorge du Guier Mort in the Chartreuse, Darsac, 1983; Boisseau, 1987). On these slopes, just east of the Isère lineament a laterally discontinuous narrow strip (<2km wide) of high energy bioclastic facies and even

rudist facies (Valanginian) were developed, the lowstand wedge(s) of Arnaud-Vanneau & Arnaud (1991). Carbonate platform sedimentation on the Jura Platform during the lower Cretaceous is interpreted to have mostly developed during times of rapid relative sea-level rise (the TST) and highstands of relative sea-level (Fig. 4.22).

Figure 4.23. The sequence boundary BE5 developed at the La Chambotte section (southern Fench Jura) between sequences BE4 and BE5. The sequence boundary is an exposure horizon which was vegetated upon exposure as evidenced by the partially drusy calcite filled rhizoliths developed into shallow, reddened subtidal-intertidal micrites with birdseye fenestrae. The maximum flooding surface to the next sequence at the base of the *picteti* zone (Fig. 4.22) lies approximately 5m above. Pen, approximately 8cm long for scale.

The Hauterivian represents a time during the lower Cretaceous when the Jura platform was transgressed to such an extent that shallow water carbonate sedimentation was drowned across much of the Jura (eg. Fig. 4.8 & 4.21). In the

southern Jura the Hauterivian is characterized by the development of outer shelf type facies, arranged into 5-10m shallowing up cycles from subwave base siliciclastic rich lime mudstones-wackestones to shallow water crossbedded grainstones which are often oolitic, typically capped by a hardground which represents the beginning of the next cycle (eg. Arnaud-Vanneau & Arnaud, 1990). These represent the outer part of the Pierre Jaune de Neuchâtel platform which is dated as lower to ? upper Hauterivian in age (possibly to *sayni* - *anguilcostata* zones, Arnaud-Vanneau & Arnaud, 1990). In the Dauphinois Basin the Hauterivian is typified by the development of nodular limestones with interbedded shales (Fig. 4.24) (the 'calcaire à miches' of the French). The upper Hauterivian is variably and incompletely developed below the Urgonian platform across the Jura Platform and Dauphinois Basin and is unfortunately generally poorly dated but varies between the *sayni*, *balearis* and *anguilcostata* zones of the upper Hauterivian along and across the strike of the Jura Platform and Dauphinois Basin (eg. Clavel *et al.*, 1987, Fig. 4.26).

The Urgonian platform is interpreted to have developed after a major relative sea-level fall during which a large area of the Dauphinois Basin was exposed (eg Arnaud & Arnaud-Vanneau, 1989). This interpretation elegantly accounts for the absence of a lower Barremian fauna in the Jura and northwestern Dauphinois Basin (Fig. 4.22) and the irregular absence of some upper Hauterivian biozones below the Urgonian limestones upon the Jura Platform and across the Dauphinois Basin (Arnaud & Arnaud-Vanneau, 1989; Arnaud-Vanneau & Arnaud, 1990; Arnaud-Vanneau & Arnaud, 1991) (Fig. 4.22). This interpretation is, however, not uncontroversial and is discussed further in Section 4.4. The lower Barremian is represented in the southern Vercors by the Borne and Glandasse Bioclastic Limestone Formations (Figs 4.20 & 4.22) and overlain by the *Matheronites limentinus* marls which are everywhere interpreted to be at the base of the Urgonian Limestone Formation (Fig. 4.22). The Urgonian platform is itself divided and overlain by the lower and upper *Orbitolina* marls respectively and is divisible into a number of unconformity-bound sequences.

Figure 4.24. Typical outcrop photograph of the 'calcaire à miches', the upper Hauterivian nodular limestones interbedded within shales, here photographed in the northern Vercors on the northern side of the tunnel de mortier approximately 3m below the base of the Urgonian platform. The calcareous nodules have frequently nucleated upon several irregular echinoderms. Rucksack for scale.

The Urgonian platform is overlain by Gargasian and younger glauconitic outer shelf deposits on the Jura Platform and across much of the Dauphinois Basin, and these pass upwards into condensed Albian phosphates containing a pelagic fauna. Where the Urgonian platform was developed this time is associated with a decrease of sedimentation rates whereas in the Vocontian Basin this time is associated with an increase of sedimentation rates (eg. compare Figs 4.10 & 4.15).

4.4. The Urgonian Platform, Definition, History Of Research, And The Palaeontological Controversy.

4.4.1. Definition of the Urgonian platform.

The term Urgonian is commonly used in reference to any limestone facies which contains rudists, the highly asymmetric bivalve which is characteristic of many Cretaceous carbonate platforms. Upon an Urgonian platform rudist facies are typically restricted to a specific environment, such as the high energy shelf-margin (eg. lower Cretaceous of Gulf Coast USA, Bay, 1977, see Fig. 3.22. p. 81, Masse & Philip, 1981) or low energy shelf-lagoon environment as is generally the case for the Barremian-Aptian Urgonian platform of SE France, the subject of this study.

In the case of the Barremian-Aptian carbonate platform of SE France the lower Barremian is characterized by coarse bioclastic facies and true Urgonian facies are restricted to a very thin stratigraphic interval (approximately 5m) near to the top of the Glandasse Bioclastic Limestone Formation (see following Chapters). Urgonian facies are only abundant (and preserved) in the upper Barremian and lower Aptian above the *Matheronites limentinus* level which marks both the top of the Glandasse Limestone Formation and base of the Urgonian Limestone Formation (Arnaud, 1981) (eg. Fig. 4.22). Throughout this thesis the upper Barremian - lower Aptian is referred to as the Urgonian platform *sensu stricto*, comprised of the Urgonian Limestone Formation. Reference to the Urgonian platform *sensu lato* includes both Borne and Glandasse Bioclastic Limestone Formations together with the Urgonian Limestone Formation, bound by the major sequence boundary below the platform (eg. Fig. 4.20 & 4.22).

4.4.2. History of research.

The Urgonian platform was first described and assigned to the upper Neocomian by Lory (1846) in his regional geological study of the Grenoble region. Lory (1846) described the abundant fauna of shells and corals which he noted

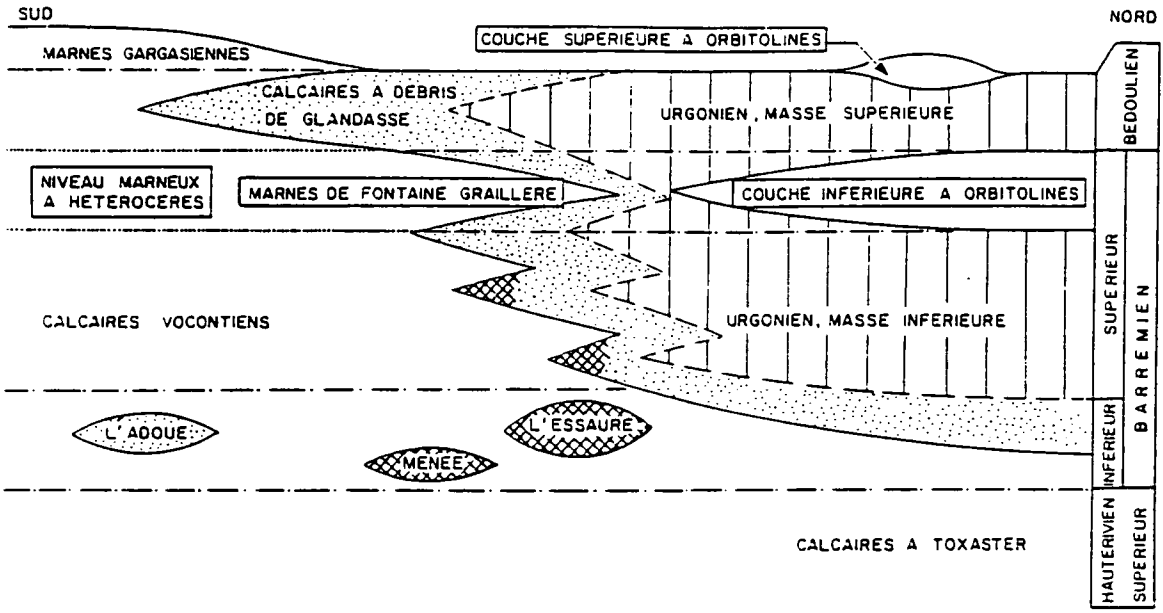

Figure 4.24a. The stratigraphic scheme for the Urgonian platform of Paquier (1900) (from Arnaud, 1980), based upon correlation of Urgonian facies from the Chartreuse to the Glandasse plateau in the southeastern Vercors.

are frequently associated with dolomitization. Lory (1846) also reported the division of the Urgonian limestones by a marly layer containing abundant Orbitolinid foraminifera; the lower *Orbitolina* beds ('couches inferieur a Orbitolines'), and a second marly level, the upper *Orbitolina* beds ('couches superieur a Orbitolines') developed above the last Urgonian facies of the platform. Paquier (1900) focused upon the fauna contained within marly layers of the platform from which he erected the first stratigraphic and lithological scheme for the platform, illustrated in Figure 4.24a. Paquier (1900) interpreted the rudist facies of the Chartreuse and Vercors

below the lower *Orbitolina* level to be of upper Barremian age ('masse superieur', Fig. 4.24a) and laterally equivalent to the bioclastics of the southern Vercors below the Fontaine Graillère marls which he believed to be the same age as the lower *Orbitolina* level (Fig. 4.24a). The upper Urgonian limestones ('masse superieur') of the Sub-Alpine Chains he interpreted to be of Bedoulien age (L. Aptian) and the inner platform equivalents of the bioclastic grainstones of the Glandasse plateau region above the Fontaine Graillère marls (Fig. 4.24a).

Revil (1911) in his thesis study of the southern Jura and Sub-Alpine chains was the first to use thin sections to study Urgonian microfacies and he observed that the limestones are composed of a mélange of Miliolid and Orbitolinid foraminifera, calcareous algae, coral fragments and other grains. Perhaps the most significant conclusion of Revil (1911) was that the lower part of the Urgonian platform is lower Barremian rather than upper Barremian in age (eg. Paquier, 1900, Fig. 4.24a), based upon the recovery of a lower Barremian ammonite from just below the Urgonian platform in the northern Chartreuse. Further studies cast increasing doubts upon the stratigraphy of Paquier (1900) with, for example, Jacob (1905) interpreting the upper *Orbitolina* level to be upper Gargasian in age. The debate surrounding the 'birth' or 'emplacement' of the Urgonian platform in the Sub-Alpine chains and Jura was a foretaste of the controversy which again surrounds the platform (eg. see Section 4.4.3).

The spate of stratigraphic publications at the beginning of the century was fuelled by collation of data necessary for the publication of geological maps. From this time to the late 1970's stratigraphy of the Urgonian platform and Sub-Alpine Chains in general was simplified as research interest focused upon structural aspects of Alpine geology. From the late 1950's research elsewhere in the Tethyan realm upon Urgonian platforms developed a good micropalaeontological biostratigraphic base upon which the later micropalaeontological biostratigraphic work of Arnaud-Vanneau (1980) in the Sub-Alpine Chains was based. In the mid-late 1970's re-mapping of the Dauphinois area once again highlighted stratigraphic problems of the

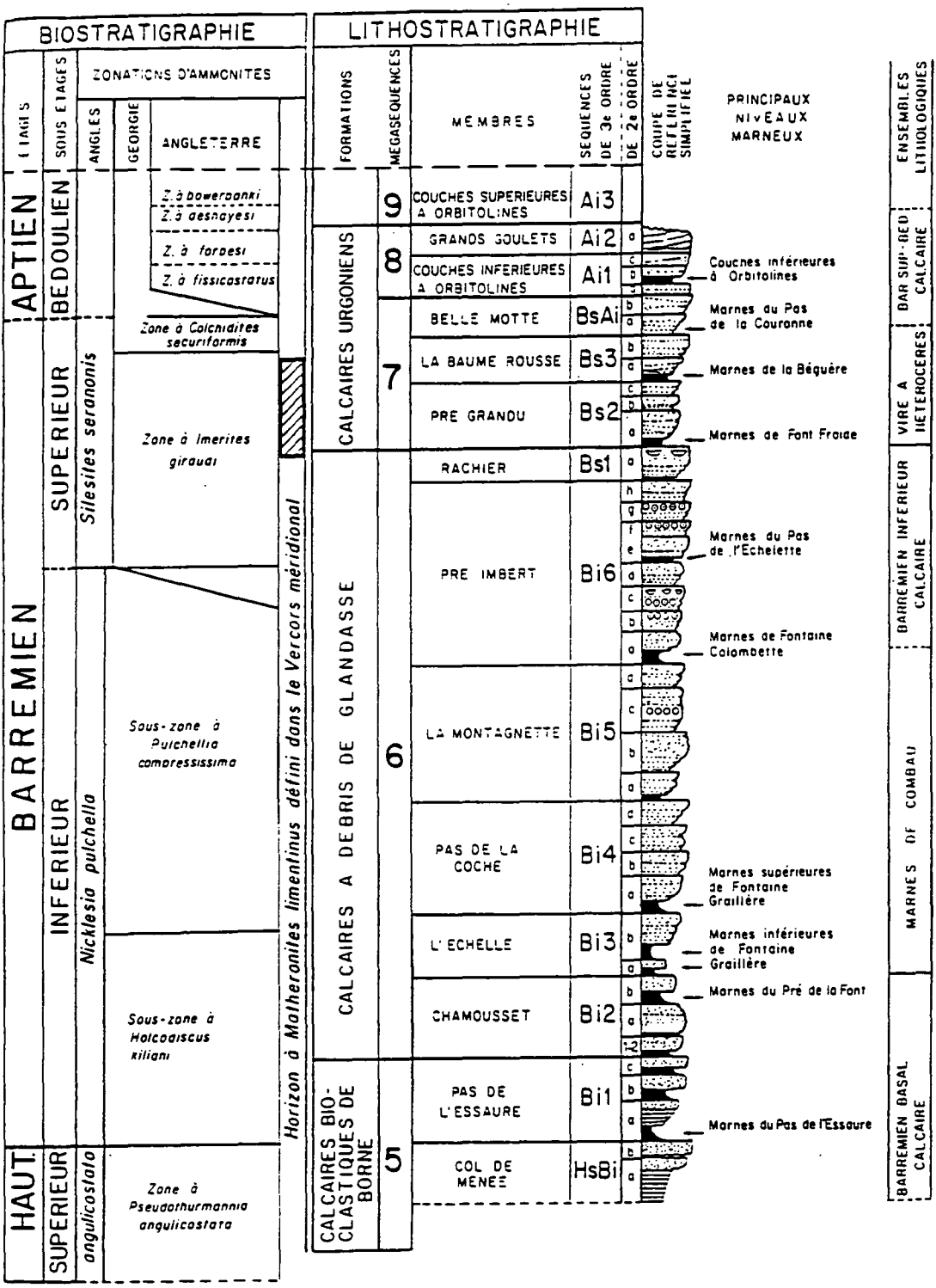

Figure 4.25. The Stratigraphy for the Urgonian platform of the southern Vercors of Arnaud (1981).

Urgonian platform. The most important recent work upon the Urgonian platform of the French Sub-Alpine Chains began at this time (eg. S. Ferry, 1976-southwestern Vercors and Diois; A. Arnaud-Vanneau, 1980-northern Vercors and Chartreuse; H. Arnaud, 1981-southern Vercors, Diois and Dévoluy; Vieban, 1983-southern Jura) and led to a major re-interpretation of the Urgonian stratigraphy in the French Sub-Alpine Chains.

Arnaud-Vanneau *et al.* (1976) and Thieuloy (1979) established the Borne and Glandasse Bioclastic Limestone Formations to be lower Barremian in age, and geographically, palaeontologically and sedimentologically distinct from the overlying Urgonian Limestone Formation (eg. Fig. 4.19) from which they are separated by the *Matheronites limentinus* level (eg. Fig. 4.22). The macropalaeontology from the southern Vercors where ammonites are frequently found in shales interbedded with Urgonian outer shelf facies (eg. Arnaud-Vanneau *et al.*, 1976; Thieuloy, 1979) allowed correlation of the platform with the Angles Barremian type section in the Vocontian Basin (eg. Busnardo, 1965). This biostratigraphy was then used in comparison with work on other Mediterranean Urgonian platforms to construct a micropalaeontological biostratigraphy for the platform (eg. Arnaud-Vanneau, 1980). This biostratigraphy (Arnaud-Vanneau, 1980) provided an excellent correlation tool between the outer and inner platform where pelagic macrofauna (eg. ammonites) is generally rare and allowed the erection of a new stratigraphy for the platform (eg. Arnaud-Vanneau, 1980; Arnaud, 1981) (Fig. 4.25).

In a similar manner to the controversy surrounding the base of the Urgonian platform at the beginning of the century, doubts have subsequently been cast by Clavel *et al.* (1986, 1987) upon the stratigraphy of Arnaud-Vanneau (1980) and Arnaud (1981). Using an almost identical argument to that of Revil (1911) Clavel *et al.* (1986) and Clavel *et al.* (1987) showed a macrofauna from below the base of the platform to be of lower Barremian age. These authors use this fauna to argue for a similar age of the platform (see Section 4.4.3 for further discussion). Since the late 1980's attention has focused upon sequence stratigraphic interpretations of the

platform using the superb lateral continuity of platform exposure to test the sequence stratigraphic models outlined in Chapter 2 (eg. Arnaud & Arnaud-Vanneau, 1989; Arnaud-Vanneau & Arnaud, 1990; Jacquin *et al.*, 1991; Arnaud-Vanneau & Arnaud, 1991; Hunt & Tucker, 1992) and is the subject of this thesis.

4.4.3. The Urgonian Palaeontological Controversy.

There is at present quite a controversy surrounding the 'emplacement' or 'birth' of the Urgonian platform in the Jura, Sub-Alpine Chains and margins of the Vocontian Basin as touched upon in the preceding section. Two very different interpretations of the basic palaeontological data have been suggested, each giving a very different chronological development of the Urgonian platform and Hauterivan-Barremian palaeogeography.

In the late 1980's Clavel *et al.* (1986) and Clavel *et al.* (1987) used ammonite and echinoid biostratigraphic data to challenge the stratigraphy developed by Arnaud-Vanneau (1980) and Arnaud (1981). Clavel *et al.* (1986) and Clavel *et al.* (1987) demonstrated that sediments from just below the Urgonian platform vary from lower Hauterivian in the Jura to lower Barremian in age in the Dauphinois Basin, typically between *sayni, balearis* and *angulicostata* zones of the upper Hauterivian along and across the strike of the Sub-Alpine Chains (eg. Fig. 4.26). These authors used this fauna to argue for the same age of development the Urgonian platform from which they suggested a revised palaeogeographic development for the platform radically different from that previously proposed by Arnaud-Vanneau (1980) and Arnaud (1981) (Fig. 4.27). Clavel *et al.* (1986) proposed that the Urgonian platform prograded gradually east and southeast into the Dauphinois Basin from the Jura platform.

Further to this study, work by Schroeder *et al.* (1989) upon the Pont de Laval Urgonian section in the Ardèche region of France cast further doubts upon the biostratigraphy of Arnaud-Vanneau (1980) and Arnaud (1981). Schroeder *et al.* (1989) demonstrated that the Orbitolinid species *Valserina brönnimanni*, used by

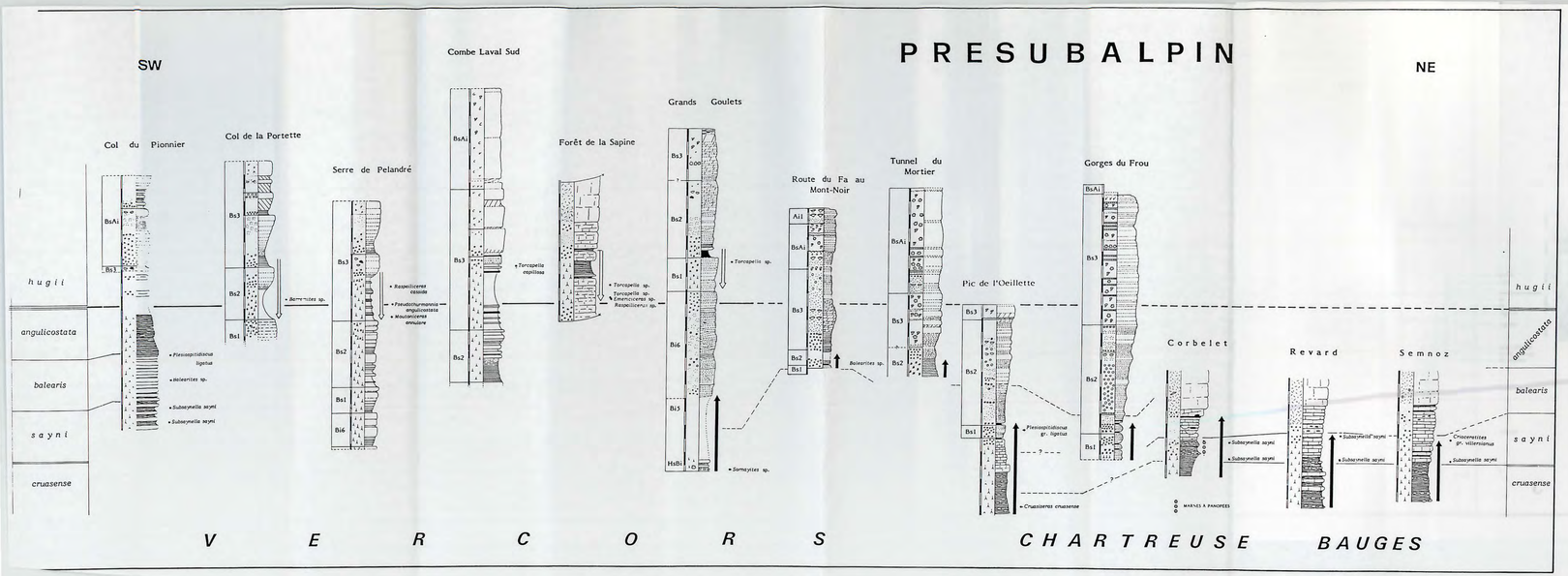

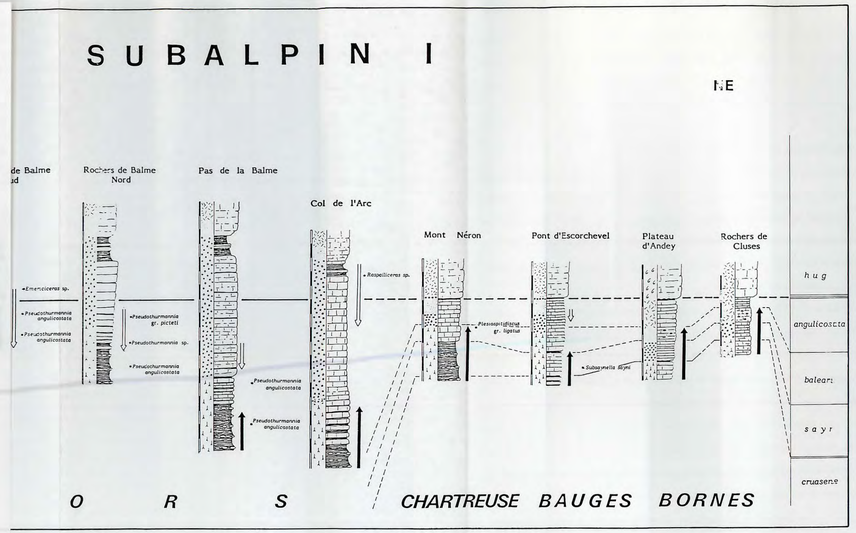

Figure 4.26. Reinterpretation of the stratigraphy of Arnaud-Vanneau (1980) and Arnaud (1981) by Clavel *et al.* 1987 based upon the dating of echinoderms and ammonite faunas from below the base of the Urgonian platform. These data were used by Clavel *et al.* (1986) to develop the revised palaeogeographic evolution of the platform illustrated in Figure 4.27. The first 'Presubalpin' section is taken from the east of Vercors, Chartreuse, and bauges massifs of the Sub-Alpine Chains and the 'subalpin' section from the eastern extremity of these massifs. Note that the youngest age of the facies dated by these fauna varies along and across the strike of the Dauphinois basin and are used to constrain Figure 4.27.

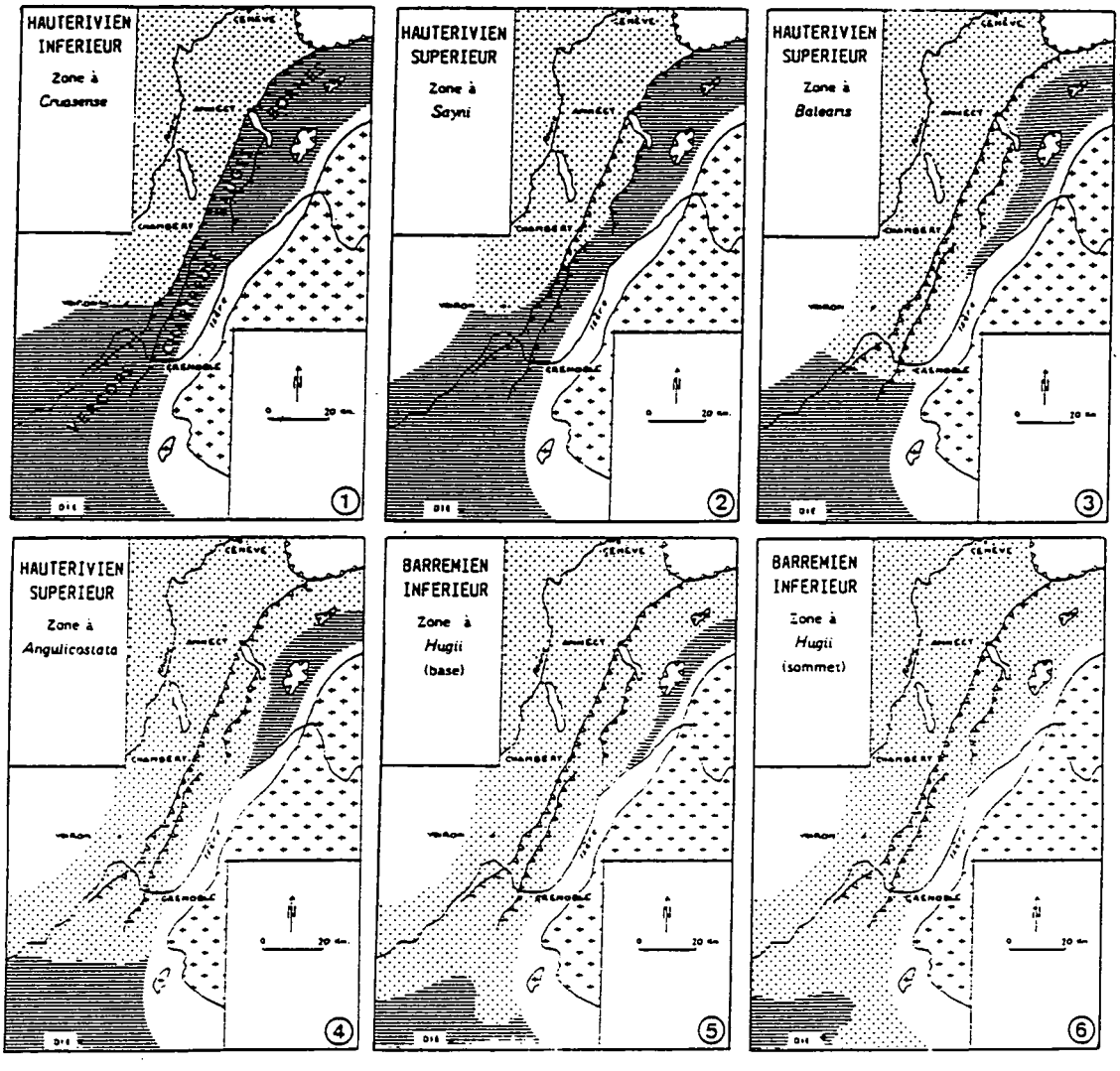

Figure 4.27. Palaeogeographic reconstruction of the Urgonian platform in the French Jura and Sub-Alpine Chains. This reconstruction is based upon the dating of ammonites and echinoderms from below the true Urgonian platform facies (eg. Fig. 4.26). Note the gradual progradation of Urgonian facies east and southeast from the Jura Platform (From Clavel *et al.*, 1987).

Arnaud-Vanneau (1980) and Arnaud (1981) to indicate an upper Barremian age for the Urgonian Limestone Formation in the Sub-Alpine Chains, occurs alongside undisputed lower Barremian ammonites in the Pont de Laval section. Schroeder *et al.* (1989) concluded from this evidence, coupled with that of Clavel *et al.* (1986) and Clavel *et al.* (1987) that the stratigraphy of Arnaud-Vanneau (1980) and Arnaud (1981) is invalidated.

The conclusions of Clavel *et al.* (1986) and Clavel *et al.* (1987) have been strongly rebuked by Arnaud-Vanneau & Arnaud, (1986), Arnaud & Arnaud-Vanneau, (1987) and Arnaud-Vanneau & Arnaud (1991, pers comm.) who argue that the conclusions of these workers are incorrect for a number of reasons. Firstly, Clavel *et al.* (1986) and Clavel *et al.* (1987) maintain that dating of the Urgonian Limestone Formation by ammonites is precise. Such a conclusion is difficult to envisage as the platform is itself conspicuous by the absence of ammonites with the exception of the southern Vercors, where the stratigraphy of Arnaud (1981) is not disputed. Ammonite faunas are very environmentally sensitive so that species found on the platform and borders of the platform are often notably different from those of the Angles Barremian type section in the Vocontian Basin (eg. Busnardo, 1965). Secondly, the range of ammonites within the Angles section is itself debatable as biostratigraphic ranges of specific species vary from author to author and, at the present time this section is undergoing substantial but as yet unpublished biostratigraphic revision (H. Arnaud pers comm. July 1990). Finally, the stratigraphic range of the echinoids quoted by Clavel *et al.* (1986) and Clavel *et al.* (1987) is large; *Toxaster amplus* has a range which covers all of the Hauterivian, and *Toxaster seynenis* a large part of the Barremian. Thus, their use as biostratigraphic markers on the scale of this problem is questionable (Arnaud-Vanneau & Arnaud, 1986).

The dates that Clavel *et al.* (1986) and Clavel *et al.* (1987) have obtained from <u>below</u> the platform Arnaud-Vanneau & Arnaud (1986) do not dispute. In fact, on the contrary, they argue that these data confirm the conclusions of Arnaud-Vanneau (1980) and Arnaud (1981). However, these biostratigraphic data cannot be used to constrain the beginning of Urgonian platform sedimentation and <u>only</u> demonstrate the age of the youngest sediments <u>below</u> the Urgonian platform, not that of the platform itself (Arnaud-Vanneau & Arnaud, 1986; Arnaud-Vanneau *et al.*, 1987; Arnaud & Arnaud-Vanneau, 1989; Arnaud-Vanneau & Arnaud, 1990; Arnaud-Vanneau & Arnaud, 1991). The timing of the beginning of Urgonian platform sedimentation by

Clavel *et al.* (1986) and Clavel *et al.* (1987) is an upward extrapolation from biostratigraphic data below into the platform, where there is no biostratigraphic data of the type used by Clavel *et al.* (1986) and Clavel *et al.* (1987) (eg. Fig. 4.26).

In the case of the index fossil *Valserina brönnimanni,* first noted by LaFarge (1978) Arnaud-Vanneau (1991, pers comm.) pointed out that it is well known to her, since she performed the species determinations of this section for LaFarge (1978). Arnaud-Vanneau (1991, pers. comm.) argued that in the Jura and Sub-Alpine Chains this species is not associated with any other lower Barremian fauna, but notably with other proven fauna of upper Barremian age, notably *Eopalorbitolina.* The species *Eopalorbitolina* is in eastern Spain described from the upper Barremian in association with *V. brönnimanni* and is also associated with the upper Barremian-Aptian *Palorbitolina lenticularis.* Such associations suggest that the species *V. brönnimanni* has a wide chronostratigraphic distribution. However, in Savoie, Dauphiné and the Jura mountains Arnaud-Vanneau (1991, pers comm) argued that this species is exclusive to the upper Barremian *Colchidites* zone of the Barremian stratotype section in the Vocontian Basin.

In conclusion to the palaeontological controversy surrounding the Urgonian platform the use of ammonites from below the platform to give the age of the platform (particularly in the light of sequence stratigraphic concepts) appears inappropriate. However the interpretations of Schroeder *et al.* (1989) do give some cause for concern.

In this thesis the stratigraphy of Arnaud-Vanneau (1980) and Arnaud (1981) is followed and geometric constraint suggests that for much of the platform this stratigraphy holds true. The facies model which Arnaud-Vanneau (1980) and Arnaud (1981) developed to analyse the platform is briefly discussed in the following Section.

4.5. Facies Of The Urgonian Platform.

4.5.1. Introduction.

The stratigraphy developed by Arnaud-Vanneau (1980), Arnaud (1980) and Vieban (1983) divided the Urgonian platform into a number of 'shallowing-up' members as illustrated in Figure 4.25. The evolution of each of these members can be analysed in more detail by comparison of their microfacies evolution to the standard microfacies model developed for the Urgonian platform by Arnaud-Vanneau (1980) and Arnaud (1981). This model divides the platform in to eleven standard microfacies (Figs 4.28 & 4.29). The model of Arnaud-Vanneau (1980) and Arnaud (1980) is used throughout this thesis with some modification. Additional facies to the Arnaud's model have been distinguished in the slope and basin-floor environments and are discussed in Sections 5.3 and 5.4 respectively, and also within the appropriate stratigraphic discriptions in Chapter 6. The standard eleven microfacies of the Urgonian platform as well as some of their variations are briefly discussed and illustrated in the following section. More detailed documentation and discussion of Urgonian microfacies is given in the six volume memoirs of Arnaud-Vanneau (1980) and Arnaud (1981).

Figure 4.28 (Facing page) The eleven standard microfacies of the Urgonian platform and its foreslope as according to Arnaud-Vanneau *et al.*, (1987), shown within their appropriate positions upon an idealised profile of a rimmed shelf. **F11**: Micrites with *Pseudotrioculina* and micrites with birds eye fenestrae; **F10**: Biomicrites-sparites with oncolites; **F9**: Biomicrites-sparites with Miliolids and Rudists; **F8**: Biomicrites-sparites with large foraminifera, sometimes accompanied by large rudists (F11-F8 vary from mudstone to grainstone textures); **F7**: Biosparites with corals - boundstones; **F6**: Oosparites; **F5**: Biosparites with large rounded bioclasts; **F4**: Biomicrites-sparites with crinoids and bryozoans; **F3**: Biosparites with rounded echinoderm grains and small foraminifera; **F2**: Biomicrites with echinoderms; **F1**: Biomicrites with sponge spicules. **F0** (basin-floor facies): biomicrites with pelagic foraminifera. See text for further discussion.

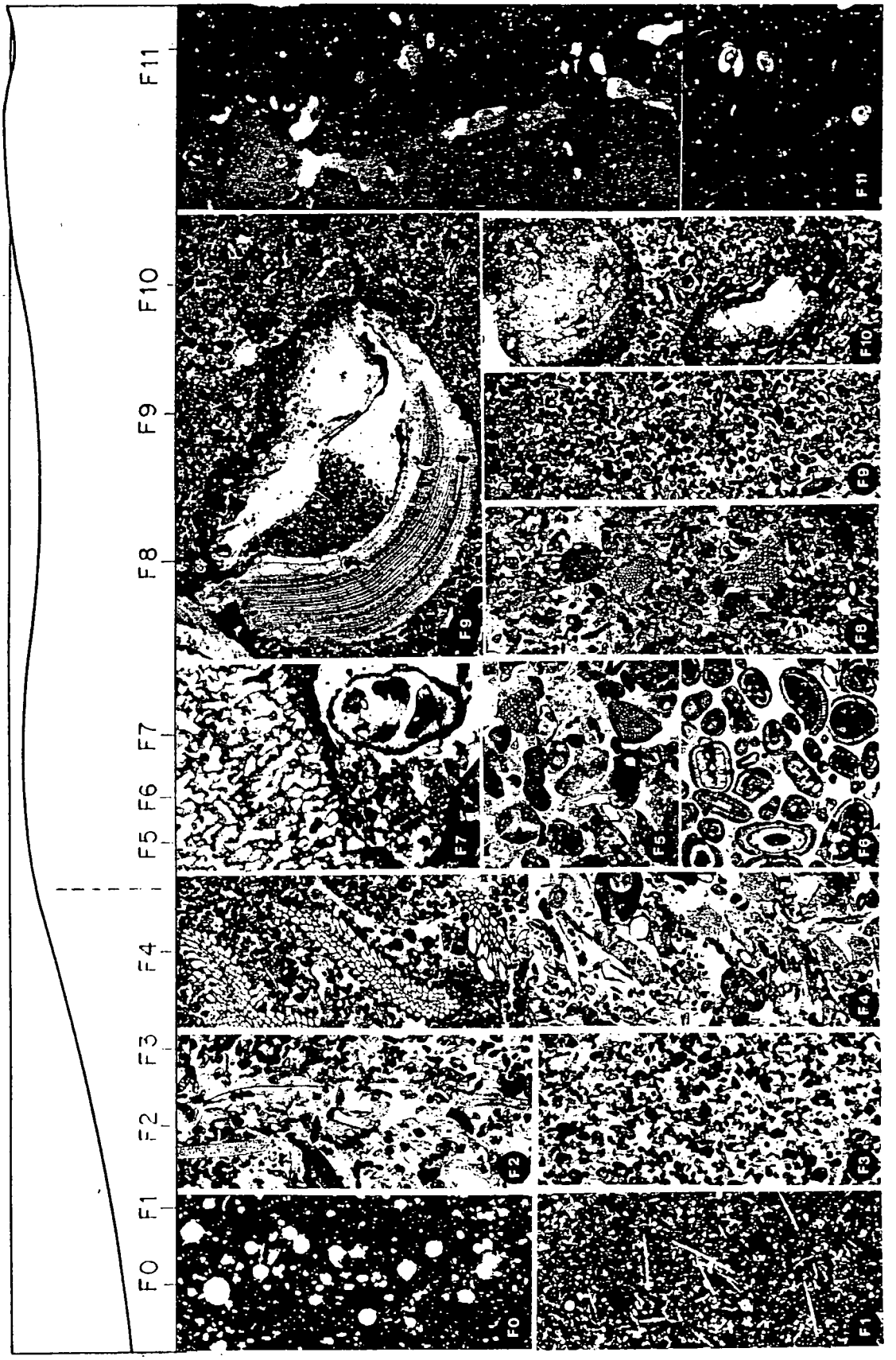
F11
F10
F9
F8
F7
F6
F5
F4
F3
F2
F1
F0

4.5.2. The facies model for the Urgonian platform.

The facies of the Urgonian platform are interpreted in terms of an accretionary rimmed shelf (eg. Figs 4.28 & 4.29) with a topographically elevated outer rim characterized by high-energy facies (F5-7), backed by a protected lagoon where the true rudist facies which characterize the Urgonian platforms are developed (F11-8). By way of contrast to many of the important hydrocarbon bearing upper Cretaceous Urgonian platforms (eg. Wilson, 1975; Bay, 1977), rudists are not developed in high-energy areas of the platform or upon the foreslope. A schematic block diagram of the Urgonian platform is illustrated in Figure 4.30. This contrasts a hypothetical steep windward local bypass margin of the shelf, backed by a high-energy lagoon (F8-10) with a shallowly dipping leeward accretionary margin, backed by a low-energy, muddy lagoon (F8-10). These two different lagoons are separated by a central

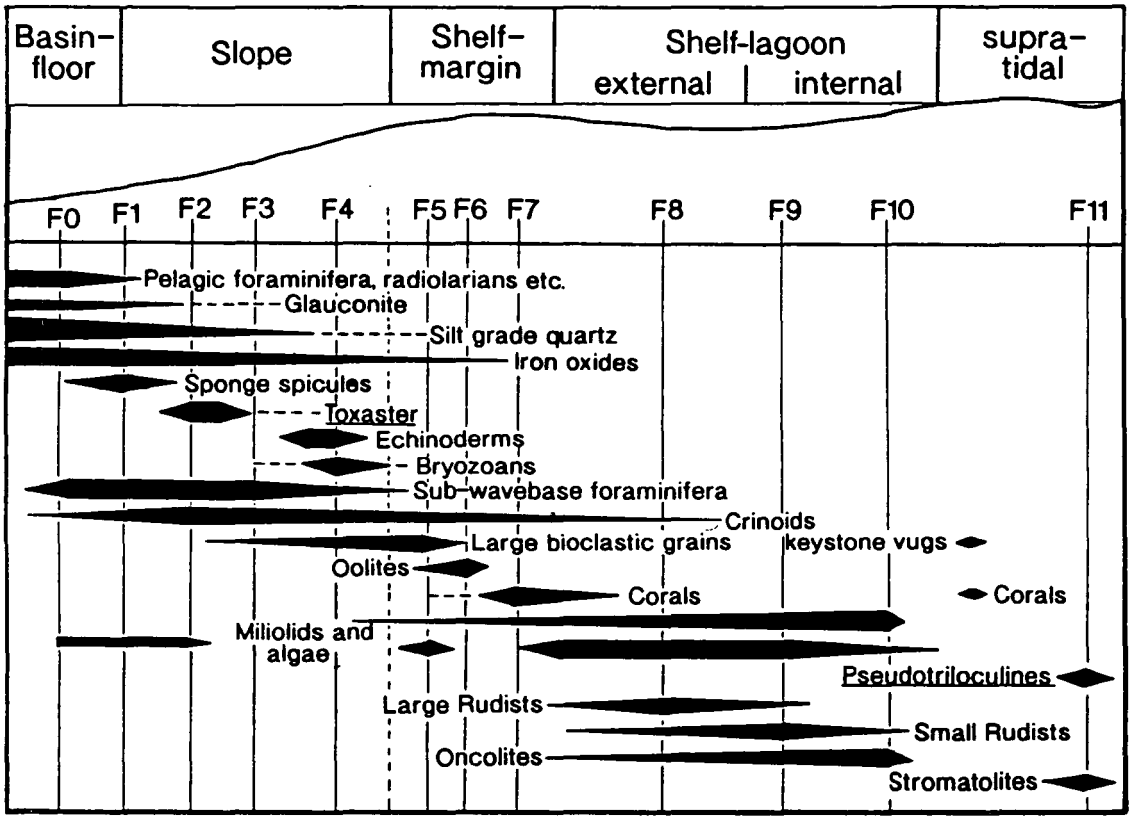

Figure 4.29. The hypothetical lateral arrangement of the eleven standard microfacies upon the Urgonian platform and basin-floor. The main components of these standard facies (eg. coated grains, oncolites), the processes which typify different parts of the platform (eg. micritization) and characteristic fabrics developed (eg. keystone vugs) are illustrated in their appropriate position. The standard microfacies are as according to Fig. 4.28 (From Arnaud-Vanneau *et al.*, 1987).

island against and upon which the F11 facies are developed (eg. compare Figs 4.28, 4.29 & 4.30). The high-energy shelf-margin of the Urgonian platform was dominated by bioclastic grainstones (F5) with some oolites (F6) and isolated corals/reefs (F7). These high-energy facies are shown to pass gradually basinwards through a variety of sub-wavebase facies to the pelagic basin-floor (F0) (F4-1) (Figs 4.28 & 4.29).

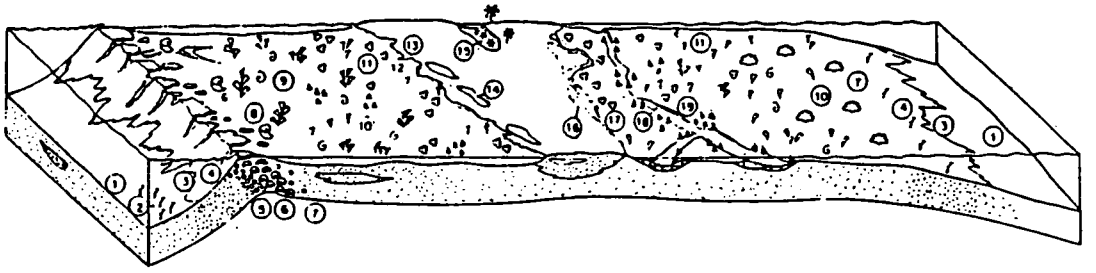

Figure 4.30. Hypothetical block diagram across the Urgonian platform contrasting a steep windward margin (left) with some upper slope bypass, backed by a relatively high-energy lagoon and a more gently dipping leeward shelf-margin (right), backed by a low-energy, muddy shelf-lagoon (from Arnaud-Vanneau, 1980). *Facies*: **1**: sandy muds with echinoids; **2**: coarse sands with Bryozoans; **3**: fine-grained sands with echinoderms and Annelids; **4**: coarse sands with Orbitolinids and Dasycladaceans; **5**: oolitic sands; **6**: coral reefs; **7**: coarse coral sands; **8**: muds with Caprotinid and Caprinid rudists; **9**: peloidal sands with *Agriopleura*, *Neotrocholina* and echinoids; **10**: fine grainstones with large rudists; **11**: fine grainstones with small rudists and oncolites; **12**: fine grainstones with Requienid rudists; **13**: beach facies with keystone vugs; **14**: muds with *Pseudotriloculina*; **15**; Muds with *Charq* (and clays); **16**: muds with birds eye fenestrae; **17**: muds with isolated rudists; **18**: mud and argillaceous muds with *Palorbitolina*; **19**: Muds with Dasycladacean alga.

4.5.2. A. Lagoonal facies-supratidal facies.

The F11-8 facies are volumetrically the most important facies upon the Urgonian platform *sensu stricto*, developed within the vast shelf-lagoon during the upper Barremian and lower Aptian (eg. Figs 4.9 & 4.20). These facies represent the true Urgonian limestones of the platform (eg. rudists facies). In the standard platform model the different types of intertidal to supratidal environments are grouped together

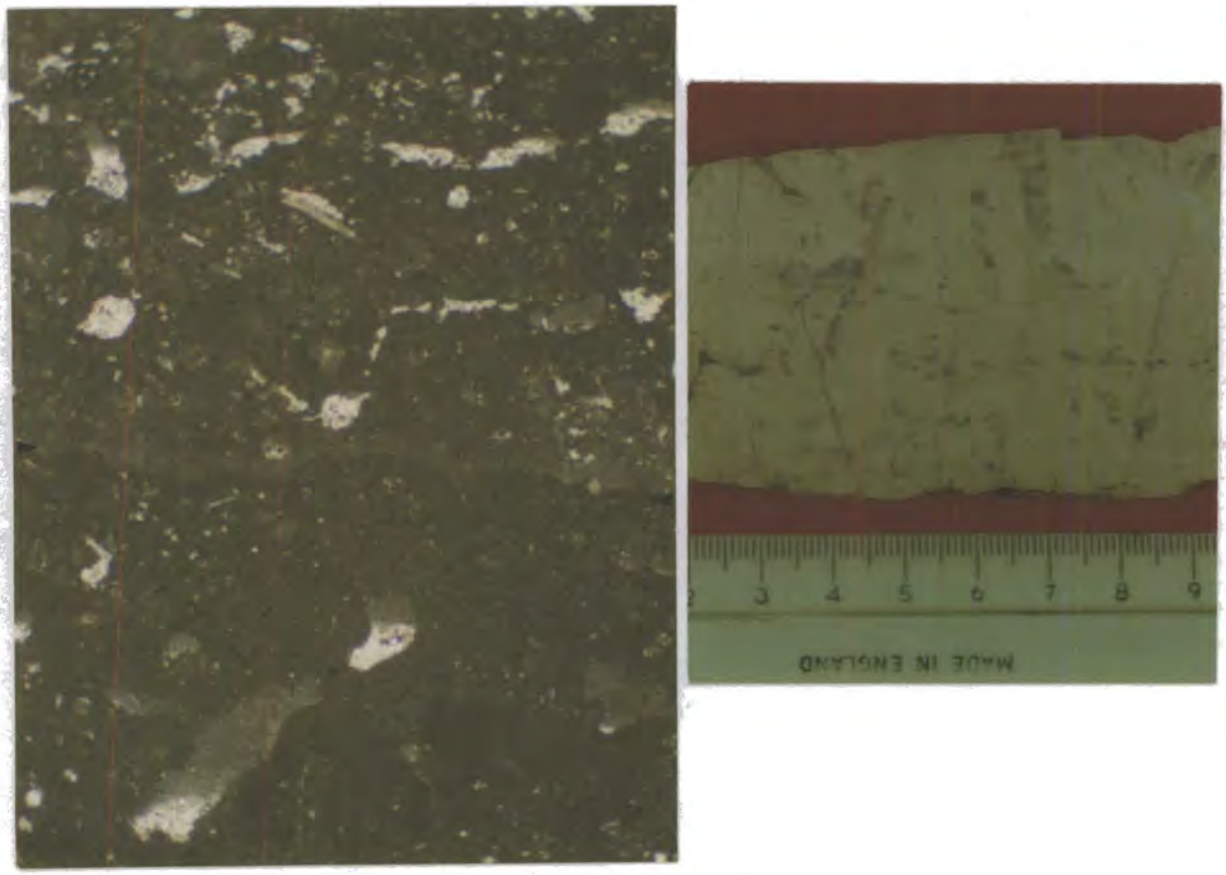

Figure 4.31A. 1: Photomicrograph of the standard F11 microfacies, (right) irregular sub-horizontal laminar birds eye fenestrae developed in *Pseudotriloculina* (P) mudstone (below) separated by sharp contact (arrowed) from F10 oncolitic wackestone containing sub-vertical and partially filled tubular fenestrae (from BsAi of the Gorge du Frou) (Field of view 15mm, PPL). **2:** Well developed sub-horizontal, flat-based irregular birds eye fenestrae separating microbial mats (BsAi, Balcon des Ecouges, northern Vercors).

under the umbrella of the F11 standard microfacies (Arnaud-Vanneau, 1980; Arnaud, 1981) (eg. Figs. 4.28 & 4.29). This most internal 'facies' of the Urgonian platform thus actually includes a wide variety of environments, from low-energy intertidal facies such as *Pseudotriloculina* mudstones with birds eye fenestrae (Figs 4.31A & 4.33B) and parallel-laminated stromatolites (Fig. 4.31B) to high-energy low-diversity restricted-shelf beach facies, composed entirely of oncolites (Fig. 4.31C) and high-

Figure 4.31(B-C) B: Well developed subhorizontal planar stromatolites from Bs3 of Gorge du Nant, northern Vercors. These stromatolites have an irregular fenestral fabric in thin section and are interpreted to be low-energy tidal-flat facies (fingers for scale). Note that these facies are very strongly compacted. **C**: Restricted shelf, high-energy beach facies of large oncolites and algal coated bioclasts. The porosity between the oncolites is partially filled by yellow calcitic vadose pendant/meniscus cements and/or by geopetal sediments with a late blocky sparry cement filling the porosity. The stylolitized contact separates these beach facies from restricted lagoon oncolitic grainstones.

energy unrestricted beach facies with a high faunal diversity. Both of these higher-energy environments have well developed asymmetric yellow cements, perched sediments and keystone vugs (eg. Fig. 4.31D). For the sake of convenience Arnaud-Vanneau (1980) and Arnaud (1981) also included features developed when the platform was subaerially exposed within the F11 facies division. This includes lacustrine limestones containing fragments of the freshwater algae *Chara* (eg. Figs 5.8F, G & Fig. 6.10) and features such as root moulds (eg. Fig. 5.8E). Furthermore, diagenetic textures indicative of subaerial exposure are also included. These include vadose diagenetic features such as preferential dissolution below grains, karstic dissolution pipes (eg. see Fig. 5.8D), preferential dissolution of shells (Fig. 4.32A) with partial fills of geopetal cements (eg. Fig. 5.8B), and also meteoric phreatic cements (eg. Fig. 4.32B).

The F9 and F10 microfacies are interpreted to be the most internal subtidal

Figure 4.31D. Photomicrograph (XP) of beautifully developed high-energy beach facies with well formed 'oversized' pores - keystone vugs. The upper part of keystone vugs are partially filled by well developed botryoidal pendant and meniscus cements. The lower part of the keystone vugs are partially filled by fine geopetal sediments. Porosity was eventually filled by a late burial cement. The diverse assemblage of shelf-lagoon type bioclasts suggests that these facies developed on an open unrestricted part of the shelf. Field of view approximately 16mm.

facies of the platform. Crinoids, an indicator of normal oxygenation and salinity are notably absent from these microfacies suggesting confinement. In the field these facies are characterized by metre sized to massive bedding and a white or beige colour. The macrofauna of these facies is dominated by small rudists and/or oncolites developed along side peloids and a microfauna dominated by small Miliolid foraminifera. In thin section *all* grains in these facies are pervasively micritized, and it is this which gives these facies their characteristic white-beige colour in the field. An example of very restricted low-energy, low diversity oncolitic wackestones (eg.

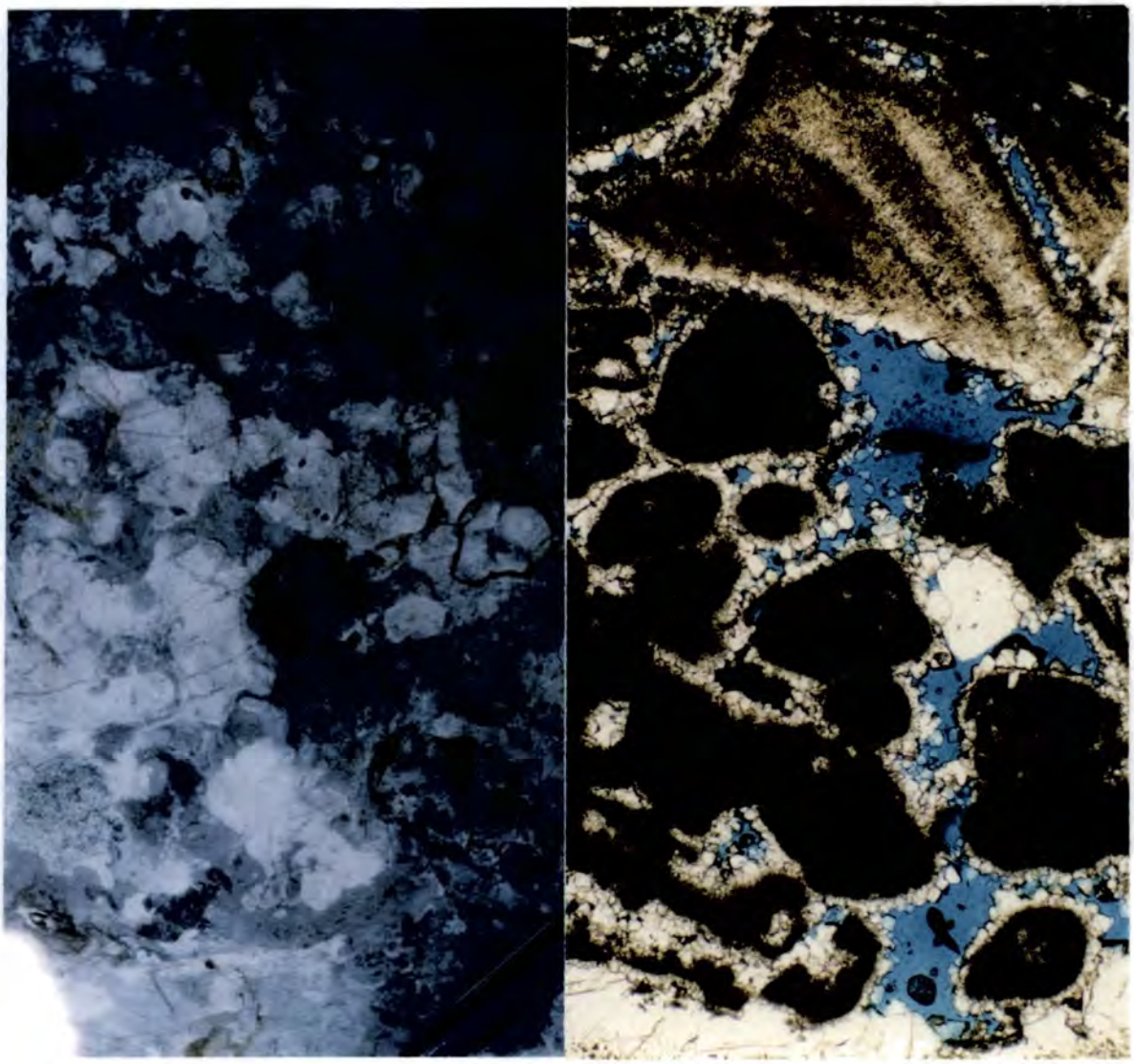

Figure 4.32(A-B). **A** (left) Fill of dissolved rudist bivalves at the top of the Urgonian platform by the 'Lumachelle' limestone. Rudist bivalves were preferentially dissolved when the platform was subaerially exposed (SbBA2, see Chapters 5 & 6 for further discussion of this boundary). Pencil approximately 8mm diameter for scale. **B** (right) photomicrograph of well developed equant non-isopachous meteoric vadose cements developed in open shelf F9 facies. Section from approximately 4m below SbAP1, Balcon des Ecouges, N. Vercors (also see Figs 4.33iD & 6.10). Note section is impregnated by blue resin, filling porosity. Field of view approximately 4mm, PPL.

F10 facies) is illustrated in Figure 4.33A. In this facies (and typical of low agitation) are highly asymmetric oncolites, nucleated upon bivalves (Fig. 4.33A). Less restricted, low-energy conditions favour the development of a more varied fauna, typically rather stunted 10-20mm rudists with asymmetric oncolites with a wackestone fabric as illustrated in Figure 4.33B. By way of contrast, high-energy

Figure 4.33A. Restricted, low-energy oncolitic wackestone from Bs3 of the northern Chartreuse (F10 facies). The growth of highly asymmetric oncolites attests to very low agitation as does the muddy fabric. The shape of these oncolites contrasts markedly to those of Figure 4.3.3C.

Figure 4.33B. Polished block and outcrop photo of low-energy restricted-shelf type facies overlying intertidal fenestral mudstones with *Pseudotriloculina* (F11 facies) within BsAi, Balcon des Ecouges, northern Vercors. The restricted lagoonal facies are characterized by small rudists up to 20mm in size and 10-20mm irregular, asymmetric oncolites nucleated on to bioclasts. The styolitized boundary between the F11 and F10 facies is the base of a 2m shallowing-up cycle (see also Figs 6.15 & 6.16).

restricted environments are characterized by the development of oncolitic grainstones (eg. Fig. 4.33C). High-energy, but slightly less restricted environments than illustrated in Figure 4.33C are typified by the deposition of well sorted pack-grainstones with or without 'oversized' rudist bivalves (eg. Fig. 4.33D, F9). Both the F9 and F10 facies are thought to have developed in poorly oxygenated and hypo/hypersaline sea-waters on the basis of the absence of crinoids, diagnostic of normal marine, well oxygenated sea-waters.

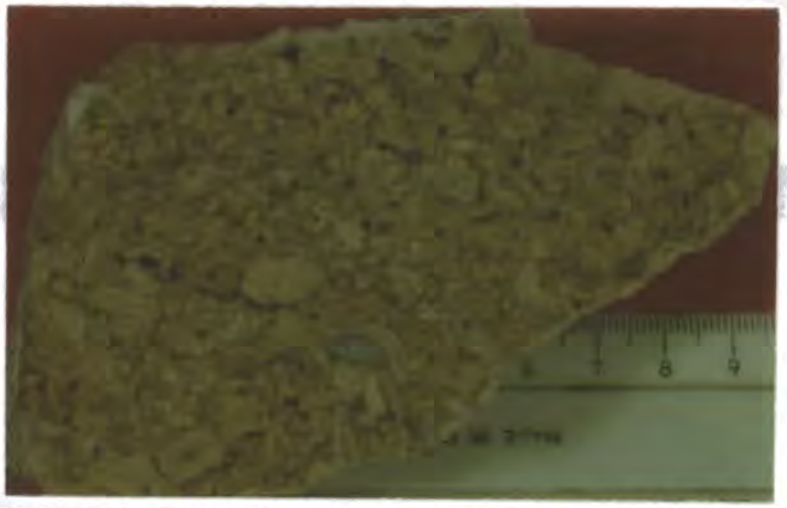

Figure 4.33C. Polished block of BsAi oncolitic grainstone (F10) from the Tunnel du Mortier in the northern Vercors. In direct contrast to Fig. 4.33A, oncolites are well rounded, suggesting constant agitation. The low diversity fauna and dominance of oncolites with a grainstone fabric are suggestive of high-energy but restricted (eg. hypo/hyper saline) conditions on the shelf.

F8 facies are considered to have been deposited in the less restricted parts of the Urgonian lagoon as evidenced by the frequent inclusion of crinoids in to these facies suggesting more normal salinities and well oxygenated conditions. The vast majority (but not all) of bioclastic grains are also micritized in these facies. However, in comparison to F9 and 10 these facies contain both quite large foraminifera (eg. Orbitolinids) and larger rudists (eg. *Agriopleura*, Fig. 6.33) along-side Miliolids. The vertical stacking patterns of a low-energy (?leeward) shelf-lagoonal succession are beautifully exposed at the Balcon des Ecouges where they comprise 1-3m thick shallowing-up cycles as illustrated in Figures 5.15 & 5.16. In this stratigraphic section the F8 facies mark the least restricted conditions and pass-upward into

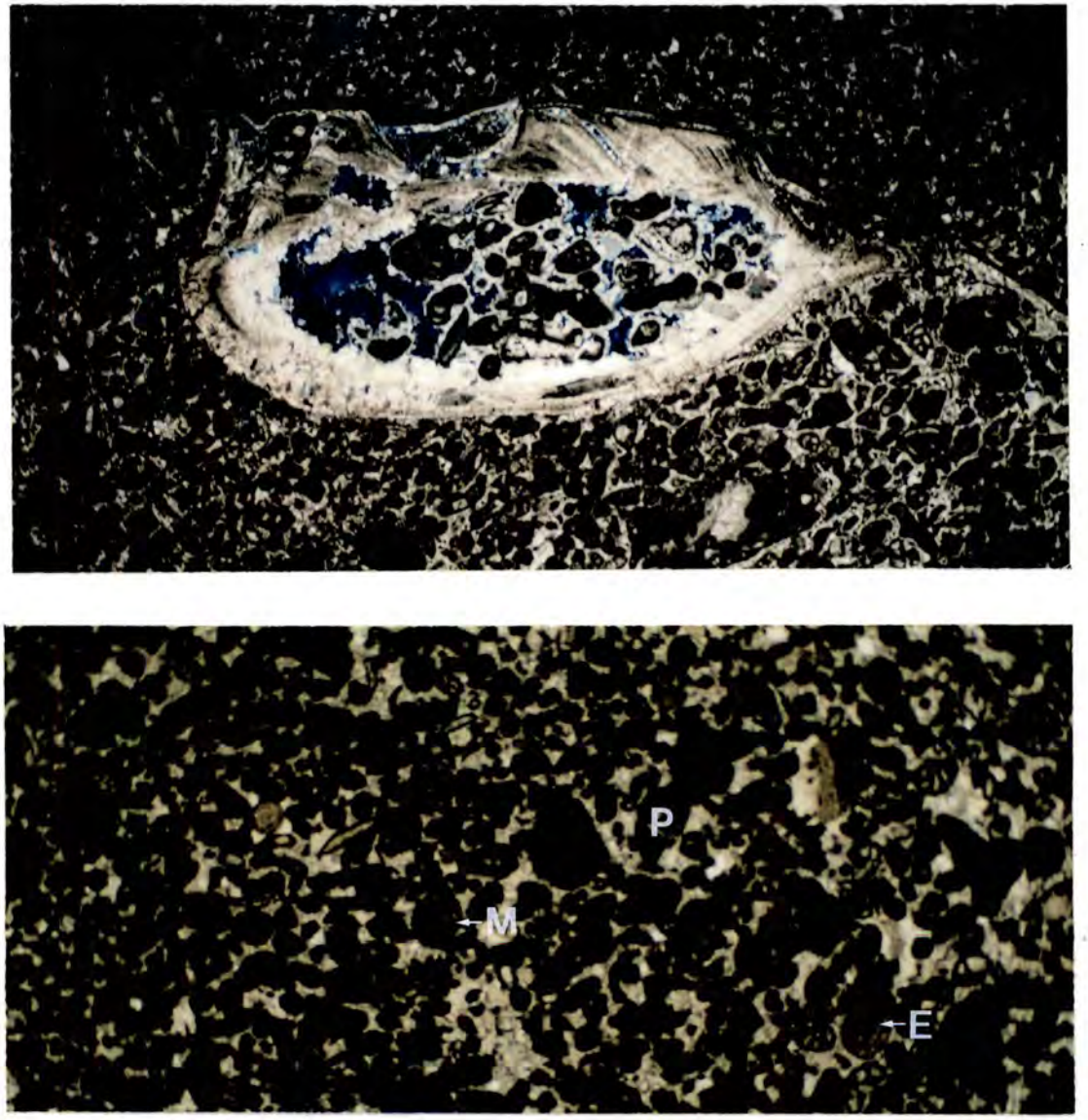

Figure 4.33D. The F9 type standard microfacies of the Urgonian platform. These facies are characterized by an absence of echinoderm debris suggesting relatively restricted circulation. The grainstone fabrics and good sorting of both **1** and **2** suggest fairly constantly agitated conditions during the development of these facies. Note that the baffling of muds around the small rudist bivalve pictured (**1**, above), locally develops a packstone microfacies. This suggests that the rudist bivalve stood proud of the depositional surface. Internally, the rudist bivalve in **1** has a well developed non-isopachous meteoric vadose cement, detail of which is illustrated in Figure 4.32B. Note that this section is impregnated by blue resin, which fills porosity (Field of view approximately 18mm, BsAi, Balcon des Ecouges, northern Vercors). **2**(below): Restricted circulation, high-energy, well sorted peloidal(P)-Miliolid(M) grainstone shelf facies (Echinoid spine E, also labelled). Field of view approximately 6mm, (Ai2 Pas d l'Echelle, Chartreuse). Both photomicrographs in PPL.

F9-10 facies characterized by small rudists and oncolites, generally capped by intertidal fenestral muds (F11).

4.5.2. B. The shelf-margin facies.

The F5, 6 and 7 facies of Arnaud-Vanneau & Arnaud (1981) are characteristic of the high-energy external rim of the Urgonian shelf (eg. Figs 4.28, 4.29 & 4.30). These facies are thought to have been constantly reworked by currents and developed in well oxygenated waters of normal salinity. These facies are particularly important in terms of sediment volume as they constitute a considerable proportion of the Glandasse Bioclastic Limestone Formation. In this formation the F5 and F6 facies represent almost all of the shallow-water sedimentation and a considerable proportion of the slope facies. Caution must be used in identifying the F5 and F6 facies on the basis of fabric and fauna alone due to the prolific overproduction of these facies in shallow-waters resulting in their shedding from the shelf on to and down the slope (eg. see Section 4.5.2D). This is the cause of a fundamental difference in interpretation between this thesis and that of Arnaud-Vanneau & Arnaud (1976), Arnaud (1981) and Arnaud-Vanneau & Arnaud (1991) who interpreted all of the F5-6 bioclastic sands of the Glandasse Bioclastic Limestone Formation (Bi2-Bs1) to have been deposited in shallow-water (eg. the 'southern Vercors shoal' of Arnaud & Arnaud-Vanneau, 1976). Subhorizontal bedding and interbedding of the F5 and F6 facies with F7 boundstones and/or incorporation of oversized corals and stromatoporoids in life orientation (eg. Fig. 5.29) is the only way to show unequivocally that the F5 and F6 facies were deposited in shallow-water.

The high-energy shelf-margin facies are dominated by grainstone or locally boundstones (F7) (Fig. 4.33iA). Grainstones are predominant at the shelf-margin, whereas organic buildups (F7) are relatively rare. Oolites (F6) are also volumetrically much less important than F5 facies and constitute only a small part of shelf-margin facies. The main development of oolites is at the base of the Urgonian platform *sensu stricto* (eg. Bs2 of Arnaud-Vanneau, 1989; Arnaud, 1980; Fig. 4.33iB), when high-

Figure 4.33iA. Characteristically off-white massively bedded coral-stromatoporoid boundstone facies (F7) of BsAi of Arnaud (1980), from the vicinity of Baumme Rousse, Glandasse plateau, southern Vercors. Corals and early marine cements are bored by *Lithophagid* bivalves (L). These boundstones are developed within in well-sorted bioclastic grainstone (F5 type facies). Lens cap approximately 50mm diameter for scale.

energy open marine conditions prevailed across a wide area of the platform. Thus, by far the most important facies in terms of sediment volume at the Urgonian platform margin are the F5 type microfacies (eg. Fig 4.33iC). In the field these facies are thought to have been formed at about fair-weather wavebase (<10m). Wavebase deposits of these facies are characteristically off-white to creamy-yellow in colour and sub-horizontally bedded. Beds are typically lenticular, a maximum of 200-300mm thick and pinch-out laterally in strike-sections over 2-4m. Sub-wavebase deposits of these facies (immediately below the lenticular wavebase deposits) are characteristically planar cross bedded. Macroscopically the F5 facies is a very well sorted creamy-yellow coloured grainstone composed of rounded bioclasts.

Microscopically this facies is normally dominated by large Orbitolinid foraminifera and Dasycladacean algae along side a wide assortment of rounded bioclasts such as coated grains, corals and shallow-water lithoclasts (eg. Fig. 4.33iC). The development of F5 facies on the slope is normally associated with some oxidation and the impregnation of bioclasts by iron-oxides. This gives the sub-wavebase F5 facies a characteristic orange colour in the field (eg. see Section 4.5.2.D).

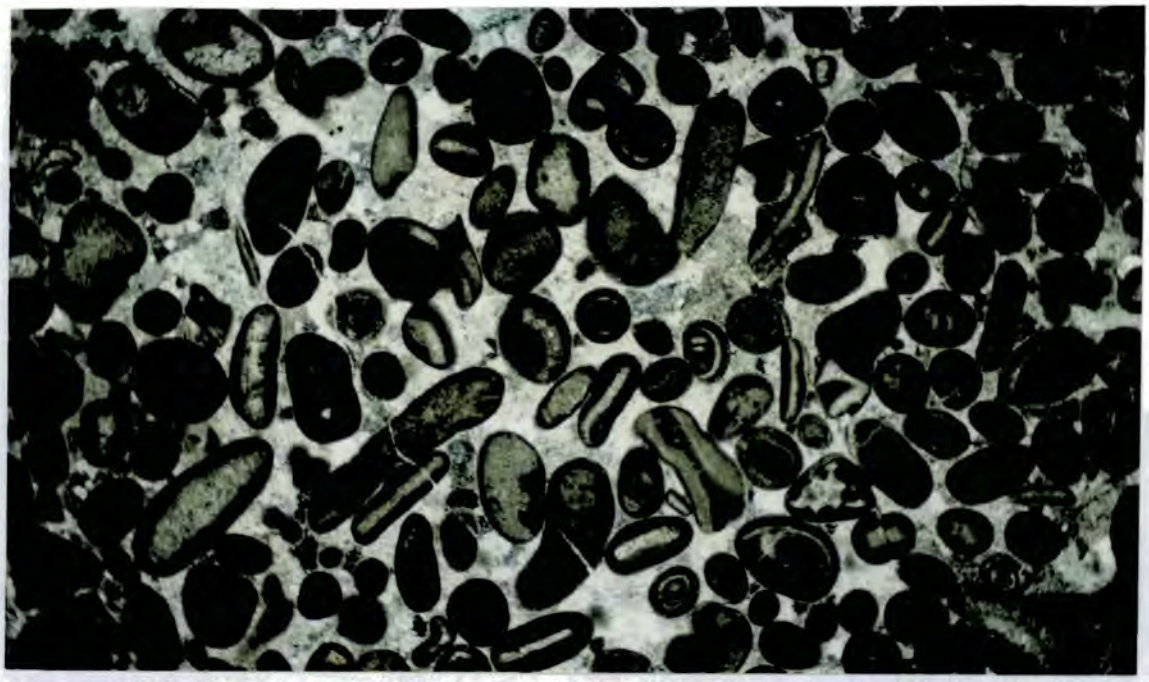

Figure 4.33iB. Photomicrograph of well sorted, high-energy oolitic grainstone (F6) from the Gorge du Frou in the northern Chartreuse (Bs2, Arnaud-Vanneau, 1980) (field of view approximately 18mm, PPL). Oolitic grainstones are most significantly developed at the base of the Urgonian platform in the northern Vercors and Chartreuse when high-energy open-marine conditions were developed across the shelf.

4.5.2. C. Slope and basin-floor facies.

The facies model for the slope is accretionary, and the F4-1 slope facies reflect this model, as indicated by the fining down the slope from fine grainstones, containing rounded bioclasts (F4) to mudstones with sponge spicules (F1). The slope is characterized by sub-wavebase deposits which in the field are typically dark-blue gray nodular limestones interbedded with shales in variable proportions (eg. Fig. 4.34A-B) (F3-1 facies). This contrasts to basin-floor pelagic limestones (F0) which

tend to form laterally continuous tabular beds and have a mottled light-grey to even white colour, and a chalky / powdery texture (eg. Fig. 5.41).

Figure 4.33iC. Photomicrograph of high-energy F5 shelf-margin facies from Bi5 toplap strata of the northern Cirque d'Archiane, approximately 1km north of the sub-horizontal toplapping strata illustrated in Figure 6.14, as seen in Figure 6.15. The bimodal grainstone illustrated above contains a diverse fauna of Orbitolinid (O) and Miliolid (M) foraminifera, Dasycladacean algae (D), coral fragments (C) and bivalves fragments (B). Generally micritization is limited to the rims of grains. Lithoclasts (L) are entirely composed of shallow-water facies with early marine isopachous cements. Field of View approximately 18mm, PPL.

The F4 facies are the uppermost microfacies identified by Arnaud-Vanneau (1980) Arnaud (1981) on the slope below fair-weather wavebase (eg. Figs 4.28 & 4.29). Two quite different F4 facies are recognized (eg. see Fig. 4.28): The first being a well sorted grainstone composed mainly of rounded slope bioclasts such as bryozoans and crinoids with occasional shelf-margin type lithoclasts. In the field this facies is characterized by 1-2m long concave-up 50-80mm thick lenticular limestones beds which characteristically weather to an orange-ochre colour. This colour is a reflection of the impregnation of most grains by iron oxides. This type of the F4 facies is interpreted to have been deposited at about storm-wavebase and was

Figure 4.34A-B. The typical appearance of F1-4 slope facies in the field. Sub-wavebase slope facies are characterized by the interbedding of shales with nodular limestones which are probably partly diagenetic in origin. Right: Nodular limestones with interbedded shales from the upper Hauterivian / lower Barremian Col des Aravis, northern Sub-Alpine Chains (60km northeast of Chambery, rucksack approximately 1m high for scale); Left: the upper part of the Bi4 shallowing-up slope cycle below La Montagnette, southern Vercors. The base of the exposure is shale dominated with few, discontinuous, nodular beds of limestone whereas the top of the gully is characterized by tabular limestones with interbedded shales. The trees mark the approximate base of Bi5. Person for scale.

probably quite regularly reworked by currents as it contains no *in situ* slope fauna. This is a complete contrast to the second type of F4 facies which are characterized by the preservation of elongate 'stick' bryozoans in life orientation (eg. Fig. 4.34C). These are the *in situ* fauna of the sub-wavebase slope (eg. Fig. 4.30) and are thought to have grown in areas of the slope free of currents and/or where currents were very

infrequent and as such can be developed in a wide variety of slope facies, from mudstones (eg. Fig. 4.28) through to pack-grainstones (eg. Fig. 4.34C).

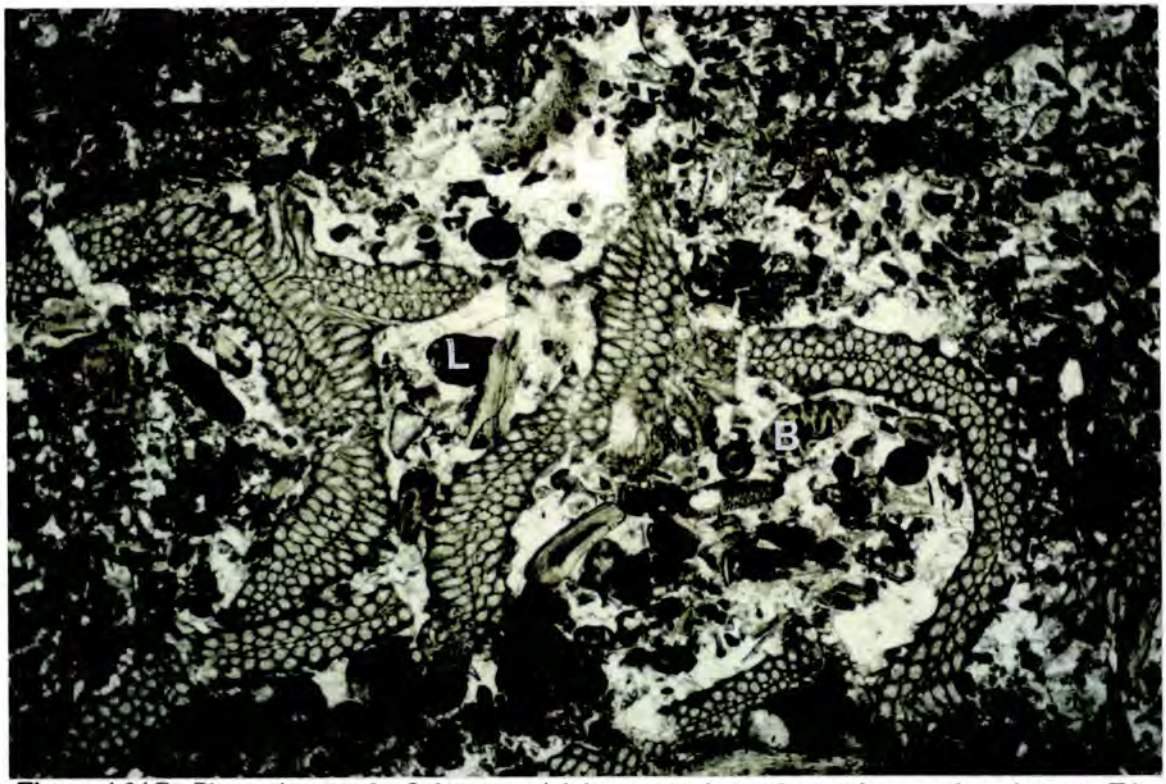

Figure 4.34C. Photomicrograph of elongate stick bryozoans in a sub-wavebase pack-grainstone (F4 facies). The pack-grainstone is quite well sorted and is composed of rounded bryozoans (B), peloids, crinoids with occasional rounded slope lithoclasts (L). These facies are interpreted to have developed at and/or just below storm wavebase. Specimen from the base of Bs2 of Arnaud-Vanneau (1980), Pic d'Oeillette, Chartreuse approximately 3m above flooding surface arrowed in Figure 5.9. (Field of view 18mm, PPL).

The F3-1 facies are illustrated in Figures 4.28 & 4.34A, B, D & E, and contain between 20 and 30% clays and up to 10% silt grade quartz (eg. Fig. 4.34D). In the field they are characterized by blue-grey shales containing a low diversity fauna dominated by the irregular burrowing echinoid *Toxaster* (eg. Fig 4.34A, C, D & E). The limestones vary between a yellow and grey colour and are typically wavy to nodular bedded, but notably less so than the upper Hauterivian slope facies (eg. compare Fig. 4.24 & Fig. 4.44E). The FO basin-floor facies is characterized in the field by thick-bedded limestones interbedded with shales and is generally less nodular than slope facies (eg. Fig. 5.41). In thin section these are mudstones composed of a

variable proportion of pelagic foraminifera and calcispheres (*Oligostegina*) (Fig. 4.34F).

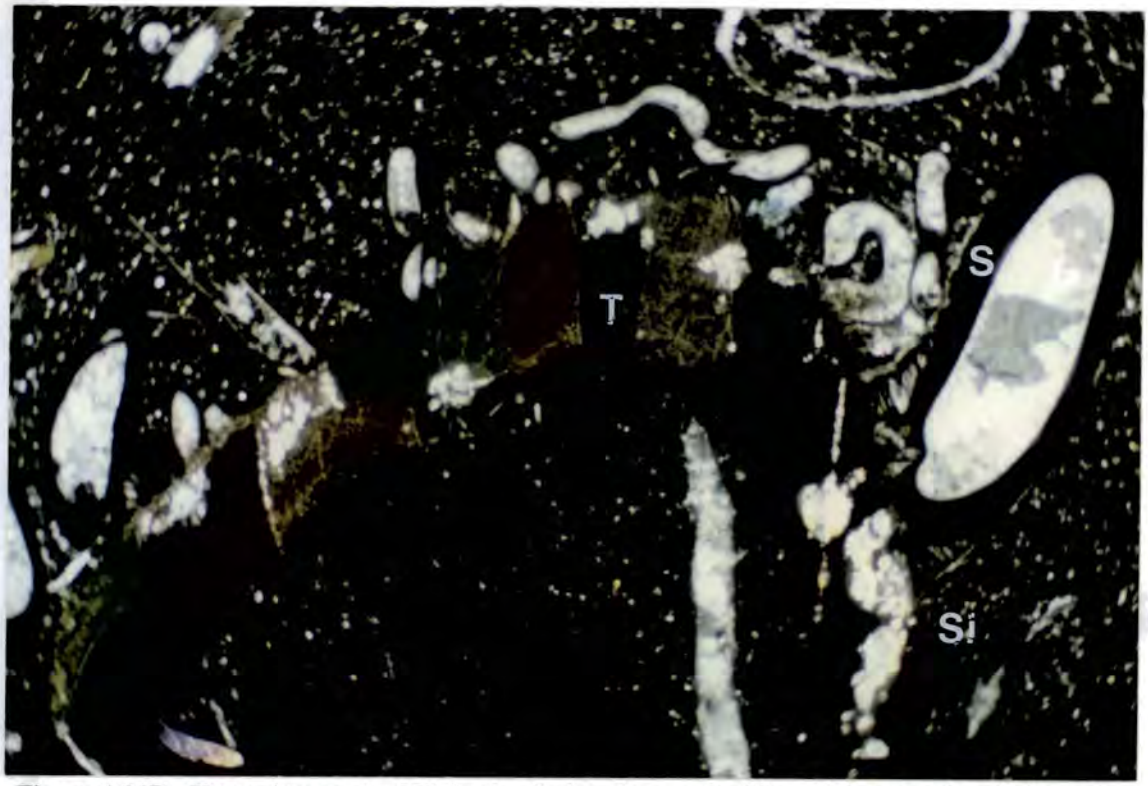

Figure 4.34D. Photomicrograph of F1-2 microfacies, characterized by a high proportion of silt grade quartz and sponge spicules. This particular section is dominated by the test of the irregular echinoid *Toxaster* (T), which is itself encrusted by serpulids (S). Note the partial replacement of the test of the echinoid by silica (Si). Field of view approximately 18mm.

4.5.2. D. Processes of sedimentation upon an accretionary slope.

The sub-wavebase accretionary slope extends basinward from sub-horizontal toplap strata developed at about fair-weather wavebase and characterized by F5-7 facies to the basin-floor. Classically, an accretionary slope flattens out asymptotically basinwards (eg. Figs 6.13, 6.14 & 6.15). Bioclastic sands overproduced in shallow-waters (<10m, - above wavebase) were moved to the offlap break (fair-weather wavebase), from where they became redeposited down-slope. On the mid-slope of clinoforms to Bi5, individual beds vary from 0.1-0.5m thick and have sharp, undulose bases (eg. Fig. 4.35). Occasionally, where the depositional fabrics are not destroyed by bioturbation normal grading can be seen. These undulose beds are separated by laterally persistent orange or green thin (5-50mm) shale horizons (Fig. 4.35),

Figure 4.34E. Lower Barremian (Bi5-Bi6) F1-F2 facies of the lower (sub-storm wavebase) slope as developed in the Grands Goulets, western Vercors. The thick and continuous nature of limestone beds readily distinguishes these deposits from Hauterivian slope facies (eg. compare to Fig. 4.24). Close-up (below) of dark-grey shales immediately adjacent to the hammer (arrowed above) illustrates the characteristic fauna of these facies, the irregular burrowing echinod *Toxaster* (T). Hammer approximately 350mm long for scale in both photographs.

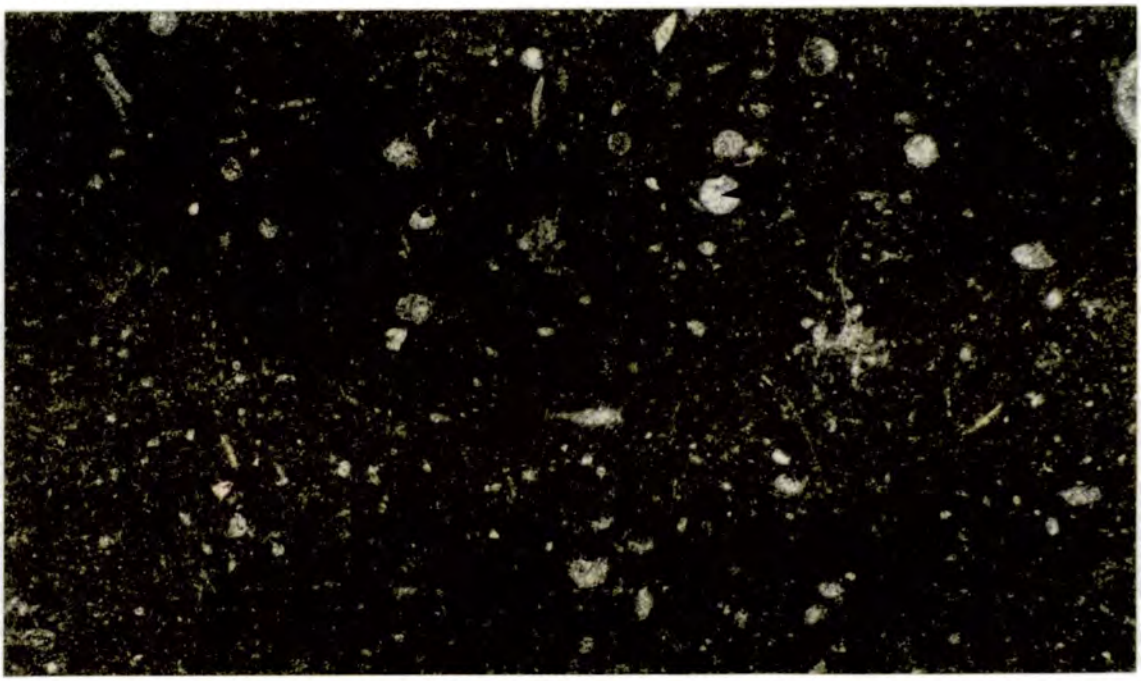

Figure 4.34F. Photomicrograph of basin-floor lower Barremian pelagic mudstone of La Chaudière, Diois. This facies is dominated by the calcisphere *Oligostegina*(O). Field of view 4mm.

Figure 4.35. Characteristic strata of the mid part of Bi5 clinoforms of the northern Archiane valley, southern Vercors (eg. see Fig. 6.14). Beds are tabular, but undulose and separated by shales which are laterally very persistent. This suggests that the bases of the limestone beds are not erosive. Internally the depositional fabric of the limestones, originally a grainstone is now preserved as islands within a wacke-mudstone, see Fig. 4.36. The undulose nature of these beds is thought to be a reflection of the pervasive bioturbation of these beds.

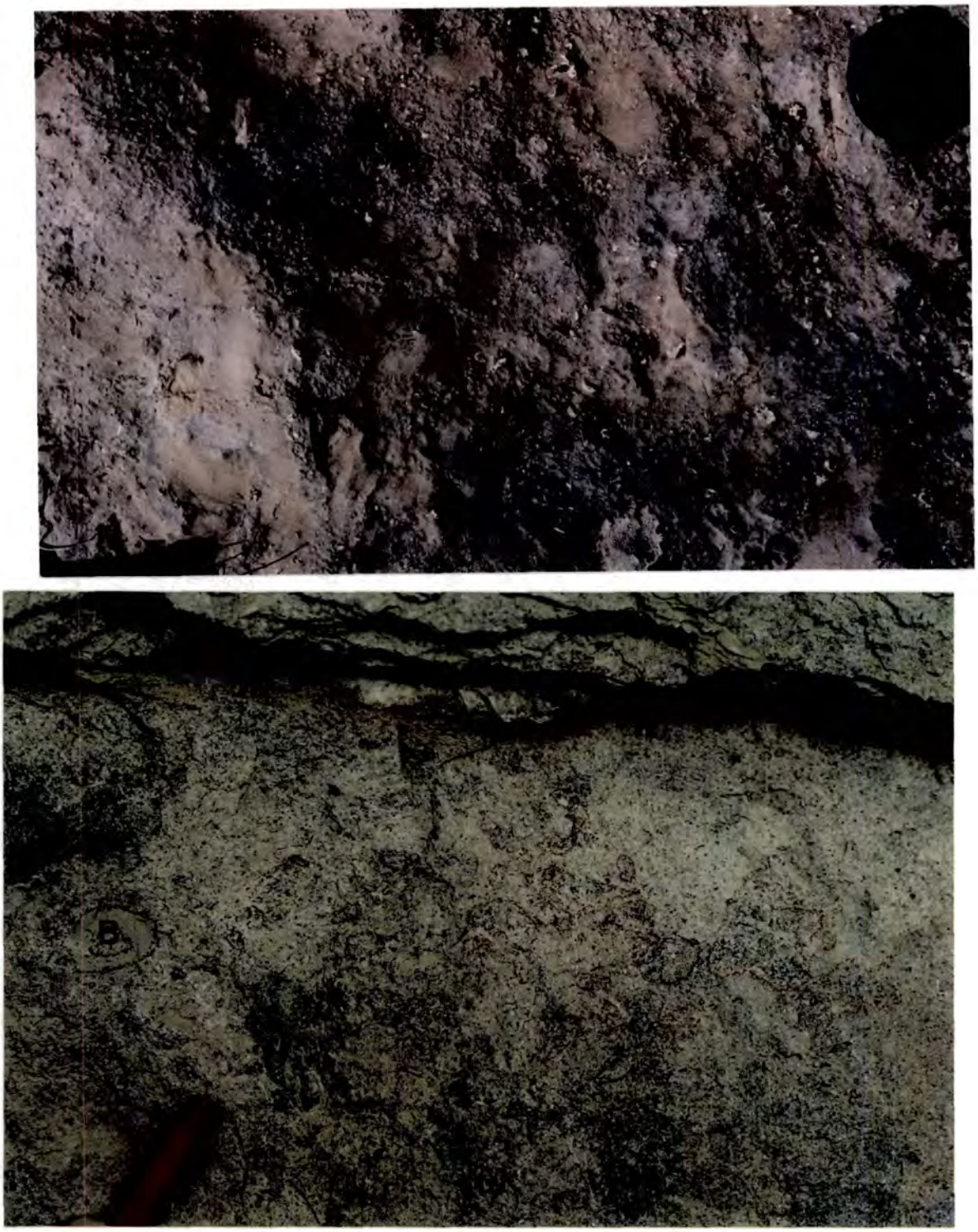

Figure 4.36. Photographs of a bed and bedding surface of the slope sands illustrated in Figure 4.35. On the bedding surface (above) characteristically ochre-orange coloured, iron rich mudstones are bioturbated into the depositional grainstone fabric. Lens cap approximately 50mm in diameter for scale. In vertical section (below) 'islands' of the original grainstone texture of these slope sands are outlined in red and are separated by a post-depositional biogenically formed mud-wackestone fabric. Bryozoans and a single burrow (B) are outlined in green pencil. The pervasive bioturbation of these facies is thought to develop the irregular upper surface of these beds, Pencil approximately 30mm long for scale.

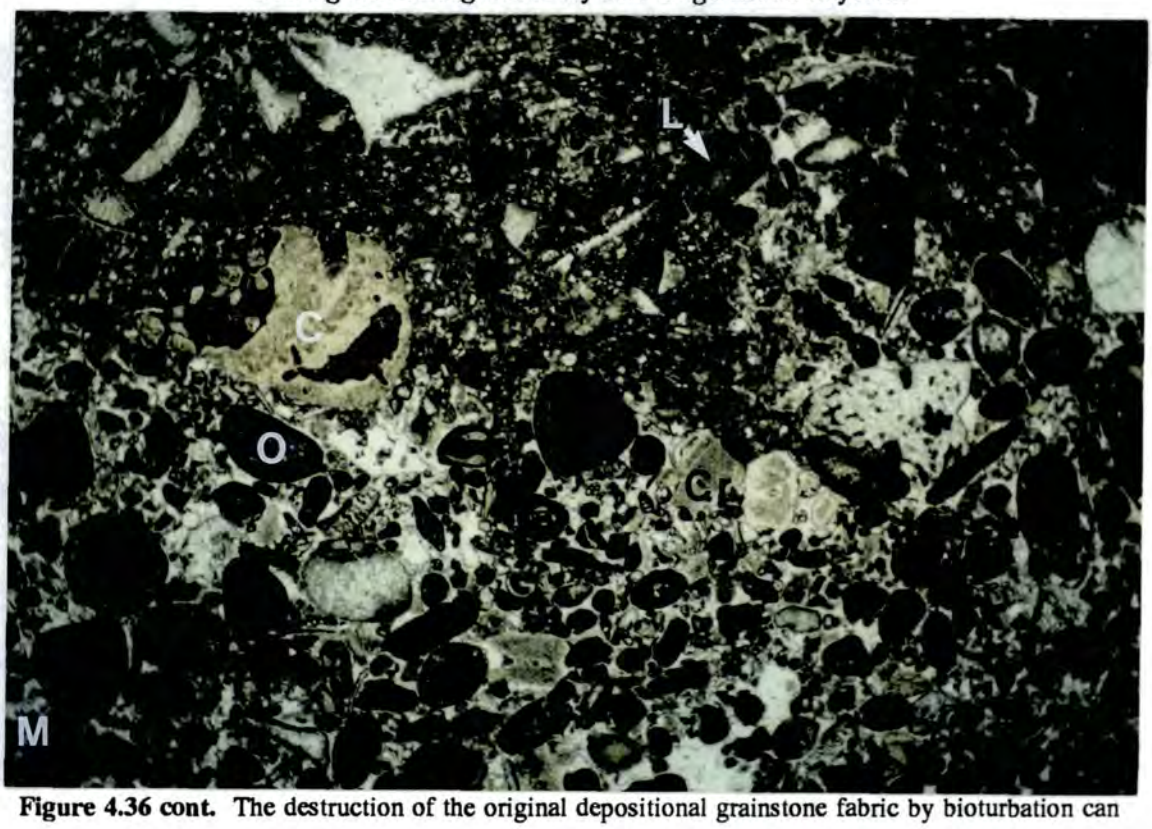

Figure 4.36 cont. The destruction of the original depositional grainstone fabric by bioturbation can also be clearly seen in thin-section. This photomicrograph of an original bimodal grainstone illustrates the biogenic mixing of foreslope muds in to F5 type grainstone facies. The original grainstone is composed of Orbitolinid (O) and Miliolid (M) foraminifera, crinoids (Cr), bioclasts of corals (C) and lithoclasts of shallow-water facies with early isopachous marine cements (L). Field of view 18mm, PPL.

suggesting that the bases of the limestone beds are not erosive, but fill the topography of the preceding bed. Internally, the fabrics of these sharp-based beds are complex and can vary from grainstone to mudstone textures (Fig. 4.36). The top 50-150mm of beds is normally composed of the highest proportion of muds and also contains 'oversized' bryozoan colonies (eg. Fig 4.36). The upper surface of these beds is illustrated in Figure 4.36 and can be seen to be composed of approximately 50-60% mudstone, bioturbated into the slope sands which are preserved as 'islands' of pack-grainstone fabrics separated by mud-wackestones (Fig. 4.36B). The irregular upper surface of these limestone beds (eg. Fig. 4.35) is thought to be a reflection of their pervasive post-depositional bioturbation which increased the volume of the beds by mixing in slope muds (eg. Fig 4.36). The development of mudstones highly enriched in iron oxides between limestone beds and the bioturbation of these muds

Figure 4.37. Photograph looking northwards up the slope of clinoforms at La Montagnette in the southern Vercors (see also Fig. 6.13). At the base of the slope (where clinoforms flatten out, see Fig. 6.13) individual clinoform packages marked by prominent and laterally very persistent shale horizons. These can be traced up the slope to the shallow-water shelf (eg. Figs 6.13, 6.14 & 6.15). In the foreground the limestone-shale couplets build to form a 2-2.5m thick bundle bound by prominent shale horizons which can be traced up the slope. On the shallow-water shelf (eg. Figs 6.14 & 6.15) the prominent shales separating clinoforms are the base of 5-10m thick shallowing-up cycles (eg. Figs 6.13, 6.14 & 6.15).

into the underlying slope sands suggests prolonged periods of non-deposition between the deposition of the bioclastic sands on the mid-slope. Both the mid-slope sands and muds are interpreted to have been deposited below storm wavebase.

Where clinoforms flatten-out (eg. at the base of the Bi5P cliff of La Montagnette, Figs 4.37 & 6.13) this pattern is more readily distinguished, for here limestones are rhythmically interbedded with shales (Fig. 4.37); a pattern not immediately apparent on the mid-slope (eg. Fig. 4.35). At the toe-of-slope, four to five limestone-shale couplets build to form a package approximately 2.5m thick, which is bound above and below by prominent shale horizons (Fig. 4.37). These shales, which bound the bundles of 4-5 limestone-shale couplets at the toe-of-slope

are laterally persistent and can be traced up from the toe-of-slope to the upper slope, and separate the major clinoforms (eg. Figs 4.37, 6.13, & 6.14). The thickness of these major shale bound clinoforms increases up-slope to approximately 4m on the mid-slope. As the clinoforms are followed further up-slope the 4-5 rhythmic limestone-shale alternations identified at the toe-of-slope are gradually lost (eg. Fig. 4.37). This is interpreted to reflect the gradual up-slope increase of bioclastic sedimentation rates, the normal pattern developed on an accretionary slope.

The major bounding surfaces of clinoforms packages, marked by sub-wavebase shales as identified at La Montagnette (eg. Fig. 4.37) can also be identified at the chronostratigraphic equivalent exposure in the Cirque d'Archiane (eg. Figs 6.14 & 6.15). In the northern Cirque d'Archiane these surfaces which divide clinoform packages can be traced from the slope and into shallow-water facies where they divide asymmetric 5-10m shallowing-up cycles (eg. Figs 6.14 & 6.15). The shedding of limestones from the shallow-water 'shelf' on to the slope is thus interpreted to occur during times when there was excess sediment in this region of the platform. Such times were separated by the temporary drowning of carbonate sedimentation in shallow-water areas and are marked by the deposition of laterally persistent sub-wavebase shales on the slope. The thickness of mid-slope clinoform bundles is approximately 4m whereas those at the toe-of-slope are approximately 2-2.5m. These correspond to an equivalent thickness of shallow-water toplap strata of 5-10m suggesting that the toe-of-slope sedimentation rates vary from approximately 20-40% of the shallow-water shelf-margin sedimentation rate during Bi5, negating the effects of differential compaction between these environments.

4.6. Stratigraphic Evolution Of The Urgonian Platform.

4.6.1. Introduction.

In this section the general stratigraphy and palaeogeographic evolution of the Urgonian platform as developed by Arnaud-Vanneau & Arnaud (1976), Arnaud-Vanneau (1980) and Arnaud (1981) is described. This provides a basic background for the following two chapters where a sequence stratigraphy for the Urgonian platform is built. As discussed in Section 4.4, Arnaud-Vanneau *et al.* (1976) and Thieuloy (1979) established palaeontologically that the bioclastic sands of the southern Vercors, the Borne and Glandasse Bioclastic Formations (Arnaud-Vanneau, 1980; Arnaud, 1981, Fig. 4.25, previously named the Haut-Fond du Dévoluy and Haut-Fond du Vercors Meridional respectively, Fig. 4.38) are lower Barremian in age. These two lower Formations of the Urgonian platform *sensu lato* are separated from the Urgonian Limestone Formation by a widely developed marly horizon; the *Matheronites limentinus* level (Font Froide marls of Fig. 4.25) (Fig. 4.38). The Borne and Glandasse Bioclastic Limestone Formations crop out in Dévoluy, Borne and the southern Vercors (Glandasse plateau), whereas the younger Urgonian Limestone Formation is developed from the Glandasse plateau northwards across the northern Vercors and Chartreuse of the Sub-Alpine chains and on to the Jura (Fig. 4.38).

Figure 4.38. (Facing page) Two schematic NW-SE cross-sections of the Urgonian platform according to Arnaud-Vanneau & Arnaud (1976). The Haut-Fond du Dévoluy is equivalent to the Borne Bioclastic Formation, and the Haut-Fond du Vercors Meridional to the Glandasse Bioclastic Limestone Formation of Arnaud-Vanneau (1980) and Arnaud (1981) (eg. Fig. 4.25). The Haut-Fond du Dévoluy was originally interpreted to be a shallow-water shoal (Arnaud-Vanneau & Arnaud, 1976), but has since been re-interpreted as a deep-water (>> storm wavebase) slope and basin-floor fan (eg. Arnaud, 1981).

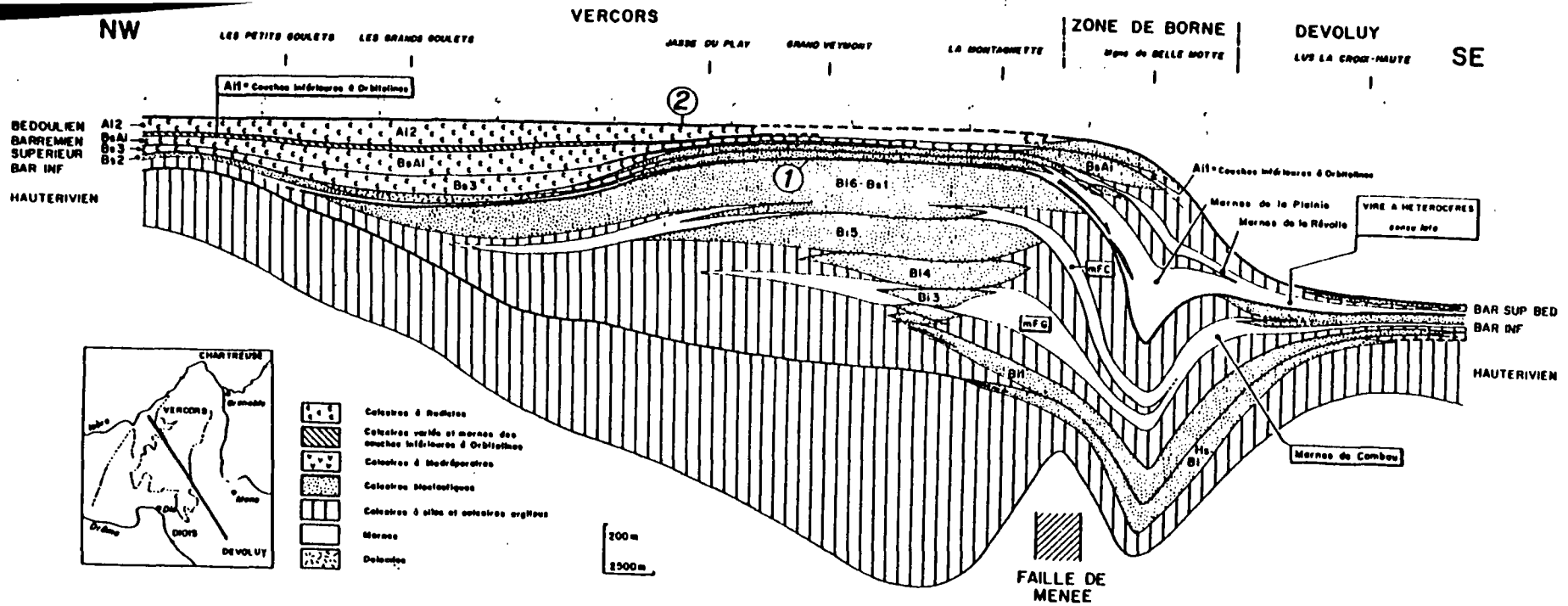
NW
VERCORS
ZONE DE BORNE
DEVOLUY
SE
LES PETITS GOULETS
LES GRANDS GOULETS
JASSE DU PLAT
GRAND VEYMONT
LA MONTAGNETTE
Mgne de BELLE MOTTE
LUS LA CROIX-HAUTE
BEDOULIEN
BARREMIEN SUPERIEUR
BAR INF
HAUTERIVIEN
Al2
BsAl
Bs3
Bs2
Bi6-Bi1
Bi5
Bi4
Bi3
mFC
mFG
BH
Ha
Bl
Marnes de la Plaine
Marnes de la Révolle
VIRE A HETEROCERES
BAR SUP BED
BAR INF
HAUTERIVIEN
Marnes de Combau
FAILLE DE MENEE
CHARTREUSE
VERCORS
DIOIS
DEVOLUY
Calcaires à Rudistes
Calcaires variés et marnes des couches inférieures à Orbitolines
Calcaires à Madréporaires
Calcaires Bioclastiques
Calcaires à silex et calcaires argileux
Marnes
Dolomies
200 m
2500 m

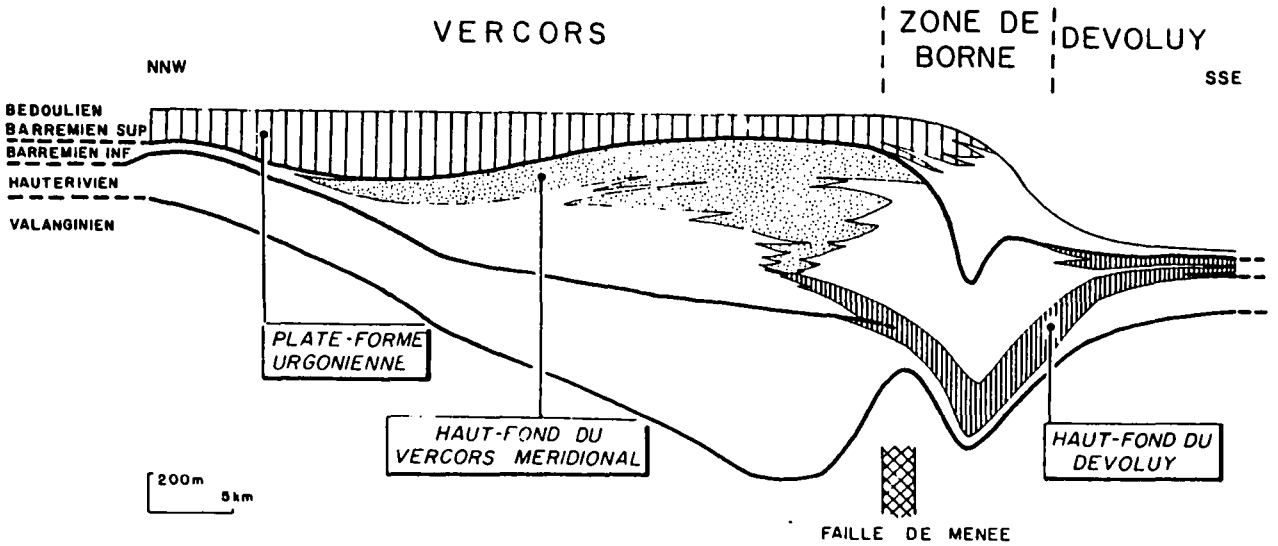
VERCORS
ZONE DE BORNE
DEVOLUY
NNW
SSE
BEDOULIEN
BARREMIEN SUP
BARREMIEN INF
HAUTERIVIEN
VALANGINIEN
PLATE-FORME URGONIENNE
HAUT-FOND DU VERCORS MERIDIONAL
HAUT-FOND DU DEVOLUY
200m
5km
FAILLE DE MENEE

4.6.2. The tectonostratigraphic evolution of the lower Barremian Borne and Glandasse Bioclastic Limestone Formation.

These two Formations are exposed on the northern flanks of the Vocontian basin, and, as their nomenclature suggests, are dominated by bioclastic sands and crop-out (eg. Fig. 4.38). The lower Borne Formation (Haut-Fond du Dévoluy, Fig. 4.38) is divided into two members, HsBi and Bi1 (Figs 4.25 & 4.38), and are the lowermost deposits of the Urgonian platform *sensu lato* (Arnaud-Vanneau & Arnaud, 1976). The approximate areal extent of this member and its progressive development as originally envisaged by Arnaud-Vanneau & Arnaud (1976) is shown in Figure 4.39.

The bioclastic sands of the Glandasse Formation (Haut-Fond du Vercors, Fig. 4.38) overlie the Borne Formation at its northern-most extremity. The Glandasse Formation is composed of six members, Bi2-Bs1 (Fig. 4.25) and has a maximum thickness of approximately 650-700m of bioclastic sands in the vicinity of La Montagnette (Mo, Figs 4.25 & 4.40). This area, just to the north of la Montagnette (Mo, Fig. 4.40) is interpreted to be where shallow-water sedimentation of the Glandasse Formation initiated and subsequently aggraded and prograded. As such, it is the palaeogeographic centre of this Formation (Fig. 4.40a), and is offset by approximately 10km from the lower Barremian depocentre (eg. Fig. 4.40b). Above Bi2, (the lowest member of the Glandasse Formation) each succeeding member prograded further basinward (S-SE) than its immediate precursor (Fig. 4.40). This southward progradation was not, however, as marked as the shelfward (N-NW) shedding of bioclastic sands from the southern Vercors shoal (eg. Fig. 4.40a). This is interpreted to reflect the preferred leeward shedding of bioclastic sands off the shallow-water shoal from northerly directed winds. These are interpreted to have developed a steeper windward margin which cause the local bypassing of sands to the basin-floor during Bi5 and Bi6 (Arnaud, 1981, see Fig. 4.43).

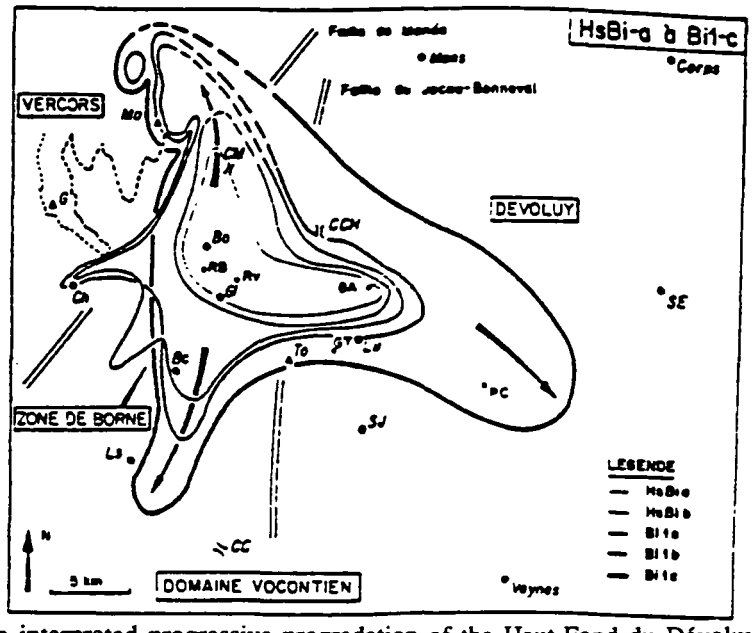

Figure 4.39. The interpreted progressive progradation of the Haut-Fond du Dévoluy according to Arnaud-Vanneau & Arnaud (1976) (compare to Fig. 4.42).

Originally, both the Borne and Glandasse Bioclastic Limestone Formations were interpreted to have been deposited in shallow-waters (eg. <10m) on two palaeogeographically separate isolated platforms (Arnaud-Vanneau & Arnaud (1976). This led Arnaud-Vanneau & Arnaud (1976) to suggest complex and differential movements along both the Menée and Jocou faults during the upper Hauterivian / lower most Barremian (eg. Fig. 4.41). The 'zone de Borne' was interpreted to have become topographically elevated in the uppermost Hauterivian, upon which shallow-water bioclastic sedimentation was established and shed into surrounding topographic lows (eg. Figs 4.39 & 4.41b). In the lower Barremian (Bi2) the 'Chenal de Borne' was interpreted to have formed from the reactivation of the Menée and Jocou-Bonneval faults (Fig. 4.41c-d). This tectonically formed depression separated two interpreted shallow-water areas where bioclastic sands were developed; the Glandasse plateau area to the north, site of the Haut-Fond du Vercors and Zone de Borne to the south (eg. Figs 4.39 & 4.41).

Subsequently, in a major re-interpretation, Arnaud-Vanneau (1980) and Arnaud (1981) recognized that the shallow-water grains of the Borne Formation had been redeposited in a deep-sea fan complex. They suggested that this fan complex was derived from a shallow-water platform (no longer exposed) which lay to the

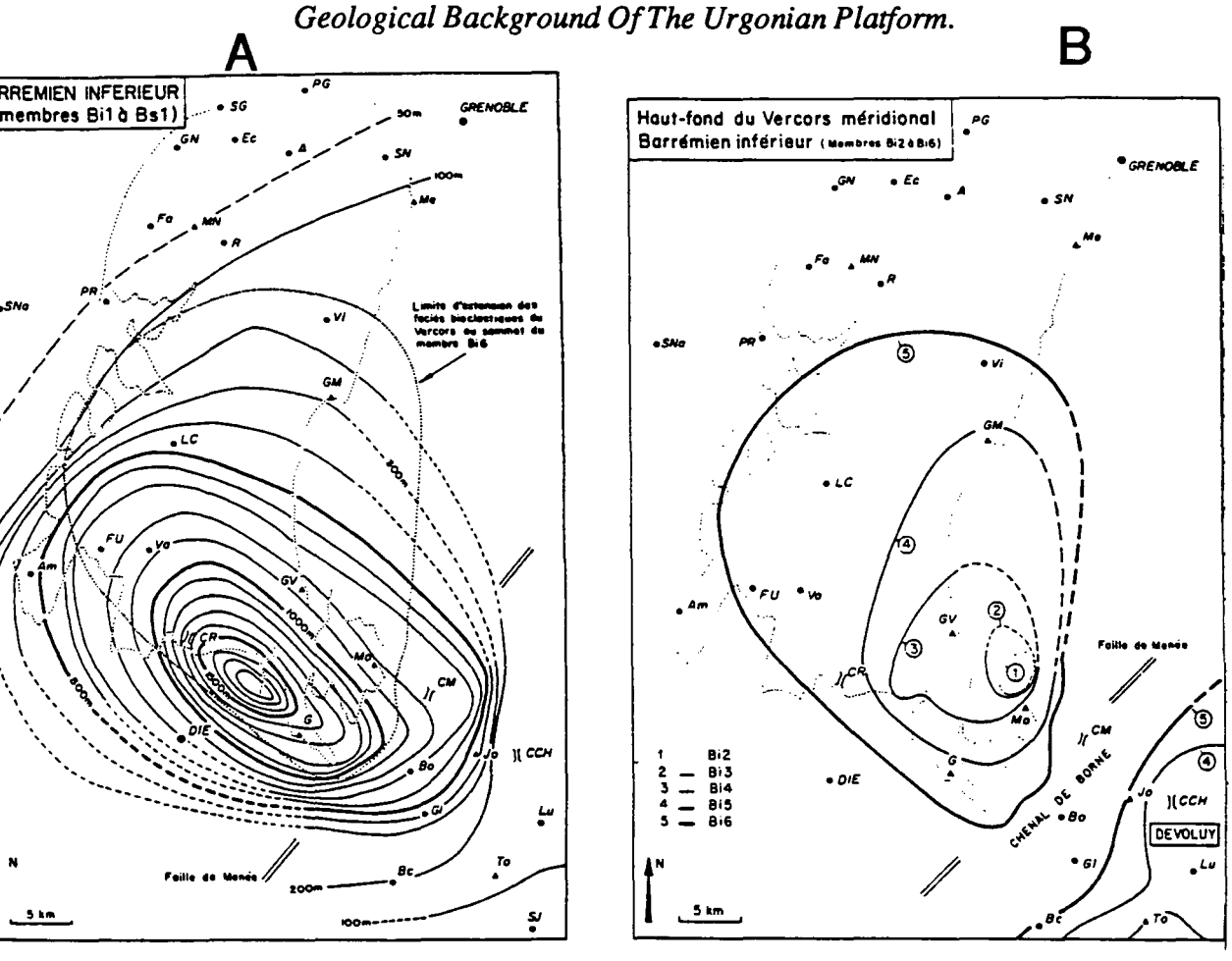

Figure 4.40. Paired maps of the southern Vercors showing (A) the isopachs of the Haut-Fond du Dévouly and Haut-Fond du Vercors Meridional of Arnaud-Vanneau & Arnaud (1976); the Borne and Glandasse Bioclastic Limestone Formations of Arnaud-Vanneau (1980) and Arnaud (1981) and, (B) the progressive progradation of the first five members (Bi2-6) of the Glandasse Formation (compare to Fig. 4.38). From Arnaud-Vanneau & Arnaud (1976).

Place names: A: Autrans; Am: Montagne de Ambel; Bo: Borne; Bc: Boulc; CM: Col de Menée; CR: Col du Rousset; Ec: Balcon des Ecouges; Fa: La Fa; FU: Font d'Urle; G: Glandasse Gl: Glandage; GM: La Grand Moucherolle; GN: Gorge du Nant; GV: Grand Veymont; Jo: Jocou; LC: La Chapelle; Lu: Lus-la-Croix-Haute; ME: Le Moucherotte; Mo: La Montagnette; MN: Mont Noir; PG: Pré de Gève; PR: Pont-en-Royans; R: Les Rimets; SN: Saint Naziere; SNa: Saint-Nazaire-en-Royans; To: Toussiere; Va: Vassieux; Vi: Villard-de-Lans.

northeast of the Glandasse plateau area (eg. Fig. 4.42). As a consequence of this major palaeogeographic re-interpretation there was no longer a need to invoke the complex reactivation of the Menée and Jocou-Bonneval basement faults during the late Hauterivian and lower Barremian (eg. Fig. 4.41). Arnaud-Vanneau (1980) and Arnaud (1981) argued that the lowermost Barremian sedimentary bypass of shallow-

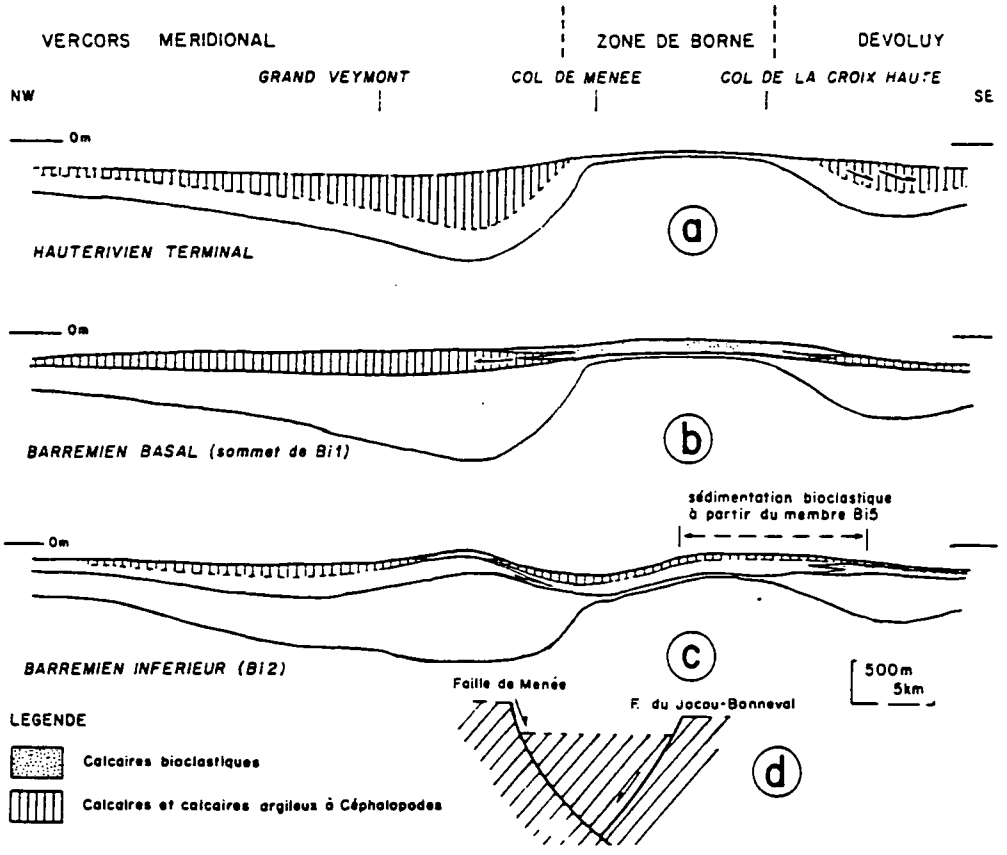

Figure 4.41. The progressive conceptual development of the Haut-Fond du Dévoluy and Haut-Fond du Vercors Meridional according to Arnaud-Vanneau & Arnaud (1980). Note that the 'zone de Borne' was interpreted to have been a tectonic high at the end of the Hauterivian (a), upon which shallow-water sedimentation (<10m) developed in the uppermost Hauterivian/lowermost Barremian (HsBi-Bi1 of Arnaud, 1981). Subsequently, (Bi1-Bi2) the reactivation of the Menée and Jocou-Bonneval faults drowned this most southerly shoal in and located shallow-water sedimentation upon a tectonically induced high to the north of la Montagnette (eg. Bi2, Fig. 4.40) (Arnaud-Vanneau & Arnaud, 1976).

water sands to the slope and basin-floor (Borne Formation, Fig. 4.42), and the subsequent development of a shallow-water bioclastic sand shoal in the north, the Glandasse plateau (Bi2, Fig. 4.41) was a direct consequence of the tectonic uplift of the southern Vercors area. Arnaud-Vanneau (1980) and Arnaud (1981) suggested that this uplift was localised along the NE-SW orientated Clery and Jasneuf faults (Fig. 4.19). The inversion of these faults is interpreted to have raised the depositional surface in the region of La Montagnette to fair-weather wavebase, allowing the development of a shallow-water bioclastic sand shoal: Bi2 (Fig. 4.40), the lowermost

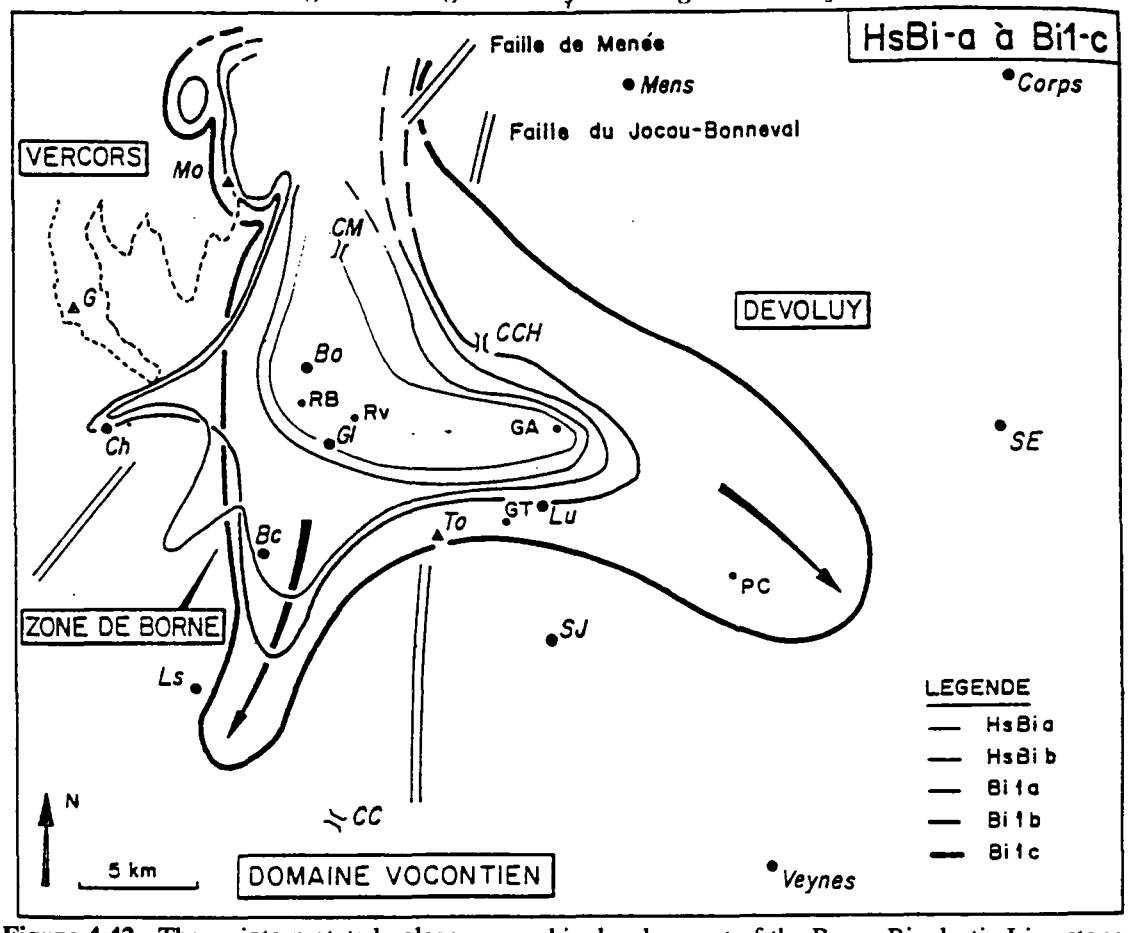

Figure 4.42. The re-interpretated palaeogeographic development of the Borne Bioclastic Limestone Formation (HsBi-Bi1) according to Arnaud (1981) (compare to Fig. 4.39 & 4.41). This Formation originally interpreted to have been deposited in shallow-water in the 'zone de Borne' (eg. Fig. 4.41) was re-interpreted by Arnaud to be a deep-sea slope (La Montagnette area) and basin-floor fan (Borne area), derived from a shallow-water platform area which lay to the northeast of the Glandasse plateau area.

member of the 'southern Vercors shoal' (Arnaud-Vanneau & Arnaud, 1976, Bi2, Figs 4.38 & 4.40). The establishment of this bioclastic shoal was followed by the gradual subsidence of this area at a lower rate than that of the shallow-water sedimentation, which resulted in the progradation of the shallow-water sands over a progressively larger area (Figs. 4.38 & 4.40). The member Bi6 of Arnaud (1981) is interpreted to mark the greatest areal extent of this southern Vercors shoal and its palaeogeography is schematically illustrated in Figure 4.43. Arnaud (1981) interpreted the more rapid northern progradation of the Glandasse Formation to reflect the preferential leeward movement of sediment in response of a northward trade wind at this time ('vent dominant', Fig. 4.43).

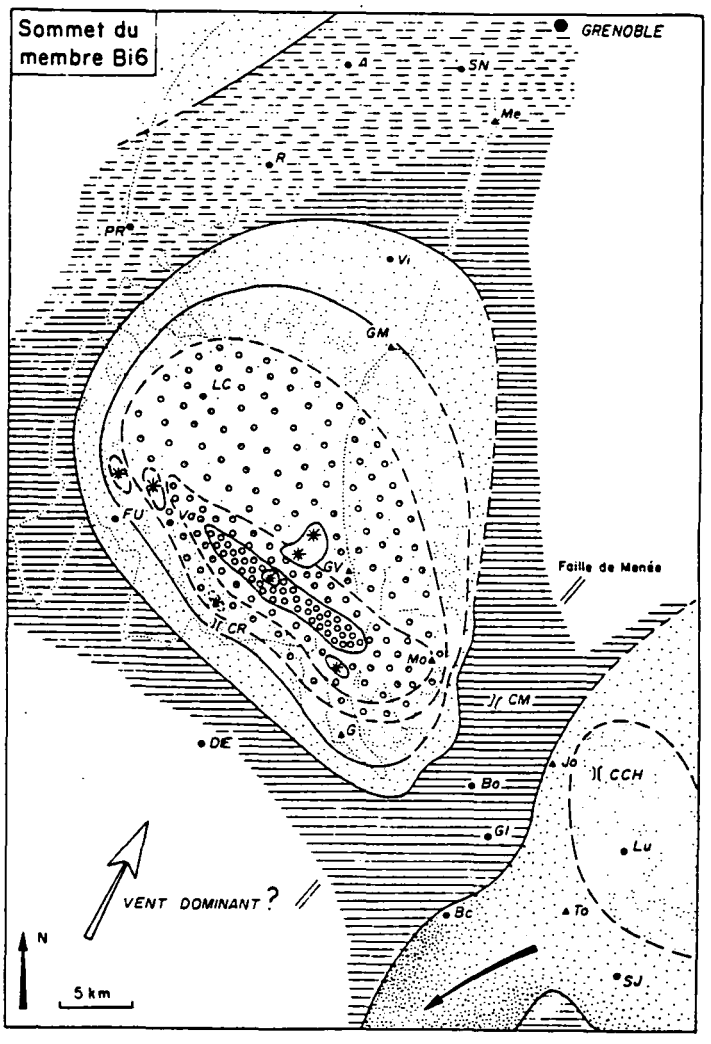

Figure 4.43. The interpreted palaeogeography of the southern Vercors area for the uppermost member (Bi6) of the Glandasse Bioclastic limestone Formation as according to Arnaud-Vanneau & Arnaud (1976). *Key to symbols*, (moving away from the centre of the shoal): stars: coral boundstones; open circles: rounded coralline bioclasts; dotted open circles (alone): oolites; dotted open circles with dots: bioclastic grainstones with ooliths; dots (closely spaced): bioclastic limestones; dots (widely spaced): fine bioclastic limestones; horizontal lines (continuous): sub-wavebase limestones and shales; horizontal lines (dashed): sub-wavebase shales with limestones. *Place names:* as according to Fig. 4.41 and: CCH: Col de la Croix -Haute; SJ: Saint-Julien-en-Beauchêne.

The Borne and Glandasse Bioclastic limestone Formations of the southern Vercors are interpreted by Arnaud-Vanneau (1980) and Arnaud (1981) to have developed from a structurally-induced shallowing of the southern Vercors whilst the more northerly Vercors, Chartreuse and Jura remained drowned after an upper Hauterivian transgression, and were thus characterized by relatively condensed sedimentation. The very different sedimentation rates between the northern Vercors,

Chartreuse, Jura and the southern Vercors (eg. Figs 4.8 & 4.10) were thus attributed to the structural independence of the southern Vercors area the rest of the Dauphinois basin (eg. Arnaud, 1988).

4.6.3. The upper Barremian Urgonian Limestone Formation.

The Urgonian Limestone Formation is entirely upper Barremian in age and is the third distinct palaeogeographic stage to the development of the platform *sensu lato* (Arnaud-Vanneau & Arnaud, 1976; Arnaud-Vanneau *et al.*, 1976; Arnaud-Vanneau, 1980; Arnaud, 1981). This Formation has an average thickness of 300m on the shelf, is essentially aggradational and was interpreted by Arnaud-Vanneau & Arnaud (1976), Arnaud-Vanneau (1980) and Arnaud (1981) to have developed after a relative sea-level rise during lowermost upper Barremian (Bs1-Bs2, Figs 4.25 & 4.38). The reasons for the 'start-up' of Urgonian sedimentation across areas 'drowned' during the lower Barremian (eg. northern Vercors, Chartreuse and Jura) as a result of this further relative-sea-level rise are not, however, clear. As shallow-water sedimentation initiated in the previously drowned areas, the southern Vercors shoal became attached to the 'mainland' of the Jura platform (eg. compare Fig. 4.38 & 4.43).

The lower member of the Urgonian Limestone Formation (Bs2-BsAi, Figs 4.25 & 4.38) thins over the inherited topography of the Glandasse Formation (Figs 4.38 & 4.44) and also in the northern Vercors where the northerly extension of the Rochers de Chironne fault intersects with the Isère lineament (Figs 4.19 & 4.44). This lower member of the Urgonian platform *sensu stricto* is divided by the lower *Orbitolina* beds from the upper member of the Formation (Fig. 4.38) which is a prominent marly horizon within the platform succession. These marls were interpreted to have developed during a distinct relative sea-level rise during the development of the Urgonian platform (eg. Arnaud-Vanneau *et al.*, 1987).

The upper member of the Urgonian platform succession is the upper *Orbitolina* marls, interpreted to have been confined to tidal channels upon the upper

surface of the Urgonian platform (Arnaud-Vanneau, 1980). These marls are in-turn overlain by an outer-platform sand-shoal complex, the 'Lumachelle' limestones which mark the demise of Urgonian sedimentation.

The stratigraphic schemes described above have since been modified by sequence stratigraphic interpretations of the platform. These are described in the following two chapters of this thesis, and which divide the platform into unconformity bounded units (sequences) emphasising times when the platform became subaerially exposed, previously interpreted to have been of little importance to the development of the platform.

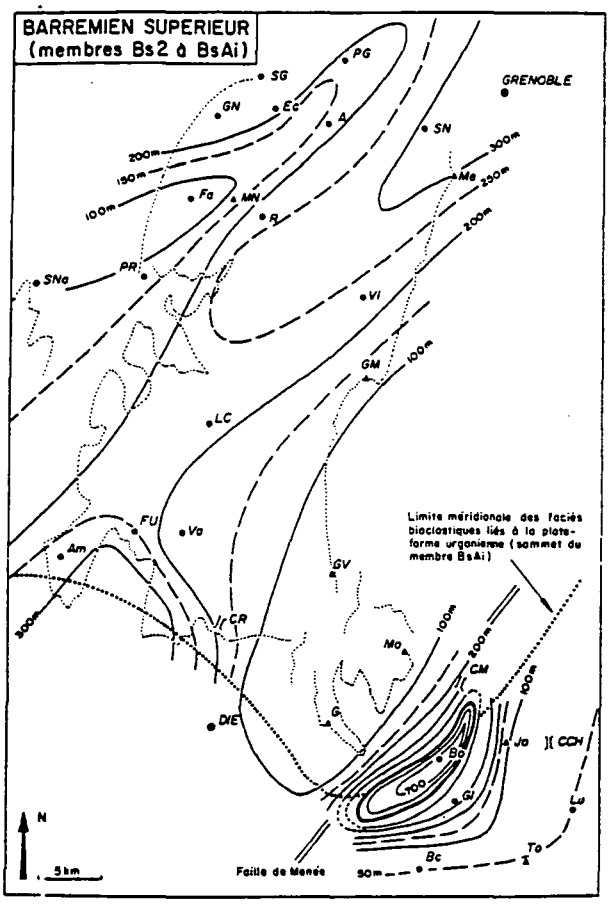

Figure 4.44. Isopachs of the lower member of the Urgonian Limestone Formation as according to Arnaud-Vanneau & Arnaud (1976). The average thickness of the whole Urgonian Limestone Formation (eg. including Ai1, 2 & 3) across the shelf is approximately 300m. Note the thinning of the lower part of the Urgonian Limestone Formation across the Glandasse plateau area where the Glandasse Formation developed (eg. compare to Fig. 4.38) and in the northern Vercors, approximately where the Rochers du Chironne fault intersects the Isère fault (see Fig. 4.19). The approximate limit of the BsB1 member is also marked with a dotted line.

Chapter 5.
Criteria For The Identification Of Stratal Surfaces And Stratal Patterns Upon The Urgonian Platform.

5.1. Introduction.

In the preceding Chapter the general stratigraphy and evolution of the Urgonian platform were discussed. Following from this introduction the criteria used to identify sequence boundaries, maximum flooding surfaces etc. upon the Urgonian platform are discussed. On the basis of stratal patterns and facies associations the platform is divided into three components: shelf, slope and basin-floor and each is discussed in turn. For each part of the platform the 'Galloway' and 'Exxon' models are compared in terms of both the prediction of stacking patterns and ease of identifying the sequence bounding surface (eg. flooding surfaces v exposure surfaces).

The shelf is the least controversial area of the platform as is illustrated by the convergence of recent sequence stratigraphic interpretations on this part of the platform (eg. Arnaud-Vanneau & Arnaud, 1991; Jacquin *et al.*, 1991; Hunt & Tucker, 1992). The sequence stratigraphic schemes of these workers, however, diverge markedly upon the slope. Here the interpretation of sequence boundaries and their component systems tracts is more controversial. In the Exxon paradigm sequence boundaries on the slope are normally interpreted on the basis of erosional truncation of older strata and/or by onlap of younger strata onto the sequence boundary (see Section 2.2.4 for a fuller discussion). Such an approach has been widely applied to the spectacular seismic scale lower Barremian exposures of the southern Vercors and Glandasse plateau (eg. Ravenne *et al.*, 1987; Jacquin *et al.*, 1991). Doubts are, however, cast upon this geometric approach from the study of the Cirque d'Archiane and Rocher du Combau where unambiguous shallow-water bioclastic facies can be followed semi-continuously from the shelf-margin

on to and down the slope. Here the development of onlap and/or erosional truncation upon the slope is put into a sequence stratigraphic context by evaluating relative sea-level changes upon the shallow-water shelf. Basin-floor stratal patterns are afforded less attention as seismic scale exposure is generally poor.

5.2. Shelf.

5.2.1. Introduction.

The shelf extends landward of the shelf-slope break, is characterized by water depths of normally <10m and includes both marine and non-marine depositional environments. The Urgonian shelf is characterized by a high-energy shelf-margin dominated by bioclastic sands which is backed by a protected lagoon where Urgonian facies *sensu stricto* are developed (eg. rudist facies). Stratal patterns are typically parallel-parallel in the shelf-lagoon whereas the downlap and toplap of progradational-aggradational sand shoals is characteristic of the shelf-margin. Recent sequence stratigraphic schemes for the Urgonian shelf have tended to be similar which reflects a general consensus of interpretation(s) upon the shelf (eg. Arnaud & Arnaud-Vanneau, 1989; Arnaud & Arnaud-Vanneau, 1990; Jacquin *et al.*, 1991; Hunt & Tucker, 1992) (eg. Fig. 5.1, compare A & B).

In the stratigraphic scheme of Arnaud-Vanneau (1980) and Arnaud (1981) the Urgonian shelf was subdivided into component members (shallowing-up cycles of Arnaud-Vanneau, 1980) by prominent flooding surfaces in a similar way to the genetic stratigraphic sequences of Galloway (1989a) (eg. Figs 2.8, p. 31 & 4.25, p.149). Contrastingly, the Exxon sequence stratigraphic methodology divides the shelf into unconformity bounded units, emphasising the omission of stratigraphy and subaerial

Key Stratal Patterns, Packages And Surfaces; Shelf, Slope And Basin-Floor.

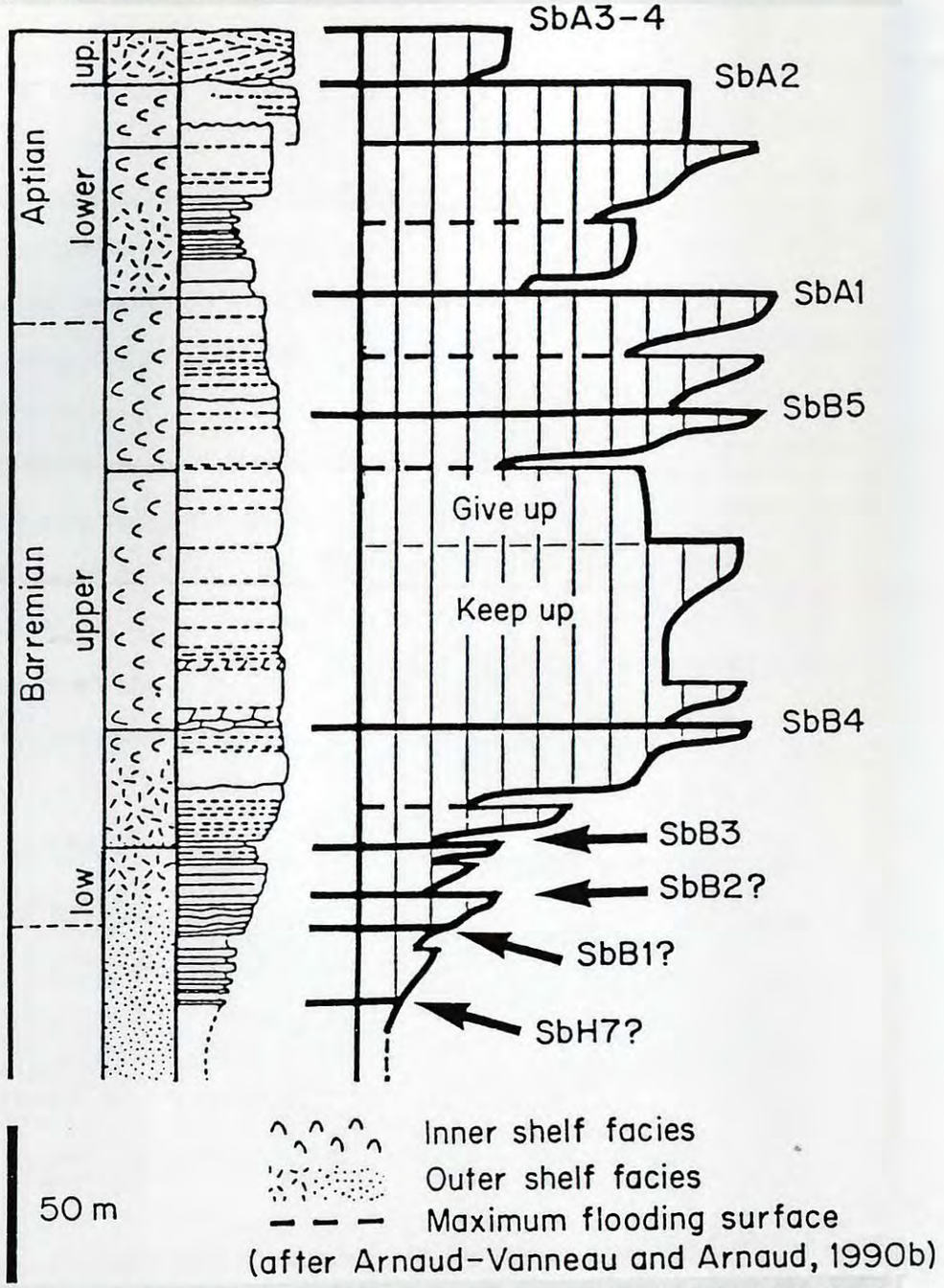

Figure 5.1. Comparison of the shelf sequence stratigraphic schemes of Hunt & Tucker (1992) (A) with that of Jacquin *et al.* (1991) (B). Note that although the nomenclature of the sequence boundaries of these two schemes is different the placing of sequence boundaries SbBA3, SbBA5, SbAP1 and SbAP2 of A are placed in an identical position to those SbB4, SbB5, SbA1 and SbA2 respectively of B. The vertical scale is identical on both sections.

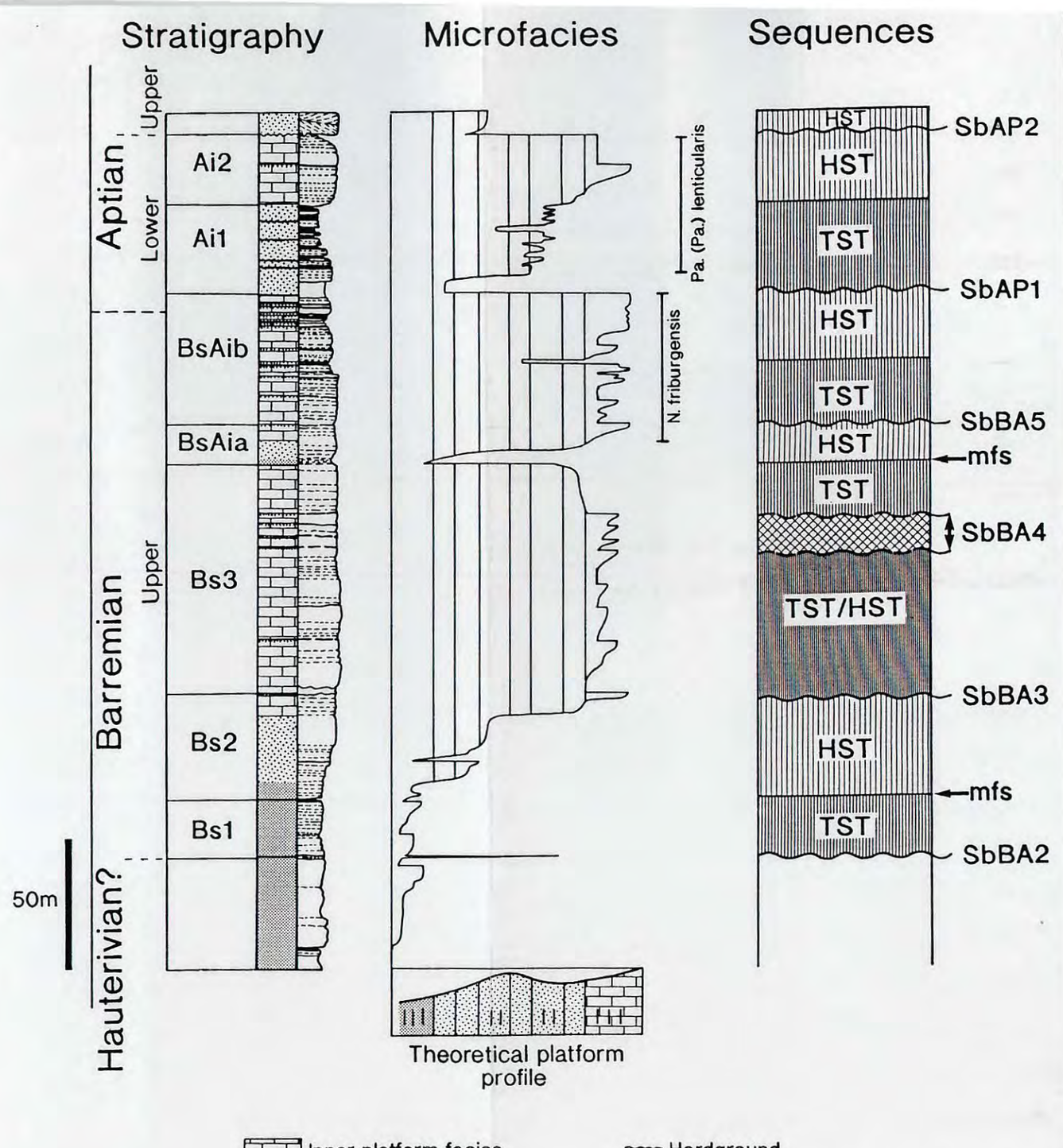

exposure of the shelf during lowstand of relative sea-level (eg. Fig. 3.5 A & B, p. 41). Arnaud & Arnaud-Vanneau (1989), in their initial re-interpretation of the Urgonian platform using this approach developed the basic sequence stratigraphic framework for the shelf as shown in Figure 5.2. In this scheme Arnaud & Arnaud-Vanneau (1989) were able to establish from palaeontological arguments that the lowstand systems tract is absent from the shelf for their sequences BA1-BA2 and AP1 and, thus, demonstrated that the stratigraphy of the Urgonian shelf is composed of transgressive and highstand systems tracts for these sequences, broadly analogous to the Exxon stratigraphic model for a carbonate shelf (eg. compare Figs 3.5B & 5.2). Subsequent sequence stratigraphies of the Urgonian platform have built upon this basic scheme of Arnaud & Arnaud-Vanneau (1989). Common to all of these is the interpretation that the lowstand systems tract is either absent or volumetrically insignificant on the shelf (eg. Fig. 5.1A) (Arnaud-Vánneau & Arnaud, 1990; Arnaud-Vanneau & Arnaud, 1991; Jacquin *et al.*, 1991; Hunt

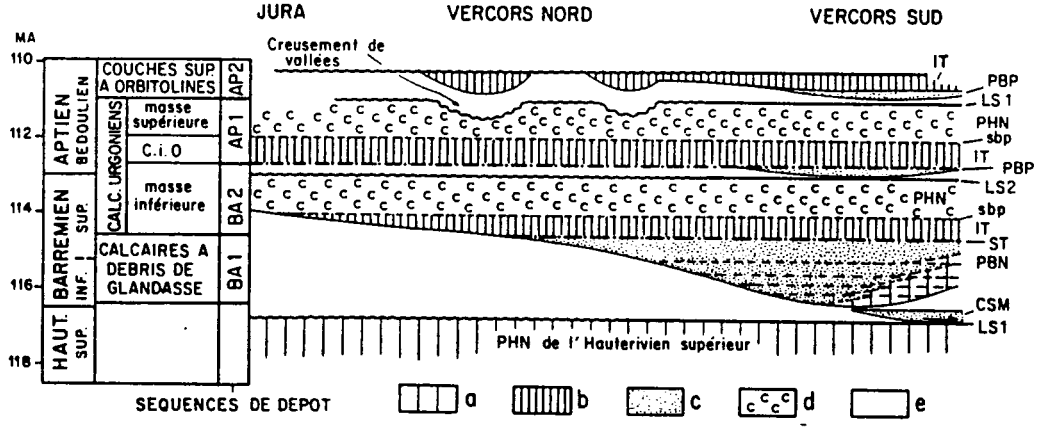

Figure 5.2. The sequence stratigraphic scheme for the Urgonian platform of Arnaud & Arnaud-Vanneau (1989) with respect to geologic time (time scale of Haq *et al.*, 1987). CSM: submarine fan; IT: transgressive systems tract; LS1; type 1 sequence boundary; LS2: type 2 sequence boundary; PBN: lowstand wedge; PBP: shelf margin wedge; PHN: highstand systems tract; sbp: downlap surface: ST: transgressive surface; a: hemipelagic facies; b: transgressive systems tract; c: outer platform facies; d: inner platform facies; e: omission surface.

& Tucker, 1992).

5.2.2. Stratal patterns.

As discussed above only the transgressive and highstand systems tracts are represented upon the Urgonian shelf. In the Exxon stratigraphic model for carbonate shelves the transgressive systems tract is depicted as a retrogradational parasequence set, onlapping the preceding shelf sequence landwards and downlapping basinwards (eg. Fig. 3.5B). The highstand systems tract is, by way of contrast, characterized by a sigmoidal to sigmoidal-oblique offlapping stratal pattern with clinoforms downlapping onto the condensed section (Fig. 3.5B). Whilst similar patterns to these models can be recognized at the Urgonian shelf-margin these patterns are not observed within the platform's shelf-lagoon. Common to both the shelf-lagoon and the shelf-margin is the absence of significant organic buildups which can be important upon other Urgonian carbonate platforms (eg. Masse & Philip, 1981; Bay, 1977, see Fig. 3.22, p. 81).

Parallel-parallel stratal relationships of the Urgonian shelf-lagoon between the main stratal packages (sequence boundaries, systems tracts and parasequences) could, however, be partly an artifact of the dearth of dip sections across the shelf in the northern Vercors and Chartreuse, for here seismic scale exposures of the shelf are good, but mostly orientated parallel to the strike of the platform. A consequence of this parallel-parallel stratal pattern of the shelf-lagoon is that seismic scale geometric observations of the shelf generally cannot be used to distinguish sequence or any other stratal boundaries. A notable exception to this general rule are the incised valleys developed into the top of the Urgonian platform (sequence boundary AP2, Figs 5.2, 5.3 & 5.4). These were originally mapped and interpreted as tidal channels by Arnaud-Vanneau (1980) (eg. Fig. 5.4) but have been subsequently re-interpreted as incised valleys by Arnaud & Arnaud-Vanneau (1989). As can be observed on Figure 5.4 these incised valleys cover less than 5% of the shelf and as such areally represent only a small part of the sequence boundary

Figure 5.3. View of the Les Rimets exhumed incised valley, looking north. Bedding dips at about 25° to the east at this exposure and can be seen as an intersection lineation in the wall of the incised valley which is up to 15m in height here. See text for further discussion.

upon the shelf which is elsewhere represented by a parallel-parallel pattern unconformity. The most spectacular of these valleys crops out in the vicinity of Les Rimets, northern Vercors (Fig. 5.3). This valley is partly exhumed and has a minimum length of 2.5 km, width of up to 250m and is up to 50m deep (Fig. 5.5). The depth of contemporaneous valleys tends to vary between 30 & 50m (Arnaud, 1981) which suggests a sea-level fall of a similar magnitude to develop this sequence boundary (AP2, Fig. 5.2 = SbAP2 and SbA2 Fig. 5.1 A & B respectively) (Arnaud-Vanneau & Arnaud, 1990). The most striking feature of the exhumed valley at Les Rimets is its marked asymmetry (eg. Figs 5.3 & 5.5). The northern flank of the valley is generally steep and even sub-vertical in places (eg. Fig. 5.5), and in this side of the valley the bedding intersection of the preceding sequence is observed (Fig. 5.3). By way of contrast, its southern flank dips gently to the bottom of the valley (Fig. 5.5) and as a consequence is rather poorly

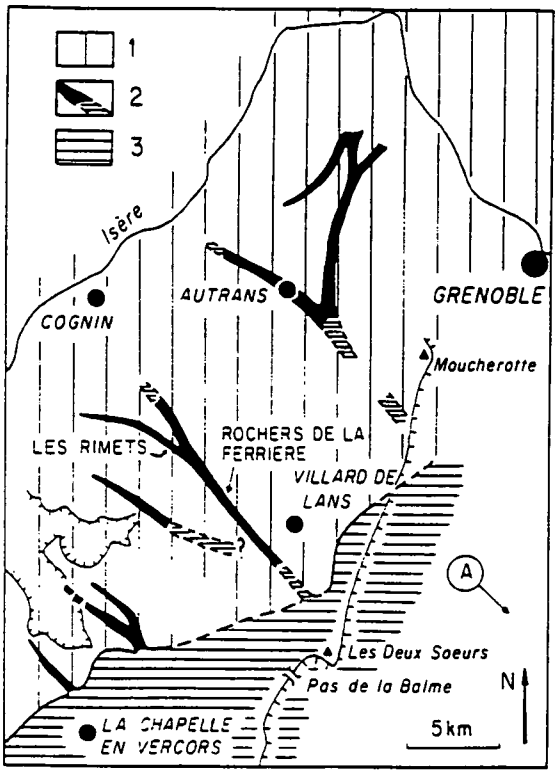

Figure 5.4. Map of the Aptian incised valleys of the northern Vercors. Note that width of valleys is exaggerated. (1) Sequence boundary typified by parallel-parallel stratal pattern and development of karst; (2) incised valleys containing the upper *Orbitolina* beds, interpreted as a part of the transgressive systems tract; (3) glauconitic sandy marls considered contemporaneous to the *Orbitolina* marls within the incised valleys. (A) Direction of the Urgonian shelf margin (From Arnaud-Vanneau & Arnaud, 1990).

exposed. The Les Rimets incised valley and its counterparts (Fig. 5.4) are interpreted to have developed contemporaneously, eroded during times of falling and lowstand of relative sea-level when silt grade siliciclastic sediments were introduced onto the shelf. This influx of siliciclastics is interpreted to be related to climatic changes at this time (see Section 5.2.3.B for further discussion).

By way of contrast to the shelf-lagoon, the shelf-margin is dominated by progradational and aggradational packages of bioclastic sands. These sands are best exposed in the northern Cirque d'Archiane, in the vicinity of Pierre Ronde Rocher (eg. Fig. 5.6). The TST can be associated with the development of a single flooding surface or an aggradational package overlain by the mfs (eg. Bi5P, Fig. 5.7). Retrogradational packages are not normally developed although the stratal unit Bs1 is a notable exception

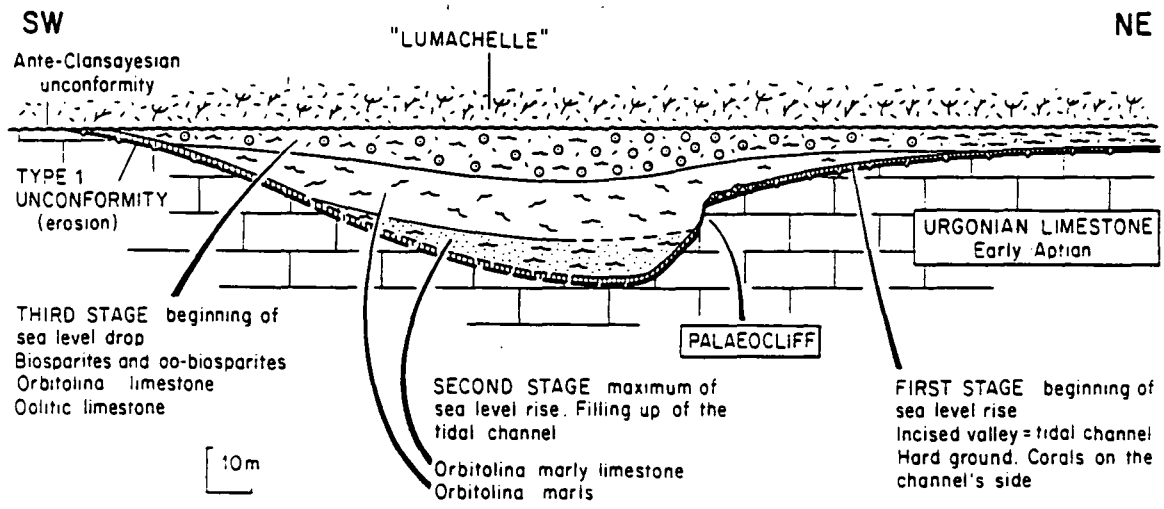

Figure 5.5. Schematic cross section through the incised valley of Les Rimets from Arnaud-Vanneau & Arnaud (1990). (1) type 1 erosional unconformity formed during lowstand of relative sea-level; (2) the three main stages of filling by the upper *Orbitolina* beds at which time the valley acted as a tidal channel (Arnaud-Vanneau, 1980); (3) interpreted onlap of the *Orbitolina* levels onto the sides of the valley; (4) unconformity below the glauconitic 'Lumachelle' limestones.

as is seen at the Rocher du Combau. Progradational packages are characterized by clinoforms with 15-20m relief which downlap asymptotically onto sub-wavebase facies and pass upward into subhorizontal toplapping strata (Fig. 5.6). Relative sea-level rises with a lesser rate than that of sedimentation can be measured (in amplitude) from the thickness of toplap strata to each parasequence (eg. Bi5 P-A, see Fig. 5.7). Only one sequence boundary has been recognized in well exposed shelf margin strata, a type 2 sequence boundary as illustrated in Figure 5.6 and is further discussed in Section 5.3.3B. However, it is worthy of note here that at the seismic scale it would not be possible to distinguish between normal toplap and the erosional truncation at this sequence boundary (eg. compare the toplap and erosional truncation of Figure 5.6). To conclude, upon the shelf seismic stratigraphic criteria cannot generally be used to distinguish between types

Figure 5.7. (opposite, bottom) Sketch of the northern [illegible] Cirque d'Archiane in the southern Vercors. Here the subhorizontal to descending cliff geometry of the 'shelf'-margin to members Bi5 and Bi6 of Arnaud (1981) can be seen. Bi5 is composed of a lower progradational package (P) and an aggradational part (A) overlain by the Lower Fontaine Colombette marls. The location of Figure 5.6 (above) is also shown.

Figure 5.6. (Above) Bi6 prograding-aggrading bioclastic sand shoals at the Pierre Ronde Rocher in Cirque d'Archiane, southern Vercors. The lower sand shoal downlaps asymptotically onto the Lower Fontaine Colombette Marls, a flooding surface overlying the aggradational upper part of Bi5 (=*Dnb*, Fig. 5.26). The clinoforms of this lowest shoal are erosionally truncated above by the sequence boundary SbBA2 (Hunt & Tucker, 1992, their figs 16 & 17, =*et5*, Fig. 5.26) and is overlain by 5-10m of shelf-lagoon type rudist facies. These rudist limestones are downlapped by orange weathering bioclastic sands which pinchout in a shelfward direction (north). The second prograding sand shoal complex downlaps onto these bioclastic sands and the rudist limestones (=*Dnc*, Fig. 5.26). Clinoforms of this shoal pass upward into subhorizontal toplapping strata which are in-turn overlain by an aggradational package of sands.

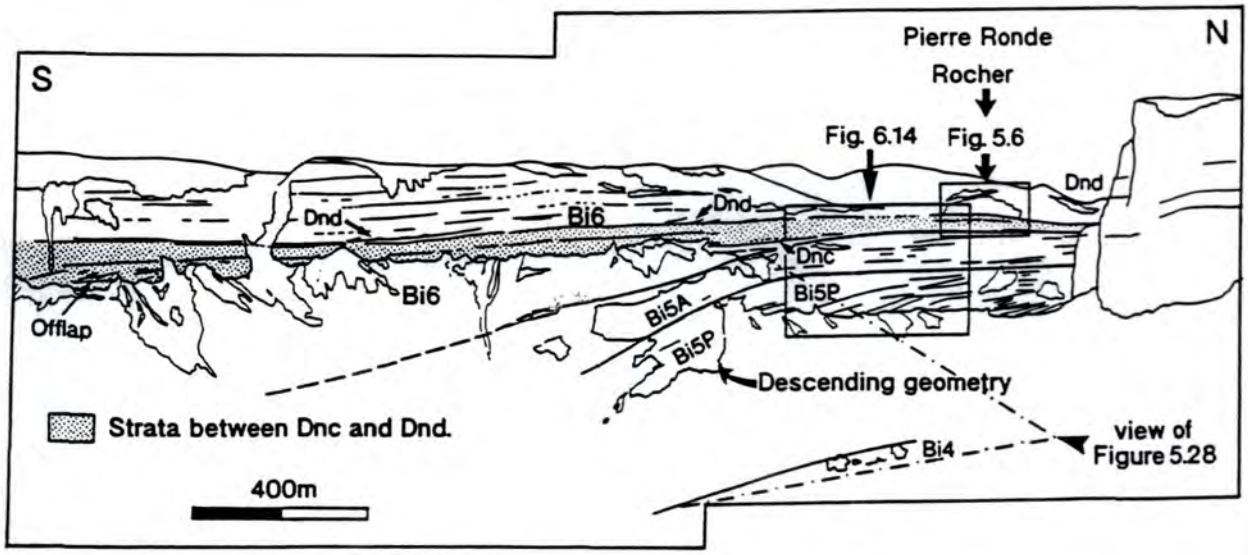

1 and 2 sequence boundaries unless siliciclastic sediments are introduced onto the shelf during times of falling and lowstand of relative sea-level (eg. AP2, Figs 5.2 & 5.3).

5.2.3. The sequence boundary.

5.2.3. A. Introduction, definition and controversy.

As discussed above, almost all of the sequence boundaries identified on the Urgonian shelf have little erosional topography (<0.5m) and have a parallel-parallel stratal pattern at the seismic scale. As such, the type of sequence boundary generally cannot be determined from examination of the shelf alone. In chapter 3 the definition of a sequence boundary upon carbonate shelves was briefly discussed (Section 3.6.2, p. 59) and it was concluded that a type 1 boundary is developed only when the whole of the shelf is exposed, not just the shelf-margin, which commonly develops an elevated topography to the shelf-lagoon (eg. Fig. 3.2, p. 37). Defining a type 2 sequence boundary upon a healthy carbonate rimmed shelf is more problematic, for if defined as a downward shift of relative sea-level which only exposes the topographically elevated parts of the shelf (i.e. not the shelf-lagoon), then similarities to the patterns of exposure developed during the late highstand have the potential to be confused with a type 2 sequence boundary. As such this relaxation for the definition of a sequence boundary is not particularly useful. Upon the Urgonian shelf type 2 sequence boundaries are distinguished from type 1 sequence boundaries only if relative sea-level falls before shelf sedimentation has aggraded near to sea-level (eg. relative sea-level falls before the HST).

The second controversy which has arisen in the development of a sequence stratigraphy for the Urgonian platform surrounds the frequency of sequence boundary development. P. Vail (pers comm, March 1991), suggests that 'parasequence scale sequence boundaries' (eg. 4^{th}-5^{th} order unconformity bounded units) should not be used to separate sequences but included as parasequences within a third order sequence: the frequency band of seismic sequences (eg. Vail *et al.*, in press). However, such a

chronological restriction to the definition and recognition of sequences is artificial as is evidenced by the development of 'parasequence scale' sequences from the late Tertiary to the present day which formed from high-frequency high-amplitude glacio-eustatic sea-level changes (i.e. changes of up to 150m at a 150-200 000 year frequency, see Fig. 2.2, p. 7) (eg. Mitchum & Van Wagoner, 1991 in a siliciclastic setting; Humphrey & Kimbell, 1990 in a carbonate setting). Upon the Urgonian shelf a high-frequency sequence is developed (eg. BA3, Fig. 5.1A), although its origin is very different from those discussed above. This Urgonian sequence is interpreted to have formed in response to a low amplitude relative sea-level fall (<10m) which exposed the whole shelf as it was aggraded very close to sea-level across much of its width (eg. an aggraded shelf Fig. 3.3, p. 38).

5.2.3. B. Identification of the sequence boundary.

The sequence boundary upon the Urgonian shelf is almost invariably marked by meteoric diagenesis unless the boundary is substantially reworked during the ensuing transgression when sedimentological evidence for subaerial exposure can be lost (eg. SbB1 and SbB2 in the northern Vercors, Chartreuse and Jura). The penetration of meteoric vadose diagenesis is generally low at the sequence boundary and restricted to within 0.5m of the exposure surface. Thus, it is not possible to evaluate the amplitude of relative sea-level fall from the penetration of meteoric diagenesis which is for the most part neither substantial nor obviously related to the amplitude of sea-level fall and/or the length of subaerial exposure. This pattern of non-penetrative meteoric diagenesis does suggest one or a combination of the following:

1) the shelf had a low diagenetic potential (i.e. was very well cemented prior to exposure and/or had a relatively stable mineralogy in the meteoric diagenetic realm i.e. predominantly calcite, see Fig. 3.16, p. 65) and/or

2) that the palaeowater-table(s) within the platform remained high during times of falling and lowstand of relative seal-level so there was only a narrow meteoric vadose zone (eg. water table kept to within 1-2m of the exposure surface, see Fig. 5.10) and/or

3) that rainfall rates were low (see below) and/or

4) reworking of the exposure surface during the transgressive systems tract was substantial, removing much evidence of subaerial exposure.

Generally, when compared to the preservation potential of sequence boundaries upon siliciclastic shelves that of those upon a carbonate shelf is high. This reflects the normally early cementation of shallow-water carbonates and, commonly, the continuation of this process in the meteoric environment (see Tucker, 1992 for review). Early cementation tends to reduce greatly the degree to which the sequence boundary is reworked during the ensuing transgressive systems tract (see Section 5.2.4.C for further discussion). In the field a sequence boundary on the shelf can be associated with juxtaposition of very different facies which are most obviously marked by changes of colour and bedding patterns (eg. SbBA2, SbAP1 & SbAP2, Fig. 5.1A and see following examples). In contrast, across other sequence boundaries the changes of facies, bedding, or colour may not be significant (eg. SbBA3, SbBA4 & SbBA5, Fig. 5.1A). All sequence boundaries are, however, normally marked by a subaerial exposure surface which can be associated with one or more of the following at an individual locality and/or contemporaneously developed and areally distributed across an individual sequence boundary:

A) Dissolution of the underlying limestones (eg. Fig. 5.8A), particularly aragonitic grains and/or bioclasts (eg. Fig. 5.8B) and development of vadose cements (eg. Fig.

5.8C).

B) The development of a micro-karstic or karstic topography (eg. Fig. 5.8D).

C) The development of pedogenic features such as rhizoliths (eg. Fig. 5.8E).

D) Formation of freshwater limestones on to the exposure surface (eg. Fig. 5.8F & G).

E) Influx of siliciclastic sediments (eg. Fig. 5.8H).

F) Development of incised valleys (eg. Figs 5.3, 5.4 & 5.5).

Normally the topography developed at a sequence boundary is less than 0.5m upon the Urgonian shelf. The exception to this general rule is the uppermost sequence boundary of the platform which (as discussed in Section 5.2.2) can be up to 50m (eg. Fig. 5.5). Away from the incised valleys this sequence boundary is typically represented by a karstic topography with narrow dissolution pipes (eg. Fig. 5.8B) which can penetrate 2m into the preceding sequence. Studies of the European Barremian palaeoclimate (eg. Ruffel & Batten, 1990) suggest that the Urgonian platform developed during a distinct arid climatic phase as did the Tithonian platform (see Section 4.3.2C-D pgs. 125-131). During these arid phases input of siliciclastic sediments to the passive margin is interpreted to have fallen in response to reduction of precipitation rates (Ruffel & Batten, 1990). Such a reduction of precipitation can also explain the general lack of penetrative meteoric vadose diagenesis generally characteristic of subaerial exposure on the Urgonian platform. Interestingly, the final sequence boundary upon the Urgonian shelf (SbAP2, Fig. 5.1A) has the most penetrative meteoric diagenesis (2m) frequently associated with the development of meteoric vadose cements, pedogenic features (eg. Fig. 5.8E) and also the influx of siliciclastics onto the shelf. This corresponds to a major change of sedimentation in the Vocontian Basin (shift to shale dominated sedimentation,

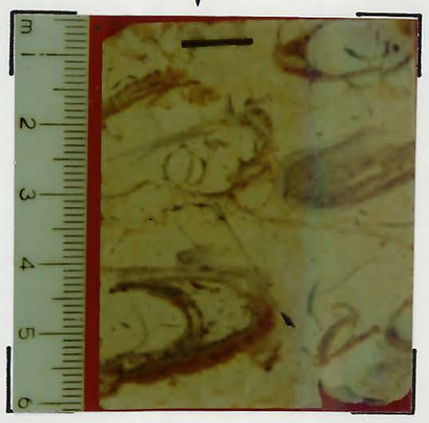

▼B

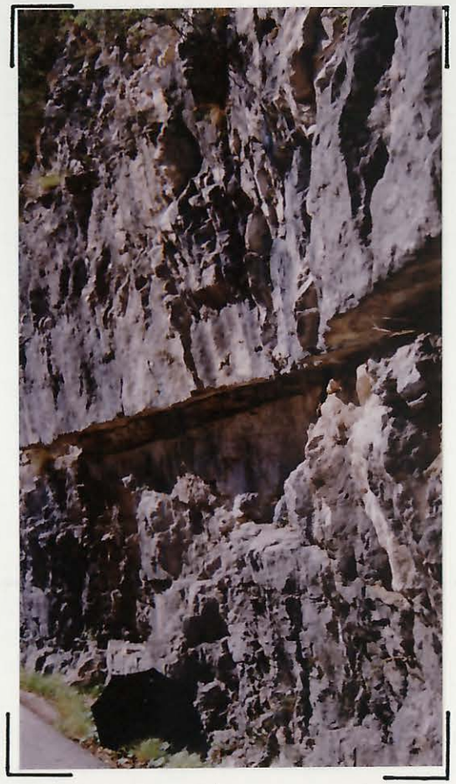

▲F

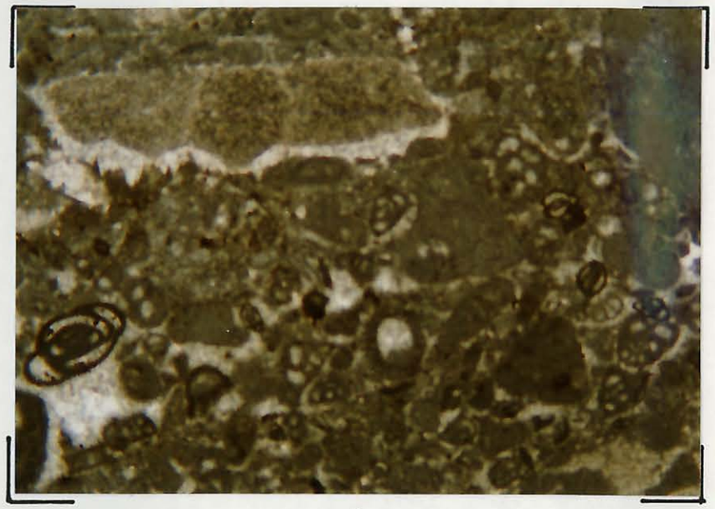

▲C

▲A

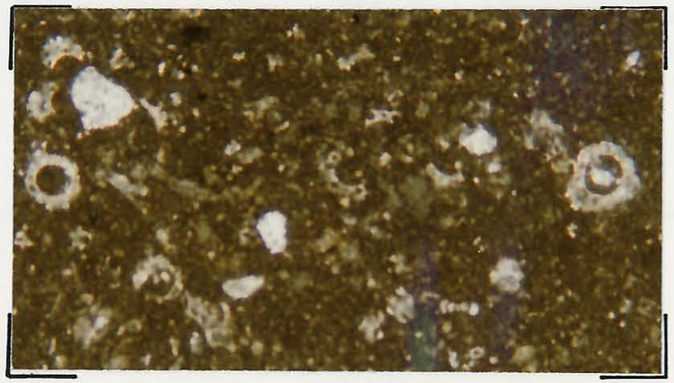

▲G

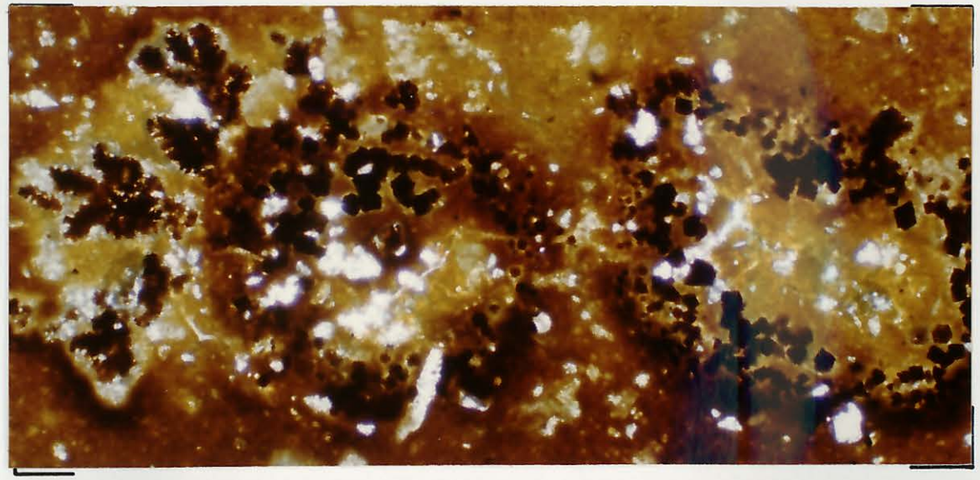

▲E

▲D

▲H

Figure 5.8. (preceding page) Features which are commonly developed at sequence boundaries upon the Urgonian shelf, nomenclature of boundaries as according to Fig. 5.1A. A: vadose meteoric dissolution breccia cemented by yellow calcite SbBA5, Gorge du Frou, Chartreuse; B: dissolution of the aragonitic wall and partial filling of voids by silts which were later selectively dolomitized (brown). SbBA3, Gorge du Nant, N. Vercors (specimen courtesy of S. Moss). Scale bar is 10mm long. C: Photomicrograph of asymmetric freshwater vadose cements below SbAP2, Tunnel du Mortier, N.Vercors. Field of view is approximately 4mm; D: Karstic dissolution pipes developed into the top of the Urgonian platform (SbAP2), Charmont Sommet, Chartreuse. Pencil for 130mm long for scale; E: Organically controlled (?bacteria) iron oxide precipitation around rhizoliths developed at SbAP2, Charmont Sommet. Field of view 18mm across; F: thin lens of freshwater limestones (arrowed) developed at SbBA5, Borne Gorge, Vercors. Umbrella for scale; G: photomicrograph of freshwater limestones containing fragments of thin walled bivalves and the freshwater algae *Chara*, from the level arrowed in F. Field of view is approximately 2.5mm; H: Siliciclastic clays enclosing nodular limestone (?clasts) with microkarstic textures, SbBA2, Gorge du Frou, Chartreuse. Hammer, approximately 350mm long for scale.

an increase of pelagic sedimentation rates and the domination of smectite-rich clay minerals). Together, these changes of patterns of diagenesis and sedimentation on the shelf and within the Vocontian Basin strongly suggest a change from arid to more humid climatic conditions at this time.

Upon the Urgonian shelf two sequence boundaries have been established palaeontologically by Arnaud & Arnaud-Vanneau (1989) (their sequence boundaries BA1-2 and AP1, Fig. 5.2). The lower of these sequence boundaries in the northern Vercors, Chartreuse and Jura is at the base of the upper Barremian Urgonian Limestone Formation below which all fauna are Hauterivian in age (eg. Figs 4.26, p.152 & 5.2, Clavel *et al.*, 1986; Clavel *et al.*, 1987, see Section 4.4.3 for further discussion). Between these dated units a 5-10m package of undated dark grey medium-thickly wavy bedded mudstones-wackestones is commonly developed (eg. Fig. 5.9). This package is sedimentologically distinct from both the underlying Hauterivian interbedded limestones and shales and the overlying Urgonian Limestone Formation (Fig. 5.9) and is interpreted to have developed during the transgressive systems tract from the reworking

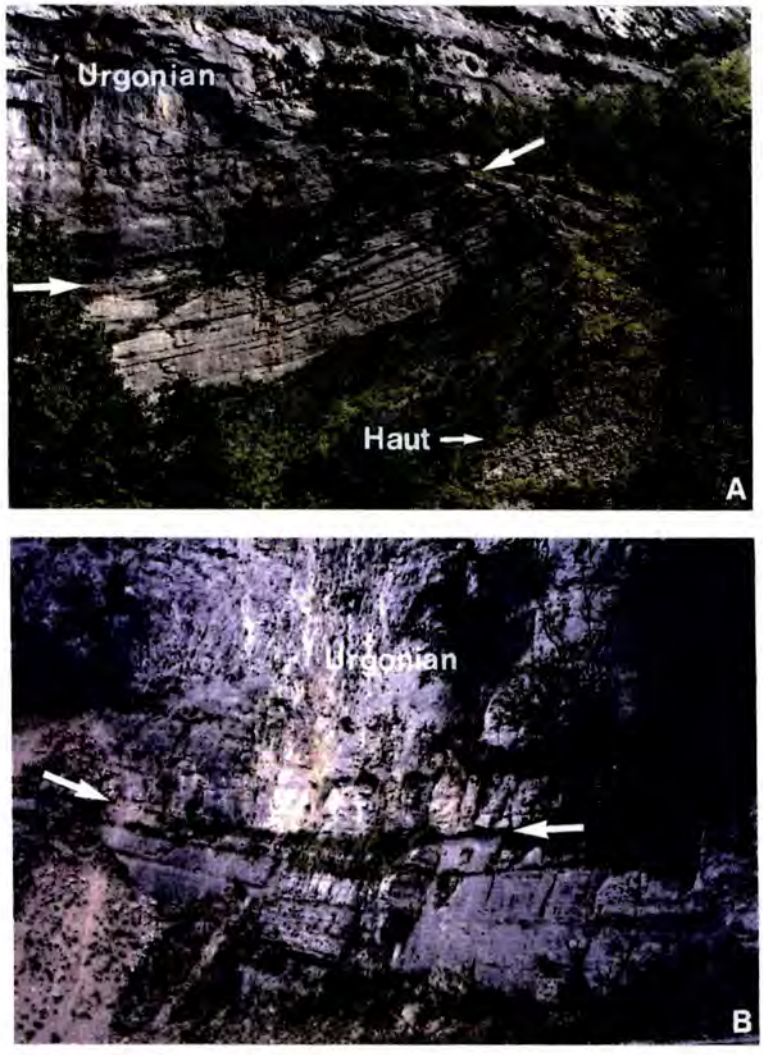

Figure 5.9. The base of the Urgonian platform at the Balcon des Ecouges, N. Vercors (A) and the Gorge du Guiers Mort (Pic d'Oeillette) (B). These two sections are approximately 40km apart along the strike of the Urgonian shelf. In Figure A the typical upper Hauterivian nodular limestones and interbedded shales can be seen in the bottom right of the photograph. These are overlain by a distinctive 10m package of grey packstones separated from the Urgonian Limestone Formation by a thin vegetated shale horizon (arrowed). The succession at (B) is almost identical with the upper Hauterivian and upper Barremian Urgonian Limestone Formation again separated by the undated 10m package of packstones overlain by a thin level of shales. This distinctive 10m package below the Urgonian limestone Formation is interpreted as a transgressive unit which reworked the sequence boundary, destroying the sedimentological evidence of subaerial exposure (see text for further discussion). In both sections the weathered out horizon at the top of the 10m transgressive package is interpreted to represent the mfs.

and destruction of the sedimentological sequence boundary as it was transgressed (see Section 5.2.4.C for further discussion of reworking of the sequence boundary during the transgressive systems tract).

The second palaeontologically distinguished sequence boundary upon the platform, AP1 (Fig. 5.2, & SbAP1 Fig. 5.1A) is commonly also marked by sedimentological evidence for subaerial exposure such as meteoric diagenesis and the development of small lenses of freshwater limestones frequently associated with siliciclastic clays upon the boundary (Balcon des Ecouges, N. Vercors, Fig. 5.10). At this locality and elsewhere upon the shelf this sequence boundary separates two species of foraminifera, *Neotrocholina friburgensis*, below the sequence boundary from *Palorbitolina (Palorbitolina) lenticularis* above the sequence boundary (eg. Fig. 5.1A). Contrastingly, in the autochthonous slope wedge developed during this lowstand (eg. Fig. 5.2) these two species have an overlapping range (Arnaud-Vanneau, 1980; Arnaud, 1981), demonstrating that this wedge developed chronologically between the two shelf packages (eg. Fig. 5.2).

5.2.4. Shelf systems tracts.

5.2.4. A Introduction.

Shelf sedimentation is composed almost entirely of the transgressive and highstand systems tracts, although locally the lowstand systems tract can also be represented (eg. Figs 5.8F & 5.10). The base of the transgressive systems tract is the transgressive surface and this surface can be associated with the reworking of the sequence boundary (see example in preceding Section). The thickness and facies of the transgressive systems tract upon the shelf tends to reflect the ratio of the rate of sedimentation to that of relative sea-level rise and is separated from the highstand systems tract by the maximum flooding surface (mfs). The identification of the mfs may be problematic for shelf sedimentation rates can match rates of relative sea-level rise so

that no clear flooding surface is developed. In such cases distinction of the systems tracts is arbitrary and is often of little real value as is particularly the case for high-frequency (4th-5th order) sequences (eg. sequence BA3, Fig. 5.1A).

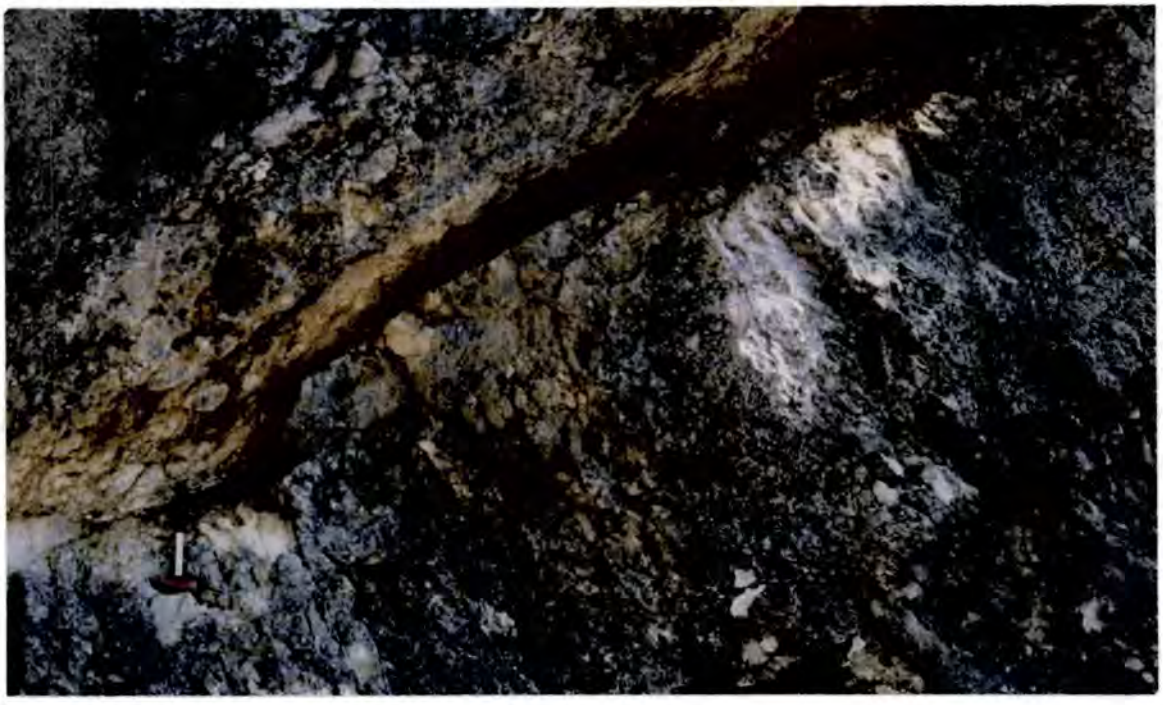

Figure 5.10. (A) Outcrop photo of the sequence boundary SbAP1 (as according to Fig. 5.1A) at the Balcon des Ecouges, N. Vercors. Lenses of freshwater limestones containing the freshwater algae *Chara* are preserved in small depressions. These sit on siliciclastic clays draped across the sequence boundary below which are 2m of prominently weathered limestones with vadose meteoric cements. Below this level is a recessive weathering level with a strong vertical jointing pattern and good biomoldic porosity. Cements within and below this level have well developed meteoric phreatic cements (eg. see Figs 4.32B & 4.33D). This weathered out level is therefore interpreted to represent the palaeowater-table below the sequence boundary SbAP1.

5.2.4. B. Lowstand shelf sedimentation.

The lowstand systems tract normally comprises only a small and volumetrically almost insignificant part of sedimentation on the Urgonian shelf. Only above a few sequence boundaries is lowstand sedimentation preserved where it is typically represented by a thin level (<0.5m thick, i.e. Figs 5.8F & 5.10) of conspicuous grey-green coloured freshwater limestones containing the freshwater algae *Chara*, fragments

of thin-walled bivalves and rarely ostracods (eg. Fig. 5.8G). Such limestones are normally preserved in small (<6m wide) shallow, spoon shaped depressions eroded into the preceding sequence (eg. Fig. 5.10). The development of freshwater limestones on the platform does suggest either the platform was at least locally tightly cemented and/or that the palaeowater-table was very high (eg. Fig. 5.10) for a least part of the lowstand so that lacustrine facies were able to develop 'perched' on top of the platform.

5.2.4. C. The transgressive surface.

The extent to which the sequence boundary is reworked by the transgressive surface and the succeeding systems tract depends upon several variables such as the facies and cementation of the preceding sequence, the speed of relative sea-level rise compared to the 'start-up' rate of shelf sedimentation and the depositional dynamics of the succeeding sedimentary system(s). Whilst the preservation potential of the sequence boundary is generally high upon a carbonate shelf (see Section 5.2.3B) this does depend, to a large extent upon the facies of the preceding sequence. For example, slope facies with a high proportion of clays (eg. the Hauterivian slope facies, Fig. 4.24, p.145) are generally poorly cemented in both the marine and meteoric environment and as such are particularly susceptible to reworking during the transgressive systems tract after subaerial exposure. Such a scenario is envisaged for the SbBA1-2 (Fig. 5.1A) sequence boundary between Hauterivian slope sediments and the unconformably overlying upper Barremian Urgonian Limestone Formation in the northern Vercors and Chartreuse (Figs 5.2 & 5.9). At this sequence boundary almost all direct sedimentological evidence for subaerial exposure is absent and is interpreted to have been reworked and destroyed during the ensuing transgressive systems tract (eg. Fig. 5.9).

In other examples upon the Urgonian shelf when the rate of relative sea-level rise is greater than that of sedimentation the shelf becomes drowned so that outer-shelf or

even slope type facies are developed onto the shelf-lagoon of the preceding sequence (eg. SbAP1 and SbAP2, Fig. 5.1A). In such situations substantial modification of the sequence boundary can occur leading to the development of a *compound surface*, a hybrid sequence boundary retaining evidence of subaerial exposure, but reworked during the transgressive systems tract, frequently as a hardground (eg. SbAP2, Tunnel du Mortier Fig. 5.11A; Les Rimets Figs 5.5, 5.11D). Upon the Urgonian shelf development of reworked sequence boundaries appears to be associated with environmental changes for both reworked sequence boundaries SbAP1 and SbAP2 are associated with an influx of siliciclastic sediments onto the shelf which are interpreted to have reduced carbonate sedimentation rates so that the shelf-lagoon became drowned and outer-shelf type facies developed on the shelf.

The reworking of the sequence boundary during the transgressive systems tract can be mechanical (A & B, below), chemical (C, below), biological (C, D & E below) or a combination of these;

A) Shoreface erosion (eg. also see Section 5.2.3.B, Figs 5.9, 5.11A & B)

B) Current scouring (eg. Fig. 5.11B & ?C).

C) Mineralisation (eg. Figs 5.11A & D).

D) Boring of marine bivalves (eg. Fig. 5.11A, E & F).

E) Encrustation by marine fauna (eg. Figs 5.5 & 5.11A).

The sequence boundary SbAP2 is probably the best example of a compound sequence boundary, modified during the transgressive systems tract and is particularly well developed as such at Les Rimets and Tunnel du Mortier in the Vercors and up on Charmont Sommet in the Chartreuse. At the Tunnel du Mortier reworking of the sequence boundary is complex and several different stages can be observed (eg. Fig. 5.11A). Coarse shallow-water bioclastic sands are the first and partial fill of the karstic dissolution pipes formed during lowstand of relative sea-level into sequence AP1. These bioclastic sands have oversized pores (Keystone vugs), yellow, pendant cements and

perched lenses of sediment, indicative of a high-energy shoreface environment. This first stage of reworking is interpreted to mark the passage of the transgressive surface (eg. the shoreline) over the shelf and a brief 'start-up' of shelf type sedimentation. At this stage shoreface sands are interpreted to have scoured and 'smoothed' the karstic dissolution pipes. The second distinct phase of reworking of the karstic topography is characterized by *Lithophaga* bivalve borings into both the preceding sequence and beach facies. These are filled by outer-shelf type glauconitic muds and sands indicating that the 'give-up' and drowning of the Urgonian shelf had occurred by this time. The final stage of this *compound surface* is the erosional scouring and planation of both the preceding sequence and the earlier glauconitic sands (eg. Fig. 5.11C) and the subsequent mineralisation and encrusting of this surface by oysters (eg. Fig. 5.11A). This final erosional event is interpreted to have been developed by traction currents which moved glauconitic sand wave complexes (the Lumachelle bioclastic limestones) across the current dominated shelf at this time.

Figure 5.11 (following pages) Features associated with the reworking of the sequence boundary during the transgressive systems tract. A: Complex compound surface form the Tunnel du Mortier, N. Vercors (SbAP2). Several distinct phases of reworking can be distinguished in this specimen from the passage of the transgressive surface (abrasion and smoothing of dissolution pipes and their partial fill with shoreline facies), followed by the 'give-up' of carbonate sedimentation and boring of the surface by *Lithophaga* bivalves and finally the scouring of the surface by along shelf currents and the mineralisation of the surface and encrusting of it by oysters; B: rounded karst dissolution pipes filled by coarse bioclastic sands (Lumachelle), Charmont Sommet, Chartreuse, pen for scale (130mm long); C: planar erosion surface at the Tunnel du Mortier into which the underlying Urgonian Limestones are truncated. This surface is interpreted to have been developed by the incursion of long-shelf oceanic currents onto the shelf (see also Delamette, 1988) Wall is approximately 1.3m high; D: Strongly mineralised hardground surface at Les Rimets in the northern Vercors. Lens filter of 60mm diameter for scale; E: *Lithophaga* bivalve borings into the sequence AP1 at sequence boundary SbAP2, at Les Clapiers, N. Vercors. Pencil 130mm long for scale; F: Photomicrograph of *Lithophaga* bivalve borings (L) (the fill of which is partially plucked) into sequence AP1 at the Tunnel du Mortier. Field of view is approximately 18mm.

A

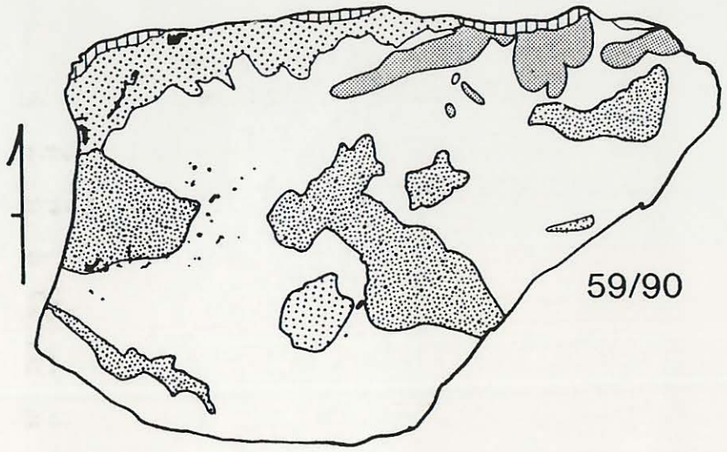

- Sequence Ap1.
- Shoreface sands with yellow, calcitic cements.
- Lithophaga borings.
- Glauconitic sands.
- Encrusting fauna.

B

D

C

E

F

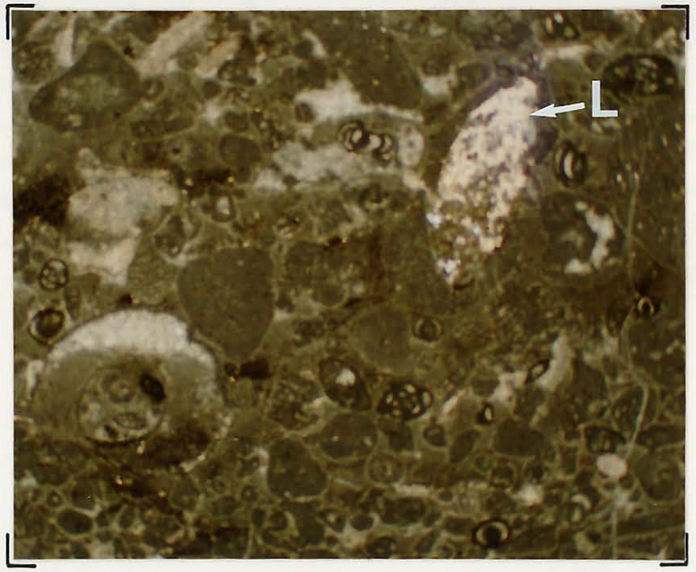

Figure 5.12. The interpreted mfs of sequence AP1 (as according to Fig. 5.1A) at the Gorge du Frou section in the northern Chartreuse. The mfs is placed at the top of the lower *Orbitolina* beds, the dark-grey shales below the beige shelf limestones. The height of the exposure is approximately 5.5m.

5.2.4. D. The maximum flooding surface.

This surface separates the transgressive and highstand systems tracts upon the shelf and in the Exxon stratigraphic model is characterized by the most widespread development of open marine facies upon the shelf (Fig. 3.5 A & B). Upon the Urgonian shelf this surface typically divides shelf stratigraphy into two approximately equal parts (eg. Fig. 5.1A) and is often represented by the development of outer-shelf or even slope type facies on the shelf (Figs 5.1, 5.9 & 5.12). An example of such a mfs is that of sequence BA4, developed after a gradual 'opening' of shelf sedimentation as the rate of relative sea-level rise is interpreted to have accelerated to a point where 'give-up' of carbonate sedimentation occurred (Fig. 5.1A). Contrastingly, in the sequence BA3 no obvious maximum flooding surface is developed so that the TST and HST cannot be

discriminated on the shelf. This illustrates that within unconformity bounded sequences a clear flooding surface is not always necessarily developed as sedimentation rates can keep pace with or even outpace rates of relative sea-level rise.

Whether the mfs upon the Urgonian shelf always reflects solely changes in the rate of relative sea-level rise is, however, questionable. For example, the abrupt facies jumps which mark the mfs to sequences BA5 (Fig. 5.1A) and AP1 (Figs 5.1A & 5.12) could also reflect environmental changes which altered the sedimentation rate(s). In particular, the change of facies which characterizes the mfs to sequence AP1 at the top of the lower *Orbitolina* beds is both abrupt (Fig. 5.12) and associated with a marked decrease of siliciclastic input to the shelf. As such, this boundary is interpreted to have developed largely as a response to environmental change(s) (?reduction of precipitation rates), rather than from a change in the rate of relative sea-level rise.

5.2.5. Parasequences.

Parasequence boundaries are interpreted in the Exxon model to be developed by punctuated, rapid relative sea-level rises which have a rate significantly greater than that of sedimentation (eg. Fig. 2.3, p. 11). Such rises are thought to be followed by times of relative sea-level stillstand when facies belts prograde basinwards (Fig. 2.3). Parasequences upon siliciclastic shelves typically range from 20-30m thick (eg. Van Wagoner *et al.*, 1990, their figs 3, 6, 7, 11 and table 1). At the Urgonian shelf-margin similar scale asymmetric cycles are spectacularly developed from the lateral (basinward) progradation of bioclastic sand shoals (eg. Cirque d'Archiane, member Bi6 of Arnaud, 1981, Fig. 5.6). By way of contrast, as discussed in Section 3.6.3 (p. 61), within the lagoons of carbonate rimmed shelves and across aggraded shelves parasequences and/or their component shallowing-up cycles can be developed by *in situ* vertical aggradation (eg. Fig. 5.13) (the punctuated aggradational cycles of Goodwin & Anderson, 1985). Generally, within the Urgonian shelf-lagoon parasequences and their component

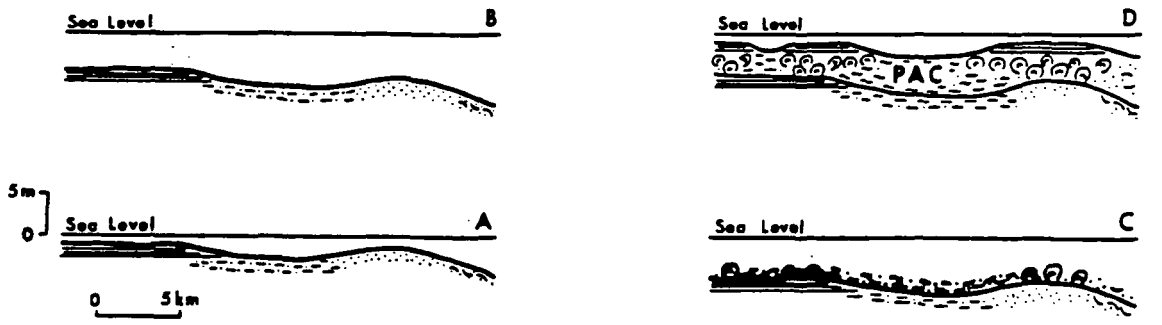

Figure 5.13. Schematic development of a punctuated aggradational cycle according to Goodwin & Anderson (1985). A: equilibrium between aggradation and a stable sea-level; B: geologically instantaneous sea-level rise; C: resumption of aggradation at the new base-level; D: aggradation to equilibrium conditions resulting in a punctuated aggradational cycle.

shallowing-up cycles are poorly developed although sequence SbB5 is a notable exception and is discussed below. The general paucity of such cycles upon the Urgonian shelf reflects a combination of the dominance of subtidal facies and that most sections are based along relatively unweathered road sections. In naturally weathered sections shallowing-up cycles can be recognized from weathering profiles (Fig. 5.14) although the facies between the top and bottom of these cycles are frequently extremely difficult to differentiate where cycles are entirely subtidal.

Classically, upon carbonate platforms asymmetric cyclic packages of sediments are termed shallowing-upward cycles (eg. Goodwin & Anderson, 1985) and in a similar manner to their siliciclastic counterparts evolve from deep(er) to shallow(er) water facies (Figs 2.3 & 5.13). Upon carbonate platforms, many 5-20m thick shallowing-up cycles (from here on termed a parasequence) are divisible into a number of higher order, smaller 1-5m shallowing-up cycles (eg. Goodwin & Anderson, 1985; Goldhammer *et al.*, 1990). Frequently, an individual parasequence unit contains between 3 and 5 of these smaller shallowing-up cycles and, classically, each of these in-turn contains a higher proportion of shallow-water or supratidal facies (i.e. the Triassic Latemar platform, Italy, Goldhammer *et al.*, 1990, their fig.1 & Fig. 5.15). Such systematic, rhythmic stacking of

Figure 5.14. Five distinctive 1.5-3m thick asymmetric shallowing-up cycles within a shallow-water subtidal-supratidal shelf-lagoon succession at the Pas d l'Echelle in the Chartreuse (Member Ai2, Arnaud-Vanneau, 1981; sequence AP1 Fig. 5.1A, Hunt & Tucker, 1992). Blue coat by 0.5m high rucksack upon the top of the second cycle for scale.

1-4m shallowing-up cycles is not, however, often well developed during normal Urgonian platform sedimentation. In fact, where developed, many of the smaller scale (1-2m) shallowing-up cycles (eg. Fig. 5.16) are also atypical and do not develop the classical asymmetric deep-shallow stacking pattern as illustrated in Figure 5.13. Classical asymmetric cycles are only well developed on the Urgonian shelf during the lower Aptian, the Lower *Orbitolina* Beds and Ai2 (Fig. 5.14).

The most spectacular lagoon cycles of the Urgonian shelf are developed at the Balcon des Ecouges in the northern Vercors as illustrated in Figure 5.15 (sequence BA5 as according to Fig. 5.1A). Here parasequences are generally poorly organised and comprised of between five and thirteen 1-2m thick shallowing-upward cycles. In a 'type' asymmetric profile these shallowing-up cycles evolve from subtidal unrestricted shelf facies with large rudists to restricted subtidal shelf facies with small rudists and/or

Figure 5.15. Complex stacking of 5th order shallowing-up cycles within sequence BA5 (according to Fig. 5.1A) at the Balcon des Ecouges in the northern Vercors. Fourth order parasequence boundaries are marked by siliciclastic clays which are weathered out. The complexity of stacking patterns at this locality probably reflects high rates of sedimentation compared to those of relative sea-level rise. One fourth order cycle at this locality (labelled) has a classical stacking pattern, containing five higher order cycles which contain a higher proportion of inter-supratidal facies upwards. In the preceding and succeeding parasequences, however, this pattern is not repeated as the most open marine deposits are not developed at the base of the parasequences. Such patterns are thought to reflect a close match between rates of relative sea-level rise and sedimentation.

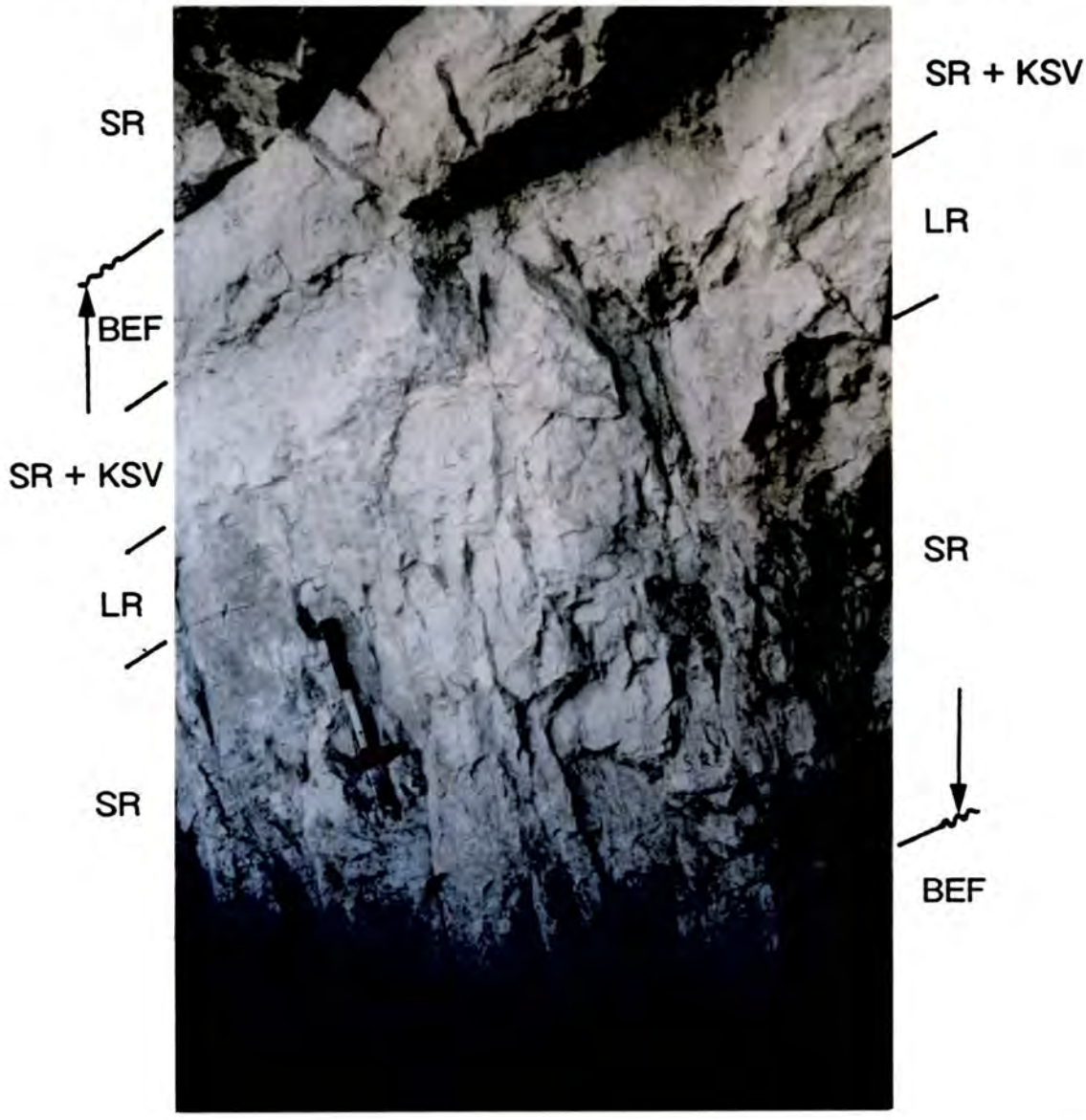

Figure 5.16. Detail of a complexly developed shallowing-up cycle at the Balcon des Ecouges in the northern Vercors. This cycle is located at the exit to the tunnel in Figure 5.15 with the intertidal facies at the top of the cycle forming the prominent bedding surface in the roof of the tunnel. In this shallowing-up cycle the most open shelf facies, marked by large rudists are developed approximately 3/4 through the cycle reflecting the near balance of rates of aggradation and of relative sea-level rise. BEF: birdseye fenestrae; KSV: keystone vugs; SR: small rudists; LR: large rudists. Hammer approximately 0.35m long for scale.

oncolites, and are capped by intertidal facies with birdseye fenestrae, high-energy beach facies with keystone vugs or a combination of the two. This classical evolution of a shallowing-up cycle is not, however, normally developed at this locality and their facies

evolution is more complex as shown in Figure 5.16. The most open marine conditions of the cycle illustrated in Figure 5.16 are not developed at the base of cycle (as in a classical cycle) but approximately three quarters of the way through it (facies with large rudists). This shallowing-up cycle is interpreted to have developed from a slowly rising, but accelerating rate of relative sea-level rise which eventually exceeded the sedimentation rate of the restricted rudist facies to develop facies with large rudists suggesting less restricted circulation. This relative sea-level rise is interpreted to have been followed by a stillstand (or even a small relative sea-level fall?) when the depositional surface aggraded to sea-level, developing peritidal facies with birdseye fenestrae. Such cycles suggest that the rate of 'start-up' and subsequent sedimentation was approximately equal to that of relative sea-level rise. The similar general lack of classical asymmetric structuring within parasequences at this locality (excepting that illustrated in Figure 5.15) is also interpreted to have developed as the rates of sedimentation were (for the most part) able to aggrade as fast as relative sea-level rise(s).

Upon the Urgonian shelf, asymmetric, subtidal shallowing-up cycles similar to those described by Osleger (1991) are only well developed in the Lower *Orbitolina* Beds which represent the TST to sequence AP1 (Fig. 5.1A). These cycles vary in thickness between 1 and 3m and pass upward from shales to nodular limestones and shales, normally capped by 1-2m of outer-shelf type bioclastic limestone facies (eg. Fig. 5.17). The top of the cycles is typically a hardground surface commonly impregnated by iron hydroxides (i.e. goethite-limonite, Fig. 5.18) and/or encrusted by bivalves. These more classical asymmetric cycles differ significantly from those of the Balcon des Ecouges. This suggests that either rates of relative sea-level rise were greater at this time and/or that sedimentation rates were reduced. The abundance of siliciclastics within the shallowing-up cycles of the lower *Orbitolina* beds does suggest that environmental changes played an important role at this time, probably reducing sedimentation rates. If correct, then similar rates of relative sea-level rise to those which developed the atypical

Figure 5.17. Asymmetrical 1-3m thick shallowing-upward cycles of the lower *Orbitolina* beds in the Gorge du Frou section, northern Chartreuse. These cycles pass from an omission surface, a hardgound developed on the top of the preceding cycle (see Fig. 5.18 for detail) to siliciclastic rich shales which weather recessively (thick arrows). These shales pass upward into outer-shelf type bioclastic and/or oolitic limestones which generally have abrupt bases. Rucksack, approximately 0.75m in height to scale.

shallowing-up cycles of the preceding sequence at the Balcon des Ecouges could drown carbonate sedimentation to produce the more classical (but subtidal) asymmetric shallowing-up cycles typical of the lower *Orbitolina* beds across the Urgonian shelf.

As discussed in Chapter 4 limestone-shale couplets in the Vocontian basin are interpreted to represent 20 000 year climatic cycles (Section 4.2.3.C). These couplets build to form asymmetric cycles (eg. Fig. 4.11, p. 121) interpreted by Ferry & Rubino

Figure 5.18. Ferruginised upper surface at the top of an asymmetric shallowing-upward cycle within the lower *Orbitolina* beds, Gorge du Frou, Chartreuse. This undulose upper surface at the top of a cycle is interpreted to have developed due to sediment starvation and to represent a stratigraphic omission surface after a punctuated relative sea-level rise (eg. similar to Fig. 5.13) and/or an environmental change. This omission surface is directly overlain by recessively weathering shales. Pen for scale is approximately 100mm long.

(1989) as equivalent to the parasequences of the Exxon model. However, Fourier transform analysis of these cycles by Rio *et al.* (1989) failed to reveal obvious Milankovitch cyclicities (Fig. 4.16, p. 129), often invoked as the major control upon parasequence development (Goodwin & Anderson, 1985; Goldhammer *et al.*, 1990). The general lack of classical asymmetric structuring of shallowing-up cycles and parasequences within Urgonian shelf-lagoon succession(s) and for evidence of Milankovitch driven cyclicities in the Vocontian basin does suggest that the role of astronomically driven glacio-eustatic sea-level fluctuations was much reduced in importance during Urgonian times, at least in this area. Such an interpretation agrees with Global Cretaceous climate models which also suggest an absence of continental ice-

sheets and therefore a weakening of the astronomically driven glacio-eustatic sea-level cycle signature (eg. Barron *et al.*, 1981). It is suggested that at this and other such times (i.e. greenhouse times, see Fig. 3.16, p. 65) both the rate(s) and amplitude(s) of glacio-eustatic sea-level changes were considerably reduced in comparison to ice-house times (eg. see Tucker *et al.*, 1992, their fig. 2). At such times it is possible that autocyclic processes such as shoreline progradation (eg. Balcon des Ecouges?) played a more important role in the development of stacking patterns than rates of relative sea-level change (allocyclic processes).

5.2.6. Conclusions: shelf.

1. The characteristic stratal pattern of the shelf-lagoon upon the Urgonian platform is parallel-parallel, from the shallowing-up cycle scale upward. The exception to this general rule is during times of falling and lowstand of relative sea-level if siliciclastics are introduced onto the shelf. The dominant stratal pattern at the shelf-margin is downlap of clinoforms to prograding bioclastic sand shoals onto flooding surfaces. These clinoforms pass upward into subhorizontal toplapping strata which cannot at the seismic scale be differentiated from the sequence boundary.

2. The Exxon sequence boundary is preferred to the Galloway sequence bounding surfaces on the shelf as; A: On a carbonate shelf as compared to a siliciclastic shelf exposure surfaces have a much greater preservation potential as meteoric diagenesis is often associated with cementation so that the sequence boundary is not normally destroyed by transgressive reworking; B: Within the Urgonian shelf-lagoon a clear flooding surface it not necessarily developed and may be 'concealed' within a thick succession of lagoonal facies where it can be almost impossible to differentiate; C: It is easier to correlate exposure surfaces from the shelf-lagoon to shelf-margin than flooding surfaces. Exposure is normally marked by the development of a discrete surface whereas

contrastingly, several different flooding surfaces can be developed at the shelf-margin during a relative sea-level rise.

3. Type 1 and type 2 sequence boundaries are not easily distinguished, except after times when the shelf-margin was drowned. Otherwise stratal patterns and termination patterns appear to be similar for both type 1 and 2 boundaries.

4. The times of falling and lowstand of relative sea-level on the shelf are marked by meteoric diagenesis which is generally only weakly penetrative. Freshwater limestones can also be developed during lowstand of relative sea-level.

5. The transgressive and highstand systems tracts are the main components of shelf sedimentation. Lowstand sedimentation is generally absent or volumetrically insignificant.

6. At the shelf-margin only two types of stratal packages are normally developed, aggradational and progradational. These packages are separated by sub-wavebase limestones developed when the shelf was drowned as sedimentation abruptly 'gives-up'. Bi1 is, however, an exception to this general rule. Contrastingly, in the shelf-lagoon in terms of facies assemblages retrogradational or 'give-up' stratal packages are relatively common (eg. TST to sequence BA4, Fig. 5.1A).

7. Shallowing-upward cycles and parasequences are for the most part poorly developed upon the Urgonian platform. Where observed these cycles are very atypical and this is thought to reflect a combination of low rates of relative rise in comparison to high sedimentation rates.

8. Climate changes can exert a strong control upon shelf stratal patterns. Change to humid climatic conditions can be related with the influx of siliciclastic sediments onto the shelf and more penetrative meteoric diagenesis. During times of falling and lowstand of sea-level such changes are associated with the development of incised valleys on the shelf (eg. SbAP2). At other times the influx of siliciclastics can reduce carbonate sedimentation rates and allow the development of classical asymmetric shallowing-up cycles as sedimentation rates were reduced.

5.3. Slope.

5.3.1. Introduction.

The slope extends basinward from the sub-wave base shelf-margin to the basin-floor and is dominated by gravity driven processes. Contrasting with the shelf, all the systems tracts are interpreted in the Exxon model to be represented on the slope (eg. Vail, 1987; Haq *et al.*, 1987, 1988 etc., see Section 2.4). In the Exxon model (Fig. 2.1, p. 6) the slope is the area where sediment is accommodated during lowstand of sea-level. In this model the most important stratal patterns formed on the slope are: erosional truncation, associated with channel/canyon incision and developed during times of falling sea-level, and onlap of the lowstand wedge against the slope, formed during the slow relative sea-level rise subsequent to sequence boundary formation. The times of falling and lowstand of relative sea-level are associated with the highest sedimentation rates upon the slope (see Chapter 2 for a fuller discussion). By way of contrast, the TST is characterized by a decrease of sedimentation rates and development of a condensed section often associated with chemical precipitation (eg. glauconite, phosphates). Finally, a gradual increase of sedimentation rates associated with basinward progradation typifies the highstand systems tract (eg. Figs 2.1 & 2.5, p. 14).

The stratal geometries and termination patterns of the Exxon model have been used to interpret the seismic scale lower Barremian slope exposures of the Urgonian platform *sensu lato*, the Borne and Glandasse Bioclastic Limestone Formations of the southeastern Vercors (eg. Ravenne *et al.*, 1987; Arnaud-Vanneau & Arnaud, 1990; Jacquin *et al.*, 1989; 1991). The exposures of these formations rival those of any other ancient carbonate slope facies in the world. In this section the stratal patterns of these exposures are introduced and firstly interpreted using the Exxon model (Section 5.3.2) as applied by Ravenne *et al.* (1987) and Jacquin *et al.* (1989; 1991). These interpretations are followed by a discussion of the stratal packaging and facies of the Cirque d'Archiane and Rocher du Combau (see Section 5.3.3) which allow the only well exposed semi-continuous seismic scale dip-section from the shelf to the slope. The final part of this section reappraises the sequence stratigraphic interpretations of Ravenne *et al.* (1987), Arnaud-Vanneau & Arnaud (1991), Jacquin *et al.* (1991) and Hunt & Tucker (1992) upon the slope in the light of the stratal patterns and relationships observed in Cirque d'Archiane and Rocher du Combau. The timing of slope collapse is also discussed in Section 5.4.

5.3.2. The identification of sequence boundaries upon the slope: The geometric approach.

Recent sequence stratigraphic interpretations of the Borne and Glandasse Bioclastic Limestone Formations by Ravenne *et al.* (1987) and Jacquin *et al.* (1989, 1991) have relied heavily upon the geometric stacking patterns of the Exxon model (eg. Fig. 2.1) and these are reviewed here. From these interpretations lower Barremian relative sea-level changes have been determined (eg. Jacquin *et al.*, 1991, Fig. 6.8). Ravenne *et al.* (1987) identified the position of sequence boundaries on the slope using solely geometric criteria whereas Jacquin *et al.* (1989; 1991), in their stratigraphically more complete study, used a combination of geometric criteria and the basic sequence

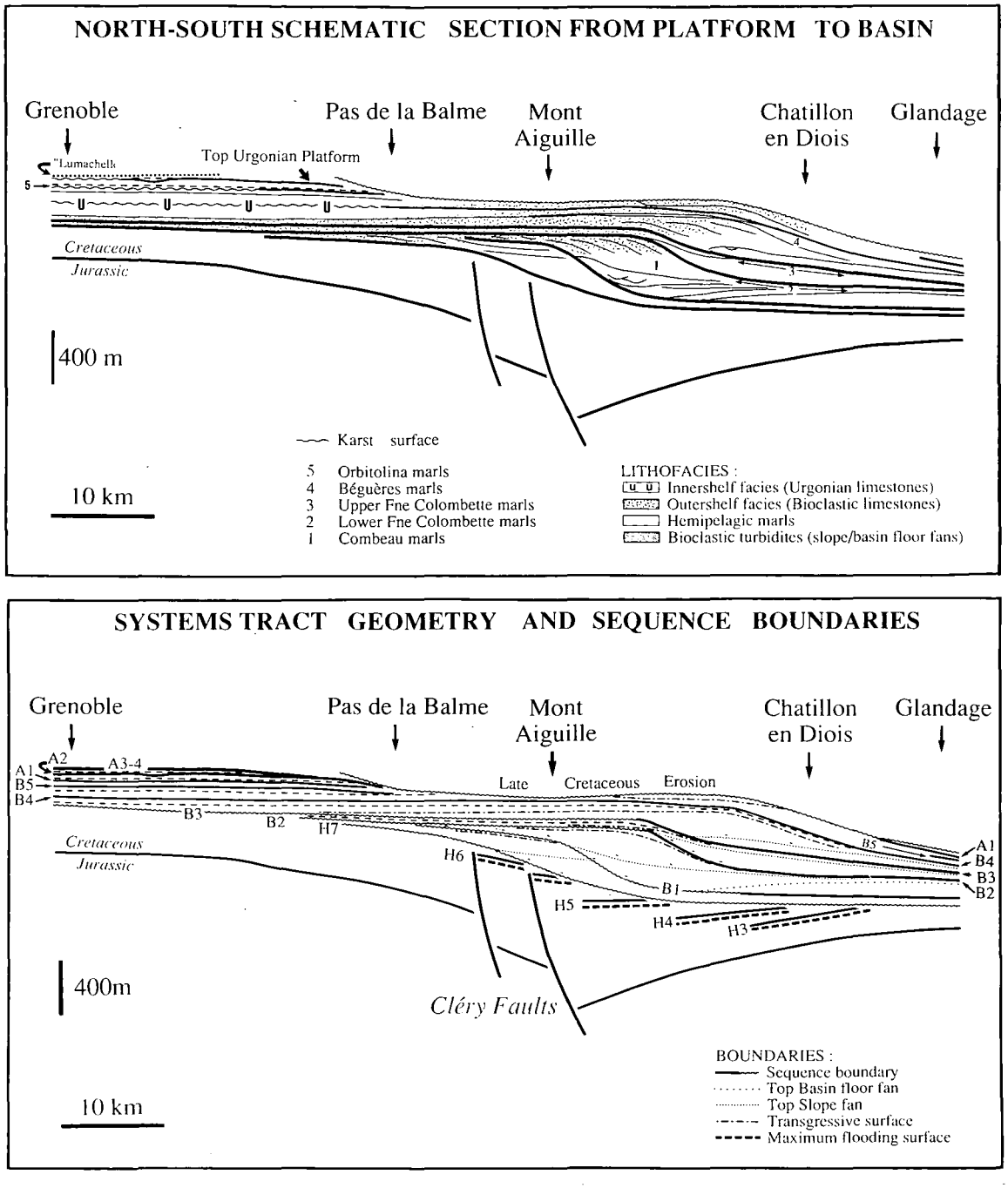

Figure 5.19. Schematic north-south cross-sections of Jacquin *et al.* (1991) of the southern Vercors along the eastern side of the Vercors plateau. The upper diagram illustrates the main lithofacies, stratigraphy of Arnaud-Vanneau (1980) and Arnaud (1981) and stratal units of the platform. The lower diagram shows the main boundaries between stratal units, their relative positioning and stratal termination patterns. Note that sequences H7 and B1 are restricted to the slope and the erosional truncation of the three interpreted Hauterivian sequences (H3-6) below the base of sequence H7.

stratigraphy of Arnaud & Arnaud-Vanneau (1989) and Arnaud-Vanneau & Arnaud (1990) (eg. Fig. 5.2) which is based largely upon palaeontological arguments.

Arnaud & Arnaud-Vanneau (1989) and Arnaud-Vanneau & Arnaud (1990) established that the Borne and Glandasse Bioclastic Limestone Formations forms a 'general' lowstand wedge, geographically restricted to the southern Vercors (Figs 4.20, p. 138 & 5.2). Further to this work Jacquin *et al.* (1991) established four sequence boundaries SbH7, SbB1, SbB2 and SbB3 within the 'general' lowstand wedge of Arnaud & Arnaud-Vanneau (1989) and Arnaud-Vanneau & Arnaud (1990), as illustrated in Figure 5.19. In the interpretation of Jacquin *et al.* (1989; 1991) the lower two sequences (SH7 & SB1) are comprised of lowstand and transgressive systems tracts only upon the slope. Contrastingly, the overlying two sequences (SB2 & SB3) are interpreted also to have highstand systems tracts developed within the 'general' lowstand wedge of Arnaud-Vanneau & Arnaud (1990) in the southern Vercors (eg. compare Figs 4.20 & 5.2 with 5.19).

5.3.2. A. The lower-upper Barremian slope sequence boundaries of Jacquin *et al.* (1989; 1991).

Jacquin *et al.* (1989; 1991) interpreted the cliffs along the eastern edge of the Vercors and north-south trending cliffs through the Cirque d' Archiane and Rocher du Combau to represent a dip section through the Urgonian platform from the shelf through the slope to the basin-floor (Fig 5.19). This interpretation is based upon the orientation of clinoforms which in the southern Glandasse plateau area dip almost exactly south (members Bi5 & Bi6 of Arnaud, 1981) (eg. see Figs 5.6, 5.7 & 5.21).

At outcrop Jacquin *et al.* (1989; 1991) have recognized four different stratal patterns, all associated with abrupt facies changes which mark sequence boundaries upon the slope in the southern Vercors:

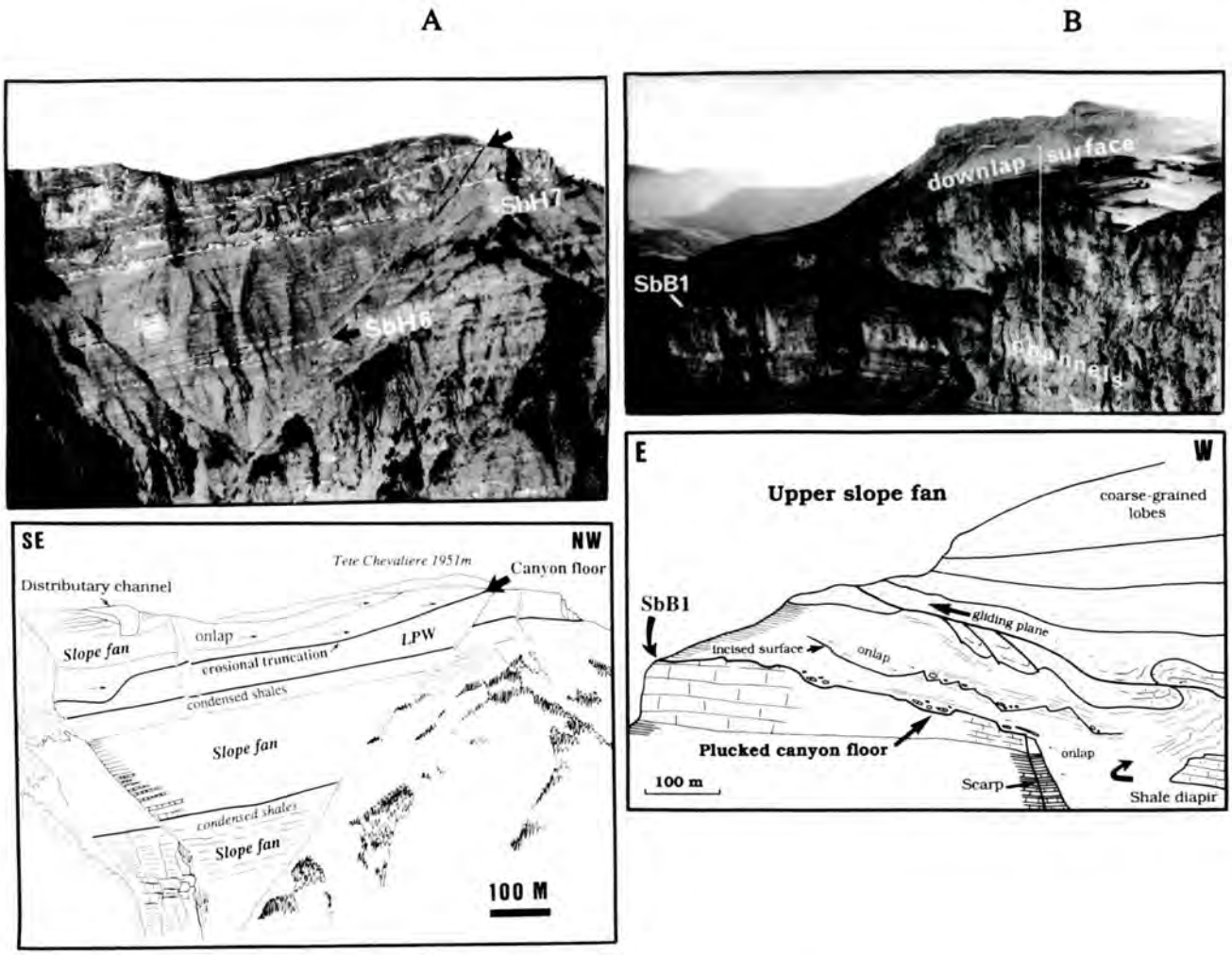

Figure 5.20. A) Sequence stratigraphic interpretation of the Tête Chevalière according to Jacquin *et al.* (1991). The sequence boundary SbH7 at the base of the prominent cliff, marked by an abrupt facies change and a parallel-parallel stratal pattern is the base of the Urgonian platform *sensu lato*. Note that the next sequence boundary SbB1 is marked by strong erosional truncation of the preceding H7 sequence. SbB1 is interpreted to correspond to the erosional truncation of a submarine canyon. This erosional surface is further illustrated in Figure B a view looking south from just to the left of the 'distributary channel' illustrated in A. In this view the SbB1 is observed and can be seen to be overlain by draping shales with interbedded nodular limestones which contain several internal erosion surfaces. Note the marked loading structures at the base of the B1 slope fan (see also Fig. 5.40).

1). Parallel-parallel stratal pattern (eg. SbH7, Tête Chevalière, Fig. 5.20).

2). Erosional truncation of preceding stratigraphic units (eg. SbB1, Tête Chevalière, Fig. 5.20; SbB3 Cirque d'Archiane and Rocher du Combau, Figs 5.21 & 5.22).

3). Onlap of the boundary by the succeeding sequence (eg. against SbB1 and SbB2, Tête de Praozel, Fig. 5.23; SbB2, Cirque d' Archiane, Fig. 5.21).

4). Downlap onto the sequence boundary by the overlying sequence (eg. SbB1 at Mont Aiguille, Fig. 5.24; SbB3 Cirque d'Archiane Fig. 5.21).

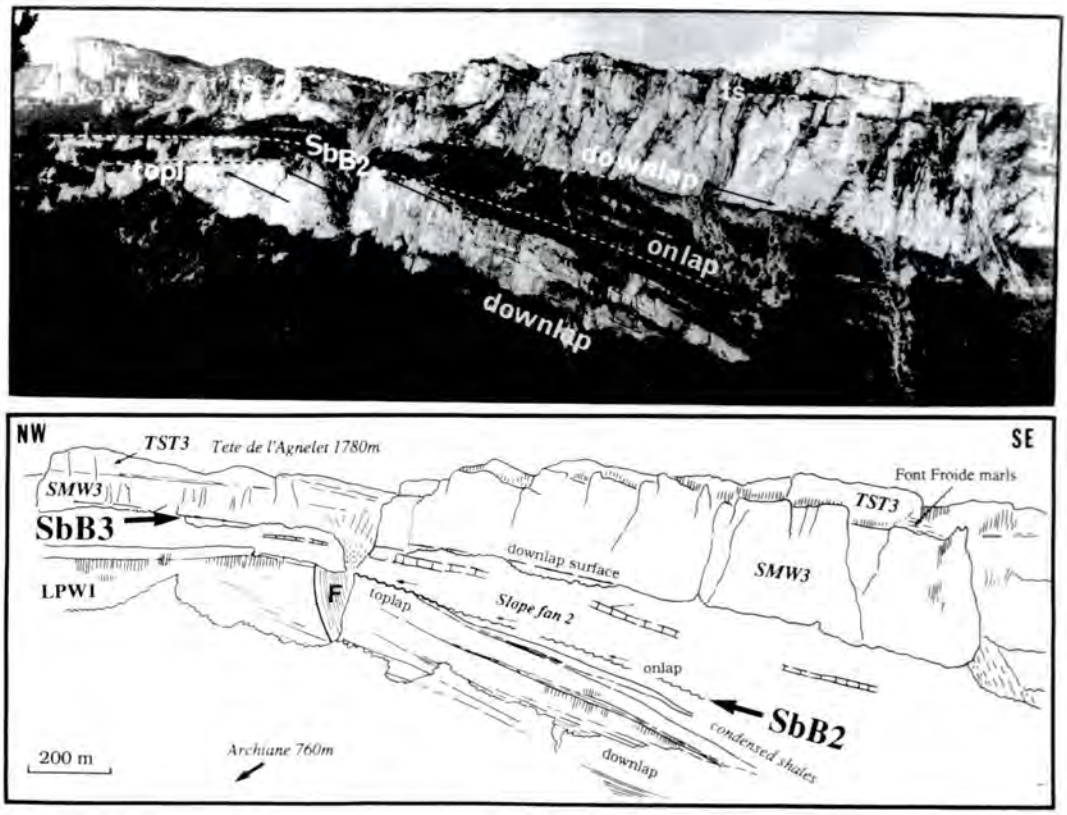

Figure 5.21. Interpreted photograph and line drawing of the eastern side of the Cirque d'Archiane of Jacquin *et al.* (1991). Note the change to a descending geometry of LPW1 (Bi5 of Arnaud, 1981) southwards. The inflexion point of this unit is interpreted as the shelf-slope break. This lower cliff (Bi5) is overlain by the Lower Fontaine Colombette marls (Arnaud, 1981) which are interpreted to be onlapped by several bioclastic slope units. This is interpreted by Jacquin *et al.* (1991) as the sequence boundary SbB2 and to be onlap of the slope fan. Also note that the succeeding sequence boundary SbB3 is a downlap surface and that all clinoforms dip south.

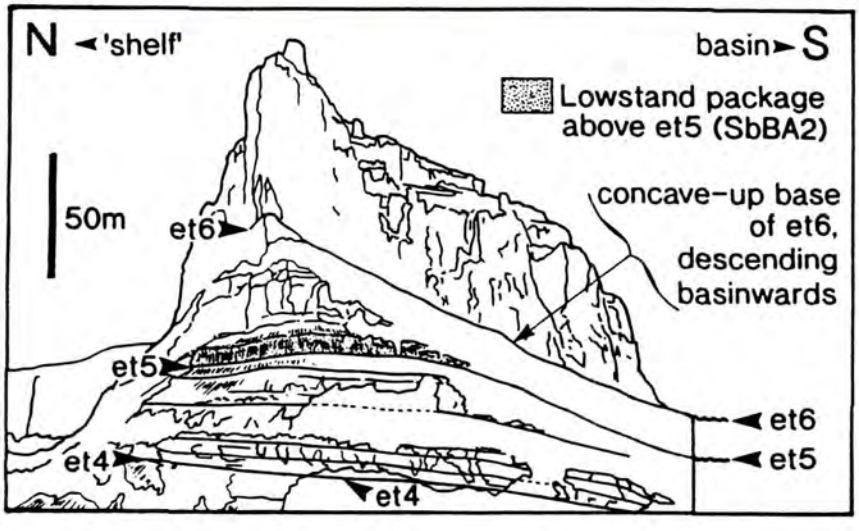

B

A

C

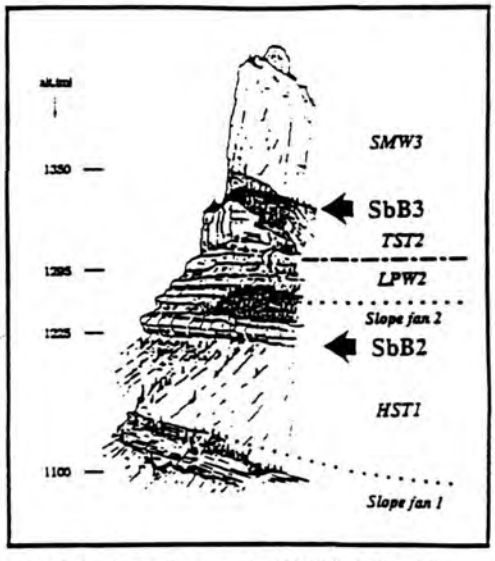

Figure 5.22. The western face of the Rocher du Combau as interpreted by Jacquin *et al.* (1989) (A) with an accompanying photograph of the face (B) and a second sketch labelling the surfaces of this exposure as discussed in Section 5.3.3 and the interpreted position of SbBA2 of Hunt & Tucker (1992) (C).

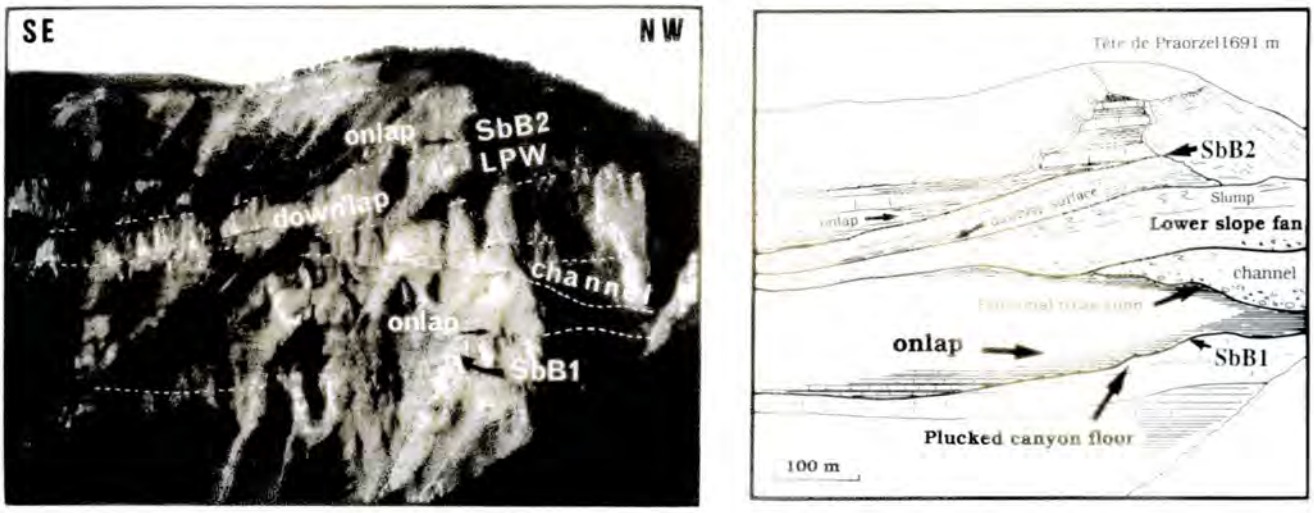

Figure 5.23. Paired photograph and line drawing of the Tête de Praorzel of Jacquin *et al.* (1991). This exposure is interpreted to represent the toe-of-slope by Jacquin *et al.* (1991). The sequence boundaries SbB1 and SbB2 are interpreted on the basis of onlap of the overlying strata. The strongest erosional truncation occurs within the sequence B1, marked by the development of the major channel and the coarsest facies. Note that this stratigraphic interpretation differs significantly from that of Arnaud (1981) who considers the basinal limestones and shales which onlap the SbB2 of Jacquin *et al.* (1991) to be equivalent to Bi2-5 whereas this interpretation would place these as equivalent to Bi6.

Further examination of changes of facies and stratal pattern(s) both at and across the sequence boundaries of Jacquin *et al.* (1989; 1991) indicates that sequence boundaries can be marked by a decrease of grainsize (2 of 8 of their illustrated examples), but are more frequently marked by an increase of grainsize (6 of 8 examples). Initially, these figures do suggest that for the most part the slopes to the Urgonian platform developed in an similar way to siliciclastic slopes as depicted by the Exxon model. Thus, the sequence boundary is associated with an increase of grainsize. However, five of the eight illustrated sequence boundaries of Jacquin *et al.* (1989; 1991) are coincident with neither the coarsest facies or the strongest erosional truncation upon the slope as is predicted by the Exxon model for siliciclastic slopes (see Section 2.2.4). A noteworthy exception of this is, however, SbB3 (eg. Figs 5.22 & 5.30) (see Section

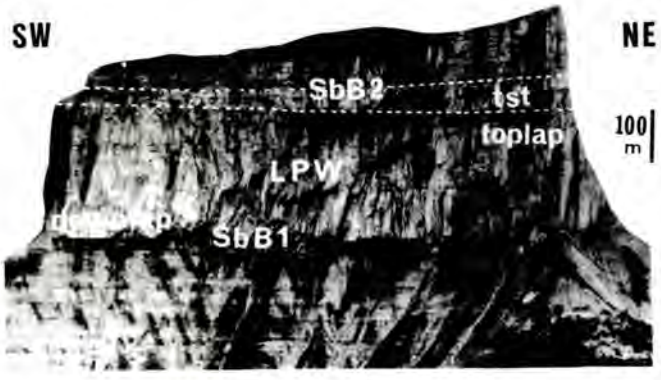

Figure 5.24. Interpreted photograph of the southern face of the Mont Aiguille a few km to the east of the Vercors plateau. This exposure is approximately 3km to the north of the Tête Chevalière. Here the sequence boundary is a downlap surface. Sequence H7 is absent at this locality and is interpreted to have pinched out. Thus, sequence B1 downlaps onto H6. This exposure is interpreted by Ravenne *et al.* (1987) and Jacquin *et al.* (1991) to represent a major submarine canyon which removed approximately 150m of the preceding stratigraphy as it was cut.

5.3.3 for further discussion of this boundary).

To conclude, Ravenne *et al.* (1987) and Jacquin *et al.* (1989; 1991) have based their interpretation(s) of slope sequence boundaries within the Borne and Glandasse Bioclastic Limestone Formations of Arnaud (1981) almost entirely upon stratal patterns and relationships of the Exxon model (outlined and discussed in Chapter 2). Their interpretations suggest that a sequence boundary is marked by an abrupt facies change which can be associated with one or a combination of the following stratal pattern(s): parallel-parallel, erosional truncation, onlap or downlap. However, contrasting to the Exxon sequence stratigraphic model, in the sequence stratigraphic interpretations of Jacquin *et al.* (1989; 1991) the coarsest facies are <u>not</u> coincident with the sequence boundary upon the slope, and similarly, erosional truncation is <u>not</u> restricted to the time of sequence boundary formation (eg. Tête Chevalière and Tête de Praorzel). In fact the reverse is frequently true with the strongest erosional truncation upon the slope being

developed within the sequences of Jacquin *et al.* (1989; 1991) (eg. Fig. 5.23) This is a very different conclusion from Jacquin *et al.* (1991) who stated that "it clearly appears that the stratal patterns and stratal termination patterns of carbonate systems tracts, especially of carbonate lowstand systems tracts, are basically similar to those of siliciclastic systems tracts".

5.3.3. The lower-upper Barremian shelf-slope transition of the Cirque d'Archiane and Rocher du Combau, southern Vercors.

5.3.3. A. Introduction.

Having briefly reviewed the position of the sequence boundary and its characteristic stratal patterns as interpreted upon the lower-upper Barremian slope(s) to the Urgonian platform *sensu lato* by Ravenne *et al.* (1987) and Jacquin *et al.* (1989, 1991) it is useful here to discuss in some detail the lower-upper Barremian 'shelf'[4] -slope cross-section of the Cirque d'Archiane and Rocher du Combau. These two exposures allow an unrivalled (upon the Urgonian platform) transect of members Bi5 & Bi6 of Arnaud (1981) from a shallow water (<10m) 'shelf' area basinwards onto the slope.

Exposures of the two valleys are dominated by cliff-forming bioclastic facies with a thin level of shelf-lagoon type rudist facies developed approximately 20m above the base of member Bi6 of Arnaud on the 'shelf' (1981) (eg. Figs 5.6 & 5.26). The rudist facies weather white and form a distinctive marker horizon, developed within yellow-orange weathering, outer-shelf bioclastic facies (Fig. 5.6). The base of the rudist package is extremely abrupt, erosional, and is interpreted to represent a type 2 sequence boundary

4. The term 'shelf' is used here in inverted commas as the members discussed in the text (Bi4-6) comprise part of the 'general' lowstand wedge of Arnaud-Vanneau & Arnaud (1990, Fig. 6.1) interpreted to have been deposited during a lowstand of sea-level when the shelf of the Urgonian platform was exposed. Thus, here 'shelf' refers to shallow-water sedimentation (<10m) developed as an autochthonous wedge on the slope to the Urgonian platform *sensu stricto*.

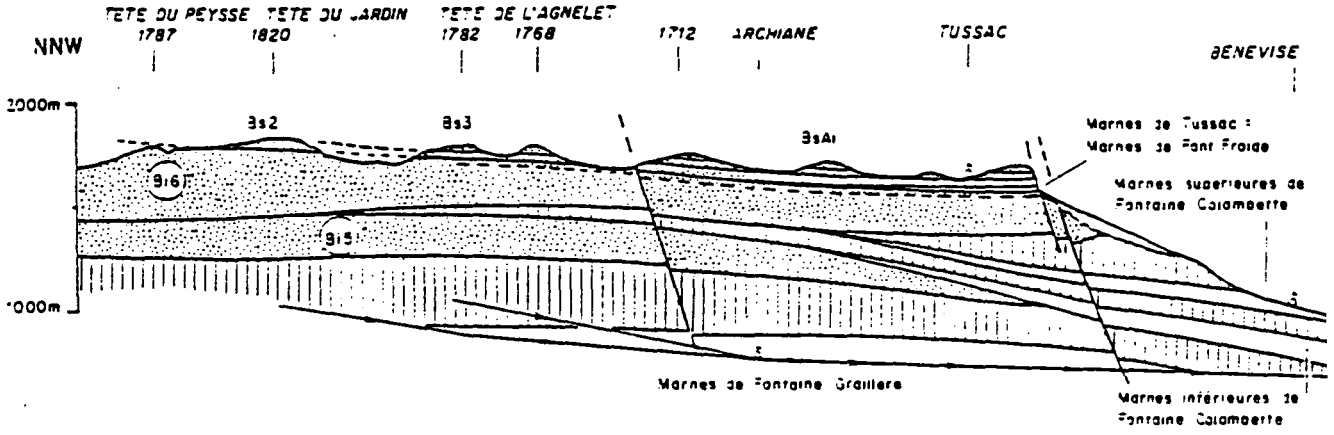

Figure 5.25. Summary north-south sketch section through the Cirque d'Archiane of Arnaud (1981) illustrating the relationships of his members Bi5 and Bi6 of the Glandasse Bioclastic Limestone Formation.

(Hunt & Tucker, 1992). This is the only unambiguous sequence boundary which can be traced almost continuously, from a shallow water 'shelf' area onto and down the slope. For this reason exposures of the Rocher du Combau and Cirque d'Archiane are discussed here in some detail and compared to other sequence stratigraphic schemes (eg. Ravenne *et al.*, 1987; Arnaud-Vanneau & Arnaud, 1990; Jacquin *et al.*, 1991; Arnaud-Vanneau & Arnaud, 1991).

The Cirque d'Archiane is dominated by three broadly progradational bioclastic wedges which correspond to members Bi4, Bi5 and Bi6 of Arnaud (1981) (eg. Fig. 5.7 & 5.26), who divided these members on the basis of flooding surfaces. In the sequence stratigraphic scheme of Arnaud & Arnaud-Vanneau (1989) and Arnaud-Vanneau & Arnaud (1990) these members (Bi4-6) represent the upper three prograding parasequences of their 'general' lowstand wedge (Figs 4.20 & 5.2). Jacquin *et al.* (1989; 1991) interpret the lower two members of Arnaud (1981) as the slope fan (Bi4) and autochthonous prograding slope wedge (Bi5) of sequence B1, the top of member Bi5 as the sequence boundary SbB2 and the upper member (Bi6) as the shelf margin wedge,

TST and HST of sequence B3 (Bi6) (Figs 5.21 & 5.22).

5.3.3. B. Stratal patterns and facies.

The stratal relationships, patterns and packages of the Cirque d'Archiane and Rocher du Combau are summarised in Figures 5.26 & 5.27. The Archiane valley is the more complete cross-section and the Rocher du Combau supplements exposures of the upper slope to Bi5 and Bi6, and its approximate position within the cross-section of Cirque d'Archiane is shown in Figure 5.26. Exposures of the Cirque d'Archiane can be divided into two crude parts; northern, which represents the 'shelf' and is characterized by sub-horizontal boundaries to the main stratal packages, comprised of progradational-aggradational bioclastic sands (Fig. 5.26), and, basinwards, a central/southern part which represents the slope to the shallow-water 'shelf'. This is characterized by descending basinwards progradation of members Bi5 & Bi6 of Arnaud (1981) (similar to Fig. 3.24C, p. 86) which dip steeply basinward (<20°) in the central region, flattening basinward into the 'southern' area (Figs. 5.26 & 27). The central region is characterized by the basinward thinning of Bi5 and represents the upper slope to this member and the mid-upper slope of Bi6. By way of contrast, the southern area represents the lower slope to Bi5 and mid-upper slope of Bi6 and is characterized by lower basinward dips than the 'central' area to member Bi5 (5°-10°), although similarly Bi6 thickens basinward (Figs 5.26 & 5.27).

Three types of stratal package are recognized in the Cirque d'Archiane: progradational, aggradational and retrogradational. The 'shelf' is dominated by prograding packages whereas slope sedimentation is composed of approximately equal proportions of progradational and aggradational stratal packages (Fig. 5.27). The proportion of retrogradational stratal packages is similar between the 'shelf' and slope. Significantly, the stratal surfaces differ quite markedly between the 'shelf' and slope (Fig. 5.26). The 'shelf' is dominated by downlap surfaces and the slope by erosional surfaces

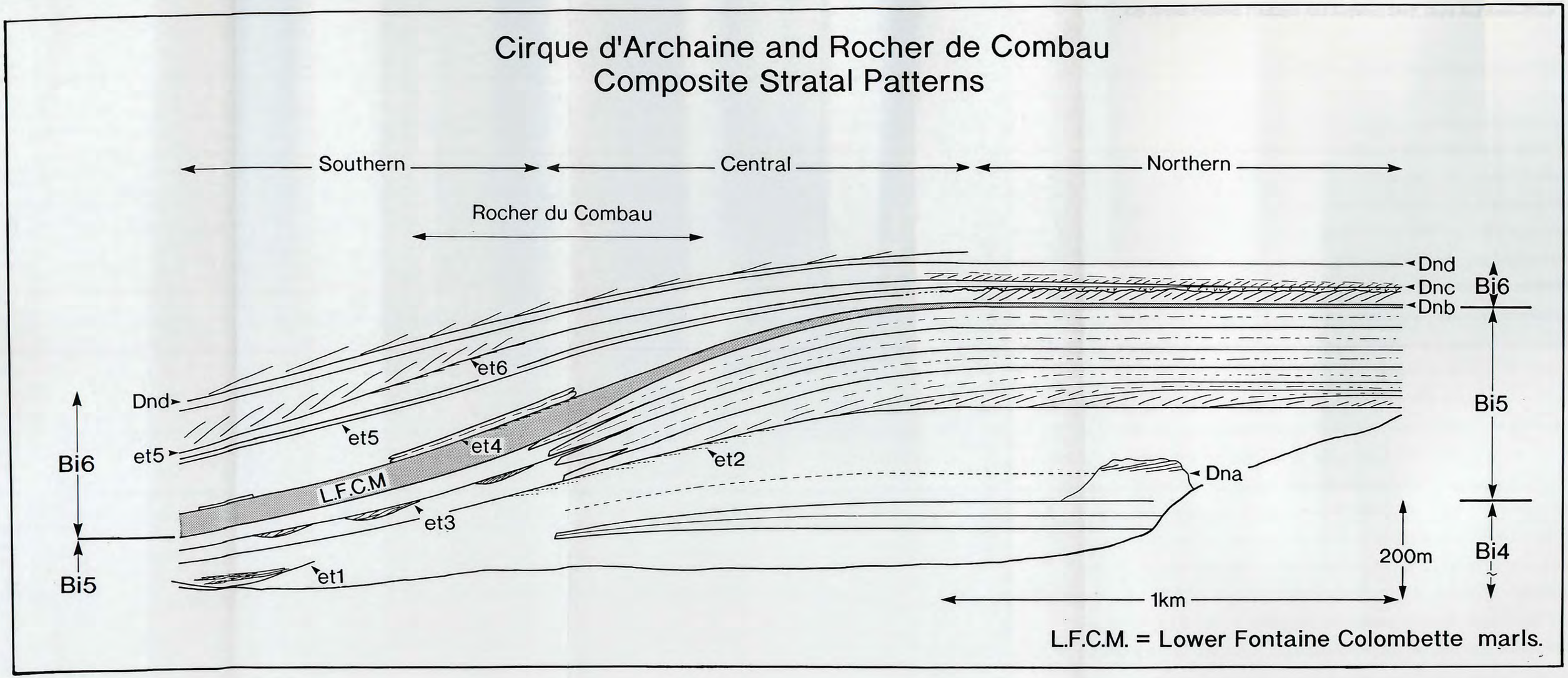

Figure 5.26. Summary of the main stratal surfaces for the lower-upper Barremian of the Cirque d'Archiane (members Bi4-6 of Arnaud, 1981). Note that of the six erosional surfaces identified upon the slope only one is also developed onto the 'shelf' of northern Archiane, characterized by sub-horizontal boundaries to stratal packages.

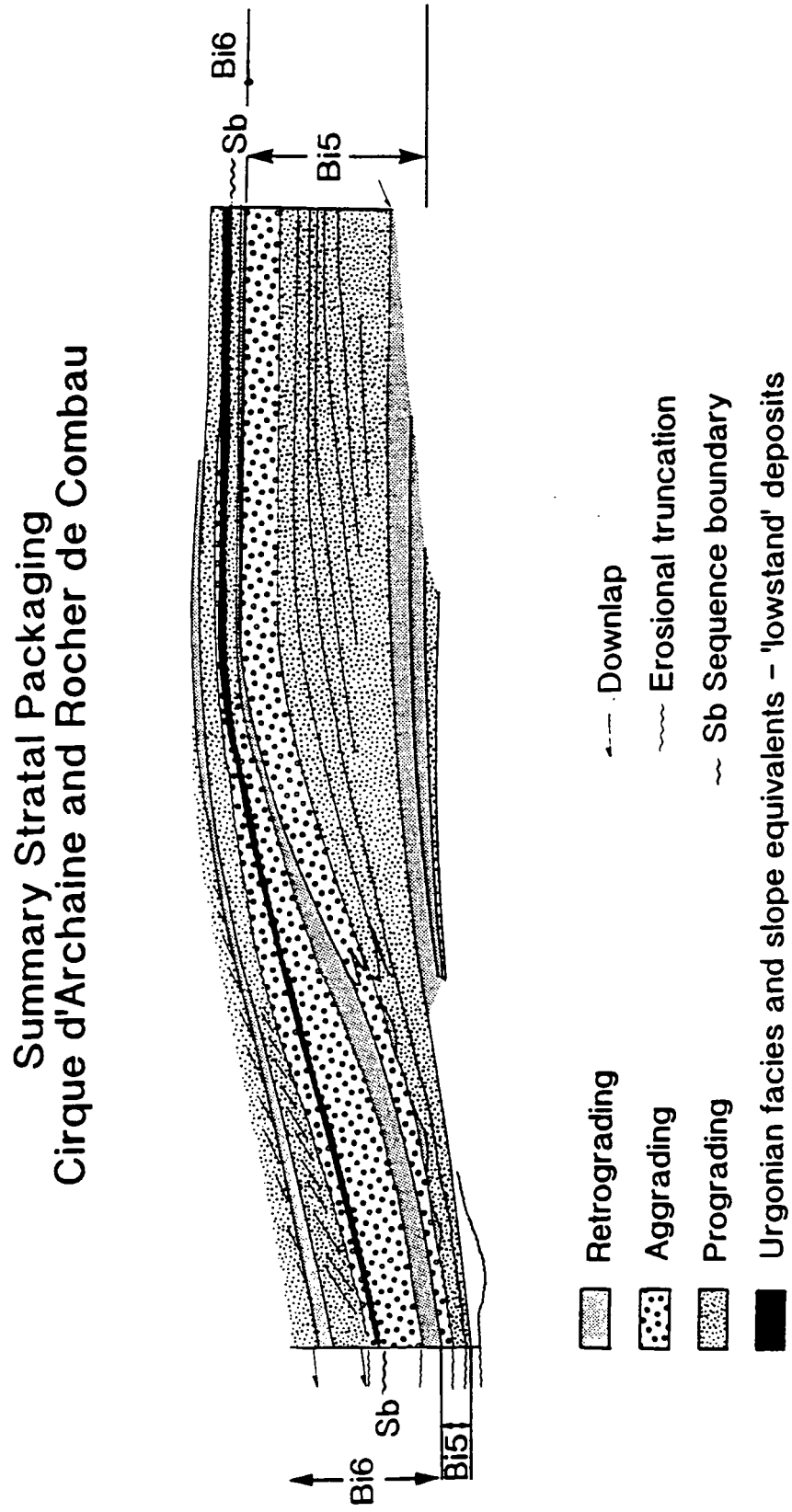

Figure 5.27. Summary of the main stratal packages identified in the Cirque d'Archiane.

(noted *Dn* and *et* respectively, Fig. 5.26). Four downlap surfaces are recognized on the 'shelf' of northern Archiane (denoted *Dna,b, c* and *d* respectively on Figures 5.6 & 5.26) and all but one of these (*Dnb*) is recognized on the slope. Contrastingly, 6 erosional surfaces are recognized on the slope (*et1-6*, Fig. 5.26), but only one of these (*et5*) is also developed upon the 'shelf' and is the type 2 sequence boundary at the base of the shelf-lagoon type rudist limestones (Figs 5.6 & 5.26) (SbBA2, see Chapter 6).

The basinward descending geometry developed within the progradational stratal package of Bi5 exerts a very strong control upon the patterns, processes and geometry of succeeding slope sedimentation (eg. Figs 5.26 & 5.27). This descending geometry of Bi5 and Bi6 differs markedly to that of the preceding slope wedge (Bi4 of Arnaud, 1981 or slope fan 1 of Jacquin *et al.*, 1989; 1991, Fig. 5.19) which has a subhorizontal base. This pattern is illustrated in Figure 5.28 where bioclastic slope sands of Bi5 descend towards and appear to downlap onto the preceding subhorizontal slope wedge (Bi4 of Arnaud, 1981). Such a configuration illustrates that the descending progradational geometry of Bi5 was not developed by tectonic rotation as the underlying strata (Bi4) have not been similarly rotated (Fig. 5.28). Furthermore, geometric considerations, such as the rate of basinward thinning of Bi5 suggest the presence (unexposed) of an intraformational erosion surface (*et2*, Fig. 5.26) within the progradational Bi5 stratal package. Such a hypothesis eliminates the need for the very rapid basinward thinning of lower slope facies which is not seen elsewhere where lower slope facies of this member are exposed (eg. Bi5 between La Montagnette and Ranconnet of the eastern Glandasse Plateau, eg. Fig. 6.13). Thus, the listric, descending, basinward flattening geometry developed by the upper part of the progradational Bi5 stratal package is interpreted to develop by progradation into a pre-existing topographic depression. The listric shape of *et2* is similar to that of slide scars identified in seismic sections (eg. Mullins *et al.* 1986; Mullins *et al.*, 1988) and is here interpreted to have developed as a portion of the slope gravitationally collapsed.

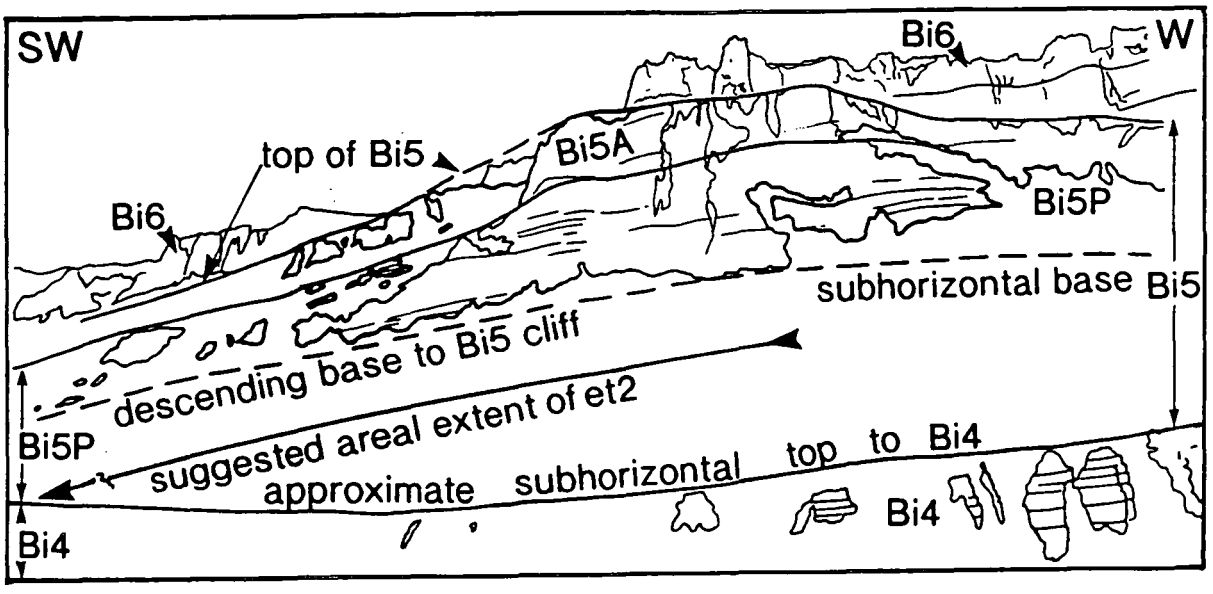

Figure 5.28. Sketch of the stratal relationships of members Bi4 and Bi5 on the western side of the Archiane valley, located on Figure 5.7. Here Bi5 descends basinwards and would appear to downlap onto the subhorizontal Bi4. This is interpreted to have developed from the progradation of slope sands of Bi5 into a pre-existing topographic depression. This is interpreted to be an intraformational slide scar (*et2*, Fig. 5.26) developed as the slope gravitationally collapsed. This developed a basal relationship similar to that illustrated in Figure 3.24, p. 86).

The 'shelf' section of the northern Cirque d' Archiane is used here as a 'control' to evaluate relative sea-level changes since they can only be unambiguously ascertained above the first *in situ* shallow-water fauna. Where found in the 'shelf' stratigraphy, shallow-water faunas such as 'oversized' corals and stromatoporoids in life position establish water depths of <10m (Fig. 5.29). From these tie-in points relative sea-level changes can be measured using criteria such as facies shifts, the thickness of toplapping strata and changes of gross stratal patterns (eg. changes from basinward shifting to stationary aggrading packages, Bi5 P-A, Fig. 5.7). During Bi5 the subhorizontal toplapping strata of the northern Archiane valley are interpreted to have formed in water depths of less than 10m as these bioclastic facies contain *in situ* oversized corals and

Figure 5.29. Bored 'oversized' corals within bioclastic grainstones in the upper part of Bi5 in the northern Cirque d'Archiane. Fauna such as this in life position are used to establish water depths of less than 10m from which relative sea-level changes can be ascertained. Hand lens for scale.

stromatoporoids (eg. Fig. 5.29). Thus, upon the 'shelf' relative sea-level falls of >10m should be recorded by the development of a subaerial exposure surface(s) (eg. type 1 sequence boundaries) and relative sea-level rises can be evaluated from the thickness of toplapping strata, changes of stratal patterns and facies changes.

Upon the interpreted shallow-water 'shelf' area of the northern Cirque d'Archiane only <u>one</u> fall of relative sea-level is identified from the base of the Bi5 progradational package to the top of Bs2, although only Bi5-6 are considered here. The fall of relative sea-level is interpreted to have developed a type 2 sequence boundary as it does not expose the 'shelf' in this area or drop sea-level below the shelf-slope break, but it is associated with a basinward facies shift. At the sequence boundary protected shelf-lagoon type rudist facies sit abruptly on a prograding outer-shelf sand shoal complex (eg. Fig 5.6). The base of the rudist facies (the type 2 sequence boundary) is an erosional surface (*et5*) with a relief of up to 5m into which clinoforms of the preceding sand-shoal

A1 ▲ A2 ▼

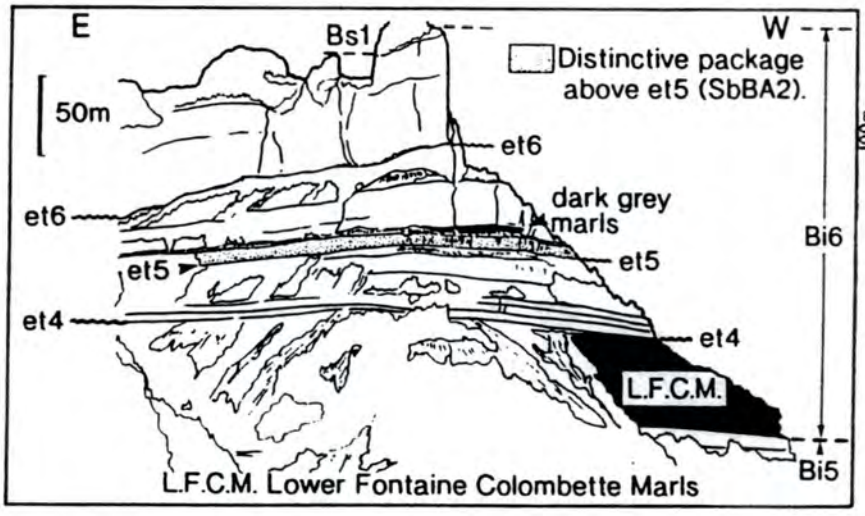

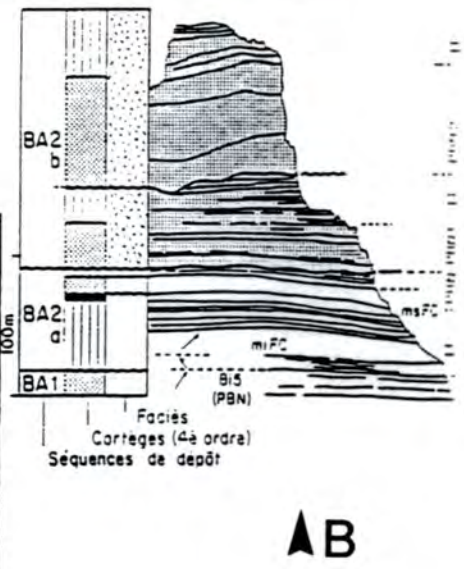

▲B

Figure 5.30. A1 & A2 Paired photograph and sketch of the northern face of the Rocher du Combau. This is approximately a strike section through this locality. On the sketch the nomenclature used in the accompanying text is given as detailed in Figures 5.26 and 5.27. B: The sequence stratigraphic interpretation of this side of the Rocher du Combau of Arnaud-Vanneau & Arnaud (1991). Key to symbols of B as according to Fig. 5.2.

Figure 5.31. The contemporaneous package of trough crossbedded light-grey bioclastic sands on the slope at the Rocher du Combau to the rudist limestones on the 'shelf' in the northern Cirque d'Archiane. The height of this exposure is approximately 5m. This package directly overlies *et5* and is itself overlain by approximately 3m of dark grey shales (eg. see Fig. 5.30).

complex are abruptly terminated (Fig. 5.6). The sequence boundary can be traced almost continuously along the over 2km of exposure north of the 'shelf'-slope break to member Bi5 where between 5 and 10m of shelf-lagoon type rudist facies are developed above the sequence boundary. The thickness of these rudist facies tends to reflect the erosional topography at the base of the package on to the sequence boundary (eg. Fig. 5.6). This distinctive package of rudist facies is interpreted to have developed during a relative sea-level lowstand and these appear to have been sheltered from storm currents as the vast

majority of rudists are in life orientation (there is also no evidence of tidal currents).

This sequence boundary is correlated from the 'shelf' (Fig. 5.6) to a very abrupt facies change on the slope (*et5*, Figs 5.26, 5.27, 5.30 & 5.31), the base of which is erosional, although very minor in comparison to the other erosional surfaces identified on the slope (eg. *et2*, *et4* & *et6*). The surface *et5* is only accessible on the eastern side of Archiane and Rocher du Combau on the lower-mid slope where its base is very sharp and loaded, but does not appear to be erosional (underlying shales too weathered out to confirm). The lowstand slope package is volumetrically relatively small (about 5m thick, Fig. 5.31) but is sedimentologically distinctive, composed of light-grey weathering trough crossbedded bioclastic sands with a characteristic absence of reddened grains which typify slope sands above and below (eg. Figs 5.30 & 5.31). The combination of its small volume and distinctive sedimentology is interpreted to reflect the small area available for sediment production and disruption of patterns of sedimentation with high-energy facies restricted to a very narrow strip basinward of the shelf-slope break. The characteristic grey colour of this lowstand package is thought to reflect the important contribution of muds swept off the adjacent 'shelf-lagoon' of northern Archiane at this time.

At the Rocher du Combau approximately 3m of dark-grey shales overlie the distinctive 'lowstand' package (Figs 5.22 & 5.30) and these are in-turn overlain by a 60m package of characteristically orange weathering bioclastic sands which generally coarsen upwards and are erosionally truncated below *et6* (Figs 5.22, 5.30, 5.32, 5.33). The orange colour of these bioclastics reflects the coating and impregnation of grains by iron oxide minerals and is suggestive of relatively slow sedimentation rates. Due to incomplete exposure it is not possible to establish fully the basinward geometry of these bioclastic slope sands. In the northern Cirque d'Archiane the upper surface of these orange bioclastic sands is convex-up in shape, developed topographically (approximately 10m) above the preceding 'shelf'-slope break (Figs. 5.6, 5.26). In this area the bioclastic

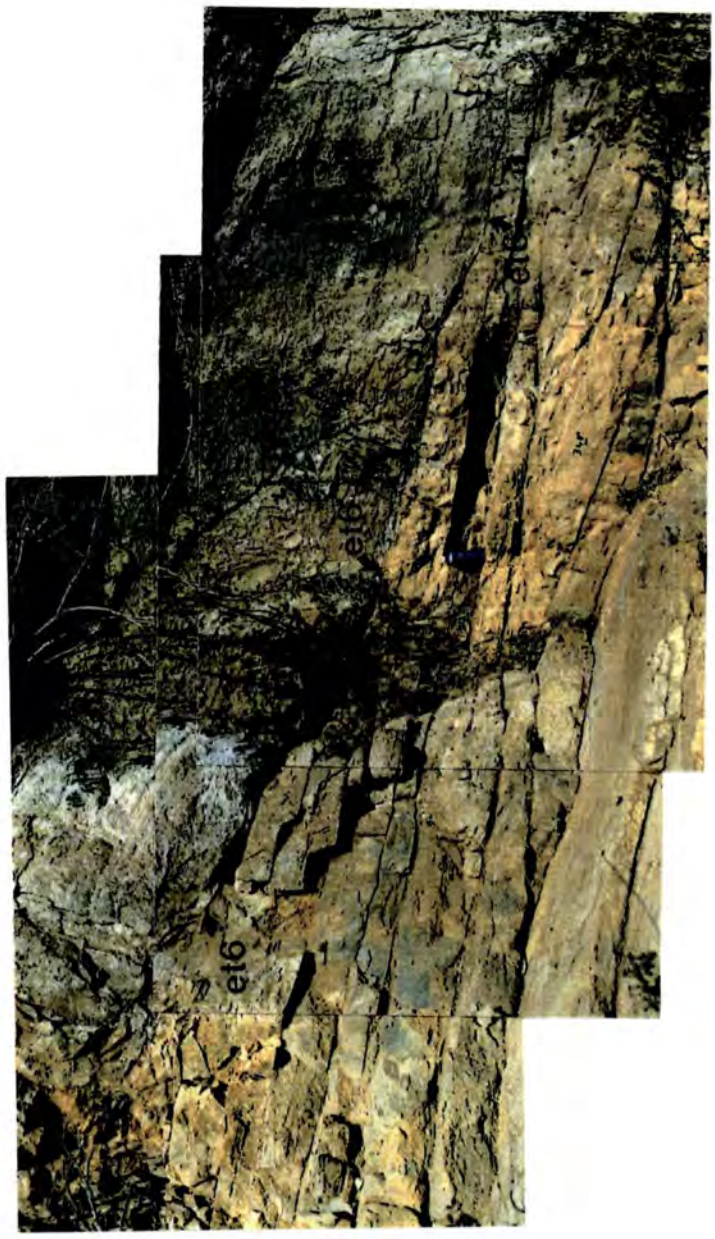

Figure 5.32. Detail of the surface *et6* in dip section on the southern face of the Rocher du Combau, located upon Figure 5.33. Trough cross-bedded orange weathering packstones are erosionally overlain by exceptionally coarse, poorly structured grainstones with slope lithoclasts (eg. Fig. 5.34). This locality is marked 'A' on Figure 5.33. Face is orientated 348° (left) and 168° (right). Blue water container approximately 300mm high for scale.

sands are also deposited on the 'shelf' on to which they both thin and downlap, pinching out some 1.2km north of the shelf-slope break of Bi5 in the vicinity of Pierre Ronde Rocher (eg. Fig. 5.6). Such a geometry and stratal termination pattern is suggestive of an 'overfill' lowstand wedge developed in the late lowstand systems tract (illustrated in Fig. 2.7, p. 30). However, the shales below these bioclastics on the upper slope (eg. at Rocher du Combau, Figs 5.30 & 5.33) appear to represent the mfs above the 'lowstand' package and correlate with the drowning of rudist facies on the 'shelf'. This correlation casts doubts on the geometric interpretation of the shelf-margin bioclastic buildup as an 'overfill' lowstand wedge, suggesting, alternatively, that this bioclastic buildup developed in the early HST and was terminated as 'shelf' sands (above *Dnc*, Fig. 5.26) prograded over it in the late HST. This interpretation, placing the bioclastic buildup within the early HST also explains the pervasive oxidation of bioclastic grains within the buildup which would not be expected if it were a high-energy lowstand bioclastic wedge where the grains are being constantly reworked.

Stratigraphically the youngest erosional surface upon the slope in Cirque d'Archiane and Rocher du Combau is *et6*, interpreted by Jacquin *et al.* (1989; 1991) as the sequence boundary SbB3 (eg. Figs 5.21 & 5.22) and by Arnaud-Vanneau & Arnaud (1991) as sequence boundary BA2b (Fig. 5.30B). In both the Archiane valley and at the Rocher du Combau this erosional surface is developed basinward of the 'shelf'-slope break of Bi5 (eg. see also Arnaud, 1981, his fig. 52) and descends basinward with a characteristic concave-up shape both in dip and strike sections (Jacquin *et al.*, 1989, 1991, eg. Figs 5.21, 5.22, 5.30 & 5.33). At the Rocher du Combau at least 15m of stratigraphy can be seen to be erosionally truncated below the surface *et6* as it descends basinward (eg. Fig. 5.33). At outcrop this surface (*et6*) dips basinward between 10° and 20° (Figs 5.21, 5.22 & 5.33), has a very irregular topography in both dip (Fig. 5.32) and strike sections, and is overlain by 10m of exceptionally coarse grainstones which contain outer-shelf and slope lithoclasts (eg. Figs 5.32 & 5.34). The slope sands above *et6* can

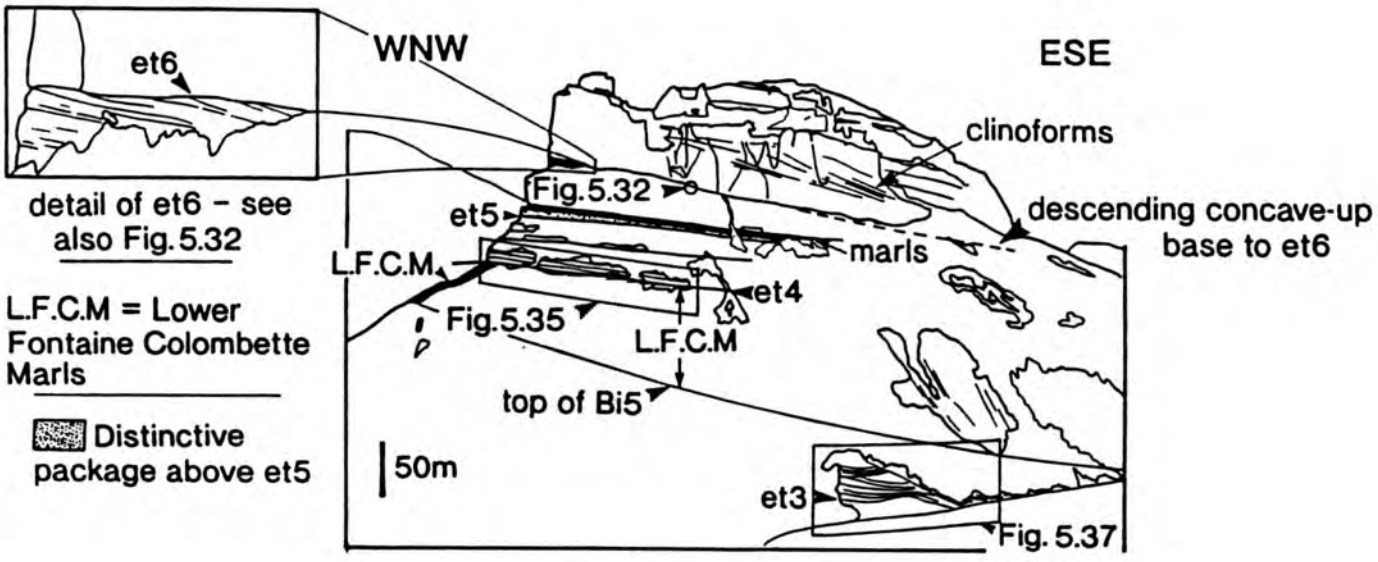

Figure 5.33. The southern face of the Rocher du Combau showing the erosional truncation of *et6* at the base of the prominent cliff and paired interpreted line drawing locating main surfaces and other Figures discussed in the text and named according to Figs. 5.26 & 5.27.

be traced up slope to the 'shelf' towards which they thin (eg. Fig. 5.26). On the 'shelf' this same package of bioclastic sands asymptotically downlaps onto either the rudist limestones or, to the south of Pierre Ronde Rocher, onto orange bioclastic limestones (*Dnc*; the early HST buildup, Figs 5.6 & 5.26). In the northern Archiane valley the surface *Dnc* is downlapped by clinoforms with some 10-15m of relief (Fig. 5.6) whereas upon the slope clinoforms have a relief of some 40-50m (eg. Figs 5.21, 5.22 & 5.33). These younger clinoforms, developed basinward of the Bi5 'shelf'-slope break downlap onto the massive coarse bioclastic sands above *et6* (Fig. 5.33). Such a relationship suggests that the erosional surface was cut prior to the progressive progradation and downlapping of sands basinward from the 'shelf'-slope break.

Contrasting with the preceding erosional surface *et5*, *et6* is only developed on the slope (Fig. 5.26, Arnaud, 1981, his fig. 52). The restriction of *et6* to the slope must reflect a change of depositional dynamics at the 'shelf'-slope break (the upper limit of *et6*) at this time as relative sea-level was at a stillstand. This is indicated by the constant thickness of toplap strata and of the sand shoal complex itself on the 'shelf' (eg. Fig. 5.6). Slope erosion appears to have occurred when the sand shoal complex (above *Dnc*) had prograded to the 'shelf'-slope break. At this time sands moved across the 'shelf' to the front of the sand shoal were delivered to not just the frontal face of the bedform but also the 'shelf'-slope break as these were coincident at this time. The initial bypassing and erosion the upper slope by sands delivered to this point is interpreted to reflect the increase of gradient at the 'shelf'-slope break, where the potential of the gravity flows which moved sediment down the frontal face of the bedform (sand shoal) abruptly increased, causing upper slope bypass and erosion.

Ravenne *et al.* (1987), Jacquin *et al.* (1989; 1991, their SbB2, Figs 5.21 & 5.22) and Arnaud-Vanneau & Arnaud (1991, their SbBA2a, Fig. 5.30) also identified an older sequence boundary in the Cirque d'Archiane and Rocher du Combau (eg. see Section 5.3.2). This sequence boundary whose 'type' locality is the Archiane valley is interpreted

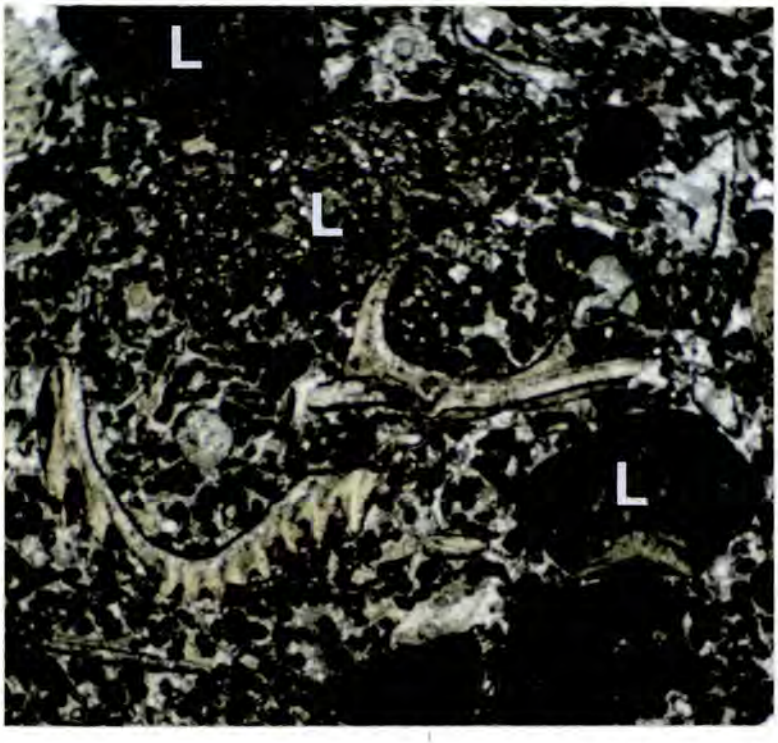

Figure 5.34. Photomicrograph of Bi6 bioclastic grainstones with slope lithoclasts (L) from just above the surface *et6* in the southern Cirque d'Archiane (eastern side). Field of view approximately 18mm.

on the basis of onlap of three prominent bioclastic limestone packages (Fig. 5.21) onto the upper slope of Bi5 (Jacquin *et al.*, 1989; 1991). This slope sand package actually appears to onlap the Lower Fontaine Colombette Marls (Figs 5.26 & 5.35). These marls thin markedly up onto the 'shelf' in northern Archiane where they are represented by sub-wavebase grey, bioturbated wackestones (Fig. 5.36) containing infrequent 50-100mm thick sharp based cross-laminated grainstone beds, interpreted as tempestites. The development of these facies upon the 'shelf' indicates that it had become 'drowned' (see Section 3.4.5, p. 47) by a relative sea-level rise to below approximately10m (see Fig. 3.8, p. 48). This relative sea-level rise did not, however, develop a retrogradational but first an aggradational parasequence set (Bi5A, Fig. 5.7) overlain by the mfs, represented by the Colombette marls when sedimentation 'gave-up'.

Examination of the base of the lowest 'onlapping' bioclastic slope-sand package at the Rocher du Combau demonstrates that the onlap of this unit is apparent, for at this

Figure 5.35. The erosional surface *et4* at the Rocher du Combau, as located on Figure 5.33. This surface can be seen to erosionally truncate the Lower Fontaine Colombette marls which appear to drape the upper surface of Bi5 in the Cirque d'Archiane. The distinctive package of wackestones-packstones above the erosional surface appear to onlap Bi5 in the Cirque d'Archiane (eg. Jacquin *et al.*, 1989; 1991, Fig. 5.21). However, as can be seen here this is apparent, an artifact of the units basinward descending geometry.

Figure 5.36. The 'shelf' equivalent of the Lower Fontaine Colombette Marls from the north of Cirque d'Archiane. This facies, interpreted to be sub-wavebase is a wackestone with reddened bioclastic grains and is also heavily bioturbated. In the north of Cirque d'Archiane these facies are interbedded with sharp based 50-100mm thick beds of cross-laminated sands, interpreted as tempestites and thought to be equivalent to the *et4* surface on the slope (eg. Fig. 5.35). Pencil approximately 130mm long for scale.

locality the base of these lowest slope sands is strongly erosional (surface *et4*, Figs 5.22, 5.26, 5.30 & 5.35). This erosive package is both overlain by and overlies marls, suggesting that it developed whilst the shelf was flooded. The surface *et4* and the overlying slope sands are correlated to the 50-100mm thick tempestite beds within limestone equivalents of the Lower Fontaine Colombette Marls up on the 'shelf'. These storm driven density currents are interpreted to have accelerated as they moved over the shelf-slope break, increasing their erosional capacity and thus eroding a significant part of the upper slope (eg. Figs 5.26 & 5.35). The steeply descending base of the slope sands above *et4* gives this stratal package the *appearence* of onlapping the slope.

The Lower Fontaine Colombette Marls overlie the upper aggradational part of Bi5. On the mid-lower slope the base to the Bi5 aggradational package appears to be contemporaneous to the development of erosively based (*et3*) decimetre scale channels,

Figure 5.37. Large erosively based channel (*et3*, located upon Fig. 5.33) developed into the limestone dominated foreslope to Bi5 at the Rocher du Combau. The channel is filled by interbedded limestones and shales suggesting that carbonate sedimentation rates were reduced during/immediately following the cutting of the channel. This channel and its lateral equivalents are interpreted to have developed at the base of the Bi5A package (eg. see also Figs 5.26 & 5.27). Truck for scale.

filled by lime muds and interbedded shales (Fig. 5.37). These channels are interpreted to have developed and filled at the time when 'shelf' (and therefore slope) sedimentation rates were reduced at the beginning of the aggradational package of Bi5 (Bi5A, Fig. 5.7). This aggradational package (Bi5A, Fig. 5.7) represents the TST, developed above a relative highstand systems tract represented by the offlapping, progradational Bi5 package (Bi5P, Fig. 5.7). Thus, the succeeding TST (Bi5P) has a type 2a geometry (eg. see Section 3.7.2. B, Fig. 3.20, p. 73), developed as the 'shelf'-margin sedimentation rates were able to keep pace with but not outpace the rate(s) of relative sea-level rise. As discussed in Section 3.7.2.B (p. 72), the development of this type of TST geometry is marked by the increase of shelf to basin-floor topography which may be associated with the bypassing of sands to the basin-floor at this time as relief increases. Such a scenario

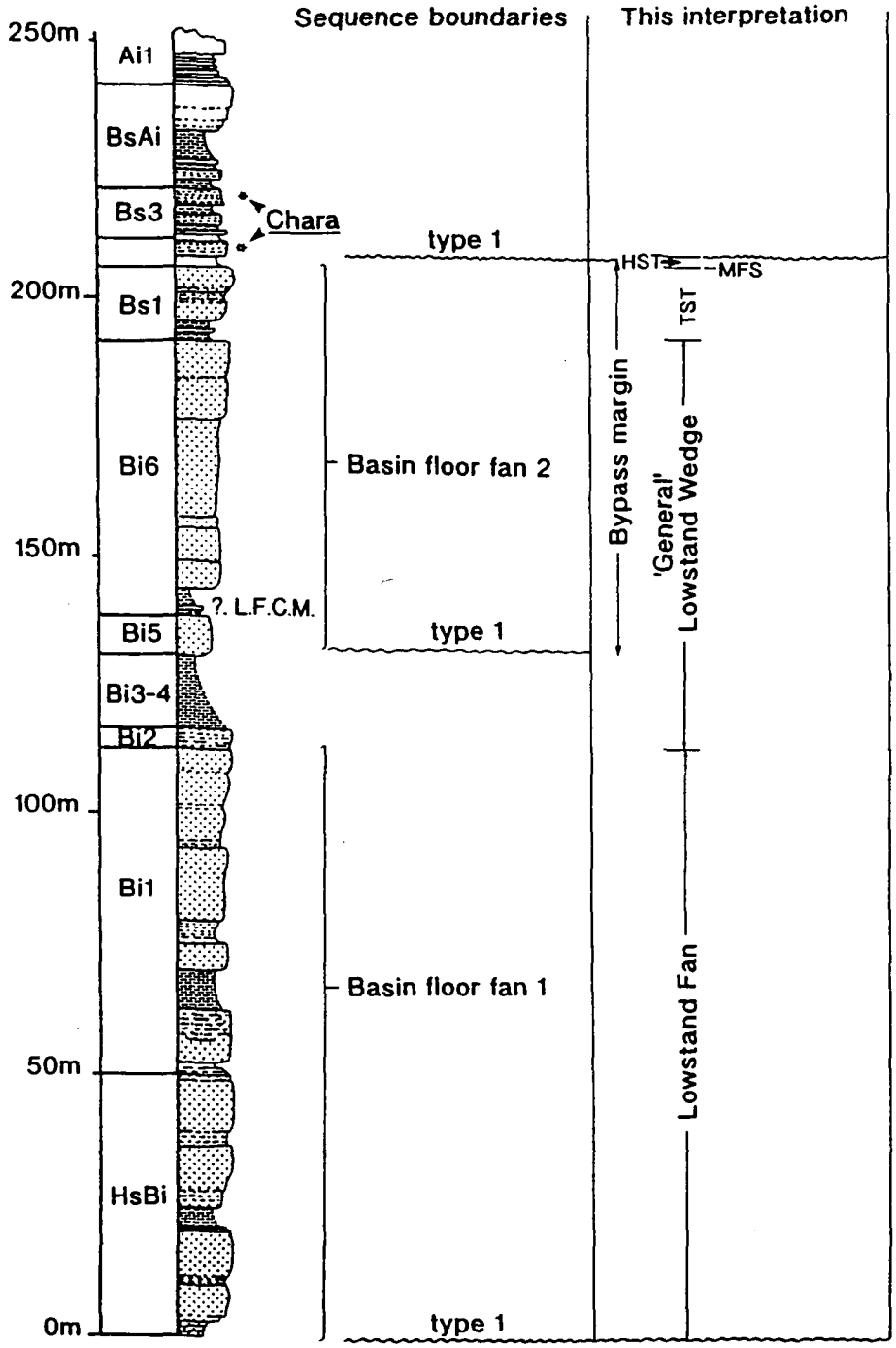

Figure 5.38. The basin-floor section of the Gorge de Amayers showing the stratigraphy of Arnaud (1981) (slightly modified) as compared to a 'typical' sequence stratigraphic interpretation and that developed by Hunt (1990) and Hunt & Tucker (1992). This section is characterized by two discrete packages of sands HsBi-Bi1 and Bi5-Bs1 (Arnaud, 1981). Classically, on the basis of basin-floor stratigraphy alone this would suggest two falls of relative sea-level and thus two sequence boundaries (eg. left hand column). However, it is argued here that the change of geometry and build-up of topography at the 'shelf'-margin during the latter part of Bi5 is the main cause of bypass during Bi5, Bi6 and Bs1. L.F.C.M.= Lower Fontaine Colombette Marls.

appears to have developed at the Urgonian 'shelf'-margin during Bi5, for at this time the deposition of basin-floor sands is resumed (Fig. 5.38) (Hunt, 1990). Classically, using the Exxon sequence stratigraphic model (Figs 2.1 & 2.5) such a resumption of basin-floor sedimentation would be taken to suggest strongly a fall of relative sea-level and the development of a sequence boundary (eg. Fig. 5.38). However, the bypassing of sands to the basin-floor at this time appears to be more closely related to a combination of the increase of topography and the inherited slope morphology (Hunt, 1990; Hunt & Tucker, 1992). The Lower Fontaine Colombette Marls represent the mfs to this TST and appear to drape shelf-slope topography. The apparent onlap of the strata above the Lower Fontaine Colombette Marls is due to slope re-equilibration and is similar in origin (and to some extent geometry) to the drowning unconformities described by Schlager (1989).

5.3.3. C. Summary.

1. Bi5P prograded basinward during a relative sea-level rise which did not exceed sedimentation rates on the 'shelf' so that sigmoidal clinoforms characterize the lower part of this member. As facies prograded basinward the slope collapsed along a listric shaped plane, leaving a slide scar into which the succeeding part of Bi5 prograded to develop a basinward descending geometry. This change to a descending geometry is associated with the change of slope facies from dark-grey interbedded limestones and shales to light-grey limestones.

2. During the latter part of Bi5 relative sea-level began to rise more rapidly (Bi5A). This is marked by the development of shales on the slope and a halt of basinward progradation. The shift of slope sedimentation from limestones to interbedded limestones and shales is associated with the cut and fill of decimetre scale channels on the mid-upper slope (transgressive surface).

3. Aggradation of the 'shelf'-margin and of the upper slope (Bi5A) increased topography

to the basin-floor, and is possibly the cause of slope bypass (type 2 TST).

4. As the rate of sea-level rise increased still further 'shelf' sedimentation was drowned and the Lower Fontaine Colombette marls were deposited (mfs). The 'shelf' was not, however, submerged to depths greater than 30m as storm currents swept across the shelf removing much sediments and redepositing it onto the slope. As these storm generated currents reached the shelf-slope break they are interpreted to have accelerated and thus eroded a significant part of the upper slope (*et4*), developing a type of drowning unconformity as the slope sands above this surface *appear* to onlap the slope.

5. A fall of relative sea-level subsequent to the progradation of the preceding sand shoal to the 'shelf'-slope break caused a major basinward 'facies jump'. Shelf-lagoon type limestones developed directly on outer 'shelf' bioclastic limestones. Equivalent slope deposits are volumetrically small, but sedimentologically distinct and erosively based (sequence boundary formation and lowstand sedimentation).

6. Both slope and shelf-lagoon type sedimentation drowned as sea-level rose more rapidly.

7. A second sand shoal developed from farther back on the 'shelf' again prograded across the drowned 'shelf'. Contemporaneously, at the 'shelf'-slope break a bioclastic 'buildup' developed. As the prograding sand shoal reached the 'shelf'-slope break the bioclastic 'buildup' sedimentation was terminated and once again bioclastic sands bypassed through and eroded the upper and mid slope (late HST progradation and shedding developing a slope unconformity).

5.3.3. D. Conclusions.

The study of stratal packaging and the relationship of stratal terminations and geometries upon the slope of Cirque d'Archiane and Rocher du Combau casts serious doubts upon the reliance of stratal termination patterns alone (eg. erosional truncation) to infer relative sea-level changes upon the slopes of the Urgonian platform, and more

widely carbonate platforms in general. Inherited topography developed from slope collapse played an important role in the development of the slope to Bi5 and Bi6 in a similar manner to that noted by Mullins *et al.* (1988) upon the flanks of the Florida platform. This study has shown that of the 6 erosional surfaces observed upon the slope to members Bi4, 5 & 6 of Arnaud (1981) only one is traceable onto the 'shelf' where it is associated with a fall of relative sea-level and sequence boundary formation (*et5*). Of the other erosional surfaces recognized upon the slope above *et2* one is associated with a relative sea-level rise (*et3*) and the other 2 (*et4* & *6*) are both interpreted to have developed as sediments were shed past the 'shelf'-slope break where they underwent a 'hydraulic jump', eroding the slope to a new equilibrium profile. Most erosional surfaces identified upon the slope are thus not sequence boundaries but are developed by sedimentary bypass. This study has shown that the sequence boundaries SbB2 and SbB3 of Jacquin *et al.* (1989; 1991) interpreted from stratal patterns within the Cirque d'Archiane and Rocher du Combau are incorrectly placed. The lower sequence boundary of Jacquin *et al.* (1989; 1991) (SbB2) is interpreted to represent a variable of the drowning unconformities described by Schlager & Camber (1985) and Schlager (1989). The sequence boundary SbB3 of Jacquin *et al.* (1989; 1991) is interpreted to have developed from upper slope bypass as bioclastic sands prograded to the 'shelf'-slope break after a relative sea-level rise which had drowned the 'shelf'.

5.3.3. E. Discussion.

As discussed in the proceeding section there is a marked discrepancy between the number of erosional surfaces identified on the slope of Cirque d'Archiane, Rocher du Combau and those identified upon the 'shelf' (6:1) for the members Bi4-Bi6 of Arnaud (1981). This illustrates that erosional truncation upon the slope is not limited to times of falling relative sea-level and as such is *not* a reliable criteria for the identification of sequence boundaries on the slope as suggested in many sequence stratigraphic models

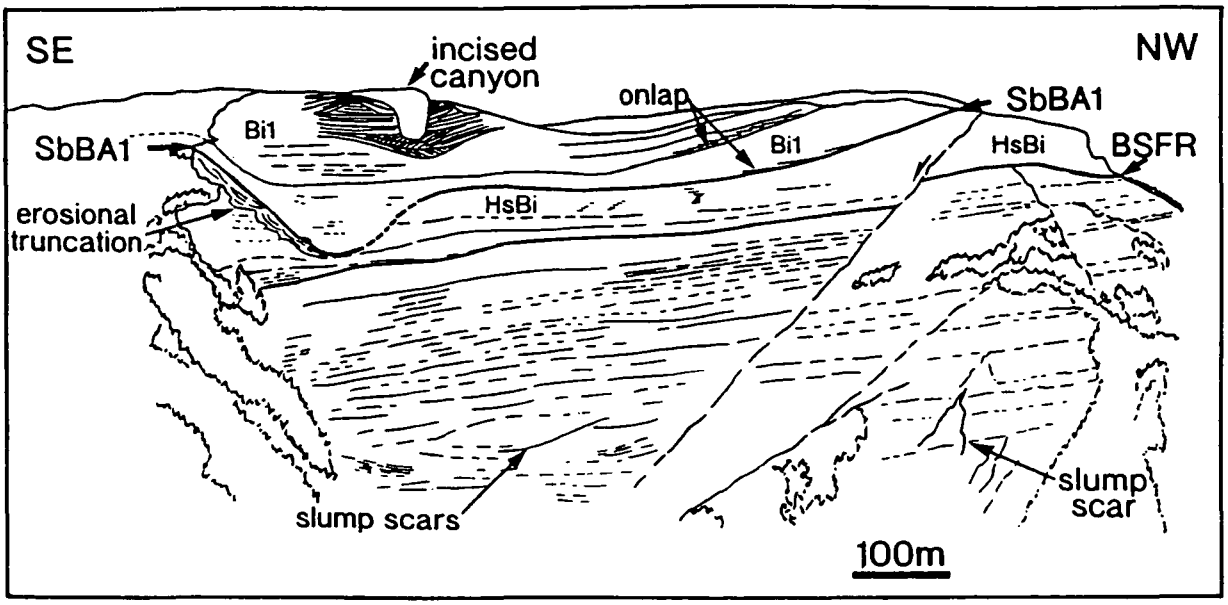

Figure 5.39. The sequence stratigraphic interpretation of the Tête Chevalière of Hunt & Tucker (1992). The BSFR (basal surface of forced regression) and SbBA1 are coincident with the sequence boundaries SbH7 and SbB1 of Jacquin *et al.* (1991) (eg. Fig. 5.20). The BSFR has a parallel-parallel stratal pattern and is associated with a major facies jump. This contrasts markedly to the sequence boundary (SbB1) which is associated with strong erosional truncation. This sequence boundary is, however, draped by shales with interbedded nodular limestones which suggests a marked reduction of carbonate sedimentation rates at, during or from the time of erosional truncation (see also Fig. 5.40).

(eg. Figs 2.1 & 2.5). Thus, geometry alone cannot be used to identify a sequence boundary on the slope. Identification of erosional surfaces upon the slope as sequence boundaries must include good correlation to the shelf or evidence of textural and compositional changes of slope sedimentation (eg. Everts, 1991). Otherwise their identification as sequence boundaries will be questionable.

Such arguments suggest that the placing of sequence boundaries upon the slopes elsewhere upon the Urgonian platform (eg. as discussed in 5.3.2) needs to be re-evaluated, in particular at the Tête Chevalière and Tête Praorzel (Figs 5.20, 5.39, 5.40 & 5.23 respectively). At the Tête Chevalière two sequence boundaries are identified by Jacquin *et al.* (1991) (SbH7 and SbB1, Fig. 5.20). These boundaries are reinterpreted as the BSFR and SbBA1 in the sequence stratigraphic scheme of Hunt & Tucker (1992)

(Fig. 5.39) (i.e. compare Figs 5.20 & 5.39). The lower boundary is associated with a marked facies shift and has a parallel-parallel stratal pattern (Figs 5.20, 5.39 & 5.40). This contrasts markedly to the overlying boundary which is characterized by strong erosional truncation (SbBA1, Fig. 5.39) and is overlain and draped by shales with interbedded nodular limestones (eg. Fig. 5.40). This suggests that the erosional truncation developed prior to or during a reduction of carbonate sedimentation rates in perhaps an analogous situation to the channels in the foreslope to Bi5 (eg. *et3*, Figs 5.26 & 5.37). The package of shales developed above the major erosional surface at Tête Chevalière contains many internal erosion surfaces (Fig. 5.40), and these, in a similar way to the main erosion surface (SbBA1, Figs 5.39 & 5.40), are interpreted as collapse scars. The irregular concave-up profile of the erosion surfaces at the Tête Chevalière which cut up and down section both to the north and south (Fig. 5.39) suggests that the section is orientated perpendicular to the main dip of the slope at the time the scars developed. This interpretation differs significantly from others (eg. Arnaud & Arnaud-Vanneau, 1989; Jacquin *et al.*, 1991) who interpret the Tête Chevalière to be a dip section, but agrees with the earlier interpretation of Arnaud (1981) who suggested it was a strike-section at this time. An interpretation equal to that of Jacquin *et al.* (1991, Fig. 5.20) and Hunt & Tucker (1992, Fig. 5.39) is that their erosional sequence boundary (SbB1, Fig. 5.20 & SbBA1, Fig. 5.39 respectively) formed thorough slope collapse during a relative sea-level rise which drowned the 'source' for the carbonates so that the scar(s) were partially filled by shales (Fig. 5.40) (i.e. analogous to *et3*, Figs 5.26, 5.27 & 5.37). Subsequently, shallow-water sedimentation resumed and sediment was again shed to the slope and became channellised into the partially-filled topographic depression above the collapse scars. The lower sequence boundary at the Tête Praorzel (SbB1, Fig. 5.23) can also be interpreted to have developed in a similar way. Contrastingly, the upper sequence boundary at the Tête Praorzel is characterized by the onlap of mudstones onto a sand dominated package. This boundary can be equally reinterpreted as a

Figure 5.40. Paired photopanorama and interpreted line drawing of the Tête Chevalière on the east of the Glandasse plateau. The cliffs here represent the HsBi of Arnaud (1981) and the HsBi-Bi1 of Hunt & Tucker (1992) (see Fig. 5.39). The lower limestone cliff has an abrupt base with a parallel-parallel stratal pattern. In direct contrast, the upper surface of this package of limestones is marked by strong erosional truncation and is draped by periplatform limestones and shales (see also Fig. 5.39). This surface is interpreted to be a collapse scar and is the SbB1 of Jacquin *et al.* (1991) and SbBA1 of Hunt & Tucker (1992) (Figs 5.20 & 5.39). The periplatform shales and limestones (shaded opposite) which overlie this erosive surface contain several intraformational truncation surfaces, also interpreted as collapse scars. One of these (arrowed), can be viewed in both dip and strike sections in the changing orientation of the face and clearly demonstrates that the dip of the slope was to the west. The periplatform shales and limestones are in-turn erosionally overlain by limestones. In the base of these a prominent flame structure is developed which changes upwards from a vertical to a sub-horizontal structure, associated with recumbent folding. This fold is cut by a discrete low angle surface, interpreted to be a slide plane. These structures are interpreted to have been developed from dewatering of the shales as they were loaded by the overlying deposits. This loading is thought to have increased fluid pressures and thus lowered the shear strength at the base of the overlying limestone package which slid down-slope on the basal 'slide plane'. The upper part of the cliff is dominated by the spectacular box canyon. This canyon has sub-vertical walls and cuts erosionally through the slope limestones (eg. see also Fig. 5.39). The canyon must have been extremely rapidly filled for the steep slopes to have been supported. The upper part of the canyon is aggradational and is associated with its own overbank levee deposits. Sedimentologically these are very similar to the preceding slope facies.

drowning unconformity developed after a rapid relative sea-level rise. Such an interpretation is suggested by the change from bioclastic sands to muds at the onlap surface which would be expected if the 'source' shelf area from which the sands were derived became drowned.

To conclude this brief discussion, the interpretation of the sequence boundaries by Jacquin *et al.* (1991) and Hunt & Tucker (1992) at the Tête Chevalière and Tête Praorzel is questionable. Onlap of stratal surfaces could have developed for a number of alternative reasons such as channellisation into a collapse scar on the slope (SbBA1, Fig. 5.39; SbB1, Fig. 5.23) or because of the drowning of carbonate sedimentation (SbB2, Fig. 5.23). Clearly without the control of a well exposed shelf section it is at present impossible to unequivocally differentiate between such interpretations and all possibilities should therefore be equally explored.

5.4. Basin-Floor.

5.4.1. Introduction.

In the Exxon sequence stratigraphic model basin-floor sedimentation is dominated by the development of the basin-floor fan and/or megabreccia(s) (eg. Fig. 3.5, p.41). These are interpreted to be developed during times of falling relative sea-level when sediments are forced to bypass both the shelf and slope, or by the increased loading of the slope as storm-wavebase was lowered (Vail, 1987; Sarg, 1988; Hunt & Tucker, 1992, see Section 3.7.2.A). In these models the external form of both basin-floor fans and megabreccia(s) is a convex-up mound (Figs 2.1, p. 6 & 3.5, p.41). Mounded stratal patterns are also internally developed within the basin-floor fan (Mitchum, 1985; Vail, 1987) (eg. Fig. 3.5, p. 41), whereas slope collapse basin-floor breccias are thought to develop an internally chaotic stratal pattern. Sedimentation at other times (TST-HST) is

considered to be characterized by a parallel-parallel stratal pattern and is normally pelagic in origin and, as such condensed (Figs 2.1 & 3.5).

5.4.2. The basin-floor to the Urgonian platform.

5.4.2. A. Introduction.

The basin-floor of the Urgonian platform crops out to the south of the Vercors Massif, the east of the Ardèche and north of the Haute Provence (eg. 'domaine vocontien' Fig. 4.4, p.110). Generally, exposure within these areas is poor both vertically and laterally (compared to the Urgonian platform) so that a good understanding of the geometry of basin-floor deposits is difficult to ascertain. The Barremian basin-floor is schematically illustrated in Figure 4.12 (p.123). This pattern of basin-floor sedimentation is notably rather different from the preceding and succeeding patterns. In particular, sands redeposited from the Urgonian platform on to the basin-floor are localised to the margins of the basin (Fig. 4.12). These sands were deposited as several discrete lobes at the toe-of-slope of the platform, and are fans on the scale of the Vocontian basin (Fig. 4.12). Previously, sands which were bypassed to the basin-floor formed elongate bodies along the centre of the basin within the long-lived submarine canyon system (Fig. 4.12). This suggests that the Urgonian created a new and independent bypass system to that which was previously established and resulted in the change from a point source (Crest palaeo-canyon) to localised line sources off the Urgonian shelf on the basin-floor. During Urgonian times the major axis of the basin-floor (Crest palaeo-canyon) was dominated by the deposition of collapse breccias derived from the slopes on the northern and western flanks of this canyon (eg. Fig. 4.12, see later this section).

5.4.2. B. Facies and timing of basin-floor allochthonous sedimentation.

There are basically three distinct types of basin-floor sedimentation to the

Urgonian platform; pelagic limestones, slumps/debrites and sands. The pelagic limestones are illustrated in Figure 5.41, and these are the basic background type of sedimentation on the Urgonian basin-floor. As discussed in Chapter 4, the Urgonian times are characterized by a marked decrease of sedimentation rates on the basin-floor (Fig. 4.15, p.127), accompanied by a shift to limestone dominated pelagic sedimentation (eg. Fig. 4.11, p.121).

Figure 5.41. Medium-thick bedded pelagic limestones and interbedded shales from the lower Barremian, La Chaudière river section. Hammer approximately 350mm long for scale.

Probably the best (in terms of vertical and horizontal continuity) exposure of basin-floor sands in the northern part of the Vocontian Basin is the Montagne de la Varaime in the Borne area (Fig. 5.42) (see Fig. 4.17, p.132, for location). This mountain face is essentially a strike-section through a mid-Barremian basin-floor sand complex. The exact age of this basin-floor sand body is, however, rather problematic. The original interpretation of Arnaud as uppermost lower Barremian age (Bi5-Bi6 of Arnaud, 1981)

see enclosures for paired photopanorama

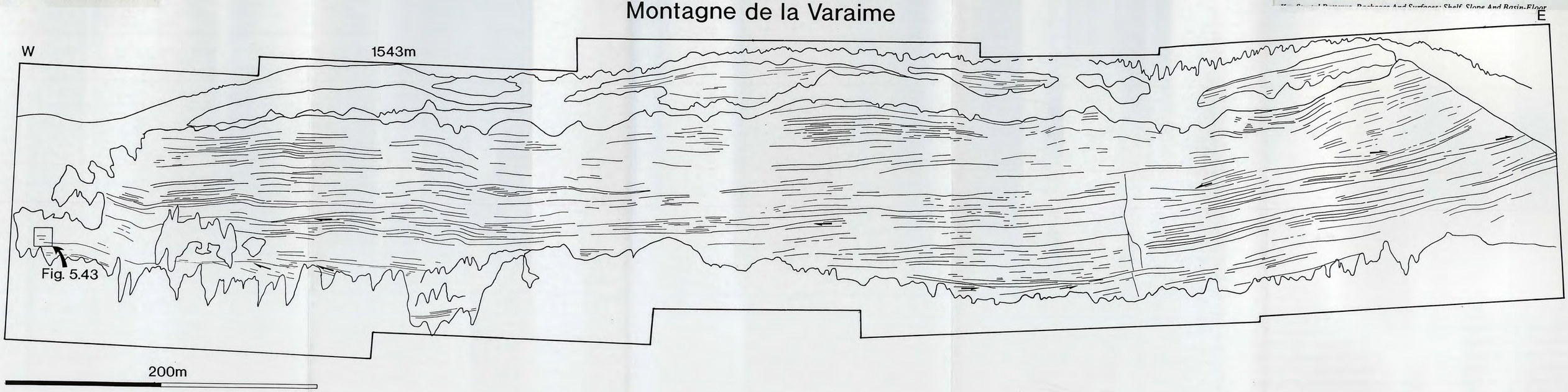

Figure 5.42. Paired photopanorama® and line drawing of the Montagne de la Varaime. This section is essentially a strike-section through a basin-floor sand complex. These sands are characterized by broad, shallow channels and parallel bedded limestones. Note there are no primary mounded stratal patterns. The cliff is composed of two different types of stratal package; thick-bedded to massive bioclastic sands and more thinly bedded packages composed of a high proportion of fine grained siliciclastics and carbonate muds (see also Figs 5.43 & 5.44). This Figure is located upon Figure 4.17 (p.132).

® see enclosure for photopanorama

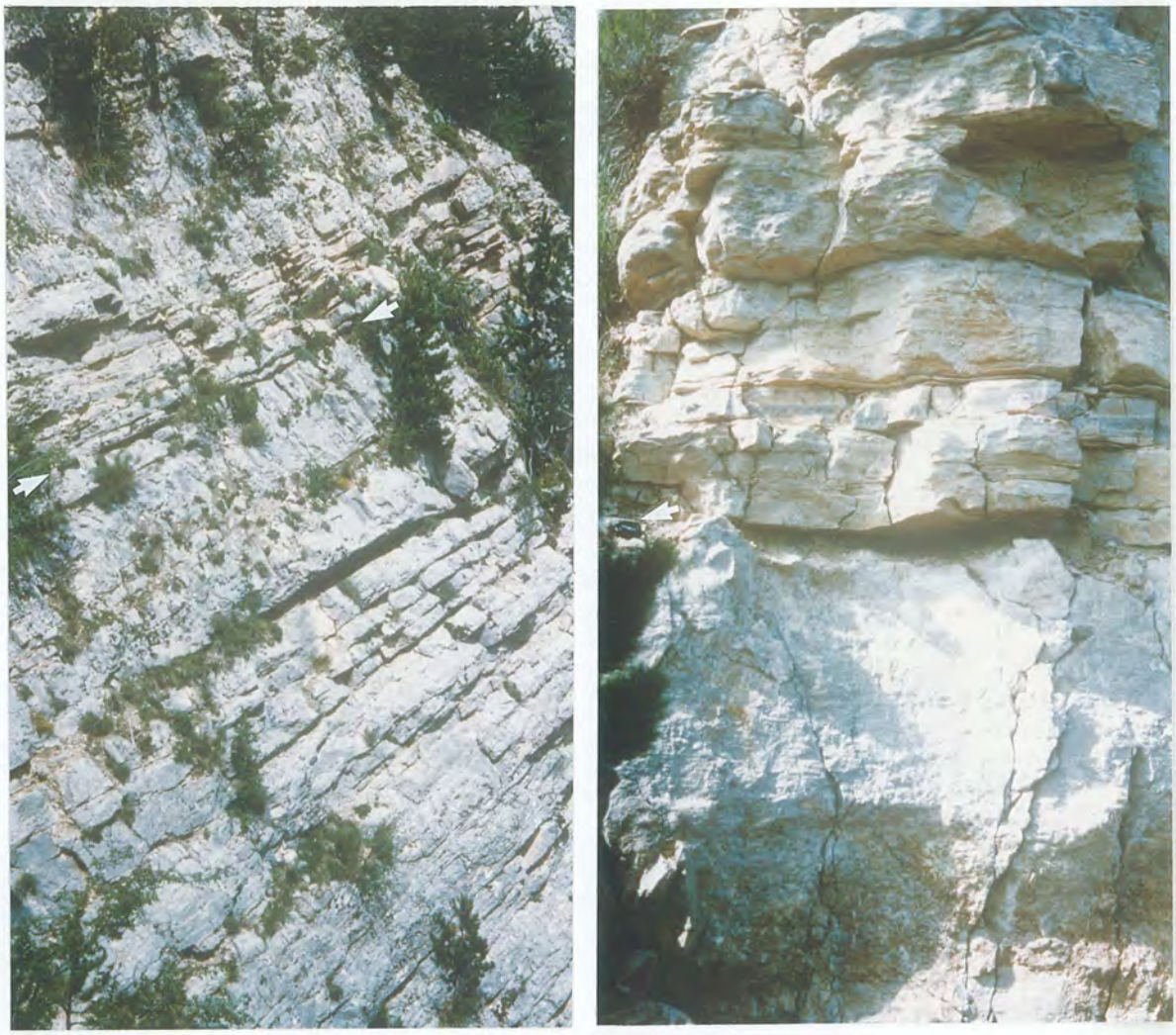

A B

Figure 5.43. Detail of the different stratal packages distinguished at the Montagne de la Varaime in the Borne area, as located upon Figure 5.42. Thicker bedded packages are composed almost entirely of shallow-water shelf type bioclastic sands (Fig. 5.44B). The thinner beds, which characteristically weather to a more orange colour, are composed of crinoidal bioclastic sands interbedded with 5-10mm thick graded beds of silt grade quartz and crinoid ossicles passing up in to carbonate muds (Fig. 5.44A). The contact between the prominent massive beds, overlain by thinner beds in 'A' (arrowed) is shown in B. Lens cap approximately 50mm diameter in B (arrowed) for scale. The different sands from this exposure (B) are illustrated in Figure 5.44.

has been thrown into doubt by the recent recovery of an upper Barremian ammonite just below the exposure, suggesting a younger age (?Bs2-3, H. Arnaud, 1990, pers. comm.). Because of the uncertainty concerning the age of these sands this exposure is not

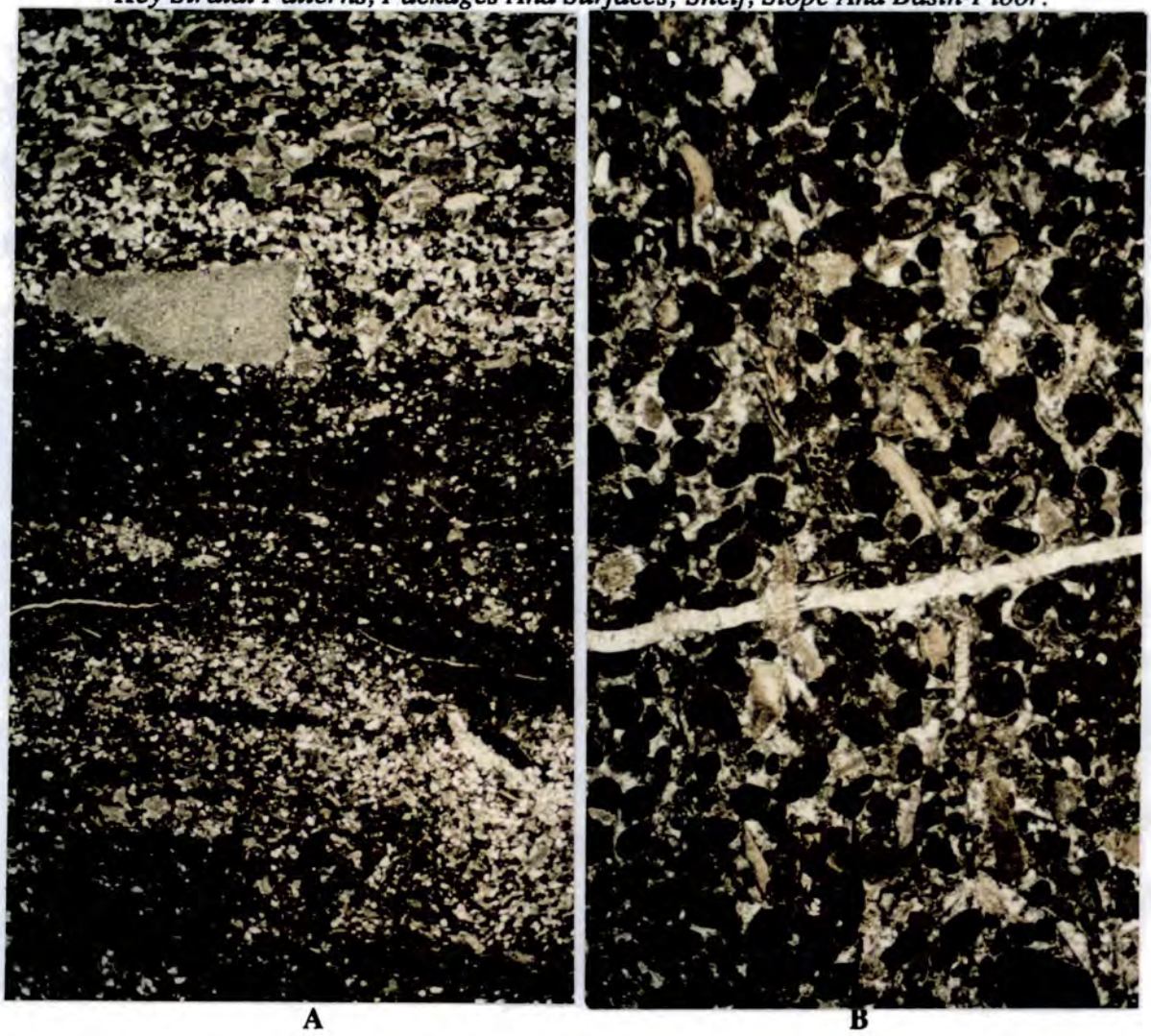

Figure 5.44. The two compositionally different types of basin-floor bioclastic sand distinguished at the Montagne de la Varaime. A: sharp-based, graded, mixed crinoidal bioclastic grains and silt grade quartz, interbedded with pelagic limestones; B: diverse assemblage of shallow-water grains from massive beds (Both views in PPL). These two very different types of sand are interpreted to be derived from the sub-wavebase slope and shallow-water shelf respectively. These cycles could be explained in terms of a transgressed and productive shelf (B) (eg. 'highstand shedding') and an exposed shelf when only a narrow strip of high-energy facies was developed on the slope so that basin-floor sedimentation was dominated by slope derived facies, *or*, alternatively, if there were no relative sea-level falls represented within this section then the slope sands (A) could represent times when the shelf-margin was drowned and, conversely, shallow-water derived sands (B) times when normal sedimentation resumed at the shelf margin (eg. a variable of 'highstand shedding'). Field of view for both photomicrographs 18mm, PPL.

interpreted in a sequence stratigraphic context, but its stratal patterns and facies are described.

The dominant stratal pattern of the Varaime section is parallel-parallel, but cut by gently concave-up surfaces which erosionally truncate older strata (Fig. 5.42). These erosional surfaces are generally broad (0.15->0.5km), but shallow (<40m) in comparison to their width (Fig. 5.42). The concave-up erosional depressions are filled by onlapping strata, oblique bedding or massive sands (Fig. 5.42). Notably, there is a distinct absence of primary mounded bedforms, although mounds can be generated as topographic highs between two erosional depressions. The diversity of stratal relationships to these concave-up erosional depressions is interpreted to reflect different types of submarine channel fills. Two different types of stratal package can be differentiated in this exposure, thick-bedded to massive bioclastic sands, which tend to overlie the most obvious erosional surfaces and thinner-bedded crinoidal and mixed crinoidal-quartz rich sands (Figs 5.42, 5.43 & 5.44). The thick to massively bedded strata weather to a light-grey colour and are composed of very well sorted packstones-grainstones, containing a wide variety of shallow-water grains (eg. miliolids, Orbitolinids, ooids, coated grains etc.) with rare <5% lithoclasts (Fig. 5.44B). By way of contrast, the thin-bedded strata weather orange (Fig. 5.43) and are composed of prominent beds of crinoidal packstones with unrounded bryozoa and lithoclasts (<<5%). These are interdedded with dark-orange, recessively weathering, very thin beds, composed of sharp-based 5-10mm thick fining-up beds from silt grade quartz-crinoidal sands to carbonate muds (Fig. 5.44A). The crinoidal and mixed crinoidal-siliciclastic rich graded sands, characteristic of the thin-bedded strata are interpreted to be derived entirely from the sub-wavebase slope.

It is rather difficult to interpret this exposure not knowing either its chronostratigraphic position or the time interval which the exposure represents. Accordingly, the cycles between shallow-water derived and slope derived sedimentation can be interpreted in three very different ways. Firstly, using a classical sequence stratigraphic approach the sands could be interpreted to represent several sequence boundaries, with the shallow-water derived sands representing lowstand of sea-level and

the slope sands the transgressive-highstand phase of sedimentation. The second possibility, based upon patterns of sedimentation observed from bypass slopes in the Tongue of the Ocean, Bahamas (eg. Droxler & Schlager, 1985) would interpret the shallow-water shelf derived sands to represent times when the shelf was flooded and exporting excess sediment ('highstand shedding'). The slope sands would thus be interpreted to represent lowstand of relative sea-level when the area of shallow-water sedimentation was reduced to a narrow strip upon the slope (eg. see Sections 3.7.2.C and 3.7.2.A respectively). The third alternative interpretation (which is tentatively advocated here) is that the cycles developed over a shorter time span (eg. are 4^{th} rather than 3^{rd} order cycles) and represent the drowning (thin-bedded crinoidal sands) and subsequent re-establishment of shallow-water sedimentation at the shelf-margin (thick-bedded bioclastic sands). These cycles are thought to be developed on a similar scale to the younger progradational-aggradational-drowning cycles observed in the Cirque d'Archiane (Figs 5.6, 5.7 & 7.15). This is a type of 'highstand shedding' more similar to the basin-floor cycles recognized by Boardmann *et al.* (1986) in the Bahamas.

The third distinctive type of basin-floor deposit are slumps and/or debrites. Probably the best examples are exposed in the vicinity of La Chaudière (Figs 5.45, 5.46 & 5.47). This area of the basin-floor (the continuation of the Crest palaeo-canyon, see Fig. 4.12) received reworked sub-wavebase slope facies from the north during the development of the Urgonian platform (Figs 5.45 & 5.47). The basin-floor debrites and slumps developed from the collapse of this slope are separated by pelagic facies (eg. Fig. 5.41) and these together record the progressive, catastrophic collapse of the slope (Ferry & Flandrin, 1979, Arnaud, 1981; Ferry & Rubino, 1989). The lowermost allochthonous basin-floor debris of la Chaudière is illustrated in Figures 5.46 and 6.6. This deposit is a bimodal matrix-supported debrite composed of dark-grey elongate, angular clasts of shale (<150mm long), small (10-15mm) asymmetric, sheared clasts of periplatform limestones with angular glauconite fragments (eg. Figs 5.46 & 6.6). The shearing of the

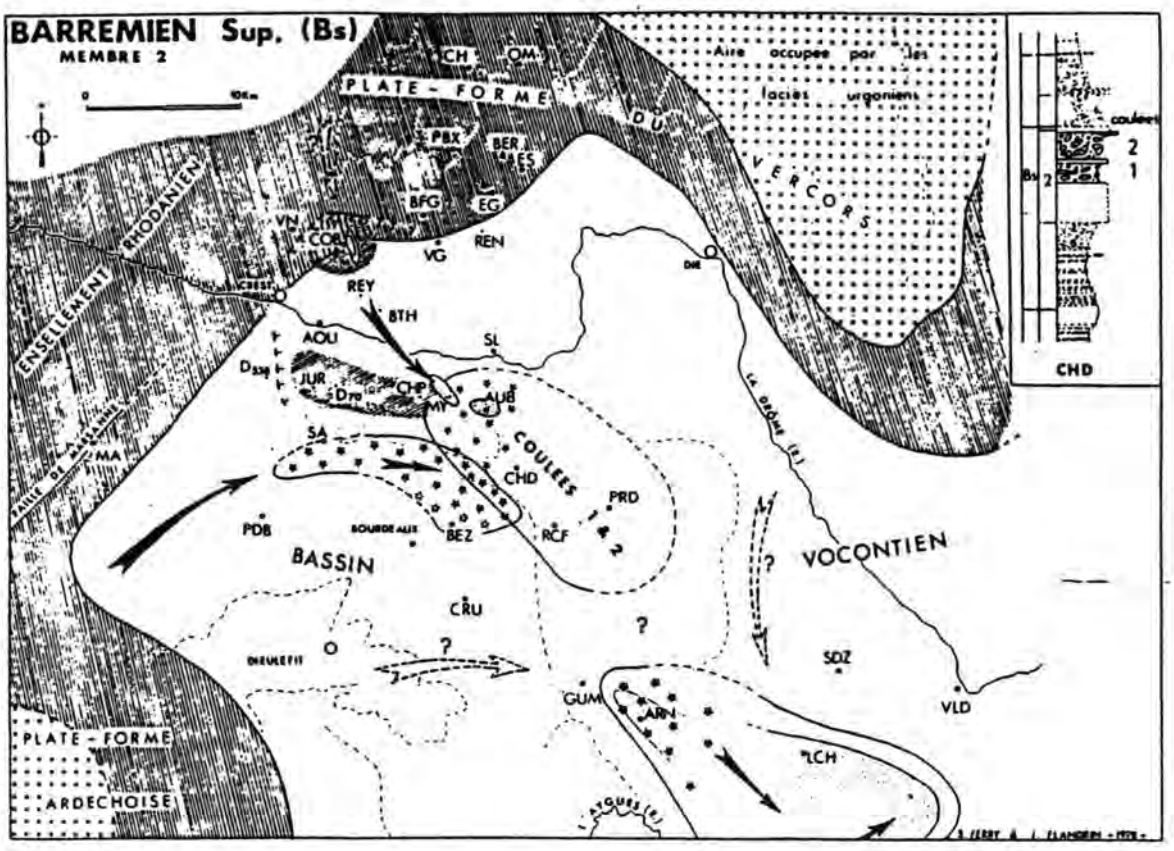
BARREMIEN Sup. (Bs)
MEMBRE 2
PLATE - FORME DU VERCORS
Aire occupée par les faciès urgoniens
ENSELLEMENT RHODANIEN
VOCONTIEN
BASSIN
PLATE - FORME ARDECHOISE
COULEES
CHD
CH
OM
PBX
BER
ES
EG
BFG
VG
REN
REY
BTH
AOU
SL
JUR
CHP
ALB
MY
SA
CHD
PRD
RCF
PDB
BEZ
CRU
SDZ
VLD
GUM
ARN
LCH
DIE
CREST
VN
COR

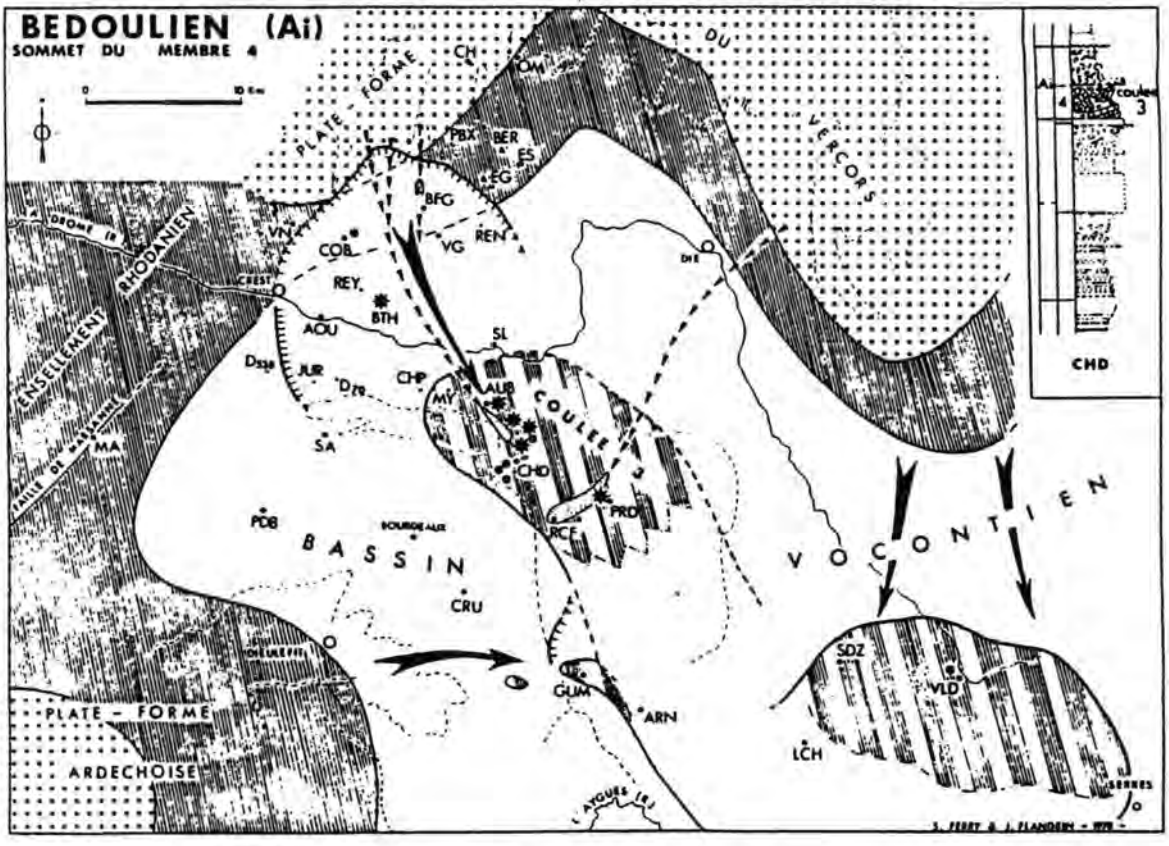
BEDOULIEN (Ai)
SOMMET DU MEMBRE 4
PLATE - FORME DU VERCORS
ENSELLEMENT RHODANIEN
VOCONTIEN
BASSIN
PLATE - FORME ARDECHOISE
COULEE
CHD
CH
OM
PBX
BER
ES
EG
BFG
VG
REN
REY
BTH
AOU
SL
JUR
CHP
ALB
MY
SA
CHD
PRD
RCF
PDB
CRU
SDZ
VLD
GUM
ARN
LCH
DIE
CREST
VN
COR

Figure 5.45. (Facing page) Palaeogeographic maps for the southwestern flanks and basin-floor of the Urgonian platform during the upper Barremian (top; =GBsc, Fig. 6.7) and lower Aptian (Ai2, Arnaud, 1981; bottom). On each of these maps the position of the slope scar () is shown and also the allochthonous debris derived from slope collapse. The position of these basin-floor allochthonous sediments are shown within the La Chaudière section (inset top right-approximately 200m thick and see Fig. 6.7). See text for further discussion.

Key: Arrows ( ) schematically show the source, transport path and location of basin-floor allochthonous debris. *Facies*; (): olistoliths; (): slumps/debrites; () sands: ( ): pelagic facies; (): periplatform limestones; (): Urgonian platform.

Locations: Aou; Aouste; Arn: Arnayon; Aub. Les Auberts; Ber; Montagne des Berches; Bez; Bezudun; Bfg; Beaufort-sur-Gervanne; Bth, Les Berthalais; Ch; Le Chaffal; Chp; Les Chapeaux; Cob; Cobonne; Cru; Crupiers; D70; D 70 road section; D538: D538 road section; Es: l'Escoulin; Gum; Gumaine; Jur, ferme Jurie; Lch; la Charce; Ma: Marsanne; Mr; Château de Montrond; My; ferme des Moyons; Om: Omblèze; Pbx: Plan-de-Baix; Pdb: Pont-de-Barret; Prd: Pradelle; Rcf: Rochefourchat; Ren, ferme Renage; Rey: ferme des Reyniers; Sa; Saou; Sdz; Saint-Dizier-en-Diois; Sl: Saillans; Vld; Valdrôme; Vn; Vaunaveys; Vg; Vaugelas.

limestone clasts suggests that these were soft during transport and that differential shear developed within the debris flow. This lowermost allochthonous unit is interpreted to have been derived from slope collapse during times of falling relative sea-level (see Section 6.2.2.B2).

The third allochthonous basin-floor slope collapse deposit at La Chaudière (CL2 of Ferry & Rubino, 1989, Fig. 5.45 or GBsc, Fig. 6.7) is composed of well cemented, sub-spherical clasts of periplatform limestone up to 3m in diameter (Fig. 5.47). This is a clast supported unit (Fig. 5.47), and almost all of the limestones clasts are completely enclosed by randomly orientated striations. This suggests that clasts were in contact with, but rotating independently to each other as the flow moved downslope to the basin-floor. The exact timing of this unit and the CL1 of Ferry & Flandrin (1979) with respect to relative sea-level changes is not clear. Ferry & Rubino (1989) place both CL1 and CL2 at the base of the *Astieri* zone, suggesting that collapse of the slope occurred at a flooding surface (Fig. 6.7). However, in the stratigraphic scheme of Arnaud-Vanneau

Figure 5.46. Photograph of the GHS/Bi basin-floor collapse deposit from the La Chaudière (located on Fig. 5.45). This unit is a bimodal, matrix-supported debrite, composed of elongate, angular dark-grey clasts of shale and asymmetric, sheared clasts of light-grey limestone.

Figure 5.47. The basin-floor CL2 collapse breccia of Ferry and Flandrin (1979) at La Chaudière (the GBsc of Fig. 6.7, Ferry & Rubino, 1989). This basin-floor allochthonous debris is composed of sub-spherical clasts of periplatform limestone up to 3m in diameter which are entirely enclosed in randomly orientated striations. This suggests that clasts were in contact, but rotating independently of each other during transport.

(1980) and Arnaud (1981) this position corresponds to the upper part of Bs2 / lower part of Bs3. This alternatively suggests that collapse occurred during the late BA2 HST/early BA3 LST (eg. see Figs 5.1A, 6.2 & 6.4).

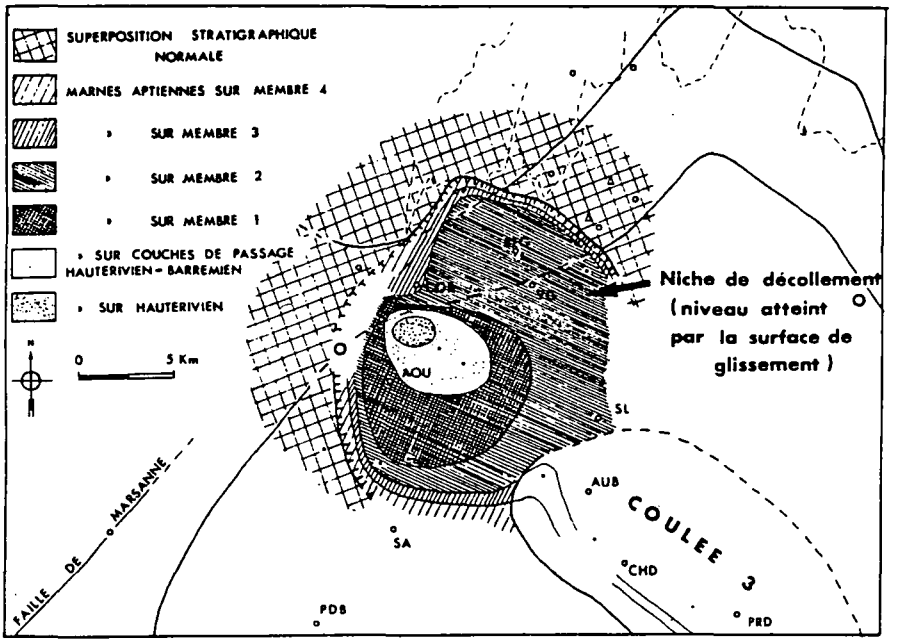

Figure 5.48. The mapped extent of the CL3 collapse scar on the slope and onto the basin-floor. A NNE-SSW cross-section through this area is illustrated on Figure 5.49. Place names as according to Figure 5.45. Key: Superposition stratigraphique normale: normal stratigraphic succession; Marnes Aptienes sur Membre 4: Aptian marls resting unconformably on member 4; Sur member 3, 2 & 1: and on to members 3, 2 and 1 respectively: sur couches de passage Hauterivian-Barremien: and on to transitional beds between the Hauterivian and Barremian; Sur Hauterivien: on to the Hauterivian (From Ferry & Flandrin, 1979).

Probably the best understood allochthonous basin-floor collapse deposits are the CL3 and CL4 units of Ferry & Flandrin (1979) and Ferry & Rubino (1989) (Figs 5.45, 5.48, 5.49, 5.50, 5.51, 5.52 & 6.7). These two basin-floor packages were deposited during times of overall relative sea-level rise (the AP2 TST, see Fig. 5.1A and Section 6.2.8.C). The lowermost of these debrites was deposited as a result of the collapse of the sub-wavebase slope across a 12km wide amphitheatre-shaped area (Fig. 5.48), along a listric shaped plane which cut down up to 500m in to the upper Hauterivian-Aptian slope

(Figs 5.48 & 5.49). This scar enlarged the area of the slope which had previously collapsed to supply CL1 and CL2 (eg. Fig. 5.45). On the basin-floor CL3 contains a complete spectrum of reworked slope facies from millimetre sized to massive blocks (olistoliths) of almost undeformed sub-wavebase slope limestone up to 10 000m^3 (eg. Fig. 5.50) (Ferry & Flandrin, 1979).

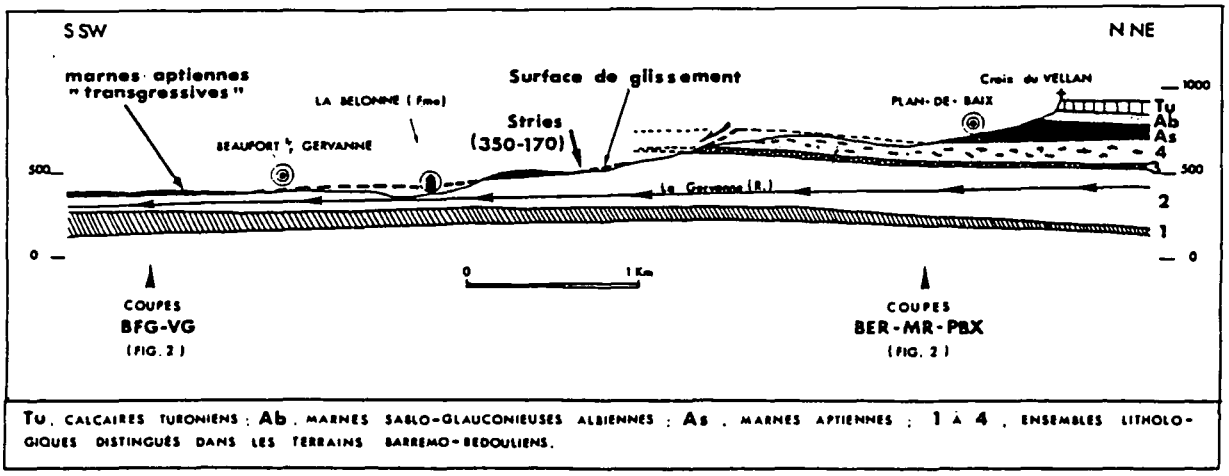

Figure 5.49. NNE-SSW dip orientated cross-section through the listric-shaped collapse scar illustrated in Figures 5.45 & 5.48 as according to Ferry & Flandrin (1979). Member Ai2 of Arnaud is the Member 4 of Ferry & Flandrin (compare to Fig. 6.45) (Section located on Fig. 4.17, p.132).

The CL3 basin-floor allochthonous debris is separated from CL4 by some mixed siliciclastic-carbonate turbidites, the 'red slabs' of Ferry & Rubino (1989) (Fig. 5.45-inset). The CL4 debrite of Ferry & Flandrin (1979) and Ferry & Rubino (1989) is, by way of contrast to CL3 composed of 5-7 discrete, separate (1-4m thick) debrites (Fig. 5.51). These are composed entirely of pelagic slope and basin-floor facies and are separated by sub-horizontal orange-brown coloured pelagic limestones (Fig. 5.51). The bases of these debrites are frequently associated with the incorporation of pelagic limestone beds in to their bases which can be complexly and intensely folded. The southward vergence of these fold structures suggests derivation of the debrites from the

Figure 5.50. Extremely large olistolith of sub-wavebase periplatform slope limestones on the basin-floor approximately 1km to the north of La Chaudière in the Ravin de la Courance, Coteau farmhouse (arrowed) for scale. This olistolith of slope limestone is internally almost undeformed but dips very steeply (up to 40°) to the basin-floor. In the background the grey area is an exposure of sub-horizontal basin-floor pelagic black shales.

north. Typically, the Cl4 debrites are inversely graded (Fig. 5.51), with a relatively clast-free base and an upper part which contains prominently weathering strung-out clasts of rounded white pelagic limestones. The series of slumps and debrites which compose CL4 are interpreted to have developed as the slope re-equilibrated to an more stable, ideal profile after the massive CL3 slope collapse. Possibly, many of the CL4 allochthonous deposits are of local origin and result from a substantial topography developed by the upper surface of CL3 around olistoliths such as that illustrated in Figure 5.50. The overall stratal pattern of CL3 is summarised in Figure 5.52. The pattern developed by the collapse of the slope, deposition of a basin-floor megabreccia and the subsequent onlap of the slope by Aptian shales is very similar to the stratal patterns developed by a type 1 sequence boundary (Ferry & Rubino, 1989) (eg. Fig. 5.52).

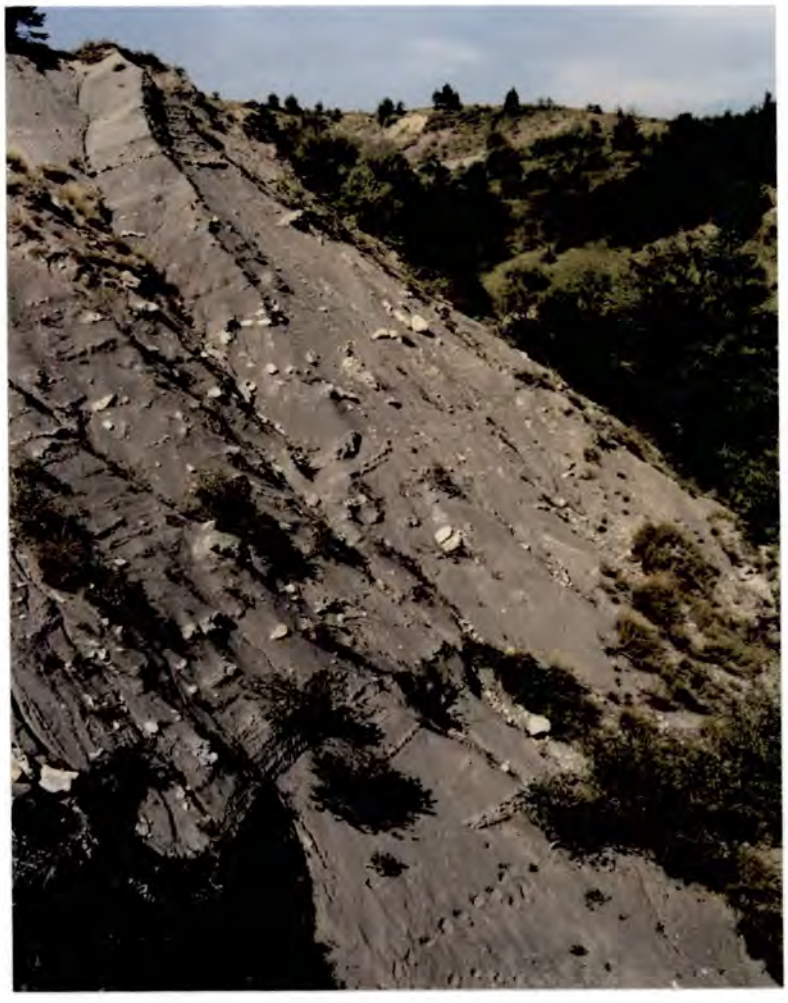

Figure 5.51. The CL4 unit of Ferry & Flandrin (1979) and Ferry & Rubino (1989) at La Chaudière. This unit is composed of 5-7 discrete inversely bedded debrites. These are separated by dark-grey pelagic shales and thin bedded limestones. The latter are frequently folded and incorporated into the base of the debris flows. The upper part of debris flows are typically characterized by white, rounded clasts of pelagic limestones which weather prominently in the exposure. These debrites, in direct contrast to CL3, are composed entirely of basin-floor pelagic facies and are interpreted to have been deposited as the slope re-equilibrated after the major CL3 slope collapse event. Possibly they originate from local highs such as around the massive olistolith of CL3 illustrated in Figure 5.50. Footprints at the base of the exposure approximately 0.5m apart for scale.

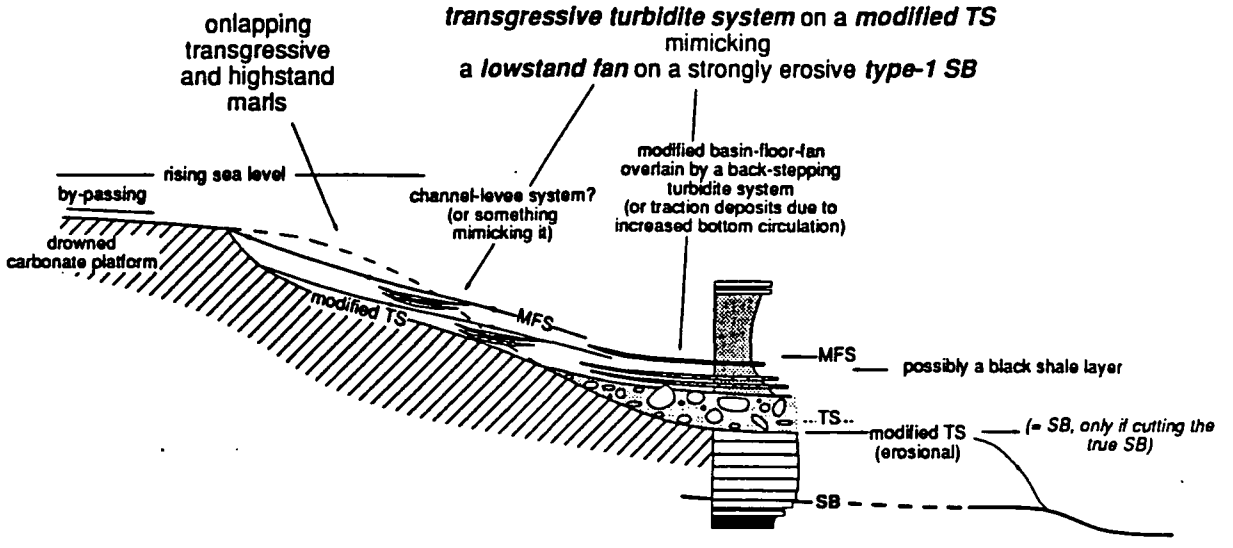

Figure 5.52. Schematic reconstruction of the stratal patterns developed by CL3 from the slope to basin-floor. This stratal pattern closely resembles the patterns suggested to be indicative of a type 1 sequence boundary (From Ferry & Rubino, 1989). The line of this section is approximately located on Figure 4.17 (p.132).

5.4.3. C. Conclusions and discussion.

Two genetically different and distinctive types of allochthonous debris are developed on the basin-floor to the Urgonian platform. Basin-floor sands develop discrete lobes at the toe-of-slope to the platform which are fans on the scale of the Vocontian basin. Sands can be redeposited on the basin-floor during times of falling and lowstand of relative sea-level (eg. HsBi-Bi1, see Fig. 5.38), but redeposition can also occur during times of rising and highstand of relative sea-level (Bi5-Bi6) (see Section 5.3.3.B, Fig. 5.38). Slumps and debrites are also associated with times of falling and lowstand of relative sea-level, although these may also be developed during the TST (eg. CL3-4). Stratal patterns developed by the bypass of sands through the slope to the basin-floor and/or by collapse of the slope and deposition of a basin-floor megabreccia can

closely resemble patterns supposedly diagnostic of lowstand of relative sea-level (eg, Fig. 5.52).

Thus, more ambiguous examples of basin-floor allochthonous debris should not be 'forcefully interpreted' and automatically assumed to be deposited during times of falling and lowstand of relative sea-level. Stratal patterns developed at times other than falling relative sea-level can also be similar to those normally associated with lowstand of relative sea-level (eg. erosional truncation, deposition of a basin-floor megabreccia and onlap of the slope). It seems entirely probable that slope collapse is an ongoing phenomenon throughout the development of a sequence, but is most readily distinguished when a sequence boundary is formed *or* when the platform becomes drowned as these times are marked by abrupt facies change which tend to preserve these features.

Chapter 6.
Sequence Stratigraphy Of The Urgonian Platform.

6.1. Introduction.

In this chapter the sequence stratigraphic evolution of the Urgonian platform is discussed, based upon a north-south profile through the platform. This sequence stratigraphy builds from the tectono-stratigraphic development of the passive margin, facies, stratigraphy, palaeogeographic evolution and facies of the platform discussed in Chapter 4, and the criteria used to identify key stratal surfaces and thus build a sequence stratigraphy introduced in Chapter 5. The sequence stratigraphic scheme presented in this Chapter builds from the basic sequence stratigraphy established by Arnaud & Arnaud-Vanneau (1989) and follows a similar line of section. Sequences are discussed in their chronological order of development and particular points of each sequence are highlighted. Alternative interpretations, comparisons and contrasts to other sequence stratigraphic schemes are also discussed.

Stratal patterns observed within sequences of the Urgonian platform frequently are seen to be similar to those depicted for siliciclastic shelves, particularly upon the slope (eg. Section 5.3). This reflects the general dearth of organic buildups, dominance of relatively uncemented rounded bioclastic grains at the shelf-margin and the interpreted leeward orientation of the best slope exposures which in other well known geological examples develop stratal patterns very similar to their siliciclastic counterparts (eg. Fig. 3.11, p.56). Careful examination of stratal patterns up on the Urgonian platform does, however, reveal that their development is normally very different with respect to relative sea-level changes from models for siliciclastic shelves as has been discussed in Chapter 3. The final section of the chapter develops a new relative sea-level chart for the platform, compares aggradation rates of the Urgonian platform to other ancient prograding carbonate platforms and the sea-level chart of the Urgonian platform to the 'eustatic' chart of Haq *et al.* (1987). The

remaining part of this introduction is a brief review of the stratigraphy and setting of the Urgonian platform as presented in the preceding Chapters. The general conclusions from the application of the sequence stratigraphic concepts and models to the Urgonian platform are given in Chapter 7.

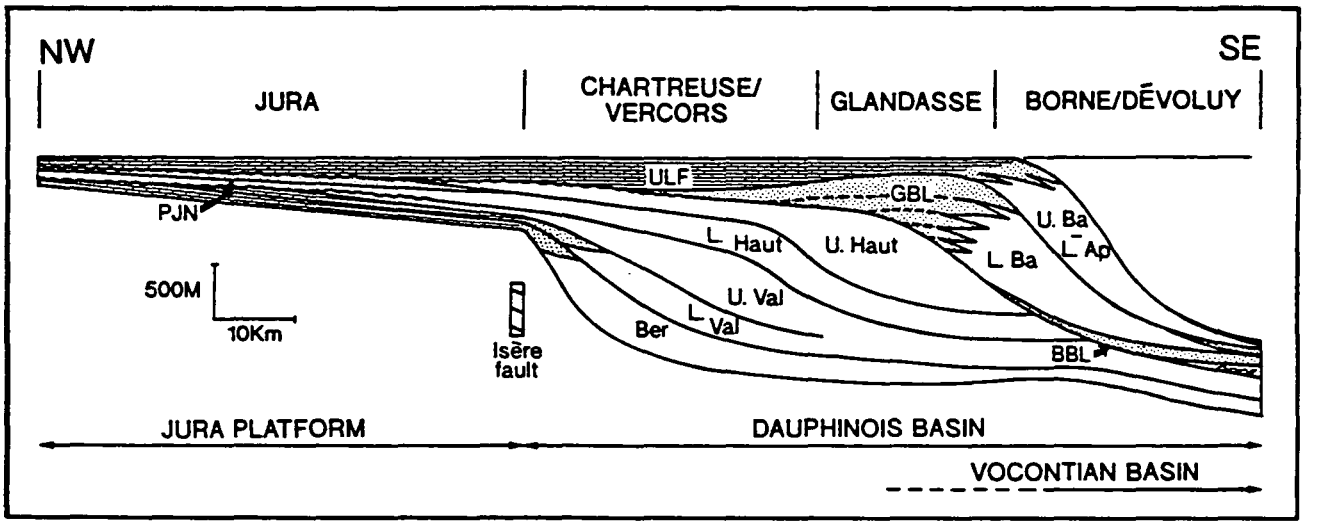

Figure 6.1. Schematic north-south cross-section from the Jura platform, across the Isère fault and into the Dauphinois basin. Prior to the development of the Urgonian platform *sensu lato* shallow-water bioclastic sedimentation was restricted to the Jura platform. A late Hauterivian / lowermost Barremian relative sea-level fall is interpreted to have shifted shallow-water sedimentation some 60-70km to the southeast, to the flanks to the Vocontian Basin. The lower Barremian is characterized by the Borne and Glandasse Bioclastic Limestone Formations, best developed on the basin-floor and slope respectively. The Glandasse Formation is the 'general' lowstand wedge of Arnaud & Arnaud (1990) from whom this figure is modified. See text for further discussion.

Throughout this chapter the systematics used for times of falling and lowstand of relative sea-level are those of Haq *et al.* (1987; 1988) (eg. Fig. 2.1, p.6). These systematics are used in preference to those developed in Chapter 2 (Section 2.3.2.A, Fig. 2.6B, p.26) as they are currently in common usage compared to the new systematics (currently in press).

6.1.1. General Urgonian stratigraphy.

The Urgonian limestones were deposited on a shelf-type platform which developed between the uppermost Hauterivian and mid-Aptian upon the early

Urgonian Sequence Stratigraphy.

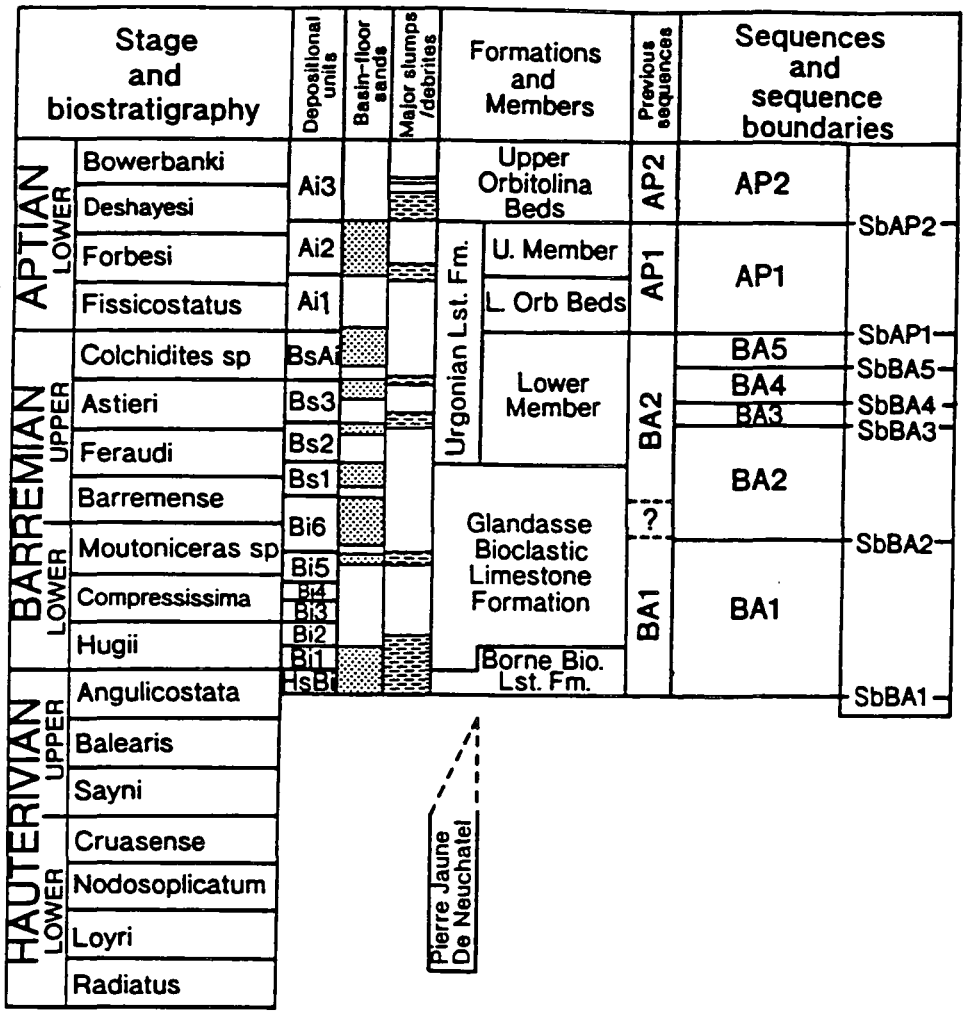

Figure 6.2. The chronostratigraphic correlation of the Urgonian platform *sensu lato*, and its component Formations, Members, depositional units and sequence boundaries. Note the timing of basin-floor sedimentation in relation to the interpreted sequence boundaries. Depositional units are named according to Arnaud-Vanneau (1980) and Arnaud (1981) and the previous sequences correspond to those of Arnaud-Vanneau & Arnaud (1990), time scale according to Haq *et al.* (1987). Modified after Hunt & Tucker (1992).

Jurassic-mid Cretaceous continental margin to Ligurian Tethys. The platform is itself divisible into two distinct parts (Figs 6.1 & 6.2): (1) lower Barremian Borne (<120m thick) and lower-upper Barremian Glandasse Bioclastic Limestone Formations, and their lateral equivalents (<1800m thick, Fig. 4.40, p.184) and (2) the upper Barremian-mid Aptian Urgonian Limestone Formation, consisting of shelf-lagoon rudistid facies (typically 300m thick) and correlative shelf-margin, slope and basinal facies (<1500m thick). The lower Barremian Borne and Glandasse Bioclastic Limestone Formations are geographically restricted to the southern Vercors, upon the

flanks of the Vocontian Basin (Figs 6.1 & 6.3). The Glandasse Formation is strongly progradational and dominated by shelf-margin and slope bioclastic sands and muds. This contrasts markedly to the essentially aggradational Urgonian Limestone Formation developed from the Jura platform across the Dauphinois Basin to the flanks of the Vocontian Basin (Figs 6.1 & 6.3), and typified by shelf-type rudist facies.

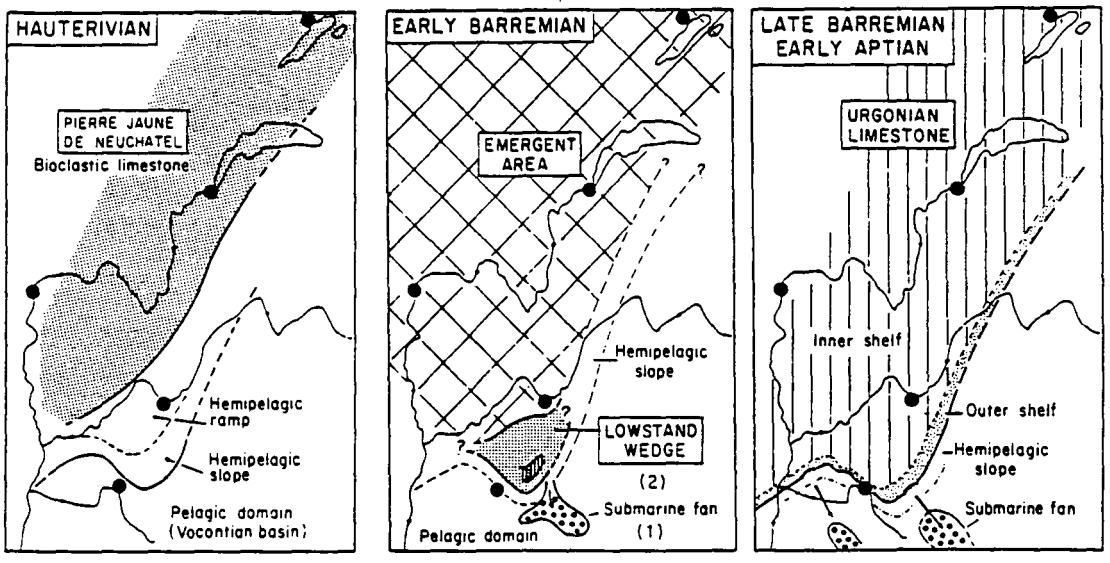

Figure 6.3. The progressive mid-Cretaceous development of palaeogeography based upon the sequence stratigraphic interpretations of Arnaud & Arnaud-Vanneau (1989). Hauterivian (middle-late): the 'Pierre Jaune de Neuchâtel' bioclastic limestones represent drowned platform sedimentation, sub-wavebase sediments were well developed in the northern Sub-Alpine Chains. Early Barremian: the Jura platform became subaerially exposed during a major fall of relative sea-level; (1) submarine fan of lowermost early Barremian age, located in the pelagic domain of the Vocontian Basin (Borne Bioclastic Limestone Formation of Arnaud, 1981); (2) 'general' lowstand wedge (Glandasse bioclastic Limestone Formation) above the preceding Hauterivian ramp and slope (the dotted area corresponds to the first occurrence of the lowstand wedge). Late Barremian-early Aptian deposition of the Urgonian Limestone Formation, subsequent to the transgression of the Urgonian shelf *sensu stricto*. (From Arnaud-Vanneau & Arnaud, 1990).

During the mid to late 1980's considerable debate surrounded the palaeontological and hence stratigraphic and palaeogeographic development of the

Urgonian platform (eg. Section 4.4.3). The palaeontological controversy centred upon the contrasting and close juxtaposition of mid-upper Hauterivian and upper Barremian biozones directly below and at the base of the Urgonian platform respectively. The sequence stratigraphic model presented by Arnaud & Arnaud-Vanneau (1989) (eg. Fig. 5.2, p.194) suggested that during the uppermost Hauterivian and lower Barremian the Jura platform and much of the neighbouring Dauphinois Basin became subaerially exposed as the result of a major relative sea-level fall, and remained so until transgressed in the mid-Barremian (eg. compare Figs 5.2 & 6.3). This model both elegantly and simply explained the close juxtaposition of very different biozones at and directly below the base of the Urgonian platform *sensu stricto* in the northern Vercors, Chartreuse, Jura and also the unique microfauna (Arnaud-Vanneau, 1980) developed within the Glandasse Bioclastic Limestone Formation of Arnaud (1981) (the 'southern Vercors shoal' of Arnaud-Vanneau & Arnaud, 1976).

6.1.2. Hauterivian platform architecture and sedimentation.

The nature of the preserved upper Hauterivian facies below the Urgonian platform and the geometry of the basal units to the Urgonian platform suggest that at this time shallow-water platform sedimentation was restricted to the Jura platform (Figs 4.27, p.153, 6.1 & 6.3). In this area shallow-water platform sedimentation is characterized by 5-10m thick shoaling-up cycles passing from sub-wavebase lime mud-wackestones to tidal cross-bedded oobioclastic grainstones (Arnaud-Vanneau & Arnaud, 1990, their fig. 18A). Across the Isère structure these shallow-water platform facies pass into periplatform shales and interbedded nodular limestones (eg. Figs 4.24, p.145 & 6.1), interpreted to have been deposited upon a sub-storm wavebase hemipelagic ramp which dipped basinward at less than 1° (SE, Arnaud-Vanneau *et al.*, 1987; Arnaud & Arnaud-Vanneau, 1989) (eg. Figs 4.20, p.138 & 6.1). Certainly, the orientation of slump scars within the thickest part of the succession suggests that the predominant dip of this part of the slope was towards the

south (eg. Fig. 5.39, p.256). The distal ramp sediments thicken markedly towards the southeast, to the margin of the Vocontian basin where they reach a maximum thickness of 900m before thinning rapidly into the basin as pelagic facies (eg. Figs 4.20 & 6.1). The thickest part of this succession is interpreted to coincide with the Hauterivian slopebreak basinwards of which the slope dipped at up to 5° (Fig. 6.1). Thus, the Hauterivian platform is interpreted to have had the overall geometry of a distally-steepened ramp (Arnaud & Arnaud-Vanneau, 1989).

The antecedent topography of the Hauterivian platform is interpreted to have been modified during the uppermost Hauterivian and lower Barremian in the Jura, N.W. Vercors and Chartreuse by subaerial exposure (eg. Fig. 6.3), and upon the flanks to the Vocontian Basin by mass wasting and incision (eg. Fig. 4.20). Thus, the architecture or template inherited by the Urgonian platform reflected structural elements inherited from Jurassic rifting, depositional patterns established during the Jurassic and lower Cretaceous (a response to the oceanographic setting, climate etc.) and the effects of relative sea-level changes.

6.2. Sequence Stratigraphic Evolution Of The Urgonian Platform.

6.2.1. Summary.

The Glandasse Bioclastic Limestone Formation of Arnaud (1981) constitutes a 'general' lowstand prograding wedge which is itself divisible into two major sequences; a lower type 1 sequence (BA1) and an upper type 2 sequence (BA2) (eg. compare Figs 5.2, p.194 & 6.1 with Fig 6.4). The upper sequence is part comprised of the Glandasse Bioclastic Limestone Formation and a part by the Urgonian Limestone Formation of Arnaud (1981) (i.e. compare Fig. 6.1 with Figs 6.2 & 6.4). The marls between the two formations represent the maximum flooding surface (mfs) to sequence BA2 (marnes de Font Froide of Arnaud, 1981, Fig. 4.25, p.149). Thus,

unrestricted and locally-rimmed during sequence BA2, to an aggraded and often highly restricted shelf during sequences BA3-5. By way of contrast, shelf sedimentation during the TST and HST to sequence AP1 was generally open and unrestricted with shelf-margin and slope type facies forming well developed subtidal shallowing-up cycles across the shelf at this time (eg. Figs 5.12, p.213 & 6.4, sections 5.2.4.C & 5.2.5). The marked difference between sequences BA3-5 and AP1 are thought to reflect a major change of environmental conditions during which the lower *Orbitolina* beds were developed across the shelf (TST to AP1, see Section 5.2.5). Finally, the shelf was again exposed, karstified and also locally incised (SbAP2), subsequent to which it became drowned during the ensuing transgression (sequence AP2). The death of Urgonian platform sedimentation is thought to reflect a combination of subaerial exposure followed by changing climatic and oceanic conditions (eg. environmental changes) during the transgressive systems tract of the AP2 sequence.

6.2.2. Sequence BA1.

6.2.2. A. Summary and introduction to the sequence.

This sequence is bound at its base by the sequence boundary SbBA1 as illustrated in Figures 6.2 & 6.4 which is coincident with the base of member HsBi of Arnaud (1981) except on the basin-floor where the collapse deposits derived from the slope are included at the base of this sequence (Figs 6.1 & 6.4). The sequence is represented by approximately 750-800m of bioclastic grainstones on the slope (Glandasse plateau) and by approximately 120m of basin-floor sands overlain by 230m of periplatform muds in the Borne area (see Fig. 6.5). Contrastingly, on the mud dominated basin-floor at the Col du Rousset the sequence is up to 1400m thick (Arnaud, 1981). The BA1 sequence is composed of three progradational units (HsBi-Bi1, Bi2-Bi5P and Bi5A-Bi6a), the lower two of which are separated by the Fontaine Graillère marls. The Lower Fontaine Colombette marls divide the final progradational cycle, Bi5A-Bi6a. Both the Graillère and Lower Colombette marls

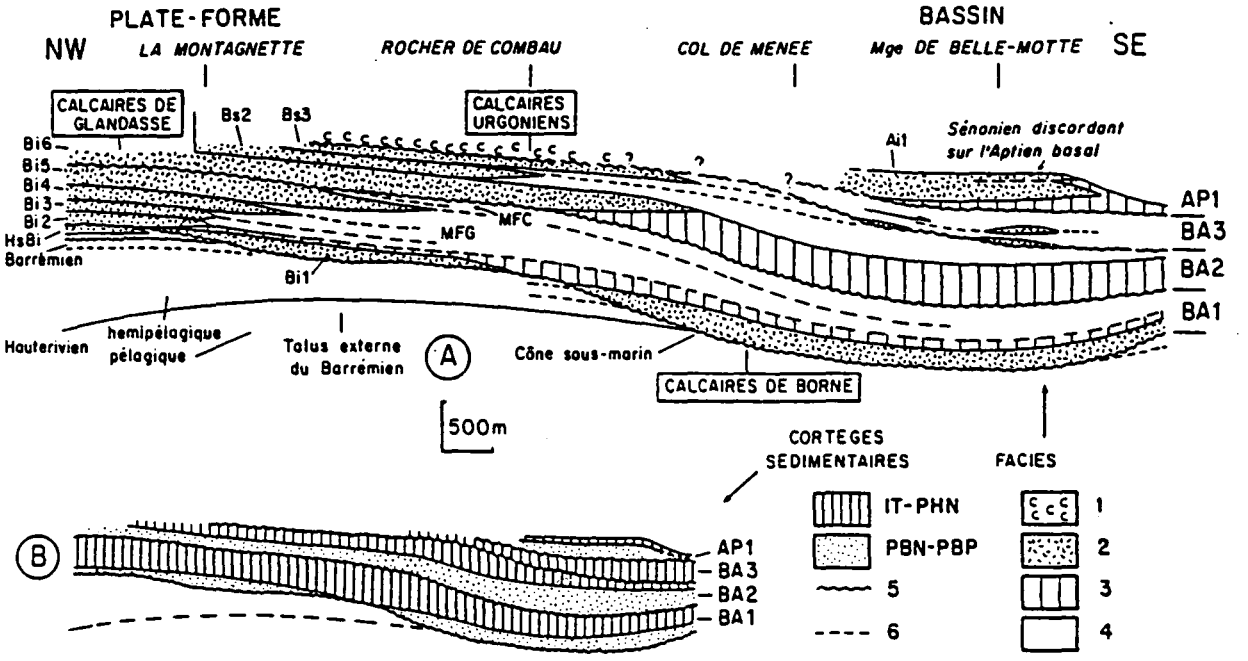

Figure 6.5. The Barremian platform margin and its sequences, systems tracts and facies as according to Arnaud-Vanneau & Arnaud (1991). A: cross-section of the Glandasse plateau (southern Vercors) to the Montagne de Belle-Motte (eastern Diois). MFG: Fontaine Graillère marls; MFC: Fontaine Colombette marls; 1 shelf-lagoon facies; 2: outer-shelf bioclastic facies (and bioclastic grainflows of the Vocontian Basin= Borne Bioclastic Limestone Formation; 3: hemipelagic limestones; 4: hemipelagic marls; 5: depositional sequence boundary; 6: parasequence set boundary. HsBi, Bi1 to Bi6, Ai1: shallowing-up cycles of Arnaud-Vanneau (1980) and Arnaud (1981). B: schematic cross-section with names of the Barremian-Lower Aptian systems tracts. See also Fig. 4.22, p.141.

are interpreted to have developed when shallow-water shelf sedimentation was temporarily backstepped and/or drowned. The lowermost of these units (HsBi-Bi1) is interpreted to have been derived from the east. This contrasts markedly with the overlying packages which both appear to have a northerly origin. Classically, the members Bi2-Bi6 have been interpreted by Arnaud-Vanneau & Arnaud (1976) and Arnaud (1981) as shallow-water bioclastic subtidal shoals (eg. the 'southern Vercors shoal', Arnaud-Vanneau & Arnaud, 1976). However, the first demonstrably shallow-water facies of these members are developed within Bi5 as can be seen in the north of the Cirque d'Archiane (eg. Fig. 5.29, p.240). Below Bi5 all bioclastic facies are here reinterpreted as sub-storm wavebase slope facies as they are characterized by an

absence of sub-horizontal bedding or a shallow-water fauna preserved in life orientation.

As a whole, this BA1 sequence is also very different from the classical sequence stratigraphic models as described in Section 2.2 and illustrated in Figures 2.1 and 3.5 (pgs 6 & 41, respectively). The BA1 sequence above the lowstand systems tract (HsBi-Bi1) is composed of a lower retrogradational-aggradational-progradational unit developed above the base of the Fontaine Graillère marls (Bi2-Bi5P), and an upper aggradational-retrogradational-progradational unit which includes the Lower Fontaine Colombette marls (Bi5P-Bi6a) (Figs 6.4 & 6.5). This lower unit (Bi2-Bi5P) is composed of a transgressive and highstand systems tract (BA1, TST-HST I). This was followed by a further (interpreted) acceleration in the rate of relative sea-level rise and subsequent stillstand to develop an upper (eg. second) transgressive and highstand systems tract (Bi5A-Bi6a) to sequence BA1 (BA1, TST-HST II). The dual development of the transgressive and highstand systems tracts is interpreted to reflect an acceleration to the rate of relative sea-level rise during Bi5 so that it first was equal to (Bi5A) and then greater than sedimentation rates, drowning shallow-water sedimentation and developing the Lower Fontaine Colombette marls. This rather different development of systems tracts is interpreted to reflect the non-sinusoidal (eg. Figs 2.1 & 3.5) form of the lower Barremian relative sea-level curve where *two* accelerations in the rate of relative sea-level rise (which exceeded sedimentation rates) are *not* separated by times of falling relative sea-level. The stratal patterns developed within sequence BA1 reflect the complex interaction of sedimentation rates and rates of relative sea-level rise. Type 2 transgressive geometries are developed within both of the BA1 transgressive systems tracts. The upper limit to the sequence is SbBA2.

6.2.2. B. Position of the sequence boundary and dynamics of lowstand sedimentation.

6.2.2. B1. General dynamics of sedimentation.

Shallow-water carbonate sedimentation continued upon the Jura platform until the uppermost Hauterivian/lowermost Barremian (Pierre Jaune de Neuchâtel Limestone- Figs 6.1 & 6.2). Sediments of lower Barremian age are not known upon the Jura platform (Arnaud & Arnaud-Vanneau, 1989; Arnaud-Vanneau & Arnaud, 1990) (eg. Fig. 6.1). During the very late Hauterivian/lowermost Barremian times a major relative sea-level fall is interpreted to have shifted outer-platform bioclastic facies 60-70km basinwards (southeast) from the Jura to the flanks of the Vocontian basin, east of the Glandasse plateau (eg. Figs 5.39, p.256, 6.1 & 6.3). At this time the Jura platform and much of the northern Dauphinois basin is interpreted to have been subaerially exposed (Fig. 6.3). Good sedimentological evidence for this exposure is, however, in the most part absent. This is possibly due to substantial reworking of the sequence boundary during the ensuing transgressive systems tract (see Section 5.2.4.C, and Fig. 5.9).

6.2.2. B2. Uppermost Hauterivian-lowermost Barremian deposits: facies and their distribution.

Deposits of uppermost Hauterivian/lowermost Barremian age are found on the slopes (southern Vercors, Fig. 5.39) and the basin-floor (Borne, Fig. 5.38, p.252) of the Vocontian Basin, and are included into member HsBi of Arnaud (1981) (Figs 6.3 & 6.4). No shallow-water deposits of this age are known (Arnaud, 1981; Arnaud-Vanneau & Arnaud, 1990) and the sub-storm wavebase gravity flow deposits of the slope and basin-floor (Borne Bioclastic Limestone Formation of Arnaud, 1981, Figs 4.25 & 4.42, p.186) are thought to have been shed from a shallow-water platform developed to the east of the Glandasse plateau (Arnaud, 1981, Fig. 4.42). On the upper to mid slope HsBi is superbly exposed at Tête Chevalière where its base is abrupt and has a parallel-parallel stratal pattern (eg. Figs 5.20, p.228, 5.39 & 5.40).

A parallel-parallel stratal pattern is also developed on the mud dominated basin-floor/toe-of-slope apron at the Col du Rousset (to the west of the Glandasse plateau). In this area the base to HsBi is abrupt, but non-erosive and marked by the change from pelagic to periplatform sedimentation; it is associated with an abrupt increase of sedimentation rates. For nearly all of the basin-floor to the west of the Col du Rousset a similar increase of sedimentation rates and parallel-parallel stratal pattern is developed at the base of HsBi (Arnaud, 1981). Sediments of this member also generally fine and thin to the west of the Col du Rousset (Arnaud, 1981). By way of contrast, on the basin-floor in Dévoluy slump and debrite deposits are the lowermost deposits of this age and rest unconformably on Hauterivian and Valanginian pelagic facies (Figs. 4.20, p.138, 5.19, p.226 & 6.1) (Arnaud, 1981; Arnaud-Vanneau & Arnaud, 1990). These allochthonous basin-floor slumps and debrites are interpreted to have been derived from the slope just prior to deposition of HsBi bioclastics (Arnaud, 1981; Arnaud-Vanneau & Arnaud, 1990; Jacquin *et al.*, 1991; Hunt & Tucker, 1992, eg. Figs 4.20 & 6.4). These allochthonous basin-floor slumps and debrites are in-turn overlain by up to 120m of coarse bioclastic sands of which the lower 60m are ascribed to HsBi (Arnaud, 1981, Fig. 5.38). In the eastern Vocontian Basin the Hauterivian-Barremian boundary is also characterized by the collapse of the slope (Beaufort-sur-Gervanne/Saillans area, Fig. 5.45, p.268) and the deposition of gravity deposits derived from this catastrophic collapse on the pelagic basin-floor (eg. GHs/Bi at La Chaudière, Ferry & Flandrin, 1979; Ferry & Rubino, 1989, Figs 5.46, p.270, 6.6 & 6.7). Rather differently, however, in this section the slope is not subsequently bypassed and so the allochthonous basin-floor package (GHs/Bi, Fig. 6.7) is overlain by deep-water parallel-bedded pelagic limestones (eg. Figs 5.41, p.262 & 6.7). Contrastingly, in true pelagic sections away from the influence of the Urgonian platform the Hauterivian-Barremian boundary is marked by a shift from limestone to predominantly shales with interbedded limestones as can be seen at the Barremian type section in Haute-Provence (Fig. 6.7).

Figure 6.6. The GHs/Bi basin-floor allochthonous debris at La Chaudière in the eastern Vocontian basin (located on Figure 4.17). This package contains elongate angular clasts of dark shales, angular clasts of glauconite and asymmetric sheared limestone clasts supported within a muddy matrix. This unit is composed of a variety of slope lithologies and is interpreted to have been a cohesive debris flow which originated from the collapse of the slope. Note that there is a preferred subhorizontal orientation to dark-grey shale clasts. These collapsed slope sediments moved downslope as a flow which had an internal shear strength so that limestone clasts became sheared. Slope collapse is interpreted to have occurred during times of falling relative sea-level and is overlain by black pelagic shales and limestones. Note that the chronostratigraphic position of this unit is shown in Figure 6.7 (opposite). Pencil approximately 120mm long for scale. Also see Fig. 4.46, p.270.

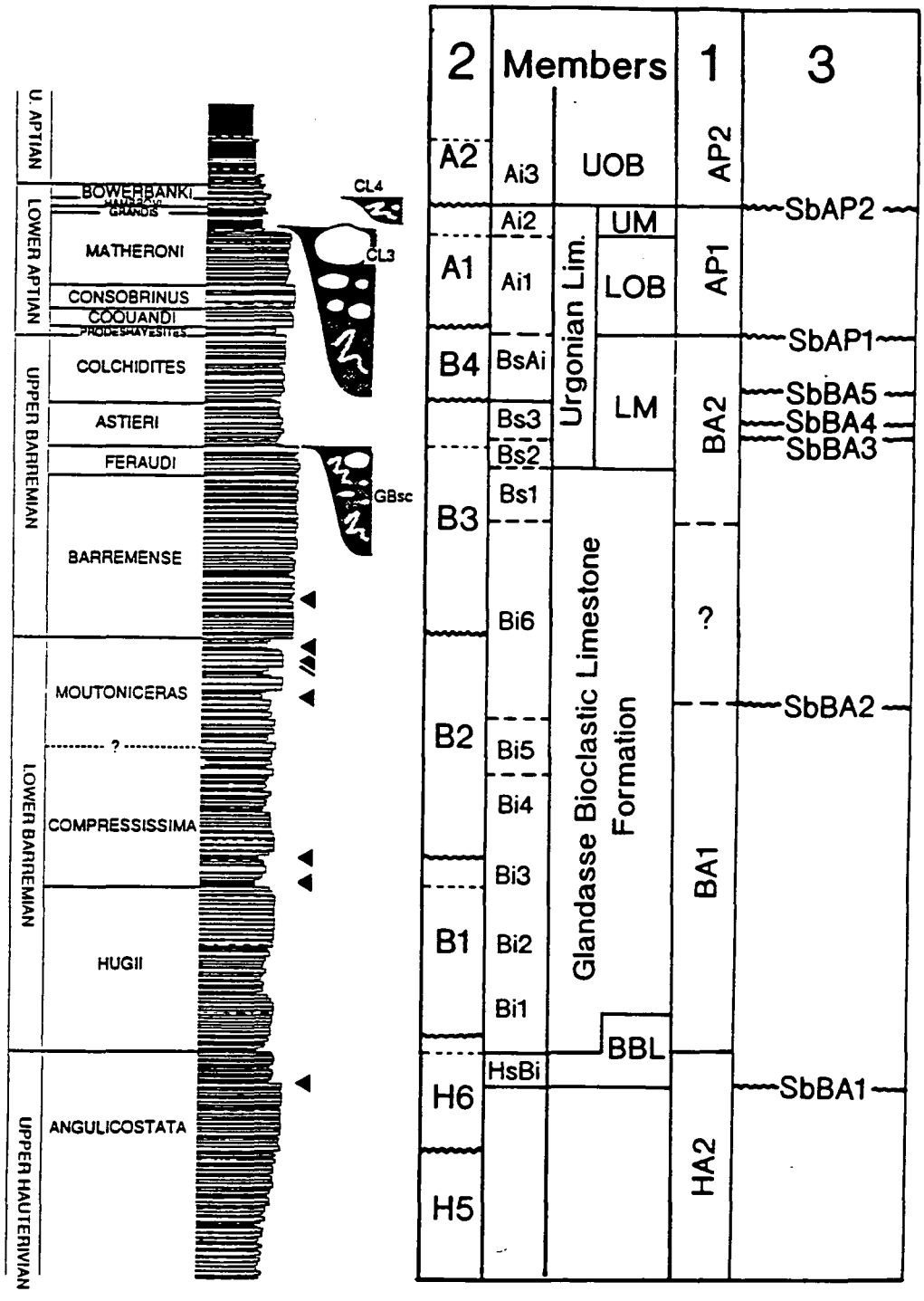

Figure 6.7. The pelagic Barremian/lower Aptian stratotype section of Angles, Alpes de Haute Provence as located within the inset. This section shows the main ammonite zones as used in Figures 6.2 & 6.4 and the interpreted chronostratigraphic positions of the basin-floor slope collapse deposits of the eastern Vocontian Basin. The position of the sequence boundaries of Arnaud & Arnaud-Vanneau (1989) (1), Jacquin *et al.* (1989)(2) and this thesis (3) are also located within this pelagic series. Triangles indicate shale levels with an total organic content of greater than 2% (Magniez-Jannin, 1991). Stratigraphy of the Angles section from Ferry & Rubino (1989). BBL= Borne Bioclastic Limestone Formation; LM= Lower Member; LOB= Lower *Orbitolina* Member; UM=Upper Member; UOB= Upper *Orbitolina* Member.

6.2.2. B3. Current sequence stratigraphic interpretations of members HsBi-Bi1 (the Borne Bioclastic Limestone Formation).

In their original sequence stratigraphic interpretation Arnaud & Arnaud-Vanneau (1989) placed the lower sequence boundary of the Urgonian platform *sensu lato* at the base of HsBi on the slope and beneath slope collapse deposits on the basin-floor (BA1, Fig. 5.2, p.194). Subsequent interpretations of Arnaud-Vanneau & Arnaud (1990; 1991) have retained this position for the lower sequence boundary to the Urgonian platform *sensu lato* (eg. Figs 4.22, p.141 & 6.5). This general scheme has been followed by Jacquin *et al.* (1991) although these and other workers (eg. Hunt & Tucker, 1992) have tended to modify the basic stratigraphy of Arnaud & Arnaud-Vanneau (1989) as discussed below. The later sequence stratigraphic schemes of both Jacquin *et al.* (1991) and Hunt & Tucker (1992) interpreted a further fall of relative sea-level and, thus, a younger sequence boundary (within members HsBi and Bi1 of Arnaud, 1981) above the BA1 boundary of Arnaud & Arnaud-Vanneau (1989, Fig. 5.2). These and another alternative interpretation are discussed below and in Section 6.2.2.B4 respectively.

On the slope at the Tête Chevalière Jacquin *et al.* (1989; 1991) identify two sequence boundaries (eg. Fig. 5.20, p.228). The lower of these is coincident with the abrupt lithological change at the base of the prominent cliff (the BA1 sequence boundary of Arnaud & Arnaud-Vanneau, 1989, Fig. 5.2). The stratigraphically younger sequence boundary of Jacquin *et al.* (1991) corresponds to the major erosional surface at the base of the modified Bi1 of Hunt & Tucker (1992, Fig. 5.39, p.256) which is draped by dark grey sub-storm wavebase dark-grey shales (Fig. 5.40), themselves both onlapped and erosionally truncated by the overlying channellised mudstones-wackestones (SbB1, Fig. 5.20). This younger sequence boundary (SbB1, Fig. 5.20) is interpreted to have developed from the erosion of a submarine canyon (Jacquin *et al.*, 1989; 1991). The SbB1 sequence boundary is interpreted by Jacquin *et al.* (1989; 1991) to represent the lowest point of relative sea-level further to the fall which developed its immediate precursor sequence H7 (the BA1 boundary of Arnaud

Urgonian Sequence Stratigraphy.

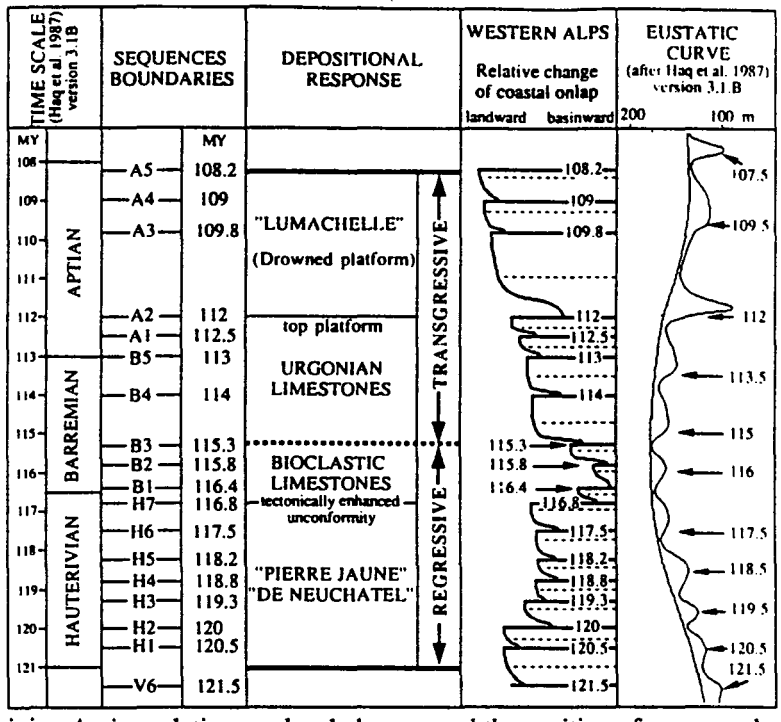

Figure 6.8. Hauterivian-Aptian relative sea-level changes and the position of sequence boundaries as interpreted from the sequence stratigraphy of Jacquin *et al.* (1991, see also Fig 5.19). Note that H7 corresponds to the base of the Urgonian platform *sensu lato* and A2 the top of the platform. These sea-level curves are also compared to the global eustatic curve of Haq *et al.* (1987).

& Arnaud-Vanneau, 1989). The H7 sequence (Figs 5.19 & 5.20) is thus interpreted to have been deposited during a time of overall falling relative sea-level (Fig. 6.8) (Jacquin *et al.*, 1989; 1991). On the basin-floor Jacquin *et al.* (1989; 1991) have correspondingly identified two sequence boundaries, one below HsBi basin-floor gravity deposits and another at the base of the Bi1 allochthonous sands (eg. Fig. 5.19, p.226).

Hunt & Tucker (1992) have followed the general geometric interpretation for the Tête Chevalière of Jacquin *et al.* (1989; 1991) (eg. compare placing of boundaries at Tête Chevalière between Figs 5.20 & 5.39). However, rather differently, Hunt & Tucker (1992) argue for an alternative interpretation based upon the new systematics for times of falling relative sea-level introduced in Hunt & Tucker (1992) and Section 2.3.2.A (eg. Fig. 2.7B, p.26). In their reinterpretation Hunt & Tucker (1992) suggested that the H7 stratal package of Jacquin *et al.* (1991) (Fig. 5.20) is not a true sequence for it developed during times of 'forced regression', prior to the lowest point of relative sea-level, coincident with their SbBA1 (SbB1 of Jacquin *et al.*, 1991, Figs

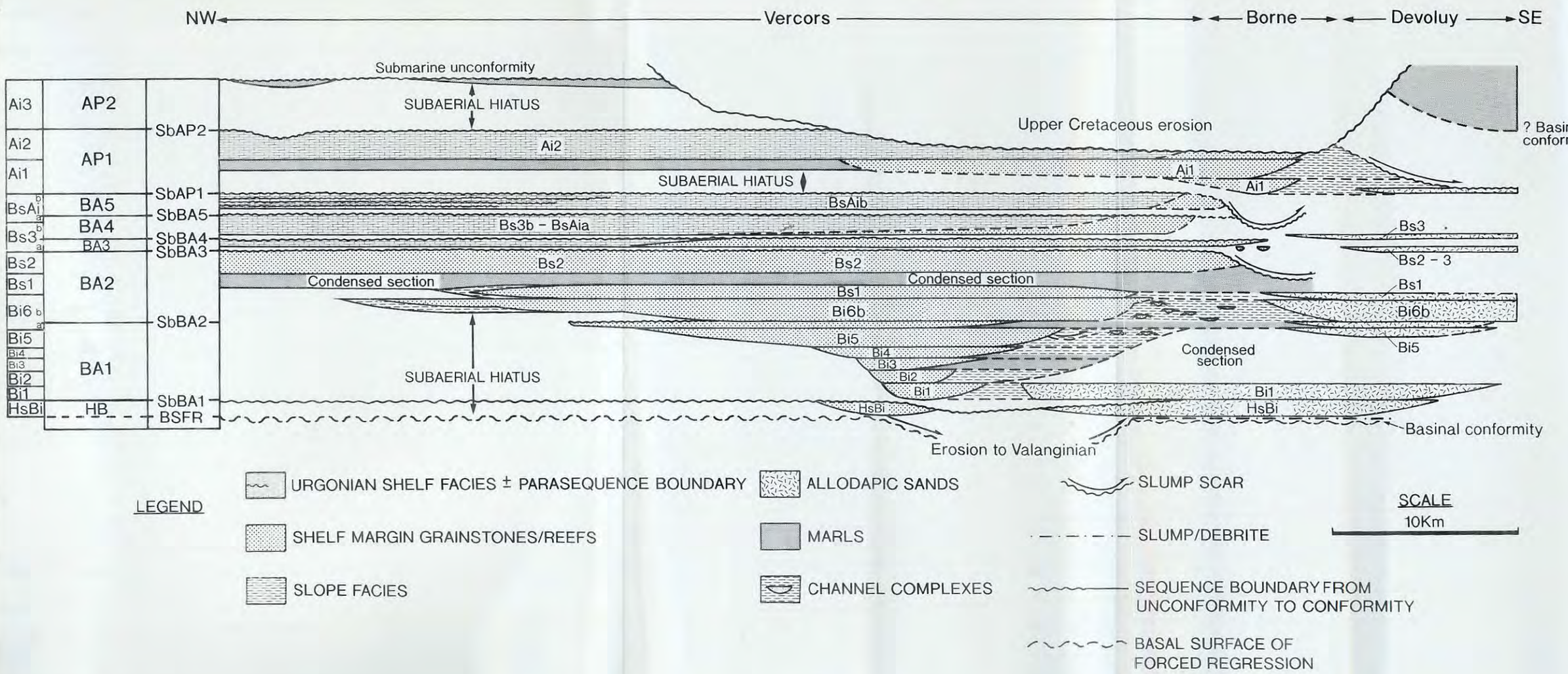

Figure 6.9. The chronostratigraphic north-south cross-section of Hunt & Tucker (1992) through the southern Vercors using the systematics for times of falling relative sea-level discussed in Section 2.3.2A, and illustrated in Figure 2.6B, p.26. This scheme can be compared to that advocated in this thesis and illustrated in Figures 6.2 & 6.4. This line of section is located on Figure 4.17 (p.132).

5.20 & 6.8) at the Tête Chevalière. As such, the H7 sequence of Jacquin *et al.* (1991) is interpreted by Hunt & Tucker (1992) as a 'stranded parasequence' (eg. Fig. 2.6A, p.26) or in the new systematics of Figure 2.6B a 'forced regressive wedge' (eg. Fig. 5.39, p.256). Accordingly, the base of HsBi (BA1 sequence boundary of Fig. 5.2 or

SbH7 of Figs 5.20 & 6.8) is reinterpreted as the 'basal surface of forced regression' (BSFR, Fig. 5.39). The BSFR is interpreted to pass basinwards from the Tête Chevalière (eg. Fig. 5.39) along the top of slump scars on the slope to beneath HsBi slumps, debrites and sands on the basin-floor (Fig. 6.9) (Hunt & Tucker, 1992). Thus, the sequence boundary is lifted above sediments interpreted to have been deposited during 'forced regression' (similarly to Fig. 2.6B) and is placed at the base of Bi1 (as modified by Hunt & Tucker, 1992) (SbBA1 Figs 5.39 & 6.9). In this reinterpretation the sequence boundary placed at the interpreted lowest point of relative sea-level. Sediments interpreted to have been deposited during 'forced regression' but prior to the lowest point of relative sea-level are placed within the 'forced regressive wedge systems tract' (Hunt & Tucker, 1992) (see also Section 2.3.2).

6.2.2. B4. Further sequence stratigraphic interpretation of HsB1-Bi1: the Borne Bioclastic Limestone Formation.

This sub-section discusses a further interpretation to that of Jacquin *et al.* (1991) and Hunt & Tucker (1992) who used the development of erosional truncation upon the slope as the main criteria to identify their B1 and BA1 sequence boundaries respectively. Using this criteria the base of Bi1 *sensu* Arnaud (1981) becomes a strong candidate for interpretation as a sequence boundary (eg. Figs 6.5, 6.10 & 6.11). This stratal package is illustrated schematically in Figure 6.5 where it is shown to sit in a lower position upon the slope and to truncate erosionally the preceding HsBi of Arnaud (1981). The most spectacular exposure of this erosionally based stratal package is at the Tête Praorzel where it is channellised and erosionally truncates at least 90m of the underlying stratigraphy (Figs 5.23, p.231 & 6.10). The base of this channel is illustrated in Figure 6.11 and can be seen to contain slope lithoclasts of up to 2m in diameter. Classically, on the basis of its erosional base and geometry this exposure at Tête Praorzel could be interpreted as a strike section through a major submarine canyon, developed during times of falling relative sea-

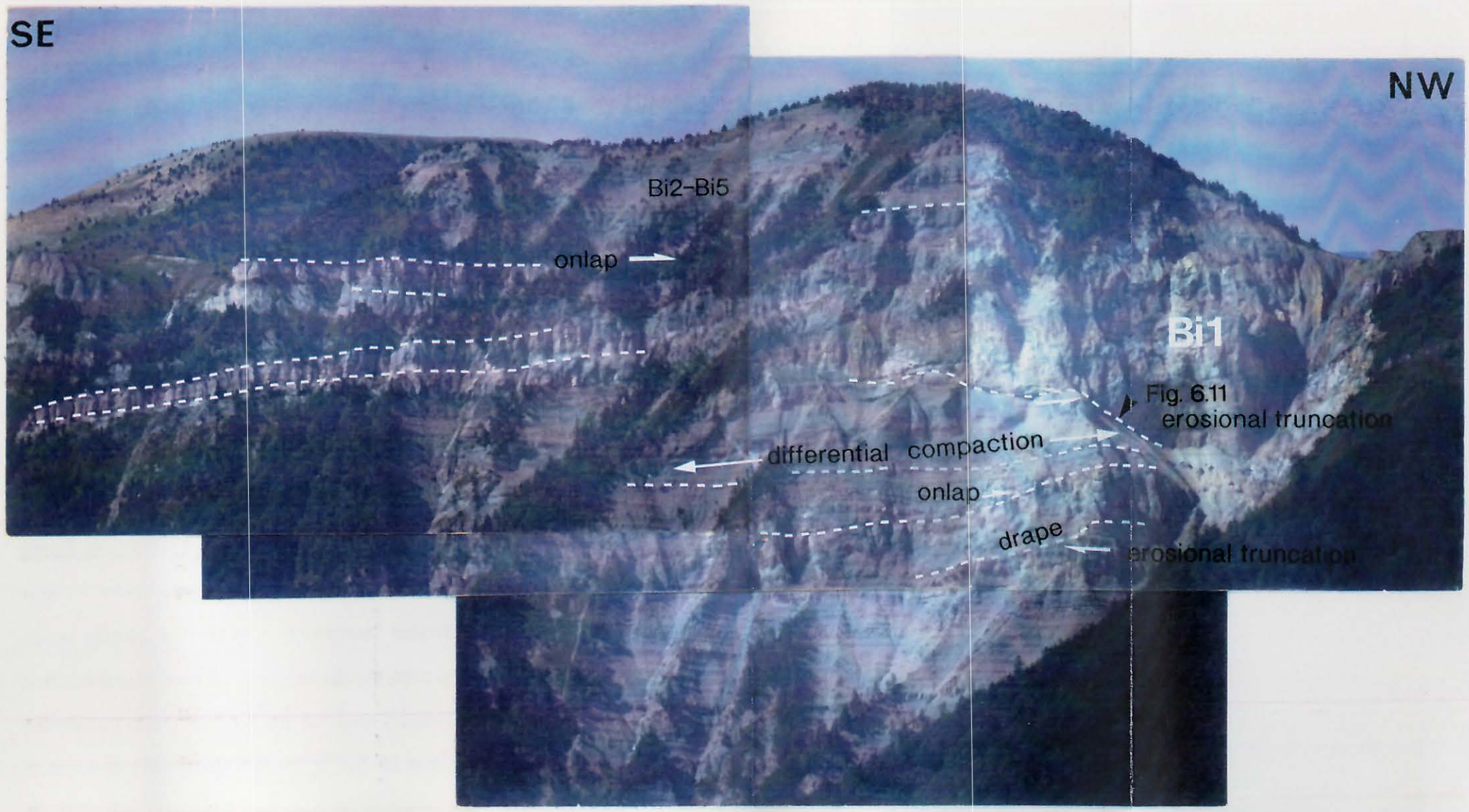

Figure 6.10. Interpreted photo-panorama of the Tête Praorzel in the southern Glandasse plateau, located on Fig 4.17 (p. 132). The major erosively based channel corresponds to the Bi1 member of Arnaud (1981). Classically, on the basis of stratal termination patterns and the coarseness of slope facies the base of Bi1 would be interpreted as a major submarine canyon cut during times of falling relative sea-level when sediments were forced to bypass the slope (eg. compare to Fig. 2.5, p.14) (see Section 6.2.2.B4 for further discussion). Member Bi1 is onlapped by dark shales and limestones, interpreted by Jacquin *et al.* (1991) as the sequence boundary SbBA2 (Figs 5.19 & 5.20). This onlap is, however, associated with an areal reduction in the extent of slope sands and is here reinterpreted as a drowning unconformity. Note the location of Figure 6.11.

Figure 6.11. Detail of erosional truncation and the large slope clasts contained within the Bi1 submarine canyon/channel at the Tête Praorzel. Classically such an erosionally based channel would be interpreted to be developed during times of relative sea-level fall. See text (Section 6.2.2.B4) for further discussion. Note that there is some camera shake. This figure is approximately located upon Figure 6.10.

level as sediments were forced to bypass through the slope to the basin-floor (eg. Fig. 2.5, p.14). If this interpretation is taken to be correct it would suggest a further fall of relative sea-level to the SbBA1 of Hunt & Tucker (1992) / SbB1 of Jacquin *et al.* (1991) (eg. Fig. 6.8). Thus, the lowest point of relative sea-level would be at the base of Bi1 of Arnaud (1981) in this further interpretation.

6.2.2. B5. Discussion.

As previously discussed in Section 5.3.3 there is a problem in using solely stratal relationships (onlap and/or erosional truncation, i.e. SbB1 & SbB2 Fig. 5.23; SbB1 Fig. 5.20, SbBA1, Fig. 5.39) for the identification of sequence boundaries on the flanks of the Urgonian platform (*sensu lato*). In the absence of correlative shelf exposures and/or a major change/jump in the type of slope facies as occurs above *et5*

in the Cirque d'Archiane (SbBA2, Figs 5.26, 5.27 & 6.15) there must be some question as to the identification of a sequence boundary on the basis of erosional truncation/onlap alone on the slope. This is because the development of erosional surfaces upon the slope is *not* restricted to times of falling and lowstand of relative sea-level (Section 5.3.3) (eg. Galloway, 1989, Fig. 2.8, p.31).

The erosional surface at the Tête Chevalière is discussed in Section 5.3.3.B (sequence boundary SbBA1 of Hunt & Tucker, 1992 or SbB1 of Jacquin *et al.*, 1991, Figs 5.20 & 5.39 respectively). In that Section it was suggested that the alternative interpretation of this surface as a collapse scar developed at a time of reduced carbonate sedimentation is certainly equal to its current interpretation as a sequence boundary. With the current exposure, and in particular the absence of correlative shelf deposits there is no way to show unequivocally that either interpretation as a sequence boundary or otherwise is incorrect. However, the fact that there is no basinward facies jump above the interpreted sequence boundary (SbB1, Fig. 5.20 & SbBA1, Fig. 5.39) so that more proximal facies sit directly on the erosional surface, but the opposite (Fig. 5.40, p.258), does suggest that the interpretation of this surface as a collapse scar is more appropriate. Furthermore, differences of stratal pattern above this erosion surface are only to be expected as gravity flow deposits would become preferentially channellised into a pre-existing topographic depression on the slope (whatever its origin) as is well documented upon siliciclastic slopes (eg. Weimer, 1989) and can be recognized elsewhere upon the Urgonian platform (*sensu lato*) (eg. *et1* and *et3*, Cirque d'Archiane, Fig. 5.26).

6.2.2. B6. Limitations to interpretation(s) of the Borne Formation (HsBi-Bi1).

In summary, members HsBi-Bi1 of Arnaud (1981) are a deep-water slope facies package (>> storm wave base). The base of HsBi is associated with a major facies 'jump' (i.e. a significant change in the character of slope sedimentation) and this is interpreted to be the basal sequence boundary of the Urgonian platform *sensu lato* (eg. Arnaud & Arnaud-Vanneau, 1989; Jacquin *et al.*, 1991). This sequence

boundary has a parallel-parallel stratal pattern both upon the slope at the Tête Chevalière and basin-floor at the Col du Rousset, but can be erosional (eg. Fig. 6.1). The orientation of channellised deposits and of collapse scars within these members (eg. Fig. 5.40, p.258), coupled with isopach data (eg. Fig. 4.40, p.184) and facies assemblages suggest that HsBi and Bi1 developed on a slope which dipped most steeply towards the west, and thus, that slope sediments were derived from a shallow-water platform developed to the east of the Glandasse Plateau (eg. Arnaud-Vanneau & Arnaud, 1976; Arnaud, 1981).

Within member HsBi of Arnaud (1981) (the whole cliff at Tête Chevalière) several erosive surfaces are developed and these can, and have been interpreted to be sequence boundaries (eg. Figs 5.20 & 5.39). The upper surface of member Bi1 of Arnaud (1981) has also been interpreted as a sequence boundary (eg. SbB2, Fig. 5.23, p.231), and as has its lower surface (Section 6.2.2.B4). In the absence of correlative shallow-water sediments these interpretations are impossible to substantiate and are driven by the predictive siliciclastic sequence stratigraphic model. The application of this model to a well-exposed, younger shelf-slope succession (eg. Section 5.3.3), however, unambiguously demonstrates that development of erosional truncation upon the slope is *not* limited to times of falling relative sea-level (eg. Fig. 5.26). Thus, it was suggested in Section 5.3.3 that in the absence of correlative shelf exposures documentation of major basinward facies shifts should be coincident with an erosional surface if is to be identified as a sequence boundary (eg. *et5*, see Section 5.3.3). This criterion is only fulfilled at the base of HsBi and Bi1 of Arnaud (1981) (Figs 6.7, 6.10 & 6.11) on the eastern Glandasse plateau.

Doubts can be cast upon the above sequence stratigraphic interpretations of Jacquin *et al.* (1991), Hunt & Tucker (1992) and Section 6.2.2.B from the progressive development of the HsBi-Bi1 submarine canyon system at the Tête Chevalière (eg. Fig. 5.39 & 5.40). The spectacular box canyon which dominates the upper part of this exposure is filled by very coarse grainstones and these were clearly contemporaneous to the muddy levee deposits developed on its flanks (eg. see Figs

5.39 & 5.40). Analogous box canyons are developed upon bypass-erosional slopes of the Bahama Banks (Schlager & Ginsburg, 1981, Fig. 3.12, p.57). Within HsBi strata below this spectacular canyon, above the dark-grey marls, erosionally-based stratal packages become increasingly channellised and areally restricted upwards (eg. Figs 5.20 & 5.39). This evolution is associated with a gradual decrease of canyon size and an increase in the steepness of canyon walls, the uppermost being U-shaped with vertical walls (the box canyon, Fig. 5.39). This is not associated with any obvious coarsening of the light grey mud-wackestone overbank facies (eg. Fig. 5.40). This vertical evolution of canyon profiles can be interpreted to represent *either* a strike-section through a basinwards prograding submarine canyon-slope fan/apron system as a series of discrete erosional events, *or* the progressive steepening and evolution of the upper slope from an accretionary slope apron (lower part of HsBi with a parallel-parallel stratal pattern) to an erosional / bypass slope. This latter scenario would suggest a gradual steepening of the slope in which the interpretation of erosional surfaces at the Tête Chevalière as collapse scars neatly fits. The development of the erosional base to Bi1 (Figs. 6.5, 6.10 & 6.11) above the HsBi of Arnaud (1981) could also be readily reconciled within this hypothesis as the complete bypass of the upper occurred. Such an interpretation does away with the need to invoke further major falls of relative sea-level to that preceding SbBA1 (Fig. 6.4 = BA1 sequence boundary of Arnaud & Arnaud, 1989, Fig. 5.2 & SbH7, Fig. 6.8) at the base of the Borne Bioclastic Limestone Formation and is here the preferred interpretation.

6.2.2. B7. Summary and conclusions.

The members HsBi-Bi1 of Arnaud (1981) are interpreted to have developed subsequent to a major fall of relative sea-level after the establishment of a shallow-water platform to the east of the Glandasse plateau. As this shallow-water platform became established excess sediments were shed onto and down its slopes. This is interpreted to be coincident with the abrupt facies shift at the base of HsBi at the Tête Chevalière, interpreted as the BA1 sequence boundary (SbBA1 of Fig. 6.4). Thus,

development of the BA1 sequence boundary at Tête Chevalière is probably slightly younger than the time at which sea-level reached its interpreted lowest point, and this time delay is a reflection of the time needed to establish shallow-water sedimentation and to begin exporting excess sediment. Initially, the eastern slopes (represented by the Glandasse plateau) to the hypothetical shallow-water platform are interpreted to have been accretionary. It is suggested that their gradual steepening facilitated their sporadic and catastrophic collapse and the subsequent channellisation of slope facies. Further steepening is interpreted to have caused the complete bypass of the upper slope by bioclastic facies and the erosion of a substantial part of the foreslope (base Bi1, Figs. 6.5, 6.10 & 6.11).

In terms of relative sea-level changes this interpretation agrees with the initial and subsequent interpretations of Arnaud & Arnaud-Vanneau (1989), Arnaud-Vanneau & Arnaud (1990; 1991) (eg. Fig. 6.12). A major relative sea-level fall in the uppermost Hauterivian exposed the Jura platform and relocated shallow-water bioclastic sedimentation some 60-70km to the southeast (east of the Glandasse plateau). This was followed by a relative sea-level stillstand during the deposition of HsBi-Bi1 (the Borne Bioclastic Limestone Formation) (Fig. 6.12). It is not possible to evaluate further relative sea-level changes from the sub-storm wavebase facies of HsBi-Bi1. This interpretation differs significantly from that of Jacquin *et al.* (1991) and Hunt & Tucker (1992) who suggested a further fall of relative sea-level above the major fall of relative sea-level which exposed the Jura platform (eg. SbH7 to SbB1 Fig. 6.8 or BSFR-SbBA1, Figs 5.39 & 6.9). As discussed in the proceeding sections the development of a bypass slope above the basal sequence boundary of the platform need not be related to any change of relative sea-level. Upper slope bypass could have developed from tectonic rotation of the slope or, alternatively, from the progradation of shallow-water bioclastic sands into a pre-existing topographic depression (eg. see Section 5.3.3). Thus, to reiterate, a single sea-level fall is interpreted prior to the deposition of HsBi and this was followed by a relative stillstand until the top of Bi1 as shown in Figure 6.12.

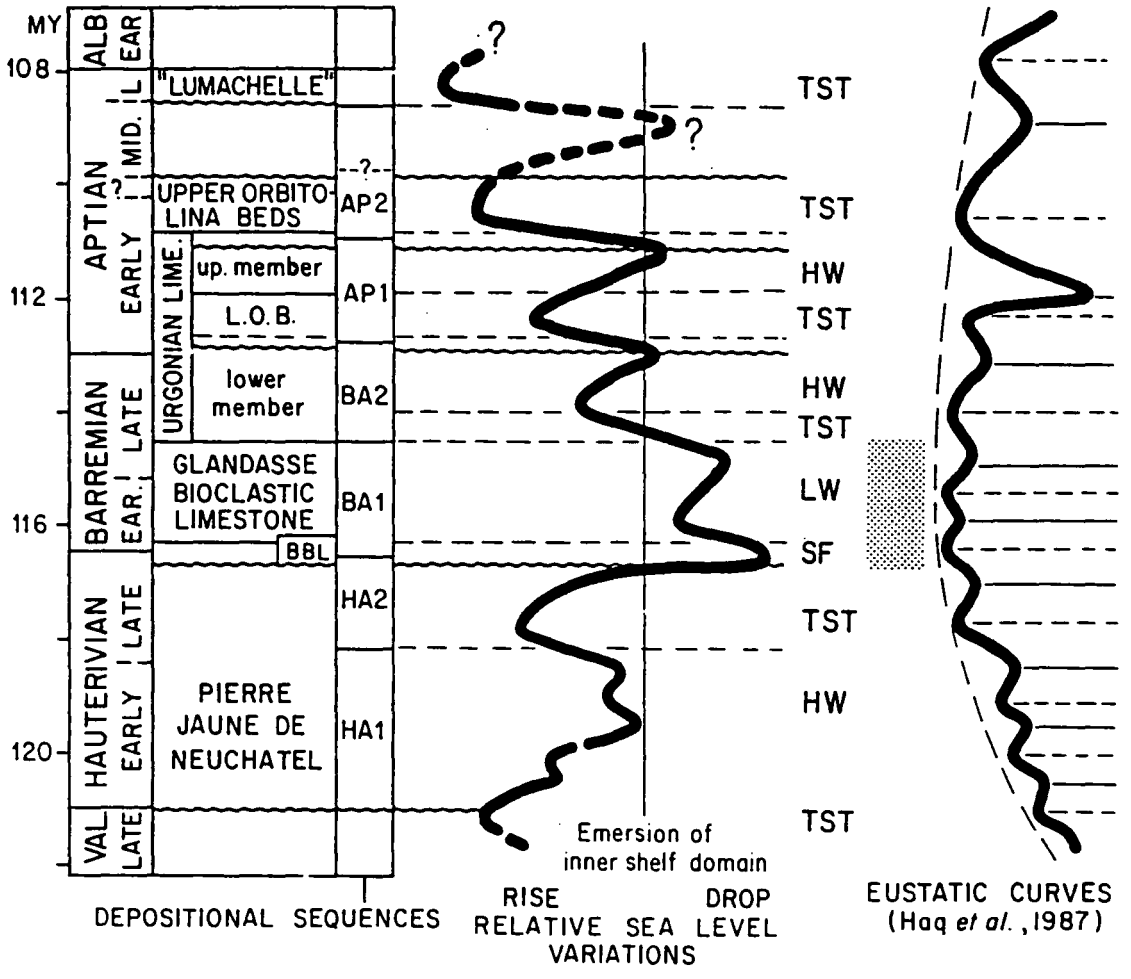

Figure 6.12. Relative sea-level curves from the upper Hauterivian to lower Aptian as interpreted by Arnaud-Vanneau & Arnaud (1990) and compared to the 'global eustatic' curve of Haq *et al.*, 1987. The shaded area corresponds to large differences between the curves. These sequence boundaries can be compared to the sequence stratigraphy of this thesis and Jacquin *et al.* (1991) upon Figure 6.7 (also see Fig. 6.2). L.O.B. : Lower *Orbitolina* beds; BBL: Borne Bioclastic Limestone Formation.

6.2.2. C. BA1 lowstand systems tract sedimentation.

This is interpreted to be represented by the members HsBi and Bi1 of Arnaud (1981) (Borne Bioclastic Formation) and has been discussed in some detail in the preceding sub-section 6.2.2.B. The lower boundary to this systems tract is SbBA1 (Figs 6.2 & 6.4) and is interpreted to have developed subsequent to the lowest point of relative sea-level after the establishment of a shallow-water platform area to the east. The lowstand systems tract is interpreted to have been marked by the evolution of the slope from accretionary to bypass type. This is most likely to have been caused

by tectonic rotation of the slope as gravity flow and collapse structures change from a north-south to an east-west orientation during HsBi1-Bi1 (Fig. 5.39 & 5.40) (see preceding Sections). The upper surface of this systems tract is a flooding surface and is associated with a return to the deposition of muds on the basin-floor and across much of the slope: the Fontaine Graillère marls (Figs 6.4 & 6.5).

6.2.2. D. BA1 transgressive systems tract I.

The upper surface of the Bi1 basin-floor fan complex (Borne Bioclastic Limestone Formation) is a flooding surface, and marks the return to hemipelagic/pelagic sedimentation on the basin-floor as the slope was no longer bypassed (eg. Fig. 5.38, p.252). On the slope this flooding surface is associated with a marked reduction to the areal extent of bioclastic sands (Bi1-2, Fig. 6.5) and the onlap of shales and muddy limestones onto the top of Bi1 at the Tête Praorzel (Fig. 6.10). This slope onlap is interpreted by Jacquin *et al.* (1991) as a sequence boundary (SbB2, Fig. 5.23, p.231). However, this slope onlap is associated with both a reduction in the areal extent of bioclastic slope sands and the development of the Fontaine Graillère marls (Figs 6.4 & 6.5). Thus, the onlap of Bi2 onto Bi1 is here interpreted as the top fan flooding surface, associated with the development of a drowning unconformity (*sensu* Schlager, 1989) on the slope (eg. Fig. 6.10).

On the slope the stacking pattern of younger bioclastic sand bodies is complex, a reflection of the interplay of sedimentation rates and rates of relative sea-level rise (eg. Fig. 6.5). The bioclastic members of Arnaud (1981) are each separated by shales (eg. Figs 4.25 & 6.5) and each is interpreted as a parasequence, developed by relative sea-level rises which temporarily drowned/backstepped shelf-margin and therefore slope sedimentation (Arnaud & Arnaud-Vanneau, 1989; Arnaud-Vanneau & Arnaud, 1990; 1991). Initially, these bioclastic sand bodies backstepped (Bi1-2), and then subsequently aggraded (Bi2-3) (Figs 6.4. & 6.5). Members Bi2-3 are contemporaneous to the development of the lower Fontaine Graillère marls and are overlain by the Bi4 and Bi5P progradational parasequences (Figs 6.4 & 6.5).

On the slope, in the absence correlative shallow-water facies there are two possible solutions for the TST I of sequence BA1. In the first interpretation the top fan flooding surface and 'backstepping' of Bi1-Bi2 is regarded to be the maximum flooding surface (mfs) (eg. the whole TST). As such, Bi2-3 are interpreted as the lower aggradational part of the BA1 highstand systems tract. An alternative interpretation is that top fan flooding surface represents the basal surface of the TST, with members Bi2-3 a type 2 (transgressive) geometry bioclastic aggradational slope package developed as sedimentation rates matched those of relative sea-level rise. In this interpretation the TST is characterized by a lower type 1 and upper type 2 transgressive geometry (eg. compare Figs 6.4 & 6.7 to Fig. 3.20, p.73). In this latter interpretation the Fontaine Graillère marls, contemporaneous to Bi2-3 bioclastic sands are interpreted to represent the mfs to the type 2 geometry TST. It is interesting to note that this interpreted position of the mfs is coincident with a marked shift to shale sedimentation at the base of the *Compressissima* zone on the basin-floor and the enrichment of these shales in organic carbon (eg. compare Figs 6.2, 6.4 with 6.7).

It is not possible to show unequivocally that either one of these interpretations is correct in the absence of correlative shelf deposits. However, the development of the Fontaine Graillère marls equivalent to the aggradational slope sands of Bi2-3 and development of organic rich black shales in the basin at this time does tend to favour the latter interpretation (eg. Arnaud-Vanneau & Arnaud, 1991, Fig. 4.22, p.149; Hunt & Tucker, 1992) and is thus here preferred. The TST appears to mark the halt of slope bypass to the basin-floor and also the change from an easterly to a westerly source of bioclastic slope sands. This is interpreted to have occurred as the easterly platform was irrevocably drowned by the BA1 TST I.

6.2.2. E. BA1 highstand systems tract I.

The highstand in this interpretation is composed of parasequences Bi4-Bi5A, favouring the latter interpretation for the BA1 TST I as discussed in the preceding sub-section. Unlike a normal highstand systems tract where the upper surface of the

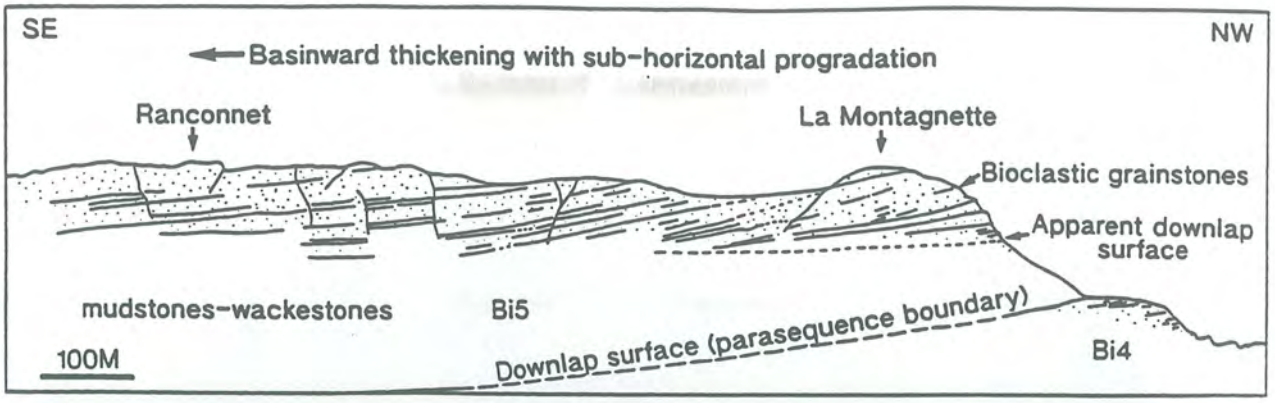

Figure 6.13. Spectacular basinward progradation of members Bi4-Bi5 of late highstand systems tract I to sequence BA1 as seen at La Montagnette on the eastern Glandasse plateau, southern Vercors. Note the slightly basinward descending base to clinoforms of Bi5. Bioclastic sands are deposited upon the upper slope and pass downslope to muds. This is the depositional pattern of an accretionary slope apron (eg. see Fig. 3.23, p.85) At the southern termination of the mountain bioclastic limestones descend more steeply basinwards. This is interpreted as the along-strike extension of surface *et2* from the Cirque d'Archiane (eg. see Fig. 5.26, p.236). The line drawing corresponds to the northern part of the mountain (From Hunt & Tucker, 1992). This Figure is located on Fig. 4.17.

systems tract is a sequence boundary, the upper surface to this sequence is the base of the second transgressive systems tract (TST II) of the BA1 sequence. In this first highstand systems tract of BA1 the lowermost demonstrably shallow-water, subhorizontally bedded toplap strata of the sequence are developed as can be

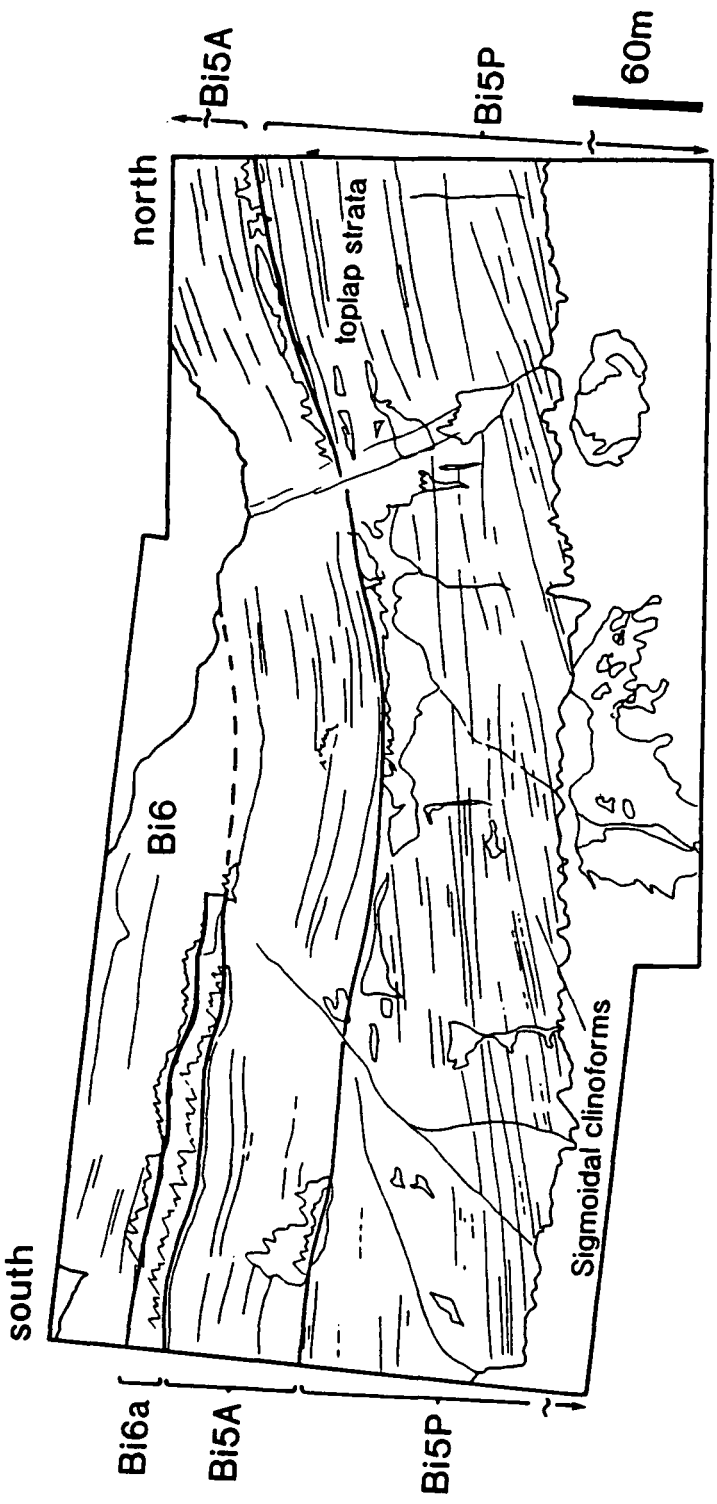

Figure 6.14. Paired photographs (opposite) and line drawing (above) of Bi5P, Bi5A and Bi6 as seen in the northern Archiane valley in the southern Glandasse plateau, southern Vercors. Note that the clinoforms have a sigmoidal to sigmoidal-oblique stratal pattern. These are equivalent to those seen at La Montagnette (Fig. 6.13). The toplap strata to Bi5P reach a thickness of 55-60m indicating a relative sea-level rise of this magnitude during the deposition of this unit. The boundary between Bi5P & A are marked on the 'shelf' by the development of a prominent bedding surface. See also Fig. 6.15. This Figure is located upon Figure 5.7, p.199

observed in the northern Archiane valley within Bi5 (eg. Fig. 5.29, p.240). The systems tract is composed of two aggradational-progradational parasequences, Bi4 and Bi5P both of which offlap basinwards. Bi4 progrades basinward by approximately 500m and Bi5P by a further 1.2km (eg. Fig. 6.5) as can be spectacularly seen both at La Montagnette (Fig. 6.13) and in the Archiane Valley (Figs 5.7, 6.13, 6.14 & 6.15). Clinoforms within this systems tract are well developed in Bi5P and dip almost exactly south as can be seen in Figures 5.7, 6.13 & 6.14, suggesting that the sediments supplied to the slope were derived from the north. This contrasts markedly with the lowstand deposits (Borne Bioclastic Limestone Formation) which are interpreted to have been derived from the east.

Member Bi4 and much of Bi5P have subhorizontal bases to their prograding clinoforms and their foreslope strata thin gradually basinward (eg. Figs 6.5 & 6.13). This is the depositional pattern of an accretionary slope apron (eg. Fig. 3.23, p.85). In the Cirque d'Archiane (Figs 5.7, p.199 & 5.26, p.236) the initially subhorizontal base to Bi5P can be seen to change its basal relationship basinwards from a subhorizontal to a descending geometry, south of the Pierre Ronde Rocher (eg. Figs 5.26, 5.28 & 6.15). This change of basal geometry is interpreted to have developed as Bi5 slope sands prograded into a pre-existing topographic depression upon the slope, a collapse scar (*et2*, Fig. 5.26, see Section 5.3.3). This change of the basal

---

Figure 6.15. (Facing page) Paired photo-panorama and line drawing of the northern Cirque d'Archiane as viewed from just north of the Pierre Ronde Rocher. In the panorama the subhorizontal to descending base developed within Bi5P can be seen. This package is overlain by the aggradational Bi5A which represents a type 2a transgressive systems tract, composed of six subtidal punctuated aggradational cycles (numbered 1-6). The upper-most of these cycles is retrogradational, composed of orange bioclastic sands and overlain by the Lower Fontaine Colombette marls (LFCM) which represent the second mfs to the BA1 sequence. The strongly progradational sand package which downlaps onto this flooding surface (*Dnb*) is the BA1HST II and is erosionally overlain by SbBA2 at the base of rudist facies which are ornamented with a 'v'. These rudist facies are the lowstand package to sequence BA2 and are downlapped (*Dnc*) by the basal surface of the thick type 2a geometry transgressive systems tract. See text for further discussion (located on Fig. 4.17, p.132).

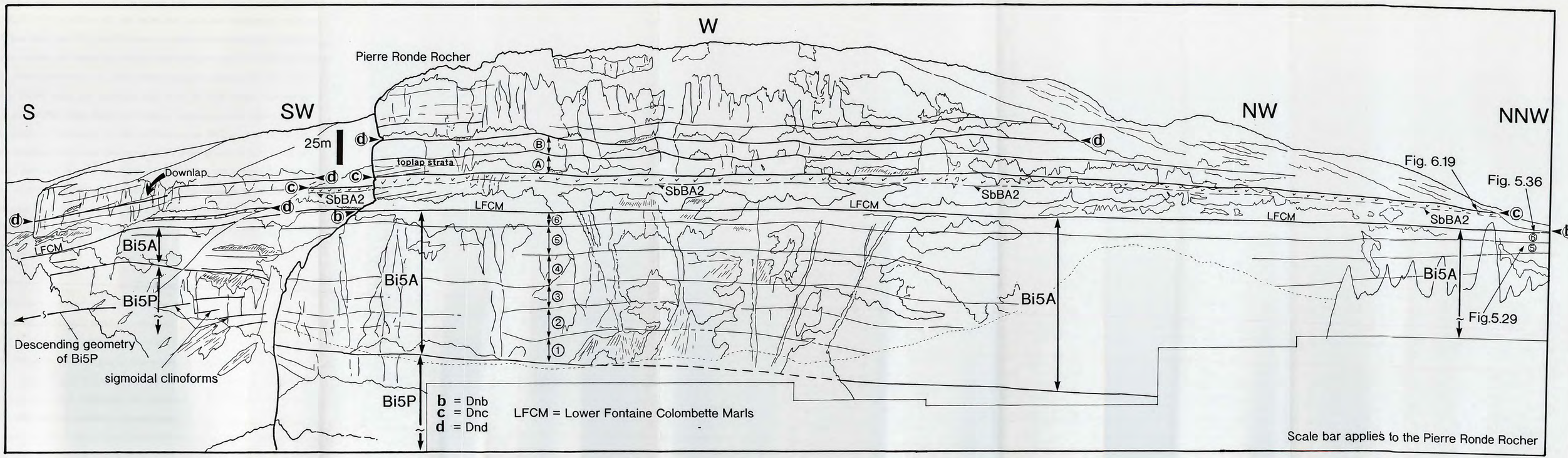
W
Pierre Ronde Rocher
S
SW
NW
NNW
25m
Downlap
toplap strata
SbBA2
LFCM
Bi5A
Bi5P
Descending geometry of Bi5P
sigmoidal clinoforms
b = Dnb
c = Dnc
d = Dnd
LFCM = Lower Fontaine Colombette Marls
Fig. 6.19
Fig. 5.36
Fig.5.29
Scale bar applies to the Pierre Ronde Rocher

geometry to Bi5P is associated with a marked change of mid-lower slope facies from dark-grey interbedded limestones and shales (eg. Fig. 4.34B, p.177) to light-grey limestones without interbedded shales, as seen in Figure 5.37, both below and above the major channel. This change of slope morphology appears not, however to have changed the gross pattern of slope sedimentation, an accretionary slope apron. Shallow-water toplap strata of Bi5P pass basinward into quite steeply dipping clinoforms which have a sigmoidal to sigmoidal-oblique stratal pattern (Fig. 6.14). These toplap strata of Bi5P are at least 55m thick in the northern Archiane valley (Figs 5.7, 5.26 & 6.14), suggesting a relative sea-level rise of this amplitude during the Bi5P. The rate of this relative sea-level rise is interpreted to have been less than the rate of shallow-water sedimentation so that excess sands were produced at the 'shelf'-margin and shed onto the slope (see section 4.5.2.D). The upper surface to this systems tract is *not* a sequence boundary, but the base to the second TST of the BA1 sequence, BA1 TST II.

6.2.2. F. BA1 transgressive systems tract II.

This systems tract is characterized by a lower type 2 (transgressive) geometry developed by Bi5A, overlain by the Lower Fontaine Colombette marls which represent the mfs to the systems tract and have a 'type 1' transgressive geometry. The base of this second transgressive systems tract of sequence BA1 is marked by the cutting of channels on the mid-lower slope (*et3*, Figs 5.26 & 5.37, p.251). These erosional channels are filled by limestones with interbedded shales, contrasting with the preceding slope facies of Bi5P where shales are absent (eg. see Fig. 5.37). These shales interbedded into the limestone-dominated foreslope are interpreted to represent a 'backstepping' of facies on the slope, as can be seen in Figure 5.37 (p.251). On the 'shelf' the base of the TST is marked by a prominent, laterally continuous bedding surface (eg. Figs 6.14 & 6.15) which divides the Bi5 cliff in two on the upper slope (eg. Bi5A-P, Figs 5.26, p.236 & 5.28, p.239). Thus, the lower, aggradational part of the TST has a parallel-parallel stratal pattern developed on the 'shelf' and upper slope

in the northern Cirque d'Archiane (Figs 5.7, 5.26, 5.28, 6.14 & 6.15). By way of contrast, on the mid-lower slope the basal surface of the TST is erosional (eg. *et3* Figs 5.26 & 5.37).

The Bi5A stratal package is approximately 60-65m thick on the shallow-water 'shelf' area of the northern Cirque d'Archiane (Figs 5.27, 6.14 & 6.15). This suggests a relative sea-level rise of 60m during the deposition of Bi5A at a rate equal to the maximum rate of 'shelf'-margin sedimentation. Bi5A can be seen to the north of the Pierre Ronde Rocher in the Cirque d'Archiane to be composed of six 10m thick subtidal punctuated aggradational cycles, suggesting that a series of higher order (fourth order) cycles were superimposed upon the lower order rise (third order) (Fig. 6.15). Within the lower five of these cycles corals and stromatoporoids become more numerous upward within the Bi5A aggradational package, but are notably absent in the sixth, the 'drowning cycle' or 'give-up' cycle at the very top of Bi5A. The stratal pattern developed by the Bi5A is a type 2a transgressive geometry (eg. compare Fig. 5.7 with Fig. 3.20, p.73) and is associated with an increase of the 'shelf' to basin-floor topography. On the basin-floor Bi5A is interpreted to be associated with the deposition of a second, but relatively thin sand package (eg. Fig. 5.38, p.252). Classically, the redeposition of sands onto the basin-floor would suggest a second fall of relative sea-level and development of a type 1 sequence boundary (eg. Fig. 5.38) (eg. Arnaud-Vanneau & Arnaud, 1991, their sequence boundary BA1a, Fig. 4.22, p.141). However, this secondary basin-floor sand package is here interpreted to reflect the buildup of topography during Bi5A, locally oversteepening the slope so that small amounts of sand were bypassed to the basin-floor at this time.

Bi5A is overlain by the Lower Fontaine Colombette marls on the slope (Fig. 5.25, p.234) and their 'shelf' equivalents, sub-wavebase grey wackestones, containing conspicuous rounded, reddened bioclasts (eg. Figs 5.26, p.236 & 5.36, p.250). The Fontaine Colombette marls thin markedly onto the 'shelf' (Fig. 5.26), and on the slope exposure of these marls is generally poor so that it is difficult to observe the stratal relationship of these marls to the underlying upper surface of Bi5A. At the Rocher du

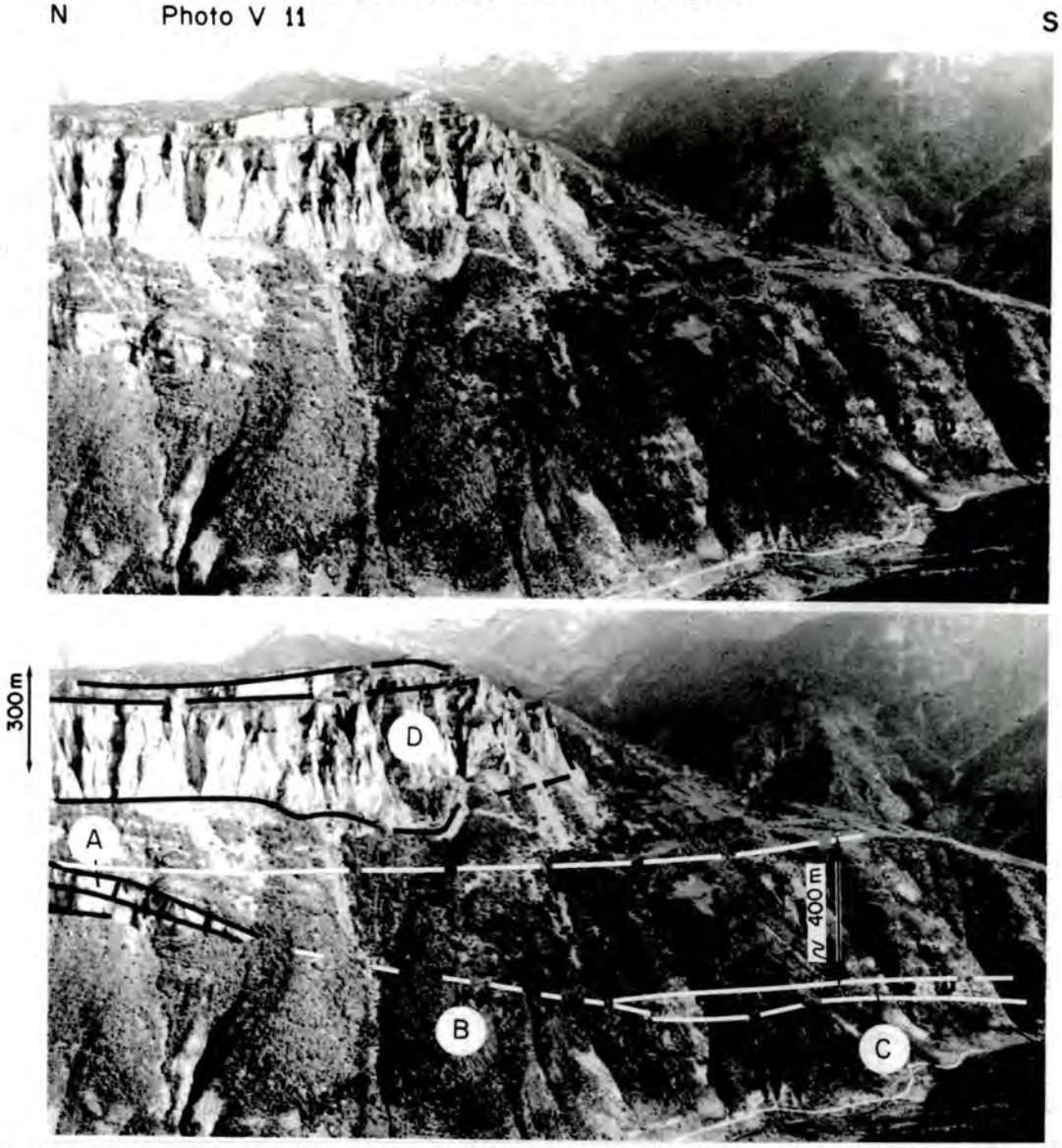

Figure 6.16. The interpretation of the southeastern termination of the Cirque d'Archiane according to Ravenne *et al.* (1987). (A) position of the palaeoshelf; (B) palaeoslope; (C) deep-sea-fan deposits; and (D) new shelf unit atop marly limestones; (B) is interpreted to represent a sequence boundary. See Figs 5.26, 6.17 & 6.18 for alternative interpretations. Section line located on Figure 4.17, p.132.

Combau these marls can be observed to dip basinwards at a lower angle than that of the top to Bi5A so that if projected, they would *appear to* onlap on the slope, developing a drowning unconformity (eg. Fig. 5.33). The development of sub-wavebase wackestones on to the 'shelf' demonstrates that this area had become 'drowned' by a further acceleration in the rate of relative sea-level rise subsequent to that at the base of Bi5A (a type 1 transgressive geometry). Drowning of 'shelf' sedimentation (eg. Fig. 5.36) is interpreted to indicate that this area had become submerged to water depths of greater than 10m, below the maximum zone of

carbonate production (eg. Fig. 3.8, p.48). Water depths upon the 'shelf' do not, however, appear to have been greater than approximately 30m (storm wavebase) as 50-100mm thick sharp-based cross-lam inated and rippled grainstone beds, interpreted as tempestites are interbedded with sub-wavebase 'shelf' facies.

On the slope the Lower Fontaine Colombette marls are overlain by a mid-upper slope wedge (eg. Fig. 5.35), and this is in-turn overlain by dark-grey marls. This slope wedge of the Cirque d'Archiane (slope fan 2 of Jacquin *et al.*, 1991) has been interpreted to onlap the slope (eg. Figs 5.21, 6.16, 6.17 & 6.18). This criterion has been used by Ravenne *et al.* (1987), Jacquin *et al.* (1991) and Arnaud-Vanneau & Arnaud (1991) to indicate a relative sea-level fall and thus a sequence boundary (boundaries B: Fig. 6.16; SbB2: Figs 5.19, 5.20, 5.30B & 6.17; SbBA2a: Fig. 4.22, p.141 & 5.30 respectively). Alternatively, Hunt & Tucker (1992) suggested that this stratal relationship represents a type of drowning unconformity developed subsequent to the drowning of the 'shelf' of the northern Cirque d'Archiane (eg. Fig. 6.18). However, as discussed in Section 5.3.3. the onlap of the slope as observed in the 'type' locality of the Cirque d'Archiane (eg. Figs. 6.16, 6.17 & 6.18) is *apparent.* This *apparent slope onlap* is an artifact of the steep, erosional base (*et4*) to the bioclastic slope wedge and the shelfwards (northerly) thinning of the Fontaine Colombette marls (Fig. 5.26, p.236). The basal relationship of the erosive slope wedge is spectacularly exposed at the along-strike slope exposure to the Cirque d'Archiane, the Rocher du Combau (eg. *et4*, Figs 5.33, p.246 & 5.35, p.249).

In their interpretation Hunt & Tucker (1992) placed the slope wedge above *et4* within their BA2 highstand systems tract. However, the correlation of the progradational-retrogradational-progradational slope cycle between *et4* and *et5* to the single, simply progradational bioclastic sand shoal on the 'shelf' which the interpretation of Hunt & Tucker (1992) demands is far from obvious (eg. compare Figs 5.6, p.199 & 5.22, p.230). The facies of the slope wedge above *et4* have a wackestone-packstone fabric and the bioclasts within this package are characteristically very reddened, similar to those contained within the limestone

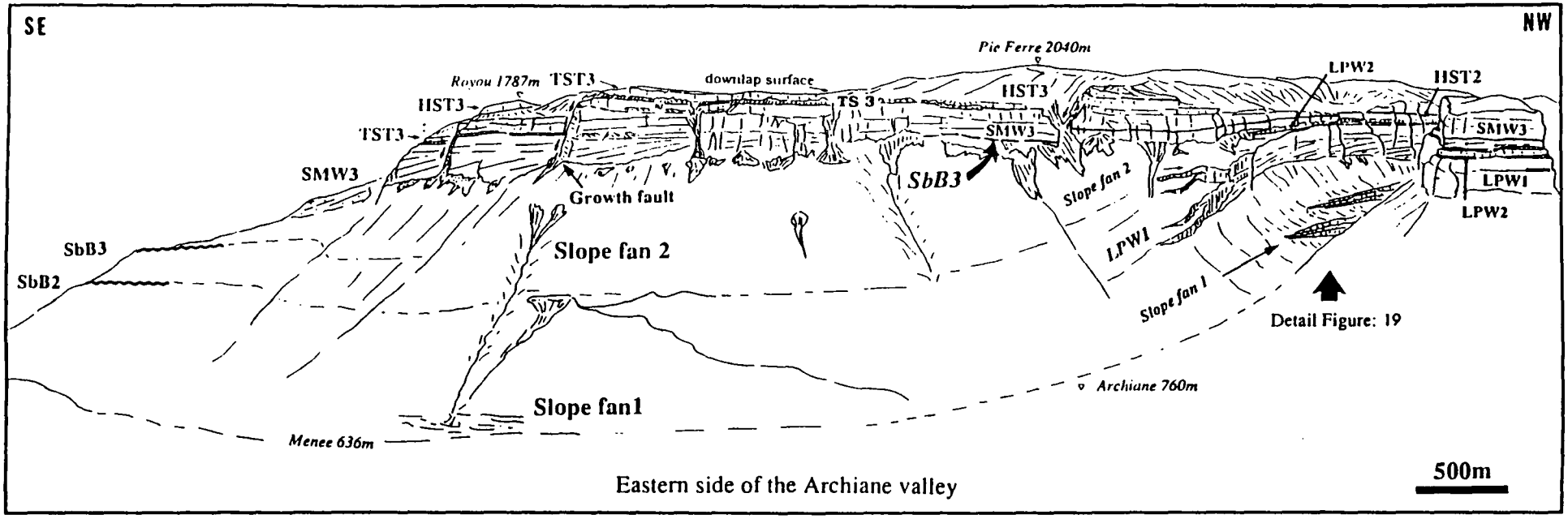

Eastern side of the Archiane valley

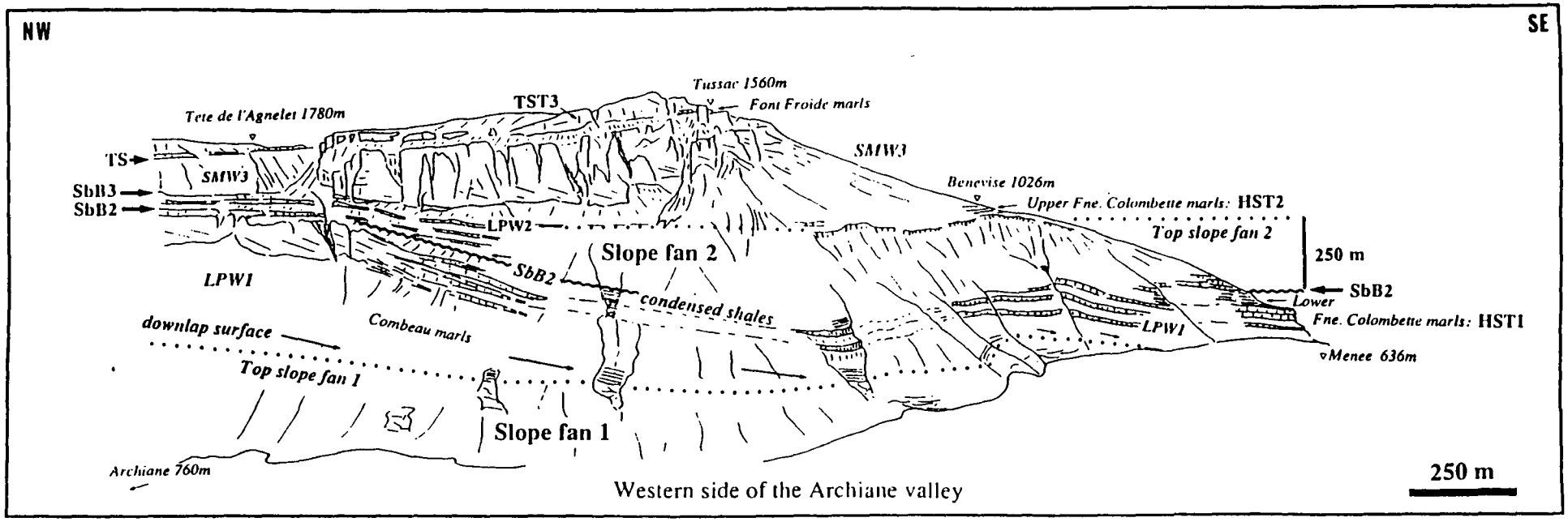

Western side of the Archiane valley

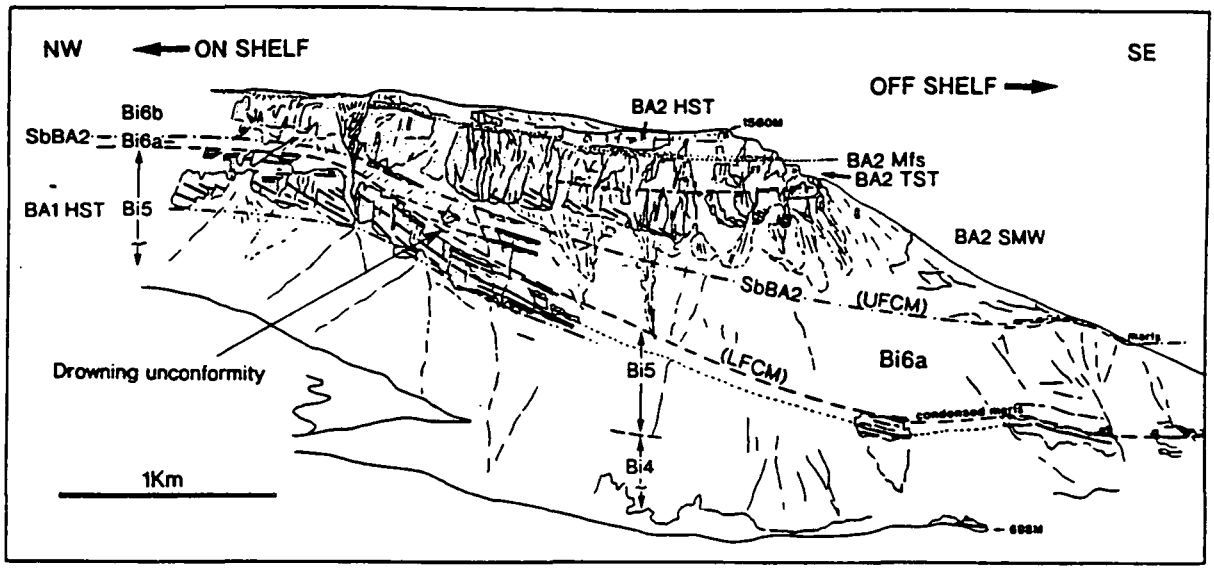

Figure 6.18. (Above) Schematic interpreted line drawing of the southeastern Archiane valley as interpreted by Hunt & Tucker (1992). Sequence boundaries as according to Fig. 6.9. Their BA2 sequence boundary is placed at the top of the distinctive rudist limestones and equivalents which they considered to have been deposited during 'forced regression'. Note the steeply descending concave-up base to Bi6b which contrasts to the western side of the valley (eg. see Fig. 6.17, opposite). Note that slope onlap interpreted by Jacquin *et al.* (1991) (eg. opposite) and Arnaud-Vanneau & Arnaud (1991) as a sequence boundary is in this figure interpreted as a drowning unconformity. See text for further discussion of this stratal relationship in particular.

equivalents to the Lower Fontaine Colombette marls upon the 'shelf'. This slope wedge is also overlain by dark-grey shales, strongly suggesting that this package above *et4* was deposited whilst the 'shelf' was still drowned and as such should be considered within the (late) BA1 transgressive systems tract II. In this interpretation the slope wedge is interpreted to be composed of muds and sands swept off the shelf by density currents generated by major storms. As these density currents moved off

Figure 6.17. (Preceding page) Interpreted line drawings of the Cirque d'Archiane as according to Jacquin *et al.* (1991). Note the position of the B2 sequence boundary, defined by the onlap of bioclastic sands onto the slope (slope fan 2) (see also Figs 5.21 & 5.22). The sequence boundary SbB2 is interpreted to be associated with the filling of the slope during the 'regressive period'. The sequence boundary B3 is interpreted to be of type 2 affinity, associated with aggradational offlap and thick shelf members. This sequence is interpreted to have developed during the early stages of the transgressive period. See Sections 5.3.3. and 6.2.2.F-G for further discussion of the *'onlap'* which characterizes the B2 sequence boundary. Note the differences of the basal geometry of the Bi6 cliff between the east and west sides of the valley and, that the B3 sequence boundary in the north of the Cirque d'Archiane is equivalent to the Surface *Dnd* as defined in this thesis (eg. Figs 5.7 & 6.15).

the subhorizontal 'shelf' onto the slope, they accelerated in response to the greater gradient, increasing their load carrying capacity and thus eroding the Lower Fontaine Colombette Marls from the upper slope. These and the muds moved off from the shelf were deposited on the mid-lower slope where the gradient, and hence the load carrying capacity of the density currents both decreased. As such, the slope wedge above *et4* is considered to be equivalent to the sharp based, cross-laminated grainstone beds interpreted as tempestites up on the drowned 'shelf'. The shales developed above this slope package are thus interpreted as the upper-most surface of the BA1TST II.

6.2.2. G. BA1 highstand systems tract II.

This second highstand systems tract (BA1HST II) is the fifth and final systems tract of the BA1 sequence and has a thickness of approximately 25m on the 'shelf' (eg. Figs 5.6, 5.26 & 6.15). By way of contrast, on the mid-lower slope this systems tract has a thickness of up to 120m (Fig. 5.26, p.236). The highstand systems tract on the 'shelf' is represented by a single strongly progradational parasequence which downlaps asymptotically onto the Lower Fontaine Colombette Marls (*Dnb*, Figs 5.6, p.199 & 6.15). The almost complete lack of toplap strata to this prograding sand-shoal indicates that basinward progradation occurred during a relative sea-level stillstand which followed the mfs (the Lower Fontaine Colombette Marls) to the second transgressive systems tract of BA1 (Fig. 6.15).

Equivalent highstand slope sediments to this progradational 'shelf' package form the second of the three prominent bioclastic slope sand packages which *appear* to onlap the slope in the Cirque d'Archiane (eg. Figs. 5.21, 6.17 & 6.18). This second slope sand package above the Lower Fontaine Colombette marls is well exposed at the Rocher du Combau where it is contained between the two shale levels within surfaces *et4* & *et5* (eg. Figs. 5.22 & 5.30). This bioclastic slope package does not have an erosional base and is interpreted to have developed as the sand shoal package above *Dnb* (Fig. 6.15) prograded to the 'shelf'-slope break of the northern Cirque

d'Archiane from where sands were fed from toplap strata straight onto the slope. Some of these sands may have been bypassed to the basin-floor (eg. see Fig. 5.38), although within the uncertainty of the basin-floor section this relationship cannot be proven or otherwise. This second distinct slope sand package above the top of Bi5A is overlain by dark-grey shales (eg. Fig. 5.30), suggesting a pause in sedimentation subsequent to the deposition of the slope sands. By way of contrast, upon the 'shelf' the highstand systems tract is terminated by *et5*, the BA2 sequence boundary (Figs 5.6, 5.26, 6.4 & 6.15).

6.2.3. Sequence BA2.

6.2.3. A. Summary.

This sequence is bounded at its base by the sequence boundary SbBA2 (eg. Figs 5.6. & 6.15) and above by a type 1 sequence boundary SbBA3 (Figs 6.2 & 6.4). It is composed of the members Bi6 (b-h), Bs1 and Bs2 of Arnaud (1981) (Figs 4.25, p.149, 6.2 & 6.4) and is dominated by shelf-margin type facies. Rudist facies are only developed as a thin package directly above the BA2 sequence boundary and locally near to the top of the highstand systems tract (eg. Figs 5.6, p.199 & 6.15 & Fig. 5.1A, p.193 respectively). The sequence reaches a maximum thickness of 600m on the slope, as can be seen in the southern Archiane valley (eg. Fig. 6.18) and its surroundings and is represented by approximately 70m of sands on the basin-floor (eg. Fig 5.38, p.252). On the Urgonian shelf *sensu stricto* (northern Vercors, Chartreuse and Jura) only uppermost transgressive systems tract and the highstand systems tract are represented and a thickness of 50-80m is typical (eg. Fig. 5.1A, p.193).

In comparison to a classical sequence as illustrated in Figure 2.1 (p.6) this sequence is also very different both in its geometry and the development and timing of erosional truncation upon the slope. The classification of the type of sequence boundary at the base of this sequence is also problematic (Section 6.2.3.B2). Above the basal sequence boundary a thin but sedimentologically distinct package of rudist

facies and their lateral slope equivalents are developed. This package is in-turn overlain by a thick (145m) succession of aggrading-prograding bioclastics sediments (Bi6b-h of Arnaud, 1981) which can be variably interpreted as a lowstand wedge (eg. Arnaud-Vanneau & Arnaud, 1991), shelf margin wedge (eg. Hunt & Tucker, 1992) or a type 2b transgressive geometry. Distinguishing between these alternatives is problematic and, as discussed in Section 6.2.3.B2 a 'hybrid' interpretation is advocated. In this interpretation the distinctive rudistid stratal package is interpreted to represent the 'lowstand' developed above a type 2 sequence boundary. Bi6b-h are interpreted to represent a thick, lower 'general' type 2 geometry, Bs1 a type 1b geometry and the Font Froide marls the mfs to the BA2 TST. This mfs is marked by the drowning of the Glandasse Bioclastic Limestone Formation (the 'general' lowstand wedge of Arnaud-Vanneau & Arnaud, 1990) and is the base to the Urgonian platform *sensu stricto*. Highstand sedimentation upon the Urgonian shelf *sensu stricto* is characterized by high-energy open marine conditions, although locally muddy, restricted rudistid shelf-lagoon type facies are developed at the top of the systems tract. The top of the systems tract is a widespread and frequently dolomitized subaerial exposure surface SbBA3 (eg. Figs 5.1A & 5.8).

6.2.3. B. Position, type of the BA2 sequence boundary and lowstand sedimentation.

6.2.3. B1. The position of the BA2 sequence boundary.

The BA2 sequence boundary is well developed and has its 'type' locality in the 'shelf' area of the northern Cirque d'Archiane were it is coincident with the erosional base of a distinctive package of rudist limestones (eg. Figs 5.6, p.199 & 6.15). This erosional surface can be traced from the 'shelf' onto the slope (*et5*, Figs 5.26, 5.30 & 6.15). Thus, the sequence boundary is associated with the abrupt, erosional imposition of protected and restricted shelf-type facies onto the preceding sub-wavebase prograding BA1HST II sand-shoal (eg. Fig. 5.6). This facies 'jump' is interpreted to have occurred as the result of a low amplitude (<10m) relative sea-level

fall. This fall of relative sea-level did not expose the 'shelf' area of the northern Cirque d'Archiane and so did not fall below the 'shelf'-slope break of the preceding sequence (Fig. 5.26). Using this criterion the BA2 sequence boundary would be described as 'type' 2 boundary from its relationship to the preceding facies and offlap break. However, if alternatively viewed on the scale of the whole Urgonian platform it could be argued that since relative sea-level is interpreted to have still been below the Urgonian shelf *sensu stricto* this second downward facies shift must develop a second type 1 sequence boundary (see 6.2.3.B2 for further discussion).

6.2.3. B2. The 'type' of BA2 sequence boundary.

The discrimination of this sequence boundary as either type 1 or 2 affinity has a profound affect upon the interpretation of the overlying strata of the sequence in terms of depositional systems tracts. By interpretating the BA2 sequence to have a type 1 sequence boundary at its base the overlying aggradational-progradational Bi6(b-h) can be interpreted to represent *either* a lowstand wedge (eg. Arnaud-Vanneau & Arnaud, 1991, Figs 4.22, p.141 & 6.5, their sequence BA2b) *or* alternatively, a type 2 lower transgressive geometry to the BA2 TST, developed above the distinctive rudist 'lowstand' package above the sequence boundary (see below). By way of contrast, if the BA2 sequence boundary is interpreted to be of type 2 affinity then Bi6(b-h) would be interpreted as a weakly progradational, strongly aggradational shelf margin wedge (eg. Hunt & Tucker, 1992) (Fig. 6.18). It should be noted here that this sequence boundary at the base of the rudist facies is not identified by Jacquin *et al.* (1991) (see Fig. 6.20) and so no direct comparison to their scheme can be made at this point.

Arnaud-Vanneau & Arnaud (1991) (Figs 4.22, p.141 & 6.5) interpreted Bi6b-h to have at its base a type 1 sequence boundary, overlain by a lowstand wedge systems tract which represents the whole of Bi6b-h (their sequence BA2b). This interpretation of the affinity of the sequence boundary is to a large extent based upon the identification of the Bi6 basin-floor sands (eg. Fig. 5.38) as a basin-floor fan

sensu Vail (1987) etc. (eg. Figs 2.1 & 2.5). However, as mentioned before in this sub-section the exact timing of this redeposition within Bi6 is problematic. By way of contrast, Hunt & Tucker (1992) interpreted the sequence boundary to be of type 2 affinity, but placed the sequence boundary at the top of the rudist facies and their slope equivalents which they suggested were deposited during 'forced regression'. Thus, the overlying Bi6b-h was interpreted to be a thick shelf margin wedge (eg. Fig. 6.18).

A compromise or 'hybrid' between these two schemes is advocated here. It is suggested that the BA2 sequence boundary should be interpreted to be of type 2 affinity. This interpretation can be justified upon the basis that the abrupt facies shift is the main criterion used to identify the BA2 sequence boundary. Firstly, since water depths upon the 'shelf' were less than approximately 10m to develop the toplap strata to the *Dnb* prograding sand package (BA1HST II), then the amplitude of the relative sea-level fall which developed the abrupt basinward facies jump was probably less than 10m. Secondly, as the 'shelf' (as seen in the Cirque d'Archiane) did not become exposed relative sea-level did not fall below the 'shelf'-slope break. Thus, using these criteria as outlined in Chapter 2 for the discrimination of type 1 and 2 sequence boundaries the BA2 sequence is interpreted to be of type 2 affinity. This boundary is placed at the base of the rudist facies and their lateral equivalents, approximately 5m lower than suggested by Hunt & Tucker (1992), and therefore below the third bioclastic slope sand package (eg. compare & contrast *et5*=SbBA2, Figs 5.26 & 5.27 with Fig. 6.18).

The identification of SbBA2 as a type 2 sequence boundary would normally demand interpretation of an overlying aggrading-prograding stratal package as a shelf margin wedge (eg. Bi6b-h, Fig. 6.18). However, the package of rudist limestones and their slope equivalents are interpreted to represent 'lowstand' sedimentation, being both sedimentologically distinct and separated from the Bi6b-h bioclastics by a flooding surface which drowned rudist sedimentation (i.e. the lowstand, see 6.2.3.B3). Thus, the top of the rudist facies and their slope equivalents is interpreted

to be the base of the BA2 TST. Further support for the interpretation of Bi6(b-h)-Bs1 as a transgressive systems tract is that these members build topographically above the shelf (eg. Fig. 6.1, the geometry of a type 2 TST, see Section 3.7.2.B) and that Bi6-Bs1 are coincident with a cluster of beds enriched in organic carbon in the Barremian-Aptian pelagic type section (Fig. 6.7), similar to the BA1TST 1 (Magniez-Jannin, 1991). Thus, the 'hybrid' interpretation for the type 2 sequence boundary followed by a type 2-1b transgressive systems tract is followed in this thesis.

6.2.3. B3. BA2 lowstand sedimentation.

Above the type 2 BA2 sequence boundary a sedimentologically distinct, relatively thin (<10m) stratal package is developed upon the 'shelf' (Figs 5.6 & 6.15). On both the 'shelf' and slope the sequence boundary is associated with minor erosion and is identified as the surface *et5* on Figures 5.22 & 5.26 (pgs 230 & 236 respectively) and SbBA2 upon Figures 5.6 (p.199) & 6.15. On the 'shelf' this stratal package is composed of shelf-lagoon type rudist wackestones-packstones (eg. Figure 6.19) and varies between 5 and 10m thick, reflecting the erosional topography developed into the preceding sequence at its base (eg. Fig. 5.6). Contemporaneous slope facies are also sedimentologically distinctive, a light-grey weathering 5m package of trough crossbedded wackestones-packstones (eg. Fig. 5.31, p.242). These sands are the third prominent bioclastic sand package developed on the slope between the top of Bi5A and the base of the Bi6 cliff (eg. Fig. 6.18), and are separated from the preceding slope sands of BA1HST II by dark-grey shales (eg. Fig. 5.30, p.241). The development of these shales suggests that there was a pause of sedimentation prior to the export of sediment from the 'shelf'. This pause of sedimentation is interpreted to represent the time needed for the establishment of rudist facies on the 'shelf'. It is interesting to note here that even though relative sea-level did not fall below the 'shelf'-slope break erosional truncation is developed upon the 'shelf' and extends onto and down the slope (eg. *et5*, Fig. 5.26). Such a pattern is ideally restricted to times when relative sea-level falls to below the shelf-slope break (type 1

sequence boundaries) (eg. see Section 2.2).

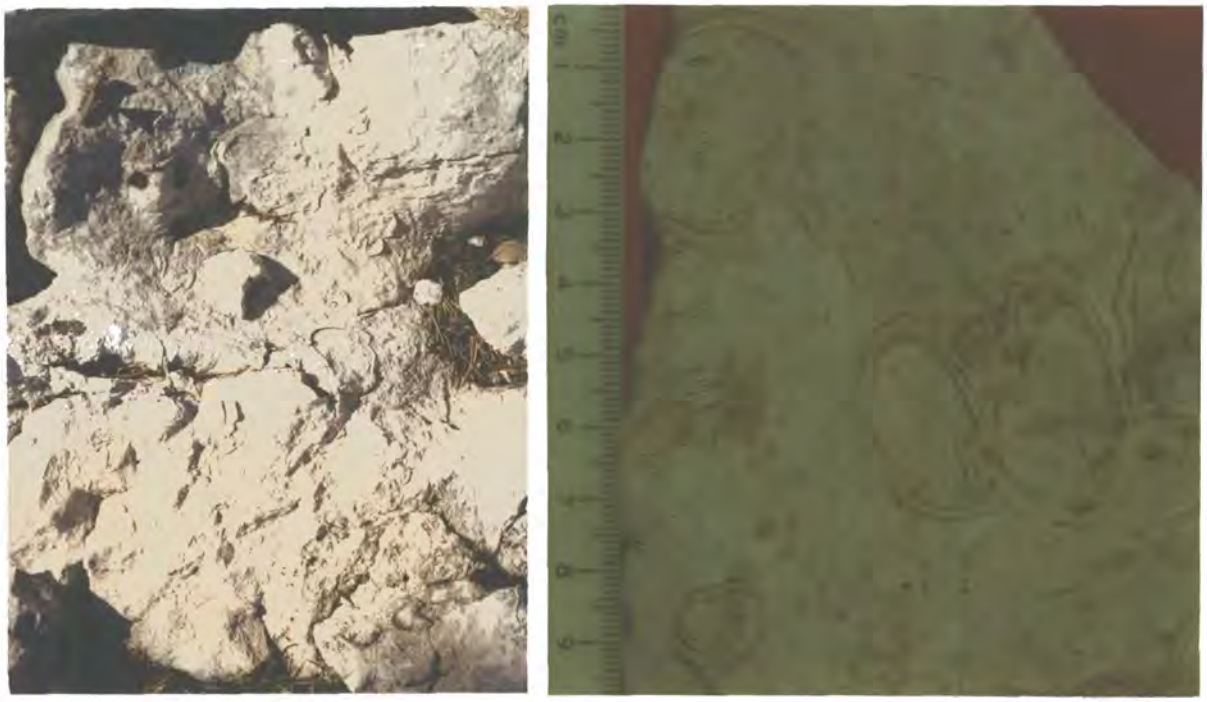

Figure 6.19. Photograph looking down onto a bedding surface of the protected, restricted shelf-lagoon type facies developed above the BA2 sequence boundary as seen in the northern Cirque d'Archiane. The correct orientation of these rudists indicates that during the development of this package the 'shelf' area of the Cirque d'Archiane was protected from storms. These facies form a discrete 5-10m 'lowstand' package. Grasshopper approximately 40mm long for scale. Note that this figure is located upon Figure 6.15.

On the slope this distinctive light-grey bioclastic package is also overlain by dark-grey shales, well exposed at the Rocher du Combau (Fig. 5.30). By way of contrast, on the 'shelf' rudist facies are overlain by downlapping orange weathering shelf-margin type bioclastic sands (eg. *Dnc*, Figs 5.6, 5.26 & 6.15). The development of dark shales on the slope and backstepping of facies on the slope are interpreted to have been contemporaneous and mark the termination of the distinctive 'shelf' rudist limestones and their slope equivalents, drowned as relative sea-level rose at a rate greater than the sedimentation rates of these facies. This flooding surface is interpreted to be the base of the BA2 TST.

6.2.3. C. The BA2 transgressive systems tract.

As discussed above the basal surface of the BA2 transgressive systems tract is marked by the development of dark-grey shales above the slope equivalents of the rudist limestones package (eg. Figs 5.22 & 5.30). These shales are interpreted to be equivalent to the drowning of shelf-lagoon type rudist facies on the 'shelf'. Subsequent to the drowning of these rudist limestones a condensed horizon was developed across the 'shelf', north of the Pierre Ronde Rocher, prior to the progradation and downlapping (*Dnc*) of the succeeding bioclastic sand shoal (eg. Figs 5.6, 5.26, 5.27 & 6.15). The drowning of the 'shelf' (as exposed in the Archiane valley) is witnessed by the absence of an aggradational package developed above the rudist limestones and below *Dnc* to the north of Pierre Ronde Rocher. This suggests that the 'shelf' was submerged by a rapid relative sea-level rise to water depths of greater than 10m (approximately).

By way of contrast to the 'shelf' (north of the Pierre Ronde Rocher) where a condensed section developed from the time of the drowning of rudist sedimentation to the downlapping of *Dnc* clinoforms, the vicinity of the 'shelf'-slope break is characterized by the development of a bioclastic 'buildup'[1] (eg. Figs. 5.26, 5.27 & section 5.3.3.A; note in that section Bi6b-h is termed 'HST' to avoid complex discussion at that point). This upper slope/'shelf' 'buildup' developed topographically above the level of the 'shelf' in the northern Archiane valley and has a convex-up upper surface (eg. Figs 5.26 & 5.27). Sands from this 'buildup' were shed back on to the drowned 'shelf' on to which they both thin and downlap, pinching out just to the north of the Pierre Ronde Rocher (eg. Figs 5.6, 5.26 & 5.27). Slope equivalents of this bioclastic buildup are up to 60m thick as can be seen at the Rocher du Combau, developed above the distinctive lowstand package, and bound above by *et6* (Figs.

[1] The term buildup is here enclosed by inverted commas as to many workers the term is synonomous with organic sedimentation. Here the term refers solely to the convex-up shape of the bioclastic wedge in the vicinity of the 'shelf'-slope break, dominated by bioclastic sediments which are not organically bound. Thus, the term 'buildup' is here used to describe the geometry of this stratal package alone.

5.26, 5.22 & 5.30). The bioclastic 'buildup' and slope equivalents are conspicuous for their characteristic orange weathering (eg. Fig 5.6 & 5.22), a reflection of the abundance of pervasively ferruginised bioclasts within this package. The abundance of such ferruginised bioclasts suggests a relatively slow sedimentation rate and that the 'buildup' developed below normal wave base (>10m), sands developed above wavebase are characteristically cream coloured and unferruginised. Thus, as the 'shelf'-margin 'buildup' is interpreted to have developed sub-fair weather wavebase it is thought to have developed in response to the focusing of storm and/or oceanic currents at/or along the 'shelf'-slope break.

The growth of the bioclastic 'buildup' at the 'shelf'-slope break was terminated by the southerly progradation of a bioclastic sand shoal from farther back on the 'shelf' (not seen on the Glandasse plateau) (eg. Figs. 5.26 & 5.27). These sands form a single 10m subtidal shallowing-up package or parasequence (eg. *Dnc* A Fig. 6.15). The constancy of the thickness of this unit across the 'shelf', of both its clinoforms and toplap strata strongly suggests that this progradational package developed during a stillstand of relative sea-level, subsequent to the punctuated rise of the relative sea-level which drowned rudist sedimentation. On the 'shelf' this progradational sand unit downlaps asymptotically onto a condensed horizon of reddened mudstones (*Dnc*, Figs 5.6, 5.7 & 6.15). Contrastingly, southwards, in the vicinity of the 'shelf'-slope break this same sand shoal downlaps onto the bioclastic 'buildup', the development of which the progradational package is interpreted to have terminated. It is notable that the base of this package is quite abrupt to the south of the Pierre Ronde Rocher where it downlaps onto the bioclastic 'buildup' (eg. Fig. 5.6), and is possibly locally erosional.

In the south of the Archiane valley and at the Rocher du Combau the base of this package is very different from that on the 'shelf' (eg. Fig. 6.15). Basinwards of the 'shelf'-slope break bioclastic sands descend steeply and have an erosional base which is concave-up both in strike and dip sections (eg. *et6*, Figs 5.22, 5.26 & 5.30, and also see Figs 6.17 & 6.18). The development of this *et6* erosional truncation upon the slope is frequently spectacular (eg. Figs 5.32 & 5.33). Correspondingly, the

stratal package (*Dnc* A-B, Figs 5.7, 5.26 & 6.15) above the erosional truncation thickens considerably basinward of the 'shelf'-slope break interface. Whereas clinoforms have a height of approximately 5-7m upon the 'shelf' (Fig. 6.15) in the south of the Archiane valley and at the Rocher du Combau clinoforms have a height of some 40-50m (eg. see Figs 5.7, 5.33 & 6.18).

As discussed in Section 5.3.3 this concave-up erosional base to Bi6b-h is interpreted as a sequence boundary by Jacquin *et al.* (1991) and Arnaud-Vanneau & Arnaud (1991). These workers interpret the development of slope erosion to be coincident with a fall of relative sea-level (eg. SbB3, Figs. 5.21, 5.22, 5.30 & SbBA2b, Figs 4.22, p.141, 5.30 respectively). However, as noted in Section 5.33 and by Arnaud (1981) the descending and erosional base of Bi6b-h is restricted to the slope and does not extend on to the 'shelf' (eg. Fig. 5.26). This relationship suggests that the development of the *et6* surface is related to a change of depositional dynamics between the 'shelf' and slope. There is also no evidence for a fall of relative sea-level in the 'shelf' succession above *Dnc* as is proposed by the interpretation of the *et6* erosional surface as a sequence boundary. On the contrary, the development of punctuated aggradational cycles on the 'shelf' with a fairly constant thickness (eg. Figs 5.26 & 6.15) suggests a series of rapid (punctuated) relative sea-level rises followed by stillstand conditions (parasequences of the Exxon paradigm).

Thus, the *et6* erosional surface at the base of Bi6b-h bioclastic slope sands is here interpreted to have developed as the prograding bioclastic sand shoal above *Dnc* reached the 'shelf'-slope break (*Dnc* A, Figs 5.7 & 6.15). At this time the frontal face of the sand shoal and the 'shelf'-slope break were coincident so that sands moved across the 'shelf' to the front of the bedform were delivered straight onto the slope. It is suggested that as grainflows moved down the front of the bedform and reached the slope they became rejuvenated, increased their load carrying capacity and cannibalised the foreslope as a consequence of the greater gradient (see Section 5.3.3 for further discussion). This initial bypassing and erosion of the upper slope is interpreted to have developed the coarse 'lag' at the base of the Bi6b-h cliff as can be

seen in Figure 5.32 (p.244). Subsequent to the erosion of the slope to a new profile and deposition of a coarse clast rich 'lag' (eg. Fig. 5.34) bioclastic sands began to prograde out from the 'shelf'-slope break as an accretionary apron onto the slope, downlapping onto the coarse sand package immediately above *et6* (eg. Fig. 5.33). The descending, erosional base to the Bi6b-h cliff appears to be steeper and more pronounced on the eastern side of the Archiane valley / Rocher du Combau than on the western side of the valley (eg. see Figs 5.33, 6.15, 6.17 & 6.18). The difference of the basal geometry to the Bi6b-h sands between the Rocher du Combau, eastern Archiane valley and western side of the Archiane valley (eg. Fig. 6.17) suggests that the slope became steeper towards the east so that, correspondingly, the descending erosive base to Bi6b-h also became more intense.

The 'shelf' equivalents of this first progradational package of the BA2 type 2 transgressive systems tract are two asymmetric, 10m thick subtidal shallowing-upward cycles (labelled A & B above *Dnc*, and below *Dnd*, Figs 5.7, p.199 & 6.15). The lower of these is characterized by well developed cream coloured toplap strata, interpreted as high-energy subtidal facies on the shelf (eg. above fair-weather wavebase, 'A', Fig. 6.15) and is very strongly progradational (eg. Fig. 5.7). By way of contrast, the second cycle ('B', Fig. 6.15) is aggradational, weathers to an orange colour and is composed almost entirely of ferruginised bioclasts on the 'shelf'. This package, by way of contrast to its precursor is interpreted to be composed of entirely sub-fair-weather wavebase facies, and was developed as sedimentation rates fell behind rates of relative sea-level rise (eg. Figs 5.6 & Figs 6.15). As such, this aggradational cycle is very similar to the sixth punctuated aggradational cycle of Bi5A which is thinner than its immediate precursors and also composed of ferruginised bioclasts (Fig. 6.15). Both of these aggradational subtidal cycles (6 & b respectively, Fig. 6.15) are interpreted to have been developed as sedimentation struggled and subsequently failed to keep pace with the rate of relative sea-level rise. As such both are directly overlain by flooding surfaces when shallow-water sedimentation was drowned and are referred to as 'drowning cycles' developed as

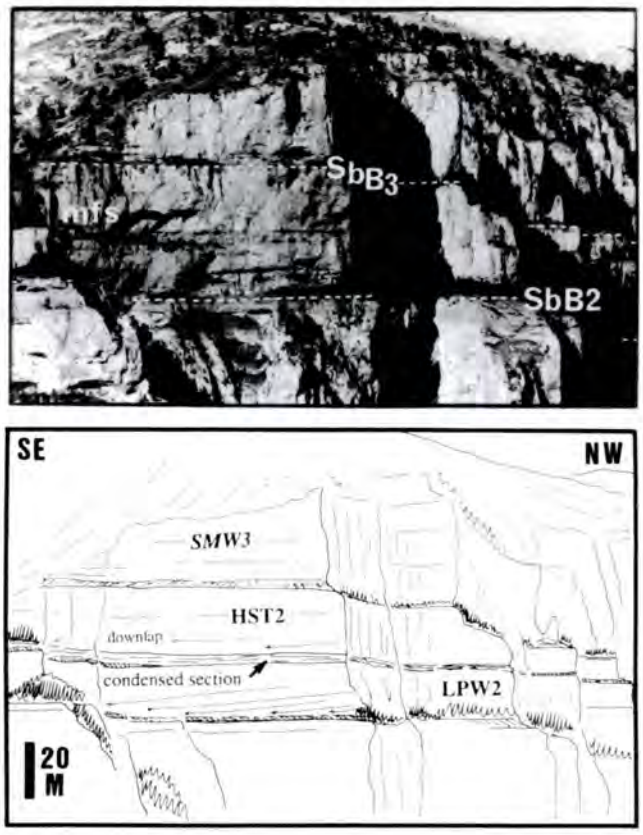

Figure. 6.20. Paired photograph and line drawing of the Pierre Ronde Rocher of the northern Cirque d'Archiane as interpreted by Jacquin *et al.* (1991). Their SbB2 is coincident with the position of the Lower Fontaine Colombette marls and located on the basis of the onlap of bioclastic slope sands on to the top of Bi5A as shown in Figures 5.21 & 6.17. Their HST2 contains the rudist facies above the SbBA2 sequence boundary as shown in Figure 6.15. The SbB3 of this Figure is a downlap surface as shown on Figure 6.15 (*Dnd*). As discussed in this Section this downlap surface is associated with the drowning of shelf facies, not a fall of relative sea-level as the interpretation shown in this Figure suggests.

sedimentation 'gave-up' (Fig. 6.15). The second of these 'drowning cycles' (*Dnc* B, Fig. 6.15) is developed immediately below the downlap surface *Dnd*, a condensed horizon developed subsequent to the drowning of shelf sedimentation on to which a younger prograding sand shoal downlaps (eg. Fig. 5.7). Thus, the *Dnd* surface can be interpreted as a type 1b geometry developed within the overall type 2 geometry TST from an interpreted acceleration in the rate of relative sea-level rise. In complete contrast, the surface *Dnd* has been interpreted by Jacquin *et al.* (1991) to represent the B3 sequence boundary upon the 'shelf' (eg. Figs 6.17 & 6.20), equivalent to the descending base of Bi6b-h as seen at the Rocher du Combau and the southern Archiane valley (eg. Figs 5.21 & 5.22). However, besides being some 10m higher than the 'lowstand' rudist facies (eg. compare Figs 5.7 & 6.15 with Figs 6.17 & 6.20) it can clearly be demonstrated that this surface (*Dnd*) developed from the drowning of

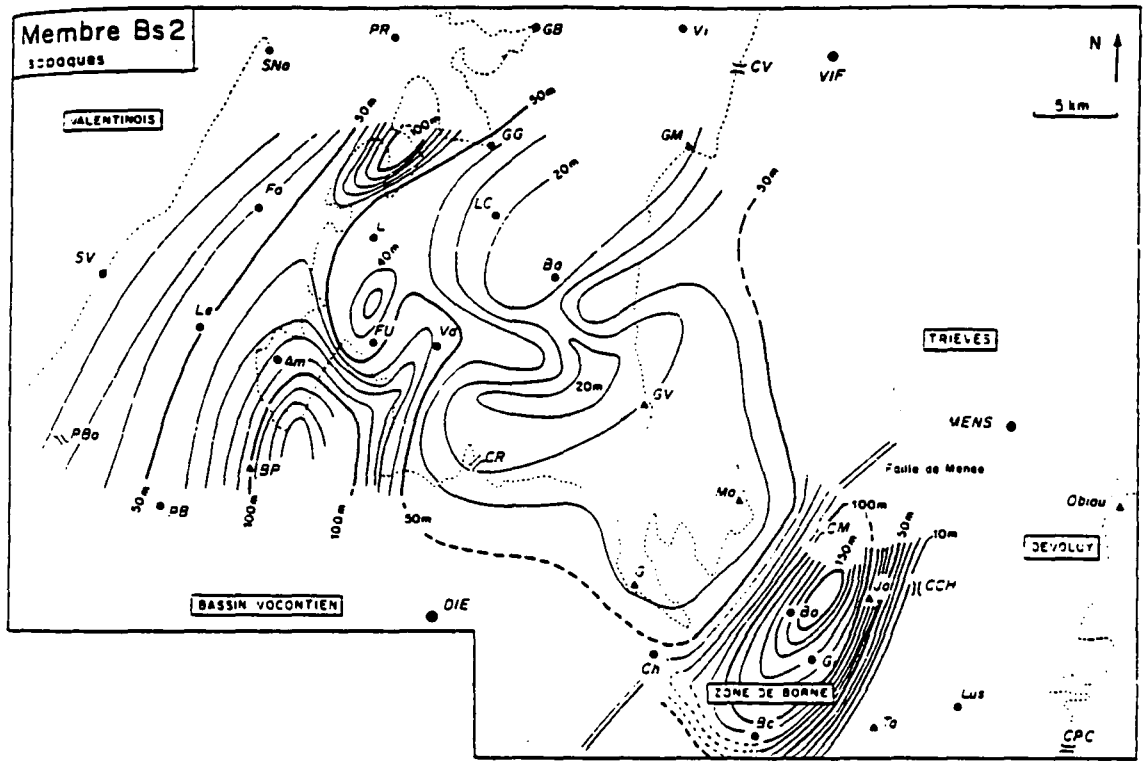

Figure 6.21. Isopach map of the member Bs2 of Arnaud (1981) in the southern Vercors, the BA2 highstand systems tract. Note the thinning of this highstand systems tract onto the raised topography of the 'general' lowstand wedge of Arnaud-Vanneau & Arnaud (1990). This thinning of Bs2 is interpreted to be a reflection of the elevated topography of this area developed during the preceding highstand systems tract. During the highstand systems tract this area is interpreted to have been characterized by high sedimentation rates, but did not shoal to sea-level as currents constantly swept the overproduced sediments off this area. Sediments moved off this area during the highstand are interpreted to have been deposited in surrounding lower-energy areas which are correspondingly thicker than average for the systems tract (eg. see Fig. 6.23). Thus, the BA2 HST systems tract is characterized by a fall of sedimentation rates in this area (eg. Figs 4.8 & 4.10) and this is thought to reflect a combination of the small amount of space available to accommodate sediments and the fact that it was an area of net sediment export. From Arnaud (1981).

'shelf' sedimentation. As such the interpretation of Jacquin *et al.* (1991) appears a mis-correlation and is 180° out of phase to the direction of relative sea-level change as interpreted here.

The succeeding part of Bi6 marks a return to aggradational-progradational sedimentation and the further development of the type 2 geometry, subsequent to the development of a type 1b transgressive geometry, and the drowning of bioclastic sedimentation marked by the surface *Dnd* (Figs. 5.7 & 6.15). The uppermost part of the BA2 transgressive systems tract is characterized by the second development of a

type 1b transgressive geometry, represented by the member by Bs1 of Arnaud (1981) (eg. Fig. 6.4). This geometry can only be resolved at the Rocher du Combau (Arnaud, 1981). In the Cirque d'Archiane differentiation of this unit is difficult as sedimentation rates were higher and no obvious flooding surface at the base of the member can be identified. This is the classical pattern of a type 1b transgressive geometry. The overall dominance of type 2 and 1b aggradational geometries during the transgressive systems tract is interpreted to have developed a topography above the Urgonian shelf as schematically shown in Figure 6.1. This relief was at least of the magnitude of 40m as this the amount by which the succeeding highstand systems tract thins over the 'general' lowstand wedge (eg. Fig. 6.21) when compared to standard shelf sections. Possibly the topography was originally more, but became subdued by differential compaction and/or tectonic subsidence.

The upper surface of the transgressive systems tract is the maximum flooding surface and this is represented by the Font Froide marls. These are developed at the upper surface of the Glandasse Limestone Formation in the southern Vercors as illustrated in Figure 6.22. Their lateral equivalents upon the Urgonian shelf *sensu stricto* are interpreted to occur at the base of the Urgonian Limestone Formation as seen in Figure 5.9 (p.206). At such localities these shales overlie an interpreted transgressive package of uncertain age which is thought to have been derived from the reworking of the Hauterivian sub-wavebase ramp facies as the shoreline moved across the shelf (eg. Fig. 5.9, see Section 5.2.4.C). Carbonate sedimentation did not start-up on the shelf until the mfs was developed and this is interpreted to reflect high water turbidities develop during the reworking of the Hauterivian platform.

6.2.3. C1. Interpretation of relative sea-level changes.

The Bi6b-h to Bs1 bioclastics sands above the distinctive lowstand stratal package and preceding the development of the Font Froide marls (the mfs) have a thickness of approximately 145m in the 'shelf' area of the northern Cirque d'Archiane. This suggests a relative sea-level rise of at least this amplitude from the top of the

Figure 6.22. The BA2 maximum flooding surface, the Font Froide marls of Arnaud (1981) at the Grands Goulets (A) and Baume Rousse (B) of the central Vercors and southwest Glandasse plateau respectively. These are both localities where the 'general' lowstand wedge of Arnaud-Vanneau & Arnaud (1990) is developed (eg. see Fig. 6.3). Compare the development of the mfs here to where the 'general' lowstand wedge is interpreted to have been absent (eg. Fig. 5.9, p.206). Scale in A is geological hammer approximately 350mm long. Scale in B is a small wall to a goat hut approximately 2.5m high (bottom right).

lowstand rudist facies to the mfs. This relative sea-level rise was divided into six distinct phases each marked by the development of a different geometric stratal package and/or surface. Initially the rate of relative sea-level rise was less than sedimentation (*Dnc* A), developing a type 2b geometry (1), but accelerated to develop a type 1b aggrading-backstepping package (2), subsequent to which shelf-margin bioclastic sedimentation drowned (*Dnd*) (3). After this temporary drowning of sedimentation, rates of relative sea-level rise again fell below those of sedimentation and bioclastic sands once more prograded basinwards, downlapping onto the condensed section (*Dnd*) and developing a second type 2b geometry (4). This is succeeded by the second development of a type 1b geometry (Bs1) (5), as the rate of relative sea-level began to exceed sedimentation, ultimately drowning sedimentation, and developing the mfs, the Font Froide Marls (6). The relative sea-level rise which characterized the TST was compartmentalised into a succession of 10m amplitude (approximately) punctuated relative sea-level rises which were superimposed onto the lower order signature. This lower order signature is interpreted to have taken the form of a stillstand followed by a gradual acceleration to the rate of relative sea-level rise to drown sedimentation, developing progradational-aggradational-retrogradational stratal packages (eg. *Dnc* A to *Dnc* B to *Dnd*).

The interpretation of the Bi6b-h as a transgressive systems tract with an overall progradational-aggradational geometry is controversial. However, it is interesting that the interpretation of Bi6-Bs1 as a transgressive systems tract is equivalent to a cluster of beds with a total organic carbon content of greater than 2% in the Barremian pelagic type section (Magniez-Jannin, 1991) (see Fig. 6.7). This is similar to the interpreted position of the BA1 TST I. The deposition of organically derived carbon on the basin-floor is frequently ascribed to times of rapidly rising relative sea-level (eg. the TST).

6.2.3. D. The BA2 Highstand systems tract.

The HST is the first shallow-water carbonate unit to cover the whole of the Urgonian shelf *sensu stricto*, and is interpreted to have at its base everywhere the Font Froide marls and their lateral equivalents (eg. Figs 5.9, p.206, 6.4 & 6.22). However, unlike carbonate highstands in general it did not prograde significantly farther than the preceding 'general' lowstand wedge over which it thins, a pattern also common to sequences BA3, BA4 and BA5 which are also essentially aggradational (eg. Figs 6.4 & 6.5). This highstand systems tract is typically between 40 & 80m thick on the shelf, but as illustrated in Figures 6.21 & 6.23 thins significantly to between 10 & 20m on the central area of the 'general' lowstand wedge, interpreted to have developed an elevated topography during the preceding TST.

The Grand Goulets of the central Vercors, illustrated in Figure 6.23 is one location where the BA2 highstand systems tract can be seen to thin onto the BA2 TST (Bi6-Bs1 of Arnaud, 1981). The thinning of the highstand systems tract onto the elevated topography of the TST and vice versa (eg. Figs 6.21 & 6.23) is interpreted to primarily reflect the small space available for the accommodation of sediments during the highstand due to the inheritance of the topography built-up by the BA2 HST. As illustrated in Figures 4.8. & 4.10 (pgs 115 & 118 respectively) sections located upon the palaeo-topographic high of the Glandasse Formation are characterized by a decrease of sedimentation rates during the BA2 HST compared to other sections located away from the 'general' lowstand wedge. Somewhat paradoxically, the bioclastic sands which characterize BA2 highstand sedimentation over the built-up

Figure 6.23. (Facing page) Schematic cross-section through the Gorge de les Grands Goulets of Arnaud (1981), located up on Figure 4.17 (p.132). In this section the uppermost units of the Glandasse Formation (Bi6-Bs1) which represent the BA2 TST can be seen to thin westward. Conversely, the member Bs2 of Arnaud which represents the BA2 HST and is composed of bioclastic sands developed above the mfs (eg. see Fig. 6.22) thickens westwards. This reflects the decreased space available for the accommodation of sediments above elevated area of the BA2 TST so that excess bioclastic sands formed upon this topographic high were shed into surrounding topographic lows of which the Grands Goulets was one (see also Fig. 6.21).

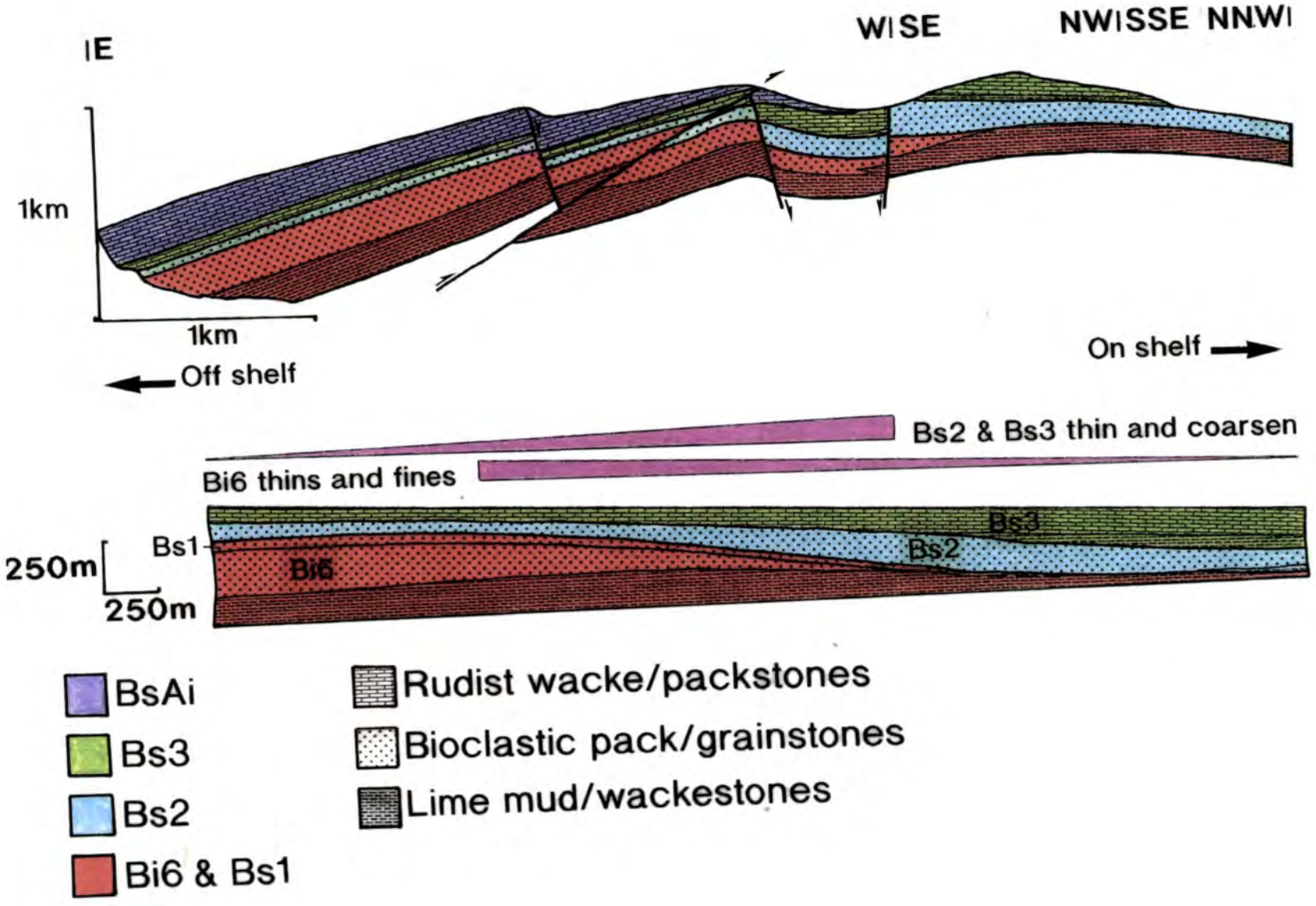
IE
WISE
NWISSE NNWI
1km
1km
Off shelf
On shelf
Bs2 & Bs3 thin and coarsen
Bi6 thins and fines
Bs1
Bi6
Bs3
Bs2
250m
250m
BsAi
Bs3
Bs2
Bi6 & Bs1
Rudist wacke/packstones
Bioclastic pack/grainstones
Lime mud/wackestones

topography of the BA2 TST (eg. Fig. 6.22B) are normally associated with high sedimentation rates. Thus, it is even more surprising that this area did not build to sea-level during the BA2 highstand to develop peritidal facies. This contrasts markedly with equivalent internal shelf-lagoon sections where peritidal facies cap the systems tract (eg. Fig. 5.1A). Thus, it would appear that for some reason the southern Vercors lost its 'advantage' of being both topographically elevated and dominated by facies normally associated with high sedimentation rates so that it did not shallow sufficiently to develop peritidal facies.

The difference between the shelf sections (eg. Fig. 5.1A) which did shallow to develop peritidal facies and the Glandasse plateau area is that the interior of the shelf-lagoon was a region of net sediment import, with muds being washed back into this area by storms etc., whilst the latter was essentially an area of net sediment export. The shallow-water, high-energy Glandasse plateau area is interpreted to have been constantly swept by currents which regularly removed bioclastic sands and deposited them in surrounding topographic lows such as the Grand Goulets (eg. Fig. 6.23). This and other such areas became the depocentres for excess sediments shed off the Glandasse plateau (eg. Fig. 6.21), geographically removed from the shallow-water area of maximum sediment production. This is a form of 'highstand shedding' as described from the Bahamas by Droxler & Schlager (1985) for example. Away from the area where the BA2 type 2b transgressive systems tract is present, in areas such as the northern Vercors and Chartreuse, the highstand systems tract is characteristically dominated by unrestricted, high-energy facies. Only locally, along the northwestern border of the Dauphinois basin are restricted shelf-lagoon type facies developed in this systems tract (eg. Fig. 5.1A).

Another immediate contrast between this highstand systems tract and those which succeed it is that the maximum flooding surface marks the 'start-up' of carbonate sedimentation upon the shelf. Characteristically, within the Urgonian Limestone Formation carbonate shelf sedimentation resumes, at least temporarily, as the shelf was transgressed (Section 5.2.4) (Fig. 5.1A). However, the BA2

transgressive systems tract (away from the area where the Glandasse Bioclastic Limestone Formation is developed) is marked by the reworking of the Hauterivian ramp facies which is interpreted to have sufficiently raised water turbidities to prevent the start-up of normal shallow-water carbonate (eg. see Fig. 5.9, p.206 & Section 5.2.C). Thus, the transgressive systems tract 'drowned' the shelf, submerging it to below storm wavebase. This drowned shelf was inherited by the highstand systems tract and led to the 'unusual' development of the BA2 highstand systems tract which is particularly notable for the lack of facies differentiation over a large area of the Urgonian shelf *sensu stricto.*

The BA2 highstand systems tract is characterized by a shoaling of facies succession from dark-grey sub-storm wavebase facies to white high-energy bioclastic facies in a broadly similar pattern across the entire shelf. The Font Froide marls and equivalents facies (eg. Figs 5.9, p. & 6.22) mark the maximum flooding surface and as such the base of the highstand systems tract. The base of the highstand systems tract is characterized by a 10-15m package of dark-grey-orange mudstones-wackestones interbedded with shales (eg. Fig. 5.9). These limestone facies typically contain an 'oversized' sub-wavebase fauna of bryozoans and serpulids (eg. Fig 4.34C, p.172) and are characterized by black rounded bioclasts. In-turn the interbedded limestones and shales are normally overlain by 5-10m of thin (50-80mm), undulose to lenticular bedded yellow-orange weathering limestones which contain well rounded bioclasts. This facies is interpreted to have been deposited just below normal wavebase. The final part of the shallowing-up cycle is characterized by creamy-yellow to white coloured high-energy bioclastic sands which pass upwards into oobioclastic grainstones and oolites (eg. Fig. 4.33B, p.169) which dominate the systems tract and typically range between 20 and 40m thick. Frequently the top 5-10 m of this package contains flat-lying corals suggesting that there was little or no restriction of circulation on the shelf at this time.

By way of contrast to most of the shelf, sections located in the northwest Vercors and Chartreuse (along the western most part of the Dauphinois basin, eg.

Gorge du Frou and Gorge du Nant, Fig. 5.1A) are characterized by the development of rudist shelf-lagoon facies in the uppermost part of the systems tract. The development of these facies may result from the gradual decrease of energy as the shelf aggraded closer to relative sea-level or from the progradation of restricted type conditions from the Jura platform.

6.2.4. Sequence BA3.

6.2.4. A. Summary.

This sequence is bounded at its base by the sequence boundary BA3, and at its upper surface by the BA4 sequence boundary. The sequence is composed of the member Bs3a of Arnaud (1981) as distinguished in the southern Vercors (eg. see Fig. 6.26) and the lower part of Bs3 of Arnaud-Vanneau (1980) in the northern Vercors and Chartreuse (eg. Fig. 5.1A). The sequence reaches a typical thickness of between 20 and 40m of the shelf (eg. Fig. 5.1A, p.193) upon which facies are almost entirely low-energy and restricted, a complete contrast to the preceding BA2 highstand systems tract (eg. see Fig. 6.26). However, no obvious flooding surface is developed within the BA3 succession in the shelf-lagoon and so the TST and HST cannot be readily differentiated. A further difference between this and other Urgonian sequences is the duration of this sequence (eg. Fig. 6.4). This BA3 sequence developed over a period of some (200-400 000 yrs) and as such is a fourth order sequence (10^5 yrs). This length of time is more typically associated with the development of parasequence sets and parasequences than sequences which are supposedly developed in response to third order (10^6 yrs) relative sea-level changes (eg. Van Wagoner *et al.*, 1990, their table 1, and see also Fig. 6.46)

6.2.4. B. The BA3 sequence boundary: recognition and preservation.

The basal boundary of this sequence is a widespread subaerial exposure surface developed and recognized across the Urgonian shelf *sensu stricto*. The sequence boundary on the shelf is frequently marked by red-brown weathering

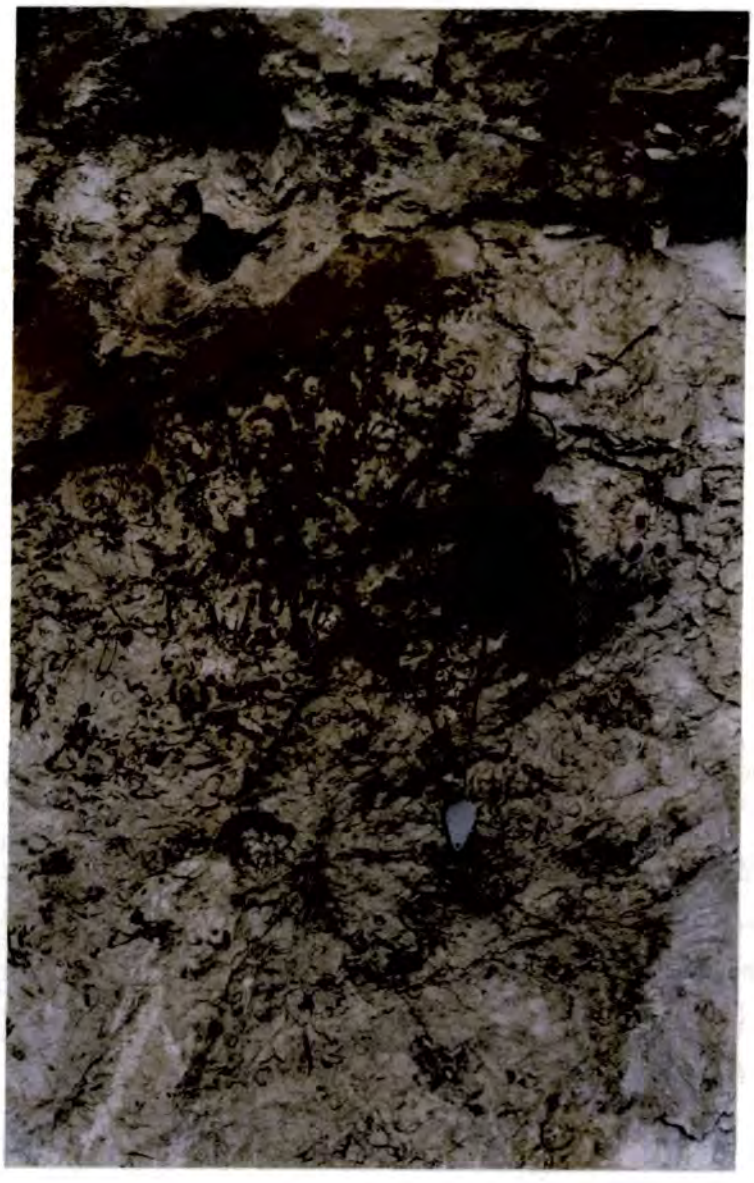

Figure 6.24. The upper-most part of the BA2 highstand systems tract at the Gorge du Nant. At this locality the aragonitic component rudist bivalves below the sequence boundary were leached in the meteoric vadose environment leaving a mouldic porosity which became partially filled by geopetal silts, which themselves became preferentially dolomitized in the burial environment (brown). Also see Fig. 5.8B. This Figure can be located within the Gorge du Nant section upon Figure 5.1A.

dolomites, a diagenetic feature which developed subsequently to the early and selective meteoric dissolution of the preceding BA2 sequence, the feature which identifies this surface as a sequence boundary (eg. Figs 5.8, p.204 & 6.24). Dissolution of the uppermost part of the preceding BA2 highstand systems tract is interpreted to have occurred during subaerial exposure. Generally, meteoric dissolution at the sequence boundary is only weakly penetrative (<1m), did not

Figure 6.25. The BA3 sequence boundary as identified at the Baume Rousse in the southwestern Glandasse plateau. At this locality the sequence boundary is identified by the inclusion of the freshwater algae *Chara* in the strata directly overlying the sequence boundary. These are interpreted to have been reworked as the sequence boundary (subaerial exposure surface) was reworked upon transgression. The sequence boundary itself is a somewhat corrugated erosion surface below which there are no obvious signs of meteoric diagenesis (note this boundary was not petrographically studied). Much of the evidence for subaerial exposure is interpreted to have been removed by shoreface erosion and the subsequent establishment of high-energy facies over the inherited raised topography of the BA2 TST.

develop a karstic topography and is highly selective so that only aragonitic components such as the inner-wall of rudist bivalves were leached and partially filled by geopetal silts (eg. Figs 5.8 & 6.24). This pattern of meteoric diagenesis is interpreted to reflect a relatively small amplitude relative sea-level fall, short period of exposure and relatively low precipitation rates during exposure (see Sections 5.2.3.B & 6.2.4.D for further discussion).

By way of contrast to the sequence boundary as identified in the shelf-lagoon, above the Glandasse plateau area the sequence boundary is typically a low relief (<80mm) corrugated erosional surface (Fig. 6.25). The sequence boundary itself is, however, otherwise inconspicuous save for the inclusion of *Chara* (i.e. freshwater

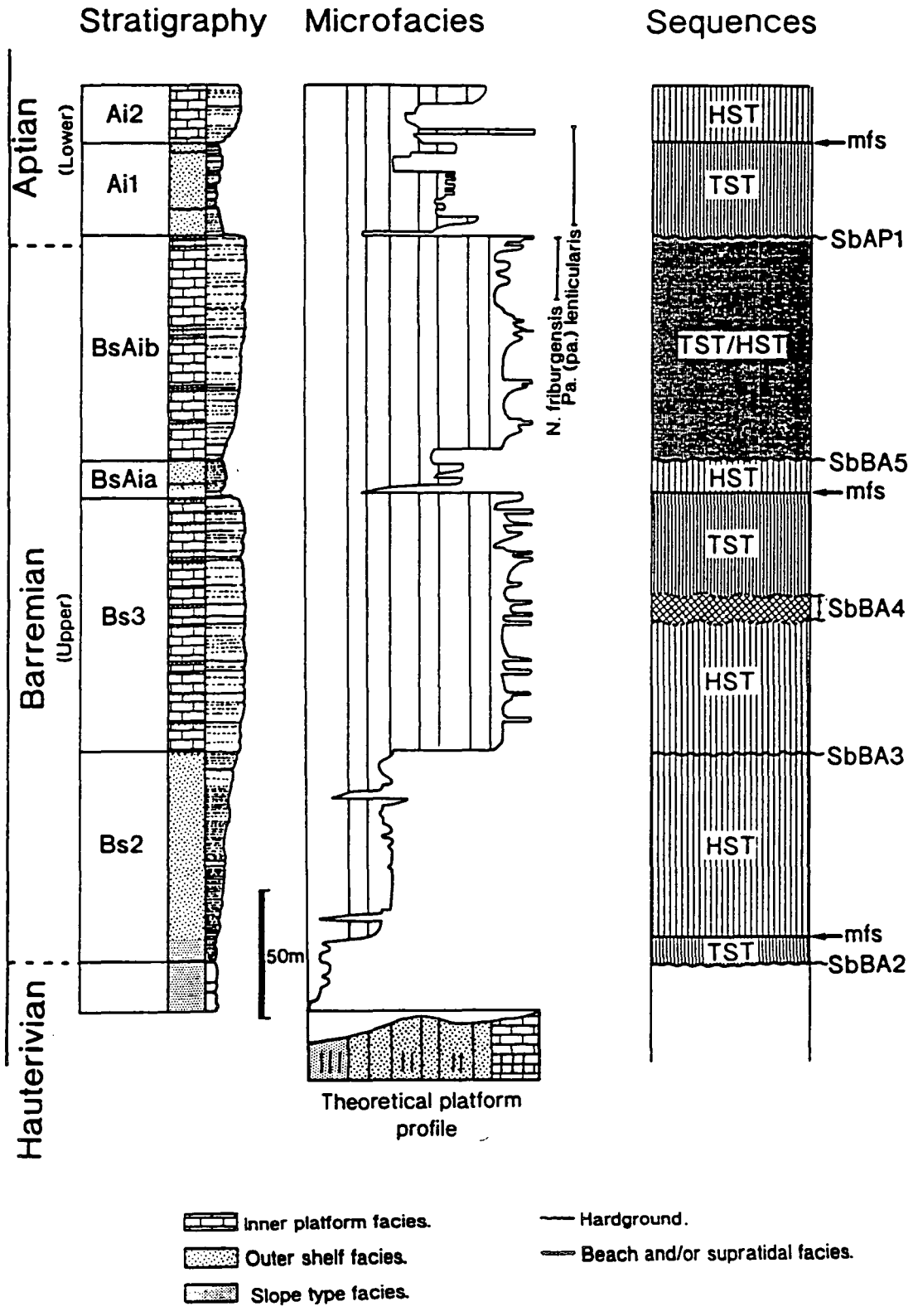

Figure 6.26. The stratigraphic division of the Gorge du Frou section of the northern Chartreuse as according to Arnaud-Vanneau (1980) with the interpreted position of sequence boundaries and systems tracts of this thesis shown in the left column. See Section 4.5 for microfacies.

algae) into the base of the BA3 sequence immediately overlying the erosion surface and the slight facies 'backstepping' across the boundary (eg. Fig. 6.25). The main difference in the preservation and hence identification of the sequence boundary between the shelf-lagoon and shelf-margin is thought to reflect primarily the dynamics of the succeeding depositional system (see also Section 5.2.4.C). In the Gorge du Nant and Gorge du Frou for example (typical examples of shelf-lagoon sections, see Figs 5.1A & 6.26 respectively) the transgression of the shelf is marked by the start-up and subsequent keep-up of restricted, muddy, low-energy facies with the rate(s) of relative sea-level rise. In such cases keep-up of sedimentation prevents the establishment of high-energy conditions back on the shelf so that the sequence boundary in these areas has a high preservation potential. This type of situation is thought to reflect times of 'environmental' stability up on the shelf. In the southern Vercors the re-establishment of high-energy facies over the outer-shelf area is interpreted to be associated with the substantial reworking the sequence boundary.

A pattern of initial preservation, followed by destruction of a sequence boundary is being, and has been developed across the Florida shelf (Parkinson & Meeder, 1991). In Florida Bay a sequence boundary is currently preserved in the low-energy shelf-lagoon where mud banks are established (early TST) (Fig. 6.27). However, as high-energy bioclastic sands transgress back across the shelf and into Florida Bay the early transgressive systems tract (mud banks) and the underlying sequence boundary are both reworked and destroyed (Parkinson & Meeder, 1991) (eg. Fig 6.27). Thus, the development of a high-energy depositional environment directly above an exposure surface (eg. BA2, and BA3 in the Glandasse area, and Florida Bay for example) generally appears to result in the reworking of the sequence boundary to develop at the least a *compound surface* (see Section 5.2.4.C) or may destroy much of the sedimentological evidence for subaerial exposure.

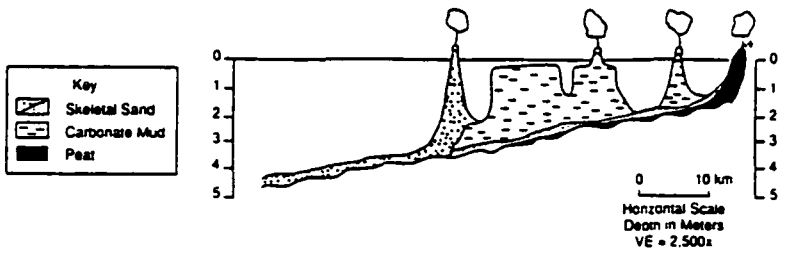

Figure 6.27. Schematic cross-section of the regressive-transgressive stratigraphy of Florida Bay. The sequence boundary is marked by the development of peats and is preserved where directly overlain by low-energy mud banks (early TST). By way of contrast both the early TST and the sequence boundary are destroyed by the migration of high-energy facies across the shelf (late TST) (From Parkinson & Meeder, 1991).

6.2.4. C. The BA3 sequence.

No autochthonous slope wedge is discernible for this sequence from which it is concluded that (if developed) the lowstand wedge must have been volumetrically small. This may reflect a short duration of exposure within this particularly short sequence and, as such, be related to the lack of penetrative diagenesis developed at the sequence boundary upon the shelf (eg. Fig. 6.24). On the basin-floor marls of this age contain abundant fragments of the freshwater alga *Chara* such as in the Gorge de Amayers section (eg. Fig. 5.38, p.252) (uppermost Bs2 of Arnaud, 1981). These freshwater algae are interpreted to have been transported off the shelf whilst it was exposed and / or during the early transgressive systems tract as the shelf was flooded. As can be seen on Figures 6.2 & 6.4 the end of Bs2 as according to Arnaud (1981) is coincident with the deposition of basin-floor slumps/debrites and sands. These can now be re-interpreted to be deposited during times of falling sea-level at the base of the BA3 sequence.

On almost the entire shelf the differentiation of transgressive and highstand sedimentation is difficult, if not impossible (eg. Figs 5.1A & 6.26). The shelf succession is essentially aggradational and dominated by restricted inner-shelf rudist facies with frequent emergence (eg. Figs 5.1A & 6.26). This is a complete contrast to the preceding sequence which is dominated by subtidal high-energy outer-shelf type facies. Thus, the sequence boundary on the shelf is generally marked by both an

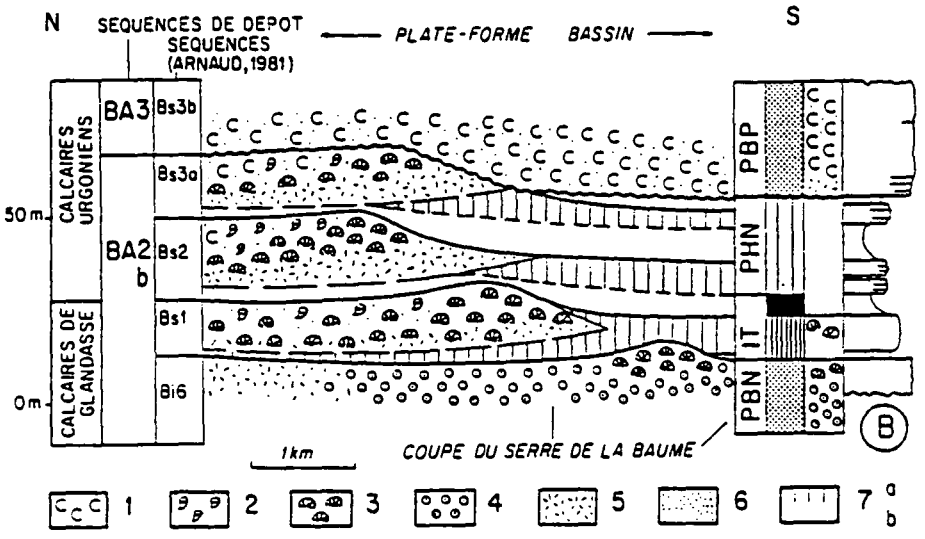

Figure 6.28. Schematic cross-section through the Serre de la Baume showing the members of Arnaud (1981) and the sequences as interpreted by Arnaud-Vanneau & Arnaud (1991) and located on Figure 4.17. Note that the Bs2 to Bs3 are essentially aggradational and are thin relative to their shelf equivalents (eg. see Figs 5.1A & 6.26). This is thought to be a reflection of the elevated topography in the Glandasse area developed during the BA2 TST. *Facies*; 1: small Rudist-Miliolid facies; 2: large rudist facies; 3: coral reef or coral debris facies; 4: oolitic facies; 5: coarse bioclastic facies; 6: fine-grained bioclastic facies; 7: hemipelagic limestones (a) or marls (b). *Systems tracts*: IT: transgressive systems tract; PHN: highstand systems tract; PHN: 'general' lowstand wedge of Arnaud-Vanneau & Arnaud (1990); PBP: shelf margin wedge.

exposure surface and an abrupt 'jump' of facies (eg. Figs 5.1A & 6.26). The transgressive surface upon the shelf is marked by the start-up of low-energy shelf-lagoon type sedimentation over almost its entire area, in the northern Vercors and Chartreuse. This type of facies is maintained throughout the sequence (Figs. 5.2A & 6.26) and is interpreted to reflect a balance between sedimentation rates and rates of relative sea-level rise during the development of this sequence on the shelf. In such areas the transgressive and highstand systems tracts cannot be differentiated (eg. Figs. 5.1A & 6.26). A similar situation is developed over much of the Glandasse plateau area where outer-shelf type bioclastics sit abruptly onto the reworked sequence boundary, although the slight backstepping of facies at the base of the sequence here suggests that the mfs and transgressive surfaces are approximately coincident (eg. Fig. 6.25). At the Serre de la Baume this relationship is more clearly developed, for

here the BA3 sequence does have a well developed flooding surface at its base (eg. Fig. 6.28, unit Bs3a of Arnaud, 1981). The development of sub-storm wavebase facies at the base of the BA3 sequence is interpreted to represent the mfs. This rather different pattern of sedimentation to that developed upon the shelf does suggest that the base of the aggradational restricted lagoonal facies on the shelf (eg. Figs 5.1A & 6.26) is the mfs so that only the HST is represented on the shelf.

6.2.4. D. Discussion of the BA3 sequence.

The sequence boundary is a regional subaerial exposure surface developed across the shelf. The lowstand is not marked by the development of any known autochthonous slope wedge and the penetration of meteoric diagenesis is small. This suggests that the shelf was only briefly subaerially exposed. The BA3 sequence on the shelf is marked by the development of restricted, low-energy facies across the shelf as it was transgressed and rates of relative sea-level rise remained low so that the shelf remained aggraded throughout the sequence (eg. Fig. 5.1A). This package therefore probably represents the highstand systems tract.

Facies of the preceding BA2 HST suggest that water depths were less than 10m so that a sea-level fall of this amplitude could develop the BA3 sequence boundary. The amplitude of the relative sea-level falls which bound the sequence above and below were probably less than 10-20m, and the duration of exposure was probably very short. This overlap of the duration, thickness of the sequence and the interpreted amplitude of relative sea-level change is thought to be characteristic 4^{th} - 5^{th} order sequences developed upon aggraded shelves (and epeiric platforms). Upon such platforms which have built very close to sea-level across much of their width 4^{th} or even 5^{th} order 'sequences' can develop since only a very small amplitude fall of relative sea-level is needed to expose almost the entire platform (eg. 5-10m). Such 'aggraded' sequences are thought to be best developed when the rates and amplitudes of relative sea-level rise are low in comparison to those of sedimentation and there are no significant 'environmental' changes.

6.2.5. Sequence BA4.

Sequence BA4 is composed of the members Bs3b and BsAia of Arnaud (1981) (Figs 5.1A, 6.2, 6.4 & 6.26). The sequence boundary as developed across much of the shelf-lagoon is marked by the stacking of subaerial exposure surfaces (eg. Figs 5.1A & 6.26). As such, it is normally difficult to pin-point the sequence boundary in this part of the platform, as shown in Figures 5.1A and 6.26. On the basin-floor the sequence boundary (and lowstand of relative sea-level?) is represented by the deposition of a second upper Barremian thin sand package which includes fragments of the freshwater alga *Chara* (eg. Fig. 5.38, p.252). At the shelf-margin of the preceding BA3 highstand in the southern Vercors the sequence boundary is marked by a downward shift of facies as illustrated in Figures 6.28 & 6.29. In this area the sequence boundary is marked by the abrupt and erosional juxtaposition of restricted shelf-lagoon type facies onto high-energy (unrestricted) shelf-margin type bioclastic sands (Figs 6.28 & 6.29). At the Serre de la Baume (Fig. 6.28) Bs3b shelf-lagoon facies are developed on to Bs3a sub-wavebase facies. This is interpreted to suggest a relative sea-level fall in the order of 10-20m. The juxtaposition of these facies and stratal patterns across the shelf-lagoon and at the shelf-margin are suggestive of a type 2 sequence boundary.

In complete contrast, at the Font d'Urle the upper part of the Bs3a of Arnaud (1981) (=base Bs3b, Fig. 6.30) is associated with the cutting of a large submarine canyon/channel. The base of this channel cuts up to 50m through the preceding sequence and into the interpreted TST of sequence BA2 (Fig. 6.30). The depth of incision (50m) is more than double the fall of sea-level interpreted from facies shifts of the Glandasse plateau (10-20m) (eg. Figs 6.28 & 6.29). The contrast between the Glandasse plateau area and the Font d'Urle area is interpreted to reflect differences in slope morphology and sedimentation rate(s). This relationship suggests that the magnitude of erosional truncation upon the slope developed during times of falling relative sea-level is not simply related to the amplitude of the fall and/or whether (or not) relative sea-level fell below the shelf-slope break.

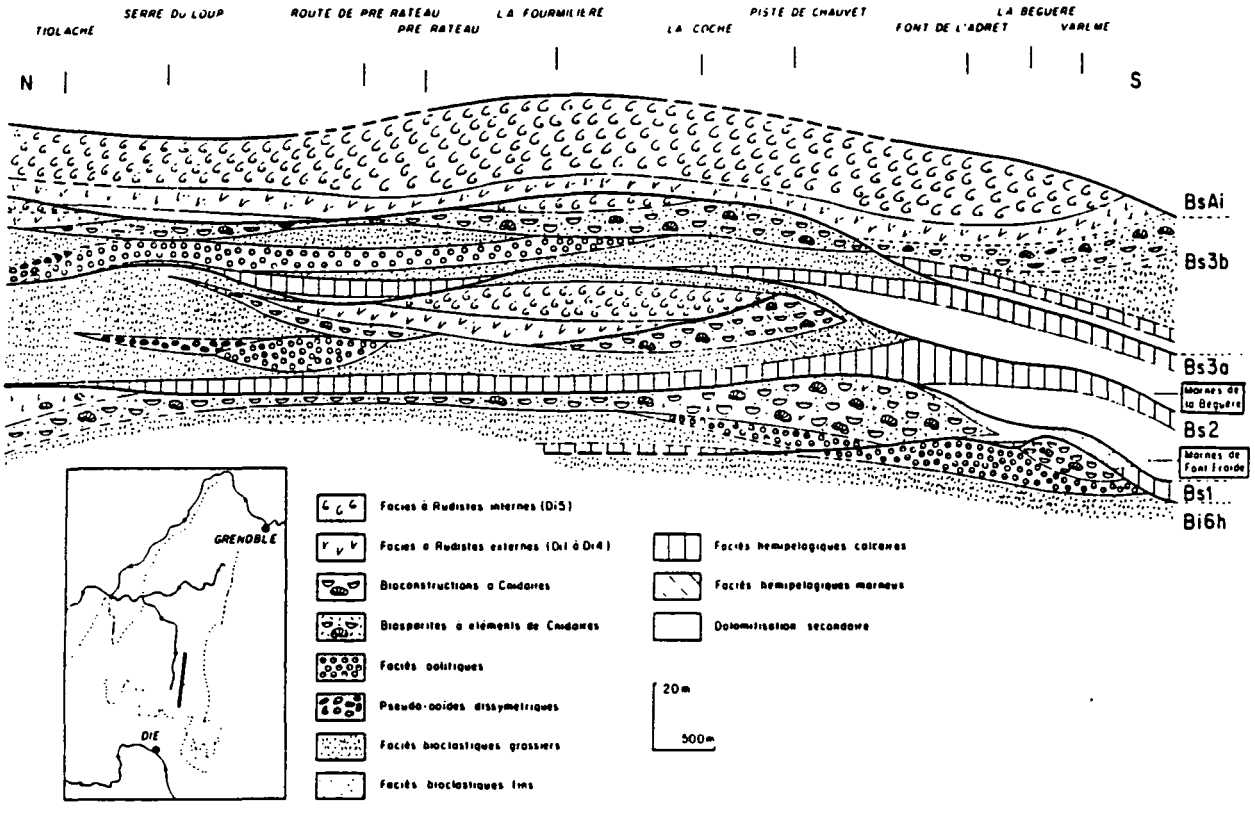

Figure 6.29. Schematic cross-section through the southern Vercors along the Vernaison valley, as located within the inset and on Figure 4.17. This section clearly shows the abrupt juxtaposition of shelf-lagoon type facies over and onto outer-shelf bioclastic sands and corals at the base of Bs3b. The base of Bs3b is interpreted as a type 2 sequence boundary (also see Fig. 6.28).

Facies (from top-left down and across): Faciès à Rudistes internes: shelf-lagoon type facies with rudists and oncolites (restricted circulation); Faciès à Rudistes externes: shelf-lagoon type rudist facies (unrestricted circulation); Bioconstructions à Cnidaires: buildups with *in situ* corals; Biosparites à éléments de Cnidaires: grainstones with coralline grains; Faciès oolitiques: oolitic facies; Pseudo-ooides dissymétriques: facies with asymmetric, deformed ooids; Faciès bioclastiques grossiers: coarse bioclastic facies; Faciès bioclastiques fins: fine grained bioclastic facies; Faciès hémipélagiques calcaires: periplatform limestones; Faciès hémipélagiques marneux: periplatform shales; Dolomitisation secondaire: replacive dolomites. Note that the last two captions on the figure are reversed.

Within the shelf-lagoon, the BA4 TST is essentially aggradational and reaches a thickness of between 25 and 35m (eg. Figs 5.1A & 6.26). Here the base of the TST is associated with the almost immediate start-up of restricted, low-energy lagoonal sedimentation. The start-up of such restricted, low-energy sedimentation across the

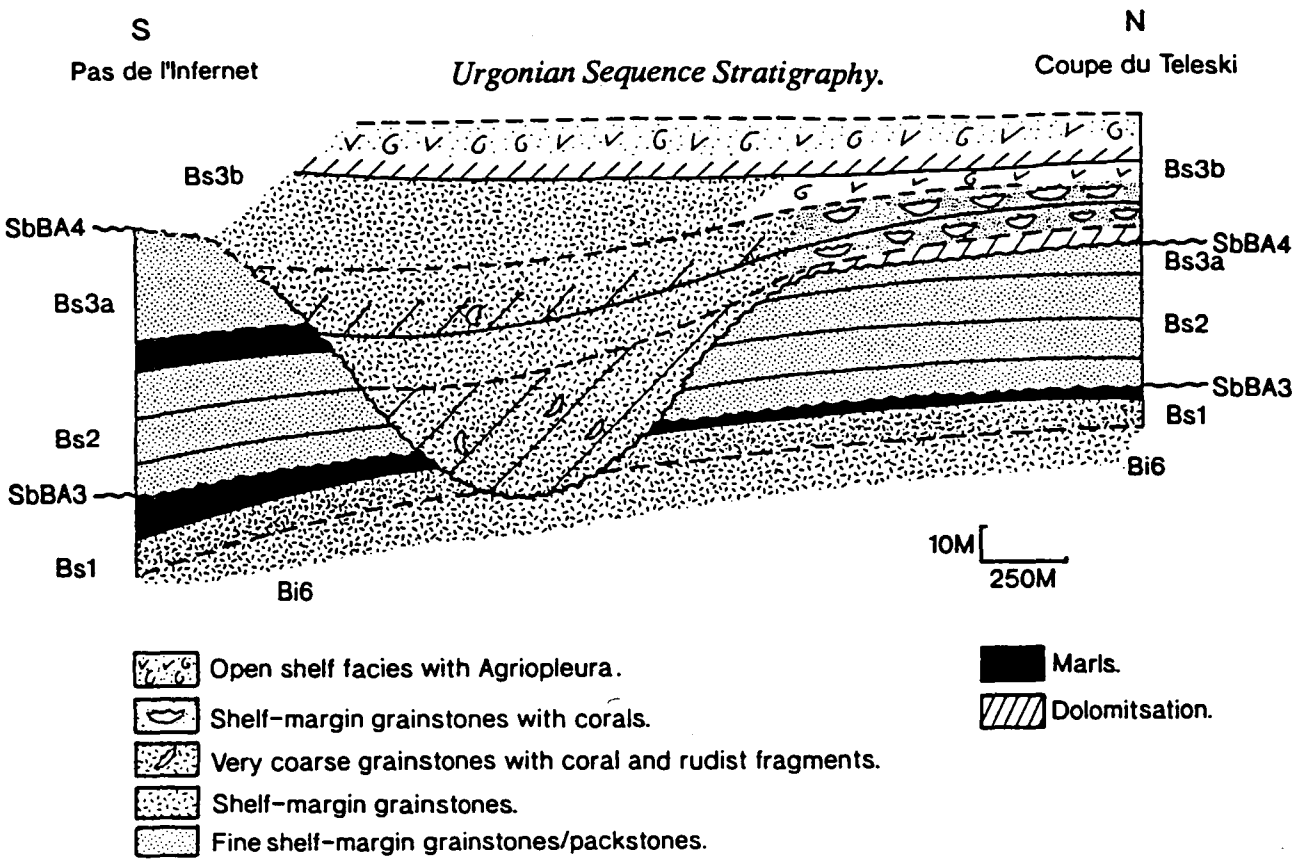

Figure 6.30. Schematic north-south cross-section in the vicinity of Font d'Urle, located on Figure 4.17 (p. 132). At this locality a submarine channel, interpreted to have formed during times of falling and lowstand of relative sea-level cuts up to 50m into the preceding sub-wavebase slope facies. This is interpreted to be associated with a relative sea-level fall of between 10 and 20m which developed a type 2 sequence boundary upon the shelf (eg. see Figs 6.28 & 6.29). The strong erosional truncation at this locality is thought to reflect locally higher sedimentation rates. Note that the stratigraphic members have been slightly modified from Arnaud (1981), after whom this figure is adapted.

shelf during the TST is interpreted to reflect a combination of environmental stability and a slow relative sea-level rise. This prevented the development of high-energy facies across the shelf. Across the shelf-lagoon development of the TST was differential. For example, in the Gorge du Nant section (Fig. 5.1A) facies gradually open and become higher-energy upwards below the mfs (base BsAia). This is interpreted to indicate that sedimentation rates were slightly less than the rate of relative sea-level rise so that facies deepen upwards. Rather differently, at the Gorge du Frou the TST is characterized by an aggradational package of sediments which remained aggraded close to relative sea-level up to the mfs where high-energy outer-shelf type facies are developed abruptly on to low-energy restricted lagoonal peritidal facies (Fig. 6.26). Thus, the differential development of the transgressive systems

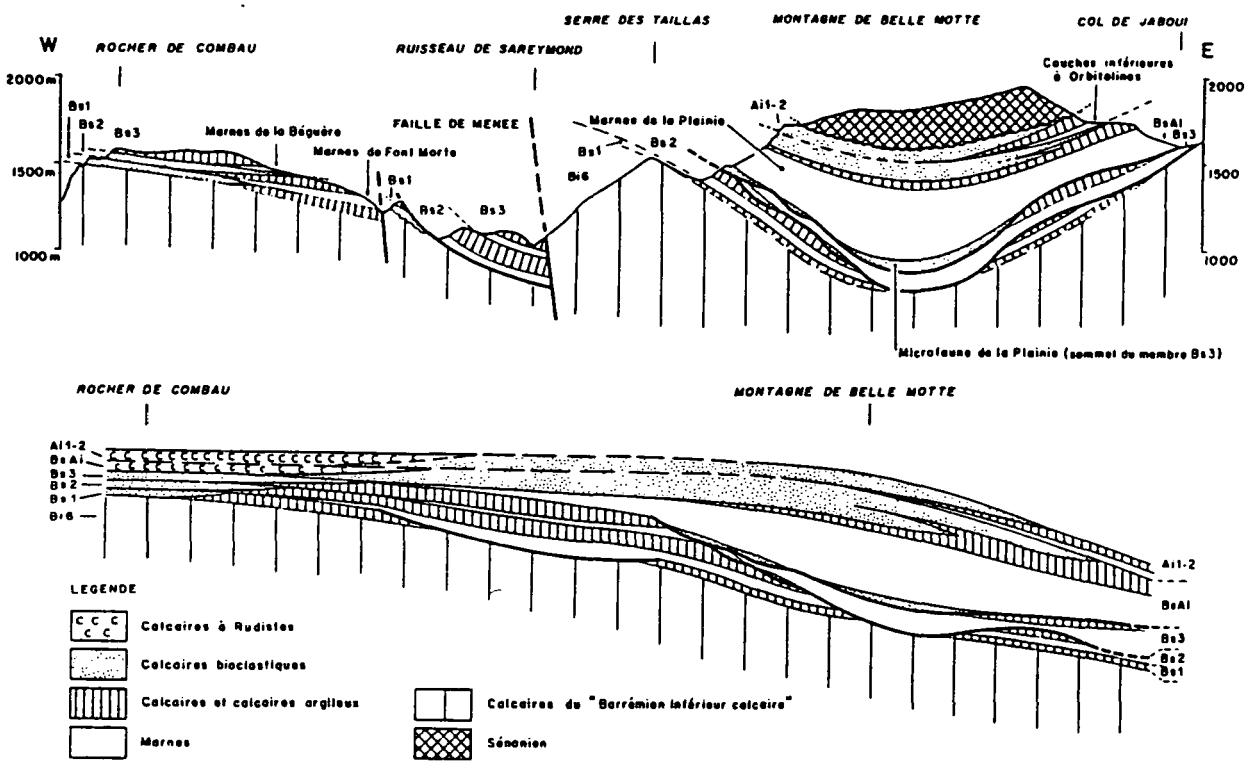

Figure 6.31. East-west cross-section and reconstruction of the margin to the Urgonian platform *sensu lato*, south of the Glandasse plateau, southern Vercors. Note that there are three discrete collapse scars upon the slope at the top of members Bs1, Bs2 and Bs3 of Arnaud (1981) respectively. Slope collapse appears to be preferentially developed during times when the shelf-margin was flooded, as suggested by Galloway (1989). Note that the uppermost collapse scar developed below the Plainie marls (Marnes de la Plainie) is partially filled by bioclastic sands which contain the unique 'Microfauna de la Plainie', indicative of the latter part of Bs3 (Arnaud, 1981). Thus, the uppermost episode of collapse illustrated is ascribed to the TST of the BA4 sequence, just prior to the mfs so that some sands were bypassed from the shelf-margin onto the slope (From Arnaud, 1981, after Arnaud, 1979). Note that the BsAi of this figure is reinterpreted to be a lowstand/shelf margin wedge. It therefore probably is not laterally correlative to rudist facies as shown in the schematic reconstructed cross-section, but onlap these (see Section 6.2.7).

Facies: Calcaires à Rudistes: rudist limestones; Calcaires bioclastiques: bioclastic limestones; Calcaires et calcaires argileux: limestones and fine-grained limestones; Marnes: marls; Calcaires du "Barremien inférieur calcaire": lower Barremian limestones.

tract is interpreted to reflect differences of sedimentation rates within the shelf-lagoon at this time. On the slope, to the south of the Glandasse plateau the upper part of Bs3 is associated with collapse and the minor bypassing of sands through the upper-mid slope (eg. Fig. 6.31) (Arnaud, 1979; 1981). Such collapse and bypassing of sands to the mid-slope would normally, and has been interpreted to have developed at a

sequence boundary (eg. Arnaud-Vanneau & Arnaud, 1991, Fig. 6.5). However, the sands deposited upon the mid-slope contain the unique 'microfauna de la Plainie', characteristic of the uppermost part of Bs3 (Arnaud, 1981). This strongly suggests that slope collapse occurred during the late BA4 TST, rather than during times of falling relative sea-level.

The highstand systems tract of this sequence is represented by a single shallowing-up unit typically between 10 and 40m thick in the shelf-lagoon and is composed of the member BsAib (eg. Figs 5.1A & 6.26). This package normally shoals from high-energy, open-shelf bioclastic and oolitic grainstones to restricted, low-energy muddy platform rudist facies. The top of the sequence is marked by a widespread exposure horizon, the sequence boundary SbBA5.

6.2.6. Sequence BA5.

Sequence BA5 is composed of unit BsAib of Arnaud-Vanneau (1980) and Arnaud (1981) (Figs 5.1A, 6.2 & 6.4). The sequence is contained between two geographically widespread exposure surfaces and/or erosion surfaces, the sequence boundaries SbBA5 and SbAP1 (Figs 6.4 & 6.26). Upon the shelf the BA5 sequence boundary is normally well developed and conspicuous, marked by freshwater limestones, the influx of siliciclastic clays and/or well preserved meteoric diagenetic features (eg. Fig. 5.8A & F, p.204). The lowstand systems tract is represented on the shelf by green-grey coloured freshwater limestones, commonly developed above siliciclastic clays and confined to within small depressions (1-2m wide by 0.1m deep). These are, however, volumetrically insignificant. The freshwater limestones and siliciclastic sediments deposited within the shelf-lagoon are equivalent to incision of up to 40m in the southwestern Vercors, where rudist facies are developed on sub-wavebase slope facies (eg. Fig. 6.32). This basinwards facies jump and incision suggests a significant fall of relative sea-level (20-40m). However, as shown from preceding sequences (SbBA2, SbBA4) the depth of erosional truncation upon the outer shelf/slope is not a particularly reliable criteria to use as a guide to the

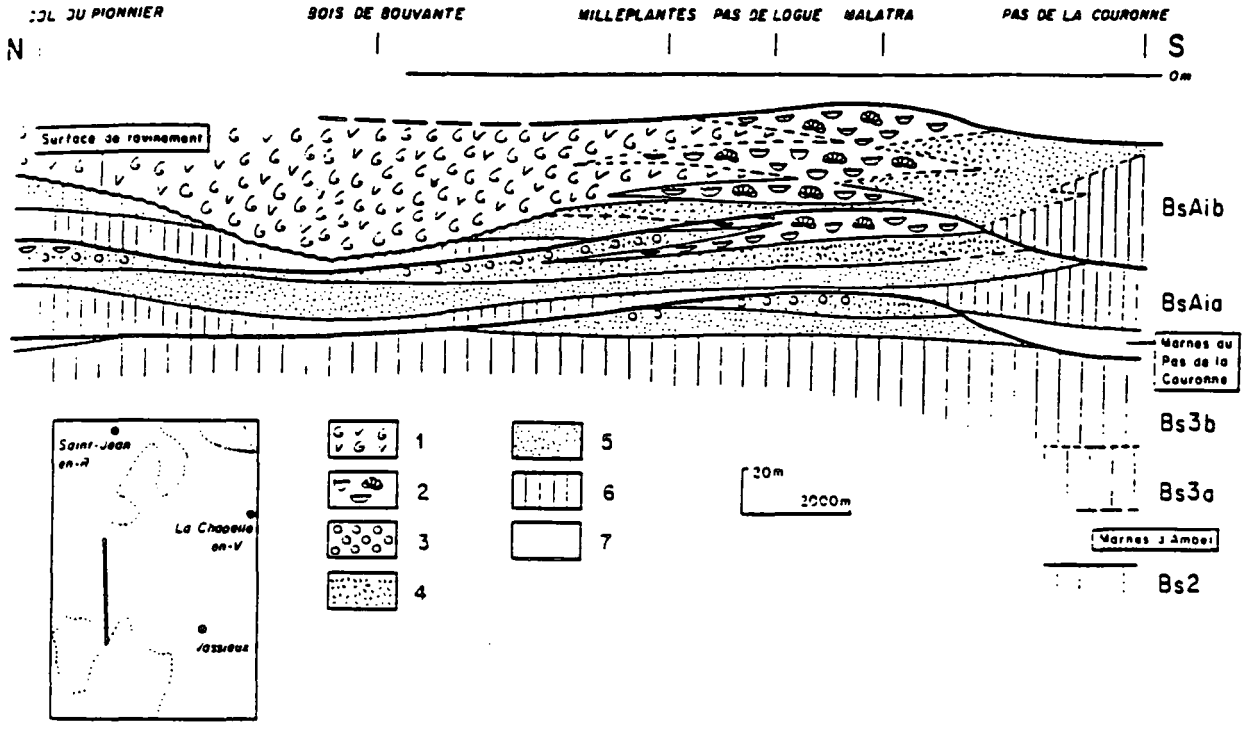

Figure 6.32. Schematic north-south cross-section through the Bois de Bouvante region of the southwestern Vercors as located in the inset and on Figure 4,17 (p.132). This section of Arnaud (1981) clearly illustrates the erosional truncation at the base of his BsAib, the sequence boundary SbBA5 of this thesis. This erosional surface is interpreted to cut at least 30m through the preceding bioclastic slope sands in to sub-wavebase limestones.

Facies: 1: Rudist facies; 3: Coralline facies; 3: oolitic facies; 4: coarse bioclastic sands; 5: fine bioclastic sands; 6: sub-wavebase periplatform limestones and shales; 7: marls. Note that replacive dolomites are omitted in this section.

amplitude of relative sea-level fall at a sequence boundary. Exposure elsewhere of slope facies and lowstand deposits of this sequence is generally poor and so, correspondingly, is the overall geometry and position of lowstand sedimentation.

On the shelf, above the lowstand deposits the transgressive and highstand systems are of approximately equal thickness where the two can be differentiated (eg. Fig. 5.1A). The base of BsAib upon the shelf (the transgressive surface) contains many fragments of the freshwater alga *Chara* (Arnaud, 1981). These are interpreted to have been reworked as the shelf was transgressed. At the Gorge du Nant the transgressive and highstand systems tracts are separated by the development of lagoonal facies containing elongate *Agriopleura* rudists (Figs 5.1A & 6.33). These

Figure 6.33. The maximum flooding surface as identified within the Gorge du Nant section of the northwestern Vercors. Here the surface is developed within a thick succession of generally restricted shelf-lagoonal facies (eg. Fig. 5.1A) and is marked by the development of *Agriopleura* rudists (arrowed). These rudists have an elongate, thin and narrow external form and are characteristic of unrestricted circulation upon the Urgonian shelf (eg. Fig. 4.30, p.159). Lens cap approximately 50mm diameter for scale.

rudists are characteristic of unrestricted protected environments within the Urgonian shelf-lagoon. By way of contrast, at the Gorge du Frou the transgressive and highstand systems tracts cannot be differentiated as there is no obvious 'backstepping' of facies (Fig. 6.26). The contrast between these two sections illustrates the differential sedimentation rates developed across the Urgonian shelf-lagoon. The pronounced and abrupt development of the mfs in the Gorge du Nant (Fig. 5.1A) may reflect a local environmental change and hence reduction of sedimentation rates facilitating drowning. The highstand systems tract is typically between 20 and 50m thick, where differentiated.

The transgressive and highstand systems tracts on the shelf are normally composed of four-five 5-10m thick 4^{th} order shallowing-up cycles (eg. Figs 5.15,

p.217 & 6.4), each of which is capped by a prominent subaerial and areally quite widely developed subaerial exposure surface. Internally, almost all of these 4th order cycles are generally poorly structured. The fourth order cycles illustrated in Figure 5.15 is a notable exception, and demonstrates the classical asymmetric facies profile with an upward increasing proportion of intertidal-supratidal facies accompanied by a decreasing thickness of its component fifth order cycles. Four-five or even more of these fifth order cycles build to form fourth order cycles. These fifth order cycles are typically 1-2m thick and capped by intertidal-supratidal facies (Figs 5.15 & 5.16, p.218). As discussed in Section 5.2.5 and illustrated in Figure 5.16 these higher order cycles are also atypical and do not show the classical asymmetric deep to shallow evolution illustrated in Figure 5.13 (p.125). The rather varied and quite unstructured development of both fourth and fifth order cycles within this BA5 sequence is interpreted to reflect a close balance between sedimentation rates and rates of relative sea-level rise (see 5.2.5 for further discussion).

6.2.7. Sequence AP1.

6.2.7. A. Introduction, the AP1 sequence boundary and lowstand sedimentation.

The AP1 sequence boundary is marked by a convergence of the current sequence stratigraphic interpretations for the Urgonian platform, as is the case for the succeeding AP2 sequence (eg. Arnaud & Arnaud-Vanneau, 1989; Arnaud-Vanneau & Arnaud 1990; 1991; Jacquin *et al.*, 1991, Hunt & Tucker, 1992) (eg. compare Figs 5.1A & B). The AP1 sequence is comprised of the members Ai1, Ai2 and the upper part of the member BsAi of Arnaud-Vanneau (1980) and Arnaud (1981) at the shelf-margin: the BsAi bioclastics below the 'couches inférieures à Orbitolines' as illustrated in Figure 6.31. These BsAi bioclastics (Fig. 6.31) of Arnaud (1981) are reinterpreted to represent a lowstand/shelf-margin wedge as the species of foraminifera *Neotrocholina friburgensis* and *Palorbitolina (Palorbitolina) lenticularis*

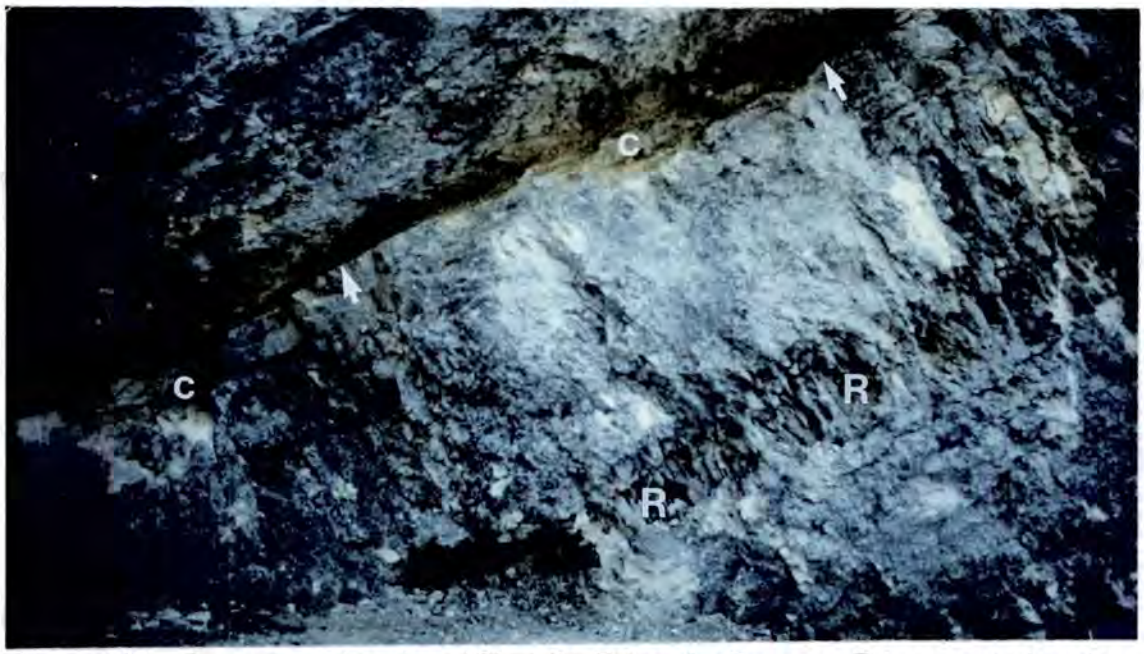

Figure 6.34. The sequence boundary AP1 at the Balcon des Ecouges. This sequence boundary separates the BA5 HST (BsAib) from the lower *Orbitolina* beds (Ai1). The sequence boundary (arrowed) is characterized by a low relief, low amplitude erosional topography and is partially filled by siliciclastic clays. The upper part of these topographic depressions are filled by lacustrine limestones bearing the alga *Chara*(C). Note that approximately 1.5m below the sequence boundary is a recessively weathering zone with strong vertical jointing (R). This separates the meteoric vadose from the meteoric phreatic diagenetic environments and is thus interpreted to represent a palaeo-watertable. Blue notebook 0.3m long (max length) for scale.

have an overlapping range in these bioclastic slope sands (Arnaud & Arnaud-Vanneau, 1989). This is a complete contrast to the shelf where these two species of foraminifera do not have an overlapping range and are separated by the BsAi-Ai1 boundary (Arnaud-Vanneau, 1980; Arnaud, 1981) (Figs 5.1A & 6.26). This boundary, between member BsAi and the lower *Orbitolina* beds (Ai1) on the shelf is commonly marked by meteoric diagenesis and/or freshwater limestones (Figs 5.10 & 6.34) and is interpreted to be the AP1 sequence boundary (Figs 5.1A, 6.2, 6.4 & 6.26). Thus, the slope sands where the species ranges of *Neotrocholina friburgensis* and *Palorbitolina (Palorbitolina) lenticularis* overlap (BsAi of Fig. 6.31) were deposited whilst the shelf was exposed and are therefore interpreted to be an autochthonous slope wedge, developed during a lowstand of relative sea-level. Sedimentologically, the sequence boundary on the shelf is also a conspicuous surface for it separates the typical shelf carbonates of sequence BA5 (eg. Figs 5.15 & 5.16)

from the lower *Orbitolina* beds which, within the Urgonian platform succession are sedimentologically unique (AP1 TST) (eg. Figs 5.1A, 6.2 & 6.4) (Arnaud-Vanneau, 1980; Arnaud, 1981).

The AP1 sequence boundary on the shelf is frequently marked by the development of freshwater limestones (eg. Figs 5.10, p.208 & 6.34). These are commonly contained within small, low amplitude erosive depressions (<0.2m deep) and overlie thin levels of siliciclastic clays (eg. Figs 5.10 & 6.34) (as also noted at SbBA5). At the Balcon des Ecouges (Figs 5.10 & 6.34) the position of the palaeo-watertable appears to be preserved below the AP1 sequence boundary. This is marked by a recessive weathering zone which is sub-horizontal with respect to bedding, approximately 0.3m wide and characterized by strong vertical jointing (eg. Figs 5.10 & 6.34). This preferentially weathered and highly jointed level separates the meteoric vadose and meteoric phreatic (eg. Figs 4.32B, p.163 & 4.33D, p.166) diagenetic environments immediately below the AP1 sequence boundary and is therefore interpreted as the palaeo-watertable developed at this locality whilst the shelf was exposed (Figs 5.10 & 6.34). The development of meteoric diagenesis and/or freshwater limestones across the shelf is interpreted to have been contemporaneous to the progradation of the autochthonous slope wedge in the southern Vercors (eg. Figs 6.4 & 6.31). The exact stratal relationships of this autochthonous wedge to the slope cannot, however, be observed due to subsequent movement and disruption along the Menée fault (eg. Fig. 6.31).

6.2.7. B. The transgressive systems tract.

The transgressive systems tract is characterized by the development of the lower *Orbitolina* beds and their lateral equivalents. At the shelf-margin the transgressive systems tract is associated with the backstepping of bioclastic facies and the deposition of marls above bioclastics sands of the autochthonous lowstand wedge (Fig. 6.31, 'couches inférieures à Orbitolines'). On the shelf the transgressive surface is commonly associated with the reworking of the sequence boundary to develop a

compound surface as outlined in Section 5.2.4.C. For example, at the Font Renard the sequence boundary is reworked as a hardground during the TST and bored by *Lithophaga* bivalves. This particular section is, however, otherwise notable for the atypical development of the transgressive systems tract which is overlain by some 25-30m of marls *below* the lower *Orbitolina* beds. These marls are finely laminated, moderately organic rich, and interbedded with thin limestones. Both limestones and shales contain fragments of the freshwater alga *Chara* and terrestrial plant detritus (eg. Arnaud-Vanneau & Medus, 1977; Arnaud-Vanneau, 1980). These marls and limestones also, however, contain restricted marine foraminifera, and are therefore interpreted to have been deposited within a protected brackish lagoon which received

Figure 6.35. Well developed asymmetric subtidal shallowing-up cycles of the AP1 TST at the Balcon des Ecouges in the northeastern Vercors. These cycles are very different from the subtidal-supratidal cycles of this section, characteristic of the preceding BA5 sequence (eg. Figs 5.15 & 5.16, pgs 217 & 218 respectively). The dominance of entirely subtidal, low to high-energy open marine shallowing-up cycles within the lower *Orbitolina* beds is thought to reflect a reduction of carbonate sedimentation rates due to siliciclastic contamination of the shelf. Each cycle passes upward from siliciclastic rich shales to subtidal limestones. Note that the base of each limestone package is very abrupt, even though there is considerable bioturbation and downward mixing of limestones at their base. The upper passage at the top of each cycle into shales is more gradual. Hammer for scale, approximately 350mm long.

occasional replenishment of saline waters from the open ocean (Arnaud-Vanneau & Medus, 1977). These facies are at this locality overlain by the lower *Orbitolina* beds which typify the AP1 TST, but are slightly thinner than normal (Arnaud-Vanneau, 1980). This lagoonal succession was probably deposited during the very late lowstand systems tract and early TST, with the lower *Orbitolina* beds representing the late TST.

The classical AP1 TST is well developed on the shelf in the western Vercors (eg. Gorge du Nant & Balcon des Ecouges, Figs 5.1A & 6.35) and Chartreuse (Gorge du Frou, Figs 5.12, p.213, 5.17, p.220, 5.18, p.221 & 6.26). At these and other similar localities, the shelf-lagoon of the preceding sequence is dominated by restricted, low-energy sedimentation (eg. see Figs 5.15 & 5.16). The base of the AP1 sequence on the shelf is, however, marked by an abrupt facies jump; the base of the Lower *Orbitolina* beds (eg. Fig. 6.26). The lower *Orbitolina* beds form a distinctive transgressive package some 30-50m thick (Figs 5.1A & 6.26), comprised of high-energy open-marine facies such as bioclastic and ooidal sands interbedded with low-energy, sub-wavebase shales which are often heavily bioturbated. This is in complete contrast to the preceding BA3, BA4 and BA5 sequences where the transgressive surface and transgressive systems tract is associated with the resumption of protected, restricted shelf type facies (eg. Figs 5.1 & 6.26). This change in character of the transgressive systems tract at the base of the AP1 shelf sequence is interpreted to reflect a major environmental change at the base of the AP1 TST to more humid climatic conditions (see Sections 5.2.4.C-D & 5.2.5). This climatic change is thought to have introduced siliciclastic sediments onto the shelf and contaminated carbonate deposition, reducing sedimentation rates and preventing the 'start-up' of normal carbonate sedimentation in previously restricted parts of the shelf. Thus, relatively open-marine conditions became established across the Urgonian shelf as the accretion rate of the depositional surface fell behind the rate(s) of relative sea-level rise. As a whole, the *Orbitolina* beds are characterized by the development of 1-3m thick, subtidal (entirely), asymmetric shallowing-up cycles as discussed in Section 5.2.5

(Figs 5.17, 5.18 & 6.35). These subtidal cycles which do not shoal to peritidal facies are thought to have developed as carbonate sedimentation rates were retarded by the influx of siliciclastic sediments onto the shelf at this time. The rates of relative sea-level rise may therefore have been similar to those during BA5, but the rate(s) of carbonate sedimentation were certainly reduced.

The uppermost part of the *Orbitolina* beds is characterized by the development of dark-grey marls (Fig. 5.12, p.213). These are interpreted to represent the mfs, which is abruptly overlain by 'normal' Urgonian shelf facies (eg. Fig. 5.12). The sudden change/jump of facies which frequently marks the upper surface of the TST is interpreted to reflect a major environmental change, rather than a simple change in the rate of relative sea-level rise (probably a decrease of siliciclastic sedimentation rates as rainfall rates fell, see also Section 5.2.4.C, Ruffell & Batten, 1990 and Deconinck, 1984). It is therefore suggested that the TST as defined by the development of the lower *Orbitolina* beds was prolonged by the persistence of more humid climatic conditions rather than high rates of relative sea-level rise.

6.2.7. C. AP1 highstand sedimentation.

The AP1 HST is up to 40m thick and its base is marked by an abrupt return to normal carbonate sedimentation on the shelf, probably a reflection of a major climatic change, the return to semi-arid climatic conditions. The AP1 highstand systems tract is comprised of the last true Urgonian facies of the platform and is overlain by the AP2 sequence boundary (Fig. 6.4). Where observed in weathered sections the systems tract can be seen to be composed of classical, asymmetric, 1-2m 5^{th} order subtidal-peritidal shallowing-up cycles on the shelf (eg. Fig. 5.14, p.216). These contrast markedly to the entirely subtidal cycles of the AP1 TST (eg. Fig. 5.12) and the poorly structured subtidal-peritidal cycles of the BA5 sequence (eg. Fig. 5.16). The cycles of AP1 develop in a more classical asymmetric pattern than equivalent cycles of BA5. This is interpreted to suggest that *either* shelf-lagoon sedimentation rates were lower during AP1 as compared to BA5 and/or that rates of relative sea-

level rise had become greater and/or more punctuated during AP1 in contrast to BA5.

6.2.8. Sequence AP2.

6.2.8. A. Summary of sequence development.

This is the final sequence of the Urgonian platform, and is characterized by the deposition of the upper *Orbitolina* beds (AP2 TST) (eg. Fig. 6.36). This sequence is comprised of the Ai2 and Ai3 members of Arnaud-Vanneau (1980) and Arnaud (1981) (Figs 6.2, 6.4). The upper *Orbitolina* beds are confined to elongate NW-SE trending topographic lows on the shelf (Figs 5.4 & 6.4). These depressions are interpreted to have been cut during lowstand of relative sea-level (Arnaud & Arnaud-Vanneau, 1989). The upper *Orbitolina* limestones (AP2 TST, Fig. 6.26) are in-turn unconformably overlain by the upper Aptian 'Lumachelle' (Figs 6.4 & 6.6). This is a bryozoan-crinoidal sand-wave complex, which passes upwards into an Albian condensed interval, reflecting the final drowning of the platform. By way of contrast, on the basin-floor the sequence is associated with the deposition of breccias derived from the catastrophic collapse of the slope (the CL3 and CL4 of Ferry & Flandrin,

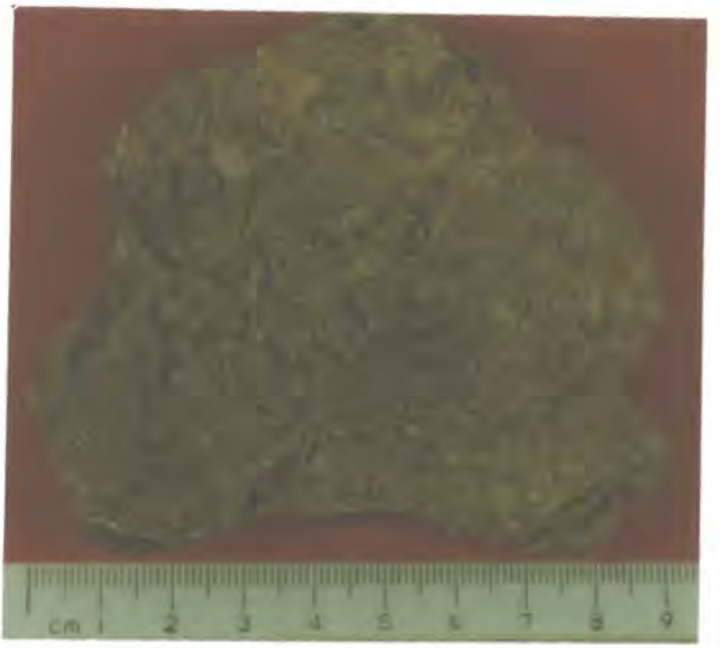

Figure 6.36. Upper weathered surface of an *Orbitolina* packstone bed from the fill of the Les Rimets palaeovalley in the northern Vercors. The *Orbitolina* are the large disc shaped grains. The other main bioclasts are crinoids and bivalves.

1979; Ferry & Rubino, 1989, Fig. 6.7). These are overlain by a thick succession of dark-grey and black shales which onlap the slope and on to the shelf in the southern Vercors. This sequence, like AP1 is marked by a general consensus of current sequence stratigraphic schemes which are all broadly based upon the original sequence stratigraphic interpretations of Arnaud & Arnaud-Vanneau (1989), although interpretation of the unconformable base of the 'Lumachelle' is rather different.

6.2.8. B. The AP2 sequence boundary and lowstand sedimentation.

This is probably the best exposed and most spectacular sequence boundary developed and preserved upon the Urgonian shelf. Unlike its precursors (on the shelf) this sequence boundary is associated with the localised erosion of a considerable portion of the preceding AP1 sequence (up to 50m) (eg. Figs 5.3, p.196, 5.5, p.198 & 6.37). The strongest erosional truncation is compartmentalized into a series of sub-parallel NW-SE trending erosional troughs, interpreted to be incised valleys (Arnaud & Arnaud-Vanneau, 1989) (eg. Figs 5.3, 5.4, 5.5 & 6.37). These palaeovalleys are thought to have been cut during times of falling and lowstand of relative sea-level. The absence of similar scale erosional truncation upon the shelf during the preceding lowstands of relative sea-level (eg. BA1-5 & AP1) suggests that very different environmental and sedimentological conditions prevailed during the AP2 lowstand when the shelf was exposed.

The cutting of incised valleys is interpreted to have occurred as siliciclastic sediments were introduced on to the shelf during lowstand of relative sea-level. The influx of a significant quantity of siliciclastic sediments on to the shelf during lowstand of relative sea-level is unique to the AP2 sequence and, like the influx of siliciclastics during the AP1 TST (Section 6.2.7.B) is thought to be the sedimentological response of a change to more humid climatic conditions. It has been suggested by Deconinck (1984) and Ruffell & Batten (1990) that a shift to more humid conditions caused the stronger erosion of the hinterland to the platform. Siliciclastic sediments eroded from this hinterland area are interpreted to have been

introduced on to and bypassed through the exposed shelf via a series of sub-parallel NW-SE trending rivers which incised the exposed shelf.

The most spectacular of the incised valleys on the Urgonian shelf is exposed near to the Les Rimets farm in the Vercors where a palaeovalley is partly exhumed (Figs. 5.3, 5.4, 5.5 & 6.37). This valley has a width of some 250m and a maximum depth of 50m (Fig. 5.5, see Section 5.2.2 for further discussion). In the more steeply dipping northern side of this palaeovalley the erosional truncation of the AP1 HST strata is clearly visible (Figs. 5.3 & 6.37). The development of incised valleys on the shelf is classically indicative of a type 1 sequence boundary (eg. Figs 2.5b & 3.5, pgs 14 & 41 respectively). The maximum depth of the Les Rimets palaeovalley (approximately 50m, Fig. 5.5) can be used in conjunction with the depths of contemporaneous palaeovalleys to estimate the amplitude of the relative sea-level fall, which developed the AP2 sequence boundary (Arnaud & Arnaud-Vanneau, 1989). This fall of relative sea-level is, thus, interpreted to have been between 30 and 50m.

Figure 6.37. View looking northwest (parallel to the valley axis) along the northeastern flank of the Les Rimets exhumed palaeovalley. In this photo of its steep northern side the erosional truncation of AP1 highstand strata is clearly visible (see also Figs 5.3, 5.4. & 5.5). Rucksack approximately 1m long for scale.

Figure 6.38. Sub-vertical section through karstic hollows in the AP1 sequence, developed during the AP2 lowstand, modified and filled by *Orbitolina* marls during the early stages of the AP2 TST. The karstic dissolution of the AP1 sequence does not penetrate more than 2m in to AP1 in the vicinity of this locality, approximately 2km to the south of Les Clapiers in the northern Vercors. Note that karstic dissolution pipes and brecciated clasts are quite rounded. This is rounding of both the clasts and karst is thought to have occurred as the shelf was transgressed. Pencil approximately 130mm long for scale.

Spectacular as the incised valley at Les Rimets and its counterparts are, these only cover 5% or less of exposed shelf and, as such, are but a small fraction of the AP2 sequence boundary. In the vast majority of localities on the shelf (where preserved, see Sections 5.2.4.C & 6.2.8.C) the sequence boundary is marked by the development of a karstic topography (eg. Figs 5.8D, E, p.204 & 5.11B, p.212). This karstic dissolution is, however, generally far from spectacular (eg. Fig. 6.38) and generally penetrates less than 2m in to the preceding AP1 sequence. This change in the morphology of the sequence boundary from a gently undulose topography which tends to characterize preceding sequence boundaries (eg. Figs 5.8G, 5.10, 6.24, 6.25 & 6.34) to karstic dissolution pipes (Figs 5.8D, 5.11B & 6.38) tends to suggest a change to more humid climatic conditions during the AP2 lowstand systems tract, as the influx of siliciclastic sediments on to the shelf at this time is also interpreted. However, it is interesting to note that this interpreted change to more humid

conditions is not associated with a change to more penetrative vadose meteoric diagenesis. Theoretically, the vadose meteoric zone developed during the AP2 lowstand could be up to 50m, the interpreted amplitude of relative sea-level fall. Compared to this, the maximum penetration of karst to 2m is remarkably small. It is certainly a possibility that the lower *Orbitolina* marls acted as a major permeability barrier whilst the shelf was exposed which kept the palaeo-watertable high within the platform. A high palaeo-watertable would lead to the development of only a narrow meteoric vadose zone. If correct, this would imply that the incised valleys cut through and below the palaeo-watertable.

Figure 6.39. Oblique (N-S) section through Ai2 trough crossbedded prograding clinoforms approximately 1km north of Gigors in the southwestern Vercors (also see Figs 5.49, p.272 & 6.45). These coarse, sub-wavebase bioclastic sands are interbedded with fine grained orange mudstones and are interpreted to represent the AP2 lowstand autochthonous slope wedge. Author contemplating the exposure for scale.

The AP2 lowstand deposits are not preserved in the east of the Vercors plateau for (if they were developed) late Cretaceous erosion has removed the upper part of the platform succession (eg. Figs 6.4 & 6.31). In the eastern Vercors lowstand sedimentation is interpreted to be represented by the member Ai2 of Arnaud (1981)

(Figs 5.48, 6.39 & 6.45). This relatively thin package of coarse prograding bioclastic sands developed conformably onto sub-wavebase slope facies (eg. Figs 5.48 & 6.45) is interpreted to be the AP2 autochthonous lowstand slope wedge.

6.2.8. C. The AP2 transgressive systems tract.

6.2.8. C1. The shelf.

The TST of this sequence is represented by the second appearance of the *Orbitolina* facies (eg. Fig. 6.36). These facies are not widely developed across the shelf (as during the AP1 TST), but are mostly contained within the topographic lows of the incised valleys upon the shelf (Figs 5.4 & 5.5). These incised valleys were re-utilised as tidal channels during the AP2 TST (Arnaud-Vanneau & Arnaud, 1990).

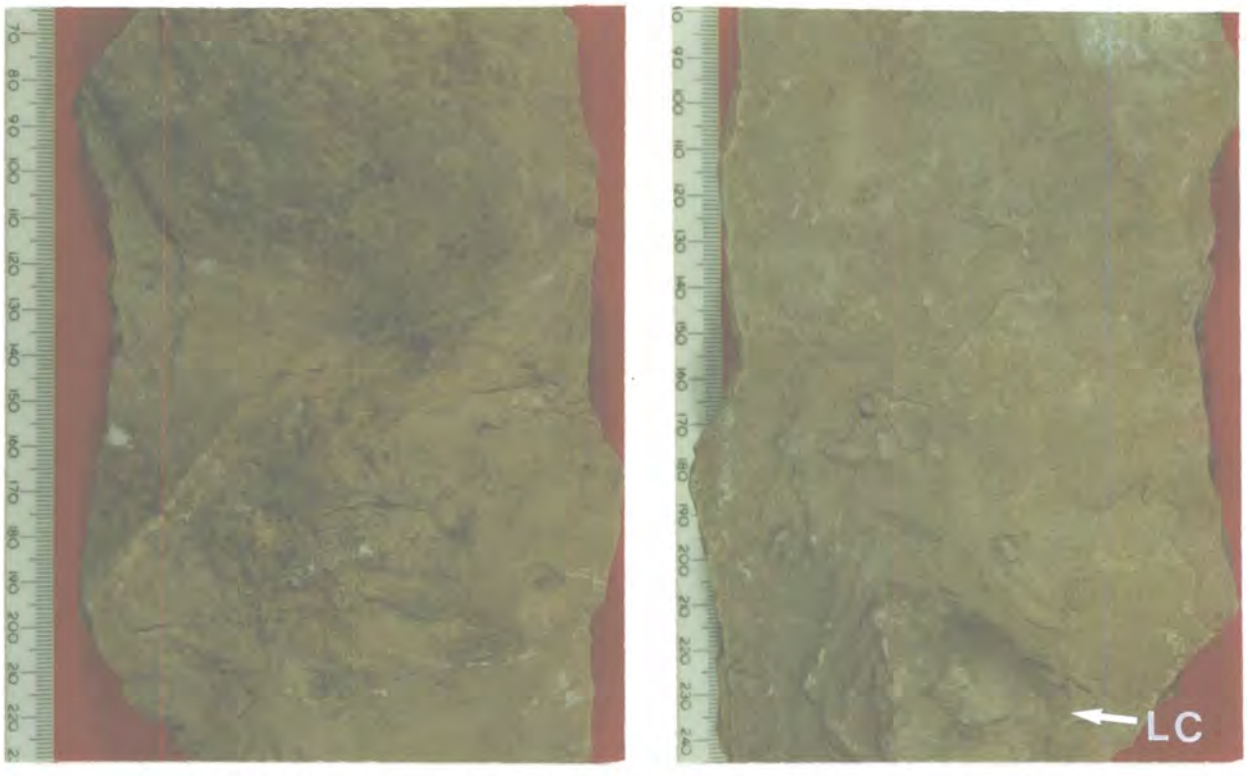

Figure 6.40. Upper (U) and lower (L) surfaces of a sharp-based sand bed within the lowest part of the upper *Orbitolina* marls. The base of the bed is also loaded (LC), with some minor bioturbation features. Internally, the bed is composed of a lower, tabular parallel-laminated part (<10mm thick) and an upper cross-laminated part (2-25mm thick). The upper surface of the bed is rippled but these have no well developed preferred orientation and are thus dome shaped in three dimensions. Both the interior structure of the bed and its external form is characteristic of hummocky cross-stratification. Accordingly, this bed is interpreted to be a shelf tempestite deposit.

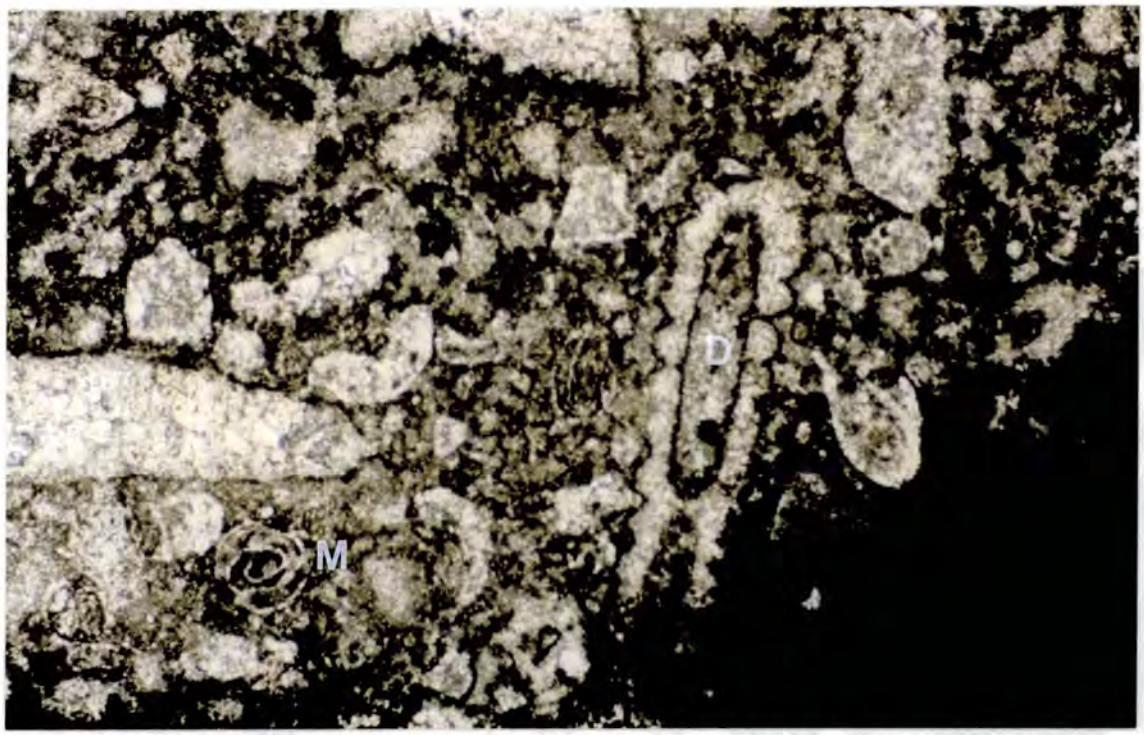

Figure 6.41. Photomicrograph of the hardground from the northern wall of the incised valley at Les Rimets (see also Figs 5.11D & 6.37). Note that the partial impregnation of the micritic walls of carbonate grains such as Miliolids (M) and Dasycladacean alga (D) by ferro-manganese minerals. This replacement was initially fabric selective, preferentially replacing the micritic walls of grains, but was ultimately fabric destructive. Maximum field of view is approximately 4mm.

Unlike the lower *Orbitolina* beds, the upper *Orbitolina* beds are not characterized by the development of 1-3m asymmetric shallowing-up cycles. Fill of the AP2 LST palaeovalleys is divisible into three distinctive phases which overall shallow and coarsen upwards from *Orbitolina* marls and wackestones with occasional storm beds (eg. Fig. 6.40) to oolitic grainstones and *Orbitolina* pack-grainstones (Figs 5.4 & 6.36). The filling of the Les Rimets palaeovalley is contemporaneous with the development of a ferro-manganese hardground on the valley sides (eg. Figs 5.11D & 6.41) and the colonisation of the upper flanks of the valley by high-energy corals and rudists (eg. Fig. 5.5). The *Orbitolina* foraminifera within the palaeovalleys include siltgrade siliciclastics (mainly quartz) into their ultrastructure and, as such, appear tolerant of siliciclastic sediments and were possibly specifically adapted to such environments. This contrasts with the corals and rudists contemporaneously developed on the flanks of the palaeovalley (Fig. 5.5), which are organisms generally

highly sensitive to siliciclastic sediments. This suggests that siliciclastic sediments were moved through the lower parts of the Les Rimets palaeovalley as it was utilized as a tidal channel during the AP2 TST. The transgressive systems tract over much of the shelf is associated with the reworking of the sequence boundary to a *compound surface* (eg. Fig. 5.11A, B, C, E, F & Fig. 6.38, see Section 5.2.4.C). Modification of the sequence boundary is interpreted to reflect a high rate of relative sea-level rise compared to the rate of sedimentation 'start-up'.

The latter part of the AP2 TST is marked by the drowning of the shelf and is equivalent to the development of black shales in the basin which onlap the slope and develop a type of drowning unconformity (eg. Fig. 6.43, see Section 6.2.8.C2). The first part of the drowning succession on the shelf is represented by the 'Lumachelle' limestones (eg. Fig. 5.11B, C, p.212 & 6.42). These are a 10-12m thick bioclastic sand-wave complex which contains a low diversity fauna of rounded bryozoans, crinoids and glauconitic grains (eg. typical slope type organisms, Fig. 6.42, see Section 4.5). The 'Lumachelle' rests unconformably on to both the Urgonian shelf and the *Orbitolina* limestones (eg. Fig. 5.5, p.198) (Arnaud & Arnaud-Vanneau, 1989). The base of the sand package is normally marked by the further reworking and modification of the AP2 sequence boundary (eg. see Fig. 5.11A, C & E). The 'Lumachelle' sand-wave complexes and associated erosion of the shelf is interpreted to have developed as a response to the incursion of oceanic currents on to the shelf (eg. Delamette, 1988; Föllmi, 1989). In some particularly scoured areas little evidence remains of the sequence boundary and the upper surface of the platform is a reddened, bored hardground (eg. Fig. 5.11E, p.212). These oceanic currents moved the bioclastic sands along the shelf, and so have scoured and eroded the Urgonian shelf, so modifying the exposure surface (eg. see also Delamette, 1988; Föllmi, 1989). The 'Lumachelle' is in-turn overlain by an extremely condensed, phosphatic pelagic bed which represents the ultimate drowning of the Urgonian platform and records the prolonged development of a pelagic environment on top of the relict Urgonian shelf. The condensation within these phosphates is also induced by the

incursion of oceanic currents on to the shelf (Delamette, 1988; Föllmi, 1989). The drowning succession from sandy glauconitic limestones to phosphates is typically in total less than 10m and sedimentation rates are typically less than 1m/Ma (Delamette, 1988) (eg. Fig. 4.10, p.118). This marked reduction of sedimentation rates (Fig. 4.8) coupled with the development of condensed deep-water, current dominated sedimentation on the shelf clearly illustrates that the shelf had drowned, for there was plenty of space available for the accommodation of sediment, but very little sediment being produced to fill it; the shelf was sediment starved.

Figure 6.42. Photomicrograph of the 'Lumachelle' limestone. This grainstone contains a low diversity fauna of bryozoans and crinoids with glauconitic grains. These sands were deposited within a sand-wave complex on top of the Urgonian limestones. Field of view approximately 4mm.

The inception of the oceanic currents on to the Urgonian shelf is thought to be directly related to the onset of compression within the Ligurian Tethys, closing oceanic pathways and causing a major re-arrangement of oceanic currents (Delamette, 1988; Föllmi, 1989). This, coupled with an initially rapid pulse of relative sea-level rise and the influx of siliciclastic sediments on to the Urgonian shelf allowed

incursion of the possibly nutrient-rich oceanic currents (Föllmi, 1989) on to the Urgonian shelf from which it never recovered.

6.2.8. C2. The slope and basin-floor.

Classically, the slope is interpreted to collapse during times of falling relative sea-level as the storm-wavebase is lowered down the slope (eg. Fig. 3.5, p.41 & see Section 3.7.2.A). However, during the AP2 transgressive systems tract which marks the drowning of the Urgonian platform two geographically and geologically distinct parts of the Urgonian slope collapsed. These do not appear to be related to any topographic buildup(s) developed during the TST which could have steepened the slope (eg. type 2 TST, Fig. 3.20, p.73), *or* to a lowering of storm-wave base. In fact, exactly the converse situation appears to be true. However, the stratal patterns developed by slope collapse during the AP2 transgressive systems tract and subsequent onlap of the slope by pelagic sediments does closely mimic stratal patterns supposedly characteristic of times of falling relative sea-level (Ferry & Rubino, 1989) (see Section 5.4.2.B & Fig. 5.51).

The collapse of the slope between the Bedoulian and Gargasian in both the Borne and Gigors regions is thought to be contemporaneous (Ferry & Flandrin, 1979). This synchroneity of slope collapse is interpreted by Ferry & Flandrin (1979) and Arnaud (1981) to have been triggered by the reactivation of two similarly orientated basement lineaments, the Glandage and Gigors/Marsanne faults (Fig. 6.43 & Figs 5.45 & 5.47 respectively). The collapse scar which is developed on the slope to south of Borne is shown in Figure 6.43. This collapse scar is preserved by the subsequent deposition of Gargasian marls (Marnes gargasiennes, Fig. 6.43) on to the erosional surface (Fig. 6.43). This scar has an amphitheatre shape in map pattern and dips to the south (Fig. 6.43B). In strike section, schematically shown in Figure 6.43A the scar cuts up and down stratigraphy to the east and west, and has an erosional topography of some 150-175m. This scar is developed entirely within the lowermost

part of the slope (probably the toe-of-slope) through the transition from thin periplatform to pelagic facies (Fig. 6.43B, Arnaud, 1979). These facies are interpreted to have been deposited in water depths of between 1000m and 1200m (Arnaud-Vanneau *et al.*, 1987; Arnaud & Arnaud-Vanneau, 1989, see Fig. 4.40, p.138). Thus, changes of relative sea-level were probably *not* a contributing factor to the cause(s) of slope collapse.

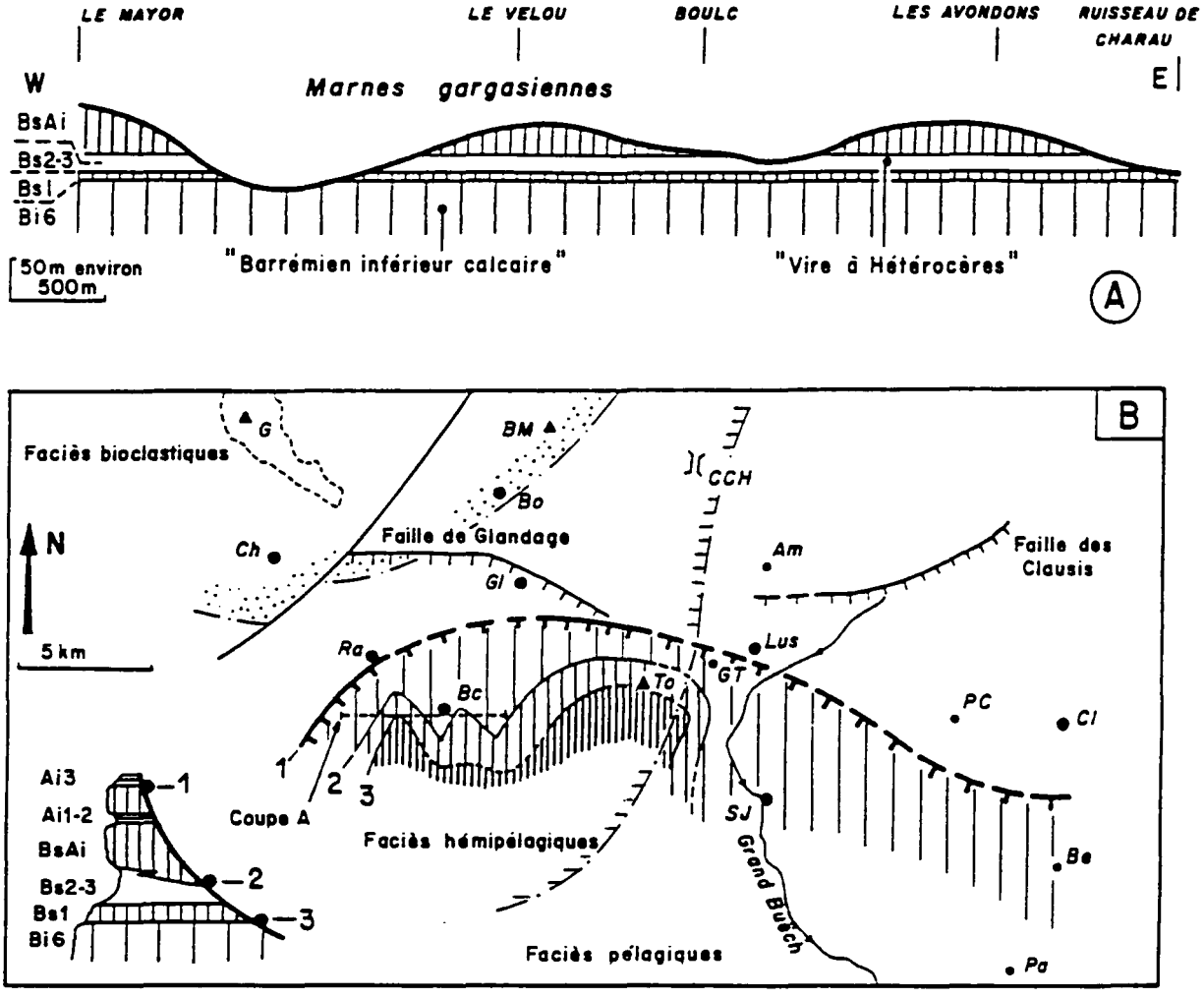

Figure 6.43. Schematic east-west strike-parallel cross-section (A) and map of the post-Bedoulian, pre-Gargasian slide scar of the southern Borne area (located up on B). The map (B) illustrates the extension of the slide plane below the Gargasian marls. This collapse scar is interpreted to have been developed in interpreted water depths of 1000-1200m (eg. see Fig. 4.20, p.138).

Locations: Am: Gorges de Amayers; Bc: Boulc; Be: Bernards section; Be: Montagne de Belle Motte; Bo: Borne; CCH: Col de la Croix-Haute; CD: Châtillion-le-Desert; Ch: Châtillion-en-Diois; Cl: La Cluse; CM: Col de Menée; G: Glandasse; Gl: Glandage; GT: Gorges de Toussière; Pa: Pascaux section; PC: Col de la Plate Contier; Ra: Ravel; SJ: Saint-Julien-en-Bochaîne; To: Montagne de Toussière (From Arnaud, 1979).

Figure 6.44. The CL3 basin-floor megabreccia as developed at La Chaudière. This collapse breccia is a matrix-supported diamictite and contains a wide variety of sub-wavebase slope lithoclasts. Limestone clasts tend to be sub-spherical, but unlike CL2 (Fig. 5.47, p.270) these are not striated. This suggests that clasts were supported within the matrix whilst being transported to the depositional site. The sub-spherical/lense shape of limestone clasts is thought to originate as limestone beds became stretched out and boudinaged during the initial stages of collapse. The shale clasts, rather differently, are angular and elongate. This suggests that these were brittle in extension whereas the limestones were plastic. Lens cap 50mm in diameter for scale (see also Fig. 5.50).

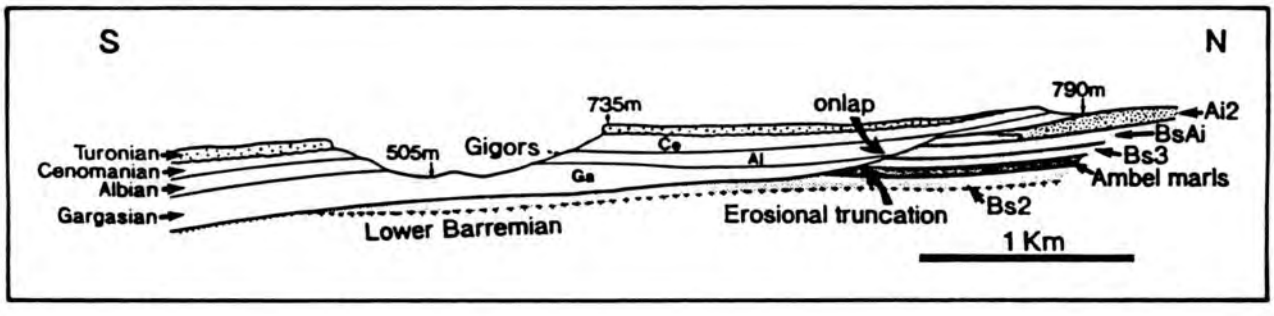

Figure. 6.45. Schematic north-south cross-section through the Gigors region, where the CL3 slide scar erosionally truncates the sub-storm wavebase part of member Ai2 (Arnaud, 1981). This member, illustrated in Figure 6.39 is interpreted to be the AP2 lowstand autochthonous slope wedge. This collapse scar is subsequently onlapped by pelagic black shales, developing a type of drowning unconformity. Section line loctaed on Figure 4.17 (p.132).

The contemporaneous collapse scar upon the southwestern flanks of the Urgonian platform which developed the CL3 megabreccia (Figs 5.50, p.273 & 6.44) is also developed entirely within sub-storm wavebase facies, and is interpreted to extend from the basin-floor to the upper-mid slope (eg. from water depths of ?800m to ?70m) (see Section 5.2.4.B, Figs 5.44, 5.47 & 6.45). The CL3 collapse scar cuts through the AP2 lowstand autochthonous slope wedge (Ai2, Fig. 6.45), and this clearly demonstrates that collapse occurred after times of falling and lowstand of relative sea-level. The CL3 collapse scar and its associated basin-floor megabreccia developed a stratal pattern which closely mimics that of a type 1 sequence boundary (Ferry & Rubino, 1989) (Fig. 5.52, p.275), and the onlap of Aptian-Albian black shales on to the slope scar is similar to of a lowstand wedge systems tract in geometry (eg. compare Figs 5.52 & 6.45 to Fig. 3.5, p.41).

Thus, the demise of the Urgonian platform is related to a relative sea-level fall, followed by a relative sea-level rise. This would probably not have drowned the Urgonian platform on its own. However, these times were also marked by two important environmental changes; firstly a return to more humid climatic conditions as marked by the influx of siliciclastics during the AP2 lowstand and early TST and, secondly the inception of an oceanic current which incurred on to the Urgonian shelf sweeping it clean of muds and developing a condensed section.

6.3. An Evaluation Of Relative Sea-Level Changes, Rates Of Relative Sea-Level Rise And Aggradation As Interpreted From The Urgonian Platform.

6.3.1. Introduction.

Relative sea-level rises, the sum of tectonic subsidence and/or eustatic sea-level rises provided the space into which the Urgonian platform aggraded and prograded. In complete contrast, relative sea-level falls 'forced' shallow-water sedimentation from the shelf onto the flanks of the Urgonian platform. In the preceding section (6.2) the stratigraphic signature of Hauterivian-Barremian-Aptian relative sea-level changes, the depositional sequences and their component systems tracts and parasequences of the Urgonian platform (*sensu lato*) were discussed. The varying role of factors other than relative sea-level changes in development of these sequences such as climate, siliciclastic input, oceanic currents have also been discussed. It is the aim of this section to work backwards from these stacking patterns and to develop a relative sea-level curve for the Urgonian platform. Firstly, the previous interpretations of relative sea-level changes upon the platform are discussed.

6.3.2. Previous interpretations.

Two different interpretations of the relative sea-level changes which shaped the Urgonian platform are illustrated in Figures 6.8 (p.293) & 6.12 (p.302). These have been developed from the building and subsequent interpretation of sequence stratigraphic schemes for the Urgonian platform (eg. Arnaud & Arnaud-Vanneau, 1989; Arnaud-Vanneau & Arnaud, 1990, Figs 5.2, p.206 & 6.12 and Jacquin *et al.*, 1991, Figs 5.19, p.226 & 6.8). Arnaud & Arnaud-Vanneau (1989) developed the basic sequence stratigraphy for the Urgonian platform (Fig. 5.2), from which they evaluated relative sea-level changes with respect to the emergence of the 'inner shelf

domain' (eg. Fig. 6.12). In this scheme the absolute amplitude of relative sea-level changes is not addressed. Relative sea-level changes are qualitatively interpreted with respect to the exposure of the shelf and depth(s) to which it was transgressed during the TST-HST. Sequence boundaries, and hence falls of relative sea-level are recognized using this approach at times when the 'inner shelf' was subaerially exposed (Fig. 6.12). By way of contrast, Jacquin *et al.* (1991) constructed their chart of relative sea-level changes from the interpreted changes of coastal onlap using the methodology as originally described by Vail *et al.* (1977) (eg. compare Figs 6.8 & 6.19). The chart produced by Jacquin *et al.* (1991) (Fig. 6.8) thus illustrates the interpreted relative shifts of coastal onlap. The slightly different approach taken by Arnaud & Arnaud-Vanneau (1989), Arnaud-Vanneau & Arnaud (1990) and Jacquin *et al.* (1991) does, however, produce a rather similar qualitative interpretation of the 2nd order relative sea-level changes which molded the form of the Urgonian platform (eg. compare Figs 6.8 & 6.12), briefly summarized in the following paragraph.

The uppermost Hauterivian/lowermost Barremian is characterized by a general fall of relative sea-level, to its lowest point. This low point of the 2nd order relative sea-level curve is interpreted to be approximately coincident with the base of the Urgonian platform *sensu lato* (eg. Figs 6.8 & 6.12). This 2nd order lowstand was followed by a gradual relative sea-level rise, which peaked in the upper Aptian/ lower Albian. This 2nd order relative sea-level rise is itself divisible in to a lower 'regressive' phase subsequent to the lowest point of relative sea-level, but prior to the interpreted transgression of the Urgonian shelf (approximately equivalent to the Glandasse Limestone Formation; the 'general' lowstand wedge of Arnaud-Vanneau & Arnaud, 1989, Figs 5.2 & 6.1), and an upper 'transgressive' part developed after relative sea-level had risen above the slopebreak of the preceding Hauterivian platform (the Urgonian Limestone Formation, 'Lumachelle' and condensed Albian phosphatic beds) (eg. Figs 6.1, 6.8 & 6.46E). The 'regressive' times are the lowstand; the 'transgressive' times are the transgressive systems tract of a 2nd order megasequence (eg. Figs 6.8 & 6.46). It is interesting to note at this point that both of

these qualitative relative sea-level curves show exactly the opposite trend to the 'eustatic' sea-level curve of Haq *et al.* (1987) (eg. see Figs 6.8 & 6.12). This observation led Arnaud & Arnaud-Vanneau (1989), Arnaud-Vanneau & Arnaud (1990) and Jacquin *et al.* (1991) to suggest a strong tectonic component within the relative sea-level fall at the base of the platform where the differences between the 'Urgonian' and 'Eustatic' curves are most acute (the 'tectonically enhanced' unconformities of Jacquin *et al.*, 1991). This interpretation of course assumes that the 'eustatic' sea-level curves of Haq *et al.* (1987) are correct for the lower Cretaceous (see Schlager, 1991 for discussion of lower Cretaceous sea-level curves). The 'general' second order relative sea-level rise which characterizes the Urgonian platform (*sensu lato*) is divisible into a number of higher order regressive-transgressive cycles; the 3^{rd}-4^{th} order sequences of the Urgonian platform. At this higher order scale the interpretations of Arnaud-Vanneau (1989), Arnaud-Vanneau & Arnaud (1990) and Jacquin *et al.* (1991) diverge, both in their identification of sequences and the presentation of their sea-level curves.

6.3.3. Limitations and characteristics of the different approaches.

At the sequence or 3^{rd} order scale the different approach taken by Arnaud & Arnaud-Vanneau (1989), Arnaud-Vanneau & Arnaud (1990) and Jacquin *et al.* (1991) has produced very different shapes of relative sea-level curves (eg. Figs 6.8 & 6.12). The relative sea-level curve of Arnaud-Vanneau & Arnaud (1990) has a near sinusoidal form and depicts relative sea-level to fall gradually from the upper part of a sequence (Fig. 6.12). This would appear to suggest that much of the highstand systems tract is developed during times of falling relative sea-level. However, such an interpretation of relative sea-level change from this curve (Fig. 6.12) would be incorrect, for the curve actually illustrates the interpreted depth of depositional surface of the shelf with respect to relative sea-level. Thus, when the shelf is, for instance, drowned during transgression (eg. AP1, Fig. 6.12) the curve shifts far to the left as the shelf is submerged below wavebase and there is a wide separation between

relative sea-level and the depositional surface of the shelf (eg. compare Figs 6.12 & 6.26). As the shelf then aggrades to meet relative sea-level (eg. upper member of the Urgonian Limestone Formation, AP1, Fig. 6.12) the curve shifts towards the right. Thus, the apparent 'fall' of relative sea-level at the top of a sequence actually represents the aggradation of the shelf to relative sea-level during a relative sea-level stillstand, the highstand systems tract. This aggradation of the depositional surface on the shelf demonstrates how in a classical asymmetric shallowing-up transgressive-highstand systems tract only a small relative sea-level fall is needed to expose the shelf during the late HST when the shelf is aggraded close to sea-level. By way of contrast, a similar amplitude of relative sea-level fall during the TST (when the curve of Figure 6.12 was shifted to the left) would not have exposed the shelf and therefore not have formed a sequence boundary.

In complete contrast, the qualitative relative sea-level chart of Jacquin *et al.* (1991) developed from the interpreted shifts of coastal onlap has a 'saw-toothed' shape (Fig. 6.8). Their sequence boundaries are marked by instantaneous basinward shifts of coastal onlap from the shelf to the slope (Fig. 6.8). These are followed by a gradually accelerating and subsequently decelerating landward shift of coastal onlap. This shift is interpreted to represent the transgressive and highstand systems tracts of the third order sequences which are separated by the mfs (dashed lines, Fig. 6.8). It is worthy of note here that the shifts of coastal onlap of Jacquin *et al.* (1991) are entirely interpreted, for there are *no* locations on the Urgonian platform *sensu lato* where shoreline facies can be seen to onlap a slope and/or the exposed shelf *sensu* Vail (1987, eg. Fig. 3.5B, p.41).

6.3.4. Construction of a new relative sea-level chart for the Urgonian platform.

A new relative sea-level curve for the Urgonian platform is illustrated in Figure 6.46. This attempts to interpret quantitatively relative sea-level changes, both the rises and falls which contributed to the development of the Urgonian platform. The new relative sea-level chart (Fig. 6.46) is built from the sequence stratigraphy of

the Urgonian platform discussed in Chapter 5 and the preceding part of this sixth Chapter, as summarized in Figures 6.2 (p.279) & 6.4 (283). This sequence stratigraphic scheme is integrated into the palaeontological framework of Arnaud-Vanneau (1980), Arnaud (1981) and Arnaud-Vanneau (1990) and placed within the time scale of Haq *et al.* (1987) (Fig. 6.46).

6.3.4. A. Methodology.

1). A single stratigraphic section can be composed of all the sequences developed on the Urgonian platform, but will not record the magnitude of all relative sea-level rises or falls. Lowstands of relative sea-level are characterized by deposition upon the slope, whereas transgressive and highstands of relative sea-level are best recorded on the shelf. Accordingly sections from both the slope and shelf have been chosen to evaluate rises of relative sea-level; the Cirque d'Archiane (see Section 5.3.3) and Gorges du Frou and Nant respectively (Figs 5.1A & 6.26). These locations were chosen, for a combination of their stratigraphic continuity, dominantly shallow-water facies and the understanding of their sequence stratigraphic development. Each stratigraphic section considered individually only gives a partial picture of relative sea-level changes, but integrated together a quite complete record can be built.

The limitations of the chosen sections with respect to the interpretation of relative sea-level changes of both slope and shelf sections are illustrated in Figure 6.46D. For the slope, relative sea-level changes are not interpreted below Bi5 as these members are interpreted to be sub-wavebase where evaluation of relative sea-

Figure. 6.46. (facing page) The building of a new relative sea-level chart for the Urgonian platform as compared to the timing of sequence boundaries as according to Haq *et al.* (1987, version 3.1B). Note that the building of this chart assumes instantaneous sea-level falls at sequence boundaries and that relative sea-level begins to rise immediately from the 'low-point' of relative sea-level. See text for further discussion.

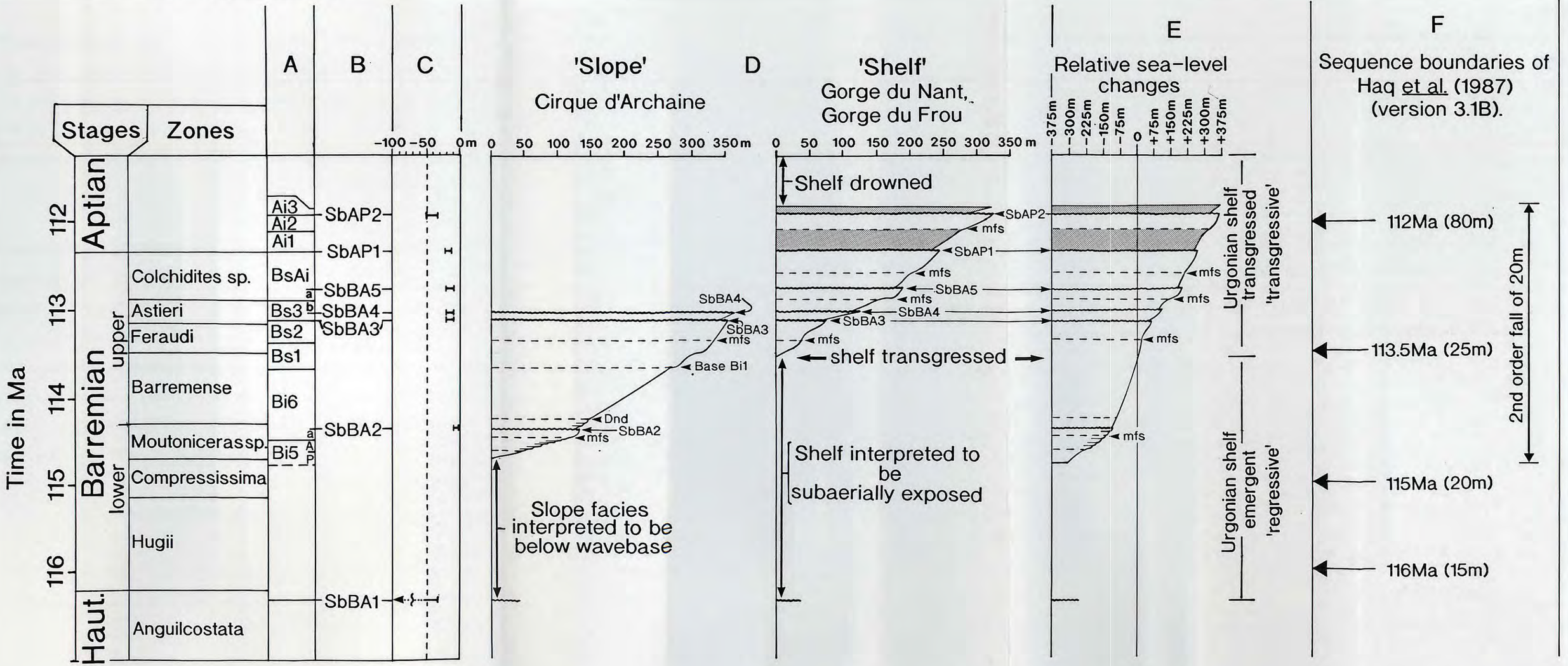

A = Members according to Arnaud-Vanneau (1980) and Arnaud (1981).

B = Sequence boundaries of this study.

C = Ranges of relative sea-level falls at sequence boundaries (in metres).

D = Relative sea-level rises for the Urgonian platform sensu lato with the average sea-level falls superimposed (in metres).

E = Integrated relative sea-level changes interpreted from the Urgonian platform sensu lato.

F = Position and measured amplitude of the 'eustatic' sea-level falls of Haq et al. (1987).

▒ Orbitolina beds

level changes is qualitative or above Bs1 as this member develops an 'overfill' TST, reducing the space available for the accommodation of succeeding sequences. Relative sea-level changes cannot be ascertained for the shelf during the lower Barremian for it was interpreted to have been subaerially exposed or for the Aptian 'Lumachelle' and Albian phosphates as the shelf was drowned and accurate constraint of water-depths is lost.

2). Falls of relative sea-level are interpreted from downward/basinward facies shifts at sequence boundaries from various slope localities. Only the interpreted 5-10m range of sea-level fall at SbBA2 is observed at the Cirque d'Archiane (eg. see Figs. 6.6 & 6.15). The interpreted ranges of relative sea-level falls at other sequence boundaries are discussed within the appropriate sub-sections of Section 6.2. The interpreted ranges of relative sea-level fall determined for each sequence boundary are plotted in column C of Figure 6.46 in their chronostratigraphically correct position. The mid-point of these ranges of relative sea-level fall are then transposed to their appropriate position within column D of Figure 6.46 and subtracted from the accrued relative sea-level rise of the preceding sequence.

3). Relative sea-level rises are determined from the thickness of shallow-water sediments within each sequence combined with the interpreted water depths of the microfacies within each sequence. At the base of each sequence the 'mid-point' of the interpreted relative sea-level fall at the sequence boundary (eg. Column C, Fig. 6.46) is subtracted from the maximum rise of relative sea-level (the 'high-point') of the preceding sequence. This is the lower control point of a sequence. This subtracted figure is then added to the total thickness of the succeeding sequence are then plotted at the chronostratigraphic upper boundary of the sequence. This gives the two end-points of the sequence. If developed, the mfs of the sequence can then be plotted. This is determined by simply adding the thickness of the TST on to the 'high point' of relative sea-level of the preceding sequence, plotted at its correct chronostratigraphic

level. This gives a third control point within a sequence. The actual form of the relative sea-level rise between three tie-points can then be qualitatively evaluated by estimating water depths of microfacies to the TST and HST of the sequence (eg. Figs 5.1A & 6.26).

For example, for BA2 the transgressive systems tract is associated with the drowning of the shelf to below storm wavebase (eg. below 30m). The average thickness of the sequence is 50-80m on the shelf (BA2 HST, Figs 5.1A & 6.26). The upper part of the HST is composed of shallow-water, high-energy facies interpreted to have been deposited in less than 10m water depths. This suggests that the shelf was fairly rapidly transgressed to 30m, followed by a relative stillstand when the shelf aggraded to within 10m of sea-level, followed by a further 20-40m of relative sea-level rise after the stillstand when the shelf aggraded (eg. Fig. 6.46D & E).

4). The two relative sea-level curves for the slope and shelf are integrated at the point where the shelf is interpreted to be transgressed. The shelf is transgressed to approximately 30m by the BA2 TST. Thus the two sections are integrated from the upper 30m of the BA2 relative sea-level rise of the slope section. This produces a single continuous quantitative record of relative sea-level changes from the mid-lower Barremian to the mid Aptian (eg. Fig. 6.26E).

6.3.4. B. Assumptions and errors.

There are basically three assumptions which have been taken to develop the relative sea-level chart of Figure 6.46 and these are listed below:

1. Relative sea-level fall is instantaneous.
2. Sea-level begins to rise immediately from the 'low-point' of relative sea-level.
3. The shelf had aggraded to within 10m of relative sea-level at the time of sequence boundary formation.

Unfortunately, it is necessary to assume that the relative sea-level fall was instantaneous as the sequences developed upon the Urgonian platform are developed

at or even below the palaeontological resolution of the platform (1Ma or less, Fig. 6.46). The interval of time represented by times of falling relative sea-level is but a fraction of a sequence and as such almost impossible to determine. Errors in assessing the amplitude of relative sea-level fall at sequence boundaries are developed if the shelf did not aggrade to within 10m of relative sea-level. This can be evaluated from the examination of facies directly below the sequence boundary upon the shelf where erosion during subaerial exposure is generally slight (eg. see Section 5.2). The maximum underestimate of relative sea-level fall is approximately 10m but for the sequences quantitatively depicted in Figure 6.46 is probably less as these develop shallow subtidal or peritidal facies directly below the sequence boundary (eg. Figs 5.1A, p.193 & 7.26). SbBA1 is a notable exception to this general rule, but it is not considered in Figure 6.46.

6.3.5. Interpretation of the relative sea-level curve: Implications for minimum sedimentation rates and subsidence.

It is interesting to compare the form of the coastal onlap charts of Jacquin *et al.* (1991) (Fig. 6.8) and the relative sea-level curves of Figure 6.46. A notable comparison between these two curves is the general relative sea-level rise during Urgonian (*sensu lato*) times through both the 'regressive' and 'transgressive' phases of sedimentation (Figs 6.8 & 6.46). This is an interpretation common to all of the charts developed to date for the Urgonian platform. The third order sequence signatures are also generally similar in shape aside from the differences of their position. However, the relative sea-level falls at sequence boundaries are very much more strongly emphasised upon the chart of Jacquin *et al.* (1991) as compared to those of Figure 6.46. This reflects the different criteria used to identify the magnitude of sequence boundaries. In the chart of Jacquin *et al.* (1991) the amplitude of a relative sea-level fall is weighted according to the 'jump' of coastal onlap at a sequence boundary. This contrasts to Figure 6.46 where the downward or basinward 'jump' at a sequence boundary is the average interpreted range of sea-level fall at a sequence boundary (eg.

its amplitude is a direct measurement of relative sea-level fall). The differences between these two approaches illustrates how upon a shallow-rimmed or an aggraded carbonate platform a low amplitude fall of relative sea-level fall (eg. 10-20m) can expose a large area of the shelf and hence cause a very significant basinward shift of 'coastal onlap'. During the 2nd order relative sea-level rise the Urgonian platform is thus interpreted to have maintained a position close to relative sea-level, and as a consequence thus, recorded low amplitude falls of relative sea-level (in comparison to the amplitude of relative sea-level rise) by developing sequence boundaries (eg. Fig. 6.46).

More quantitatively, the integration of the two relative sea-level curves for slope and shelf suggests a total relative sea-level rise of approximately 650m from the mid-lower Barremian to the mid Aptian (Fig. 6.46E). This relative sea-level rise occurred over a period of 2.9Ma (Fig. 6.46), giving an average rate of relative sea-level rise of 225 bubnoffs[5]. This compares to a second order 'eustatic' sea-level fall of approximately 20m during this time according to Haq *et al.* (1987), an average rate of 6.9 bubnoffs. If it is assumed that the 2nd order 'eustatic' fall of Haq *et al.* (1987) is correct this implies an average subsidence rate for the Urgonian platform of at least 232 bubnoffs between the upper part of SbBA1 (Bi5=BA1 HSTI) and the upper *Orbitolina* marls of sequence AP2. Assuming the 2nd order 20m fall of Haq *et al.* (1987) to be correct suggests a subsidence rate of approximately 250 bubnoffs during the 'regressive' phase of the Urgonian platform (prior to the transgression of the Urgonian shelf), and a subsidence rate of 195 bubnoffs for the Urgonian platform *sensu stricto*, plotted on Figure 6.47. This suggests that the southern Vercors (slope) subsided more rapidly than the Urgonian shelf (eg. differential subsidence between the shelf and slope) *and/or* that the lower Barremian was characterized by a higher subsidence rate than the upper Barremian and lower Aptian. Alternatively, if the subsidence rate is assumed to be constant (eg. at the average rate of 225 bubnoffs for the whole platform) then a higher rate of *eustatic* sea-level rise is implied during the

[5] 1 bubnoff = 1mm per 1000 years.

upper-lower Barremian compared to the upper Barremian and Aptian (suggesting that the 2nd order relative sea-level curve of Haq *et al.* 1987 is incorrect, 180° out of phase). Currently it is not possible to differentiate between these alternatives.

If it is assumed that the sections used to develop the relative sea-level chart of Figure 6.46 remained aggraded to within 10m of relative sea-level from the uppermost-lower Barremian to lower Aptian (eg. see Figs 5.1, 5.26 & 6.26), then the 3rd order relative sea-level falls of Haq *et al.* (1987) (eg. Fig. 6.46F) should closely match the amplitude of sea-level falls and timing of sequences developed up on the Urgonian platform (eg. Haq *et al.*, 1987; Posamentier & Vail, 1988; Posamentier *et al.*, 1988 etc.). The chronostratigraphic positions and approximate amplitudes of the 'eustatic' falls of sea-level have been measured off the chart of Haq *et al.* (1987) (version 3.1B) and are placed in their appropriate chronostratigraphic position in Column F of Figure 6.46. This shows that although the approximate amplitude of the 'eustatic' sea-level falls of Haq *et al.* (1987) are similar to the relative sea-level falls calculated from the Urgonian platform they are both fewer and have a very different chronostratigraphic distribution (eg. Fig. 6.46, compare columns E & F). This strongly suggests that the 3rd order 'eustatic' chart of Haq *et al.* (1987, version 3.1B) for the uppermost-lower Barremian to the lower Aptian is incorrect as none of the 'eustatic' sea-level falls of Haq *et al.* (1987) coincide with the development of a sequence boundary upon the Urgonian platform (assuming the interpretation of sequence boundaries and their chronostratigraphic positions of this study are accurate).

A comparison of the minimum sedimentation rates of the Urgonian platform to the aggradation rates of well known prograding carbonate platforms from the geological record is shown in Figure 6.47. The Urgonian platform exceeds all but the very highest aggradation rates of prograding carbonate platforms (Fig. 6.47), with an average aggradation rate of 225 bubnoffs, and extreme values of approximately 190 and 245 bubnoffs. This is a significantly higher than average aggradation rate for Cretaceous prograding carbonate platforms which tend to have aggradational rates of

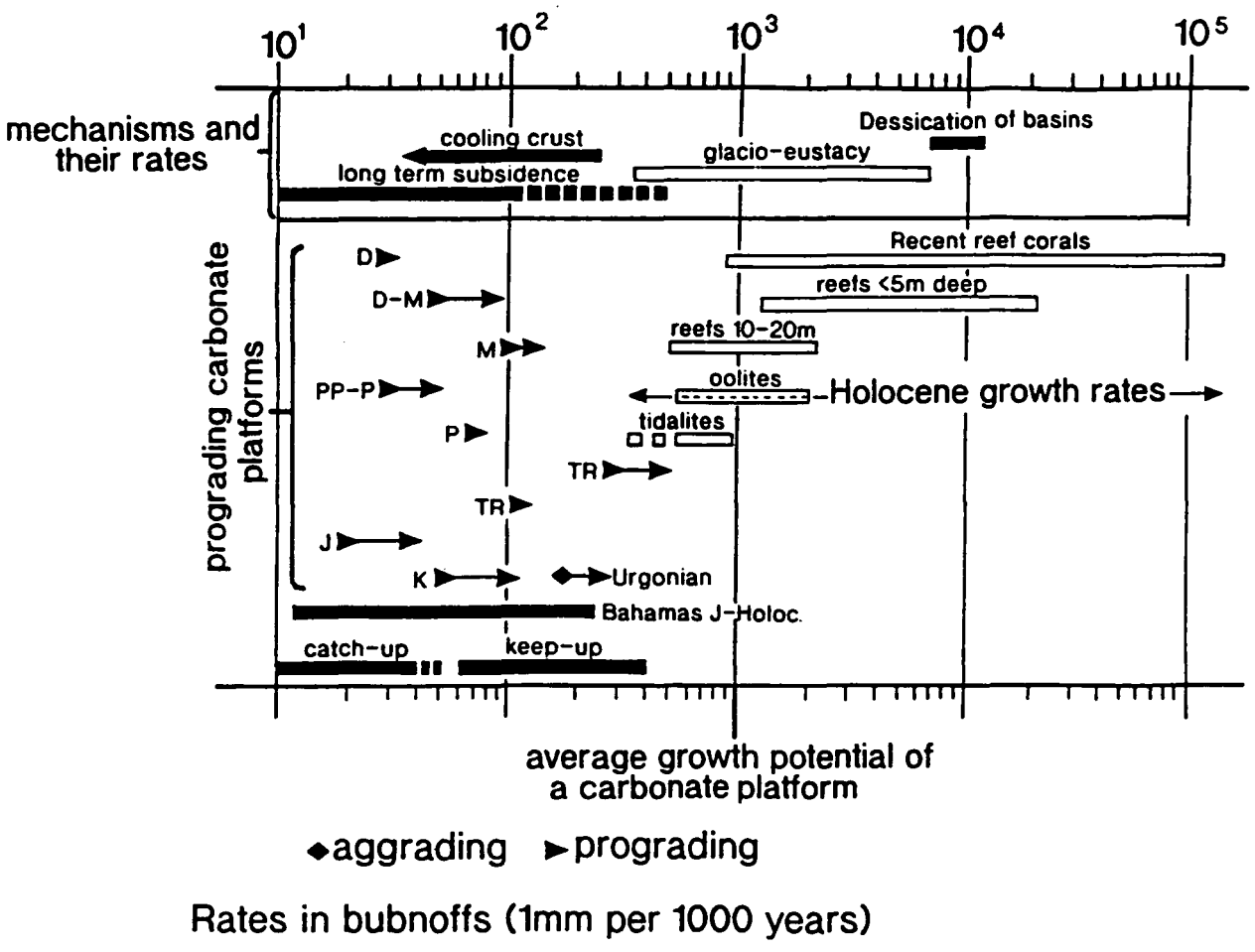

Figure 6.47. Comparison of the rates of aggradation from the Urgonian platform (In bubnoffs) to both other ancient prograding carbonate platforms (black boxes) and rates of aggradation from Holocene carbonate platforms (open boxes) (From Schlager, 1981). The aggradation rates for the Urgonian platform plot within the keep-up range of values for ancient prograding platforms as recognized by Sarg (1988). Aggradation rates for the Urgonian platform are also quite higher than comparative rates for other Cretaceous prograding carbonate platforms. Note that the lowermost aggradation rate for the Urgonian platform (*sensu lato*) corresponds to the upper aggradational ('transgressive') part of the platform (eg. Fig. 6.1) whereas the higher aggradational rate corresponds to the lower progradational ('regressive') part of the platform. This paradox may reflect higher sedimentation rates in the lower Barremian or a change in the orientation of the prevailing winds. See text for further discussion.

between 60 and 155 bubnoffs, tending towards the lower end of these values (Schlager, 1981; Sarg, 1988) (eg. see Fig. 6.47). According to Sarg (1988) the average aggradation rates for the Urgonian platform are typical of a 'keep-up' carbonate platform (Fig. 6.47). Sarg (1988) suggests that 'keep-up' times are

characterized at the platform margin by 'relatively small amounts of early submarine cement and generally dominated by grain-rich, mud-poor parasequences.....(and) displays a mounded/oblique geometry at the bank margin'. This description certainly approximates to the lower 'regressive' phase of Urgonian sedimentation, and would appear to be a fair description of a leeward orientated platform margin. A decrease to the rate of relative sea-level rise for the Urgonian platform *sensu stricto* should, theoretically, be marked by a change to stronger basinward progradation at the platform margin as a greater excess of sediments are shed into the basin allowing the progradation of the platform. Paradoxically, the reverse situation is observed upon the Urgonian platform. The decrease of aggradation rates in the upper Barremian-Aptian from 245 to 190 bubnoffs is associated with the change from a progradational to an aggradational, stationary shelf margin (eg. Figs 6.1, 6.4 & 6.47). Possibly this change marks an environmental change and a switch away from the preferred southward movement of shallow-water grains seen in the lower Barremian. Such a change could be associated with the interpreted change to more arid conditions during the development of the Urgonian platform. The average accretion rates of the Urgonian platform (uncorrected for compaction, and averaged over a few hundred thousand years) were far below the average growth potential of a Holocene carbonate platform (approximately 1000 bubnoffs, measured over 5000 years, Fig. 6.47). This further suggests that the drowning of the Urgonian platform was related to an increase of environmental stresses rather than rates of relative sea-level rise (see Section 6.2.8).

Chapter 7.
Conclusions.

As stated in Chapter 1 it has been the primary objective of this thesis to examine and test the current sequence stratigraphic models for carbonate shelves (eg. Vail, 1987; Sarg, 1988) by both literature review and their application to the mid-Cretaceous Urgonian carbonate platform of southeast France. The current widely used model depicting the sequence stratigraphic evolution of a carbonate shelf is largely derived from its conceptual siliciclastic counterpart: The model for a siliciclastic shelf has been used as the template from which the carbonate model was directly transposed. An evaluation of the current sequence stratigraphic models and development of new revised models specific to carbonate shelves in open-ocean settings, accounting for the differences between the carbonate and siliciclastic shelf depositional systems are discussed in the first part of this thesis (Chapters 2-3). The latter part of this thesis applies, compares and contrasts both the current and revised sequence stratigraphic models discussed in Chapters 2 and 3 to the Urgonian carbonate platform. Accordingly, the conclusions of this thesis are divided into two parts:

A1) The Current Exxon model.

This model depicts three systems tracts during the development of a sequence; the lowstand, transgressive and highstand systems tracts. These are divided by stratal discontinuities (eg. downlap, onlap or erosional surfaces). Areally significant erosion surfaces are thought to be formed during times of falling and lowstand of relative sea-level and form sequence boundaries. Type 1 sequence boundaries are characterized by the development of both subaerial and submarine erosion surfaces whereas in type 2 sequences the erosion is thought to be entirely subaerial. The erosion of the slope and deposition of a basin-floor sand complex are thought to be diagnostic of times of falling and lowstand of relative sea-level in a type 1 sequence, currently depicted by a single systems tract. This systems tract, however, contains two discrete stratal

packages; a basin-floor fan and a slope wedge which downlaps on to the preceding fan. Times of falling relative sea-level can be associated with the deposition of stranded parasequences on the shelf and/or upper shelf and their chronostratigraphic counterpart, the basin-floor fan. Currently these are placed below and above the sequence boundary respectively, although chronostratigraphically equivalent. Thus, new systematics were developed in Chapter 2 which separate the current lowstand systems tract in two, and these are; the *forced regressive wedge systems tract*, formed during times of falling relative sea-level, bounded below by the *'basal surface of forced regression'* and above by the *sequence boundary* representing the lowest point of sea-level fall, and the *lowstand prograding wedge systems tract*, developed as relative sea-level begins to rise after sequence boundary formation. This systems tract downlaps the basin-floor forced regressive deposits in a basinward direction and onlaps the forced regressive wedge sediments on the slope. Two end-members of lowstand prograding wedge are also distinguished; the *overfill* and *underfill* types and their development reflects the rate of sedimentation in comparison to that of relative sea-level rise.

A2) Development of new sequence stratigraphic models for carbonate shelves in open-ocean settings.

The differences between carbonate and siliciclastic depositional systems suggest that application of the previously-published sequence stratigraphic models for carbonate shelves are overly simplistic. These differences between siliciclastic and carbonate shelves can lead to the incorrect interpretation of systems tracts, sequences and ultimately relative sea-level curves from their direct and uncritical application to both subsurface and surface data. Carbonate platforms develop a wide range of geometric stacking patterns in response to both relative sea-level and environmental changes. Carbonate sedimentation rates cannot be assumed to be constant due the strong environmental sensitivity of carbonate secreting organisms in particular. Sedimentation rates are also very differentiated across a a shelf.

Conclusions.

Carbonate shelves in open ocean settings will tend to be characterized by volumetrically small lowstand wedges. Carbonate sedimentation during lowstand of relative sea-level is restricted to a narrow strip upon the slope. Little or no sediment is received off the shelf whilst it is subaerially exposed. The sequence boundary on the shelf is generally marked by meteoric diagenesis which is normally climatically controlled. Times of falling and lowstand of relative sea-level are commonly associated with the collapse of the slope, deposition of megabreccias on the basin-floor (*allochthonous debris*) and the development of *autochthonous wedges* on the slope. Two end-members of lowstand sedimentation can be differentiated: low angle mud-dominated slopes, characterized by basin-floor debrites, turbidites and a volumetrically significant autochthonous wedge and, high angle slopes characterized by basin-floor megabreccias and volumetrically insignificant or even absent autochthonous slope wedges.

Several different stratal patterns can also be distinguished during the transgressive systems tract and these reflect the complex interplay of relative sea-level rise, sedimentation rate and environmental change. Two different types of geometric stacking pattern are recognized: *type 1 transgressive geometries*, developed when the rate of relative sea-level rise is greater than sedimentation rates, *and type 2 transgressive geometries*, formed when sedimentation rates of the shelf-margin facies are equal to, or greater than rates of relative sea-level rise. The type 2 geometries can be associated with the oversteepening of the slope, leading to its collapse and the deposition of basin-floor megabreccias and/or the bypass of the slope and deposition of carbonate sands on the basin-floor. The highstand systems tract is the time of maximum productivity of carbonate platforms and is normally associated with rapid basinwards progradation. Two different progradational stratal patterns are distinguished, *slope aprons* and *toe-of-slope aprons*. Thus, carbonate shelves in open-ocean settings *can* develop stratal patterns similar to those reported from siliciclastic shelves, but in the majority of cases they are very different.

A more detailed listing of conclusions from this part of the thesis is given at the end of Chapter 3 (pgs. 101-104).

B) The development of a sequence stratigraphy for the Urgonian platform.

B1A. Stratal patterns and key stratal surfaces: Shelf.

1. The characteristic stratal pattern of the shelf-lagoon is parallel-parallel, from the shallowing-up cycle to the sequence scale. Erosional truncation can, however, be developed during times of falling and lowstand of relative sea-level if siliciclastic sediments are introduced on to the shelf. By way of contrast, at the shelf-margin the dominant stratal pattern is downlap of prograding sand shoal complexes on to the preceding drowning / exposure surface.

2. The sequence boundary as defined by Exxon production research (eg. Vail *et al.*, 1977) is preferred to the division of 'genetic sequences' by flooding surfaces as proposed by Galloway (1989a, b) because; A: On a carbonate shelf the sequence boundary has a higher preservation potential as compared to a siliciclastic shelf due to the early diagenesis of shallow-water carbonate sediments and the frequent continuation of this process during subaerial exposure. Thus, the sedimentological sequence boundary is not normally significantly reworked and lost during transgression; B: Upon the Urgonian shelf a clear flooding surface is not always developed, but may be 'concealed' within a thick succession of lagoonal sediments (eg. the TST and HST are not always easily distinguished); C: It is easier to correlate a single exposure surface from the shelf-lagoon to the shelf-margin. Exposure is normally marked by the development of a discrete surface whereas, in complete contrast, several different flooding surfaces can be developed at the shelf-margin during a relative sea-level rise and/or no well developed flooding surface may develop.

3. Type 1 and type 2 sequence boundaries cannot normally be distinguished on the shelf unless sea-level falls before the shelf has aggraded close to sea-level. Stratal patterns developed by the two types of sequence boundary on the shelf are otherwise characteristically parallel-parallel. Erosional, type 1 unconformities are only developed when siliciclastics are introduced on to the shelf during times of falling and lowstand of relative sea-level.

4. The sequence boundary and lowstand of relative sea-level is normally marked on the shelf by vadose meteoric diagenesis which is only weakly penetrative (1-2m). Thin and laterally discontinuous beds of lacustrine limestones may also be developed at this time.

5. The transgressive and highstand systems tracts are the main components of shelf sedimentation. Lowstand sedimentation is generally absent from the shelf or volumetrically very insignificant.

6. The distinction of transgressive and highstand systems tracts on the shelf can be difficult as sedimentation rates were frequently able to keep pace with rates of relative sea-level rise. In such cases no clear mfs is developed and so the TST and HST cannot be differentiated.

7. The transgressive surface is normally associated with the start-up of protected low-energy shallow-water carbonate sedimentation on the shelf. If sedimentation rates on the shelf were greater than rates of relative sea-level rise then the sequence boundary is normally preserved with little modification. In complete contrast, if sedimentation did not start-up during the transgressive systems tract or if sedimentation rates quickly fell behind rates of relative sea-level rise then the sequence boundary is frequently substantially modified as high-energy, open-shelf environments became established on the shelf, developing a *compound surface*.

8. At the shelf-margin two main types of stratal package are generally developed, aggradational and progradational. These packages may be separated by sub-wavebase limestones developed when the shelf-margin drowned as sedimentation 'gave-up'. Bs1 is, however, an notable exception to this general rule. The shelf-lagoon is typified by aggradational (early TST and HST) and give-up packages (late TST).

9. Shallowing-upward cycles and parasequences are for the most part poorly developed up on the Urgonian platform. Where observed these cycles are very atypical and this is thought to reflect a combination of low rates of relative sea-level rise in comparison to sedimentation rates. At the shelf-margin well developed subtidal shallowing-up cycles area developed. These are typically 10m thick and are thought to have been developed in an area of net sediment export, preventing their aggradation to develop peritidal facies.

10. Climatic changes can exert a strong control upon shelf stratal patterns. Change to humid conditions can be related to the influx of siliciclastics on to the shelf and the development of karstic dissolution features. During times of falling and lowstand of relative sea-level such changes are associated with the development of incised valleys on the shelf (eg. SbAP2). At other times the influx of siliciclastics can reduce carbonate sedimentation rates and allow the development of subtidal asymmetric shallowing-up cycles as sedimentation rates were retarded.

B1B. Stratal patterns and key stratal surfaces: Slope.

1. Erosional truncation is the obvious stratal relationship developed upon the slope. In the Exxon model erosion of the slope and bypass of sediments through it to the basin-floor are classically interpreted to occur during times of falling and lowstand of relative sea-level. However, upon the flanks to the Urgonian platform neither erosional truncation or bypass are restricted to times of falling and lowstand of relative sea-level (on the slope). Both can also be developed during the transgressive and highstand systems tracts, thus producing stratal patterns and/or facies associations

which closely mimic those supposedly diagnostic of the lowstand systems tract. Slope bypass can also be related to inherited slope morphology and/or the sedimentary steepening of the slope due to build-up at the shelf-margin. Collapse of the flanks of the Urgonian platform can also be related to allocyclic processes such as steepening of slope angles through tectonic rotation and/or seismic shocks.

2. The sequence boundary is not necessarily associated with the erosion of the slope but can be associated with the development of a parallel-parallel stratal pattern, onlap or downlap.

3. The sequence boundary is, however, normally associated with an abrupt facies change. This is perhaps its most diagnostic feature because of the wide range of stratal patterns which can be associated with the development of a sequence boundary on the slope.

4. The upper slope is characterized by the development of the shallow-water autochthonous slope wedge during lowstand of relative sea-level. Upon the flanks of the Urgonian platform these are volumetrically quite significant due to the low angle of slopes on its flanks. Normally, these autochthonous wedges are dominated by mobile, relatively uncemented bioclastic sands.

5. The most characteristic feature of the transgressive systems tract is the development of the mfs, which can be associated with the development of condensed sedimentation (eg. glauconite, phosphates). The systems tract itself can be characterized by a wide variety of stratal patterns depending upon the interplay of sedimentation rates and rates of relative sea-level rise at the shelf-margin.

6. The highstand systems tract is normally characterized by the downlap of clinoforms on to the slope. Bypassing of sands to the basin-floor may occur depending upon the slope morphology inherited by this systems tract.

B1C. Stratal patterns and key stratal surfaces: Basin-floor.

1. The Urgonian platform is associated with a major re-organisation of basin-floor sedimentation patterns, from elongate fans in the centre of the basin to discrete fans at the toe-of-slope.

2. The basin-floor is characterized by two distinct types of allochthonous sediment; slumps and debrites derived from collapse of the slope and, sands bypassed from the shelf through the slope. Allochthonous basin-floor sedimentation can occur during times of falling relative sea-level, but equally can be deposited during the transgressive and highstand systems tracts. The timing of basin-floor sedimentation is, to a large extent, dependant upon the processes on the slope.

3. According to the Exxon model the dominant stratal pattern on the basin-floor is convex-up mounds, developed by distributary channels upon a basin-floor fan. The dominant stratal pattern developed by allochthonous basin-floor sands to the Urgonian platform is, however, parallel-parallel, cut by concave-up channels. Chaotic patterns are developed by megabreccias.

Neither the slope or the basin-floor are associated with a predictable development of stratal surfaces and/or facies associations as for instance suggested by Haq *et al.* (1987), Posamentier *et al.* (1988) or Galloway (1989a,b). The development of stratal packages and stratal termination patterns upon the slope and/or basin-floor reflects a complex interaction of variables which can be, and often are, independent of changes in relative sea-level.

B2. Sequential development of the Urgonian platform.

1. The Urgonian platform *sensu lato* is characterized by a lower regressive, progradational phase of sedimentation when sea-level was below the slopebreak of the preceding Hauterivian platform and an upper transgressive phase. These correspond to the lowstand and transgressive systems tracts of the second order relative

sea-level curve. The lower progradational phase paradoxically has a higher aggradation rate than the upper aggradational part of the platform. Aggradation rates are far higher than for other Cretaceous prograding carbonate platforms and second only to those of the Triassic platforms in the Dolomites.

2. The base of the Urgonian platform *sensu lato* (BA1) corresponds to the lowest point of the 2nd order relative sea-level curve, above which a large general lowstand wedge is developed, the Glandasse Limestone Formation. This is divided by a type 2 sequence boundary.

3. The lowstand deposits of the first sequence are characterized by the deposition of a thick basin-floor fan, and the bypass of the upper slope. Possibly this bypassing is related to the tectonic rotation of the slope, rather than being solely of sedimentary origin.

4. This lowermost sequence is characterized by the development of two transgressive and highstand systems tracts. Both transgressive systems tracts are characterized by a type 2 aggradational geometry. The formation of the two sets of systems tracts is thought to be due to an acceleration in the rate of relative sea-level rise mid-way through the sequence, eventually drowning carbonate sedimentation and developing the Lower Fontaine Colombette marls. This illustrates the non-sinusoidal (eg. ideal) form of the relative sea-level curve.

5. The maximum flooding surface of the second systems tract of this first urgonian sequence (BA1) is associated with the development of a type of drowning unconformity upon the slope. This is commonly mistaken for a type 1 sequence boundary.

6. The second highstand systems tract of this BA1 sequence is relatively thin and downlaps onto the mfs. Its upper surface is the erosional type 2 sequence boundary

BA2, overlain by a relatively thin package (5m) of rudist limestones, representing lowstand sedimentation. Erosional truncation of this sequence boundary is minor and entirely submarine, both on the shelf and the slope.

7. The drowning of lowstand sedimentation marks the base of the BA2 transgressive systems tract characterized by the development of a thick and complex aggradational-progradational package of sands at the shelf-margin (Bi6b-h and Bs1). The upper part of the transgressive systems tract is marked by the flooding of the shelf, marking the end of the regressive phase of sedimentation and the base of the Urgonian shelf *sensu stricto*.

7. The Urgonian platform (*sensu stricto*) is divisible into six third-fourth order sequences. These sequences developed in times of an overall relative sea-level rise, separated by low-amplitude relative sea-level falls which developed sequence boundaries on the shelf as it was aggraded close to relative sea-level (<10m) at these times.

8. Normal Urgonian sedimentation is interrupted by the Lower *Orbitolina* beds at the base of sequence AP1. These are characterized by subtidal asymmetric shallowing-up cycles and are thought to have developed in response to an influx of siliciclastic sediments on to the platform which reduced carbonate sedimentation rates. This influx of siliciclastic sediments on to the shelf is thought to reflect a change to more humid climatic conditions, as are the upper *Orbitolina* beds, developed on the top of the platform.

9. The drowning of the Urgonian shelf occurred after the subaerial exposure of the shelf, developing the final sequence boundary of the shelf. This is thought to have occurred in response to the combination of influx of siliciclastics on to the shelf, relative sea-level rise and the inception of a major oceanic current which swept over the platform.

References

ACKER, K.E. & STEARN, C.W. (1990). Carbonate-siliciclastic transition and reef growth on the northeast coast of Barbados, West Indies. *J. Sed. Petrol.* **60**, 18-25.

AHR, W.M. (1989). Sedimentary and tectonic controls on the development of an early Mississippian carbonate ramp, Sacramento Mountains area, New Mexico. *In: Controls on Carbonate Platform and Basin Development* (Ed. by P.D. Crevello, J.L. Wilson, J.F. Sarg & J.F. Read). Spec. Publ. Soc. Econ. Paleont. Mineral. 44, 203-213.

ARNAUD, H. (1979). Surfaces d'ablation sous-marines et sédiments barrémo-bédouliens remaniés par gravité du Barrémian au Cénomanien entre le Vercors et le Dévoluy (SE de la France). *Géologie Alpine* **55**, 5-21.

ARNAUD, H. (1981). De la plate-forme urgonienne au bassin vocontien: le Barrémo-Bédoulien des Alpes occidentales entre Isère et Buëch (Vercors méridional, Diois oriental et Dévoluy). *Géologie Alpine*, mém. 11, 804 p.

ARNAUD, H. (1988). Subsidence in certain domains of southeastern France during the Ligurian Tethys opening and spreading stages. *Bull. Soc. géol. France* **IV** (8), 725-732.

ARNAUD, H. & ARNAUD-VANNEAU, A. (1989). Séquences de dépôt et variations du niveau relatif de la mer au Barrémien à l'Aptien inférieur dans les massifs sub-alpins septentrinoux et la Jura (SE de la France). *Bull. Soc géol. France* **V** (8), 651-660.

ARNAUD-VANNEAU, A. (1980). Micropaléontologie, paléoécologie et sédimentologie d'une plate-forme carbonatée de la marge passive de la Téthys: l'Urgonien du Vercors septentrional et de la Chartreuse (Alpes occidentales). *Géologie Alpine*, mém 10, 874 p.

ARNAUD-VANNEAU, A. & ARNAUD, H. (1976). L' evolution paléogéographique du Vercors au Barrémien et à l'Aptien inférieur (Chaînes subalpines septentrionales, France). *Géologie Alpine*, Grenoble **52**, 5-30.

ARNAUD-VANNEAU, A. & ARNAUD, H. (1986). Age des couches hémipélagiques infra-urgoniennes et mise en place de la plate-forme urgonienne du Jura au Vercors. *C.R. Acad. Sc. Paris* **303** (II), 1803-1806.

ARNAUD-VANNEAU, A. & ARNAUD, H. (1990). Hauterivian to Lower Aptian carbonate shelf sedimentation and sequence stratigraphy in the Jura and northern Subalpine chains (southeastern France and Swiss Jura). *In: Carbonate Platforms* (Ed. by M.E. Tucker, J.L. Wilson, P.D. Crevello, J.F. Sarg & J.F. Read). Int. Assoc. Sedim. Spec. Publ. 9, 203-233.

ARNAUD-VANNEAU, A. & ARNAUD, H. (1991). Sedimentation et variations relatives du niveau de la mer sur les plate-formes carbonatées du Berriasien-Valanginien

inférieur et du Barrémian dans les massifs subalpins septentrionaux et la jura (Sud-Est de la France). *Bull. Soc. géol. France* **VII** (8), 535-545.

ARNAUD-VANNEAU, A., ARNAUD, H., ADATTE, T., ARGOT, M., RUMLEY, G. & THIELOY, J.-P. (1987). *The Lower Cretaceous from the Jura platform to the Vocontian basin (Swiss Jura, France).* Third International Cretaceous Symposium Fieldguide Guide. pp. 128.

ARNAUD-VANNEAU, A., ARNAUD, H., MEUNIER, A.- R. & SEGUIN, J.-C. (1987). Caractères des transgressions du Crétacé inférieur sur les marges de l'océan ligure (Sud-Est de la France et Italie centrale). *Mém. Géol. Université de Dijon* **11**, 167-182.

ARNAUD-VANNEAU, A., ARNAUD, H. & THIEULOY, J.-P. (1976). Bases nouvelles pour la stratigraphie des calcaires urgoniennes du Vercors. *Newsl. Stratig.* **5**(2-3), 143-149.

ARNAUD-VANNEAU, A. & MEDUS, J. (1977). Palynoflores barrémo-aptiennes de la plate-forme urgonienne du Vercors Palynostratigraphie de queques formes de *Classopollis* et de quelques pollens angiosperms. *Géologie Alpine* **53**, 35-55.

BALLY, A.W. (1987) *Atlas of Seismic Stratigraphy I.* Am. Assoc. Petrol Geol. Studies in Geology 27.

BARFETY, J.-C. & GIDON, M. (1983). La stratigraphie et la couverture dauphinoise au Sud de Bourg d'Oisans. Leurs relations avec les déformations synsédimentaires jurassiques. *Géologie Alpine* **59**, 5-32.

BARRON, E.J. (1987). Cretaceous plate tectonic reconstructions. *Palaeogeog. Palaeoclim. Palaeoecol.* **56**, 3-29.

BARRON, E.J., THOMPSON, S.L. & SCHNEIDER, S.H. (1981). An ice-free Cretaceous? Results from climate model simulations. *Science* **212**, 501-508.

BAY, T.A. (1977). Lower Cretaceous stratigraphic models from Texas and Mexico. *In: Cretaceous Carbonate of Texas & Mexico* (Ed. by D.G. Bebout & R.G. Loucks). Bureau of Economic Geology, Rept of Investigations 89, Austin, Texas, 12-30.

BLES, J.L., BONIJOLY, C., CASRAING, C. & GROS, Y. (1989). Successive post-Varsican stress fields in the French Massif Central and its borders (Western Europoean Plate): comparison with geodynamic data. *Tectonophysics* **169**, 79-111.

BOARDMAN, M.R., NEUMANN, A. C., BAKER, P. A., DULIN, L. A., KENTER. R. J., HUNTER. G. E. & KIEFER. K. B. (1986). Banktop response to Quaternary fluctuations in sea-level recorded in periplatform sediments. *Geology* **14**, 28-31.

BOISSEAU, T. (1987). *La plate-forme jurassienne et sa bordure subalpine au Berriasian-Valanginian (Chartreuse-Vercors).* -Thèse Université Grenoble.

BOSELLINI, A. (1984). Progradation geometries of carbonate platforms: examples from the Triassic of the Dolomites, northern Italy. *Sedimentology* **31**, 1-24.

BOSELLINI, A. (1989). Dynamics of Tethyan carbonate platforms. *In: Controls on Carbonate Platform and Basin Development* (Ed. by P.D. Crevello, J.L. Wilson, J.F. Sarg & J.F. Read). Spec. Publ. Soc. Econ. Paleont. Mineral. 44, 3-13.

BOSENCE, D.W.J., ROWLANDS, R. & QUINE, M. (1985). Sedimentology and budget of a recent carbonate mound, Florida Keys. *Sedimentology* **32**, 317-343.

BROOKS, G.R. & HOLMES, C.W. (1989). Recent carbonate slope sediments and sedimentary processes bordering a non-rimmed platform: southwest Florida continental margin. *In: Controls on Carbonate Platform and Basin Development* (Ed. by P.D. Crevello, J.L. Wilson, J.F. Sarg & J.F. Read). Spec. Publ. Soc. Econ. Paleont. Mineral. 44, 259-272.

BROWN, L.F. & FISHER, W.L. (1980). *Seismic stratigraphic interpretation and petroleum exploration.* AAPG Continuing Education Course Notes Series #16, 179p.

BUBB, J.N. & HATLELID, W.G. (1977). Seismic recognition of carbonate buildups. *In: Seismic stratigraphy-Applications to Hydrocarbon Industry* (Ed by C.E Payton). Am. Assoc. Petrol. Geol. Mem. 26, 185-204.

BUSNARDO, R. (1965). Le stratotype du Barrémien. Lithologie et macrofaune - Colloque sur le Créacé inférieur, Lyon 1963. *Mém. Bull. Rech. Géol. Min.* **34**, 101-116.

BUTLER, R.W.H. (1989). The influence of pre-existing basin structure on thrust systems evolution in the Western Alps. *In: Inversion Tectonics* (Ed. by M.A. Cooper & G.D. Williams). Spec. Pub. Geol. Soc. Lond. 44, 105-122.

CALVET, F., TUCKER, M.E. & HENTON, J.M. (1990). Middle Triassic carbonate ramp systems in the Catalan Basin, northeast Spain: facies, systems tracts, sequences and controls. *In: Carbonate Platforms* (Ed. by M.E. Tucker, J.L. Wilson, P.D. Crevello, J.F. Sarg & J.F. Read). Int. Assoc. Sedim. Spec. Publ. 9, 79-108.

CARTER, R.M. (1988). Plate boundary tectonics, global sea-level and the development of the eastern Siuth Island continental margin, New Zealand, southwest Pacific. *Marine Petrol. Geol.* **5**, 90-105.

CLAVEL, B., BUSNARDO, R. & CHAROLLAIS (1986). Chronologie de la mise en place de la plate-forme urgonienne du Jura au vercors (France) *C. R. Acad Sc. Paris* **302** (II), 583-586.

CLAVEL, B., CHAROLLAIS, J. & BUSNARDO, R. (1987). Données biostratigraphiques nouvelles sur l'apparation des facies urgoniens du Jura au Vercors. *Eclogae Gèol. Helv.* **80**, 59-68.

COLACICCHI, R., PIALLI, G. & PRATURLON, A. (1975). *Megabreccias as a product of tectonic activity along a carbonate platform margin.* 11th Internat. Sediment. Congress, Nice, pp. 61-70.

COTILLION, P. (1987). Bed-scale cyclicity of pelagic Cretaceous successions as a result of world-wide control. *Marine Geology* **78**, 109-123.

COTILLION, P., FERRY, S., GALLIARD, C., JAUTEE, E., LATREILLE, G. & RIO, M. (1980). Fluctuation des paramètres du milieu marin dans le domaine vocontien (France Sud-Est au Crétacé inférieur: mise en évidence par l'étude des formations marno-calcaires alternantes. *Bull. Soc. géol. France* **XXII**(7), 735-744.

CREVELLO, P.D. & SCHLAGER, W. (1980). Carbonate debris sheets and turbidites, Exuma Sound, Bahamas. *J. Sed. Petrol.* **50**, 1121-1148.

CURNELLE, R. & DUBOIS, P. (1986). Evolution mésozoïque des grands bassins sédimentaires français; bassins de Paris, d'Aquitaine et du Sud-Est. *Bull. Soc géol. France* **II**(8), 529-546.

CURRAY, J.R. (1965). *Late Quaternary history, continental shelves of the United States.* Princeton. Univ. Press, 723-735.

DARSAC, C (1983). *La plate-forme berriaso-valanginienne du Jura méridional aux massifs subalpins (Ain, Savoie).* Thèse 3e cycle, Univ. Grenoble, 319p.

DAVIES, P.J., SYMONDS, P.A., FEARY, D.A. & PIGRAM, C.J. (1989). The evolution of the carbonate platforms of northeast Australia. *In: Controls on Carbonate Platform and Basin Development* (Ed. by P.D. Crevello, J.L. Wilson, J.F. Sarg & J.F. Read). Spec. Publ. Soc. Econ. Paleont. Mineral. 44, 233-258.

DECONINCK, J.-F. (1984). *Sédimentation et diagenèse minéraux argileux du Jurassique supérieur-Crétacé dans le Jura méridional et le domaine subalpin (France-Sud-Est). Comparison avec le domaine atlantique Nord.* 3rd cycle thesis, University of Lille, France, 150p.

DEBELMAS, J. (1983). *Alpes du Dauphiné.* Guides Géologiques Régionaux de France. 198p.

DELAMETTE, M. (1988). Relation between the condensed Albian deposits of the Helvetic domain and the oceanic-current influenced continental margin of the northern

Tethys. *Bull. Soc. géol. France.* **IV**(8), 739-745.

DOGLIONI, C., BOSELLINI, A. & VAIL, P.R. (1990). Stratal patterns: a proposal of classification and examples from the Dolomites. *Basin Research* **2**, 83-95.

DOMINGUEZ, L.L., MULLINS, H.T. & HINE, A.C. (1988). Cat Island platform, Bahamas: an incipiently drowned Holocene carbonate shelf. *Sedimentology* **35**, 805-819.

DROXLER, A. & SCHLAGER, W. (1985). Glacial versus interglacial sedimentation rates and turbidite frequency in The Bahamas. *Geology* **13**, 799-802.

EBERLI, G.P. (1987). Carbonate turbidite sequences deposited in rift-basins of the Jurassic Tethys Ocean (eastern Alps, Switzerland). *Sedimentology* **34**, 363-388.

EBERLI, G.P. & GINSBURG, R.N. (1989). Cenozoic progradation of northwestern Great Bahama Bank, a record of lateral platform growth and sea-level fluctuations. *In: Controls on Carbonate Platform and Basin Development* (Ed. by P.D. Crevello, J.L. Wilson, J.F. Sarg & J.F. Read). Spec. Publ. Soc. Econ. Paleont. Mineral. 44, 339-351.

ELMI, S. (1990). Stages in the evolution of late Triassic and Jurassic carbonate platforms: the western margin of the subalpine basin (Ardèche, France). *In: Carbonate Platforms* (Ed. by M.E. Tucker, J.L. Wilson, P.D. Crevello, J.F. Sarg & J.F. Read). Int. Assoc. Sedim. Spec. Publ. 9, 109-144.

ENOS, P. (1977). Holocene sediment accumulations of the South Florida shelf margin. *In: Quaternary Sedimentation in South Florida* (Ed. by P. Enos and R.D. Perkins). Mem. Geol. Soc. Am. 147, 1-130.

ENOS, P. (1983). Shelf. *In: Carbonate Depositional Environments* (Ed. by P.A. Scholle, D.G. Bebout & C.H. Moore). Mem. Am. Assoc. Petrol. Geol. 33, 507-538.

ERLICH, R.N., BARRETT, S.F. & GUO BAI JU. (1990). Seismic and geological characteristics of drowning events on carbonate platforms. *Am. Assoc. Petrol. Geol. Bull.* **74**, 1523-1537.

ESTEBAN, M. (1991). *Mesozoic and Early Tertiary Karst bauxites of the Mediterranean area and related regional unconformities: eustatic versus tectonic control.* Keynote address: Mesozoic and Early tertiary karst bauxites of the Mediterranean area and related regional unconformities; eustatic versus tectonic control. *Terra Nova* **3**, 235.

EVERTS, A.J.W. (1991). Interpreting compositional variations of calciturbidites in relation to platform stratigraphy: an example from the Paleogene of S.E. *Spain. Sedimentary Geology* **71** 231-242.

FERRY, S. (1976). *Cônes d'épandage bioclastiques en eau profonde et glissements sous-marins dans le Barrémienet l'Aptien inférieur vocontiens de la Drôme. Implications paléostructurales.* Thése 3e cycle, Lyon, 144p.

FERRY, S. & FLANDRIN, J. (1979). Mégabrèches de resédimentation, lacunes mécaniques et pseudo "hardgrounds" sur la marge vocontienne au Barrémien et à l'Aptien inferieur (Sud-Est de la France). *Géologie Alpine* **55**, 75-92.

FERRY, S. & RUBINO, J.L. (1989). *Mesozoic eustacy record on western Tethyan margins. Post-meeting field trip in the Vocontian trough.* Assoc. Sediment. Francais, pp. 141.

FOLLMI, K.B. (1989). Mid-Cretaceous platform drowning, current-induced condensation and phosphogenesis, and pelagic sedimentation along the eastern Helvetic shelf (northern Tethys margin). *In:Cretaceous of the Western Tethys* (Ed. by J. Wiedmann). E. Schweizbart'sche Verlagsbuchhanslung press, Stuttgart. 585-606.

FRANSEN, E.V. & MANKIEWICZ, C. (1991). Depositional sequences and correlation of middle to late miocene carbonate complexes, Las Negras and Níjar areas, southeastern Spain. *Sedimentology* **38,** 871-898.

FRIEDMAN, G.M. (1988). Histories of coexisting reefs and terrigenous sediments: the Gulf of Elat (Red Sea), Java sea, and Neogene basin of the Negev, Israel. *In: Carbonate-Clastic Transitions* (Ed. by L.J. Doyle & H.H. Roberts). Developments in Sedimentology 42, 77-98.

GALLOWAY, W.E. (1989a). Genetic stratigraphic sequences in basin analysis. 1: architecture and genesis of flooding-surface bounded depositional units. *Am. Assoc. Petrol. Geol. Bull.* **73**, 125-142.

GALLOWAY, W.E. (1989b). Genetic stratigraphic sequences in basin Analysis II: Application to northwest Gulf of Mexico Cenozoic basin. *Am. Assoc. Petrol. Geol. Bull.* **73**, 143-154.

GARDULSKI, A.F., MULLINS, H.T. & WEITERMAN, S. (1990). Carbonate mineral cycles generated by foraminiferal and pteropod response to Pleistocene climate: west Florida ramp slope. *Sedimentology* **37**, 727-743.

GAMBOA, L.A., TRUCHAN, M. & STOFFA, P.L. (1985). Middle and Upper Jurassic depositional environments at outer shelf and slope of Baltimore Canyon Trough. *Am. Assoc. Petrol. Geol. Bull.* **69**, 610-621.

GEBELEIN, C.D. (1974). *Guidebook for modern Bahamian platform environments.* Geol. Soc. Amer. Ann. Mtg. Fieldtrip Guide, 93p.

GILLCHRIST, R., COWARD, M. & MUGNIER, J.-L. (1987). Structural inversion and its controls: examples from the Alpine foreland and the French Alps. *Geodinamica Acta* **1**(1), 5-34.

GINSBURG, R.N. & JAMES, N.P. (1974). Holocene carbonate sediments of continental shelves. *In*: *Continetal margins* (Ed. by C.A. Burk and C.L. Drake). Springer-Verlag, Berlin, 137-154.

GLASER, K.S. & DROXLER, A.W. (1991). High production and highstand shedding from deeply submerged carbonate banks, northern Nicaragua Rise. *Jour. Sed. Petrology*, **61**, 128-142.

GLYNN, P.W. (1977). Coral growth in upwelling and non-upwelling areas off the Pacific coast of Panama. *Jour. Marine Research* **35**, 567-585.

GLYNN, P.W. & DE WEERDT, W.H. (1991). Elimination of Two Reef-Building Hydrocorals following the 1982-83 El Niño warming event. *Science* **253**, 69-71.

GOLDHAMMER, R.K. & HARRIS, M.T. (1989). Eustatic controls on the stratigraphy and geometry of the Latemar buildup (Middle Triassic), the Dolomites of northern Italy. *In: Controls on Carbonate Platform and Basin Development* (Ed. by P.D. Crevello, J.L. Wilson, J.F. Sarg & J.F. Read). Spec. Publ. Soc. Econ. Paleont. Mineral. 44, 323-338.

GOLDHAMMER, R.K. DUNN, P.A. & HARDIE, L.A. (1990). Depositional cycles, composite sea-level changes, cycle stacking patterns, and the hierarchy of stratigraphic forcing: Examples from Alpine Triassic platform carbonates. *Geol. Soc. Amer. Bull.* **102**, 535-562.

GRACIANSKY, P.-C. & LEMOINE, M. (1988). Early Cretaceous extensional tectonics in the southwestern French Alps: a consequence of North Atlantic rifting during Tethyan spreading. *Bull. Soc. géol. France* **IV**, 733-739.

GREENLEE, S.M. & LEHMANN, P.J. (1990). Stratigraphic framework of productive carbonate buildups (Abstract). *Am. Assoc. Petrol. Geol. Bull.* **74**, 618.

HALLAM, A. (1977). Secular changes in marine inundation of USST and North America through the Phanerozoic. *Nature* **269**, 762-772.

HANCOCK, J.M. & KAUFFMAN, E.J. (1979). The great transgressions of the Late Cretaceous. *J. Geol. Soc. Lond.* **136**, 175-186.

HAQ, B.U., HARDENBOL, J. & VAIL, P.R. (1987). Chronology of fluctuating sea levels since the Triassic. *Science* **235**, 1156-1167.

HAQ, B.U., HARDENBOL, J. & VAIL, P.R. (1988). Mesozoic and Cenozoic chronostratigraphy and cycles of sea-level change. *In: Sea-level Changes: an Integrated Approach* (Ed. by C. K. Wilgus, B. S. Hastings, C. G. St.C. Kendall, H. W. Posamentier, C. A. Ross & J. C. Van Wagoner). Spec. Publ. Soc. Econ. Paleont. Mineral. 42, 71-108.

HALLOCK, P. & SCHLAGER, W. (1986). Nutrient excess and the demise of coral reefs and carbonate platforms. *Palaios* **1**, 389-398.

HILBRECHT, H. (1989). Redeposition of late Cretaceous pelagic sediments controlled by sea-level fluctuations. *Geology* **17**, 1072-1075.

HINE, A.C. & MULLINS, H.T. (1983). Modern carbonate shelfbreaks. *In: The Shelfbreak: Critical Interface of Continental Margins* (Ed. by D.J. Stanley & G.T. Moore). Spec. Publ Soc. Econ. Paleont. Mineral. 33, 169-188.

HINE, A.C. & STEINMETZ, J.C. (1984). Cay Sal Bank, Bahamas-A partially drowned carbonate platform. *Mar. Geol.* **59**, 135-164.

HINE, A. C., WILBERT, R.J. & NEUMAN, A.C. (1981). Carbonate sand-bodies along contrasting shallow-bank margins facing open seaways; northern Bahamas. *Am. Assoc. Petrol. Geol. Bull.* **65**, 261-290.

HIRD, K. & TUCKER, M.E. (1988). Contrasting diagenesis of two Carboniferous oolites from South Wales: a tale of climatic influence. *Sedimentology* **35**, 587-602.

HUBBARD, R.J. (1988). Age and significance of sequence boundaries on Jurassic and early Cretaceous rifted continental margins. *Am. Assoc. Petrol. Geol. Bull.* **72**, 49-72.

HUMPHREY, J.S. & KIMBELL, T.N. (1990). Sedimentology and sequence stratigraphy of Upper Pleistocene carbonates of S.E. Barbados, West Indies. *Am. Assoc. Petrol. Geol. Bull.* **74**, 1671-1684.

HUNT, D. (1990). *Stratal patterns, and sedimentation associated with development of a gullied bypass margin: similarities to a type 1 sequence boundary.* (Abstract) Proceedings of the British Sedimentological Research Group, p 37.

HUNT, D. (1991). *A proposed classification for rates of relative sea-level change for carbonate depositional systems, with particular respect to rimmed shelves. Terra Absracts* **3**, 275.

HUNT, D. & TUCKER, M.E. (1991). *Responses of rimmed shelves to relative sea-level rises; a proposed sequence stratigraphic classification* (Abstract). Proceedings Dolomieu Conference, the Dolomites, Italy, p.114-115.

HUNT, D & TUCKER, M.E. (1992). The sequence stratigraphy of carbonate shelves with an example from the mid-Cretaceous of S.E. France. *In: Stratigraphy and Facies associations in a sequence stratigraphic Framework* (Ed. by H. Posamentier, C.P. Summerhayes, B.U. Haq & G.P. Allen). Int. Assoc. Sedim. Spec. Publ. 15, in press.

HUNT, D. & TUCKER, M.E. (1992). The responses of rimmed shelves to relative sea-level rises; implications for sequence stratigraphic models. Submitted MS.

JACOB, C (1905). *Etudes paléntologiques et stratigraphies sur la partie moyenne des terrains crétacés dans les Alpes françaises et les régions vosienes.* Thèse, Fac. Sc. Paris, série A, no 540, no d'ordte 1264, 314p.

JACQUIN, T. (1989). *Sequence stratigraphy in the southern Vercors: Study of continuous outcrops from platform to basin at the scale of seismic sections.* Unpublished fieldguide, University of Dijon, 48p.

JACQUIN, T., ARNAUD-VANNEAU, A., ARNAUD, H., RAVENNE, C. & VAIL, P.R. (1991). Systems tracts and depositional sequences in a carbonate setting: a study of continuous outcrops from platform to basin at the scale of seismic lines. *Marine Petrol. Geol.* **8**, 122-139.

JAMES, N.P. (1983). Reef environment. *In: Carbonate depositional Environments* (Ed. by P.A Scholle, D.G. Bebout, C.H. Moore). Am. Assoc. Geol. Petrol. Mem. 33, 345-462.

JAMES, N.P. & CHOQUETTE, P.W. (1984). Diagenesis 9. Limestones- the meteoric diagenetic environment. *Geoscience Canada* **11**, 161-194.

JAMES, N.P. & GINSBURG, R. N.(1979). *The seaward margin of the Belize barrier and atoll reefs.* Special Publication, International Association of Sedimentologists, 3, 191p.

JORDAN, C.F. (1978). Tropical lagoon sedimentation. *In: The encyclopedia of sedimentology* (Ed by R.W. Fairbridge & J. Borugeois). Dowden, Hutchinson & Ross, Stroudberg, 821-27.

JOSEPH, P., BEAUDOIN, B., FRIES, G. & DECONINCK, J.F. (1985). Megasequences and resediments in the subalpine basin, France (Malm - Cretaceous). *Proceedings 6th European regional meeting of sedimentology.*

JOSEPH, P., BEAUDOIN, B., FRIES, G. & PARIZE, O. (1989). Les vallées sons-marines enregistrent au Crétacé inférieur le fonctionnement en blocs basculés de domaine vocontien. *C. R. Acad. Sci. Paris.* **309**, 1031-1038.

JOSEPH, P., BEAUDOIN, B. SEMPERE, T. & MAILLART, J. (1988). Vallées sous-marines at systèmes d'épandages carbonatés du Berriasien vocontien (Alpes

méridionales françaises). *Bull. Soc. géol. France* **IV**(8), 363-374.

KENTER, J.A.M. (1990). Carbonate platform flanks: slope angle and sediment fabric. *Sedimentology* **37**, 777-794.

KENDALL, C.G. & SCHLAGER, W. (1981). Carbonates and relative changes in sea-level. *Mar. Geol.* **44**, 181-212.

KINSMAN, D.J.J. & PARK, R.K. (1976). Algal belt and coastal sabkha evolution, Trucial Coast, Persian Gulf. *In: Stromatolites* (Ed. by M.R, Walter). 421-433.

LaFARGE, D (1978). *Etude géologique du Plateau de Saint-Remèze, Ardèche. Stratigraphie, cartographie, sédimentologie, tectonique.* Thèse 3e Cycle, Lyon, pp. 119 (unpublished).

LEMOINE, M., BAS, T., ARNAUD-VANNEAU, A., ARNAUD, H., DUMONT, T., GIDON, M., BOURBON, M., DE GRACIANSKY, P.-C., RUDIEWICZ, J.-L., MEGARD-GALLI, J. & TRICART, P. (1986). The continental margin of the Mesozoic Tethys in the Western Alps. *Marine Petrol. Geol.* **3**, 179-199.

LEMOINE, M. & TRUMPY, R. (1987). Pre-oceanic rifting in the Alps. *Tectonophysics* **133**, 305-320.

LONGMAN, M.W. (1981). A process approach to recognising facies of reef complexes. *In: European Fossil Reef Models* (Ed. by D.F. Toomey). Spec. Publ. Soc. Econ. Paleont. Mineral. 30, 9-40.

LORY, C (1846). *Description géologique du Dauphiné pour servir à l'explication de la carte géologique de cette province.* Savy édit., Paris? 1ère partie p.1-240, 2è partie p.241-500, 3è partie p.501-747.

MAGNIEZ-JANNIN, F. (1991). Renouvellements fe foraminifères et séquences de dépôt dans le Crétacé inférieur du Bassin vocontien (SE de la France). *Bull. Soc. géol. France* **V**, 887-895.

MASCLE, G., ARNAUD, H., DARDEAU, G., DEBELMAS. J., DELPECH, P.-Y., DUBOIS, P., GIDON, M., GRACIANSKY, P.-C., KERCKOVE, C. & LEMOINE, M. (1988). Salt tectonics, Tethyan rifting and Alpine folding in the French Alps. *Bull. Soc. géol. France* **IV** (8), 747-758.

MASSE, J.-P. & PHILIP, J. (1981). Cretaceous coral-rudist bulidups of France. *In: European Fossil Reef Models* (Ed by D.F. Toomey). Spec. Publ. Soc. Econ. Paleont. Mineral. 30, 399-426.

MAY, J.A. & EYLES, D.R. (1985). Well log and seismic character of Tertiary

Terumbu carbonate, South China Sea, Indonesia. *Am. Assoc. Petrol. Geol. Bull.* **69**, 1339-1358.

MCLREATH, I.A. (1977). Accumulation of a Middle Cambrian, deep-water limestone debris apron adjacent to a vertical submarine carbonate escapement, southern Rocky Mountains, Canada. *In: Deep-water Carbonate Environments* (Ed. by H.E. Cook & P. Enos). Spec. Publ. Soc. Econ. Paleont. Mineral. 25, 113-124.

MIALL, A.D. (1986). Eustatic sea level changes interpreted from seismic stratigraphy: A critique of the methodology with particular reference to the North Sea Jurassic record. *Am. Assoc. Petrol. Geol. Bull.* **70**, 131-137.

MILLER, K.G. & FAIRBANKS, R.G. (1985). Cainozoic $\delta\ ^{18}O$ record of climate and sea-level. *South African. Journal of Science* **81**, 248-249.

MITCHUM, R.M. (1977). Seismic stratigraphy and global changes of sea-level, part 11: Glossary of terms used in seismic stratigraphy. *In: Seismic Stratigraphy- Applications to Hydrocarbon Industry* (Ed. by C.E. Payton). Am. Assoc. Petrol. Geol. Mem. 26, 205-212.

MITCHUM, R.M. (1985). Seismic stratigraphic expression of submarine fans. *In: Seismic stratigraphy II; an intergrated approach* (Ed. by O.R. Berg & D.G. Woolverton). Am. Assoc. Petrol. Geol. Mem. 39, 117-136.

MITCHUM, R.M., VAIL, P.R. & SANGREE, J.B. (1977). Stratigraphic interpretation of seismic reflection patterns in depositional sequences. *In: Seismic Stratigraphy-applications to hydrocarbon exploration* (Ed. by C.E. Payton). Am. Assoc. Petrol. Geol. Mem. 26, 117-133.

MITCHUM, R.M. & VAN WAGONER, J.C. (1991). High-frequency sequences and their stacking patterns: sequence stratigraphic evidence of high-frequency eustatic cycles. *Sedimentary Geology* **70**, 131-160.

MOUGENOT, D., BOILLOT, G. & REHAULT, J-P. (1983). Prograding shelfbreak types on passive continental margins: some European examples. *In: The Shelfbreak: Critical Interface of Continental Margins* (Ed. by D.J. Stanley & G.T. Moore). Spec. Publ. Soc. Econ. Paleont. Mineral. 33, 61-77.

MUGNIER, J.-L., GUELLEC, S., MENARD, G., ROURE, F., TARDY, M. & VIALLON, P. (1990). A crustal scale balanced cross-section through the external Alps deduced from the ECORS profile. *Mém. Soc. géol. Fr.* n° 156, 203-216.

MUIR, I., WONG, P. & WENDTE, J. (1985). Devonian Hare Indian-Ramparts (Kee Scarp) evolution, Mackenzie Mountains and subsurface Norman Wells, N.W.T.:basin-fill and platform-reef development. *In: Rocky Mountain carbonate Reservoirs: A core*

workshop (Ed. by M.W. Longman, K.E. Shanley, R.F. Lindsay & D.E. Eby). Soc. Econ. Paleont. Mineral. Core Workshop 311-342.

MULLINS, H.T., NEWTON, C.R., HEATH, K. & VAN BUREN, H.M. (1981). Modern deep-water coral mounds north of Little Bahama Bank: criteria for recognition of deep water coral bioherms in the rock record. *Jour. Sedim. Petrol.* **51**, 999-1013.

MULLINS, H.T. (1983). Comment on 'Eustatic control of turbidites and winnowed turbidites'. *Geology* **11**, 57-58.

MULLINS, H.T. & COOK, H.E. (1986). Carbonate apron models: alternatives to the submarine fan model for palaeoenvironmental analysis and hydrocarbon exploration. *Sedimentary Geology* **48**, 37-79.

MULLINS, H.T., GARDULSKI. A. F., HINE, A. C., MELILLO, A. J., WISE, W. W. & APPLEGATE, J. E. (1988). Three-dimensional sedimentary framework of the carbonate ramp slope of central west Florida: a sequential seismic stratigraphic perspective. *Geol. Soc. Amer. Bull.* **100**, 514-533.

MULLINS, H.T., HEATH, K.C., VAN BUREN, M. & NEWTON, C.R. (1984). Anatomy of a modern open-ocean carbonate slope: Northern Little Bahama Bank. *Sedimentology* **31**, 141-168.

MULLINS, H.T. & NEUMANN, A.C. (1979). Deep carbonate bank margin structure and sedimentation in the northern Bahamas. *In: Geology of Continental Slopes* (Ed. by L.J. Doyle & O.H. Pilkey). Spec. Publ. Soc. Econ. Paleont. Mineral. 27, 165-192.

NEUMANN, A.C. & MACINTYRE, I.G. (1985). Response to sea-level rise: keep-up, catch-up or give-up. *Proc. 5th Coral Reef Cong., Tahiti* 3, 105-110.

OSLEGER, D. (1991). Subtidal carbonate cycles: Implications for allocyclic vs. autocyclic controls. *Geology* **19**, 917-920.

PAQUIER, V. (1900). *Recherches géologiques dans le Diois et les Baronnies orientales.* Thèse, Imp. Allier Grenoble, 402p.

PARKINSON, R.W. & MEEDER, J.F. (1991). Mud-bank destruction of a transgressive sand sheet, southwest Florida inner shelf. *Geol. Soc. Amer. Bull.* **103**, 1543-1551.

PARKINSON, N. & SUMMERHAYES, C. (1985). Synchronous global sequence boundaries. *Am. Assoc. Petrol. Geol. Bull.* **69**, 685-687.

PITMAN, W.C. (1978). Relationship between eustacy and stratigraphic sequences of passive margins. *Geol. Soc. Amer. Bull.* **89**, 1389-1403.

PLAYFORD, P.E. (1980). Devonian 'Great Barrier Reef' of Canning Basin, Western Australia. *Am. Assoc. Petrol. Geol. Bull.* **64**, 814-840.

POSAMENTIER, H.W., JERVEY, M.T. & VAIL, P.R. (1988). Eustatic controls on clastic deposition I-conceptual framework. *In: Sea-level Changes, an Integrated Approach* (Ed. by C. K. Wilgus, B. S. Hastings, C. G. St.C. Kendall, H. W. Posamentier, C. A. Ross & J. C. Van Wagoner). Spec. Publ. Soc. Econ. Paleont. Mineral. 42, 108-124.

POSAMENTIER, H.W. & VAIL, P.R. (1988). Eustatic controls on clastic deposition II: sequence and systems tract models. *In: Sea-level Changes, an Integrated Approach* (Ed. by C. K. Wilgus, B. S. Hastings, C. G. St.C. Kendall, H. W. Posamentier, C. A. Ross & J. C. Van Wagoner). Spec. Publ. Soc. Econ. Paleont. Mineral. 42, 125-154.

PURDY, E.G. (1974). Reef configurations: cause and effect. *In: Reefs in Space and Time* (Ed. by L.F. Laporte). Spec. Publ. Soc. Econ. Paleont. Mineral. 18, 9-76.

PURSER, B.H. (1973). Sedimentation around bathymetric highs in the southern Persian Gulf. *In: The Persian Gulf* (Ed. by B.H. Purser). Springer-Verlag, pp. 157-177.

PURSER, B.H., SOLIMAN, M. & M'RABET, A. (1987). Carbonate, evaporite siliciclastic transitions in Quaternary rift sediments of the northwestern Red Sea. *Sedimentary Geology* **53**, 247-268.

RAVENNE, C., LEQUETTFE, P., VALLERY, P. & VIALLY, R. (1987). Deep clastic carbonate deposits of the Bahamas - comparison with Mesozoic outcrop of the Vercors and Vocontian trough. *In: Atlas of Seismic Stratigraphy* (Ed. by A. V. Bally). Am. Assoc. Petrol. Geol. Studies in Geology 27, 104-140.

READ, J.F. (1982). Carbonate platforms of passive (extensional) continental margins; types, characteristics and evolution. *Tectonophysics* **81**, 195-212.

READ, J.F. (1985) Carbonate platform facies models. *Am. Assoc. Petrol. Geol. Bull.* **69**, 1-21).

READING, H.G. (Ed.) (1986). *Sedimentary Environments and Facies* (2nd edition). Blackwell Scientific Publications, Oxford. 615pp.

REVIL, J. (1911). *Géologie des chaînes jurassiennes et subalpines de la Savoie.* 1ére et 2 è parties. Mém. Acad. Sciences, Belles-Lettres et arts de savoie, 5ème série, t.1, p. 139-774).

RIO, M., FERRY, S. & COTILLON, P. (1989). La périodicité dans les sèries pélagiques alternantes. Exemple du Crétacé inférieur de la région d' Angles/Saint-André-les-Alpes (Sud-Est de la France). *C. R, Acad. Sci. Paris*, **309** (II), 73-79.

ROBERTS, G.P. (1990). *Deformation and diagenetic histories around foreland thrust faults*. Unpublished Ph.D thesis, University of Durham.

ROBERTS, H.H. & MURRAY, S.P. (1988). Gulfs of Northern Red Sea: depositional settings of distinct siliciclastic-carbonate interfaces. *In: Carbonate-Clastic Transitions* (Ed. by L.J. Doyle & H.H. Roberts). Developments in Sedimentology 42, 99-142.

ROUX, M., BOURSEAU, J-P., BAS, T., DUMONT, T., GRACIANSKY, P.-C., LEMOINE, M. & RUDKIEWICZ, J.-L. (1988). Bathymetric evolution of the Tethyan margin in the Western Alps (data from stalked crinoids): a reappraisal of eustatism during the Jurassic. *Bull. Soc. géol. France* **IV**(8) 633-641.

RUDKIEWICZ, J.-L. (1988). Quantitive subsidence and thermal structure of the European continental margin of the Tethys during early and middle Jurassic times in the western Alps (grenoble-Briançon transect). *Bull. Soc. géol. France* **IV**(8) 623-632.

RUDOLPH, K.W. & LEHMANN, P.J. (1989). Platform evolution and sequence stratigraphy of Natuna platform, South China Sea. *In: Controls on Carbonate Platform and Basin Development* (Ed. by P.D. Crevello, J.L. Wilson, J.F. Sarg & J.F. Read). Spec. Publ. Soc. Econ. Paleont. Mineral. 44, 353-364.

RUDOLPH, KW., SCHLAGER, W. & BIDDLE, KT. (1989). Seismic models of a carbonate foreslope-to-basin transition, Picco di Vallandro, Dolomite Alps, northern Italy. *Geology* **17**, 453-456.

RUFFEL, A. H. & BATTEN, D. J. (1990). The Barremian-Aptian arid phase in western Europe. *Palaeogeog. Palaeoclim. Palaeoecol.* **80**, 197-212.

SALLER, A H., BARTON, J.W. & BARTON, R.E. (1989). Slope sedimentation associated with a vertically-building shelf. Bone Spring Formation, Mescalero Escarpe Field, southeastern New Mexico. *In: Controls on Carbonate Platform and Basin Development* (Ed. by P.D. Crevello, J.L. Wilson, J.F. Sarg & J.F. Read). Spec. Publ. Soc. Econ. Paleont. Mineral. 44, 275-288.

SANDBERG, P.A. (1983). An oscillating trend in Phanerozoic non-skeletal mineralogy. *Nature* **305**, 19-22.

SARG, J.F. (1988). Carbonate sequence stratigraphy. *In: Sea-level Changes: an Integrated Approach* (Ed. by C. K. Wilgus, B. S. Hastings, C. G. St.C. Kendall, H. W. Posamentier, C. A. Ross & J. C. Van Wagoner). Spec. Publ. Soc. Econ. Paleont. Mineral. 42, 155-181.

SCHLAGER, W. (1981). The paradox of drowned reefs and carbonate platforms. *Geol. Soc. Amer. Bull.* **92**, 197-211.

SCHLAGER, W. (1989). Drowning unconformities on carbonate platforms. *In: Controls on Carbonate Platform and Basin Development* (Ed. by P.D. Crevello, J.L. Wilson, J.F. Sarg & J.F. Read). Spec. Publ. Soc. Econ. Paleont. Mineral. 44, 15-25.

SCHLAGER, W. (1991). Depositional bias and environmental change-important factors in sequence stratigraphy. *Sedimentary Geol.* **70**, 109-130.

SCHLAGER, W. & CAMBER, O. (1986). Submarine slope angles, drowning unconformities and self-erosion of limestone escarpments. *Geology* **14**, 762-765.

SCHLAGER, W. & CHERMAK, A. (1979). Sediment facies of platform-basin transition, Tongue of the Ocean, Bahamas. *In: Geology of Continental Slopes* (Ed. by L.J. Doyle & O.H. Pilkey). Spec. Publ. Soc. Econ. Paleont. Mineral. 27, 193-207.

SCHLAGER, W. & GINSBURG, R.N. (1981). Bahama carbonate platforms - the deep and the past. *Mar. Geol.* **44**, 1-24.

SCHLANGER, S.O. & KONISHI, K. (1975). The geomorphic boundary between the coral-algal and bryozoan-algal limestone facies-A palaeolatitude indicator. *IX International Congress of Sedimentology, Theme 1*, p. 187-191.

SCHROEDER, R., BUSNARDO, R., CLAVEL, B. & CHAROLLAIS, J. (1989). Position des couches à *Valserina brönnimanni* Schroeder et Conrad (Orbitolinidés) dans la biozonation du Barrémien. *C. R. Acad. Sci. Paris.* **309**, 2093-2100.

SHANMUGAM, G. & MOIOLA, R.J. (1982). Eustatic control of turbidites and winnowed turbidites. *Geology* **10**, 231-235.

SHANMUGAM, G. & MOIOLA, R.J. (1991). Types of submarine fan lobes: models and implications. *Am. Ass. petrol. Geol. Bull.* **75**, 156-179.

SLOAN, L.C. & BARRON, E.J. (1990). "Equable" climates during Earth history? *Geology* **18**, 489-492.

STANLEY, D.J., ADDY, S.K & BEHRENS, E.W. (1983). The mudline: variability of its position relative to shelfbreak. *In: The Shelfbreak: Critical Interface of Continental Margins* (Ed. by D.J. Stanley & G.T. Moore). Spec. Publ. Soc. Econ. Paleont. Mineral. 33, 279-298.

STOAKES, F.A. (1980). Nature and control of shale basin fill and its effect on reef growth and termination: Upper Devonian Duvernay and Ireton Formations of Alberta, Canada. *Canad. Petrol. Geol. Bull.* **28**, 345-410.

THIEULOY, J.-P. (1979). Matheronites limentinus n. sp. (Ammonoidea) Espèce type

d'un horizon-repère Barrémien supérieur du vercors méridional (massif sub-alpin français). **Geobios**, Mém. **3**, 305-317.

THORNE, J.A. & SWIFT, D.J.P. (1992). Sedimentation on continental margins, part VI: A regime model for depositional sequences, their component systems tracts, and bounding surfaces. in prep.

TUCKER, M.E. (1985). Shallow-marine carbonate facies and facies models. *In: Sedimentology: Recent Developments and Applied Aspects* (ed. by P.J. Brenchley & B.P.J. Williams). Spec. Pub. Geol. Lond. 18, 139-161.

TUCKER, M.E. (1991). Sequence stratigraphy of carbonate-evaporite basins: the Upper Permian (Zechstein) of northeast England and adjoining North Sea. *J. Geol. Soc. Lond.* **148**, 1019-1036.

TUCKER, M.E. (1992). Carbonate diagenesis and sequence stratigraphy. In: *Sedimentary Reviews* (Ed. by V.P. Wright). 1, in press.

TUCKER, M. E. & HUNT, D. (in prep) Sequence stratigraphic models for carbonate platforms.

TUCKER, M.E., CALVERT, F. & HUNT, D. (1992). Sequence stratigraphy of carbonate ramps and application to the Triassic Muschelhalk platforms of eastern Spain. *In: Stratigraphy and Facies associations in a Sequence Stratigraphic Framework* (Ed. by C. P. Summerhayes, H.W. Posamentier, B. U. Haq & G. P. Allen). Int. Assoc. Sedim. Spec. Publ. 15, in press.

TUCKER, M.E. & WRIGHT, V.P. (1990). *Carbonate Sedimentology.* Blackwell Scientific Publications, Oxford. 482pp.

VAIL, P.R. (1987). Seismic stratigraphy interpretation procedure. *In: Atlas of Seismic Stratigraphy I* (Ed. by A.W. Bally). Am. Assoc. Petrol. Geol. Studies in Geology 27, 1-10.

VAIL , P.R., AUDEMARD, F., BOWMAN, S.A., EISNER, P.N. & PEREZ-CRUZ. G. (in press). The stratigraphic signatures of tectonics, eustasy and sedimentation.

VAIL, P.R., HARDENBOL, J. & TODD, R.G. (1984). Jurassic unconformities, chronostratigraphy and sea-level changes from seismic stratigraphy and biostratigraphy. *Intetregional Unconformities And Hydrocarbon Accumulation* (Ed. by J.S. Schlee). Am. Assoc. Petrol. Geol. Mem. 36, 129-144.

VAIL, P.R., MITCHUM, R.M., TODD., R.G., WIDMEIR, J.M., THOMPSON, S., HATFIELD, W.G. (1977). *In: Seismic Stratigraphy - Application to Hydrocarbon Exploration* (Ed. by C.E. Payton). Am. Assoc. Petrol. Geol. Mem. 26, 49-212.

VAIL, P. R. & TODD, R.G. (1981). North Sea Jurassic unconformities, chronostratigraphy and sea-level changes from seismic stratigraphy and biostratigraphy. *In: Petroleum Geology Of The Continental Shelf Of North-West Europe* (Ed by L.V. Illing and C.D. Hobson). Heydon Institute Of Petroleum, London, 216-235.

VAN WAGONER, J.C. (1985). *Reservoir facies distribution as controlled by sea-level change.* (Abstract) Society of Economic Palaeontologists and Mineralogists Mid-year Meeting, Golden, Colorado. p91-92.

VAN WAGONER, J.C., POSAMENTIER, H.W., MITCHUM, R.M., VAIL, P.R., SARG, J.F., LOUTIT, T.S. & HARDENBOL, J. (1988). An overview of the fundamentals of sequence stratigraphy and key definitions. *In: Sea-level Changes - an Integrated Approach* (Ed. by C. K. Wilgus, B. S. Hastings, C. G. St.C. Kendall, H. W. Posamentier, C. A. Ross & J. C. Van Wagoner). Spec. Publ. Soc. Econ. Paleont. Mineral. 42, 39-45.

VAN WAGONER, J.C, MITCHUM, R.M., CAMPION, K.M. & RAHMANIAN, V.D. (1990). *Siliciclastic Sequence Stratigraphy in Well Logs, Cores and Outcrops.* Am. Assoc. Petrol. Geol. Methods in Exploration Series, no. 7, pp. 45.

VIAU, C. (1983). Depositional sequences, facies and evolution of the upper Devonian Swan Hills Reef buildup, Central Alberta, Canada. *In: Carbonate Buildups: a Core Workshop* (Ed. by P.M. Harris). Soc. Econ. Paleont. Mineral. Core Workshop, 112-143.

VIEBAN, F. (1983). *Installation et évolution de la plate-forme urgonienne (Hauterivien à Bédoulien) du Jura méridional aux chaînes subalpins (Ain, Savoie, Haute-Savoie).* These 3e cycle, Université Grenoble, 291p.

WARD, R.F., KENDALL, CG. St.C. & HARRIS, P.M. (1986). Upper Permian (Guadalupian) facies and their association with hydrocarbons-Permian Basin, west Texas and New Mexico. *Am. Assoc. Petrol. Geol. Bull.* **70**, 239-262.

WARD, W.C., WEIDIER, A.E. & BLACK, W. (1985). *Geology And Hydrology Of The Yucatan.* New Orleans Geol. Soc. pp. 160.

WATTS, K.F. (1988). Triassic carbonate submarine fans along the Arabian platform margin, Sumeini Group, Oman. *Sedimentology* **34**, 43-71.

WEIMER, P. (1989). Sequence stratigraphy of the Mississippi fan (Plio-Pleistocene), Gulf of Mexico. *Geo-Marine Letters* **9**, 185-272.

WIENS, H.J. (1962). *Atoll environment and Ecology.* Yale University press. 532pp.

WILBER, RJ., MILLIMAN, J.D. & HALLEY, R.B. (1990). Accumulation of

bank-top sediment on the western slope of Great Bahama Bank: rapid progradation of a carbonate megabank. *Geology* **18**, 970-974.

WILGUS, C.K., HASTINGS, B.S., KENDALL. C.G., POSAMENTIER, H.W., ROSS. C.A. & VAN WAGONER, J.C. (1988) *Sea-Level Changes: An Integrated Approach.* Spec. Publ. Soc. Econ. Paleont. Mineral. 42. pp 407.

WILKINSON, B.H. (1979). Biomineralisation, palaeooceanography and the evolution of calcareous marine organisms. *Geology* **7**, 526-527.

WILLIAMS, D.F. (1988). Evidence for and against sea-level changes from the stable isotopic record of the Cenozoic. *In: Sea-level Changes - an Integrated Approach* (Ed. by C. K. Wilgus, B. S. Hastings, C. G. St.C. Kendall, H. W. Posamentier, C. A. Ross & J. C. Van Wagoner). Spec. Publ. Soc. Econ. Paleont. Mineral. 42, 31-36.

WILSON, J.L. (1975). *Carbonate Facies in Geologic History.* Springer-Verlag, Berlin. 471p.

WRIGHT, V.P. (1988). Palaeokarsts and palaeosols as indicators of palaeoclimate and porosity evolution: a case study from the Carboniferous of South Wales. *In: Paleokarst* (Ed. by N.P. James & P.W. Choquette). Springer-Verlag, Berlin. 329-341.

WRIGHT, V.P. & WILSON, R.C.L (1984). A carbonate submarine fan sequence from the Jurassic of Portugal. *J. Sedim. Petrol.* **54**, 394-412.

RESPONSES OF RIMMED SHELVES TO RELATIVE SEA LEVEL RISES; A PROPOSED SEQUENCE STRATIGRAPHIC CLASSIFICATION

D. Hunt & M. Tucker

Department of Geological Sciences, Science Laboratories, South Road, Durham DH1 3LE, UK

Carbonate depositional systems differ from siliciclastic equivalents in many respects. One of the most important contrasts is to be seen at the margin to carbonate shelves; these are typically rimmed by high energy reef and/or grainstone shoal complexes. Growth rates at rimmed shelf margins commonly have the capacity to outpace rates of relative sea level rise (RSL = subsidence + eustasy), which can result in the development of geometries different from those recognized on siliciclastic shelves where the transgressive systems tract (TST) is characterized by retrogradational parasequences. Carbonate depositional systems show a great sensitivity to the rates of relative sea level rise.

The sequence stratigraphic approach distinguishes between type 1 and type 2 sea level falls that are thought to reflect different rates of relative sea level fall. Higher rates of sea level fall result in a lowstand fan complex and lowstand wedge (type 1), and lower rates a shelf margin wedge (type 2). Rates of relative sea level rise have never been distinguished since siliciclastic depositional systems (upon which sequence stratigraphic models are largely based) appear not to develop characteristic stratal patterns in response to differing rates of relative sea level rise. Carbonates, however, develop different geometries and stratal patterns that reflect both differing rates of relative sea level

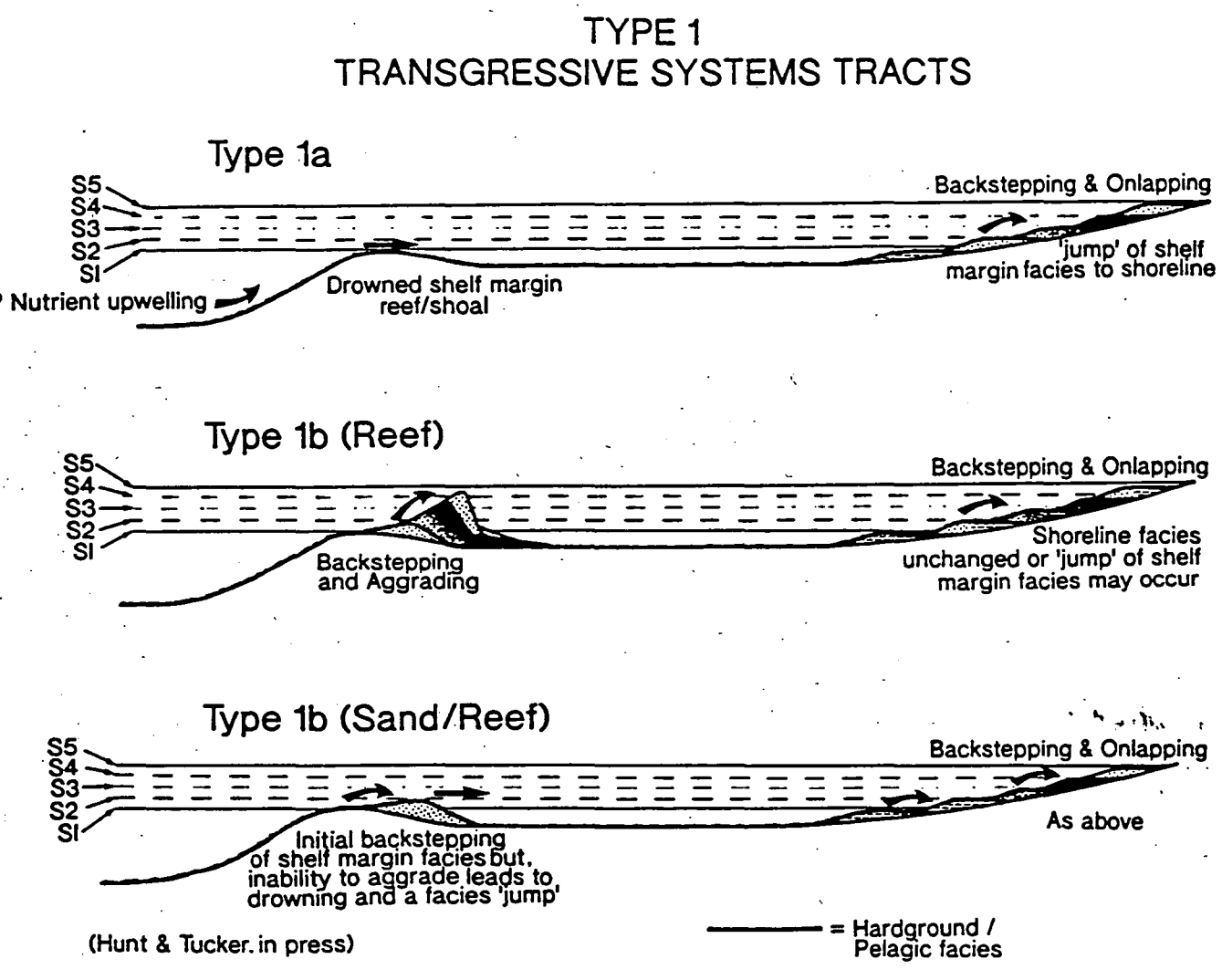

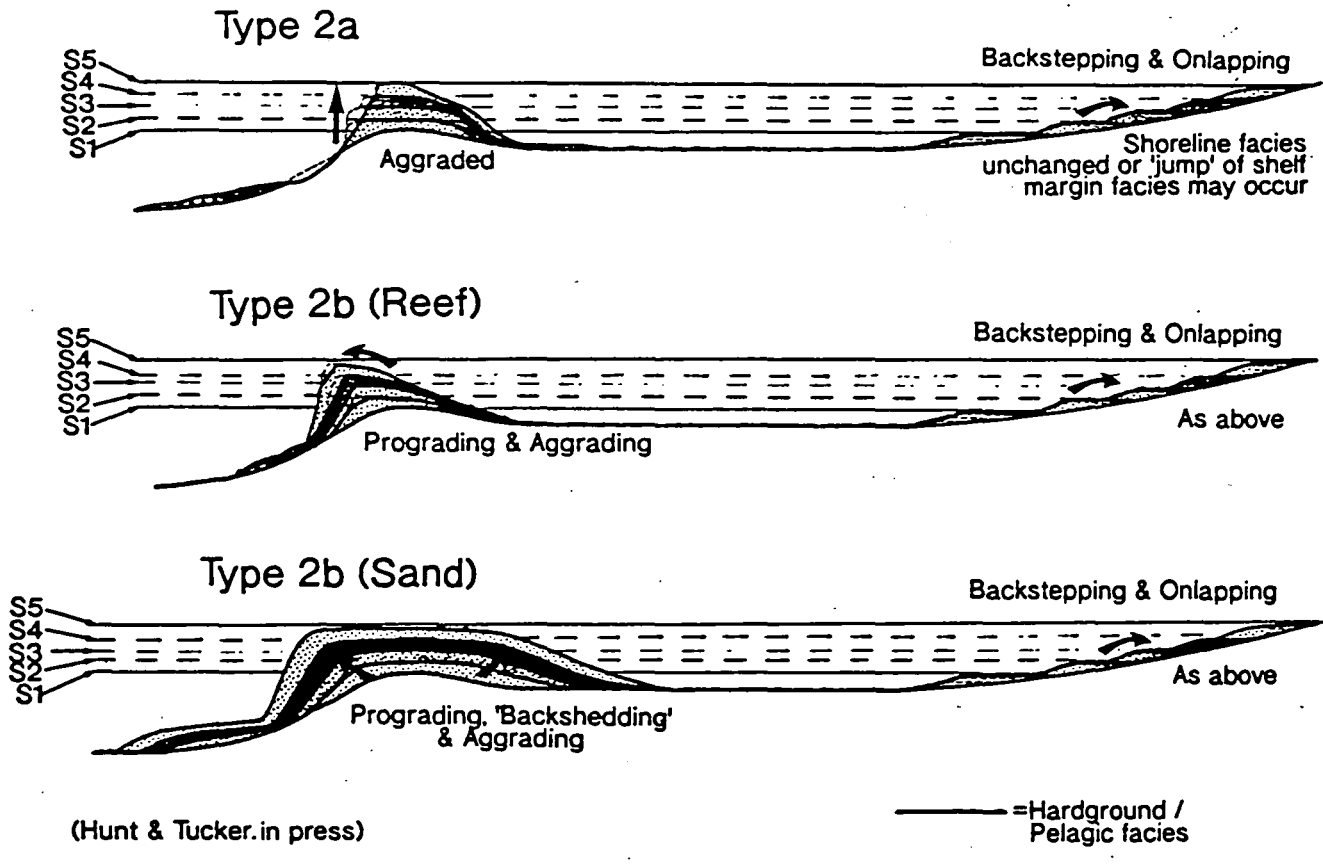

rise and the position of sea level upon the slope/shelfbreak at the beginning of the TST. Models presented in fig. 1 are for a starting point of the TST at the point when sea level is at the shelf break of the earlier highstand. In sequence stratigraphic models for shelves (siliciclastic or carbonate), the LSW is depicted as developing up to the shelf break before the more rapid sea level rise of the TST. However, this may not always be the case, and the geometries of the TST will differ if the LST has not reached the shelf-break.

Two types of relative sea level rise can be distinguished, types 1 and 2 (Fig. 1). As with relative sea level falls, a type 1 rise is associated with high rates of relative sea level change (greater than production rates) resulting in either in situ reef/shoal drowning (type 1a), or an onlapping/backstepping margin (type 1b). Rates of relative sea level change in a type 2 rise are equal (type 2a), or less than (type 2b) rates of production at the shelf margin, developing a vertical aggradational or an aggrading-prograding geometry respectively.

Type 1 relative sea level rises may develop stratal patterns within the TST similar to siliciclastic depositional systems (eg. retrogradational parasequence sets), whereas **type 2 rises** develop geometries, and stratal patterns completely different from those reported from siliciclastic shelves.

26

New trends in stratigraphy and sedimentology (Convenors: S. Smith, H. Weissert, R. Reyment and M. Mutti)

26/1 SEQUENCE STRATIGRAPHIC MODELS FOR CARBONATE PLATFORMS

M. TUCKER
(Department of Geological Sciences, University of Durham, Durham DH1 3LE, UK)

Sequence stratigraphy has largely been applied to siliciclastic formations and there is still much fundamental work to be done in applying it to carbonate formations. Carbonate depositional systems do respond in different ways to changes in relative sea-level, compared to siliciclastic systems, as a result of the strong biological-physicochemical control on sedimentation and the potential high rates of carbonate production relative to the rates of relative sea-level rise. Highstand shedding, leeward-windward effects on highstand progradation rates, lowstand bypass wedges, facies jumps due to rapid relative sea-level changes, and aggradation rather than retrogradation, are important processes in carbonate systems giving rise to particular sequence/parasequence patterns and geometries. In addition, the common early cementation of carbonates gives rise to special features (hardgrounds, reef walls, high slope angles, lithoclasts, megabreccias), which are not present in siliciclastic systems.

The three main classes of carbonate platform are rimmed shelf, ramp and epeiric platform/aggraded shelf. Now there are important differences between the geometry and internal stratigraphy of the depositional sequences of these different platform types. These are most clearly shown in the lowstand and in the relative importance of transgressive versus highstand systems tracts. Ramps usually show poorly-developed LST, just downramp migration of facies belts with little resedimentation, contrasting with the megabreccias and LSW of rimmed shelves. The magnitude of relative sea-level change is very significant on shelves, giving rise to the rimmed versus aggraded shelf types. Drowning events and facies jumps are more conspicuous on shelves. Many carbonate sequences consist of parasequences (shallowing-upward cycles), and the internal structure and stacking patterns of these vary between the platform types and give useful information on the directions, rates and causes of relative sea-level change. The sequence stratigraphic models for carbonate platforms are applied to Carboniferous, Permian, Triassic and Cretaceous examples from western Europe.

6/2 A PROPOSED CLASSIFICATION FOR RATES OF RELATIVE SEA-LEVEL CHANGE FOR CARBONATE DEPOSITIONAL SYSTEMS, WITH PARTICULAR RESPECT TO RIMMED SHELVES

D. HUNT
(Department of Geological Sciences, University of Durham, Durham DH1 3LE, UK)

Carbonate depositional systems differ from siliciclastic equivalents in many respects. One of the most important contrasts is to be seen at the margin to carbonate shelfs, these are typically rimmed by high energy reef or grainstone shoal complexes. Growth rates at rimmed shelf margins commonly have the capacity to outpace rates of relative sea-level rise (RSL=subsidence + eustacy), which can result in development of geometries different from those recognised on siliciclastic shelf margins where relative sea-level rises result in retrogradational parasequences, whatever the rate of relative sea-level rise. Carbonate depositional systems show a sensitivity to the rates of relative sea-level rise.

The sequence stratigraphic approach distinguishes between type 1 and 2 sea-level falls that are thought to reflect rates of relative sea-level change. Higher rates of RSL fall result in a lowstand fan complex (type 1), and lower rates a shelf margin wedge (type 2). Rates of relative sea-level rise have never been distinguished as siliciclastic depositional systems (from which the sequence stratigraphic approach evolved) appear not to develop characteristic stratal patterns in response to differing rates of relative sea-level rise. Carbonates, however, develop geometries, and stratal patterns that reflect rates relative sea-level rise.

It is proposed that two types of relative sea-level rise can be distinguished, types 1 and 2. As with relative sea-level falls, a type 1 rise is associated with high rates of relative sea-level change (greater than production rates), resulting in either insitu reef/shoal drowning (type 1a), or an onlapping/backstepping margin (type 1b). Rates of relative sea-level change in a type 2 rise are equal (type 2a), or less than (type 2b) rates of production at the shelf margin, developing a vertical aggradational or progradational geometry respectively.

Type 1 relative sea-level rises develop stratal patterns within the transgressive systems tract similar to siliciclastic depositional systems (eg. retrogradation of the margin), whereas, type 2 rises develop geometries, and stratal patterns considerably different from those reported from siliciclastic shelf margins.

26/3 THE WESTERN MARGIN OF THE FRIULI-PLATFORM, VENETIAN ALPS: A RECORD OF VARIOUS ORDERS OF SEA LEVEL FLUCTUATIONS IN CARBONATE SEDIMENTS

U. SCHINDLER
(Geologisches Institut, ETH-Zentrum, 8092 Zürich, Switzerland)

The Tithonian to Aptian sequence of the Monte Cavallo Group (Venetian Alps) consists of a number of prograding reef bodies separated and finally overlain by lagoonal to intertidal sediments. This pattern reflects the westward progradation of the Friuli platform. Two megacycles, interpreted as second order sequences in the sense of Haq et al. (1987), are defined by the stacking pattern of the reefs and the inserted and overlying thick intertidal intervals.

The megacycles can be subdivided into assumed third-order sequences. In the lower part of the section such a third-order sequence consists of a single reef body overlying an emersion horizon and is capped by a prism of lagoonal to intertidal sediments. In the upper part, where reefs are lacking, the six third-order sequences recognized are composed of shallowing upward lagoonal to intertidal cycles. Within the third-order sequences, the individual cycles become thinner bedded up-section and intertidal facies prevail.

Obviously two higher (4th and/or 5th) orders of sedimentary cycles are present. Their lithologies vary according to their depositional environment and can range from the classic intertidal cycles to rhythmic alternations of coarse back-reef and fine-grained lagoonal sediments. Their stacking pattern appears to be well organized and probably reflects superimposed sea level fluctuations; thus these cycles may be useful for the subdivision of sedimentary sequences. They suggest that minor sea level fluctuations may be recorded by a variety of different carbonate cycles.